Ecological Studies 209

Akira Osawa, Olga A. Zyryanova
Yojiro Matsuura, Takuya Kajimoto
and Ross W. Wein
Editors

Permafrost Ecosystems

Siberian Larch Forests

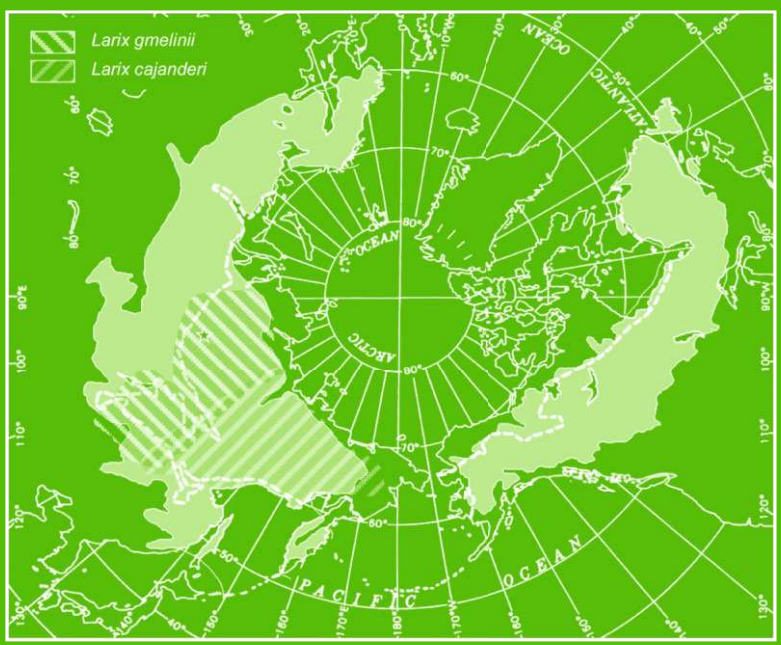

Springer

Ecological Studies, Vol. 209

Analysis and Synthesis

Ecological Studies

Further volumes can be found at springer.com

Volume 191
Wetlands: Functioning, Biodiversity Conservation, and Restoration (2006)
R. Bobbink, B. Beltman, J.T.A. Verhoeven, and D.F. Whigham (Eds.)

Volume 192
Geological Approaches to Coral Reef Ecology (2007)
R.B. Aronson (Ed.)

Volume 193
Biological Invasions (2007)
W. Nentwig (Ed.)

Volume 194
Clusia: A Woody Neotropical Genus of Remarkable Plasticity and Diversity (2007)
U. Lu¨ttge (Ed.)

Volume 195
The Ecology of Browsing and Grazing (2008)
I.J. Gordon and H.H.T. Prins (Eds.)

Volume 196
Western North American Juniperus Communites: A Dynamic Vegetation Type (2008)
O. Van Auken (Ed.)

Volume 197
Ecology of Baltic Coastal Waters (2008)
U. Schiewer (Ed.)

Volume 198
Gradients in a Tropical Mountain Ecosystem of Ecuador (2008)
E. Beck, J. Bendix, I. Kottke, F. Makeschin, R. Mosandl (Eds.)

Volume 199
Hydrological and Biological Responses to Forest Practices: The Alsea Watershed Study (2008)
J.D. Stednick (Ed.)

Volume 200
Arid Dune Ecosystems: The Nizzana Sands in the Negev Desert (2008)
S.-W. Breckle, A. Yair, and M. Veste (Eds.)

Volume 201
The Everglades Experiments: Lessons for Ecosystem Restoration (2008)
C. Richardson (Ed.)

Volume 202
Ecosystem Organization of a Complex Landscape: Long-Term Research in the Bornho¨ved Lake District, Germany (2008)
O. Fra¨nzle, L. Kappen, H.-P. Blume, and K. Dierssen (Eds.)

Volume 203
The Continental-Scale Greenhouse Gas Balance of Europe (2008)
H. Dolman,R.Valentini, and A. Freibauer (Eds.)

Volume 204
Biological Invasions in Marine Ecosystems: Ecological, Management, and Geographic Perspectives (2009)
G. Rilov and J.A. Crooks (Eds.)

Volume 205
Coral Bleaching: Patterns, Processes, Causes and Consequences (2009)
M.J.H van Oppen and J.M. Lough (Eds.)

Volume 206
Marine Hard Bottom Communities: Patterns, Dynamics, Diversity, and Change (2009)
M. Wahl (Ed.)

Volume 207
Old-Growth Forests: Function, Fate and Value (2009)
C. Wirth, G. Gleixner, and M. Heimann (Eds.)

Volume 208
Functioning and Management of European Beech Ecosystems (2009)
R. Brumme and P.K. Khanna (Eds.)

Volume 209
Permafrost Ecosystems: Siberian Larch Forests (2009)
A. Osawa, O.A. Zyryanova, Y. Matsuura, T. Kajimoto, R.W. Wein (Eds.)

Akira Osawa · Olga A. Zyryanova
Yojiro Matsuura · Takuya Kajimoto
Ross W. Wein
Editors

Permafrost Ecosystems

Siberian Larch Forests

Springer

Editors
Akira Osawa
Kyoto University
Kyoto
Japan
aosawa@kais.kyoto-u.ac.jp

Olga A. Zyryanova
V.N. Sukachev Institute of Forest
Krasnoyarsk
Russia
zyryanova-o@yandex.ru

Yojiro Matsuura
Forestry and Forest Products
Research Institute
Ibaraki
Japan
orijoy@ffpri.affrc.go.jp

Takuya Kajimoto
Forestry and Forest Products
Research Institute
Tsukuba
Japan
tkaji@ffpri.affrc.go.jp

Ross W. Wein
University of Alberta
Edmonton, AB
Canada
rosswein@shaw.ca

ISBN 978-1-4020-9692-1 e-ISBN 978-1-4020-9693-8
DOI 10.1007/978-1-4020-9693-8
Springer Dordrecht Heidelberg London New York

Library of Congress Control Number: 2009942785

Cover illustration: Distribution patterns of boreal forests (shaded area) and southern boundaries of the zones of continuous permafrost (thick broken line) in northern hemisphere. Natural range of *Larix gmelinii* and that of *L. cajanderi* are also shown. Location of the major study area at Tura is indicated by a star. Distribution of *L. cajanderi* and that of boreal forest do not match exactly at Chukotskoye Nagor'ye between 165°E and 180°E due to different sources of information. (Modified from Larson 1980; Brown et al. 1997; Abaimov et al. 1998; See also Fig. 1.1 for details.)

Printed on acid-free paper

Springer is part of Springer Science+Business Media (www.springer.com)

Dedicated to Prof. Anatoly P. Abaimov who led ecological research in the permafrost forest biome of Siberia.

Preface

This volume summarizes the results of ecological research on Siberian larch forests that has been conducted jointly by a team of Russian and Japanese scientists in northern Central Siberia during the past decade. In the following pages, we report our findings, including assertions, discoveries, and re-discoveries on the patterns and processes of the larch forests that were so common to Russian ecologists but very remote, inaccessible, and unusual to foreign scientists. Inaccessibility of the Siberian ecosystems stemmed, of course, from the world politics particularly those after the Second World War. The Soviet Union had practically prohibited foreign scientists from conducting any scientific investigation in Siberia. Ecological knowledge from this region had been published nearly exclusively in the Russian language, and was not distributed widely. In the meanwhile, ecological concepts and methods progressed in the western-block countries somewhat independently of the ecological knowledge within the Soviet Union. As a result, some major discrepancies have developed in the ecological knowledge. There were also discrepancies in the methods of analyses in forest soils and ecophysiological measurements. By working together, we have overcome some differences. We have also realized that the larch ecosystems of Siberia are unusually nutrient-limited systems. This fact has led to some discoveries in both forest structure and function, which will be discussed in some depth in the following chapters.

Opportunity for a joint research came rather suddenly. Michael Gorbachev, then the president of the Soviet Union, visited Japan in 1989, and proposed with Prime Minister Toshiki Kaifu to set aside funds for joint scientific investigation of the territory of Siberia. Gorbachev fell from power shortly thereafter, and the Soviet Union has disappeared from the world map – but the promises were kept in both sides. A major research program on atmospheric and terrestrial carbon dynamics in Siberia was organized in 1991 by funds from the Environment Agency (now Ministry of the Environment) of Japan. Japanese ecologists started visiting Siberia, first in Yakutia in 1991, then began to concentrate the efforts near a village of Tura in 1995 at 64°N and 100°E, about 800 km east of the Yenisei River and in the midst of the continuous permafrost zone. Russian Government has also contributed funds through V.N. Sukachev Institute of Forest at Krasnoyarsk.

The purpose of our investigation has been to describe *Larix gmelinii* (Rupr.) Rupr. (Gmelin larch) ecosystems in northern taiga of Central Siberia and to discern

the potential role those forests may play under the climate that is considered to be warming. A series of study sites and study plots were established near Tura by adding necessary study areas to those already been established by the scientists of V.N. Sukachev Institute of Forest. Stand structure, stand development, forest production, forest floor vegetation, tree ecophysiology, and soils have been examined. Carbon budget study with CO_2 flux measurement and nitrogen dynamics study with fertilization experiment have been initiated recently as well. This volume describes mostly the former part of our investigation, but some materials from the latter will also be included.

Readers should be reminded that this book does not provide the whole picture of larch forests in Siberia. It reviews where our knowledge stands, and adds some new information and implications that were obtained through our investigation. We do not pretend that the work has been completed. A series of investigations answered some questions. But this process created further questions. Many of them have not yet been answered. We hope to make a point in this book that the larch ecosystem over continuous permafrost is a distinct and wide-spread biome, and should be recognized as such in ecological disciplines. With this hope, we included discussions comparing larch ecosystems of Siberia to other biomes. Implications of the structure and functioning of the larch forests under global warming are also added toward the end of the book. We hope that these discussions are enlightening and useful to the readers.

The book is composed of five major parts. Part I describes ecological setting of Siberian ecosystems that are dominated by the larch species. Part II is devoted to the description of dynamics and function of the larch forest ecosystems. Part III describes tree ecophysiology and the environment for the larch species in Siberia. Part IV deals with comparisons of our findings to forest ecosystems on the other parts of the globe and implications with respect to responses to the anticipated climate change in the following decades. Finally, Part V synthesizes characteristics of larch species and larch forests in Siberia, including their potential responses to climate change.

Our activities in Siberia owe numerous individuals and organizations. Gen Inoue of Nagoya University (then at National Institute for Environmental Studies) was the key person organizing the initial scientific program with the Japanese Environment Agency during 1991–1992. Without him, there would have been no program. Kunihide Takahashi of Hokkaido University (then a member of Forestry and Forest Products Research Institute of Japan) was instrumental in creating a vital program in forest ecology. Masami Fukuda of University of Alaska, Fairbanks (then at Hokkaido University) supplied us ample insight and suggestions on the field work in Siberia. Ruzhena V. Gordeeva, director of Evenkia Department of Nature Protection at Tura, provided logistical help in our field activities. Viktor M. Borovikov and Sergey Tenishev of Evenkia Department of Forestry helped us in many ways at the field station in Tura. Galina M. Gruncheva and Galina A. Borovikova, among others, worked as cooks at our field station at separate field seasons, to whom we are grateful. Scientific field assistance were provided by many students, including T. Chikhachova, K. Fukuzaki, A. Ishizaki, E. Mizumachi,

O. Rezvykh, Y. Seo, A. Shcherbacheva, A. Shinkareva, V. Shkikunov, Y. Yanagihara, and V. Zyryanov. Following colleagues helped us focus on particular aspects of research activities through many discussions: M. Araki, A. Bondarev, K. Fukuyama, M. Ishizuka, G. Iwahana, S. Kagawa, G. Kofman, K. Kushida, V. Kuzmichov, O. Martinsson, T. Miyaura, K. Noguchi, K. Ono, N. Saigusa, H. Saito, H. Sakai, H. Sawada, T. Sofronova, R. Tabuchi, G. Takao, A. Takenaka, T. Toma, S. Yamamoto, Y. Yamamura, and T. Yokota. We tried to list all persons who contributed to our study greatly; however, if there are any relevant names missing from the above list, it is solely a mistake of the editors.

O. Martinsson, T. Lei, N. Kurachi, and S. Sugita read the manuscript and provided invaluable comments. Parts of the manuscript were also read and commented by students in a graduate course in boreal forest ecosystems at Kyoto University, including T. Agata, K. Fukuzaki, S. Takahashi, M. Takenaka, and M. Togo. We thank particularly E.-D. Schulze who carefully reviewed the entire manuscript, and helped us to improve the quality of the book substantially. Funding for our scientific work came mostly from Ministry of Environment of Japan through projects S-1 and B-053 as noted earlier. However, additional funds were also provided from Science and Technology Agency of Japan; Ministry of Education, Science, Sports, and Technology of Japan; Ryukoku University; Sukachev Institute of Forest, Siberian Branch of Russian Academy of Sciences; Russian Fund of Basic Research; and Forestry and Forest Products Research Institute of Japan. We are thankful to all these donors. Institutional and managerial support for our activities was also provided by E. Petrenko of V.N. Sukachev Institute of Forest, and N. Kanaya of Forestry and Forest Products Research Institute of Japan. We are particularly grateful to A. Onuchin, the director of V.N. Sukachev Institute of Forest, who oversaw our activities and helped us in invaluable ways. Ria Kanters of Springer provided editorial support that made our book much more readable than its original form. Last, but not to the least, we thank our families to have endured various inconveniences while we were away in Siberia for field work over many field seasons: Without their support, this work would have been impossible.

Kyoto, Japan — Akira Osawa
Krasnoyarsk, Russia — Olga A. Zyryanova
Tsukuba, Japan — Yojiro Matsuura
Tsukuba, Japan — Takuya Kajimoto
Edmonton, Canada — Ross W. Wein

Contents

Part II Ecosystem Dynamics and Function

Part IV Ecosystem Comparisons and Responses to Climate Change

Contributors

Anatoly P. Abaimov (deceased)
V.N. Sukachev Institute of Forest, Siberian Branch, Russian Academy of Sciences, Akademgorodok, Krasnoyarsk 660036, Russia

Hiro Arai
Division of Forest and Biomaterials Sciences, Graduate School of Agriculture, Kyoto University, Sakyo-Ku, Kyoto 606-8502, Japan

N.N. Bugaenko
Institute of Computaional Modelling, Siberian Branch, Russian Academy of Sciences, Akademgorodok, Krasnoyarsk 660036, Russia

Tatiana N. Bugaenko
V.N. Sukachev Institute of Forest, Siberian Branch, Russian Academy of Sciences, Akademgorodok, Krasnoyarsk 660036, Russia

Dong Su Choi
Institute of Symbiotic Science and Technology, Tokyo University of Agriculture and Technology, Fuchu, Tokyo 183-8509, Japan

Hiromu Daimaru
Department of Soil and Water Conservation, Forestry and Forest Products Research Institute, Tsukuba, Ibaraki 305-8687, Japan

Norikazu Eguchi
Graduate School of Agriculture, Hokkaido University, Kita-Ku, Sapporo 060-8589, Japan

Keitaro Fukushima
Field Science Education and Research Center, Kyoto University, Sakyo-Ku, Kyoto 606-8502, Japan

Ryo Funada
Institute of Symbiotic Science and Technology, Tokyo University of Agriculture and Technology, Fuchu, Tokyo 183-8509, Japan

Muneto Hirobe
Department of Environmental Ecology, Division of Biological and Human Environment, Graduate School of Environmental Science, Okayama University, Kita-Ku, Okayama 700-8530, Japan

Satoru Hobara
Department of Biosphere and Environmental Sciences, Faculty of Environmental Systems, Rakuno Gakuen University, Ebetsu, Hokkaido 069-8501, Japan

Shoko Homma
Department of Bioresource Science, Graduate School of Agricultural Science, Kobe Universuty, Nada-Ku, Kobe 657-8501, Japan

Mayuko Jomura
Department of Forest Science and Resources, College of Bioresource Sciences, Nihon University, Fujisawa, Kanagawa 252-8510, Japan

Takuya Kajimoto
Department of Plant Ecology, Forestry and Forest Products Research Institute, Tsukuba, Ibaraki 305-8687, Japan

Yoichi Kanazawa
Department of Bioresource Science, Graduate School of Agricultural Science, Kobe University, Kobe, Hyogo 657-8501, Japan

Alexander V. Kirdyanov
V. N. Sukachev Institute of Forest, Siberian Branch, Russian Academy of Sciences, Akademgorodok, Krasnoyarsk 660036, Russia

Satoshi Kitaoka
BRAIN Research Fellow, Hokkaido Research Center, Forestry and Forest Products Research Institute, Toyohira-Ku, Sapporo 062-8516, Japan

Takayoshi Koike
Department of Forest Science, Hokkaido University, Kita-Ku, Sapporo 060-8589, Japan

Kazuma Kondo
Corning Japan K.K., Kakegawa, Shizuoka 437-1302, Japan

Joni Kujansuu
Department of Forest Science, Faculty of Agriculture, Shinshu University, Minami-minowa, Kami-ina, Nagano 399-4598, Japan

Kobayashi Makoto
Department of Forest Science, Graduate School of Agriculture, Hokkaido University, Kita-Ku, Sapporo 060-8589, Japan

Oxana V. Masyagina
V.N. Sukachev Institute of Forest, Siberian Branch, Russian Academy of Sciences, Akademgorodok, Krasnoyarsk 660036, Russia

Yojiro Matsuura
Department of Forest Site Environment, Forestry and Forest Products Research Institute, Tsukuba, Ibaraki 305-8687, Japan

Shigeta Mori
Department of Plant Ecology, Forestry and Forest Products Research Institute, Tsukuba, Ibaraki 305-8687, Japan

Tomoaki Morishita
Department of Forest Site Environment, Forestry and Forest Products Research Institute, Tsukuba, Ibaraki 305-8687, Japan

Yuichiro Nakai
Department of Meteorological Environment, Forestry and Forest Products Research Institute, Tsukuba, Ibaraki 305-8687, Japan

Takeshi Ohta
Graduate School of Bioagricultural Sciences, Nagoya University, Chikusa-Ku, Nagoya 464-8601, Japan

Akira Osawa
Division of Forest and Biomaterials Sciences, Graduate School of Agriculture, Kyoto University, Sakyo-Ku, Kyoto 606-8502, Japan

Elena I. Parfenova
V.N. Sukachev Institute of Forest, Siberian Branch, Russian Academy of Sciences, Akademgorodok, Krasnoyarsk 660036, Russia

Anatoly S. Prokushkin
V.N. Sukachev Institute of Forest, Siberian Branch, Russian Academy of Sciences, Akademgorodok, Krasnoyarsk 660036, Russia

Stanislav G. Prokushkin
V.N. Sukachev Institute of Forest, Siberian Branch, Russian Academy of Sciences, Akademgorodok, Krasnoyarsk 660036, Russia

Laiye Qu
Key Lab of Systems Ecology, Chinese Academy of Sciences, Haidian District, Beijing 100085, China

Ali M. Quoreshi
Symbiotech Research Inc., 2020 Seed Labs Inc., Nisku, AB, T9E 7N5, Canada

Gerald E. Rehfeldt
Rocky Mountain Research Station, USDA Forest Service, Moscow, ID 83843, USA

Kaichiro Sasa
Hokkaido University Forests, FSC, Kita-Ku, Sapporo 060-0809, Japan

Fuchen Shi
Department of Environmental Resource Botany, College of Life Sciences, Nankai University, Nankai District, Tianjin 300071, China

Mark A. Sofronov
V.N. Sukachev Institute of Forest, Siberian Branch, Russian Academy of Sciences, Akademgorodok, Krasnoyarsk 660036, Russia

Nadja M. Tchebakova
V.N. Sukachev Institute of Forest, Siberian Branch, Russian Academy of Sciences, Akademgorodok, Krasnoyarsk 660036, Russia

Naoko Tokuchi
Field Science Education and Research Center, Kyoto University, Sakyo-Ku, Kyoto 606-8502, Japan

Tatsushiro Ueda
Dalton Co., Hokkaido Branch, Kita-Ku, Sapporo 060-0808, Japan

Vladimir A. Usoltsev
Botanical Garden, Ural Division, Russian Academy of Sciences, ul. Vos'mogo Marta, Yekaterinburg 620144, Russia

Eugene A. Vaganov
Siberian Federal University, Svobodny Prospect, Krasnoyarsk 660041, Russia

Alexandra V. Volokitina
V. N. Sukachev Institute of Forest, Siberian Branch, Russian Academy of Sciences, Akademgorodok, Krasnoyarsk 660036, Russia

Wenjie J. Wang
Key Laboratory of Forest Plant Ecology, Northeast Forestry University, Harbin 150040, China

Koh Yasue
Department of Forest Science, Faculty of Agriculture, Shinshu University, Minami-minowa, Kami-ina, Nagano 399-4598, Japan

Ken'ichi Yazaki
Department of Plant Ecology, Forestry and Forest Products Research Institute, Tsukuba, Ibaraki 305-8687, Japan

Yuan-Gang Zu
Key Laboratory of Forest Plant Ecology, Northeast Forestry University, Harbin 150040, China

Olga A. Zyryanova
V. N. Sukachev Institute of Forest, Siberian Branch, Russian Academy of Sciences, Akademgorodok, Krasnoyarsk 660036, Russia

Part I
Ecological Settings

Chapter 1
Introduction

A. Osawa and O.A. Zyryanova

1.1 Permafrost Forest Biome

Majority of the eastern half of Siberia is covered with forests of larch species. The forests are also growing mostly on continuous permafrost. However, the natural environment is quite different in the rest of the northern hemisphere. Tundra or arctic desert is virtually the only biome-type where the continuous permafrost predominates. Therefore, a biome of extensive forests over permafrost has never been recognized outside Siberia. Its ecology has been practically unknown. Classical textbooks of ecology, such as those by Odum (1971), Whittaker (1975), and Begon et al. (1990), describe a biome type called boreal forest (or taiga, or northern coniferous forest) for high latitudes of northern hemisphere. The boreal forest is commonly dominated by evergreen coniferous trees in both North America and Eurasia. Generally speaking, distribution of boreal forest and that of continuous permafrost are also mutually exclusive. However, we know today that approximately 20% of the boreal forests in the world are dominated by deciduous forest of larch species, and that they grow on continuous permafrost. We anticipate many differences not only in ecology of the tree species, but also in characteristics of the environmental factors between the traditional boreal forest and the permafrost forest biome of eastern half of Siberia. Area of such forests is too large to be treated as exception as well. Therefore, we propose permafrost forest as a separate division of the boreal forest biome.

Let us first see the extent of permafrost forest biome, and its relationship to the distribution of continuous permafrost in northern hemisphere. Figure 1.1 shows these patterns. Permafrost is widely distributed in Siberia. Nearly 40% of the land has the continuously frozen soils underneath. It is particularly widespread in the eastern half of the region. The distribution is also continuous in most of the areas above the 60th parallel (Wein and MacLean 1983). Its thickness varies dramatically; a range of 100 to >300 m has been described as that of the continuous permafrost (Brown et al. 1997). Therefore, much of the boreal forests in Siberia have developed over the perennially frozen soils, and our study site is located within such a region. The landscape of the continuous permafrost zone is dominated by two major species, *Larix gmelinii* (Rupr.) Rupr. (Gmelin larch) and *L. cajanderi*

A. Osawa et al. (eds.), *Permafrost Ecosystems: Siberian Larch Forests*,
Ecological studies, Vol. 209, DOI 10.1007/978-1-4020-9693-8_1,

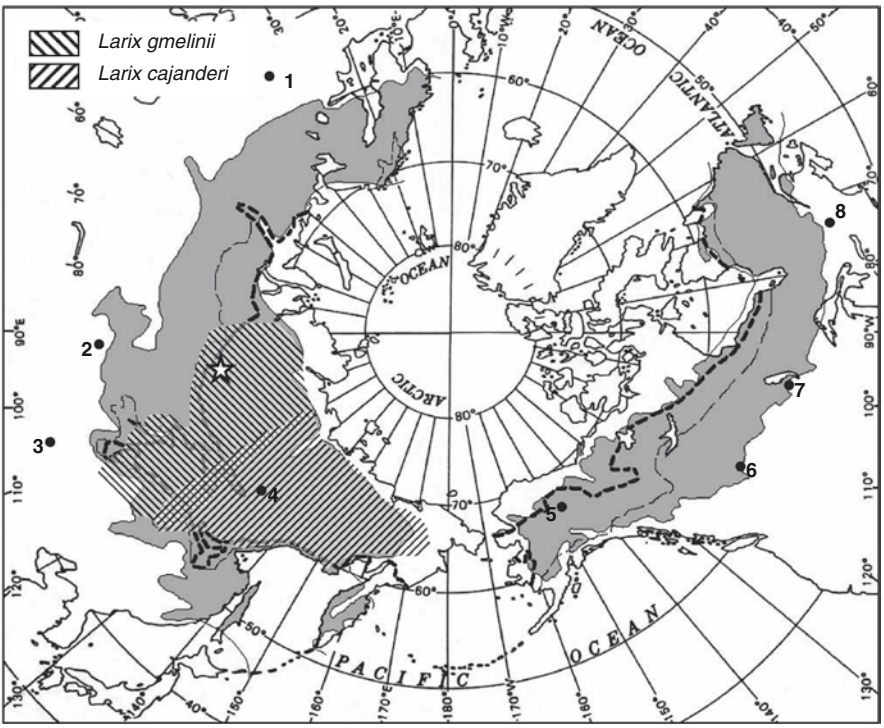

Fig. 1.1 Distribution patterns of boreal forests (*shaded area*) and southern boundaries of the zones of continuous permafrost (*thick broken line*) and those of discontinuous permafrost (*thin broken line*) in northern hemisphere. Natural range of *Larix gmelinii* and that of *L. cajanderi* are also shown. Location of the major study area at Tura is indicated by an *asterisk*. *Dots* and *numerals* indicate locations of Moscow (1; 37°E), and counter-clockwise, Krasnoyarsk (2), Ulaanbaatar (3), Yakutsk (4), Fairbanks (5), Edmonton (6), Winnipeg (7), and Montreal (8). Distribution of *L. cajanderi* and that of boreal forest do not match exactly at Chukotskoye Nagor'ye between 165°E and 180°E due to different sources of information. (Modified from Larsen, 1980; Brown et al. 1997; Abaimov et al. 1998)

Mayr (Fig. 1.1; also see Abaimov et al. 1998; Osawa et al. 2000). On the other hand, boreal forests do not commonly occupy areas of continuous permafrost in North America (Wein and MacLean 1983) except for areas of boreal peatlands (Wieder and Vitt 2006), or in areas of Eurasia west of the Yenisei River (Abaimov et al. 1998) (Fig. 1.1). Tundra and polar dessert are the biomes found over the continuous permafrost there. We know little about the reasons for these contrasting patterns. However, Paton et al. (1995) suggested that absence of continental ice sheet during the most recent ice age, and the resulting extremely low soil temperatures may have caused development of thick permafrost in eastern half of Siberia. We also do not know why the larch species can grow over the continuous permafrost so abundantly in Central and Northeastern Siberia, but not in the comparable regions of Arctic North America. Relatively small areas of *Picea mariana* (Mill.)

B.S.P. (black spruce) forests occupy the perennially frozen soils as the forested ecosystems in North America (Zoltai and Pettapiece 1974; Zoltai 1975; Van Cleve et al. 1983). It may well be that species comparable to *L. gmelinii* or *L. cajanderi* are simply absent from the New World.

1.2 The Environment and Ecology

The climate of the eastern half of Siberia is extremely continental. According to a long-term summary of climate for the former Soviet Union (Lydolph 1977; see also Figs. 9.1 and 10.4), the climate of our major study area at Tura at 64°N, 100°E is characterized by mean annual air temperature of −9.2°C and annual precipitation of 317 mm. Annual variation of the temperature is extreme. Monthly mean air temperature of the coldest month (January) is −36.8°C, whereas that of the warmest month (July) is 15.8°C. Absolute minimum of the air temperature of −67°C was observed in February, whereas absolute maximum of 35°C was recorded in July (Lydolph 1977). Diurnal temperature variation is large as well. Mean daily range of air temperature is the largest in April, with a value of 22.0°C. Precipitation is moderate with values more than 48 mm during the summer months of June, July, and August, whereas there is little precipitation (<10 mm) during the winter months of January, February, and March, with maximum snow depth (10-day average) of 44 cm (Lydolph 1977).

Prokushkin et al. (Chap. 11) show that monthly mean air temperature in January is −36.0°C, and that in July is 16.5°C based on data of much longer period including those from more recent years (1929–2006). The January and July mean temperatures are, respectively, 0.8 and 0.7°C warmer than the older statistics (Lydolph 1977). Prokushkin et al. (Chap. 11) also show that mean annual precipitation for this longer period is 366 mm, a value 49 mm more than that of Lydolph (1977). A trend of becoming warmer and more humid at Tura in recent years may be similar to that being observed in the Arctic and other boreal regions (Nemani et al. 2003; Hinzman et al. 2005). Effect of this trend may be complex, since increased precipitation in winter may shorten summer growing period under the background of warmer temperature (see Chap. 17). Potential effects of the warming climate on ecology of the permafrost larch forest will be discussed in the following chapters, and be synthesized finally (Chap. 24). See also Wielgolaski (2005) for a similar synthesis for the Nordic mountain birch forests. Chapters 10 and 11 provide further discussions on the meteorological condition of Tura.

Description of vegetation zones for Siberia follows a system of Nazimova (1996; Fig. 1.2) throughout this book by broadly following those of Shennikov and Vasil'ev (1947) and Lavrenko and Sochava (1954). See also Hytteborn et al. (2005) for details of classification by Nazimova and colleagues. Coniferous forests of Eurasia were divided into three subareas by Shennikov and Vasil'ev (1947):

(1) European–Siberian dark-coniferous taiga distributing west of the Yenisei River;
(2) Eastern-Siberian light-coniferous taiga consisting mostly of larch-dominated forests;

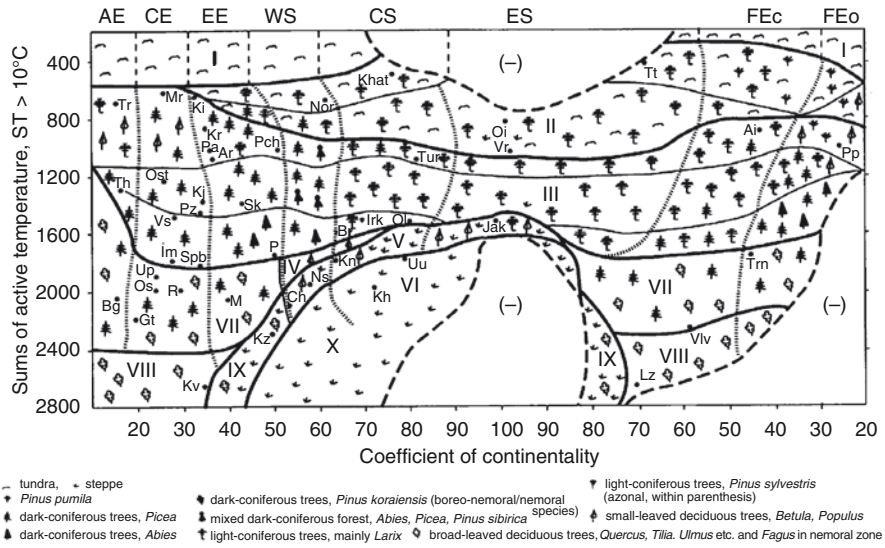

Fig. 1.2 Schematic representation of vegetation zones, subzones, and sectors in a climatic space with Coefficient of Continentality according to Conrad (1946) as the horizontal axis and temperature sums of daily mean temperatures above 10°C as the vertical axis. Explanations of zones and sub-zones: *I* tundra; *II* forest-tundra and northern open woodlands; *III* boreal zone with northern, middle, and southern subzones; *IV* small-leaved deciduous and light coniferous subzone; *V* cool Siberian forest-steppe; *VI* cool continental steppe; *VII/VIII* boreo-nemoral/nemoral zones, in Europe and Far East; *IX* warm temperate forest-steppe; *X* warm temperate steppe. Explanation of sectors: *AE* Atlantic-European; *CE* Central-European; *EE* East-European; *WS* West-Siberian; *CS* Central-Siberian; *ES* East-Siberian; *FEc* Far East continental; *FEo* Far East oceanic. Location of Tura, major study site described in this book, appears in northern taiga of Central Siberia. The sector ES is referred to as Northeastern Siberia throughout this book. See Hytteborn et al. (2005) for details. (From Hytteborn et al. 2005)

(3) Far-East dark-coniferous taiga. The boreal forests of Siberia are further divided into three latitudinal subzones: northern, middle, and southern taiga (Lavrenko and Sochava 1954). Northern open woodland and forest tundra are also recognized north of northern taiga. As a result, latitudinal zonation of vegetation types observed in Central Siberia appears, from north to south: tundra, forest-tundra, northern open woodlands, northern taiga, middle taiga, southern taiga, cool Siberian forest-steppe, and cool continental steppe, with small region of small-leaved deciduous and light coniferous subzone south of southern taiga toward western border of Central Siberia (Fig. 1.2). Major place names included in each latitudinal subzone are as follows: forest-tundra, Norilsk, Khatanga; northern open woodland, Oymyakon, Verkhoyansk; northern taiga, Tura; southern taiga, Bratsk, Irkutsk, Olekminsk; cool Siberian forest-steppe, Chelyabinsk, Novosibirsk, Kansk, Yakutsk.

Forest fires in Siberia are the integral part of ecosystem dynamics (Schulze et al. 1995; Abaimov et al. 1998; Osawa et al. 2003; see also Chap. 4). Characteristics

and the effects of fire on boreal forests appear common to the forests of both Eurasia and North America. Any forest may burn in every several decades, and is often replaced by regenerating trees in Siberia (Abaimov et al. 1998; see Chap. 3) and in North America (Cayford and McRae 1983; Viereck et al. 1983; Wein and MacLean 1983). The forests are adapted to rapid regeneration after fire disturbances. Viable seeds are not readily dispersed after ripening, and are stored in the cones for many years (called "cone serotiny") until the parent trees die of forest fires. *Pinus banksiana* Lamb. (Jack pine) and *Picea mariana* of the New World are good examples (Wein and MacLean 1983); *Larix gmelinii* also has cone serotiny (Abaimov et al. 1998; also see Chap. 3), and often regenerates as extremely dense stands after major fires.

Larix gmelinii and *L. cajanderi* hybridize introgressively in the region of contact at ca. 120°E meridian (Abaimov et al. 1998; see also Chap. 3). Southern distribution boundaries of these species roughly correspond with the southern limit of continuous permafrost zone in Siberia (Brown et al. 1997). Another larch species, *Larix sibirica* Ledeb., shows contrast by being distributed between the Ural Mountains and Yenisey River, in regions mostly free of continuous permafrost (Abaimov et al. 1998). Biomes of this region are often dominated not by the larches, but by the evergreen conifers such as *Pinus sylvestris* and *Picea obovata* (Abaimov et al. 1998; Schulze et al. 1999; Wirth et al. 1999, 2002).

1.3 Natural Regions of Siberia

We define, in the following, terminology and extent of specific areas within Siberia that we use throughout this book. The geographical terms associated with Siberia have some confusion, leading to misunderstanding. The following definitions are to avoid such potential problems. Siberia is a large area of approximately 10 million km^2 in northeastern Eurasia (Mikhailov 1976). It stretches from the latitude of roughly 77°N on the Arctic coast southward to about 48°N at the State border of the Russian Federation where it meets the Mongolian territory. It also ranges between the Ural Mountains to the west (ca. 60°E longitude) and the Pacific Ridges to the east (ca. 160°E). In total, Siberia occupies a belt as wide as 3,500 km and as long as 7,000 km (Mikhailov 1976). The northernmost point of the Asian continent – Chelyuskin Cape at 77°°43′N, 104°18′E – is located in Siberia.

Owing to the diverse environments in terms of topography, climate, and soil conditions, Siberia can be divided into four natural regions. They are Western Siberia, Central Siberia, Mountainous Southern Siberia, and Northeastern Siberia (Gvozdetskiy and Mikhailov 1978). Western Siberia is located between the Ural Mountains to the west and the Yenisei River to the east, while Central Siberia occupies a vast territory between Yenisei and Lena Rivers. Northeastern Siberia is the region east of the Lena River, but excluding the maritime region of the Russian Far East. Mountainous Southern Siberia stretches along an east–west belt of 4,500 km long with the highest point at 4,500 m a.s.l., and along the State border of the

Russian Federation. These four regions of Siberia will be referred to in this book with the first letter capitalized, e.g., “Central Siberia.” It means the region between the Yenisei and Lena Rivers excluding the southern mountains. However, a term e.g., “central Siberia,” will also be used if a general area of the central part of Siberia is referred to.

1.4 Main Region of Study

Majority of studies described in the chapters of this book were conducted near a village of Tura at approximately 64°N and 100°E (indicated by a star in Fig. 1.1) in the midst of the continuous permafrost zone in Central Siberia. Because of the history of development of the studies summarized in this book, naming of study sites and forest plots has not been as organized as it should have been. We considered renaming them. However, some results were already published with original plot identification. Renaming is likely to create confusion and possible misunderstanding. Therefore, we decided to retain most of the original site and plot names, but to give a detailed description of which is where in the following paragraphs. Table 1.1 summarizes all sites and plots mentioned in chapters that discussed substantial data from the vicinity of Tura. Those of some other chapters are not included in Table 1.1, because they were examined more or less independently of the study at Tura that we describe intensively in this book.

Within a general region surrounding the village of Tura, there were four major study sites. They were referred to as Site 1, Site 2, Site 3, and Carbon Flux Site. Site 1 through Site 3 were located along the Kochechum River, a branch of the Nizhnyaya Tunguska River into which it merges at Tura (Fig. 1.3). Site 1 was on the east-bank, and Sites 2 and 3 were on the west-bank of the Kochechum River, and are located at 5–10 km north of the village. Carbon Flux Site was located about 20 km east-southeast of Tura and upstream of the Nizhnyaya Tunguska River (Fig. 1.3). It was on a flat to gently north-facing slope, and was located about 2 km south of the river bank. Each Site consisted of up to 16 plots that varied in site condition or stand structure, or those that were considered replicates of similar stands.

Site 1 was on a north-west facing slope of about 13° slope inclination. Most of Site 1 experienced a stand-replacing forest fire in 1899 (see Chaps. 6 and 7), and was 105-year-old in 2004. We established 15 plots in the 105-year-old portion of Site 1. Plot CR1899 was located at an upper middle portion of the slope. Throughout this book, the symbol CR represents a plot that was established as a part of chronosequence. Therefore, CR1899 means a chronosequence plot in a stand that became established after a fire of 1899. Plot W1 was located at the bottom of the same slope, and on a flat area near the Kochechum River, representing a stand of poor growth condition (Chaps. 6 and 16). Plots NF1 through NF12 were established along a band of similar altitude in the middle portion of the slope, and represented replicates of similar stands. These 12 plots were collectively referred to as NF plots (Chap. 6). They were at slightly worse growth condition than that of plot CR1899

Table 1.1 Identification and cross-listing of study plots near Tura that were referred to in various chapters

Site	Plot identification	Stand age in 2004 (year)	Chapter number[d]												
			4	5	6	7	8	9	10	11	12	14	15	16	17
Site 1	CR1899	105				x	x								
	NF1-NF12[a]	105			x		x			x					
	L14[a]	105				x									
	W1	105			x		x							x	
	CR1990	14		x	x	x	x								
Site 2	C1[b]	>220			x	x	x						x	x	
	II-5[b]	>220	x												
	TB-1[b]	>220	x												
	North facing slope	>220										x			x
	South facing slope	>220										x			x
	CR1830	174			x	x	x								
	CR1994[c]	10		x	x	x	x								
	II-4[c]	10	x												
Site 3	CR1978	26		x	x	x	x							x	
Carbon flux site	CF	105			x		x	x	x		x			x	x
	South facing slope	105													x

The "x" symbol indicates that data from a plot in question were used in that chapter.

[a–c]Plots labeled with these superscripts mean that the plots with the same letter were located in the same stand, but specific areas delineated for study differed. See specific chapters for detail of each plot

[d]Chapters 4 and 6 examined additional plots located far from Tura. Chapter 11 used Kulingdakan watershed that included a portion of Site 1

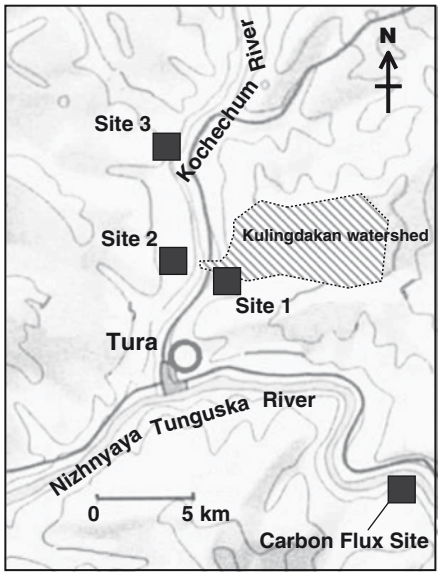

Fig. 1.3 Location of major study sites in the vicinity of Tura in Central Siberia. See text and Table 1.1 for identification of specific plots within these sites used in various chapters of the book

described above, as judged by mean tree height. Plot L14 was next to the NF plots with very similar stand structure. Patterns of stand development were examined in this plot (Chap. 7).

There was an area of younger stand age away from the Kochechum River in Site 1, consisting of 14-year-old stands that regenerated after a fire of 1990. We established a stand CR1990 there for examination of plant succession, and stand biomass and development (Chaps. 5, 6, and 7) (Table 1.1). A larger area of watershed was delineated within which Site 1 was included. It is referred to as Kulingdakan Watershed based on the name of the main stream (Chap. 11). The watershed is shown as a hatched area in Fig. 1.3. It included not only 105-year-old and 14-year-old stands, but also those of other ages.

Site 2 was on a generally east-facing gentle slope on the side of the Kochechum River opposite from Site 1. This site consisted of three stands that varied in age structure. First was an old multi-aged stand including canopy trees of >220-year-old. This stand often had lower canopy stratum of younger trees. Stand structure, biomass, root system development, and tree respiration were examined there (plot C1 in Chaps. 6, 7, 15, and 16; plots II-5 and TB-1 in Chap.4, this Vol.) (Table 1.1). A medium-sized stream flowed eastward through this site into the Kochechum River, creating north-facing and south-facing slopes of moderate inclination. Tree ecophysiological characteristics such as needle photosynthesis and phenology, and xylem growth in stems were compared between the slopes there (Chaps. 14 and 17). Second stand was a 174-year-old forest (as of 2004) to the north of the above-mentioned stream, and grew

after a fire of 1830. This stand was used as one of the chronosequence stands (CR1830; Chaps. 6 and 7). Third stand was a young regeneration developing after a fire of 1994 (Plot CR1994 in Chaps. 5, 6, and 7; and Plot II-4 in Chap. 4).

Site 3 was located farther north, and at about 10 km from Tura (Fig. 1.3). It is represented by a 26-year-old stand (in 2004) that became established after a 1978 fire (CR1978; Chaps 5, 6, and 7).

Carbon Flux Site (Fig. 1.3) was a 105-year-old forest, and was used for the evaluation of ecosystem carbon budget (Chap. 24). Major components of carbon stock and flow were estimated: soil carbon storage (Chap. 8), plant biomass and net primary production by the ecological method (Chap. 6), soil respiration by the closed chamber method (Chap. 9), and net ecosystem exchange by eddy covariance technique (Chap. 10). Nitrogen dynamics was examined there also (Chap. 12). Southern end of the Carbon Flux Site went over a small hill, and included a slope of south aspect. Therefore, this portion was used in comparison with generally north-facing slope of Carbon Flux Site to examination of the effect of slope aspect on xylem growth patterns (Chap. 17).

The chapters of this book also utilized other sites further away from Tura that could not be shown in Fig. 1.3. Chapter 2 utilized information gathered throughout a large region of Krasnoyarsk and Evenkia Territories. Chapter 3 included data from even larger regions of Siberia. Chapter 4 discussed forest plots located as north as 67°N (Kureyka River basin; Plots K1 through K4) and as west as 98°E (80 km west of Tura; Plots P1 through P3). Chapter 5 included three plots along Kochechum, Nizhnyaya Tunguska, and Tembenchi Rivers that could not be shown in Fig. 1.3. Chapter 6 added stand data from Chersky and Oymyakon regions in Northeastern Siberia. Chapter 13 based its discussion mostly on data gathered near Yakutsk in Northeastern Siberia. Chapter 18 included sites from wide area of Evenkia Territory (see Fig. 18.1). Chapters 19, 20, 21, 22, and 23 discussed data from other or even larger regions, since most of them treated biomes other than those in Siberia. Please refer to individual chapters for explanation of those various site locations and characteristics. Nomenclature of plant species follows Czerepanov (1985) throughout this book.

1.5 Brief History of Investigation

The first scientific data on the forests of high latitudes of Siberia were reported in the latter half of the nineteenth century (Middendorf 1867). Systematic investigation of the vast permafrost forests of the region followed in the early twentieth century. Sukachev (1912), Drobov (1927), Abolin (1929), Birkengof (1932), Nedrigailov (1932), and Povarnitsin (1933) made the pioneering descriptions of forest vegetation in various regions of Yakutia, while Avramchik (1937), Tjulina (1937) described northern forests of Krasnoyarsk region. Sukachev (1912) first mentioned ability of the larch species to form adventitious roots, which was later recognized as protective adaptation to extremely cold environments (Dylis 1981).

Studies of other Russian scientists were devoted to systematics and variability of Siberian *Larix* species (Kolesnikov 1946; Dylis 1961), to ecosystem diversity and natural regeneration of Siberian larch forests (Tjulina 1937, 1957; Tchugunov 1961; Krylov 1962; Panarin 1965; Utkin 1965; Shcherbakov 1975; etc.), and to examination of forest soils in Yakutia (Zol'nikov 1954; Konorowskii 1963; Elovskaya and Petrova 1965; etc.).

A series of detailed investigation using long transects and field stations were carried out by Pozdnyakov since 1950, leading to various discoveries in the "permafrost-forest" ecosystems. He studied the permafrost forests of Yakutia in Northeastern Siberia for more than 40 years and supervised research projects on hydrothermal regime of frozen soils, tree stand composition and structure, primary productivity of larch forests, seed production and seed quality, and on destructive insect populations. He also investigated soil processes including root distribution, soil thermal regime, and surface and subsurface runoff.

Detailed studies of hydrological regime made under supervision of Pozdnyakov tried to answer the following questions: (1) how does the canopy affect distribution of precipitation on the forest floor?; (2) how does precipitation penetrate through the tree canopy?; (3) how much is the stem flow?; (4) does snow depth differ in various larch ecosystems?; (5) how does litter influence the hydrological regime of forest soils? His studies of permafrost depth dynamics established that, under various environments, the seasonal permafrost thawing completed at the end of September or in the beginning of October. Maximum depth of the soil active layer was 240 cm and more in pine (*Pinus sylvestris*) forests on sandy soils. The maximum depth was only 128 cm in 50-year-old larch forests with *Duschekia fruticosa* in the understory (Pozdnyakov 1963). The depth of soil active layer in Yakutia appeared to depend on tree and shrub density as well as on the thickness of moss–lichen layer and forest floor.

Pozdnyakov was the first to have estimated the aboveground biomass of the most widespread larch forests in the permafrost area of Yakutia. According to his data, stem biomass makes up 85–91% of the total aboveground biomass. The share of the needles did not exceed 1.5–3.0% (Pozdnyakov 1967, 1975). Nevertheless, under the hydric soil conditions, the biomass of forest floor vegetation can account for 13% and more.

Based on the long-term investigation of Siberian permafrost forests, Pozdnyakov outlined the basic knowledge of the Permafrost Forest Science, a new branch of traditional forestry (Pozdnyakov 1986). He also proved that the alternative management options should be identified and developed for the cryolithic zone of Siberia to avoid inappropriate exploitation of natural resources of this territory. Today, the pioneering studies of Pozdnyakov and other scientists on permafrost forest biome of Siberia provide important bases to understand the possible responses of these ecosystems to the climate that is believed to be warming. The large proportion of the geographical area and that of the accumulated amount of carbon of the permafrost forest in world biomes also make the pioneering studies invaluable in the consideration of global carbon dynamics.

References

Abaimov AP, Lesinski JA, Martinsson O, Milyutin LI (1998) Variability and ecology of Siberian larch species. Swedish University of Agricultural Sciences, Department of Silviculture Reports 43, Umeå, 118pp

Abolin RI (1929) Geobotany and soils of the Lena-Vilyui plain. The issues on Yakutiyan Autonomous Republic studies 10:1–372 (in Russian)

Avramchik MN (1937) Geobotanic and pasture patterns of Dudypta river region. Arctic Institute Issues 63 (Geobotany), pp 47–81 (in Russian)

Begon M, Harper JL, Townsend CR (1990) Ecology, individuals, populations and communities. Blackwell, Boston 957 pp

Birkengof AL (1932) The forest cover and forest resources of the northern and eastern parts of Yakutiya 3. USSR Academic Press, Leningrad

Brown J, Ferrians OJ, Heginbottom JA, Melnikov ES (1997) Circum-arctic map of permafrost and ground-ice conditions. Circum-Pacific Map Series MAP CP-45, US Geological Survey

Cayford JH, McRae DJ (1983) The ecological role of fire in jack pine forests. In: Wein RW, LacLean DA (eds) The role of fire in northern circumpolar ecosystems. Scope 18. Wiley, New York

Conrad V (1946) Usual formulas of continentality and their limits of validity. Trans. Am. Geophys. Union 27:663–664

Czerepanov SK (1985) Vascular plants of Russia and adjacent states (the former USSR). Cambridge University Press, Cambridge 516 pp

Drobov VP (1927) Vegetation of Lena-Aldan Plateau: a brief description. In: The issues on Yakutiyan Autonomous Republic studies, vol 8. USSR, Russia, pp 1–60 (in Russian)

Dylis NV (1961) Larch species of Eastern Siberia and Far East. USSR Academic Press, Moscow (in Russian)

Dylis NV (1981) Larch species. Lesnaya promyshlennost, Moscow (in Russian)

Elovskaya LG, Petrova EI (1965) Soil and geographic subdivision of Yakutiyan Autonomous Republic territory. In: Shcherbakov IP (ed) The soils of Lena and Aldan rivers basins. Yakutknigoizdat, Yakutsk (in Russian)

Gvozdetskiy NA, Mikhailov NI (1978) Physical geography. Asian part. Mysl' Press, Moscow (in Russian)

Hinzman LD, Bettez ND, Bolton WR, Chapin FS III, Dyurgerov MB, Fastie CL, Griffith B, Hollister RD, Hope A, Huntington HP, Jensen AM, Jia GJ, Jorgenson T, Kane DL, Klein DR, Kofinas G, Lynch AH, Lloyd AH, McGuire AD, Nelson FE, Oechel WC, Osterkamp TE, Racine CH, Romanovsky VE, Stone RS, Stow DA, Sturm M, Tweedie CE, Vourlitis GL, Walker MD, Walker DA, Webber PJ, Welker JM, Winker KS, Yoshikawa K (2005) Evidence and implications of recent climate change in northern Alaska and other Arctic regions. Clim Change 72:251–298

Hytteborn H, Maslov AA, Nazimova DI, Rysin LP (2005) Boreal forests of Eurasia. In: Anderson F (ed) Ecosystems of the World 6, Coniferous forests. Elsevier, Amsterdam, pp 23–99

Kolesnikov BP (1946) Systematics and development history of *Larix* sp. Sect. Pauciseriales Patschke. In: Proceedings on history of flora and vegetation of the Soviet Union 2. USSR Academic Press, Moscow (in Russian)

Konorowskii AK (1963) On the soil erosion in Yakutiya. In: Shcherbakov IP (ed) The problems of wild nature conservation in Yakutiya. Yakutknigoizdat, Yakutsk (in Russian)

Krylov GV (1962) Forest resources and forestry subdivision. Nauka Press of the SB of RAS, Novosibirsk (in Russian)

Larsen JA (1980) The boreal ecosystem. Academic, New York 500pp

Lavrenko EM, Sochava VB (1954) Geobotanicheskaya karta SSSR, scale 1:4000000. Akad. Nauk SSSR, Moscow (in Russian)

Lydolph PE (1977) Climates of the Soviet Union. World survey of climatology, vol 7. Elsevier, Amsterdam, 417pp

Middendorf AF (1867) The travel to the northeastern part of Siberia. St. Petersburg's Botanical Garden Press, St. Petersburg (in Russian)
Mikhailov NI (1976) Nature of Siberia. Nauka, Moscow (in Russian)
Nazimova DI (1996) Sectoral and zonal classes of forest cover in Siberia and Eurasia as a basis of clarifying landscape pyrological characteristics. In: Goldammer JG, Furyaev VV (eds) Fire in the ecosystems of the boreal Eurasia. Kluwer, Dordrecht, pp 253–259
Nedrigailov SN (1932) The forest cover and forest resources of Yakutiya. The forest resources of Yakutiya 3:121–124 (in Russian)
Nemani RR, Keeling CD, Hashimoto H, Jolly WM, Piper SC, Tucker CJ, Myneni RB, Running SW (2003) Climate-driven increases in global terrestrial net primary production from 1982 to 1999. Science 300:1560–1563
Odum EP (1971) Fundamentals of ecology, 3rd edn. Saunders, Philadelphia
Osawa A, Abaimov AP, Zyryanova OA (2000) Reconstructing structural development of even-aged larch stands in Siberia. Can J For Res 30:580–588
Osawa A, Abaimov AP, Matsuura Y, Kajimoto T, Zyryanova OA (2003) Anomalous patterns of stand development in larch forests of Siberia. Tohoku Geophysic J (Sci Rep Tohoku Univ Ser 5) 36:471–474
Panarin II (1965) The types of larch associations of Chita oblast. Nauka, Moscow (in Russian)
Paton TR, Humphreys GS, Mitchell PB (1995) Soils, a new global view. UCL, London
Povarnitsin VA (1933) The forests of Aldan river valley from Tommot city to Uchur river. Issues of the Institute on forest study of the Academy of Sciences of the USSR 1, pp 155–231 (in Russian)
Pozdnyakov LK (1963) Hydroclimatic regime in forests of the central part of Yakutiya. USSR Academic Press, Moscow (in Russian)
Pozdnyakov LK (1967) Some patterns of biological productivity of larch forests in Yakutiya. Lesovedenje 6:36–42 (in Russian)
Pozdnyakov LK (1975) Dahurian larch. Nauka, Moscow (in Russian)
Pozdnyakov LK (1986) Permafrost forestry. Nauka, Novosibirsk (in Russian)
Schulze E-D, Schulze W, Kelliher FM, Vygodskaya NN, Ziegler W, Kobak KI, Koch H, Arneth A, Kusnetsova WA, Sogatchev A, Issajev A, Bauer G, Hollinger DY (1995) Aboveground biomass and nitrogen nutrition in a chronosequence of pristine Dahurian *Larix* stands in eastern Siberia. Can J For Res 25:943–960
Schulze E-D, Lloyd J, Kelliher FM, Wirth C, Rebmann C, Luhker B, Mund M, Knohl A, Milyukova I, Schulze W, Ziegler W, Varlagin A, Sogachov A, Valentini R, Dore S, Grigoriev S, Kolle O, Tchebakova N, Vygodskaya N (1999) Productivity of forests in the Eurosiberian boreal region and their potential to act as a carbon sink – a synthesis. Global Change Biol 5:703–722
Shcherbakov IP (1975) Forest cover of the northern-eastern part of the USSR. Nauka, Novosibirsk (in Russian)
Shennikov AP, Vasil'ev YY (1947) Eurasian coniferous-forest (taiga) province. In: Vasil'ev YY, Lavrenko EM, Lesnov AI (eds) Geobotanical Regionalization of the USSR. Izd-vo AN SSSR, Moscow (in Russian)
Sukachev VN (1912) Vegetation of the upper basin of Tungir river (Oljekma okrug of Yakutsk district). Amur Exped 1(1):1–286 (in Russian)
Tchugunov BV (1961) Forest regeneration in south-western Yakutiya. In: Proceedings on the forests of Yakutiya 8, pp 260–323 (in Russian)
Tjulina LN (1937) Forest vegetation of Khatanga region near the northern timberline. Arctic Institute Issues 63 (Geobotany), pp 83–180 (in Russian)
Tjulina LN (1957). Forest vegetation at the upper stream of Aldan River. Yakutian Biology Institute issues 3, pp 83–138 (in Russian)
Utkin AI (1965) Forests of Central Yakutiya. Nauka, Moscow (in Russian)
Van Cleve K, Dyrness CT, Viereck LA, Fox J, Chapin FS III, Oechel W (1983) Taiga ecosystems in Interior Alaska. Bioscience 33:39–44

Viereck LA, Dyrness CT, Van Cleve K, Foote MJ (1983) Vegetation, soils, and forest productivity in selected forest types in interior Alaska. Can J For Res 13:703–720

Wein RW and MacLean D (1983) The role of fire in northern circumpolar ecosystems. Scope 18. Wiley, Toronto

Whittaker RH (1975) Communities and ecosystems, 2nd edn. Macmillan, New York

Wieder RK, Vitt DH (eds) (2006) Boreal peatland ecosystems. Ecological Studies, vol 188. Springer, Berlin

Wielgolaski FE (ed) (2005) Plant ecology, herbivory, and human impact in Nordic mountain birch forests. Ecological Studies, vol 180. Springer, Berlin

Wirth C, Schulze E-D, Schulze W, von Stunzner-Karbe D, Ziegler W, Miljukova IM, Sgoatchev A, Varlagin AB, Panvyorov M, Grigoriev S, Kusnetzova W, Siry M, Hardes G, Zimmermann R, Vygodskaya NN (1999) Above-ground biomass and structure of prestine Siberian Scots pine forests as controlled by competition and fire. Oecologia 121:66–80

Wirth C, Schulze E-D, Luhker B, Grigoriev S, Siry M, Hardes G, Ziegler W, Backor M, Bauer G, Vygodskaya NN (2002) Fire and site type effects on the long-term carbon and nitrogen balance in prestine Siberian Scots pine forests. Plant Soil 242:41–63

Zol'nikov VG (1954) Soil investigations in Yakutiya: the main results and significance for practice. Reports of Fifth Scientific Session, Yakutknigoizdat, Yakutsk (in Russian)

Zoltai C (1975) Structure of subarctic forests on hummocky permafrost terrain in northwestern Canada. Can J For Res 5:1–9

Zoltai SC, Pettapiece WW (1974) Tree distribution on perennially frozen earth hummocks. Arct Alp Res 6:403–411

Chapter 2
Floristic Diversity and its Geographical Background in Central Siberia

O.A. Zyryanova, A.P. Abaimov, H. Daimaru, and Y. Matsuura

2.1 Introduction

Floristic diversity has been investigated in different latitudinal zones of Central Siberia. The area of focus in the present analysis stretches about 2,900 km from Karskoe Sea, at 77°41′N latitude, to the southern Russian state border, at 49°45′N. In terms of longitude, the area stretches approximately 2,075 km from the Yenisey River, at 82°E, to the Lena River, at 130°E. Total area makes up about 4.24 million km^2.

Bounded by the mountains at the northernmost and southernmost parts, Central Siberia coincides in territory with the Central Siberian Plateau, which is characterized by relatively uniform topography. Elevations of the most parts of the area rarely exceed 900–1,000 m, while some peaks reach 1,600–1,700 m high in the Putorana mountains (Kushev and Leonov 1964). Table-shaped watershed areas and rather deep river valleys with steep or step-like slopes often alternate with each other in the vast territory. Carbonates and basic bedrocks (such as basalts) are widely distributed in Central Siberia (Kushev and Leonov 1964).

In such vast areas, the climate varies locally. Mean annual air temperature ranges from −4°C in the south to −13.8°C in the north (Climate reference book of the USSR 1967). Total mean annual precipitation is about 300–400 mm in the southern part, gradually decreasing northwards to 180–250 mm (Climate reference book of the USSR 1969). Totally, climate of Central Siberia is strictly continental, with very low winter temperatures, short frost-free periods, and low humidity and moisture.

Location of Central Siberia at high latitudes of the Northern Hemisphere and severe climatic conditions provide continuous or discontinuous permafrost everywhere. It fully overlaps in territory with the zone of the permafrost (see Fig. 1.1). The total thickness of the permafrost declines from north to south and varies between 1,500 and 0 m (Fotiev et al. 1974). The temperature of the cryogenic layer increases gradually from −14 to 3°C.

Permafrost leads to the development of cryogenic microtopography, which is resulted from the frost action, and provides patterned environments on the forest floor. Soil temperature on the hummocks is usually 3–5°C or even 5–8°C higher than that in microdepressions (Abaimov et al. 1999; Kajimoto et al. 1998; see also Chap. 16).

A. Osawa et al. (eds.), *Permafrost Ecosystems: Siberian Larch Forests*,
Ecological studies, Vol. 209, DOI 10.1007/978-1-4020-9693-8_2,

The western and southern slopes of this microtopography are warmer and drier than that of eastern and northern slopes (Abaimov et al. 1997, 1998).

2.2 Regional Landforms Near Tura, Central Siberia

We first describe regional landforms and soil characteristics of Central Siberia, particularly in areas near the major study site, Tura. We then discuss geographical patterns of floristic diversity of the same region in Central Siberia.

2.2.1 Geological Setting

The settlement of Tura in Central Siberia lies near the mouth of the Kochechum River, where it becomes a tributary of the Nizhnyaya Tunguska River (see Fig. 1.3). This study area is underlain by the "Siberian Trap" flood basalt, which is the largest known continental flood basalt and was erupted ca. 250 million years ago at the end of the Paleozoic Era (Figs. 2.1 and 2.2) (Czamanske et al. 1998; Reichow et al. 2002; see also Shibistov and Schulze 2007, for description of the area in larger context). The basalt complex in the study area consists of alternating jointed massive lava and stratified tuff. The Nizhnyaya Tunguska River and Kochechum River incised this basalt complex to form the plateau-like mountains that are elevated about 300 m above the valley bottom.

2.2.2 Slope Landforms

Geomorphologically, the study area comprises the original plateau surface landform at a higher altitude, fluvial landforms along the Kochechm River lower down, and slope landforms connecting them (Fig. 2.3).

We divided the mountain slope in the study area into two segments: an upper and lower slope. The upper slope is relatively steep and is with a generally convex curvature profile. The lower slope is gentler, with a concave profile. In some areas, boundaries between slope segments are unclear. The slope has a stepped profile, with some break lines. The step-like topography probably reflects differences in resistance to physical weathering processes in the past periglacial environment. Since jointed basalt layers are more resistant to physical weathering than stratified clastic layers, the basalt layers tend to form convex slopes with evident break lines. Such step-like slope landforms are often called "cryoplanation terraces" (French 2007).

During the retreat of the cliffs under the past periglacial environment, the rock walls of the jointed basalt layer have yielded numerous boulders and produced longitudinal rock fields at the feet of their slopes (Fig. 2.4). These rock fields are

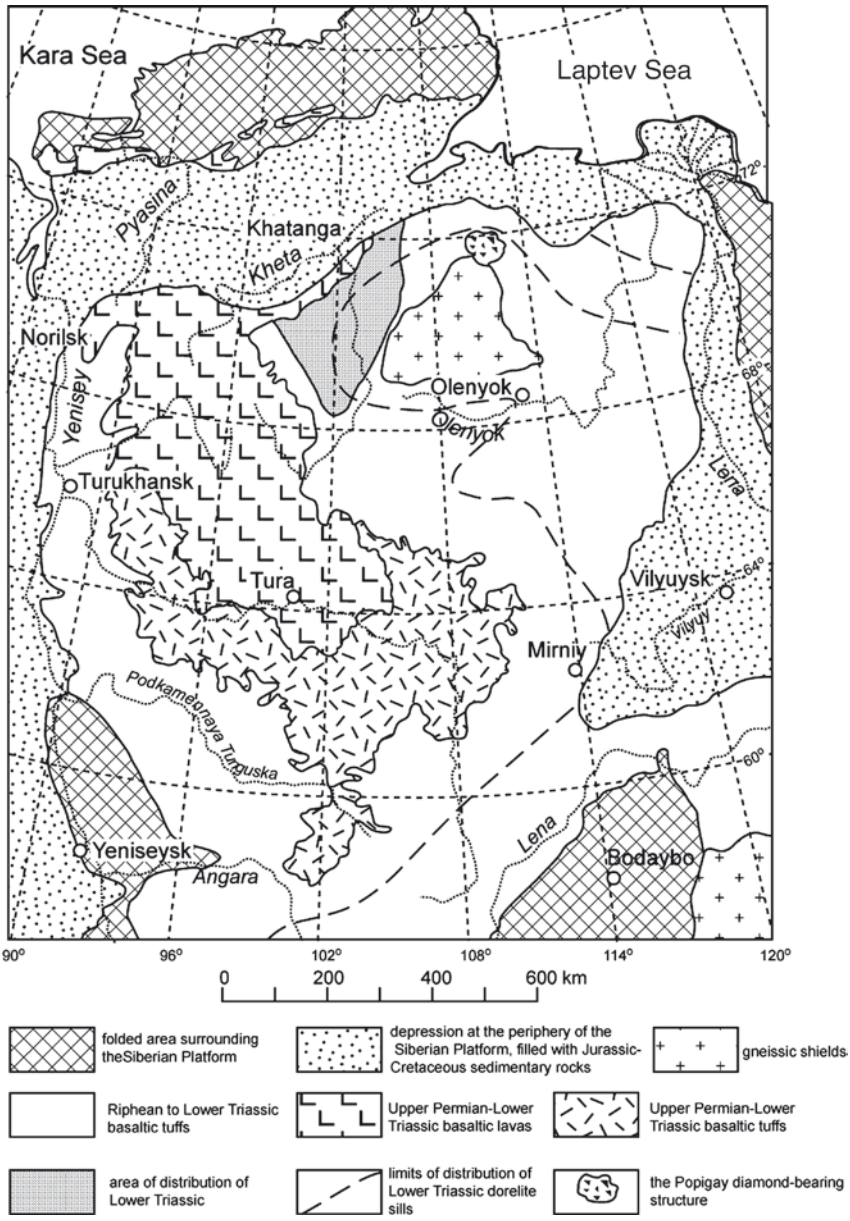

Fig. 2.1 A map showing the Siberian flood-volcanic province (modified from Czamanske 1998)

currently stable, but the scarcity of vegetation is clearly shown in the many dark bands of the normalized difference vegetation index (NDVI) image of the study area (Fig. 2.5).

Fig. 2.2 Outcrop of the Siberian Trap Basalt observed near the Nizhnyaya Tunguska River showing that jointed basalt lava forms the cliffs and stratified clastic layers form talus slopes (photo: H. Daimaru)

The steep valley slopes, located on the outside banks of the river meanders, are subject to strong lateral erosion from the Kochechum River (Fig. 2.3). Spring floods of the river (usually in late May to early June) are accompanied by flowing ice and logs. This strong erosional force (Smith 1979) creates steep slopes on the outside banks.

Figure 2.6 shows cross sections of both sides of the Kochechum River. The eastern profile (B–B′) is located on the outside bank of a channel bend where severe lateral erosion by floating ice has occurred. The eastern profile is steeper than the western profile (A–A′) located on the inside of the meander where lateral deposition of terrace prevails.

Most slopes in the study area appear to be stable in the current climate, though small landslides in the active layer occasionally occur on the steep slopes of the Kochechum and Nizhnyaya Tunguska Rivers. Slope landforms have significant effects on the thermal regime of the topsoil and the distribution of permafrost. Takenaka et al. (1999) have indicated that the thickness of the active layer tends to decrease downward along the eastern slope of the Kochechum River (B–B′, Fig. 2.3). Presumably, this reflects the thermal situation of the slope profile. Since the area at the foot of the mountains receives great quantities of melt water during summer, soil surface temperatures there tend to be lower than those in hilltop areas, where melt water drains more easily. For example, Fig. 2.7 shows that the

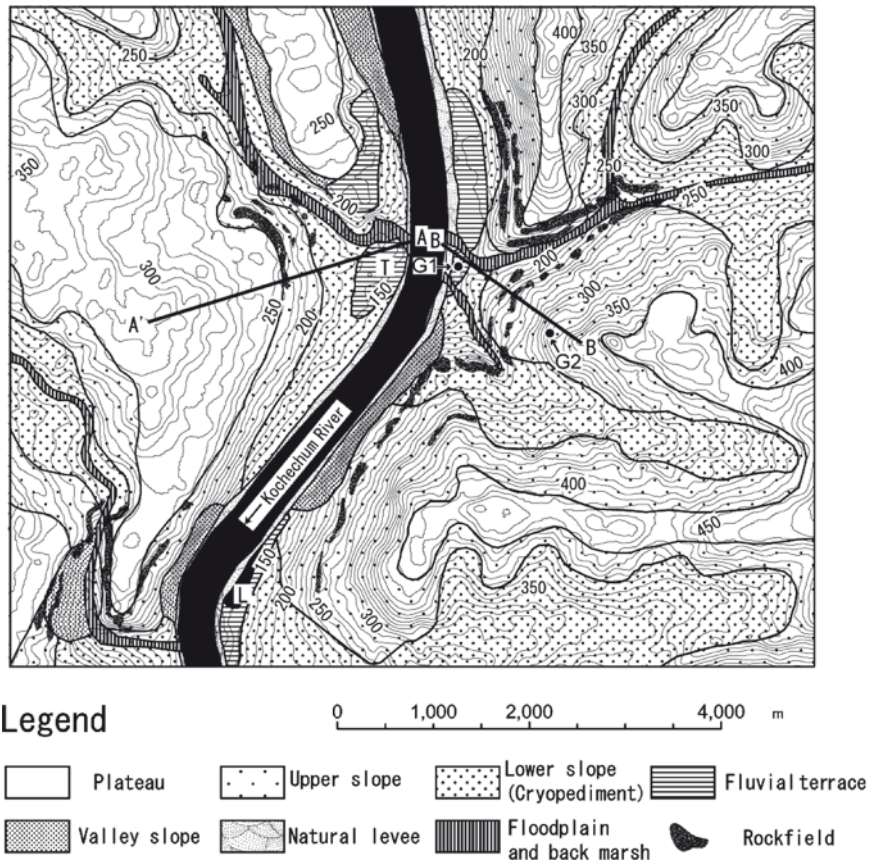

Fig. 2.3 Geomorphological map of the study area. The line segments A–A′ and B–B′ show locations where cross-sectional slope morphology was examined (results see Fig. 2.6). On the line B–B′, ground temperatures at 10 cm depth were measured at two positions; one is on fluvial terrace at the foot of the slope (indicated by G1) and the other is at the upper part of the slope (G2) (results see Fig. 2.7). These two line segments (A–A′, B–B′) were established at Site 2 and Site 1, respectively, in the major study area at Tura in Central Siberia (see Fig. 1.3). The contour lines were produced from the ASTER image by using SILCAST (Sensor Information Laboratory Corp.)

ground temperature (at 10-cm depth) measured on the fluvial terrace at the foot of the eastern slope (position indicated by "G1" in Fig. 2.3) is much lower than that on the upper part of the slope ("G2" in Fig. 2.3) during the growing season (Daimaru et al. 2007). Other factors, such as fire history and associated changes in moss and lichen cover thickness, also affect the depth of the active soil layers (Takenaka et al. 1999; see also Chap. 8). Higher soil temperature at the upper slope (G2), where young larch stand is established, is partially due to short time (ca. 15 years) since the most recent forest fire. The fluvial terrace at the foot of the slope (G1) had longer time (ca. 100 years) since the last stand-replacing fire.

Fig. 2.4 Longitudinal rock fields on the west-side slope of the Kochechum River (photo: H. Daimaru) *(see* Color Plates)

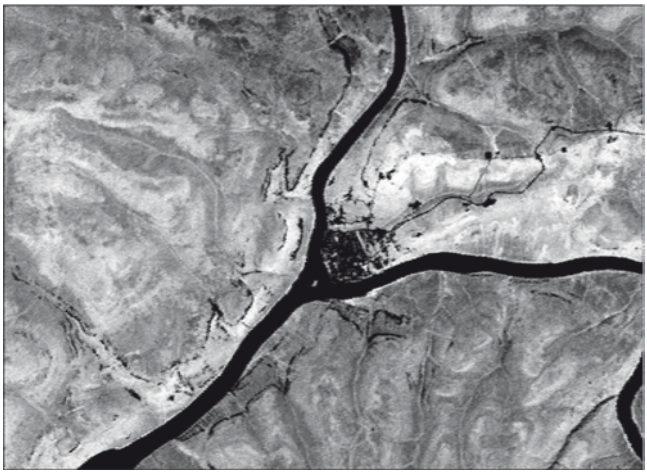

Fig. 2.5 Normalized difference vegetation index (NDVI) image of the area surrounding Tura (derived from LANDSAT TM + dataset taken on August 5, 2001)

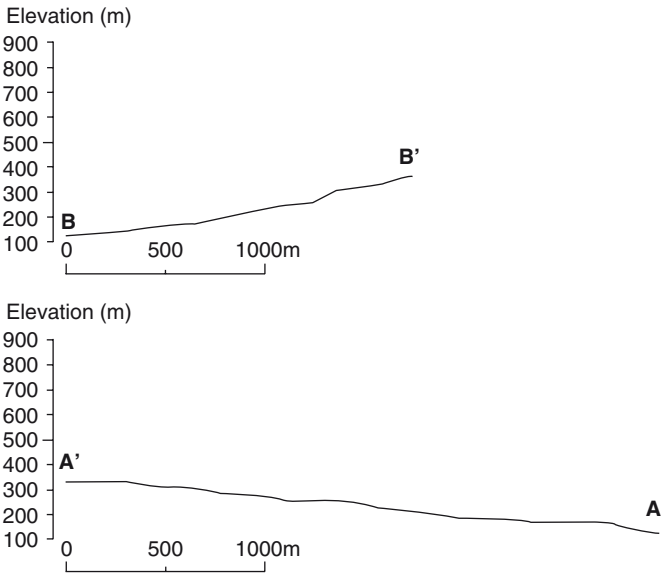

Fig. 2.6 Cross-sections of the line segments B–B′ (eastern slope) and A–A′ (western slope). Location of each line segment is shown in Fig. 2.3

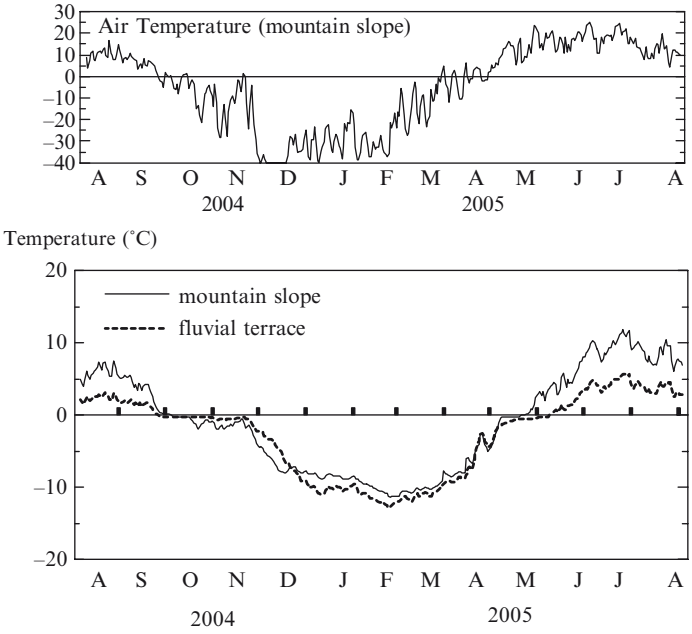

Fig. 2.7 Air temperature variation (*upper panel*) and 10 cm depth ground temperatures (*lower panel*) in the 2004–2005 season recorded at two positions along the eastern slope (B–B′); at the foot of the slope (G1; fluvial terrace) and upper slope (G2; mountain slope) (after Daimaru et al. 2007)

2.2.3 *Fluvial Landforms*

Fluvial landforms along the Kochechum River have characteristic morphologies, such as boulder pavements firmly pressed into stony sand, mounds of loose boulders, and ice-pushed driftwood along the riverbank. These are common features of cold fluvial environments at the high-latitude regions (Mackey and Mackey 1977).

The fluvial terrace is the ancient floor of the Kochechum River and can be classified into at least two surfaces with different ages. On the west side of the Kochechum River (indicated by "T" in Fig. 2.3), the terrace is elevated about 20 m above the present floodplain and is dotted with numerous earth hummocks derived mainly from the clay-rich matrix of terrace deposits. On the east side of the river, the fluvial terrace that is elevated about 10 m above the present floodplain contains a large sandbar-like mound deposit composed mainly of fine sand. We estimated that the terrace formation occurred in Holocene because the boundary between the terrace and the modern natural levee is not clear.

A natural levee runs along the Kochechum River (Fig. 2.3). As floods occasionally overtop the levee, it may continue to develop under the current environment. This is supported by the evidence that many dead tree stumps and logs are found at the bottom of the levee deposit (Fig. 2.8a). The outer part of such a buried tree stump that had existed before deposition of the upper sand layer was sampled, and was dated at 4,080 ± 80 yBP (Fig. 2.8b)(Daimaru et al. unpublished data). The radiocarbon age indicates that the deposition of current levee started at least around 4,000 yBP. The deposition of levee was most likely due to a large scale event of flood occurring around that date, which might have shifted the Kochechum River channel. For example, one small lake that was observed at the riverside (indicated by "L" in Fig. 2.3) may be a remnant of the abandoned channel in the past.

A hydrological event, such as a large ice flood and/or a breakage of dammed lakes in the upper reaches of the Kochechum River, could also have caused the channel shift at more large scale. Yamskikh et al. (1999) indicated that high floods

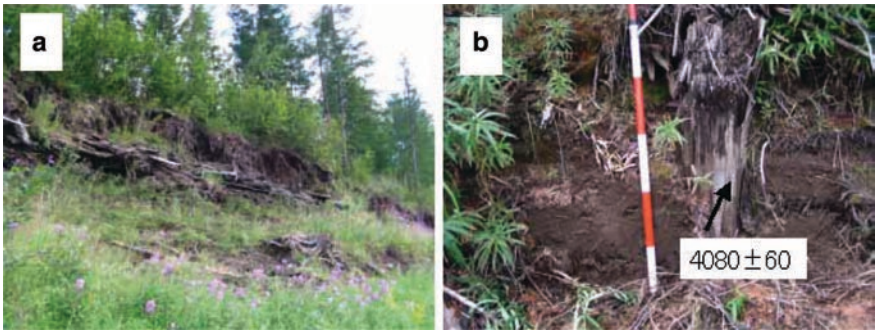

Fig. 2.8 (**a**) Ancient tree stumps and log jam buried by fluvial sand of the natural levee. (**b**) Most outside part of a buried wood stump was dated as 4,080 ± 60 yBP (Daimaru et al. unpublished data) *(see* Color Plates)

occurred around 3,000 yBP in the middle reach of the Yenisei River area, suggesting that a long-term climate change might be correlated with the fluvial change.

2.3 Soils in Permafrost Region of Siberia

Because of limitation in the integrated knowledge of soil science and plant ecology in the former Soviet Union, characteristics of ecosystems in Siberia have been misunderstood by ecologists and pedologists in the western countries until recently. With poor accessibility of the northern regions, characteristics of boreal forests in Eurasia were extrapolated from those in North America and Western Europe, and were considered essentially similar to the ecosystems of evergreen coniferous forests on podzolic or peaty soils (e.g. Jarvis et al. 2001). Only a few textbooks or reports in plant geography recognized that the permafrost region of northeastern Eurasia is covered with deciduous conifers – the larch species (e.g. Walter 1979; Tuhkanen 1984).

2.3.1 Permafrost Distribution in Siberia

There are definitions and arguments where the boundary of Central and Northeastern Siberia should be (e.g. Sokolov et al. 2004). Geological and geographical boundaries dividing Central and Northeastern Siberia lie between the Lena River and the Yenisei River systems. However, administrative boundary or forest resources inventory statistics often result in confusion regarding the division of Siberia (e.g. Alexeyev and Birdsey 1998). Those boundaries ignore geologic expansion and biographical distribution. Siberia is sometimes divided into three regions: "West," "East," and "Far East" Siberia (Shvidenko and Nilsson 1994; Kukuev et al. 1997). In that way, "East Siberia" is equal to Central Siberia in our scene, and "Far East Siberia" contains Northeastern Siberia (most of Yakutia) in usual geographical sense. We do not adopt that division of Siberia. We recognize the region of hilly plateaus between the Lena and the Yenisei Rivers as Central Siberia, and the region between the Lena and Kolyma lowland as Northeastern Siberia (see also relevant definitions in Chap. 1). Continuous permafrost dominates in both Central and Northeastern Siberian terrain.

The distinct boundary of permafrost distribution lies along the Yenisei River (Brown et al. 1997). The region above ca. 60°N to the east of the Yenisei River, both Central and Northeastern Siberia are covered by continuous permafrost. Thickness of permafrost varies much, ranging from 70 to 1,000 m. Permafrost thickness near Tura is from 220 to 500 m (Brown et al. 1997).

There is no continuous permafrost in the West Siberian Basin, except for the areas along the Arctic coast. Permafrost distribution in Siberia shows a poor relationship to the latitudinal zonality. Continuous permafrost (defined as being covered with permafrost at more than 90% of the area) expands southward in Central

and Northeastern Siberia near the Lake Baikal (Brown et al. 1997; see also Fig. 1.1). Distribution of the permafrost is determined mainly by the paleo-climate condition that affected glacier or ice sheet development. Thick continuous permafrost developed in the region where no continental ice sheet developed in the Pleistocene (Velichiko et al. 1984).

2.3.2 Unique Soil Characteristics

Recent revision of the soil classification systems in soil scientists' community also brought us a quite different view of the soil map of the world (Soil Survey Staff 1998; ISSS Working Group RB 1998). We often assume that the climate – plant community – soil complex shows zonal distribution patterns from tropical to polar regions on the Earth. Permafrost-affected soils cover relatively large area of boreal zone in more recent soil maps of the world. In a classical sense of plant geography, boreal forest zone was assigned to podzolic soils as mentioned above (Sect. 2.2.2). Although former soil maps actually did not show zonal distribution of podzolic soils on the northeastern Eurasian Continent (e.g. FAO 1993), areas of podzolic soils have shrunk much, and are only limited in Scandinavia and northeastern North America on the revised soil maps. Revision and reconstruction of the definition for the podzolic feature (spodic materials in USDA) have changed the soil maps.

Existence of permafrost table is one of higher diagnostic criteria for classification in the latest systems of soil taxonomy. Soils having the permafrost table within 1 m of the soil profile are named Cryosols in FAO-ISRIC and Gelisols in USDA classification system. Russian soil classification system was also revised in 1997, and in its English version, permafrost-affected soils were named Cryozems (Shishov et al. 2001). Soil survey of permafrost-affected regions in former Soviet Union was initiated in early 1950s, and continued until mid-1980s (Goryachkin et al. 2004). Some of those pedological studies were translated into English and published in a journal "Soviet Soil Science"; however, most of the publications were written in the Russian language, usually as a style of monographs. Under this situation, most pedologists and ecologists of the western countries could not recognize updated information on soil properties in the permafrost region, classification system of permafrost affected soils, and vegetation-soil relationships in the former Soviet Union.

Soils in the Siberian permafrost region show unique characteristics, such as nonpodzolic features under larch forests. Naumov (2004) classified soil types in Northeastern Siberia. According to his soil map, podzolic soils were distributed only in the mountainous region of Magadan near Okhotsk, where more precipitation occurs than in the Yakutian basin. Sometimes soils developed on thick alluvial deposit in the plain topography or lacustrine deposit in thermokarst topography exhibit neutral or alkaline pH regimes under the hyper-continental climate condition (details are discussed in Chap. 8)

A remarkable difference between larch forest soils in Northeastern and Central Siberia is mainly derived from differences in the soil parent materials

and geomorphology of each region. In Northeastern Siberia, soils developed on terraces of large river systems often show distinct cryoturbations – disturbed horizontal stratigraphy. On the other hand, soils developed on gently sloping topography in Central Siberia and mountain forest tundra show poor cryoturbation with more gravel content. We may roughly classify the permafrost-affected soils under larch ecosystems in Northeastern Siberia as "deposit origin soils," and permafrost soils under larch forest in Central Siberia as "weathered rock origin soils." Such difference may cause differences in organic carbon and nutrient storage in the larch ecosystems between the two regions (see Chap. 8).

2.3.3 Revised Knowledge on the Circumpolar Biomes

According to the common knowledge on plant geography in North America and Northern Europe, northern limit of forest distribution roughly coincides with southern limit of continuous permafrost distribution. Tundra biome expands on the continuous permafrost region in the Arctic (e.g., Larsen 1980). At least, such pattern of biome distribution does not appear in Central and Northeastern Siberia. Two larch species, *Larix cajanderi* in Northeastern Siberia *and L. gmelinii* in Central Siberia, dominate the continuous permafrost region (Abaimov et al. 1998; see also Chaps. 1 and 3), which is the only forest biome on the continuous permafrost in the world. The fact that forests exist on the continuous permafrost is worth examining in comparative studies among the circumpolar biomes.

Another revised knowledge in the circumpolar biome is that podzolic soils are not dominant in Central and Northeastern Siberia. Podzolic soil features do not develop under the hyper-continental climate condition there, so that larch forests are not accompanied by the podzolic soils in the continuous permafrost regions of Siberia. The dogmatic or stereotype combination between soil type and plant community, i.e., podzolic soil developing in evergreen coniferous taiga, does not apply to the permafrost regions in Central and Northeastern Siberia. The dominance of deciduous conifer (larch) means that extrapolation or prediction using parameters obtained in the evergreen boreal forests may cause over or underestimation in the evaluation of ecological processes (e.g., carbon budget and nutrient cycling) in that region.

2.4 Geographical Patterns of Floristic Diversity in Central Siberia

The distribution of zonal vegetation follows general patterns of the climate. However, in the regions of continuous permafrost, well-adapted *Larix gmelinii* (Rupr.) Rupr. dominate other tree species. When moving from north to south, as continuous permafrost and frozen soils decrease, *L. gmelinii* forests are replaced by

those of *Larix sibirica* Ledeb. and *Pinus sylvestris* L. In more humid southern montane part of Central Siberia and in Mountainous Southern Siberia (see Chap. 1), dark-conifers (such as *Abies sibirica* Ledeb., *Picea obovata* Ledeb., and *Pinus sibirica* Du Tour) prevail in the forest. Generally, three major latitudinal zones can be distinguished: tundra, forest-tundra (including northern open woodlands), and boreal forest (Hytteborn et al. 2005; see also Fig. 1.2).

Considering geographic parameters, such as area size and latitude, as the major factors that determine species diversity (Tolmachev 1970, 1974; Rosenzweig 1995), we have analyzed plant species richness in 13 sample plots from south to north in Central Siberia (Fig. 2.9). The main data sources were the literature (Lukicheva 1963; Vargina 1978; Vodopiyanova 1984) combined with our own data. The area of each sample plot was about 100 km^2 in which data on plant species diversity were summarized. Present analysis is concerned with patterns of species diversity in broad areas of Central Siberia, which is generally characterized by poor drainage due to the presence of permafrost. Species distributions at basaltic cliffs and other exceptional locations are out of the scope of the present

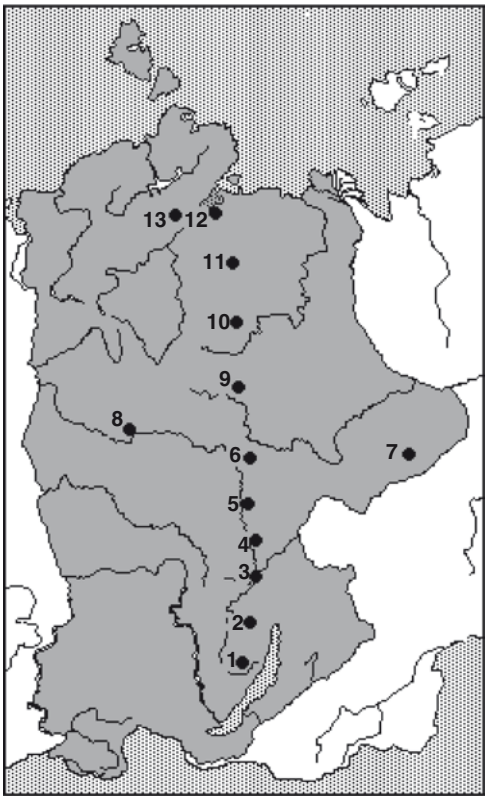

Fig. 2.9 Location of sample plots for plant species diversity estimates

discussion. The plots can be grouped into three biomes: the plots 1–8, 9–11, and 12–13 cover boreal forests, transitional forest-tundra, and tundra, respectively (Fig. 2.9). Total length of the imaginary transect is 19°30′ (or 2,120 km). Sample plots 6–8, located near the northern border of the boreal forest, characterize longitudinal patterns of floristic diversity at an ecotone.

As summarized in Table 2.1, the southern boreal floras are characterized by the largest species diversity: the flora of plot 2 is the richest (472 species), while the northernmost tundra flora of plot 12 is the poorest in species number (180 species only). Species richness also gradually decreases from south to north among the boreal floras. The southern floras (plot 1–3) have about 100 species more than the midflora (plot 4–6); smaller species number in the southernmost flora (plot 1) resulted from dryer and cooler local climatic conditions due to high elevation. Species richness of northern boreal floras (plots 7 and 8) is considerably smaller than that of the southern ones (plot 1–6). Carbonate bedrocks are likely to be responsible for such a difference between these two floras (Lukicheva 1963; Matsuura and Abaimov 1999). As has been reported earlier (Lukicheva 1963; Vodopiyanova 1984), high content of lime soil solution under continental climatic conditions leads to rocky barings, xeromorphic vegetation, as well as to the decrease in boreal species in the floras. Thus, longitudinal regularities in floristic diversity are difficult to interpret only with respect to the influence of carbonate in the bedrock.

Species richness of the forest-tundra floras (plot 9–11) declines considerably as compared to those of the boreal forest (plot 7–8). The abundance of the species varies between 228 and 257 in these forest-tundra floras (Table 2.1). Carbonate bedrocks may partially be responsible for the difference in species richness within the floras: plots 9–10 are slightly poorer in comparison to plot 11.

Floristic diversity of sample plot 13 is of special interest. This area belongs to the northernmost forest of the world (Norin 1978). Forested area as well as relatively high species richness (253 plants) could occur at such latitudes (72°30′N, 102°30′E; Table 2.1) due to the following conditions that are considered favorable to plants: (1) relatively warm winter resulted from invasion of warm air masses from the Arctic Ocean (Khairullin 1978; (2) considerable amount of snow depth (ca. 1 m) in the open and relatively dense, dwarf larch forests allow the plants to resist the frost (Lovelius 1978), while the minimum air temperature in January is as low as −57°C (Khairullin 1978); and (3) sandy soils in forest communities develop favorable hydrothermal regime (Ignatenko 1978). For example, the flora of Ari-Mas forest island (72°N, 102°E) can be characterized as being transitional between the boreal and tundra biomes in species richness, despite its distribution in tundra climatic belt.

The species richness along the transect declines northward by 292 species as a whole, i.e., 472 in the south vs. 180 in the north (Table 2.1). On average, the floristic diversity becomes 15 species poorer per latitudinal degree. Plant species diversity of boreal forests is 1.7-fold higher than that of forest-tundra, and 4.3-fold higher than tundra biome (Table 2.2). A boreal forest remains more diverse at genus

Table 2.1 Statistical patterns of the floras along the south–north transect in Central Siberia in relation to geographical parameters and vegetation cover

Plot no.	Species	Total number of Genera	Families	Vegetation patterns
13 72°30′N 102°30′E	253	107	41	Open and relatively dense larch forests (*Larix gmelinii*) with *Betula exilis*, *Salix reptans*, *S. glauca*, *S. pulchra*, *Duschekia fruticosa* shrubs and dwarf shrub-grass (*Cassiope tetragona*, *Dryas punctata*, *Ledum decumbens*, *Vaccinium uliginosum ssp. microphyllum*, *Carex ensifolia ssp. arctisibirica*, *Eriophorum vaginatum*) and moss (*Hylocomium splendens var. alaskanum*, *Ptilidium ciliare*, *Tomenthypnum nitens*, *Aulacomnium turgidum*) ground cover accompanied with shrub and sedge tundras
12 73°10′N 108°20′E	180	81	33	Shrub (*Betula nana*, *Salix* sp.) and dwarf shrub (*Cassiope tetragona*, *Dryas punctata*, *Vaccinium vitis-idaea*, *Ledum palustre*) tundras with sedge-grass (*Carex bigelowii* subsp. *arctisibirica*, *C. aquatilis* subsp. *stans*, *Eriophorum polystachyon*, *Cerastium maximum*, etc.) and moss ground cover
11 71°25′N 108°15′E	257	130	48	Open larch forests (*Larix gmelinii*) with *Betula divaricata*, *B. nana*, *Duschekia fruticosa*, *Rhododendron adamsii*, *Salix* sp. shrubs and dwarf shrub-grass (*Vaccinium uliginosum*, *V. vitis-idaea*, *Ledum palustre*, *Empetrum androgynum*, *Arctous alpina* subsp. *erythrocarpa*, *Carex ericetorum subsp. melanocarpa*, *Neuroloma nudicaule*, etc.) and moss-lichen ground cover accompanied with dryassedge (*Dryas punctata*, *D. crenulata*, *Carex macrogyna*, *C. vaginata*, etc.) tundra
10 67°50′N 108°05′E	228	128	45	ditto
9 65°30′N 108°00′E	234	117	44	ditto
8 64°18′N 100°11′E	234	146	50	Relatively dense and dense larch forests (*Larix gmelinii*) with *Duschekia fruticosa*, *Betula nana*, *Salix* sp. shrubs and dwarf shrub (*Vaccinium uliginosum*, *V. vitis-idaea*, *Ledum palustre*, *Empetrum nigrum*, *Arctous erythrocarpa*, *Arctostaphyllos uva-ursi*) and lichen-moss ground cover

7 61°50′N 122°20′E	227	126	47	Relatively dense and dense larch forests (*Larix gmelinii*) with *Duschekia fruticosa*, *Betula exilis*, *Salix jenisseensis*, *S. kolymensis* shrubs and dwarf shrub-grass (*Arctous alpina*, *Vaccinium uliginosum*, *V. vitis-idaea*, *Limnas stelleri*, *Carex glacialis*, *Trichophorum uniflorum*, etc.) and lichen-moss ground cover on the carbonates; dense larch forests (*Larix gmelinii*) with *Duschekia fruticosa*, *Ribes rubrum*, *Rosa acicularis*, *Juniperus sibirica* shrubs and dwarf shrub-grass (*Ledum palustre*, *Vaccinium sp.*, *Carex melanocarpa*, *Equisetum scirpoides*, etc.) and moss-lichen cover on the traps
6 62°40′N 108°30′E	349	194	66	Larch (*Larix gmelinii*), pine (*Pinus sylvestris*) and spruce (*Picea obovata*) forests with *Duschekia fruticosa, Betula nana* shrubs and dwarf shrub (*Vaccinium vitis-idaea*, *V. uliginosum*, *Ledum palustre*, *Maianthemum bifolium*, *Pyrola asarifolia*, *Trientalis europaea*, etc.) and moss ground cover; pine forests with *Arctostaphyllos uva-ursi*-lichens and grass (*Dendranthema zawadskii*, *Artemisia tanacetifolia*, *Carex alba*, *Polygala sibirica*) cover; larch forests with *Carex globularis* cover; birch (*Betula pendula*)-spruce forests with grass (*Pyrola asarifolia*, *Rubus humilifolius*) cover and larch-spruce forests with *Vaccinium vitis-idaea*-moss cover
5 61°10′N 108°05′E	384	217	65	ditto
4 59°20′N 108°10′E	396	232	69	ditto

(continued)

Table 2.1 (continued)

Plot no.	Species	Total number of Genera	Families	Vegetation patterns
3 57°10′N 108°30′E	455	255	73	Larch (*Larix sibirica*) and pine (*Pinus sylvestris*), sometimes accompanied by *Pinus sibirica*, *Picea obovata*, *Abies sibirica*, forests with *Spiraea media*, *Cotoneaster melanocarpus*, *Rosa acicularis* shrubs and *Vaccinium vitis-idaea*, *V. myrtillus* and grass (*Rubus saxatilis*, *Thalictrum minus*, *Aquilegia sibirica*, *Vicia venosa*, *Carex macroura*, etc.) ground cover; birch (*Betula alba*)-pine forests with *Chamaedaphne calyculata*, *Vaccinium uliginosum*, *Ledum palustre* and *Sphagnum* sp. cover; spruce-fir forests with grass (*Oxalis acetosella*, *Mitella nuda*, *Linnaea borealis*) and moss ground cover
2 55°50′N 107°40′E	472	258	72	ditto
1 53°40′N 106°30′E	375	213	61	ditto

Location of each sample plot is shown in Fig. 2.9

Table 2.2 Comparison of floristic diversity between boreal forests, forest-tundra, and tundra biomes in Central Siberia

Biome	Total number of Species	Genera	Families
Boreal forests	765	339	86
Forest-tundra	446	171	54
Tundra	180	81	33

Zyryanova et al. unpublished data

Table 2.3 Comparisons of floristic diversity between Central Siberia and boreal and temperate forests in other regions

Forest types and regions	Total number of Species	Genera	Families	Latitude (range)
Boreal forests				
Central Siberia	1,124	375	88	53°40′–72°30′N
Alaska	1,559	412	89	54°40′–71°23′N
Temperate forests				
North America	2,835	658	139	36°30′–48°N
Japan (Asia)	3,857	1,110	257	30°–45°30′

Data source: Boreal forests in Alaska (including neighboring territories) (Hulten 1974); temperate forests in northeastern parts of North America (Gleason and Cronquist 1963); temperate forests in Japan (Asian) (Ohwi 1965); Central Siberia (this study)

(2-fold and 4.2-fold) and family (1.6-fold and 2.6-fold) levels than the other biomes at high latitudes (Table 2.2).

The floristic gradient is closely related to that of the climate, and mainly to the temperature gradient (Vodopiyanova, 1984). Therefore, the closest relationship is established between the species richness and the duration of the growing season, and the sum of daily air temperature above 0°C (degree-days) is suggested as the most important variable (Malyshev 1994). However, the local environment, characterized by topography and edaphic factors (chemical composition of the bedrock), plays an important but secondary role (Larsen 1980).

The total floristic diversity of Central Siberia numbers 1,124 plant species, belonging to 375 genera and 88 families as summarized in Table 2.3 (Zyryanova 2006). These numbers seem somewhat less than those in the boreal forests of Alaska and neighboring territories, which stretch at about the same latitudes, and experience similar climatic conditions (Hulten 1974; Bliss and Matveyeva 1992). They are also 2.5-fold or even 3.5-fold less than those in the wetter and warmer temperate forests located southwards in North America (Gleason and Cronquist 1963) and Eurasia (Ohwi 1965) (Table 2.3). However, difference in the plot area used for these analyses makes it difficult to draw definitive conclusions (see also Bliss and Matveyeva, 1992).

Thus, we conclude that boreal forests of Central Siberia that are distributed on permafrost are characterized by low plant species diversity. The level of plant diversity appears to be the lowest not only within the Eurasian continent, but also among all biomes in the Northern Hemisphere.

2.5 Plant Species Diversity of Larch Association

2.5.1 Description of Species Diversity

Floristic diversity at the association's level has been studied in Tura Experimental Forest (64°N 100°E) located within the plot 8 (Fig. 2.9). Based on the estimate of species richness and species evenness (i.e., distribution of species within an area) of the associations studied, we suggest that the larch forests of the region have characteristics of both undisturbed climax and the vegetation affected by disturbance (such as fires, cuttings, etc.). To confirm this view, we compared the experimental species distribution (used in a sense equivalent to "observed" distribution throughout this chapter) with standard geometric series and MacArthur models by evaluating the species diversity utilizing Shannon's diversity index (Wittaker 1975; Zyryanova et al. 1998, 2002, 2004, 2006). See Wittaker (1975) and Magurran (1988) for details of the models. It was assumed that (1) under severe environments, distribution of species abundance in poor communities can be described by the geometric series model (Magurran 1988); (2) the geometric series considers differentiation of ecological niche resulted from interspecific plant competition (Wittaker 1975; Magurran 1988); and (3) MacArthur model supposes casual occupation (or random partitioning) of ecological niches by plants (Wittaker 1975; Magurran 1988). To avoid the sensitivity of Shannon's index to the number of species in a sample, the index was scaled by its maximum possible value, which would occur if all species had equal abundance (Zyryanova et al. 1998, 2002).

2.5.2 Observed Patterns and Interpretations

The number of species per 100 m^2, which comprised vascular plants, mosses and lichens, was estimated for 14 larch-dominated associations that occupied various forest sites. The species richness ranged between 22 and 59 plant species with its maximum values on the sites with more complex microtopography (Zyryanova and Bugaenko 2004; Zyryanova et al. 2004). The microrelief of the ground was responsible for patterned environments that led to increase in the number of ecological niches in the forest site. As a consequence, plant species found in boreal forest (*Cypripedium guttatum*, *Dactylorhiza cruenta*, *Vaccinium vitis-idaea*, etc.), forest-tundra (*Empetrum*

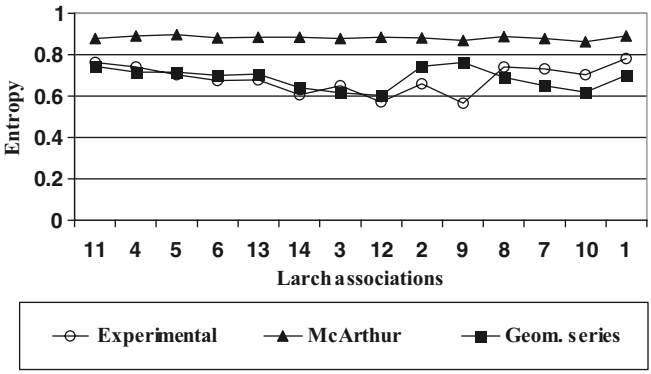

Fig. 2.10 Values of the diversity index expressed as entropy (Pielou 1977) in MacArthur, geometric series, and experimental (= observed) distributions. The diversity indices are scaled with their maximum values for the intact larch associations

nigrum, *Salix boganidensis*, *Vaccinium uliginosum*, etc.), and tundra (*Betula nana*, *Ptilidium ciliare*) could coexist in one plant association at different elements of microtopography – hummocks and microdepressions (Abaimov et al. 2000; Zyryanova 2004; Zyryanova et al. 2007). Thus, permafrost microtopography provides increase in the species number of plant associations (see also Chap. 5).

We have analyzed and compared three patterns of distribution in plant species' diversity. In some cases, the index values for the experimental pattern and geometric series model coincided (see association No. 11 and 12 in Fig. 2.10). This indicates that the forest stands are developing without any disturbance. Plant species are considered to be coadapted to their physical and temporal environments: they are niche differentiated due to interspecific competition. They are climax associations: the most stable, self-maintaining, and self-reproducing state of vegetational development.

The index values of the experimental distribution are less than those of the geometric series (association No. 2 and 9 in Fig. 2.10), indicating presence of fire influence to forest ecosystems. Weak fire damage to the ground vegetation and release of site resources would correspond to this situation. This phenomenon is the significant feature of vegetation change detected in the study of postfire forest regeneration (see also Chap. 5). If plant competition within the association decreases after the removal of a part of the community (e.g., by selective cuttings and medicinal plant gathering), values of the Shannon's index for experimental distribution become more similar to those predicted by the MacArthur model (association No. 8, 7, 10 and 1 in Fig. 2.10). This indicates that plant species share the site environment more evenly. In all, the proportions of undisturbed climax larch associations and those disturbed are 53 and 47%, respectively, in the study site at Tura. Thus, forest vegetation of the region studied comprises unique series of plant associations, which approach the climax, but without being reaching it (Abaimov et al. 1997, 2000; Zyryanova et al. 2002).

2.6 Conclusions

- Geomorphological features in Central Siberia create significant thermal regime along the cryoplanation terraces, affecting surface temperature, active layer depth, and melt water movement.
- Permafrost distribution in Central and Northeastern Siberia, at present, is roughly determined by the absence of continental ice sheet on the ground surface during the Pleistocene that enhanced permafrost development.
- We can classify permafrost-affected soils into two groups: (1) fluvial and lacustrine deposit origin soils in Northeastern Siberia and (2) weathered bedrock origin soils in Central Siberia.
- The lowest number of species among ranges of the Northern Hemisphere characterizes plant species diversity of Central Siberia.
- Species richness gradually declines northwards by following the climatic gradient. Local environments, such as topography and chemical composition of the bedrock, also affect abundance of the species.
- Complex microtopography provides the highest species richness at forest sites due to their patterned environments.
- Larch forests of Central Siberia are comprised of the climax and disturbed associations. The share of the disturbed forests among the primary vegetation appears to be about 43% of their total number

References

Abaimov AP, Prokushkin SG, Zyryanova OA, Kaverzina LN (1997) Peculiarities of forming and functioning larch forests on frozen soils. Lesovedenie (Forest Science) 5:13–23 (in Russian with English summary)

Abaimov AP, Lesinski JA, Martinsson O, Milyutin LI (1998) Variability and ecology of Siberian larch species. Swedish University of Agricultural Sciences, Department of Silviculture, Reports 43, Umeå, 118pp

Abaimov AP, Prokushkin SG, Matsuura Y, Osawa A, Takenaka A, Kajimoto T (1999) Wildfire and cutting effect on larch ecosystem permafrost dynamics in Central Siberia. In: Shibuya M, Takahashi K, Inoue G (eds) Proceedings of the seventh symposium on the joint Siberian permafrost studies between Japan and Russia in 1998. National Institute for Environmental Studies, Tsukuba, Japan, pp 48–58

Abaimov AP, Zyryanova OA, Prokushkin SG, Koike T, Matsuura Y (2000) Forest ecosystems of the cryolithic zone of Siberia: regional features, mechanisms of stability and pyrogenic changes. Eurasian J For Res 1:1–10

Alexeyev VA, Birdsey RA (1998) Carbon storage in forests and peatlands of Russia. USDA Forest Service, Northeastern Forest Experiment Station, GTR NE-244, 137pp

Bliss LC, Matveyeva NV (1992) Circumpolar arctic vegetation. In: Chapin FS III, Jeffries RL, Reynolds JF, Shaver GR, Svoboda J, Chu EW (eds) Arctic ecosystems in a changing world. Academic Press, San Diego, pp 59–89

Brown J, Ferrians OJ Jr, Heginbottom JA, Melnikov ES (1997) Circum-arctic map of permafrost and ground ice conditions. CIRCUM-PACIFIC MAP Series MAP CP-45, International Permafrost Association, USGS

Climate reference book of the USSR (1967) Gidrometeoizdat Press, Moscow, USSR (in Russian)
Climate reference book of the USSR (1969) Gidrometeoizdat Press, Moscow, USSR (in Russian)
Czamanske GK, Gurevitch AB, Fedorenko V, Simonov O (1998) Demise of the Siberian plume: palaeogeographic and palaeotectonic reconstruction from the prevolcanic and volcanic record, north-central Siberia. Int Geol Rev 40:95–115
Daimaru H, Matsuura Y, Kajimoto T, Zyryanova OA (2007) Influence of slope landform on the ground thermal regime in Tura, Central Siberia. In: Proceedings of the seventh international conference on global change: connection to the arctic (GCCA-7), International Arctic Research Center, University of Alaska, Fairbanks, pp 127–130
FAO (1993) World soil resources. An explanatory note on the FAO world soil resources map. FAO, Rome 64pp
Fotiev SM, Danilova NS, Sheveleva NS (1974) Geocryological conditions of Central Siberia. Nauka Press, Moscow, USSR, 147pp (in Russian)
French HM (2007) The Periglacial environment. Wiley, New York
Gleason HA, Cronquist A (1963) Manual of vascular plants on Northeastern United States and adjacent Canada. Willard Grant Press, Boston
Goryachkin SV, Karavaeva NA, Makeev OV (2004) The history of research of Eurasian Cryosols. In: Kimble JM (ed) Cryosols. Springer, Berlin, pp 17–28
Hulten E (1974) Flora of Alaska and neighboring territories. Stanford University Press, Stanford
Hytteborn H, Maslov AA, Nazimova DI, Rysin LP (2005) Boreal forests of Eurasia. In: Andersson F (ed) Coniferous forests. Ecosystems of the world 6, Elsevier, Amsterdam
Ignatenko IV (1978) Soils. In: Norin BN (ed) Ary-Mas. Natural environments, flora and vegetation. Nauka Press, Leningrad, USSR, pp 30–64 (in Russian)
ISSS Working Group RB (1998) World reference base for soil resources: introduction. In: Deckers JA, Nachtergaele FO, Spaargaren OC (eds) ISSS-ISRIC- FAO, Belgium, 165pp
Jarvis PG, Saugier B, Schulze E-D (2001) Productivity of boreal forests. In: Roy J, Saugier B, Mooney HA (eds) Terrestrial global productivity. Academic Press, New York, pp 211–244
Kajimoto T, Matsuura Y, Mori S, Sofronov MA, Volokitina AV, Abaimov AP (1998) Root growth patterns of *Larix gmelinii* and microsite difference in soil-temperature on permafrost soils in Central Siberia. In: Mori S, Kanazawa Y, Matsuura Y, Inoue G (eds) Proceedings of the sixth symposium on the joint Siberian permafrost studies between Japan and Russia in 1997. Tsukuba, pp 43–51
Khairullin KSh (1978) Climate. In: Norin BN (ed) Ary-Mas. Natural environments, flora and vegetation. Nauka Press, Leningrad, USSR, pp 16–21 (in Russian)
Kukuev YA, Krankina ON, Harmon ME (1997) The forest inventory system in Russia. J For 95:15–20
Kushev SL, Leonov BN (1964) Relief and geological composition. In: Gerasimov IP (ed) Central Siberia. Nauka Press, Moscow, USSR, pp 23–82 (in Russian)
Larsen JA (1980) The boreal ecosystem. Academic Press, New York 500pp
Lovelius NV (1978) Snow cover and permafrost. In: Norin BN (ed) Ary-Mas. Natural environments, flora and vegetation. Nauka Press, Leningrad, USSR, pp 21–30 (in Russian)
Lukicheva AN (1963) The vegetation of the northwestern part of Yakutia related to geology of the territory. USSR Academy Sciences Press, Moscow-Leningrad, USSR 168pp (in Russian)
Mackey JR, Mackey DK (1977) The stability of ice-push features, Mackenzie River, Canada. Can J Earth Sci 14:2213–2225
Magurran AE (1988) Ecological diversity and its measurement. Princeton University Press, Princeton 179pp
Malyshev LI (1994) Floristic diversity of the USSR. In: Proceedings third workshop "Actual problems in the comparative study of the floras." Nauka Press, St. Peterburg, USSR, pp 34–87 (in Russian)
Matsuura Y, Abaimov AP (1999) Soil characteristics in Tura experimental forest, Central Siberia. In: Shibuya M, Takahashi K, Inoue G (eds) Proceedings of the seventh symposium on the joint Siberian Permafrost studies between Japan and Russia in 1998. Tsukuba, pp 69–76

Naumov YM (2004) Soils and soil cover of northeastern Eurasia. In: Kimble JM (ed) Cryosols. Springer, New York, pp 161–184
Norin BN (ed) (1978) Ary-Mas. Natural environments, flora and vegetation. Nauka Press, Leningrad, USSR, 190pp (in Russian)
Ohwi J (1965) Flora of Japan (English edition). Smithsonian Institute, Washington 1067pp
Pielou EC (1977) Mathematical ecology. Wiley, New York
Reichow MK, Saunders AD, White RV, Pringle MS, Al'Mukhamedov AI, Medvedev AI, Kirda NP (2002) $^{40}Ar/^{39}Ar$ dates from the West Siberian basin: Siberian flood basalt province doubled. Science 296:1846–1849
Rosenzweig ML (1995) Species diversity in space and time. Cambridge University Press, Cambridge 436pp
Shibistov BV, Schulze E-D (2007) Geology and landscapes of Central Siberia. Geological Museum, Krasnoyarsk 183pp
Shishov LI, Tonkonogov VD, Lebedeva II, Gerasimova MI (2001) Russian soil classification system. V.V. Dokuchaev Soil Science Institute, RAS, Moscow, 220pp
Shvidenko A, Nilsson S (1994) What do we know about the Siberian forest? AMBIO 23:396–404
Smith DG (1979) Effects of channel enlargement by river ice processes on bank full discharge in Alberta, Canada. Water Resour Res 15:469–475
Soil Survey Staff (1998) Keys to soil taxonomy, 8th edn. USDA, National Resources Conservation Service, Washington, DC, 326pp
Sokolov IA, Ananko TV, DYe K (2004) The soil cover of central Siberia. In: Kimble JM (ed) Cryosols. Springer, Berlin, pp 303–338
Takenaka A, Matsuura Y, Abaimov AP (1999) The depth of active layer along a slope as affected by the fire history of ground vegetation. In: Shibuya M, Takahashi K, Inoue G (eds) Proceedings of the seventh symposium on the joint Siberian permafrost studies between Japan and Russia in 1998. Tsukuba, pp 33–39
Tolmachev AI (1970) About some quantitative ratios in the floras of the Earth. Vestnik Leningrad Univ 15(3):71–83 (in Russian)
Tolmachev AI (1974) Introduction into plant geography. Leningrad University Press, Leningrad, USSR, 244pp (in Russian)
Tuhkanen S (1984) A circumboreal system of climatic-phytogeographical regions. Acta Bot Fennica 127:1–50
Vargina NE (1978) Flora of Ary-Mas. In: Norin BN (ed) Ary-Mas. Natural environments, flora and vegetation. Nauka Press, Leningrad, USSR, pp 65–86 (in Russian)
Velichiko AA, Isayeva LL, Makeyev VM, Matishov GG, Faustova MA (1984) Late Pleistocene gleciation of the arctic shelf, and the reconstruction of Eurasian ice sheets. In: Velichiko AA, Wright HE Jr, Barnosky CW (eds) Late quaternary environments of the Soviet Union. Univ Minnesota Press, Minneapolis, pp 35–41
Vodopiyanova NS (1984) Zonal patterns in the flora of Central Siberian Plateau. Nauka Press, Novosibirsk, USSR, 159pp (in Russian)
Walter H (1979) Vegetation on the earth and ecological systems of the geobiosphere, 2nd edn. Springer, Berlin 274pp
Whittaker RH (1975) Communities and ecosystems, 2nd edn. MacMillan, New York 385pp
Yamskikh AF, Yamskikh AA, Brown G (1999) Siberian-type quaternary floodplain sedimentation: the example of the Yenisei River. In: Brown AG, Quine TA (eds) Fluvial processes and environmental change. Wiley, New York
Zyryanova OA (2004) Plant species diversity and recovery of forest vegetation after fire disturbance in continuous permafrost area of Siberia. In: Tanaka (ed) Proceeding of the fifth international workshop "Global change: connection to the arctic 2004 (GCCA5)." Tsukuba University, Tsukuba, pp 191–194
Zyryanova OA (2006) Plant species diversity of the Siberian cryolithic forests and its post-fire change under Global Warming. In: The best popular lectures of 2005 for the youth. Darma Press, Krasnoyarsk, pp 51–56 (in Russian)

Zyryanova OA, Bugaenko TN (2004) Plant species diversity of larch associations in cryolithic zone of Central Siberia and its post-fire transformation. In: Proceedings all-Russian conference "Structure, function and dynamics of forests," Krasnoyarsk, pp 301–303 (in Russian)

Zyryanova OA, Bugaenko TN, Bugaenko NN, Kanazawa Y, Matsuura Y (1998) Floristic diversity of Siberian larch ecosystems. In: Mori S, Kanazawa Y, Matsuura Y, Inoue G (eds) Proceedings the sixth symposium on the joint Siberian permafrost studies between Japan and Russia in 1997, Tsukuba, pp 92–100

Zyryanova OA, Bugaenko TN, Bugaenko NN (2002) About the study of species diversity in intact forests of Siberian cryolithic zone. Investigated in Russia, Electronic multi-disciplinary Scientific Journal. Moscow Physico-Technical Institute. vol 198:2194–2203 http://zhurnal.ape.relarn.ru/articles/2002/198.pdf (in Russian)

Zyryanova OA, Abaimov AP, Bugaenko TN (2004) Evaluation of the species diversity of autochthonal larch associations of cryolithic zone and its post-fire dynamics on the basis of the Shannon information index. Siberian Ecol J 5:735–743 (in Russian)

Zyryanova OA, Abaimov AP, Bugaenko TN (2006) Analysis of plant species diversity and spatial structure of larch associations in cryolithic zone of Siberia. In: Shumny VK, Shokin YuI, Kolchanov NA, Fedotov AM (eds) Biodiversity and dynamics of ecosystems: computational approaches and modeling. Publishing House of SB RAS, Novosibirsk, Russia, pp 495–504 (in Russian)

Zyryanova OA, Yaborov VT, Tchikhacheva TL, Koike T, Makoto K, Matsuura Y, Satoh A, Zyryanov VI (2007) The structure and biodiversity after fire disturbance in *Larix gmelinii* (Rupr.) Rupr. Forests, Northeastern Asia. Eurasian J For Res 10–11:19–29

Chapter 3
Geographical Distribution and Genetics of Siberian Larch Species

A. P. Abaimov

3.1 Introduction

Species of the genus *Larix* Mill. are the most abundant trees in Russian Federation. Some 263.2 million ha are occupied by forests where the larch dominate, constituting 36.6% of the whole forest area of the country (Forest Fund of Russia 1999). Vast areas of larch forests are concentrated in Siberia. Having very high adaptability, Siberian larch species (*Larix sibirica* Ledeb., *L. gmelinii* (Rupr) Rupr., *L. cajanderi* Mayr.) and their natural hybrid complexes form large tracts of monodominant and open forests at high latitudes (Dylis 1961, 1981; Bobrov 1972, 1978; Abaimov and Koropachinsky 1984; Abaimov et al. 1998).

In central and southern regions of Siberia, larch stands are subjected to harvesting for industrial purposes. In the permafrost zone, open and relatively dense forests fulfil, first of all, ecological and biospheric functions. These forests contribute to keeping up the relative stability of the "atmosphere–soil– permafrost" system; they hamper development of the permafrost processes (e.g., thermokarst, solifluction, and thermoerosion), and serve as depositor of a great amount of carbon. It should be noted that total yield in the larch stands of Siberia amounts to over 10 billion m^3 (Forest Fund of Russia 1999). In addition, larch stands and open forests of the Siberian permafrost zone are the natural habitats for small populations of aboriginal people in the Extreme North and serve as the basis for conservation and development of their national culture, tradition, and economy (e.g., hunting, fishing, and reindeer-breeding) (Abaimov 1997).

Despite the wide geographic distribution of the larch stands and open forests in Siberia, their economic, social, ecological, and biospheric roles have not been studied extensively. Presently, the most debatable points concern systematics, geography, variability, and natural hybridization of the larch species. In spite of a number of studies by Russian researchers (Dylis 1961, 1981; Bobrov 1972, 1978; Karpel' and Medvedeva 1977; Kruklis and Milyutin 1977; Abaimov 1980; Abaimov and Koropochinsky 1984; Abaimov and Milyutin 1995), there is not a unanimous opinion as to the number of larch species and boundaries of their habitats. Information is still limited on the biological peculiarities of larch species, their ecological and

A. Osawa et al. (eds.), *Permafrost Ecosystems: Siberian Larch Forests*,
Ecological studies, Vol. 209, DOI 10.1007/978-1-4020-9693-8_3,

biospheric roles as the depositor of the atmospheric carbon. These circumstances make it desirable for scientists outside of Russia to be introduced to the brief history of taxonomic studies on Siberian larch species and present understanding of their status, geographic distribution, biology, and basic ecological characteristics.

3.2 Systematic Position and Present Status of Siberian Larch Species

The question on the origin and genetic interrelationships of the species of genus *Larix* has a long history. According to the sources known to us, larch was recognized for the first time as a separate genus by an English botanist F. Muller in 1754. Earlier, the larch growing in Europe was assigned to the genus *Pinus* (Dylis 1961) by K.Linney. Only in 1749 after publication of the book "Siberian Flora" by I.G.Gmelin, it became known that larch is distributed in Siberia. However, it has long since been believed that the larch in Siberia and larch in Europe are of the same species. Only 80 years later, K.F. Ledebour described *Larix sibirica* as a separate species.

According to Bobrov (1972), F.I. Ruprecht distinguished three species of Russian larches in 1845 – *L. ledebouri, L. gmelinii,* and *L. kamtschatica.* Evidently, he denied the status of *Larix sibirica* as a separate species and found no differences among the larches growing in the Ural Mountains and in the European part of Russia. F.I. Ruprecht assigned these three larch species to the genus *Abies*.

A bit earlier than F.I. Ruprecht, in 1838, a Russian scientist N.S. Turchaninov suggested the name "*dahurica*" for the larch growing in Zabaikalie. However, according to Dylis (1961), the necessary botanical description of this larch was made later by R.E. Trautfetter in 1844 and by F.I. Ruprecht in 1845. The former suggested the epithet "*dahurica*" for this species, while the latter – the epithet "*gmelinii.*"

Almost 60 years later, the German dendrologist Mayr (1906) analyzed herbarium data gathered by the Finnish botanist A.K. Kajander in the vicinity of the town Yakutsk and described *Larix cajanderi* as a separate species.

German botanist Patschke (1913) has greatly contributed to the knowledge of systematics of the genus *Larix* in the beginning of the last century. He divided *Larix* into two sections - *Multiseriales* and *Pauciseriales*. The first section included species with big cones. To the second section, W. Patschke assigned *L. leptolepsis, L. sibirica,* and *L. dahurica*, which are characterized by small cones with a small seed-scale number and short bract-shaped scales. The rest of the species from this section recognized by that time was assigned by him to a typical *L. dahurica*.

Polish scientist Szafer (1913) recognized *L. sibirica* and *L. dahurica* as separate species. Moreover, he denied a species status of *L. cajanderi* and *L. kurilensis* and assumed that they should be assigned only to the forms of *L. dahurica*. W. Szafer was one of the first to point out high variability of morphological properties of *L. dahurica* and to distinguish a series of forms according to color of cones and structure of seed-scales. It was his important achievement to describe a natural intraspecific

hybrid of *L. sibirica* and *L. dahurica* under the name of *L. czekanowskii* Szaf. on the basis of herbarium data.

The distinguished Russian scientist Sukachev (1924) made a considerable contribution to the study of historical formation and development of the genus *Larix* in the territory of Russia. He suggested combining all larch species described by that time into two genetic series – *Eurasiaticae* and *Paucisquamatae*. *Larix sibirica* was put by him in the first series, while *L. dahurica* and other species of the Far East were assigned to the second one. He considered *L. dahurica* to be relatively young, progressive species originated at the end of pleistocene and at the beginning of holocene "… not only in terms of a migration process but, very likely, also at the site through the gradual transformation of one species into another" (see p 30, Sukachev 1924).

Dylis (1961), Sukachev's follower, recognizes and describes *Larix sukaczewii* Dylis, *L. sibirica* Ledeb., *L. dahurica* Turcz.ex Trautv., *L. kurilensis*, *L. olgensis,* and *L. maritima* as separate species in his monograph on the genus *Larix*. *Larix x czekanowskii, L.x ochotensis, L.x amurensis,* and *L.x lubarskii* were assigned by Dylis to hybrid complexes. The former is met in Siberia, and the rest – in the Far East of Russia. Within the habitat (area of distribution) of *L. dahurica*, N.V. Dylis suggested distinguishing two geographical races: the western - *L. dahurica ssp. dahurica* and the eastern - *L. dahurica ssp.cajanderi* (Mayr). To differentiate these races, Dylis (1961, 1981) considered the angle between seed-scale and the axis in mature larch cones to be the main morphological distinction. In his opinion, *L. dahurica* has evolved from separate populations of *L. kurilensis*. Its western race (*L. dahurica ssp. dahurica*) had been formed in the north-western Asia by the middle of pleistocene in the process of climate changes. The eastern race, *L. dahurica* ssp. *cajanderi* (Mayr). Dyl., had been formed by the late pleistocene as a result of intensive selection and adaptation to increasing climate continentality in initial populations of *L. dahurica* ssp. *dahurica*. Then this race occupied the central Yakutia and the basins of the Yana, Indigirka, and Kolyma Rivers.

Bobrov (1972, 1978) – a well-known Russian scientist dealing with systematics of coniferous species – does not consider *L. sukaczewii* described by Dylis (1947) to be a separate species. Bobrov thinks that larch growing in the Ural and in the European part of Russia has no essential morphological distinctions from *L. sibirica*.

Bobrov restored the original name *L. gmelinii* (Rupr.) Rupr. while examining *L. dahurica*, and suggested that the eastern race distinguished by Dylis (1961) as a separate species and was previously described by E. Mayr should be assigned a name *L. cajanderi* Mayr. In Bobrov's opinion (1978), *L. cajanderi* Mayr. should not be a subspecies, since it has a certain habitat and is morphologically isolated.

Contradictory statements on the number of species for the genus *Larix* and their taxonomic status have been resulted from different views on the historical formation of the genus as well as from highly expressed polymorphism against a background of weak reproductive isolation. Presence of intraspecific hybrids in natural and introduced populations has resulted in considerable difference in scientists' views even on the number of species. For instance, Sukachev (1924) recognized and described 14 species, Dylis (1961) – 20, Wright (1962) –15, Gaussen (1966) – 18, Bobrov (1972) – 16, Holtmeier (1995) – 12, and Schmidt (1995) –10.

According to Dylis (1961), there are three larch species in Siberia: *L. sukaczewii* Dyl., *L. sibirica* Ledeb., *and L. dahurica* Turcz. Ex Trautv. Prof. Bobrov (1972) distinguishes three species there as well, but of a bit different kind: *L. gmelinii* (Rupr.) Rupr, *L. sibirica* Ledeb, and *L. cajanderi* Mayr.

Canadian palaeobotanists LePage and Basinger (1995) recognize and describe 10 species. In their opinion, there are only two larch species in Russia – *L. sibirica* and *L. gmelinii,* as well as a natural hybrid *L. x czekanowskii*. These scientists do not consider *L. sukaczewii* and *L. cajanderi* to be separate species. Larch species and their hybrids in the Far East are assigned by them to the forms and varieties of *L. gmelinii*. In terms of philogenesis, *L. sibirica* and *L. gmelinii* are considered by these researchers to be two separate branches in development of the genus *Larix*.

Many other foreign scientists also make use of the species epithet "*gmelinii*" for the areas of *L. cajanderi* and species in the Far East (Kurahashi 1988; Uemura et al. 1994; Ewald and Kretzschmar 1995; Sindelar and Frydl 1995). It is likely to be conditioned by the limited access to the results of research conducted by Russian scientists which were published only in Russian language at different times.

The genus *Larix* was well-established in north-eastern Asia in the late Oligocene, divided into two morphologically distinct groups by the Eocene, and the northern group further divided to form *L. laricina* (North American species), *L. decidua* (Europen larch), *L. sibirica* (Siberian larch), and *L. gmelinii* (Dahurian larch) during the Pliocene and Pleistocene (LePage and Basinger 1995; Hytteborn et al. 2005). A study of allozyme variation in the Eurasian and American *Larix* species suggests that these two are well separated with negligible gene flow between them since the last glaciation (Semerikov and Lascoux 1999). In addition, *L. sibirica* shows greater genetic variation along longitude than latitude, and is genetically close to *L. olgensis*, a species distributed in Korean peninsula (Semerikov et al. 1999). The same study also identified, through the analysis of allozyme variability in Eurasian larch species, that *L. gmelinii* and *L. olgensis* could be separated, but *L. cajanderi*, *L. amurensis*, *L. kamtschatica*, and *L. ochotensis* were all closely related to *L. gmelinii*, and considered introgressive hybrids.

Recent investigation of *Larix* phylogenies based on cytoplasmic and nuclear DNA suggests pictures somewhat different from the analysis with allozyme variations. Eurasian and American species are well separated, but affinity of *L. olgensis* and *L. gmelinii* was suggested closer than that of *L. olgensis* and *L. sibirica* (Semerikov et al. 2003). The results also confirmed discrepancy between phylogenies based on chloroplast DNA and nuclear DNA.

We share Bobrov's opinion (1972) and presume that there are three larch species in Siberia – *L. sibirica, L. gmelinii, L. cajanderi*, and a hybrid complex *L.x czekanowskii*. In the zone of the habitat contact, *L. gmelinii* and *L. cajanderi* are involved in hybridization and form a treeline of transitional hybrid populations (Abaimov 1980; Abaimov et al. 1980; Abaimov and Koropachinsky 1984; Abaimov and Milyutin 1995; Abaimov et al. 1999). All three species have definite habitats, morphologically isolated, and are characterized by a series of biological and ecological peculiarities.

3.3 Geographical Distribution of Siberian Larch Species

The earlier mentioned contradictory views on the geographical distribution of Siberian larch species and their hybrid complexes in the contact zones of natural populations make it necessary not only to present a map of larch distribution (Fig. 3.1), but also to give a short description of habitat borderlines. As a basis for characterization of the habitats of Siberian larch species, we made use of available literature data, scientists' herbarium samples as well as our own collections of mature cones and young larch shoots gathered by the author in different years on the territory of Siberia and the Far East (1976–2001) in 230 geographical points. The natural populations studied by us are located mainly between the longitude of 70–179°E and latitude of 51–72°N.

3.3.1 Larix sibirica Ledeb.

Disjunctive (netted) habitat of *L. sibirica* occupies approximately 3.2 million km^2 in total (Koropachinsky 1983). *Larix gmelinii* and *L. cajanderi* usually

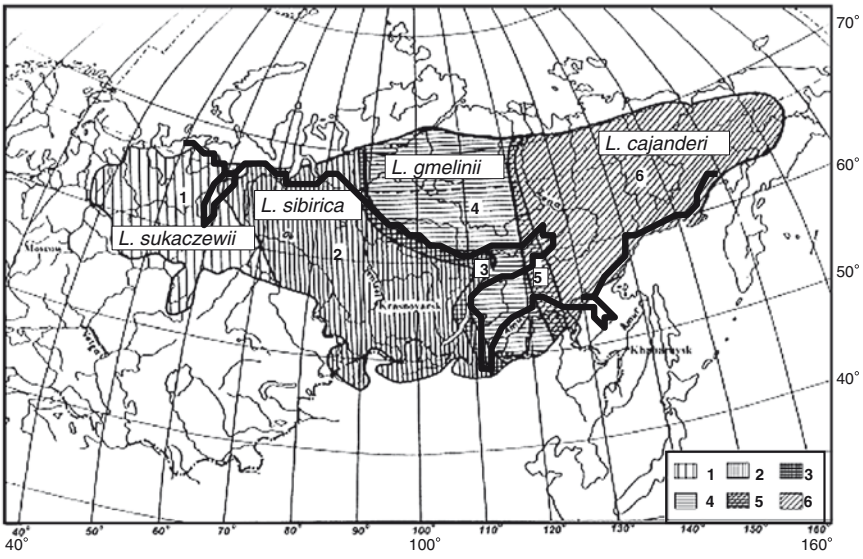

Fig. 3.1 Distribution of larch species in Siberia and adjacent territories: (1) *Larix sukaczewii* Dyl., (2) *L. sibirica* Ledeb., (3) *L. x czekanowskii* Szaf., (4) *L. gmelinii* (Rupr.) Rupr., (5) *L. gmelinii x L. cajanderi*, (6) *L. cajanderi* Mayr. Southern boundary of continuous permafrost zone (indicated as thick black line) approximately follows southern limit of *L. cajanderi* distribution and southern and western boundaries of *L. gmelinii*. See also Fig. 1.1 (this Vol.) for more exact boundary of continuous permafrost. (Modified from Abaimov et al. 1998)

have continuous habitats. Their area constitutes, correspondingly, 1.9 and 2.6 million km^2 (Abaimov et al. 1980). If the area of related hybrid complexes is included, *Larix sibirica* covers approximately 14% of the total area of larch distribution in the Russian Federation, *L. gmelinii* – 35%, and *L. cajanderi* – 48% (Abaimov et al. 1998).

In the North, *L. sibirica* together with Siberian spruce (*Picea obovata* Ledeb.) forms a polar limit of tree stand distribution over the territory between the Ob and Yenisey Rivers. The uppermost north-eastern limit of this species' distribution is located in the basin of the Pyasina River on the Taimyr Peninsula. There it reaches, according to our observations, latitude 71°N and forms sparse stands where dwarf, shrub-like forms of this species grow alongside scattered trees.

According to Putenikhin and Martinsson (1995), the western borderline of the *L. sibirica* range stretches from the towns of Kurgan and Yalutorsk to the north-east reaches of the Ishim River, and along its valley, it turns to the Irtysh River. Further, the borderline turns to the south-west and runs into the basin of the Tobol River. Then it follows a bit to the west of the town Chelyabinsk and runs to the south in the direction of the town Orenburg. Having a general direction to the south-east, the western borderline of Siberian larch runs through the southern regions of Novosibirsk Oblast and Altaysky Krai.

In the South of Altai, it reaches the Kholzunsk Ridge and the Katunsky mountains. Then the borderline turns to the South in the direction of the Republic of Kazakhstan along the slopes of the South Altai and the Saura Ridges, and crosses the basin of the Markagol Lake. Then it goes to the territory of the Mongolian Republic along the main ridge of the Mongolian Altai. According to Dugarjav (1995), separate Siberian larch stands reach the Baitak-Ula mountains (45°10′N, 91°E) in Mongolia. It is likely to be the most south-western outpost of *L. sibirica*.

The eastern borderline of *L. sibirica* habitat is the most comprehensively studied. Its detailed description is given in the works of Dylis (1947, 1961), Kruklis and Milyutin (1977), and Abaimov and Koropachinsky (1984).

In the far north-east of its distribution, reaching the upper watershed of the Pyasina River, Siberian larch grows along the western macroslope of the Putorana mountains penetrating the valleys of the Dudinka, Khantayka, and Kureyka Rivers into the plateau almost up to 90°E longitude. Then the eastern borderline crosses the Nizhnyaya Tunguska River and goes along its watershed with the Podkamennaya Tunguska River on the territory of Evenkia, Irkutsk Oblast, and the Republic of Sakha (Yakutiya). Near the latitude of 60°N, the eastern borderline of this species habitat reaches the upper flow of the Lena River basin (Fig. 3.1). Then it turns sharply to the south-west in the direction to the western shore of the Baikal Lake. From its eastern shore the borderline is directed to the south-east. In the Republic of Buryatiya it stretches toward the vicinity of the town of Ulan-Ude. Southwards, on the territory of Chitinskaya Oblast, the south-eastern edge of the *L. sibirica* habitat reaches the town Petrovsk-Zabaikalsky in the basin of the Ingoda River. It then leaves the territory of the Russian Federation near the longitude 113°E for the Republic of Mongolia.

There this species reaches the south-eastern limit of its distribution in the region of the Khentay Ridge (Dugarjav 1995).

3.3.2 *Larix gmelinii (Rupr.) Rupr.*

The northern borderline of *L. gmelinii* distribution passes through the latitude of 70°N and 71°N through the basin of the Pyasina River in the far north-west to the Lena River delta in the east (Fig. 3.1). The northernmost tracts of open forests and sparse stands of *L. gmelinii* are located on the Taimyr Peninsula. One of them, the stow of "Ary-Mas," is situated in the basin of the Novaya River (72°28′N). Another one is composed of isolated sites of dwarf, shrub-like forms of *L. gmelinii* in the lower flow of the Lukunskaya River - the right tributary of the Khatanga River (72°40′N). At present, these populations are isolated from the main *L. gmelinii* habitat by the zonal shrub tundra associations.

The northern borderline of *L. gmelinii* as well as of *L. cajanderi* habitat serves a climatic limit of the distribution of timber vegetation. It is conditioned by the warmth deficit and the short vegetation period. Within the Central and Northeastern Siberia, the northern timberline very closely coincides with the July isotherm of 10°C, with isolines of the sum of active air temperatures (over 10°C) during a growing season of 300°C and the isoline of growing season duration of 60 days (Abaimov and Koropachinsky 1984).

Views concerning the western and eastern borderlines of *L. gmelinii* habitat are the most contradictory. Many Russian and foreign scientists who studied the genus *Larix* Mill. have drawn the eastern limit of *L. sibirica* habitat and the western limit of *L. gmelinii* habitat either directly close or overlapping one another (Sokolov et al 1977; Bobrov 1978; LePage and Basinger 1991). Meanwhile, as was mentioned earlier, these species in the contact zone are involved in natural hybridization and form a stripe of hybrid populations described by Szafer (1913) as *Larix czekanowskii*. The width of the stripe of these hybrid populations varies from 50–70 km in the north to 250–300 km in the central part and in the southern region of Siberia (Fig. 3.1).

According to literature and our data (Abaimov et al. 1998), the western borderline of *L. gmelinii* on the Taimyr Peninsular passes the upper Kheta River basin. It crosses the eastern edge of the Lama Lake, reaches the central part of the Khantaysk Lake basin, turns to the south-east, and comes to the Nizhnyaya Tunguska River approximately 450 km east of the Turukhansk settlement. Further, the western *L. gmelinii* borderline passes parallel with the eastern borderline of *L. sibirica* habitat. On the watershed of rivers Nizhnyaya and Podkamennaya Tunguska, it coincides closely with the boundary of continuous permafrost distribution.

On the territory of Irkutsk Oblast, the western borderline of *L. gmelinii* habitat crosses the Nizhnyaya Tunguska River for the second time and continues toward the upper flow of the Lena River. Further, it turns to the south-west and reaches the northern shore of the Baikal Lake (see Fig. 3.1). Then the borderline of this species

as well as of *L. sibirica* turns to the south-east, and at 110°E longitude, goes to the territory of Mongolia.

Different understanding of this species by scientists results in considerable contradictions in the characteristics of the eastern borderline of *L. gmelinii,* even among Russian scientists. Suffice it to point out that Dylis (1961), having divided *L. dahurica* habitat into the western (*L. dahurica* Tursz. Ex. Traut. *ssp. dahurica*) and eastern (*L. dahurica ssp. cajanderi* (Maur.) Dyl.) races, draws a dividing line between them at 120–123°E longitude.

Bobrov (1972, 1978), having restored the species status of *L. gmelinii* and *L. cajanderi,* draws a borderline between them along the Verkhoyansk Ridge in the northern and central Yakutia (127–130°E), and further from the mouth of the Aldan River to the south-east in the direction of the shore of the Sea of Okhotsk.

Meanwhile, according to our investigation (Abaimov et al. 1980; Abaimov and Koropachinsky 1984) in the contact habitat zone, *L. gmelinii* and *L. cajanderi* are involved in hybridization and form a stripe of transitional populations situated on the left bank of the Lena River. In the north of Yakutia, its width does not exceed 50–100 km, and in southern Siberia, it enlarges to 550–600 km (see Fig. 3.1). According to our approximate calculation, the total area of hybrid populations of these species constitutes about 350,000 km^2. The stripe of transitional hybrid forms occupies approximately 7% of the mother species habitat area.

Thus, the eastern borderline of *L. gmelinii* habitat in the northern part of Yakutia passes virtually along the right bank of the Olenyok River basin at ca. 120°E longitude. Going southwards, it crosses the Lena River some 40–50 km to the west of the Olyokminsk settlement. Then it bends somewhat to the south-east and approaches the Amazar settlement (122–123°E) and then continues to the central part of the Great Khingan (or Daxingan) Mountains in China (see also Chap. 19, this Vol.).

It should be noted that the eastern borderline of *L. gmelinii* habitat coincides with the January isotherm of −30°C, and the eastern borderline of *L. cajanderi* coincides with the January isotherm −40°C. In the mountains of the Siberian south, this regularity is broken because altitudinal vegetation zonality and latitudinal zonality overlap one another.

3.3.3 Larix cajanderi Mayr.

The northern borderline of this species distribution is close to the latitude 70°N and, as it was mentioned earlier, appears to be determined climatically everywhere. *Larix cajanderi* habitat reaches the zonal tundra and forms the northern limit of the distribution of timber vegetation.

The western border of *L. cajanderi* habitat goes along the left bank of the Lena River at the distance not more than 70–100 km from its valley. There it coincides

closely with the western limit of *Pinus pumila* (Pall.) Regel. and *Betula middendorffii* Trautv. However, in central Yakutia and mountainous parts of the Siberian north, this regularity is broken. The eastern borderline of the habitat crosses the valley of the Lena River at 124°30′ E longitude. Further, it continues toward the upper flow of the basin of the Aldan River. On the territory of Amurskaya Oblast, *L. cajanderi* borderline passes through the Zeya River basin and then approaches China at the town of Shimanovsk.

The eastern borderline of *L. cajanderi* distribution remains the least studied at present. It reaches the middle flow of the Anadyr River in the far north-east. Then it turns to the south-west, crosses Penzhinsky Ridge, and at the longitude of 160°E, comes to the shore of the Sea of Okhotsk.

According to Bobrov (1978), in the environment of the Pribrezhny Ridge and somewhat southwards, *L. cajanderi* is involved in hybridization with *L. kamschatica* or other hybrid forms of the Far-Eastern Larix species. This conclusion is trustworthy since it is proved by the presence of morphological features characteristic to mature cones and young shoots which differ from *L. cajanderi* in the continental part of its area. These morphological features include the presence of spoon-shaped seed-scales with a rounded upper edge and predominance (up to 60–80%) of one-year shoots with reddish-brown color typical for a considerable number of trees in natural populations.

To clarify the south-eastern borderline of *L. cajanderi* habitat, in our opinion, it is necessary to study natural populations and development of hybridization in detail among representatives of the genus *Larix* in the Far East of Russia.

Finally, it should be stressed that *L. gmelinii* and *L. cajanderi* have definite habitats. In the zone of their contact (which was likely to occur at the end of Pleistocene), hybrid populations with combining features of mother species were formed. *Larix sibirica* and *L. gmelinii* habitats are also divided by a stripe of hybrid populations described by Szafer (1913) as *Larix czekanowskii* in the honour of a well-known Polish geologist.

3.4 Morphological and Ecological Features of Siberian Larch Species

It is a well-known fact that outwardly all larch species resemble one another. They are monoecious timber plants with needles on short shoots falling down in the autumn. Siberian larch species occupy vast habitats. Their territory is characterized by a wide range of ecological conditions. In the process of evolution and adaptation to the changing environment, Siberian larch species have acquired not only definite morphological features, but also hereditary ecological properties with respect to warmth, moisture, soils rich in elements of mineral nutrition, and permafrost. This is the reason why it is expedient to give a brief morphological and ecological characteristic of *L. sibirica, L. gmelinii,* and *L. cajanderi*. The main morphological features and some peculiarities of Siberian larch species are compared in Table 3.1.

Table 3.1 Cone and seed features of three Siberian larch species

	Siberian larch species		
Features	*L. sibirica*	*L. gmelinii*	*L. cajanderi*
Mean cone length (mm)	19.0–39.0	12.0–19.6	12.4–19.0
Mean cone width (mm)	15.2–32.0	8.8–17.8	13.2–23.3
Cone width/length ratio	0.70–0.90	0.62–0.96	1.03–2.22
Typical cone form in open state	Wide-ovate	Ovate	Flattened-round
Angle of seed-scale (°)	20–50	15–45	45–110
Form of seed-scale upper edge	Round	Slightly hollow	Deeply hollow
Shape of seed-scale surface	Spoon-shaped	Flat or transitional	Flat or transitional
Seed-scale downiness	Downy	Not downy	Not downy
Number of parastichies	3–7	2–5	2–4
Cone opening for dissemination	In autumn and at the beginning of winter	At the end of spring and the beginning of summer	In autumn during 3–5 days, only
Seed dormancy	No	Yes	No
Weight of 1,000 filled seeds (g)	3.8–10.0	1.2–6.0	1.1–6.5
Germination energy of seeds(%)	17–70	11–76	49–64
Germination ability of seeds (%)	24–73	18–77	45–81
Share of filled seeds (%)	24–73	23–84	33–69

Values (range) are compiled from the various data (Dylis 1961; Pozdnyakov 1975; Karpel' and Medvedeva 1977; Kruklis and Milyutin 1977; Abaimov 1980, 1997; Milyutin 1983; Abaimov and Koropachinsky 1984; Abaimov and Milyutin 1995; Abaimov et al. 1998, 2000)

3.4.1 Larix sibirica Ledeb.

This species is the most comprehensively studied in different parts of its habitat. The main morphological distinctions used for its diagnostics are described in the following paragraph.

Young annual shoots are usually straw-yellow colored and hairless. Young cones in natural populations are characterized by predominance of red color of different shades. Forms with green cones are rarely met. Mature cones are light-brown, their length and width vary from 10 to 50 mm. Seed-scales amounting to 9–44 are distributed spirally in 3–7 rows (parastichies). They have ovate or rounded shape,

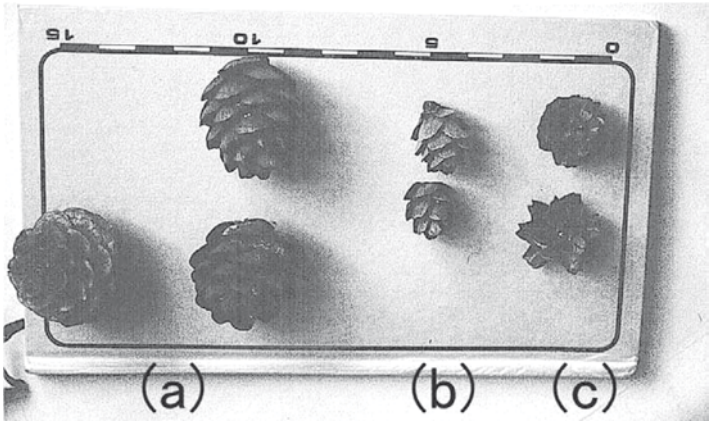

Fig. 3.2 Typical mature cones of (**a**) *Larix sibirica* Ledeb, (**b**) *Larix gmelinii* (Rupr.) Rupr., and (**c**) *Larix cajanderi* Mayr. Each cone represents one population. Details see Table 3.1 and Abaimov et al. (1998).(Photo T. Kajimoto)

domed spoon-shaped surface with rounded upper edge. Their length and width vary within 5–17 mm. Seed-scales, as a rule, have conspicuous reddish downiness at the base or over a considerable part of the surface. Protective scales are obviously visible. Typical form of mature cones is wide-ovate. The width/length ratio equals 0.70–0.90 (Table 3.1, Fig. 3.2a). During the process of cone maturation, angle of the seed-scales varies between 20 and 50°. Needles mainly grow on short shoots (brachyblasts) and their number in bundles amounts to 10–50. The needle length varies in the range of 10–58 mm, depending on the ecological conditions. The mean weight of 1,000 seeds can be 4–10 g. Energy of seed germination varies in different years from 17 to 70%. Germinating ability varies from 24 to 73%. Share of filled seeds in crops of different years is in the range 24–73% (Dylis 1961, 1981; Burovskaya 1966; Deryuzhkin 1970; Kruklis and Milyutin 1977; Milyutin 1983; Abaimov et al. 1998, 2002).

A wide range of ecological conditions is characteristic to Siberian larch. It forms stands at the zonal tundra borderline and in the zone of contact with dry steppes in the south of the habitat. Active temperature sum (over 5°C) in the larch habitat varies from 2,000°C in southern Siberia to 300–400°C at the northern borderline of the habitat and in the mountains.

Larix sibirica is more "heat-loving" than *L. gmelinii* and *L. cajanderi*. For example, according to observations in Zabaikalie, its blooming begins at the day temperature sum of 18–20°C. Likewise, hybrid *L. czekanowskii* begins to bloom at the day temperature sum of 17–19°C, while *L. gmelinii* does so at 9–13°C (Kruklis and Milyutin 1977). Unfolding of needles of these three species occurs at the following temperature sums: 50–60°, 30–35°, and 27–45°, respectively; and the process of fertilization – at 392°, 346°, and 312°, respectively. These data prove high heat demand of *L. sibirica* in comparison with *L. gmelinii*. Hybrid *L. czekanowskii* is transitional with respect to this leading ecological factor.

Larix sibirica is also characterized by high light demand. This ecological property intensifies with age (Sukachev 1938). However, young *L. sibirica* can successfully grow under dense canopy of stands (Tikhomirov et al. 1961; Popov 1982).

In the north, *L. sibirica* grows on dry sands as well as on sandy loam, clay loam, and peat soils with excessive moistening (Dylis 1981). Gentle slopes and river valleys with drained wet acid and neutral soils are optimum environment for *L. sibirica*. Lack of aeration and low temperature of active soil layer under conditions of long seasonal, interrupted and insular permafrost lead to sharp lowering of stand productivity. This is the reason why growing-stock volume in the north does not exceed 40–120 $m^3 ha^{-1}$ (Falaleev 1985; Abaimov 1997).

Under optimum ecological conditions, *L. sibirica* can reach 40 m high and more, and one meter and more in diameter. For instance, in the Republic of Tuva in the Altai and other mountain regions of southern Siberia on rich drained soils, stands with growing-stock volume of 800–1,000 $m^3 ha^{-1}$ can grow. Under excessive soil moistening, *L. sibirica* forms surface root systems as well as adventitious roots. *Larix sibirica* is sensitive to permafrost. Therefore, it gives up "edificatory" role to *L. gmelinii* along the contact zone of their habitats.

On open sites it begins to produce seeds at the age of 10–15 years; in dense stands seed production starts at about 25–30 years old. Years of heavy seed crops usually occur at every 4–5 years. Seed crops can vary from 2 to 120 kg ha^{-1} and more in different parts of the habitat (Verkhovtsev 1940; Lashchinsky 1958; Milyutin 1983). Their size is conditioned by the environment, weather conditions of a definite year, stand age, stand productivity, canopy closure, density, and other factors.

Stands with the predominance of *L. sibirica* are formed mainly in the mountains of southern Siberia. There it reaches the upper limit of the forest at the altitude of 1,900–2,400 m above sea level. Its considerable role in the formation of forests is expressed at the borderline with tundra within the West-Siberian Plain. In the taiga zone *L. sibirica* usually only participates in the formation of mixed stands. After fires and clear cuttings, this species is, as a rule, replaced by birch and other woody species (Tyrtikov 1979; Popov 1982; Sokolov et al. 1994; Babintseva et al. 1998; Abaimov et al. 1999).

3.4.2 Larix gmelinii (Rupr.) Rupr.

This species is characterized by the following morphological peculiarities. Young annual shoots are yellowish-ochre or brown colored. In different parts of the habitat they have sparse downiness. Young cones are chiefly red colored with different shades. Forms with green cones are rarely met (Abaimov 1997). Color of mature cones changes from yellow to brown. Their length varies from 8 to 35 mm, and width from 5 to 25 mm. Cones consist of 7–30 scales which are usually distributed in 2–3 rows (limit is up to 5 rows). Seed-scale surface is flat or transitional. Sometimes their surface is deformed. Scales are hairless. Scales are polymorphous

as to the form of the upper edge of seed-scales. Almost in any natural population there are larch trees with emarginate or weakly emarginate, serrate or straight-cut upper edge. However, weakly emarginate type of scales is predominant. Mature cones are compact. When maturing, the angle of the seed-scales varies from 15 to 45°. Therefore, typical form of mature cones is oval or ovate. The width/length ratio is 0.62–0.93 (Table 3.1, Fig. 3.2b). The length of seed-scales varies in different ecological conditions from 6 to 15 mm and the width from 5 to 13 mm. Needles on brachyblasts grow in bundles of 8–58. The needle length varies from 4 to 42 mm. The mean weight of 1,000 seeds constitutes 1.2–6.0 g, seed germination energy – 11–76%, germinating ability – 18–77%, and share of filled seeds changes in different years from 23 to 84%. Seeds have expressed dormancy. Their total maturity completes only by spring of the following year (Karpel' and Madvedeva 1977)

Larix gmelinii is characterized by high reproductive potential. On open sites, it begins to bear fruit at the age of 9–12 years; in tree stands - from 20–25 years old. Heavy crops occur every 4–5 years. It can produce up to 37 kg of seeds and more per one hectare in the yielding years in south-western Yakutia (Karpel' and Medvedeva 1977). According to observations in Zabaikalie, one tree can have up to 18,000 and even 38,000 cones (Kruklis and Milyutin 1977).

Small angle of seed-scales in mature cones predetermines not only cone shape, but also terms and characteristics of seed dispersal. Over the vast part of the habitat, the seeds begin to fly out only in spring and summer of the following year. A definite proportion of good quality seeds is kept in the cones for 3–4 years. In northern part of Central Siberia, 9–20% and more of the produced seeds are still viable in the autumn of the following year (Abaimov 1997; Abaimov et al 2000).

As it was mentioned earlier, *L. gmelinii* habitat almost completely coincides with the zone of continuous and interrupted distribution of the permafrost. This species is dominant in the vegetation of the northern part of Central Siberia. Under optimum ecological conditions, the trees can reach 35 m and even 40 m high with diameter of 80–100 cm (Shcherbakov 1975; Dylis 1981; Falaleev 1985).

At the northern limit of distribution and in the mountains, *L. gmelinii* forms dwarf, shrub-like and semi-dwarf forms. Therefore, in the southern part of the habitat growing-stock volume often equals 400–500 $m^3 ha^{-1}$ and more. Under extreme ecological conditions, the stand volume does not exceed 15–40 $m^3 ha^{-1}$ (Abaimov 1997; Abaimov et al. 1998). *Larix gmelinii* reaches its age-limit of 609 years old in Taimyr (Vaganov et al. 1999). Mean age of uneven-aged stands can amount to 250–260 years old, and limits of its variation in a separate stand are 383–435 years old (Bondarev 1995).

Larix gmelinii is a light-loving tree species. However, its seedlings and saplings can survive under canopy of taller trees for 100 years and more (Abaimov 1997). *Larix gmelinii* is especially resistant to low temperatures of air and soil. Under plain conditions it can form stands at the sum of effective temperatures amounting to 550–600°C and in mountains - at 250–300°C. With respect to resistance to climate continentality, it is inferior only to *L. cajanderi* (Nazimova and Polikarpov 1996). Moreover, the temperature of active soil horizon under different ecological conditions does not usually exceed 2–5°C (Abaimov et al. 1999).

Larix gmelinii grows on dry sandy, cold permafrost and swamped, stony, rich alluvial and acid podzolic soils (Dylis 1981). It grows best of all on fertile drained soils with permafrost thawing deeply. In the permafrost zone, it forms superficial root system, and when the depth of thawing decreases, it is capable of forming adventitious roots which can be distributed at 3–4 levels (see Chap. 16, this Vol.). According to Pozdnyakov (1975), *Larix dahurica* in its broad sense (i.e., *L. gmelinii* and *L. cajanderi*) was formed together with permafrost development and is well adapted to it.

3.4.3 Larix cajanderi Mayr.

The color of young annual shoots varies from yellowish-ochre to brown with predominance of ochre color. Young cones are red or close to this color. Green cones are rarely met. Mature cones change their color from yellow to brown. Their length varies from 9 to 25 mm, and width from 10 to 28 mm. The number of seed-scales is within 10–30, growing in 2–4 rows. Seed-scale surface is flat or wavy. They are hairless. Scales are 6–17 mm long and 5–15 mm wide. The upper edge is often emarginate, less often weakly emarginate, serrate, or straight cut. Bract-shaped scales are longer than protective ones and are clearly visible. The angle of seed-scale bending outside is usually 45–90°, sometimes even 100–110°. Typical form of the cones is round or flattened-round. Width/length ratio of cones varies within all forms from 1.03 to 2.22 (Table 3.1, Fig. 3.2c). Needles on brachyblasts grow in bundles of 12–59 and are from 6 to 33 mm long. The mean weight of 1,000 seeds varies from 1.1 to 8.0 g, germination energy is 49–64%, germinating ability is 45–81%, and share of filled seeds changes every year from 33 to 69%.

The main part of *L. cajanderi* habitat is situated eastwards of the Verkhoyansk Ridge in the basins of the Yana, Indigirka, and Kolyma Rivers. This territory is characterized by the most severe continental climate. Mean annual air temperature varies from −11 to −17.1°C. Outwardly, this larch changes from straight trees 35–40 m high to dwarf, shrub-like forms depending on latitude of the locality, altitude above sea level, and ecological conditions. *Larix cajanderi* is characterized by maximum durability. In the basin of the lower flow of the Indigirka River and at the upper limit of timber vegetation distribution, living trees were found at the age of 878–885 years old (Vaganov et al. 1999).

On the greater part of the habitat, *L. cajanderi* forms open forests with growing-stock volume of 10–60 $m^3 ha^{-1}$ typical of the Extreme North. On rich alluvial soils of river valleys, however, *L. cajanderi* forms stands with much larger growing-stock volume, ranging between 500 and 700 $m^3 ha^{-1}$ (Tikhomirov et al. 1961; Shcherbakov 1975; Pozdnyakov 1986). This species is the least heat-demanding. It endures perfectly well the long and extremely low air and soil temperatures; besides, it is frost-resisting.

This species does not demand rich soils. It can grow on stony skeletal soils of mountain slopes, and on carbonate, podzolic and alluvial soils. Only on dry sands in

central Yakutia, *L. cajanderi* cannot compete with Scots pine (*Pinus sylvestris* L.). It forms surface root system and adventitious roots when permafrost thawing increases.

Like other Siberian species, *L. cajanderi* is light-demanding. However, young trees can survive under forest canopy for decades.

It has a high reproductive potential. Blooming begins at the sum of positive mean day and night temperatures amounting to 90°C (Karpel' and Medvedeva, 1977). Heavy crops occur every 2–3 years, which is more frequent than *L. gmelinii*. It can produce up to 65 kg of seeds on one hectare (Pozdnyakov 1975). Seeds fly out in the beginning of autumn immediately after maturity within 3–5 days.

In the southern part of the habitat *L. cajanderi* successfully competes with coniferous (*Pinus sylvestris* L., *Picea obovata* Ledeb., *Picea ajanensis* Lindl. et Gord.) and deciduous species (*Betula pendula* Roth., *Populus tremula* L.). On slashes and burnt-over areas without sources of seeds, it gives up its edificator role to birch (*Betula pendula* Roth.) and brushes (*Duschekia fruticosa* (Rupr.) Pouzar., *Betula exilis* Sukacz., *Salix ssp.*).

3.5 Conclusions

On the territory of Siberia there are three larch species: *Larix sibirica* Ledeb., *L. gmelinii* (Rupr.) Rupr., and *L. cajanderi* Mayr. Species close to present *L. sibirica* and *L. gmelinii* were formed by the beginning of Pleistocene, and *L. cajanderi* - at the end of Pleistocene within the initial populations of mother species through the process of natural selection and divergence of features. Disjunctive habitat of *L. sibirica* occupies about 3.2 million km^2. *Larix gmelinii* and *L. cajanderi* are close species, well separated morphologically and having definite continuous habitats. Their area constitutes, correspondingly, 1.9 and 2.6 million km^2. Absence of mechanisms of reproductive isolation contributes to the development of natural hybridization of the species in the zones of contact of their natural populations. *Larix gmelinii* and *L. cajanderi*, compared to evergreen coniferous species, are better adapted to conditions of continuous distribution of the permafrost and the northern limit of the distribution of forest vegetation everywhere on the territory of Siberia.

References

Abaimov AP (1980) *Larix gmelinii* and *Larix cajanderi* (systematics, geography, variability, and natural hybridisation). PhD Thesis, Krasnoyarsk, p 24 (in Russian)

Abaimov AP (1997) Larch forests of Siberian North (diversity, features of ecology and forest-forming process). PhD thesis, Krasnoyarsk, p 537 (in Russian)

Abaimov AP, Koropachinsky IY (1984) *Larix gmelinii* and *Larix cajanderi*. Nauka, Novosibirsk, p 120 (in Russian)

Abaimov AP, Milyutin LI (1995) Present ideas on Siberian larch species and research needed. In: Proceedings of Seventh Sukachev Memorial Confeernce: Issues of dendrology. Novosibirsk, pp 41–60 (in Russian)

Abaimov AP, Karpel' BA, Koropachinsky IYu (1980) On habitat borderlines of Siberian larch species. Bot Zhurn 65:118–120 (in Russian)

Abaimov AP, Lesinski JA, Martinsson O, Milyutin LI (1998) Variability and ecology of Siberian larch species. Swedish University of Agricultural Sciences, Department of Silviculture, Reports 43, Umeå, p 118

Abaimov AP, Prokushkin SG, Matsuura Y, Osawa A, Takenaka A, Kajimoto T (1999) Wildfire and cutting effect on larch ecosystem permafrost dynamics in Central Siberia. In: Shibuya M, Takahashi K, Inoue G (eds) Proceedings of the Seventh Symposium on the Joint Siberian Permafrost Studies between Japan and Russia in 1998, Tsukuba, 1999 pp 48–58

Abaimov AP, Erkalov AV, Prokushkin SG, Matsuura Y, Osawa A, Kajimoto T, Takenaka A (2000) The conservation and quality of Gmelin larch seeds in cryolithic zone of Central Siberia. In: Inoue G, Takenaka A (eds) Proceedings of the Eighth Symposium on the Joint Siberian Permafrost Studies between Japan and Russia in 1999. National Institute for Environmental Studies, Tsukuba, pp 3–9

Abaimov AP, Barzut VM, Berkutenko AN, Buitink J, Martinsson O, Milytin LI, Polezaev A, Putenikhin VP, Takata K (2002) Seed collection and seed quality of *Larix* ssp. from Russia – Initial phase on the Russian-Scandinavian larch project. Eurasian J For Res 4:30–49

Babintseva RM, Buzykin AI, Ivanov VV, Maslenkov PG, Pshenichnikova LS (1998) Forest ecosystem formation under conditions of intensive forest exploitation. Nauka, Siberian Enterprise RAS, Novosibirsk (in Russian)

Bobrov EG (1972) History and systematics of larch species. Nauka, Leningrad (in Russian)

Bobrov EG (1978) Main conifers in forests of the Soviet Union. Nauka, Leningrad (in Russian)

Bondarev AI (1995) Structure and rules of inventorisation of the pre-tundra forests in the north-eastern part of the Krasnoyarsk Territory. PhD Thesis, Krasnoyarsk, p 22 (in Russian)

Burovskaya EV (1966) Seed crop in larch stands in the Podkamennaya Tunguska River basin. PhD Thesis, Krasnoyarsk, p 22 (in Russian)

Deryuzhkin RI (1970) Selection and larch cultures in the central part of the forest-steppe zone. In: Forest genetics, selection and seed management. Petrozavodsk, Russia, pp 203–209 (in Russian)

Dugarjav C (1995) Larch forests of Mongolia. PhD Thesis, Krasnoyarsk, p 392 (in Russian)

Dylis NV (1947) Siberian larch. Materials on taxonomy, geography, and history. Moskov, Odshch Issled Prir, Series "Botany" 2:1–137 in Russian

Dylis NV (1961) Larch species of East Siberia and the Far East. AN SSSR, Moscow, p 209 in Russian

Dylis NV (1981) Larch. Lesn. Promyshl, Moscow, p 96 (in Russian)

Ewald D, Kretzschmar U (1995) Tissue culture of adult larch as a tool for breeding purposes. In: Martinsson O (ed) Larch genetics and breeding. Research findings and ecological-silvicultural demands. Swedish University of Agricultural Sciences, Umeå, pp 153–163

Falaleev EN (1985) Forests of Siberia. Krasnoyarsk State University Press, Krasnoyarsk, p 135 (in Russian)

Forest Fund of Russia (1999) Reference. Book for Forest Fund of the Russian Federation. All-Russia Research and Information Center for Forest Researches, Federal Forest Service, Rosleskhos, Moscow, p 280 (in Russian)

Gaussen H (1966) Les Gymnosperms actuelles et fossiles. Travaux Lab Forest Touluse Tome 2:481–672

Holtmeier F-K (1995) European larch in Middle Europe with special reference to the Central Alps. In: Schmidt WC, McDonald KJ (comps) Ecology and management of *Larix* Forests: A look Ahead. USDA Forest Service, Intermountain Research Station, GTR-INT-319, pp 41–49

Hytteborn H, Maslov AA, Nazimova DI, Rysin LP (2005) Boreal forests of Eurasia. In: Andersson A (ed) Coniferous forests, Ecosystems of the worlds 6. Elsevier, Amsterdam

Karpel' BA, Medvedeva NS (1977) Seed crop in *Larix dahurica* in Yakutia. Nauka, Novosibirsk (in Russian)

Koropachinsky IYu (1983) Timber vegetation in Siberia. Nauka, Novosibirsk, p 383 (in Russian)
Kruklis MV, Milyutin LI (1977) *Larix czekanowskii* Szafer. Nauka, Moscow, 210 p (in Russian)
Kurahashi A (1988) Improvement of Larch by species hybridization. Bull Tokyo Univ For 79:1–94
Lashchinsky NN (1958) Regeneration of *Larix sibirica* in forests of the Altai Mountains. Novosibirsk, Trudy Po Lesn Khoz Sibiri 4:461–478 (in Russian)
LePage BA, Basinger JF (1991) A new species of *Larix* (Pinaceae) from the early tertiary of Axel Heiberg Island, Arctic Canada. Rev Paleobot Palynol 70:89–111
LePage BA, Basinger JF (1995) The evolutionary history of the genus *Larix* (Pinaceae). In: Schmidt WC, McDonald KJ (comps.) Ecology and management of *Larix* Forests: A look Ahead. USDA Forest Service, Intermountain Research Station, GTR-INT-319, pp 19–29
Mayr H (1906) Fremdländishe Wald- und Parkbaume fur Europa. Parey, Berlin, 662 s
Milyutin LI (1983) Interrelations and variability of allied species of timber vegetation in the contact zone of their habitats (on example of *Larix sibirica* and *Larix dahurica*). PhD Thesis, Krasnoyarsk, p 418 (in Russian)
Nazimova DI, Polikarpov NP (1996) Forest zones of Siberia as determined by climatic zones and their possible transformation trends under global change. Silva Fenn 30:201–208
Patschke W (1913) Ueber die extratropischen Coniferen und ihre Bedeutung fuer die pflanzengeographische Gliederung Ostasiens. Bot Jahrbuch fuer Systematik und Pflanzengeographie 158:651–655
Popov LV (1982) Southern taiga forests of the central part of Siberia. Irkutsk, p 330 (in Russian)
Pozdnyakov LK (1975) *Larix dahurica*. Nauka, Moscow, p 310 (in Russian)
Pozdnyakov LK (1986) The permafrost forestry. Nauka, Novosibirsk, p 130 (in Russian)
Putenikhin VP, Martinsson O (1995) Present distribution of *Larix sukaczewii*. Swedish University of Agricultural Sciences, Department of Silviculture Reports 38, Umeå, p 78
Schmidt WC (1995) Around the World with *Larix*: an introduction. In: Schmidt WC, McDonald KJ (comps.) Ecology and management of *Larix* forests: A look Ahead. USDA Forest Service, Intermountain Research Station, GTR-INT-319:6–18
Semerikov VL, Lascoux M (1999) Genetic relationship among Eurasian and American *Larix* species based on allozymes. Heredity 83:62–70
Semerikov VL, Smerikov LF, Lascoux M (1999) Intra- and interspecific allozyme variability in Eurasian *Larix* Mill. Species Hered 82:193–204
Semerikov VL, Zhang H, Sun M, Lascoux M (2003) Conflicting phylogenesis of *Larix* (Pinaceae) based on cytoplasmic and nuclear DNA. Mol Phylogen Evol 27:173–184
Shcherbakov IP (1975) The forest cover of the north-eastern part of the Soviet Union. Nauka, Novosibirsk, p 344 (in Russian)
Sindelar J, Frydl J (1995) Parental partners' effects on progenies characteristics on hybridization within the *Larix* genus. In: IUFRO Working party S 2.02-07(July 31- August 4, 1995): Larch genetics and breeding, Umeå, Sweden, pp 99–121
Sokolov SY, Svyazeva OA, Kublin VA (1977) Habitats of tree and shrub species in the Soviet Union. 1: 1–16 (in Russian)
Sokolov VA, Atkin AS, Farber SK (1994) Structure and dynamics of taiga forests. Nauka, Siberian enterprise RAS, Novosibirsk, p 168 (in Russian)
Sukachev VN (1924) About the history of the genus *Larix* Mill. In: The forest issues. Novaya Derevnya, Moscow-Leningrad, pp 12–44 (in Russian)
Sukachev VN (1938) Dendrology and basics of forest geobotany. Goslestekhizdat, Leningrad, p 574 (in Russian)
Szafer W (1913) Contribution to the knowledge of Eurasian larch species with particular attention paid to larch species occurring in Poland. Kosmos 38: 1021, 1281–1315 (in Polish)
Tikhomirov BN, Koropachinsky IY, Falaleev EN (1961) Larch forests of Siberia and Far East. Goslesbumizdat, Moscow –Leningrad, p 164 (in Russian)
Tyrtikov AP (1979) The dynamics of vegetation cover and the development of permafrost relief forms. Nauka, Moscow, p 116 (in Russian)

Uemura S, Tsujii T, Ishizuka M, Volotovsky KA (1994) Timber limit vegetation of the Northernmost taiga in the Lena River basin, Eastern Siberia. In: Inoue G (ed) Proceedings of the Second Symposium on the Joint Siberian Permafrost studies between Japan and Russia. National Institute for Environmental Studies, Tsukuba, Japan, pp 116–121

Vaganov EA, Naurzbaev MM, Eger IV (1999) Age limit in larch trees in Siberia. Lesovedenie 6:65–68 (in Russian)

Verkhovtsev EP (1940) Seed crop quantity and seed quality in Siberian larch sparse stands. In: Siberian Larch. Krasnoyarsk, pp 89–96 (in Russian)

Wright JW (1962) Genetics of forest tree improvement. vol 16, FAO Forestry and Forest Product Studies, Rome, p 399

Chapter 4
Wildfire Ecology in Continuous Permafrost Zone

M.A. Sofronov and A.V. Volokitina

4.1 Introduction

Climatic conditions are ecologically the most important factors influencing the differentiation and character of the vegetation cover at a global scale (Archibold 1995). In particular, fluctuations in climate and weather during drought periods affect vegetation both directly and indirectly through factors such as those related to forest fires.

Characteristics of permafrost and vegetation vary considerably in Siberia, creating quite heterogeneous environments in this region. For instance, the depth of soil active layer often reaches 2 m or more in the summer in the southern part of the permafrost zone. Interactions among permafrost, vegetation, and wildfire are not so obvious. On the other hand, in the northern part of the permafrost zone, the soil usually thaws to 0.3–0.6 m in depth. The mutual influence among the permafrost, vegetation, and wildfires is strong due, for example, to dominance of fire-prone plant species over a permafrost soil, resulting in the development of unique forest ecosystems. Thickness of tree's root layer and the root volume per unit of ground are both small, leading to thin tree canopies. These characteristics suggest us to categorize the forests on permafrost soil differently from the taiga forests to the south of the region. Therefore, forests on the permafrost should be considered an independent biome (Kolesnikov 1969; Parmuzin 1979; Sofronov 1991a; Sofronov and Abaimov 1991).

Peculiarities of wildfire ecology in the northern part of the permafrost zone are presented in this chapter. Typical vegetation in the region of the permafrost is the 'northern open woodlands' biome where it is characterized by forests with thin canopy (Nazimova 1996; see also Chap. 1, this Vol.). This feature is easily visible in aerial photographs. In Central Siberia, the area of the northern open woodlands extends northward from the basin of the Podkamennaya Tunguska River (63°N). The forest vegetation spreads up to 72°N due to warm summer. In the northern part of Siberia, rather sparse larch (*Larix gmelinii*) forests dominate. Typical northern taiga forests with denser canopies are located in patches only in river valleys and sites with relatively warm soils.

A. Osawa et al. (eds.), *Permafrost Ecosystems: Siberian Larch Forests*,
Ecological studies, Vol. 209, DOI 10.1007/978-1-4020-9693-8_4,

There have been few pyrological studies in the northern open woodlands zone of Siberia. Stepanov (1985) investigated reforestation through natural regeneration in burnt areas of northwestern Yakutia. Sofronov (1988, 1991b) investigated pyrological characteristics of vegetation in the Turukhan River basin and in the Taimyr Peninsula. Matveev (1992) studied the consequences of wildfires in the basins of the Kheta, Nizhnaya Tunguska, Lena, and Kolyma Rivers. Tsykalov (1987, 1991) collected data of fire experiments on fuel dry mass in the region of Tura, and estimated the damage to larch stands. Fire effects and tree regeneration in burnt-over areas of the same region were studied by Tsvetkov (1994, 1998) and the Laboratory of Permafrost Forest Science group at V.N. Sukachev Institute of Forest at Krasnoyarsk (Abaimov and Sofronov 1996; Sofronov and Volokitina 1996a, 1996b; Abaimov et al. 1997; Sofronov et al. 1998a, 1998b; 2000a, b, 2001, 2004Abaimov and Prokushkin 1999). In this chapter, we summarize studies on permafrost vegetation from the viewpoint of wildfire ecology mainly in the northern parts of Western Siberia (62°–86°E) and Central Siberia (86°–108°E). New data were collected and analyzed from a few sites in Central Siberia.

We will describe subjects regarding (1) vegetation fuel; (2) seasonal condition of fuel moistening, drying, and burning; (3) conditions of wildfire spread over the territory; (4) causes and affected area of wildfires; and (5) ecological consequences of wildfire.

4.2 Approaches to Study Wildfire Ecology

Field studies were carried out at three different sites along two tributaries of the Yenisey River in Central Siberia (central Evenkia). One site was in the Kureyka River basin (67°N, 88°E). Two other sites were located along the Nizhnyaya Tunguska River: one was within the vicinity (<10 km) of Tura settlement (64°N, 100°E) at Kochechum site (Fig. 1.2, this Vol.), and the other was farther from the settlement (about 80 km west) in the basin of the Degigli River (64°N, 98°E). Details of the field study are given in Sofronov et al. (2004).

On the Kureyka River basin site, four experimental plots (K1–K4) of *L. gmelinii* dominating and mixed forests of *Betula pendula*, *Pinus sibirica*, *Larix gmelinii*, *Picea obovata*, and *Abies sibirica* at various proportions were established (Table 4.1) to examine the function of organic layer as a "thermal insulator." Stands of various species' mixtures were included so that characteristics of the organic layer could be examined for a breadth of stand types. Soil temperature was measured in each plot at the depth of 35 cm (from the surface of moss or litter layer) during midsummer (from early to mid-August). The term "organic layer" is defined as the sum of layers of moss, lichen, litter, and duff: duff means a layer of decomposing fine vegetation remnants which are under the layer of live (growing) upper part of moss and lichen or under the layer of litter. However, not all parts are necessarily present. Soil temperature was recorded in the plot ($n = 5–8$ for plots K1–K3; $n = 1$ for plot K4). The thickness of the organic layer was also measured in a vertical

Table 4.1 Characteristics of four experimental plots in the Kureyka River basin site

Plot number	K1	K2	K3	K4
Species composition[a]				
Upper layer	9B1P	5L 5B	7B2LIS	9BIS+P
Lower layer	10S	6S4F	–	–
Tree age (yrs-old)	90–140	110–170	100–140	110–140
Sight index	V	IV	Va	V
Tree density (ha^{-1})				
Upper layer	700	600	1,300	1,100
Lower layer	600	300	–	–
Total basal areas ($m^2\ ha^{-1}$)				
Upper layer	16.6	21.3	14.0	17.7
Lower layer	8.5	2.8	–	–
Stemwood stock ($m^3\ ha^{-1}$)				
Upper layer	120	190	90	130
Lower layer	50	20	–	–
Mean tree height (m)				
Upper layer	17	20	12	14
Lower layer	12	1	–	–
Mean diameter by species (cm)	17 (B)	30 L	11 (B)	14 (B)
	13 (S)	18 (B)	17 (L)	13 (F)
	17 (B)	12 (S)	12 (S)	10 (S)
	–	12 (F)	–	–
Undergrowth tree composition[b]	10 S	6S 2F	9B 1S	5S 3F 2B
Undergrowth tree density (ha^{-1})	500	200	1400	400
Undergrowth biomass ($kg\ m^{-2}$)[c]	0.05	0.11	0.22	0.20
Organic layer biomass ($kg\ m^{-2}$)				
Moss	–	0.6	0.7	1.5
Litter	0.1	–	–	–
Duff	0.2	1.5	2.1	4.1
Organic layer thickness (cm)[d]	2–3	9–11	13–17	23–27

[a]Relative proportion of each tree species based on tree density; *L*, larch; *B*, birch; *S*, spruce; *F*, fir; *P*, Siberian pine. For example, plot with 5L 5B consists of larch (50%) and birch (50%). Layers refer to those of the canopy

[b]Tree species composition belonging to the undergrowth (i.e., height of 20–300 cm); this index is called "re-growth composition" in the Russian Forest Science)

[c]Including undergrowth trees, and other shrub species and grasses

[d]Sum of thickness of litter, moss, and duff

soil profile around each point of soil temperature measurement. When studying the organic layer it was cut with secateurs for the layer structure not to be disturbed.

At the site within the vicinity of the Tura settlement, vertical soil profiles and soil temperature were examined in two experimental plots II-4 (burned plot) and II-5 (unburned plot) in Site 2 (see Fig. 1.3). These plots had different conditions of organic layers (Table 4.2. Notes: description of tiered canopy unburned plot TB-1 is used in Sect. 4.8.3). The burned plot II-4 was located inside the burnt area created by a wildfire of 1994, and its organic layer was partially destroyed; the unburned

Table 4.2 Characteristics of three experimental plots of *L. gmelinii* forests established within the >220-year-old stand at Kochechum site near Tura

	Burned plot	Unburned plot[a]	Tiered canopy
Plot number	II-4	II-5[a]	unburned plot TB-1
Slope aspect	North–East	North–East	East
Slope gradient	12°	13°	5°
Stand parameters			
Tree age (years)			
Upper layer	170–180	170–180	180–220
Lower layer			80–90
Tree density (ha^{-1})			
Upper layer	1,030	1,000	700
Lower layer			4,900
Mean tree height (m)			
Upper layer	10.0	9.0	10.5
Lower layer			4.5
Mean stem diameter (cm)			
Upper layer	11.3	9.0	11.0
Lower layer			4.5

[a]The unburnt plot II-5 was about 20 m away from the burnt plot II-4 where fire occurred in 1994

plot II-5 was set outside of the burnt area (about 20 m away from the burned plot). Tree density, mean tree height, and stem diameter at breast height were 1,030 ha^{-1}, 10.0 m, and 10.8 cm for the burned plot, and were 1,600 ha^{-1}, 9.0 m, and 9.0 cm for the intact plot, respectively (Table 4.2). In each plot, the organic layer thickness and soil temperature were measured along a line transect at 50 cm intervals by making small soil profiles (total $n = 35$ for each transect). These measurements were carried out in the summer following the 1994 fire.

In order to examine the interactions between thawing soil depth, organic layer thickness, and micro-topography in detail, we established three plots in a mature larch forest (250–320 years-old) along the Nizhnyaya Tunguska River (80 km west of Tura). Large variation of micro-topography in this stand allowed us to examine its effect on soil and organic layer characteristics. One plot (P1) was on the river terrace close to a lake where micro-relief (shallow depressions and mounds in the area with elevation fluctuation usually not more than 1 m) was well-developed. The second plot (P2) was on the lower end of south-facing slope covered with dense shrubs (mostly *Duschekia fruticosa*), and the third plot (P3) was on the convex part of the slope (Table 4.3). In each plot, soil thawing depth and thickness of organic layer were measured along a line transect at 20 cm intervals (total $n = 200$ for each transect). Thawing depth was measured under two different soil moisture conditions (normal year and dry year) in summer. Significance of the dependence of soil thawing depth on the thickness of total organic layers (hereafter also referred to as 'organic layer thickness') was tested by simple correlation coefficient using all data of each transect.

Table 4.3 Characteristics of three experimental plots of *L. gmelinii* forests on the site 80 km west of Tura settlement

Plot number	P1	P2	P3
Slope aspect	North	South	East
Slope gradient	2°	15°	6°
Stand parameters			
Tree density (ha^{-1})	495	665	1,191
Tree age (years)	320	300	250
Mean tree height (m)	10.5	15.0	8.5
Mean stem diameter (cm)	14.0	16.6	9.5

4.3 Vegetation Fuel

Green mosses (e.g., *Hylocomium splendense*, *Pluerozium schreberi*) commonly dominate the surface cover of northern open woodlands, and are known to be a fire-hazard. Lichens can increase the fire danger by settling on the green moss cover. Simultaneously, accumulation of litter takes place. As the organic layer thickness increases, the soil becomes progressively colder. This further slows organic matter decomposition and contributes to more litter accumulation. For example, in the Turukhan basin in Western Siberia (66–67°N, 83–86°E), dry mass of the organic layer is as large as 4 kg m^{-2} in 100–120 year-old larch stands, and can amount to 6.7–7.5 kg m^{-2} in forest stands over 200 years old (Sofronov 1988). In the northern part of Northeastern Siberia, the dry mass of organic layer (green moss, lichen, and litter) varies from 2.5 to 8 kg m^{-2} (Sofronov and Volokitina 1998). Usually an average load of green moss-lichen cover, litter, fallen branches, and combined *Vaccinium uliginosum-Ledum palustre* equals 1 kg m^{-2}, 2–3 kg m^{-2}, 0.5 kg m^{-2}, and 0.1–0.3 kg m^{-2}, respectively.

Depth of soil active layer increases in the burnt-over areas where the organic layer has been removed by fire. However, this increase in the thickness of active layer is a temporary phenomenon. It provides a suitable environment for growth of tree seedlings and understory shrubs. In the basin of the Nidym River (30 km west of Tura settlement), the height of shrubs in a 12–13 year-old larch stand was 2–2.5 m, whereas the canopy height of trees reached 4–5 m. After recovery of the moss and litter layer, about 30–50 years later, the thickness of the active layer starts to decrease again.

Northern part of Western Siberia is affected strongly by widespread wetlands called “flat frost mound bogs.” This feature is defined as hillocks consisting of ice and peat, and is alternating with thermokarst lakes and depressions. About 80% of the area is occupied by well-drained flat mounds. The mounds are composed of a core of ice mixed with peat, and are often found to be covered with both lichens (1.5 kg m^{-2}) and *Ledum palustre* (1 kg m^{-2}). This indicates that fire danger of the mounds is very high. The mounds are typical for tundra, but they are not typical swamp elements (they are dry). It is more correct to call such landscape as a complex of swamp and forest tundra, and not merely swamps or bogs (Shumilova 1962).

4.4 Seasonal Conditions of Fuel Moistening, Drying, and Burning

A characteristic trait of the permafrost is high content of ice. This is the main difference of permafrost from the seasonally frozen soils, i.e., the soil that covers the permafrost is frozen in winter and melts in summer. It is due to the ice content of the permafrost that such characteristic features as thermokarst and heaving arise and develop.

Seasonally, frozen soils can actively absorb the melting water in spring. But permafrost with its high ice content does not absorb water and acts as a waterproof layer. In spring, melted water runs off to rivers. Therefore, fires do not practically occur in the northern open woodlands zone for about six weeks after snow melt, except for the limited areas of inflammable sites covered with dry herbs and sedges on the riversides and frost mound bogs in the northern part of Western Siberia.

The thin canopy of northern open woodlands creates favorable conditions for drying of the vegetation fuel. The quantity of radiation energy and illumination under the canopy of the northern larch stands is 1.5–3 times higher than those in typical taiga stands (Table 4.4) (Sofronov and Volokitina 1998).

In the beginning of summer, only lichens and mosses become dry while the litter remains wet. Therefore, this period is characterized by running surface wildfires. Wind, the main factor of spreading fires, freely penetrates the thin canopy of northern open woodlands. Surface fires may be exceedingly intense with a flame height of more than two meters. They are harmful to the forests. Wildfires are usually surface fires since the thin canopy prevents their development into crown fires.

In summer, rain water rapidly flows into rivers and lakes. Water is nearly absent in the subsoil. Therefore, precipitation and surface water run-off provide major source of water to moisten the forest floor. Location on a micro-elevation influences water regimes of the soil, duff, and moss (Table 4.5) (Sofronov et al. 2000).

During hot and dry periods of summer, the permafrost does not thaw out actively since it is protected from the sun by the layers of moss and duff. At the same time, the duff dries out and surface fire can acquire a steady form, if there is a zone of smoldering behind the flaming front. Higher above this zone, a vertical flow of hot air keeps the wind off the frontal edge of the flame. As a result, creeping surface fire spreads slowly, lowering the fire intensity.

Table 4.4 Relative illumination under forest canopy (%, compared to open)

Zonal type	Relative basal area							
	0.3	0.4	0.5	0.6	0.7	0.8	0.9	1.0
(I)	70	60	50	40	30	24	22	22
(II)	(95)	90	84	76	67	59	58	(58)

(I) – in typical taiga forests of Scots pine, spruce, Siberian pine, and larch
(II) – in larch forests (parentheses indicate calculated illumination values)
Relative basal areas are characteristic of forest density used in Russia (Zakharov 1967)

Table 4.5 Classification of relief elements according to their impact on run-off distribution and soil moistening

Relief elements	Major features	Impact on run-off and soil water regime
Convex forms	Radius of curvature	Run-off dispersal, soil drainage, and dryness
Smooth upper surfaces (plateaus)	Surface gradient	Weak run-off and moderate soil moistening
Slopes	Steepness, slope aspect, slope height; upper, middle, or lower parts of a slope	Soil moistening varies from insufficient to excessive depending upon location
Concave forms (depressions, stream valleys, etc.)	Radius of curvature and bottom gradient (for unclosed depressions)	Run-off concentration and increased or excessive (including stagnant) soil moistening
Smooth lower surfaces (terraces, flood-lands)	Surface gradient and height in relation to the maximum water level in the river	Weak run-off, moderate soil moistening, sometimes flooding

4.5 Wildfire Spread over the Territory

Wildfire spread over the territory is determined by characteristics of the landscape. In the zone of northern open woodlands, three categories of pyrological landscape can be distinguished: (1) flat lowlands; (2) mountain localities (with watersheds above the altitudinal tree line); and (3) plateaus and hilly plains (with watersheds below the altitudinal tree line).

Flat lowlands are located in the northern part of Western Siberia. The number of fire breaks in this territory is large due to thermokarst lakes and humid hollows occupied by sedge-*Sphagnum* swamps. For example, the area of thermokarst lakes and humid hollows amounts to 15–20% in the region of "flat frost-mound bogs," which is the typical landscape in Western Siberia. The average distance between fire breaks is about 1 km. Although the mounds covered with lichens and *Ledum palustre* are extremely fire-prone, lakes and humid hollows hamper the wildfire spread over the territory. However, the humid hollows and lakes are not perfect fire breaks, since wildfires can jump over them under strong winds (Sofronov 1988).

In Central and Northeastern Siberia, the territory of northern open woodlands zone includes areas of mountainous relief (Putorana Mountains, the Anabar Ridge, and mountains in the northern part of Yakutia) where vertical zonality of vegetation is common. The altitudinal tree line is at about 400 m above the sea level, and even 200 m in the Anabar Ridge. The mountain tundra followed by polar deserts is situated at even higher altitudes.

A noncontinuous vegetation floor is characteristic to the mountain tundra. Thereupon watersheds covered with noninflammable mountain tundra or mountain tundra in combination with polar deserts can be considered absolute fire breaks in the areas of open forests in the mountainous regions. A system of such noninflammable watersheds is supplemented by other fire breaks (e.g., mountain rivers and

streams that remain wet in summer, and stony screes). Altogether they create considerable pyrological barriers of the territory. Therefore, wildfires cannot spread over a vast territory (maximum 0.8–1.5 thousand ha).

Plateaus and hilly plains occupy almost the whole territory of northern open forests in Central and Northeastern Siberia (with the exception of mountain localities in the northern regions). A characteristic feature of these landscapes is that watersheds, which are situated below the mountain tundra, are the most typical routes for the spread of large wildfires since there are no elevated *Sphagnum* bogs. The *Sphagnum* bogs serve as the main fire breaks in the taiga zone.

Absence of upper *Sphagnum* bogs on watersheds is explained by permafrost heaving under the patches of *Sphagnum*. This phenomenon makes the *Sphagnum* cease its growth, and it gradually dies out. Without the subsoil waters, favorable conditions for *Sphagnum* development are created only by the active moisture supply from surface water, which flows to the lower parts of north-facing slopes. Such *Sphagnum* patches of 5–10 m^2 usually do not die during fires, and begin to grow out actively after them. We often find *Sphagnum* patches of about 1 ha on north-facing slopes. These are not bogs since a core of ice is always formed under the *Sphagnum*, though small *Sphagnum* bogs sometimes develop in the upper part of hollows, foot slopes, and slope terraces (Sofronov and Volokitina 1996a). The general extent of wetland is only about 10% of the total area of the northern open woodlands zone in Central and Northeastern Siberia (the area of peat bogs is about 4–6%).

Absence of upper *Sphagnum* bogs in watersheds is also related to drying-out of streams and shallow rivers in summer because of the absence of subsoil water. This decreases the number of fire breaks on the territory to a greater extent; therefore, wildfires freely spread along watersheds and slopes, and can burn over vast areas amounting to tens of thousands of hectares.

4.6 Causes of Wildfire and Areas of Wildfire Occurrence

The northern part of Siberia is characterized by low population density. Therefore, the main cause of forest fire is not people but lightning; however, also see Mollicone et al. (2006) and Achard et al. (2008) for indirect evidence of many human-caused fires at perimeter of intact boreal forests in Russia. Lightning activity in the Taimyr region is weak: only two days with thunderstorm during a fire season is observed (Agroclimatic reference book 1961). The size of burnt area in this region is not large. To the south, in the Putorana mountains, fire breaks are numerous because unburnable mountain tundras occupy the watersheds. Therefore, burnt area is restricted here as well. On the other hand, there are favorable conditions for high fire occurrence in the forests of central Evenkia: thunderstorms in summer occur rather often, e.g., 10 days with thunderstorms at Tura, and fifteen days at Vanavara and Baikit. The watershed area has no mountain tundras and unburnable *Sphagnum* bogs. Fire can spread freely in the watershed area and cover large areas.

In the northern part of Siberia, the continental climate is characterized by warm summers with long days and short nights. Duration of the fire season is three

months from the second half of June to the first half of September. The percentage distribution of wildfire occurrences for June, July, August, and September are 25, 40, 25, and 10%, respectively. But favorable weather conditions for fire (long hot dry periods) do not happen every year. Dry seasons seem to migrate on the Siberian territory. For example, in 1989, catastrophic fires occurred in Western Siberia to the south of 64°N parallel; and in 1990, to the north of it. In 1992, the forests of central Evenkia burnt extremely heavily (Sofronov et al. 1998a).

About 36% of the Russian forests are too remote to provide any fire protection. Unprotected areas are basically located in the northern open woodlands zone: in Western Siberia – 43 million hectares, in Central Siberia – 119 million hectares, and in Northeastern Siberia and the Far East – 249 million ha (Goskomstat of the Russian Federation 1993). Therefore, there is no official information on the size of burnt area in the zone of northern open woodlands.

Analysis of 1979–1984 space images for parts of the Taimura, Chuna, and Ilimpeya River basins in central Evenkia (9 million ha) gives relative evaluation of the burnt area amounting to about 1.5%, i.e., extremely high. It was found that burnt areas are seen during a six-year period after fire in the "Kosmos" space images for the Evenkia territory. Burnt areas are seen on the TIROS/NOAA thermal space images also during these six years after fire (Fig. 4.1).

Analysis of the TIROS/NOAA and SPOT-3 space images for the area near Tura settlement (10 million ha) showed that 51 large fires occurred from 1990 to 1995 (burnt areas over 1,000 ha for each fire). These fires covered 675,000 ha: 1.1% of the territory per year. According to "Soyuz" space images, 20 large fires occurred between 1978 and 1989 on the same territory; burnt area being about 300,000 ha: 0.3% of the territory per year. They characterize that the area surrounding Tura is highly burnable (the average fire recurrence time is 60–90 years) (Sofronov and Volokitina 1996b; Sofronov et al. 1998a).

4.7 Wildfire Impact on Larch Regeneration

There is always much light under the canopy of northern open forests; however, regrowth is not abundant. Even in old stands (> 200 years), sapling density does not customarily exceed one thousand per ha. Root competition with old larch trees may not be the cause. For example, in the Degigli River basin (the tributary of the Nizhnyaya Tunguska River), there were no larch seedlings in a stand where the larger larch trees had died of natural causes other than fire ten years earlier.

Considerable thickness of the moss and duff layers is likely to influence the larch regeneration negatively. In other words, thin organic layer on the forest floor is likely to promote establishment of larch seedlings. For example, the number of tree seedlings was 3–10 thousand per ha in larch stands after weak intensity fires, which generally reduce the moss layer thickness (Matveev and Usoltsev 1991). A comparison of a fire-disturbed site and unburned control near Tura settlement suggests a similar pattern (Sofronov and Volokitina 1996b). The control plot had

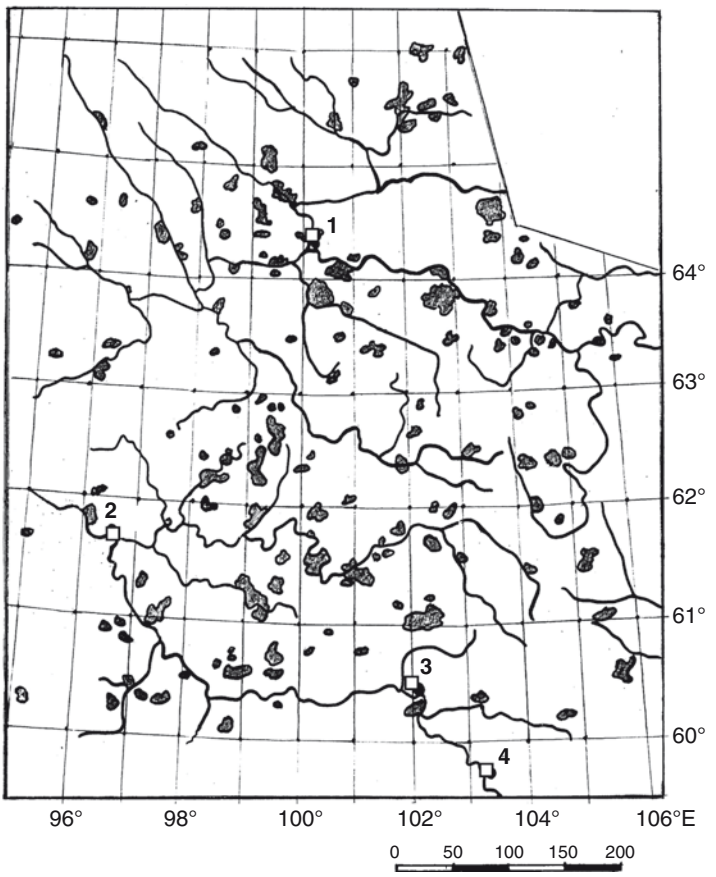

Fig. 4.1 Large burnt areas (> 1,000 ha) in Evenkia, the northern part of Central Siberia, from 1990 to 1995 (from TIROS/NOAA satellite images). Numerals 1–4 represent the towns of Tura, Baikit, Vanavara, and Chemdalsk, respectively

170 year-old larch trees, 10 m high. There were almost no regrowth (12 seedlings per ha). The mean thickness of the organic layer (moss, lichen, and duff) was 17.3 cm. The burnt plot had 37% of old trees that had died in a fire one year earlier. The number of larch seedlings was 165 thousand per ha there. We noted that the seedlings have become established successfully where thickness of the organic layer was 4.2 cm. On the other hand, seedlings were absent where the mean thickness of organic layer was 6.3 cm.

Similar impact of the organic layer thickness on forest regeneration was also observed in a nearby larch stand disturbed by a creeping ground fire 8 years ago. There was abundant larch regeneration (about 60,000 seedlings per ha) in 3.5 cm of moss and duff layer; but the regeneration was absent in 6.6 cm of moss and duff layer.

In the vicinity of the Tura settlement, there is an old 7-ha clear-cut of 1970. This clear-cut had only 180 small larch trees and saplings of various sizes (0.8–2.5 m

high) per ha. The thickness of the moss and duff layer was 15–24 cm. It is probable that the large thickness was the cause of seedlings' absence. A fire occurred in this clear-cut in August 1994. In the following summer, larch saplings were counted with a linear method. The transect to forest edges did not exceed 100 m. The transect was 236 m in total length, and sample plots (0.5 m^2 each area) were set at 4 m intervals. Seedling density was 135 thousand per ha. Analysis of the obtained data showed that larch seedlings become established only in small depressions and on flat places. The thickness of the organic layer was 2 cm when the seedlings were the densest. The thicker the organic layer, the lesser the number of seedlings. Regrowth was almost absent when the organic layer was 8–10 cm thick.

Examination of 1–5 year-old burnt areas suggests that optimal conditions for larch seedling establishment are created under partial burning of the forest floor, since the partly burnt duff plays the role of mulch, and prevents the soil from drying.

It is concluded that the main barrier to larch regeneration in the northern open woodlands is the moss and duff layer that is typically 10–25 cm thick. Satisfactory larch regeneration can take place where the organic layer thickness has decreased to 2–5 cm as a result of wildfires.

4.8 Ecological Effects of Wildfires

In the forest ecosystems of northern Eurasia, pyrogenic succession occurring after fires is predominant. Fire impact leads to dynamic biodiversity (for details, see Chap. 5, this Vol.). Fire with a certain periodicity can stabilize biodiversity within a large territory, though fire impact on each ecosystem may be destructive (Furyayev 1996).

The effects of fire on forest ecosystems depend on their periodicity and intensity. The absence of fires during a very long period not only promotes predominance of climax stages in plant communities, but also can lead to a gradual degradation of the forest vegetation and to its replacement by different nonforest vegetation types. In the forest ecosystems of northern Siberia, absence of fire promotes the increase in moss and duff layer and decrease in soil temperature. This leads to active permafrost development and exacerbates the poor soil conditions (Sofronov and Volokitina 1996a, 1996b, 1998). As a result, forest ecosystems may be replaced by a forest tundra or tundra ecosystem.

Frequency of forest fires may be categorized into three types: rare, frequent, and very frequent fires. The first type is likely to affect a given forest approximately once in a century; the second type occurs once every 20–30 years; and the third type may be as frequent as every 3–5 years. Rare fires provide "natural rotation" of boreal forests. Fires with such a periodicity act as the periodic natural factor that allows existence of stable forest vegetation and relatively high biodiversity of plants in the forest ecosystems of northern Eurasia.

Frequent fires are likely to act as a destructive factor in forest ecosystems. When young stands are destroyed by fire, regeneration is difficult for the absence of seeds.

This may lead to replacement of the forest vegetation by nonarboreal vegetation such as meadow, shrub, or tundra.

Very frequent fires will be less intense, but may function as a factor that favors stability. Very frequent fires do not allow vegetation fuel to accumulate, and therefore, exclude possibility of intense fires.

In the zone of northern open woodlands, forest vegetations are likely to be affected by three major factors: (1) soil temperature regime, (2) soil water regime, and (3) soil fertility (nutrient status). These factors are interdependent and depend also on other factors (Sukachev 1931). There is a complex relationship between the regimes of water and temperature in the soil. A schematic diagram of the complex relationships among the different factors within the permafrost of northern Siberia is shown in Fig. 4.2.

Soil thawing depths are generally less than one meter in the larch forests, except for some peculiar sites, such as stands near streams, near edges of slopes, and on sandy soils. The soil thawing depth is further affected by the thickness of the organic layer covering the ground surface.

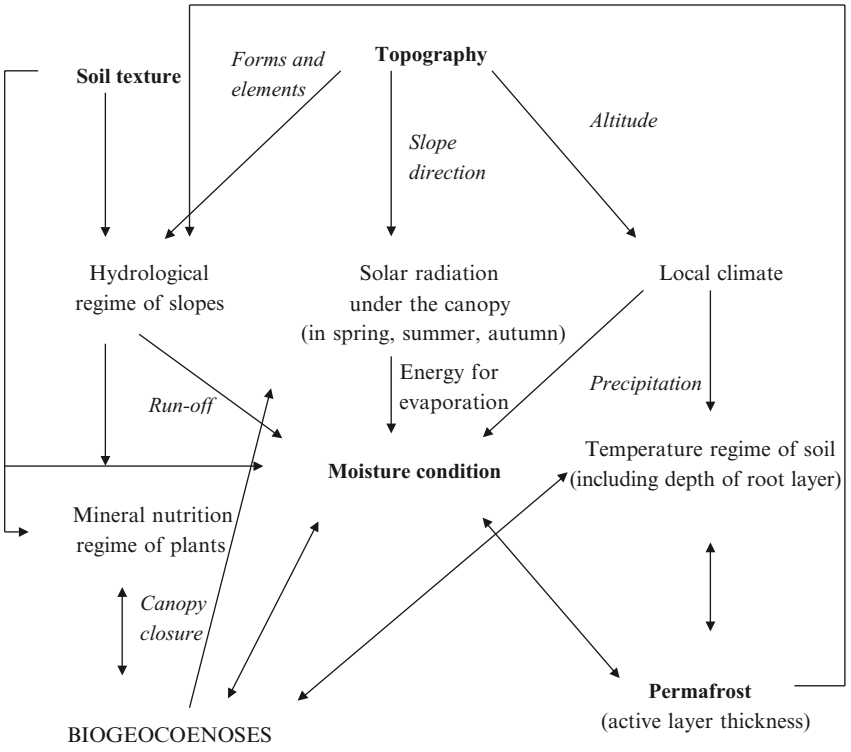

Fig. 4.2 Schematic diagram of the relationship between ecological factors and their influence on the ecosystems in the northern open woodlands of Siberia

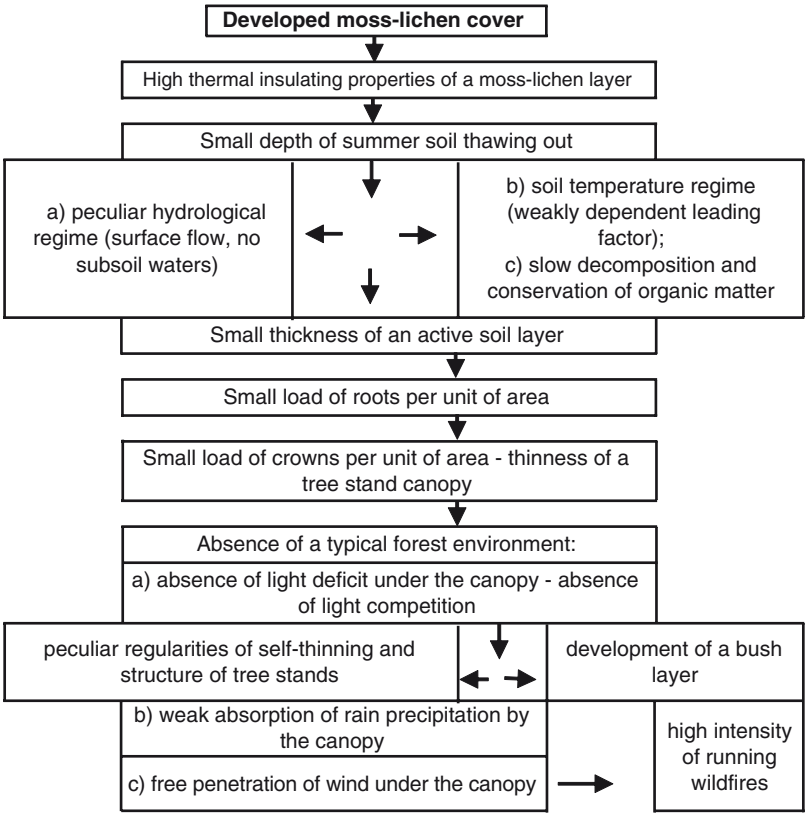

Fig. 4.3 Role of moss-lichen cover in the ecological chain of physical environments, tree growth, and fire disturbance in the larch forest ecosystem of northern Siberia

Temperature regime of the soil is more or less independent of air temperature, since the organic layer functions as a considerable thermal insulator. The organic layer weakens the influence of air temperature on soil temperature: the difference between surface air temperature and soil temperature is large in the summer (Pozdniakov 1986). The summer surface temperature often exceeds 40°C just above the moss-lichen layer with thickness of 15–30 cm on the weakly drained terrace. However, the soils can still be frozen under this cover (Sofronov 1988). This is primarily due to the low heat conductivity of moss-lichen and duff layers, especially under dry condition (Oechel and Van Cleve 1986). Therefore, such organic layer is an important component, affecting many ecological processes in the larch forest ecosystem.

If we consider the moss-lichen layer as the initial component throughout the chain of ecological processes (Fig. 4.3), it will cause both direct and indirect effects on the soil temperature and hydrological regimes (Sofronov and Volokitina 1998). However, details of each process are to be further studied, since many factors are involved interactively. The moss-lichen cover is disturbed by periodical wildfires,

and its function as the thermal insulator varies temporally: the summer soil thawing depths change after fire in response to recovery of the organic layers (Pozdnyakov 1986). If wildfires are absent for a long time, the thickness of the organic layer increases. Then, the soil becomes progressively colder, further slowing organic matter decomposition and contributing to further accumulation of duff. For example, the 100–120 year-old pyrogenic larch stands in the Turukhan basin have an organic layer thickness of 8–10 cm, whereas the stands over 200 years have a layer thickness of 22–27 cm (Sofronov 1988).

According to such recovery of moss-lichen and duff layers, the average depth of soil active layer will be reduced gradually, and growth rate of larch individuals will also decrease greatly (Sofronov 1991a). Thus, to clarify the effects of moss-lichen cover on both the physical environment and tree growth in this forest ecosystem, we need to pay attention to the influence of periodic fire disturbance on every process of the ecological chain shown in Fig. 4.3.

4.8.1 Soil Temperature

Soil temperatures at the depth of 35 cm (T35) varied within each plot, as well as among the four plots on the Kureyka River site (Fig. 4.4). If all data are compared, T35 decreased from 8 to 0°C with the increase of organic layer thickness (OL; being the sum of litter, moss, and duff; lichen was absent here) from 2 to 30 cm. This negative relationship indicates that the moss and duff organic layers play a major role as a thermal insulator, since the amount of litter accumulation in each plot (<0.1 kg m^{-2} in biomass) is much smaller than that of the moss (0.6–1.5 kg m^{-2}; except K1) or duff (0.2–4.1 kg m^{-2}) layers (Table 4.1).

Figure 4.5 compares vertical soil profile and change of soil temperature between the two larch stands in Site 2: II-5 shows the unburned site and II-4 shows the burned site. In both plots, soil temperature decreased sharply within the upper organic layers. However, the thickness of the organic layer was much thinner in burned plot II-4 (only duff, about 5 cm) than in unburned plot II-5 (moss and duff, about 18 cm), and soil temperature just below the organic layer was much higher in II-4 (about 12°C) than in II-5 (about 5°C). Consequently, the soil thawing depth in late summer differed considerably between the two plots, and the potential rooting layer (Rt) above the frozen soil (Pf) was much deeper in the burned plot than in the unburned one (Fig. 4.5). This indicates that ground-fire disturbance improves the thermal condition of the soil for plant growth by eliminating moss and duff covers.

4.8.2 Summer Soil Thawing Depth

A preliminary survey around the Tura settlement (including a site 90 km west) indicated that summer soil thawing depth on a site that burned recently and inside a larch

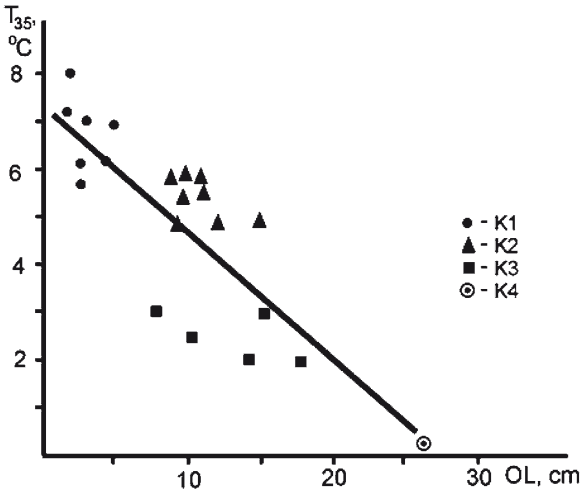

Fig. 4.4 Relationship between depth of organic layer (OL: moss, litter and duff) and soil temperatures (T_{35}: at 35 cm from the surface of moss or litter) in four experimental plots (K1-K4) of the Kureyka River basin site (See Table 4.1). Measurements were made from early to mid-August

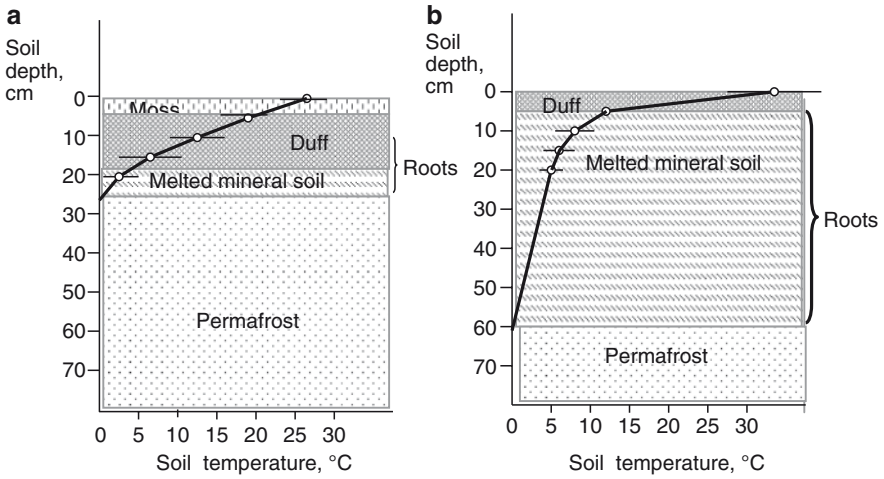

Fig. 4.5 Vertical soil profiles and soil temperatures in the two experimental plots of *L. gmelinii* forests at Site 2 near Tura, (**a**) unburned plot II-5 and (**b**) burned plot II-4 by 1994 surface fire. T: Mean soil temperature with standard deviation (*bars*)

forest was negatively related to the average thickness of the moss and duff layers. However, the thawing depth is also dependent on other factors, such as the slope aspect and earth hummock micro-topography (Sofronov et al. 2000a, 2000b).

Table 4.6 summarizes thickness of each component of the organic layers (here called "prime conductors of burning", PCB) in three larch stands near Tura (P1–P3).

Table 4.6 Coverage area and average thickness of prime fire carriers, total organic layer thickness (TOL), and summer soil thawing depth (STD) in three experimental plots on the site 80 km west of Tura settlement. (after Sofronov et al. 200b)

Plot number	P1	P2	P3
Coverage area (%)			
Lichen[a]	–	–	23
Green mosses[b]	68	74	44
Mixture of mosses and lichen	26	4	30
Litter (α-layer)	2	8	–
Duff[c]			
F-layer	94	–	95
H-layer	86	83	92
Bare ground	4	14	3
Thickness (cm)[d]			
Lichen	–	–	5.3 ± 1.6
Green mosses	5.6 ± 1.4	4.2 ± 1.3	3.5 ± 1.2
Mixture of mosses and lichen	6.6 ± 1.4	3.4±1.6	2.5±1.4
Litter (α-layer)	2.0 ± 0.5	2.0 ± 0.5	–
Duff			
F-layer	7.6 ± 3.1	–	4.6 ± 1.3
H-layer	8.0 ± 4.0	11.3 ± 3.8	10.7 ± 2.4
Average TOL (cm)[e]	21.2 ± 3.8	17.7 ± 3.6	18.8 ± 2.0
Soil thawing depth (STD) (cm)[f]			
In late July (normal condition)	46	39	44
In late July (drought condition)	44	44	50
Correlation of STD with TOL[g]			
Soil thawing depth (normal condition)	−0.22	−0.18	−0.07
Soil thawing depth (drought condition)	−0.19	−0.04	0.44*

[a]*Cladina* species
[b]*Pleurozium schreberi* prevails
[c]Duff was separated into two components: dead moss (F-layer) and decomposed moss (H-layer)
[d]Average and standard deviation for each component of organic layers
[e]Sum of the thickness of each component estimated by multiplying the average thickness by average coverage area (%) within each plot: this is not equal to the sum of absolute values of the average thickness determined separately for each component of organic layers
[f]Soil thawing depth measured under two moisture conditions (normal and dry) in late July; each value shows average of all measurement points along the transect of 40 m long
[g]Simple correlation coefficient of the relationship between TOL (absolute value) and STD using all data at each measurement point; correlation was significant at $p = 0.05$ (*)

Additionally, the results of the correlation analysis between total organic layer thickness (TOL) and soil thawing depth (STD) are shown. In each plot, duff (F- and H-layers) covered the ground surface densely (11–16 cm thick) among the components of organic layers, and TOL reached 20–30 cm. There were no significant relationships between TOL and STD, except for one case in P3 where the STD measured under dry soil condition was positively correlated with TOL ($r = 0.44$, $p < 0.05$).

No clear dependence of STD upon TOL (Table 4.6) may contradict the pattern that soil temperature (T35) generally decreased with increase in organic layer

thickness (Fig. 4.4). However, the present data (P1–P3) were obtained from multipoint measurements along line transects across the earth hummock micro-topography. Namely, the transect included both convex (elevated mounds) and concave (depressed hollows) parts, and the TOL–STD relationship differed largely between these two contrasting micro-topography. Soils on the concave parts were generally colder, and thawed more slowly during the early summer, resulting in much shallower soil thawing depths than that observed in the soils on the convex parts. Thickness of the organic layer may not be of major importance under this situation (e.g., Sofronov et al. 2000a, 2001; Kajimoto et al. 2003). As seen in Fig. 4.6, spatial variation of the thawing depth is considerable. Therefore, multiple measurements are required to determine the average thawing depth. Weak correlation between TOL and STD in each larch stand is likely to reflect the large variation in soil thermal regime due to micro-topography. Further discussion of the interaction between thickness of organic layer and summer thawing depth in relation to micro-topography requires additional data and analysis.

It should be noted that summer soil thawing depth in the permafrost zone depends not only on organic layer thickness, but also on relief (convex or concave relief, slope steepness, and aspect) of the plot. It is known that southern slopes are warmer and northern slopes are colder than horizontal plots. Upper part of slopes and convex elements are better drained. This tends to increase the soil thawing depth. Lower part of slopes and concave elements are likely to be wet. This tends to decrease the soil thawing depth. Tables 4.6 and 4.7 show the impact of a complex of factors on soil thawing depth (Sofronov and Volokitina 1998). It is deep at locations with well-developed hummocky micro-topography (Fig. 4.6c).

It is a well-known fact that the depth of summer thawing of permafrost soils increases in burnt-over areas where the organic layer was partly destroyed by fire

Table 4.7 Mean values of depth of soil thawing and thickness of soil organic layer examined in the study site at the basin of the Degigli River

Plot number[a]	1	2	3	4	5	6	6c	7
Organic layer thickness (cm)	15	16	23	19	7	7	19	12
Soil thawing depth (cm)	49	9	44	50	47	59	30	47
Length of transect (m)	30	30	30	30	300	40	40	40

[a]Notes on plots examined: Plot 1 is *Ledum*-green moss larch stand on the flat eminence; Plot 2 is *Duschekia*-green moss larch stand on the lower part of the southern slope (8°); Plot 3 is shrubmoss larch stand on the river terrace; Plot 4 is-*Ledum*-lichen-green moss larch stand on the convex slope; Plot 5 is 1990 burnt area, the lower position of the northern slope (10–20°); Plot 6 is 1990 burnt area, river terrace; Plot 6c is dwarf shrub-green moss larch forest (control for. 6); and Plot 7 is 1975 burnt area on the river terrace. All plots were located in the basin of the Degigli River (64°N, 98°E). Observation period is July 1991 for plots 1–4, and July 1992 for plots 5, 6, 6c, 7 (after Sofronov and Volokitina 1998; Sofronov et al. 2004)

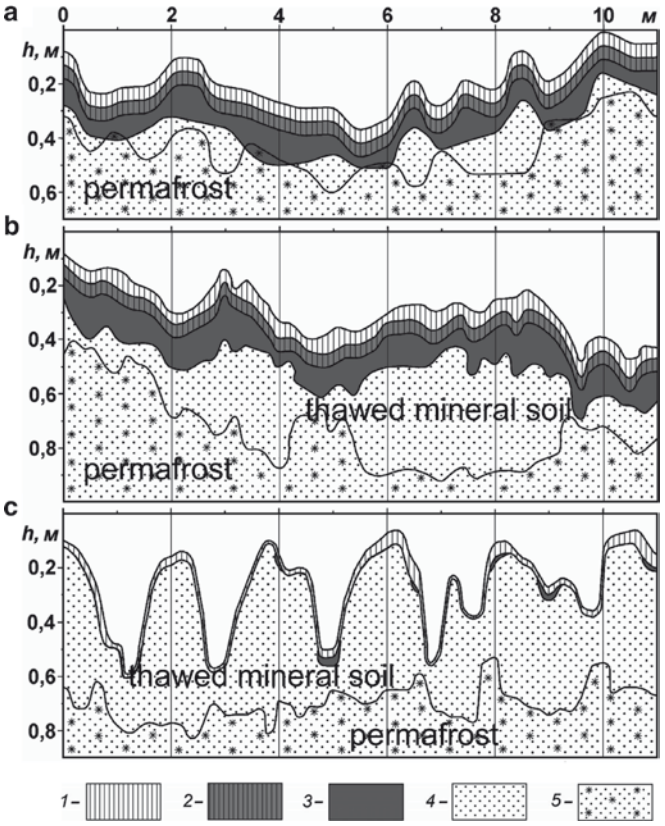

Fig. 4.6 Cross-section of transects with measured thawing depths and thickness of the moss and duff layers. Transects: (**a**) *Ledum*-moss larch forest (unburned plot II-5, Table 4), date of measurements August 3, 1995, (**b**) *Ledum*-lichen-moss larch forest (plot P3, Table 5), date of measurements August 10, 1991, and (**c**) lichen-moss larch forest with hummocky topography on river terrace gently sloping (3°) to the south (about 300 m west of the unburned plot II-5), tree stand: 175-year-old trees with an average height of 8.9 m, 1,120 trees ha^{-1}, date of measurements August 3, 1995 (location see Fig. 1.3, this Vol.). 1 – live part of moss and lichen; 2 – dead part of moss and lichen; 3 – duff; 4 – melted mineral soil; and 5 – permafrost

(Pozdnyakov 1986). For example, according to our field research in a green moss-*Ledum*-larch stand (plot II-5, Table 4.2), the mean thawing depth in early August 1995, measured from the moss surface on a transect of 20 m long, was 25 cm, and the mean thickness of the moss and litter layer was 17 cm. Nearby, in a similar larch stand affected by a creeping surface fire in August 1994 (plot II-4, Table 4.2), the organic layer decreased to 5 cm (i.e., 3.5 times). Due to this, thawing depth increased up to 72 cm (i.e., 3 times) (Sofronov et al. 2000b).

No connection was found between wildfire and "classical" forms of thermokarst (i.e., depressions, lakes). On steep slopes, wildfire often causes the development of a peculiar form of thermokarst – solifluction. When moss and litter are destroyed

by fire, the soil on the slopes is washed off by spring water and/or heavy rain. As a result, permafrost begins to thaw out actively, further intensifies the wash-out, and prevents forest floor and litter layers from developing. In places of active thawing out of large ice lenses, mud streams may develop. Sometimes they are active periodically, throwing out a large mass of material that rushes down as mud flow (Sofronov and Volokitina 1998).

4.8.3 Influence of Fires on Growth of Larch Trees

Larch trees in northern open forests in Siberia are 5–15 m high and have a shallow root system. The running surface fire that usually occurs in early summer can damage or destroy forest stands by crown heating. Therefore, creeping ground fire (with active smouldering of duff) that damages tree roots and causes tree mortality are common during the period of summer drought in July and August. Trees may tip over in case of complete burning of the roots.

In central Evenkia, fire is a major disturbing factor (Abaimov and Sofronov 1996). The average interval of fire events is about 80 years (Sofronov et al. 1998a). According to our reconnaissance along the Nizhnyaya Tunguska and Kochechum Rivers near the Tura settlement, this territory suffered from wildfire intensively early in the twentieth century (Sofronov et al. 1998b). To examine how such fire disturbance influenced the growth of larch trees, we analyzed tree-ring data obtained for some *L. gmelinii* trees growing on an old burnt site near Tura (a tiered canopy unburned plot TB-1; Table 4.2). This larch stand experienced a fire about 90 years ago (in 1910) and contains two age groups of trees (or two different layers) at present. The older trees (180–220 years old) form the upper canopy layer. They escaped the damage of the 1910 fire. The younger trees (80–90 years old) of the lower canopy layer were regenerated mostly after the fire. Tree density, mean tree height, and stem diameter were 700 ha^{-1}, 10.5 m, and 11 cm for the older age group; the values were 4,900 ha^{-1}, 4.5 m, and 4.5 cm for the younger age group, respectively (Table 4.5). For the analysis of individual growth patterns, three larch trees were selected from the older age group, and five trees were chosen from the younger age group. The diameter growth curve of each tree was reconstructed by reading the annual ring-widths on each stem disk sample. Stem disk samples were taken at a height of 1.3 m for the younger trees, while the disk samples were taken at a height of 0.5–1 m for the older trees in order to include the parts with fire scars. On this plot (TB1), the thickness of the organic layer was 15–20 cm (with only moss and duff layers as lichens did not occur at this location) and summer soil thawing soil depth was about 30 cm (Table 4.2). Figure 4.7 shows that growth rates of younger trees (No. 4 and 5) were relatively high during the early growth stage, but decreased gradually in 30–40 years after regeneration. As for two older trees (Nos. 2 and 3; ca. 200 years old), which regenerated before the fire of 1910, their growth rates were also reduced for several decades after the regeneration of each tree. However, growth rates recovered after the depressed stage (i.e., 110–150 years

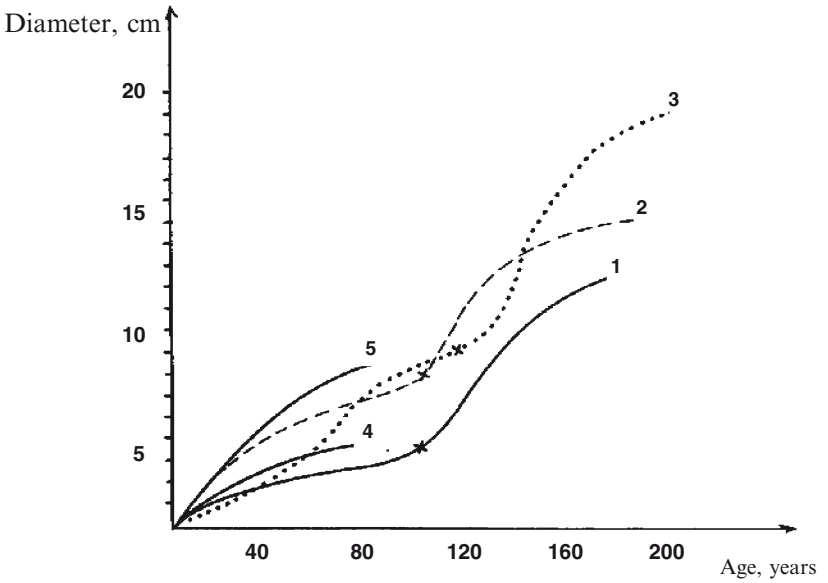

Fig. 4.7 Examples of stem diameter (D) growth curves for the *L. gmelinii* trees of the old burnt plot (TB-1) at Kochechum site near Tura. Three trees (No.1–3) of older age-group regenerated before the surface fire of 1910. Two trees (No.4–5) of younger age-group regenerated after the fire. *Cross mark* (x) in each growth curve of the three older trees (No.1–3) shows the year of 1910 surface fire

after regeneration). This growth recovery ("rejuvenation phenomena") occurred just after the 1910 fire. Likewise, the other older tree (No.1, ca. 220 years old) also showed a growth recovery after the 1910 fire (Fig. 4.7). These patterns suggest that growth activities of the larch trees, if they can escape heavy damage, are often enhanced by ground fire. The postfire growth recovery might be primarily a result of the amelioration of soil-temperature due to burning of the organic layers that act as thermal insulation (Table 4.2). In addition, other effects of fire disturbance, such as nutrient release from the organic layers (Oechel and Van Cleve 1986) and elimination of competitors for the uptake of soil nutrients, may also contribute to the rejuvenation phenomena of the surviving larch trees.

Figure 4.7 also indicates that the older trees can double in size (10–20 cm in diameter) after fire impact compared to the size before the fire (less than 7–8 cm). This supports the results of a previous study (Matveev and Abaimov 1979). They examined growth patterns of seven larch trees (up to 160 years-old) growing on four different sites within the continuous permafrost zone of Siberia, and showed that diameter growth rates after fire were 1.25–1.52 times higher than those before the fire disturbance. Likewise, such a positive effect of fire on individual tree growth was observed among old larch trees (150, 170, and 250 years-old) in central Evenkia (Abaimov et al. 1997; original data from M. Arbatskaya).

According to our data and previous findings, the growth pattern of *L. gmelinii* in central Evenkia (area directly north of Krasnoyarsk region) might be characterized

by two distinct growth stages. The early stage just after fire regeneration has relatively high growth rates (both in diameter and height) and the subsequent stage shows several decades of conspicuous growth reduction (see also Fig.6.5, this Vol.). The beginning of the second growth stage, which depends on the speed of recovery of the moss-lichen and duff layers, could differ somewhat depending on the sites (Sofronov 1988). As for the evergreen taiga in Alaska, it is also known that postfire recovery of moss and lichen layers takes place 25–50 years following fire disturbance, during which time the active layer depth returns to its original level (Viereck 1982; Dyrness et al. 1986).

Our study showed that moss-lichen layers functioned as an important "thermal insulator," and regulates conditions of the summer soil temperature in the larch forest ecosystem of central Evenkia. It also suggested that the insulative function of the moss-lichen cover was eliminated by periodic fire disturbances, which results in enhanced growth rates of the survived larch trees. In terms of forest management in this region, we conclude that prescribed fires may be a way of increasing timber production of individual trees by eliminating the thermal insulator and ameliorating the soil environment, i.e., increasing soil temperature and available soil nutrients. There are, however, some problems that should be taken into consideration before applying the prescribed fire. For example, it is necessary to calculate and/or select optimal conditions for prescribed fire carefully by noting the fact that *L. gmelinii* is a fire-resistant species and extent of fire damage is largely dependent on tree size (Sofronov and Volokitina 1990). Nevertheless, on cold permafrost soils, prescribed burning may achieve effective "thermal amelioration" of the stands with low productivity (Sofronov et al. 2001). The 50–160 year-old larch trees growing on permafrost soils are under growth depression for a long time. They might enter a typical stage of growth rejuvenation by the fire impact, leading to considerable increases in tree size.

4.9 Conclusions

In the northern part of Siberia, larch (*L. gmelinii*) forests develop on permafrost soils with shallow depth of soil thawing in summer. The forests are characterized by thin canopy regardless of tree density. Therefore, light competition that is typical for the other forest biomes is less important and replaced by root competition. Such an ecosystem seems common in the northern open woodlands, with wildfire being an important ecological factor.

The zone of northern open woodlands has the following pyrological features in the Northeasten, Central, and Western Siberia:

- Predominance of fire-susceptible green mosses and lichens on the forest floor.
- Absence of upper sphagnum bogs and limited extent of swamps in the whole territory due to the lack of water in the subsoil in the permafrost.
- Long-term moistening of the moss and duff layers in spring and their subsequent drying during summer droughts.

- Free penetration of the main factors of fire intensity and speed – solar radiation and wind – through thin canopy of tree stands.
- Lightning as the main ignition source due to low population density.
- Low frequency of fire breaks in the territory with moderate relief of mountain and hills, and high frequency of fire breaks in the mountains and in the Western Siberian Plain.
- Many large and intense wildfires occur in some years.
- Wildfire causes tree mortality, but creates favorable conditions for forest regeneration by reducing the thickness of moss and duff layers.
- Reduction in the thickness of moss and duff layers increases the depth of summer soil thawing and temporal effect of "thermal melioration".

In the zone of northern open forests, wildfire creates a traditional ecological function as well: it causes postfire succession and maintains biological biodiversity. It is likely that without fire there would be a progressive cooling of the soil in this region as a result of constant increase of the organic layer. The cooled soil then feeds back to further increase in the organic layer thickness. This process could eventually lead to the development of a treeless tundra biome.

References

Abaimov AP, Prokushkin SG (1999) Alteration of larch stands vital sate in the permafrost zone of Central Siberia under fire influence. In: Fukuda M (ed) Proceedings of the Fourth Symposium on the Joint Siberian Permafrost Studies between Japan and Russia in 1995. Hokkaido University, Sapporo, pp 57–64

Abaimov AP, Sofronov MA (1996) The main trends of post-fire succession in near-tundra forests of Central Siberia. In: Goldammer JG, Furyaev VV (eds) Fire in ecosystems of boreal Eurasia. Kluwer Academic Publishers, Dordrecht, pp 372–286

Abaimov AP, Kanazawa Y, Prokushkin SG, Zyryanova OA (1997) Postfire transformation of larch ecosystem in Siberian permafrost zone. In: Inoue G, Takenaka A (eds) Proceedings of the Fifth Symposium on the joint siberian permafrost studies between Japan and Russia in 1996. National Institute for Environmental Studies, Tsukuba, pp 129–137

Achard F, Eva HD, Mollicone D, Beuchle R (2008) The effect of climate anomalies and human ignition factor on wildfires in Russian boreal forests. Philos Trans R Soc Lond, Ser B 363:2329–2337

Agroclimatic reference book for Kranoyarsk kray and Tuva region (1961) Gidrometeoizdat. Leningrad, p 288 (in Russian)

Archibold OW (1995) Ecology of world vegetation. Chapman and Hall, London, p 510

Dyrness CT, Viereck LA, Van Cleve K (1986) Fire in taiga communities of interior Alaska. In: Van Cleve K, Chapin FS III, Flanagan PW, Viereck LA, Dyrness CT (eds) Forest ecosystems in the Alaskan Taiga. Springer, Berlin Heidelberg New York, pp 74–86

Furyayev VV (1996) Role of fires in forest formation. Novosibirsk, Nauka, p 253 (in Russian)

Goskomstat of the Russian Federation (1993) Forest management in Russian Federation in 1992. Russian State Committee on Statistics, Moscow, p 33 (in Russian)

Kajimoto T, Matsuura Y, Osawa A, Prokushkin AS, Sofronov MA, Abaimov AP (2003) Root system development of *Larix gmelinii* trees by micro-scale conditions of permafrost soils in central Siberia. Plant Soil 255:281–292

Kolesnikov BP (1969) Forestry regions of the USSR taiga zone and systems of forestry for long term forecast. In: Information of scientific counsel on complex using of forest regions. Irkutsk, pp 9–39 (In Russian)

Matveev PM (1992) Fire consequences in larch forest on permafrost zone. Abstract of doctor thesis. Polytechnic Institute, Yoshkar-Ola, p 50 (in Russian)

Matveev PM, Abaimov AP (1979) On the estimation of the role of fire in larch stands on permafrost soils. In: Proceedings of First All-Union Science-Technical Meeting, Combustion and fire in the forest, part III: Forest fires and their effects. Sukachev Institute of Forest and Wood, Krasnoyarsk, pp 123–130 (in Russian)

Matveev PM, Usoltsev VA (1991) Post-fire tree mortality and larch regeneration on permafrost soil. Soviet J Ecol 4:3–15 (in Russian)

Mollicone D, Eva HD, Achard F (2006) Human impact on 'wild' fires in boreal Eurasian forests. Nature 440:436–437

Nazimova DI (1996) Sectoral and zonal classes of forest cover in Siberia and Eurasia as a basis of clarifying landscape pyrological characteristics. In: Goldammer JG, Furyaev VV (eds) Fire in ecosystems of boreal Eurasia. Kluwer Academic Publishers, Dordrecht, pp 253–259

Oechel WG, Van Cleve K (1986) The role of bryophytes in nutrient cycling in the Taiga. In: Van Cleve K, Chapin FS III, Flanagan PW, Viereck LA, Dyrness CT (eds) Forest ecosystems in the Alaskan taiga. Springer, Berlin Heidelberg New York, pp 121–137

ParmuzinYP (1979) Tundra-forest zone of the USSR. Misl Press, Moscow, p 396 (in Russian)

Pozdniakov LK (1986) Permafrost forestry. Nauka, Novosibirsk, p 192 (in Russian)

Shumilova LV (1962) Botanical geography of Siberia. Tomsk State Univ, Tomsk, p 440 (in Russian)

Sofronov MA (1988) Pyrological characteristic of vegetation in the upper part of the river Turukhan basin. In: Forest fires and their fighting. VNIILM, Moscow, pp 106–116 (in Russian)

Sofronov MA (1991a) Forest forming process on cold soils and its relation with fires. In: Ecological and geographical problems of protection and restoration of northern forests. Abstracts of the All-Union Conference, Arkhangelsk, pp 169–171 (in Russian)

Sofronov, MA (1991b) Pyrological characteristic of forest in the south-east of Taimyr. In: Forest fire and their fighting. VNIILM, Krasnoyarsk, pp 205–211 (in Russian)

Sofronov MA, Abaimov AP (1991) The forest forming process peculiar features on the frozen soils. In: The theory on the forest forming process. Abstracts of the All-Union Conference. Arkhangelsk, pp 154–155 (in Russian)

Sofronov MA, Volokitina AV (1990) Pyrological zoning in taiga. Novosibirsk, Nauka, p 205 (in Russian)

Sofronov MA, Volokitina AV (1996a) Vegetation fires in the zone of northern thin forests. Siberian J Ecol 1:43–50

Sofronov MA, Volokitina AV (1996b) The role of fires in forest restoration of cutting down areas in the North of Central Siberia. Lesnoye Khozyaystvo 6:50–51 (in Russian)

Sofronov MA, Volokitina AV (1998) On ecological peculiarities of the northern open forests zone in Central Siberia. Siberian J Ecol 3–4:245–250 (in Russian)

Sofronov MA, Volokitina AV, Shvidenko AZ (1998a) Wildland fires in the north of Central Siberia. Commonwealth Forestry Rev 77:124–127

Sofronov MA, Volokitina AV, Shvidenko AZ, Kajimoto T (1998b) On area burnt by Wildland fires in the northern part of Central Siberia. In: Mori S, Kanazawa Y, Matsuura Y, Inoue G (eds) Proceedings of the Sixth Symposium on the Joint Siberian Permafrost Studies between Japan and Russia in 1997. Tsukuba, pp 139–146

Sofronov MA, Volokitina AV, Kajimoto T (2000a) Ecology of wildland fires and permafrost: their interdependence in the northern part of Siberia. In: Inoue G, Takenaka A (eds) Proceedings of the Eighth Symposium on the Joint Siberian Permafrost Studies between Japan and Russia in 1999. National Institute for Environmental Studies, Tsukuba, pp 211–218

Sofronov MA, Volokitina AV, Kajimoto T, Matsuura Y, Uemura S (2000b) Zonal peculiarities of forest vegetation controlled by fires in northern Siberia. Eurasian J Res 1:51–57

Sofronov MA, Volokitina AV, Kajimoto T (2001) On the possibility of "thermal melioration" of larch forests in the northern part of Siberia. In: Fukuda M, Kovayashi Y (eds) Proceedings of the Ninth Symposium on the Joint Siberian Permafrost Studies between Japan and Russia in 2000. Hokkaido University, Sapporo, pp 10–17

Sofronov MA, Volokitina AV, Kajimoto T, Uemura S (2004) The Ecological role of moss-lichen cover and thermal amelioration of larch forest ecosystems in the northern part of Siberia. Eurasian J Res 7:11–19

Stepanov GM (1985) Forest forming on post fire areas in the northern taiga of Yakutia. Abstract of PhD thesis. Sukachev Institute of Forest and Wood, Siberian Department Academic Science, USSR, Krasnoyarsk, p 17 (in Russian)

Sukachev VN (1931) Guidance for the forest types investigations. State Press of Agriculturel Literature, Moscow- Leningrad, p 328 (in Russian)

Tsvetkov PA (1994) On height of smoked part of trees after fires in larch forests of Evenkia. Lesovedenie 4:90–93 (in Russian)

Tsvetkov PA (1998) Pyrological characteristic of larch forests of Evenkia. Lesnoye Khozyaystvo 6:45–46 (in Russian)

Tsykalov AG. (1987) Fire dander of larch forests of Central Evenkia in correlation with load of surface forest fuel. In: Forest fire and their fighting. VNIILM, Moscow, pp 226–238 (in Russian)

Tsykalov AG (1991) The nature of fires in forests on permafrost zone of Central Evenkia. PhD Thesis, Institute Forest and Wood, Siberian Department Academic Science, Krasnoyarsk, p 26 (in Russian)

Viereck LA (1982) Effects of fire and firelines on active layer thickness and soil temperature in interior Alaska. In: French HM (ed) Proceedings of the Fourth Canadian Permafrost Conference. NRC, Ottawa, pp 123–135

Zakharov VK (1967) Forest inventory. Moscow, p 406 (in Russian)

Chapter 5
Recovery of Forest Vegetation After Fire Disturbance

O.A. Zyryanova, A.P. Abaimov, T.N. Bugaenko, and N.N. Bugaenko

5.1 Introduction

Fire is the dominant form of disturbance in boreal forests (Wein and MacLean 1983; Van Cleve et al. 1986; Payette 1992; Rees and Juday 2002). In the Siberian cryolithic zone, ground fires are predominant among the disturbance factors; about 1.5% of the total forested area is damaged annually by wild fires (Sofronov et al. 1998). Fire frequency of northern taiga forests varies between once every 20–200 years, with a mean frequency at about once every 80 years (Sofronov and Volokitina 1996; Abaimov et al. 2000). Understanding patterns of development in forest associations is important, because the fires not only transform forest environment such as microclimate condition, temperature and moisture of upper soil layers, and chemical properties of the soils, but also change cycling of mineral nutrients, soil respiration rate, species composition and other biological characteristics of the ecosystem (Schulze et al. 1995; Abaimov et al. 1996, 1997b, 1998; Matsuura and Abaimov 1998; Bourgeau-Chavez et al. 2000; Prokushkin et al. 2000; Shvidenko and Nilsson 2000; Zyryanova et al. 2002, 2004, 2006, 2007). Under extreme climatic conditions, fires can dramatically change directions of development in forest formation and the rate of progressive succession (Abaimov et al. 2000; Abaimov 2005).

The vegetation development following ground fires varies depending on the intensity and history of disturbance, dispersal and germination traits of regenerating species, specific site characteristics, and microtopography. Permafrost and dynamic processes of annual freeze–thaw cycles result in various surface features. Most common are the earth hummock topography and sorted and nonsorted stripes (Bliss 2000; Ershov 2004). The earth hummocks may be 10–50 cm in height and 1–2 m in diameter. Such hummocks occur at level ground or at gentle slopes (1–3°) (Fig. 5.1a; see also Chap. 16, this Vol.). Elongated stripes are common on slopes >3–5° (Fig. 5.1b). The distance between the stripes may vary from 1 m up to 10 m.

Cryogenic microtopography of boreal forests is responsible for patterned hydrothermal and edaphic conditions of forest habitats, as well as for distribution of plants, spatial differentiation of ground vegetation, and its postfire changes in northernmost Siberia (Shcherbakov 1979; Abaimov et al. 1996, 1997a, b, 1998;

A. Osawa et al. (eds.), *Permafrost Ecosystems: Siberian Larch Forests*,
Ecological Studies, Vol. 209, DOI 10.1007/978-1-4020-9693-8_5,

Fig. 5.1 Forest sites with microtopography. (**a**) *Larix gmelinii – Vaccinium vitis-idaea* + *Vaccinium uliginosum – Hylocomium splendens* + *Pleurozium schreberi* + *Peltigera* spp. + *Cladina* spp. association (spot hummock-depression microrelief). (**b**) *Larix gmelinii – Ledum palustre* + *Vaccinium uliginosum – Aulacomnium turgidum* + *Pleurozium schreberi* association (elongated stripe-depression microrelief) (Photo: O. Zyryanova)

Prokushkin et al. 2000; Zyryanova 2004; Zyryanova et al. 2002, 2007). In this chapter we synthesize the results of previous studies and unpublished data, and discuss influence of microtopographical conditions (microrelief) on recovery of forest vegetation after fire disturbances.

5.2 Approaches to Study Vegetation Recovery

We have investigated associations of *Larix gmelinii* (Rupr.) Rupr. and plant communities developing after major fires in *L. gmelinii*-dominated forests at Tura Experimental Forest, Central Siberia (Table 5.1; see also Fig. 1.3). A series of chronosequence plots were used for estimating the patterns of vegetation development that would occur over some 90 years.

Plant species diversity (the number of species) was determined in sample plots of 100 m^2 in old larch associations and in recently burned areas. Six plots were established in stands developing after forest fires. Plots 1 and 2 were in areas burned in 1994: the former was in Site 2 and the latter was at ca. 30 km east-southeast of Tura along the Nizhnyaya Tunguska River. Plot 3 was located at ca. 50 km north of Tura, and along the Tembenchi River. Plots 4 and 5 were at Site 1 and Site 3 near Tura, respectively. Plot 6 was on the left bank of the Kochechum River at a few kilometers north of Tura. See Fig. 1.3 (Chap. 1) for locations of these study stands, except for plot 3.

Vegetation was described by noting vascular plants, mosses, and lichens, including description of species abundance (percentage cover). Specific similarity (i.e., similarity of floristic composition) between different stages of progressive succession has been compared with Stogren–Radulescu coefficient ρ_{sr} (Schmidt 1984; Degteva 2005).

Table 5.1 Characteristics of the permanent plots used for description of structure in plant associations

Number of plot	Plant association, its geographical location and topography	Year and fire intensity
Sites with complex microtopography		
1	*Larix gmelinii* – *Vaccinium vitis-idaea* + *Vaccinium uliginosum* – green mosses+lichens 64° 19′ N 100° 13′ E Surface of structural step of east-facing slope of plateau, of 1–3° steepness, spot hummock-depression microrelief	1994 Steady ground, middle
2	*Larix gmelinii* – *Duschekia fruticosa–Ledum palustre* + *Vaccinium uliginosum* – lichens+green mosses 64° 10′ N 100°44′ E North-facing slope of plateau, of 10° steepness, elongated stripe-depression microrelief	1994 Running ground
3	*Larix gmelinii* – *Betula nana*+*Salix* sp. – *Ledum palustre* + *Vaccinium uliginosum* – lichens+green mosses 64° 48′ N 99°29′ E Down part of south-eastern-facing slope of plateau, of 1–2° steepness, small hillocky microrelief	1990 Strong running ground
Sites without microtopography		
4	*Larix gmelinii* – *Duschekia fruticosa*–*Ledum palustre* +*Vaccinium vitis-idaea* – green mosses 64° 19′ N 100° 14′ E Upper part of west-facing slope of plateau, of 7–9° steepness	1990 Strong running ground
5	*Larix gmelinii* – *Duschekia fruticosa*–*Ledum palustre* +*Vaccinium vitis-idaea* – green mosses 64° 23′ N 100° 12′ E Middle part of east-facing slope of plateau, of 10–12° steepness	1978 Strong running ground
6	*Larix gmelinii* – *Duschekia fruticosa*–*Ledum palustre* +*Vaccinium vitis-idaea* – green mosses 64° 18′ N 100° 14′ E Middle part of west-facing slope of plateau, of 8–10° steepness	1950 Strong running ground after winter selective cutting

To detect the key points and define key plant associations of the postfire forest regeneration, we compared the patterns of experimental species distribution (used in the sense of "observed" distribution throughout this chapter) with standard geometric series and MacArthur models by calculating Shannon's diversity index for each community at a given time (Zyryanova et al. 2004, 2006; see Chap. 2). Also see definitions of the models applied for description of the same approach (Whittaker 1975; Magurran 1988).

Nomenclature of Latin names for plant species follows Czerepanov (1985).

5.3 Patterns of Vegetation Development After Fire

5.3.1 Sites with Complex Microtopography

Conditions of various microtopography result in different burning characteristics during forest fires, and consequently affect the restoration of larch trees and ground vegetation. Under conditions of microrelief characterized by the spot hummock-depressions (meaning hummock-trough topography of small scale as in spots) (plot 1; Table 5.1), a steady ground fire of medium intensity destroyed, first of all, vegetation of the microdepressions. This was caused by a large amount of organic matter accumulated at the bottom of the depressions, which acted as fuel for burning. Dominance of such plants as *Ledum palustre* and *Vaccinium uliginosum* is also responsible for the extensive burning, because these are some of the most fire-prone species in the cryolithic zone (Kurbatski 1970; Shcherbakov 1979). Here, the height difference between the top of the hummock and the bottom of the depression is about 40–50 cm.

The vegetation at the top of the hummocks was preserved in part at least 1 year after the fire, until microtopography began to change: experimental (= observed) distribution is more similar to the geometric series model than to the model of MacArthur (Fig. 5.2). Total number of species decreased 2.5-fold as compared to that of unburned association (Fig. 5.3).

During the following 2 years, soil thermal melioration begins to destroy the microrelief of the site. Also, hydrological and thermal regimes change considerably (Abaimov et al. 2001). By the fourth year after the fire, ground vegetation develops into a secondary grass-moss association dominated by *Calamagrostis lapponica*, *Chamaerion angustifolium*, *Marchantia polymorpha,* and *Ceratodon purpureus* (Zyryanova et al. 2002, 2008). The coincidence of Shannon's indices for experimental and geometric series distributions (Fig. 5.2) suggested that the plant community was formed as a result of interspecific competition (Zyryanova et al. 2002; Zyryanova 2004; see also Whittaker 1975).

Young larch trees were abundant in the burned area: the number of seedlings amounted to 558.5 thousand per hectare (Abaimov et al. 2000). Within 3 years after fire, the number of vascular plants in the burned area became 83% of that of a mature plant community. Plant species composition of the ground vegetation nearly recovered to the prefire level of plant diversity at the fifth year after fire. The total number of species was 1.2–1.3 times larger than that of the unburned association by the eighth and ninth year after fire (Fig. 5.3). Similarity coefficient $\rho_{sr} = -0.08$ detected this pattern owing to the restored prefire species such as *Duschekia fruticosa*, *Empetrum nigrum*, *Juniperus sibirica*, *Tomenthypnum nitens*, etc. (Zyryanova et al. 2002, 2007). New species (*Atragene sibirica*, *Galium boreale*, *Potentilla inquinans*, etc.) also invaded free ecological niches: nonuniformity of experimental distribution was still significant during this period (Fig. 5.2). In 11 years after fire, the larch regrowth formed dense groups of 45% cover. *Arctous erythrocarpa* and *Vaccinium vitis-idaea* restored their dominating positions among dwarf-shrubs,

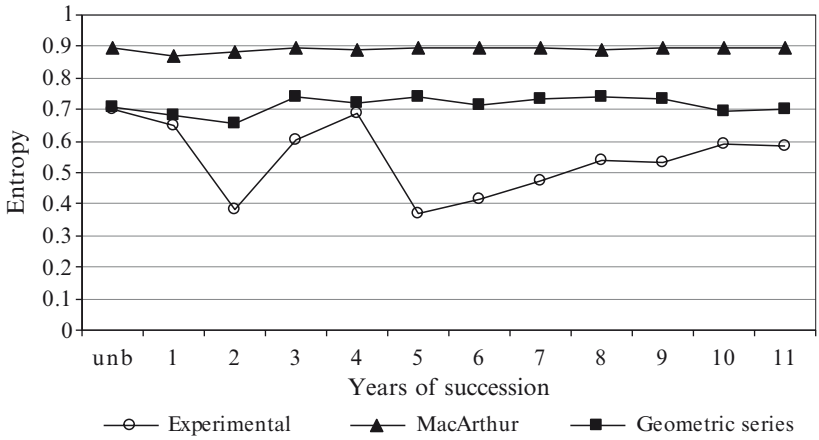

Fig. 5.2 Values of the diversity index expressed as entropy in MacArthur, geometric series, and experimental (= observed) distributions. The diversity indices are scaled with their maximum values for mature larch (unburned) and postfire plant associations at a forest site with spot hummock-depression microtopography (plot 1)

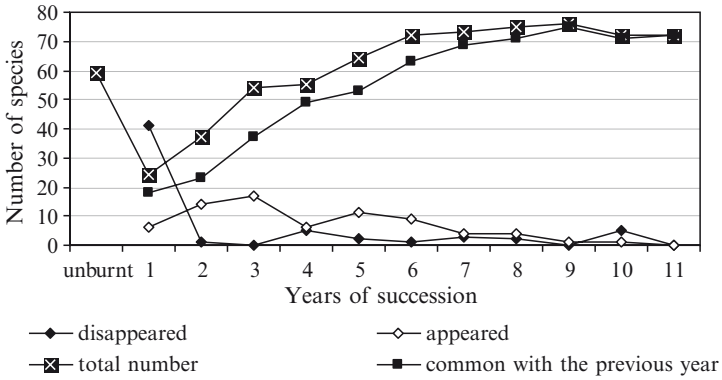

Fig. 5.3 Plant species dynamics at the initial stages of the postfire progressive succession in the forest site with spot hummock-depression microtopography. Total number of species, numbers of disappeared and appeared, as well as common species in relation to the plants of the previous year are shown for each year

while *Ceratodon purpureus*, *Aulacomnium turgidum,* and *Polytrichum uniperinum* dominated the moss cover. Thus, invasion of new species at the sites with spot hummock-depression microtopography lasted for 9 years after steady ground fire of medium intensity. Later on, total number of species showed a tendency of gradual decrease (Fig. 5.3).

Elongated stripe-depression microrelief (plot 2 Tunguska; Table 5.1) produces striped patterns of burning and subsequent regeneration in the ground vegetation (Zyryanova et al. 2002, 2007). Four years after a running ground fire, all main

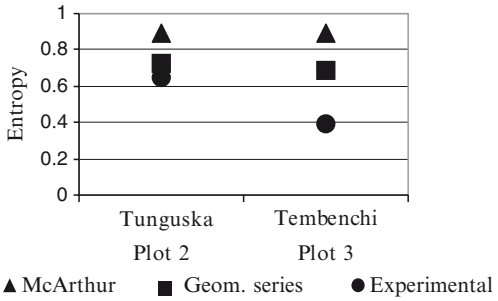

Fig. 5.4 Values of the diversity index expressed as entropy in MacArthur, geometric series, and experimental (= observed) distributions. The diversity indices are scaled with their maximum values for postfire plant associations at a forest site with elongated stripe-depression microtopography (plot 2) in 4 years after fire, and at a forest site with small hillocky microtopography (plot 3) in 8 years after the fire

dominant species (*Vaccinium uliginosum*, *Ledum palustre*, *Hylocomium splendens*) of the understory and ground vegetation were restored from the preserved refugia of these species along the linear depressions. At this year, the experimental distribution was more similar to the geometric series model (Tunguska; Fig. 5.4), suggesting that the species present in the depressions were not damaged by the fire. In contrast, the stripes, convex parts of the ecosystem, were strongly damaged by the running fire and covered by the patches of *Vaccinium vitis-idaea*, *Equisetum scirpoides*, *Rubus arcticus*, *Dryopteris fragrans*, etc. The restoration of the ground floor was not uniform and its rate was rather low.

On the other hand, small hillocky microrelief (the difference between the top of the hillock and the bottom of the depression was about 15–20 cm, plot 3 Tembenchi; Table 5.1) led to total destruction of the ground vegetation by strong running fires, while larch trees were only weakly damaged (Zyryanova et al. 2002, 2007). Eight years after the fire, *Ceratodon purpureus*, fire specialist species typical of the cryolithic area, occupied about 80% of the burned area and prevented both successful restoration of prefire plant species and invasion of the new species. Only *Vaccinium vitis-idaea*, *Vaccinium uliginosum,* and *Ledum palustre* began their regeneration near the bases of larch stems probably from the survived rhizomes. Plant community has not developed fully at this site, since experimental and geometric series distributions differed considerably (plot 3 Tembenchi; Fig. 5.4). Thus, small hillocky microtopography is responsible for rather uniform burning of ground vegetation and slackening of its subsequent restoration.

5.3.2 Sites Without Microtopography

We investigated successional sequence of the forest association designated as *Larix gmelinii – Duschekia fruticosa – Ledum palustre* + *Vaccinium vitis-idaea* – green

mosses after a strong running ground fire at three sites where microtopography was not well developed (plots 4–6; Table 5.1). Being typical for the cryolithic area, the old *Larix* forest occupied the upland sites and was considered to be the vegetation composed of a late successional fire species in the region (Abaimov et al. 1997b, 2002). Vegetation of plot 4 was described annually since the time of the fire in 1990, whereas plots 5 and 6 were found as separate stages of the chronosequence at different sites (Table 5.1). All chosen sites were completely destroyed by the running forest fire.

Total number of species in a community decreased 1.4-fold 1 year after the fire, as was shown in the flora of the unburned association (Fig. 5.5). The representatives of such families as Salicaceae, Valerianaceae, Caryophillaceae, Saxifragaceae, Pyrolaceae, and Empetraceae disappeared after the fire, while species of Apiaceae, Fumariaceae, and Onagraceae families newly appeared in the burned area (Zyryanova et al. 2004, 2006). Nontypical of prefire, larch community (composed of *Corydalis sibirica*, *Chrysosplenium alternifolium*, *Erigeron silenifolius*, *Androsace septentrionalis,* and other species) appeared at different postfire years. The process of invasion by new plant species prevailed for 9 years after fire, then the number of invading species decreased (Fig. 5.5). Maximum total number of species in the burned site was 1.2 times greater than that in unburned association 9 years after fire. This pattern resulted from the cyclic development of such sod-forming species as *Calamagrostis lapponica* and *Carex media* and coincided with the period when they lost their positions as strong competitors and dominants. The new plant species (*Achillea asiatica*, *Chamaerion angustifolium*, *Urtica dioica*, *Ribes rubrum*, etc.) occupied the newly released ecological niches and became abundant. Since the sixth year after fire, young larch seedlings established a dense layer of regrowth, completing this process by the 11th–12th year (Abaimov et al. 2001). Shrub cover of alder and willow (primarily *Duschekia fruticosa* and a number

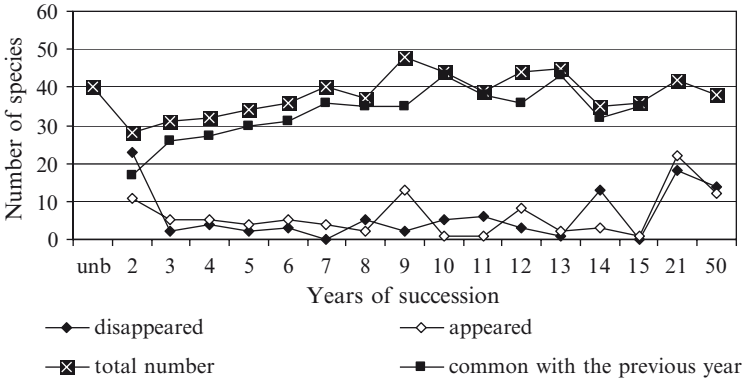

Fig. 5.5 Plant species dynamics at different stages of the postfire progressive succession in the forest site without microtopography. The total number of species, disappeared and appeared plants are shown for each year. The plants which are common to two subsequent years are shown for the early (2–15 years) succession

of *Salix* spp., but *Salix phylicifolia* being the most abundant) may reach dominance of nearly 60%.

In 21 years after a running ground fire, total number of species on the burned area still exceeded that of the prefire community (Fig. 5.5). The species composition was also different: 22 of 42 plants were invaded species (Zyryanova et al. 2004, 2006). But the main layers – the trees, the shrubs, the dwarf-shrubs, and the lichen-mosses – of the vegetative groups were similar to those in the unburned larch forest. The dominants in these layers were the restored plants that were formerly abundant in the stand before the fire (*Larix gmelinii*, *Duschekia fruticosa*, *Vaccinium uliginosum*) accompanied by postfire species of *Betula pendula*, *Salix* sp., *Chamaerion angustifolium*, and *Rubus sachalinensis*.

In 50 years after a fire, the subdominant postfire species disappeared from the species composition of the ground layer. Typical intact dominants kept their positions, but they established more dense layers than in the prefire community. For example, the extent of canopy closure of *Larix gmelinii* and *Duschekia fruticosa* was equal to 40 and 35%, respectively, in the secondary community; whereas 15 and 25% in the intact forest, respectively. The total number of species (38) almost reached the total number before the fire (39) (Fig. 5.5), but the species composition was still different: similarity coefficient (ρ_{sr}) was −0.20 (Zyryanova et al. 2006). Thus, even in a 50-year-old postfire ecosystem, the total number of plant species and their composition differed from those in a prefire larch association, though the forest layers and the dominant species of the community were the same. The spatial structure (vertical and horizontal) of the prefire larch community has been restored within 50 years after a strong running ground fire in the cryolithic area of Siberia. However, species richness and floristic composition of such a community tend to be different from the original forest before the fire. This appears to be a general pattern. Similar results were obtained for tropical forests of central Amazonia (Ferreira and Prance 1999).

Final restoration of the original species diversity and the floristic composition (assumed equal to vegetation of the unburned forest of ca. 90 years old) occurred in the period sometime between 50 and 90 years after the fire (Fig. 5.5). Larch crown and shrub canopies have markedly declined during this time, whereas cover of the ground species has become similar to that of prefire community. As was reported previously (Zyryanova et al. 2002, 2004, 2006, 2007), 90- to 100-year-old larch associations in Siberian cryolithic area represent the ultimate structure of a plant community: the most stable, self-maintaining, and self-reproducing state of vegetational development. Plant species within this community are coadapted to their physical and temporal environment: they may be described as being niche differentiated owing to interspecific competition (Zyryanova et al. 2002).

Postfire dynamics of the species composition was also analyzed with Shannon's diversity index; the index was calculated for the experimental species distribution as well as for the standard geometric series and MacArthur models (Fig. 5.6). Geometric series distribution was established to be a criterion of the community structure development of the larch forest examined. The points where experimental species distribution coincided with the standard geometric series were considered

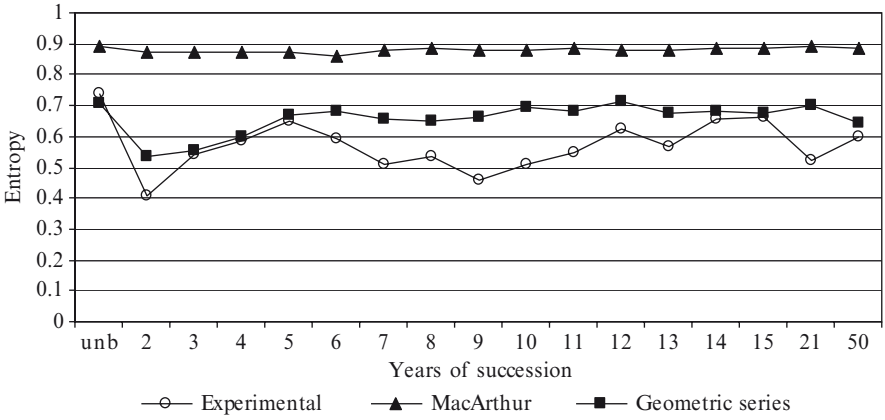

Fig. 5.6 Values of the diversity index expressed as entropy in MacArthur, geometric series, and experimental (=observed) distributions. The diversity indices are scaled with their maximum values for mature larch (unburned) and postfire plant associations at a forest site without microtopography (plots 4–6)

to define secondary plant associations – the key points of the postfire succession. Thus, nine successional stages were distinguished in the long-term process of the forest restoration (Table 5.2). Following a fire, intervening few weeks may be recognized when no live vegetation is present. A similar condition continues to the next year, which is together recognized as stage I (1 year after fire). Here, *Marchantia polymorpha* quickly invades the areas where mineral soil has been exposed by fire. This liverwort and *Corydalis sibirica* develop in stage II (2 years after fire). This annual plant apparently has viable seeds buried in the soil that were stimulated to germinate by fire. Light seeded species such as *Chamaerion angustifolium* (fireweed) is also the usual first invader at this stage. The next three stages in the developing vegetation are dominated by *Calamagrostis lapponica*, which resprouts from the rhizomes. All herbal stages (II–V; 2–5 years) do not form dense soddy mat, and larch seedlings and saplings may be abundant at this time. In about 13 years after fire (stage VI), *Duschekia fruticosa* (alder) with a component of *Salix phylicifolia* (willow) form open shrub cover of as much as 50%. The heavy shrub and seedling canopy greatly reduces the herbaceous strata: its cover drops to less than 7%. Some species of the mature larch forest such as *Vaccinium vitis-idaea* and mosses (*Aulacomnium turgidum* and *Pleurozium schreberi*) become scattered on the mounds. In 14–21 years after fire (stage VII), the main layers of the mature larch association are restored, and *Larix gmelinii*, with a component of birch trees, becomes dominant in the tree canopy. The shrubs form dense layer, while dwarf-shrubs develop a scattered layer. As the stand becomes older, birch trees become less abundant (stage VIII; 22–50 years). Alder is the common shrub; *Ledum palustre* and *Vaccinium vitis-idaea* are the most common dwarf-shrubs at this stage. A dense and thick layer of feathermosses such as *Pleurozium schreberi*,

Table 5.2 Stages of postfire progressive succession in cryolithic area of Central Siberia

Stage	Years after fire	Characteristic vegetation
I	1	Bare surface with separate *Marchantia polymorpha* patches
II	2	Herb-moss species groups with *Calamagrostis lapponica, Corydalis sibirica* and *Marchantia polymorpha* dominants
III	3	*Calamagrostis lapponica - Ceratodon purpureus + Marchantia polymorpha* association
IV	4	*Carex media + Calamagrostis lapponica - Marchantia polymorpha + Ceratodon purpureus* association
V	5	*Carex media + Calamagrostis lapponica − Ceratodon purpureus* association
VI	6–13	Herb-moss association disappeared. *Larix gmelinii, Duschekia fruticosa* and *Vaccinium vitis-idaea* became more widespread and abundant and developed open storeys
VII	14–21	*Betula pendula + Larix gmelinii + Salix phylicifolia + Duschekia fruticosa − Vaccinium vitis-idaea − Pleurozium schreberi + Ceratodon purpureus* association become established. The trees, shrubs, dwarf-shrubs, lichens, and mosses developed closed storeys with prefire and postfire species subdominated. Birch and larch trees overtop the shrubs
VIII	22–50	Prefire dominants (except birch species) become common in the storeys. *Betula pendula + Larix gmelinii - Duschekia fruticosa − Ledum palustre + Vaccinium vitis-idaea - Pleurozium schreberi + Hylocomium splendens + Aulacomnium turgidum* association become established
IX	50–90	Final restoration of prefire plant species composition and cover percentage of the species

Table 5.3 Dominant species of mature larch association and postfire association at the early stages of succession in cryolithic area of Central Siberia

Mature larch association	Postfire associations
Larix gmelinii	
Duschekia fruticosa	*Corydalis sibirica*
Ledum palustre	*Chamaerion angustifolium*
Vaccinium uliginosum, V. vitis-idaea	*Calamagrostis lapponica*
Empetrum nigrum	*Carex media*
Aulacomnium turgidum	*Marchantia polymorpha*
Cladina sylvatica, C. amaurocraea	*Ceratodon purpureus*
C. alpestris, C. rangiferina	*Leptobryum pyriforme*
Cetraria cucullata, C. islandica	

Hylocomium splendens, and *Aulacomnium turgidum* develops by 50 years after fire. Final restoration of the prefire plant species composition and the cover percentage of the species is completed during the period from 50 to 90 years (stage IX). Mature larch forest with a continuous lichen-moss mat develops in about 90–100 years following a ground fire. This is the ninth, and final, stage of the progressive succession (Table 5.3).

5.4 Conclusions

- Ground fires in the cryolithic area of Siberia (i.e., Central Siberia) change floristic diversity of larch associations drastically. In 3–4 years after the fire, the number of vascular plants in a burned area becomes 1.2–1.3 times greater than that of the unburned associations. Both restoration of the prefire species and invasion of the new ones are responsible for such increase in species number. Dominant species of the prefire larch association and subsequent postfire associations are different, particularly during the early successional stages.
- At the early successional stage, mosses are 1.5–3 times less in species number than in the prefire larch association. Feathermosses *Tomenthypnum nitens*, *Dicranum congestum,* and *Aulacomnium palustre* typically begin their restoration, and *Pleurozium schreberi*, *Aulacomnium turgidum,* and *Polytrichum commune* increase their cover drastically, as the canopy of larch seedlings closes in 12–13 years after fire. Species composition in mosses is usually restored by 50 years after a strong ground fire.
- The lichens seem to be much more damaged by fire than the mosses. The number of lichens is two to five times less after fire. Species composition in lichens is restored only in 90 years after fire.
- Generally, the total number of species is 1.1–1.2 times more in sites with and without microrelief than in the unburned association in 9 years after fire. The spot hummock-depression provides faster regeneration of plant species diversity and structure of forest association after ground fires, while small hillocky and elongated stripe-depression microrelief usually delay this process. At the early successional stages, microtopography in northern larch forests sustains plant diversity and increases the number of species and families (Fig. 5.7).

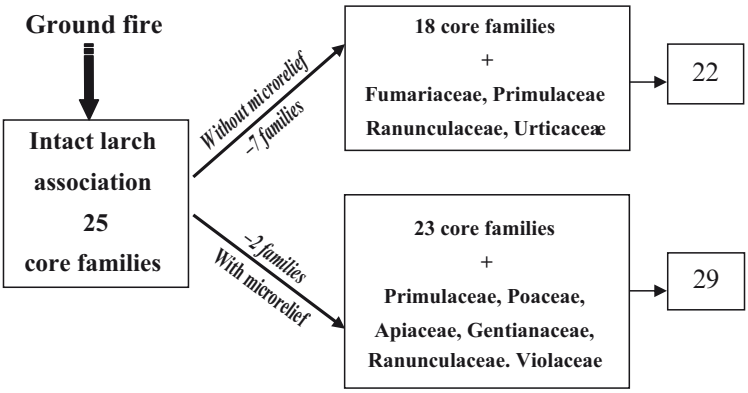

Fig. 5.7 The changes in the composition of vascular plant families at the initial stages of postfire progressive succession. After ground running fires, number of families markedly increased in sites with microtopography than in sites without it (29 vs. 22, respectively)

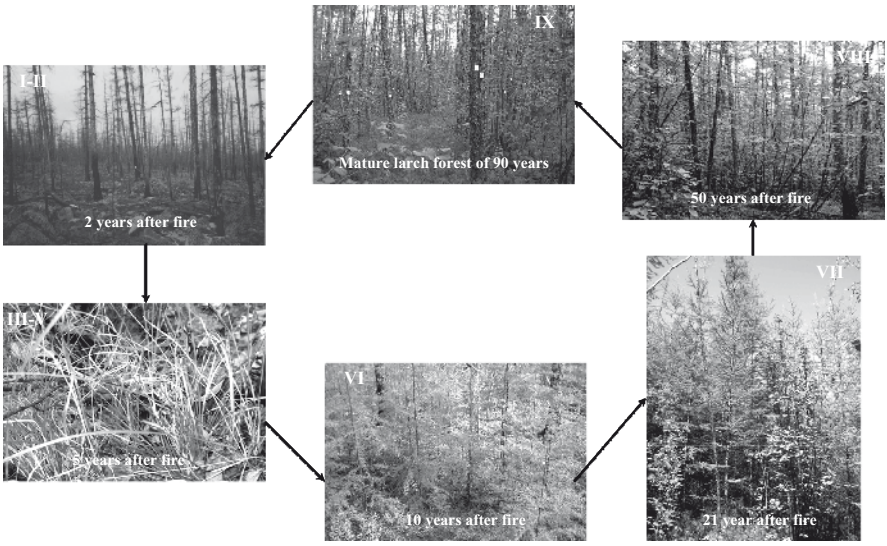

Fig. 5.8 Secondary postfire succession in *Larix gmelinii* (Gmelin larch) forests of Siberian cryolithic zone

- Restoration of plant species' diversity after fire is a long-term process (90–100 years), which may be divided into nine distinctive successional stages.
- Postfire recovery of the larch association described occurs among the even-aged *Larix gmelinii* stands, which represents one of the main trends of postfire succession in the cryolithic areas of Siberia, i.e., progressive succession of forest vegetation without changes in dominant tree species (Fig. 5.8).

References

Abaimov AP (2005) Peculiarities and basic trends of the time course of forests and thin forests in the permafrost zone of Siberia. Siberian J Ecol 4:663–675 (in Russian)

Abaimov P, Prokushkin SG, Zyryanova OA (1996) Ecological-phytocoenotic estimation of the effect of fires on the forests of cryolithozone of Middle Siberia. Siberian J Ecol 1:51–60 (in Russian with English summary)

Abaimov AP, Bondarev AI, Zyryanova OA, Shitova SA (1997a) Polar forests of Krasnoyarsk region. Nauka Siberian Enterprise, Novosibirsk, 208pp (in Russian)

Abaimov AP, Prokushkin SG, Zyryanova OA, Kaverzina LN (1997b) Peculiarities of forming and functioning larch forests on frozen soils. Lesovedenie 5:13–23 (in Russian with English summary)

Abaimov AP, Prokushkin SG, Zyryanova OA (1998) Peculiarities of postfire damages of larch forests in cryolithic zone of Central Siberia. Siberian J Ecol 3–4:315–323 (in Russian with English summary)

Abaimov AP, Zyryanova OA, Prokushkin SG, Koike T, Matsuura Y (2000) Forest ecosystems of the cryolithic zone of Siberia: regional features, mechanisms of stability and pyrogenic changes. Eurasian J For Res 1:1–10

Abaimov AP, Prokushkin SG, Zyryanova OA, Kanazawa Y, Takahashi K (2001) Ecological and forest-forming role of fires in the Siberian cryolithic zone. Lesovedenie 5:50–59 (in Russian with English summary)

Abaimov AP, Zyryanova OA, Prokushkin SG (2002) Long-term investigations of larch forests in cryolithic zone of Siberia: brief history, recent results and possible changes under global warming. Eurasian J For Res 5:95–106

Bliss LC (2000) Arctic tundra and polar desert biome. In: Barbour MG, Billing WD (eds) North American terrestrial vegetation, 2nd edn. Cambridge University Press, Cambridge, pp 1–40

Bourgeau-Chavez LL, Alexander ME, Stocks BJ, Kasischke ES (2000) Distribution of forest ecosystems and the role of fire in the North American boreal region. In: Kasischke ES, Stocks BJ (eds) Fire, climate change, and carbon cycling in the boreal forests. Ecological Studies, vol 138. Springer, Berlin, pp 111–131

Czerepanov SK (1985) Vascular plants of Russia and adjacent states (the former USSR). Cambridge University Press, Cambridge, 516pp

Degteva SV (2005) Parameters of ecological space and floristic diversity of forest formations in the Northeast of European Russia. Russian J Ecol (Ekologiya) 36:158–163

Ershov YuI (2004) Soils of Central Siberian Plateau. Sukachev Institute of Forest Press, Krasnoyarsk, 86pp (in Russian)

Ferreira LV, Prance GT (1999) Ecosystem recovery in terra firme forests after cutting and burning: a comparison on species richness, floristic composition and forest structure in the Jau National Park. Bot J Lin Soc 130:97–110

Kurbatski NP (1970) The research of the amount and the features of the fuel organic matter. Forest pyrology issues. Sukachev Institute of Forest and Wood, Krasnoyarsk, pp 5–58 (in Russian)

Magurran AE (1988) Ecological diversity and its measurement. Princeton University Press, New Jersey, 192pp

Matsuura Y, Abaimov AP (1998) Changes in soil carbon and nitrogen storage after forest fire of larch taiga forests in Tura, Central Siberia. In: Mori S, Kanazawa Y, Matsuura Y, Inoue G (eds) Proceedings of the Sixth Symposium on the Joint Siberian Permafrost Studies between Japan and Russia in 1997. Tsukuba, Japan, pp 130–135

Payette SG (1992) Fire as a controlling process in the North American boreal forest. In: Shugart HH, Leemans R, Bonan GB (eds) A system analysis of global boreal forest. Cambridge University Press, Cambridge, pp 144–169

Prokushkin SG, Sorokin ND, Tsvetkov PA (2000) Ecological sequences of wildfires in larch stands of the northern taiga of Krasnoyarsk region. Lesovedenie 4:9–15 (in Russian)

Rees DC, Juday GP (2002) Plant species diversity on logged versus burned sites in Central Alaska. For Ecol Manage 155:291–302

Schmidt VM (1984) Mathematical methods in botany. Leningrad University Press, Leningrad, 288pp (in Russian)

Schulze E-D, Schulze W, Kelliher FM, Vygodskaya NN, Ziegler W, Kobak KI, Koch H, Arneth A, Kuznetsova WA, Sogatchev A, Isaev A, Bauer G, Hollinger DY (1995) Above-ground biomass and nitrogen nutrition in a chronosequence of pristine Dahurian *Larix* stands in eastern Siberia. Can J For Res 25:943–960

Shcherbakov IP (ed) (1979) Forest fires in Yakutiya and their influence on the forest nature. Nauka, Novosibirsk, 226pp

Shvidenko AZ, Nilsson S (2000) Extent, distribution, and ecological role of fire in Russian forests. In: Kasischke ES, Stocks BJ (eds) Fire, climate change, and carbon cycling in the boreal forests. Ecological studies, vol 138. Springer, Berlin, pp 111–131

Sofronov MA, Volokitina AV (1996) Vegetation fires in the northern open forest zone. Siberian J Ecol 1:43–49 (in Russian)

Sofronov MA, Volokitina AV, Shvidenko AZ, Kajimoto T (1998) On area burnt by wild land fires in the northern part of Central Siberia. In: Mori S, Kanazawa Y, Matsuura Y, Inoue G (eds) Proceedings of the Sixth Symposium on the Joint Siberian Permafrost Studies between Japan and Russia in 1997. Tsukuba, Japan, pp 139–146

Van Cleve K, Chapin FS III, Flanagan PW, Viereck LA, Dyrness CT (eds) (1986) Forest ecosystems in the Alaskan taiga. Ecological Studies, vol 57. Springer, Berlin, 230pp

Wein RW, MacLean D (1983) The role of fire in northern circumpolar ecosystems. Scope 18. Wiley, Toronto

Whittaker RH (1975) Communities and ecosystems, 2nd edn. MacMillan, New York 385pp

Zyryanova OA (2004) Plant species diversity and recovery of forest vegetation after fire disturbance in continuous permafrost area of Siberia. In: Tanaka H (ed) Proceedings of the Fifth International Workshop on Global Change: Connection to the Arctic 2004 (GCCA5). Tsukuba University, Tsukuba, pp 191–194

Zyryanova OA, Bugaenko TN, Abaimov AP (2002) Pyrogenic transformation of species diversity in larch forest of cryolithozone. In: Pleshikov FI (ed) Forest ecosystems of the Yenisey meridian. Publishing House SB RAS, Novosibirsk, pp 135–146 (in Russian)

Zyryanova OA, Abaimov AP, Bugaenko TN (2004) Evaluation of the species diversity of autochthonal larch associations of the cryolithic zone and its postfire dynamics on the basis of the Shannon information index. Siberian J Ecol 5:735–743 (in Russian)

Zyryanova OA, Bugaenko TN, Bugaenko NN (2006) Analysis of plant species diversity and spatial structure of larch associations in cryolithic zone of Siberia. In: Shumny VK, Shokin YuI, Kolchanov NA, Fedotov AM (eds) Biodiversity and dynamics of ecosystems: computational approaches and modeling. Publishing House SB RAS, Novosibirsk, pp 495–504 (in Russian)

Zyryanova OA, Yaborov VT, Tchikhacheva TL, Koike T, Makoto K, Matsuura Y, Satoh A, Zyryanov VI (2007) The structure and biodiversity after fire disturbance in *Larix gmelinii* (Rupr.) Rupr. Forests, Northeastern Asia. Eurasian J For Res 10:19–29

Zyryanova OA, Abaimov AP, Chikhacheva TL (2008) The influence of fire on forest-formation process in larch forests of northern Siberia. Lesovedenie 1:3–10 (in Russian with English summary)

Part II
Ecosystem Dynamics and Function

Chapter 6
Biomass and Productivity of Siberian Larch Forest Ecosystems

T. Kajimoto, A. Osawa, V.A. Usoltsev, and A.P. Abaimov

6.1 Introduction

Boreal forests are expected to affect global carbon balance significantly due to their large areas (e.g., Goulden et al. 1998; Schulze et al. 1999; Chapin et al. 2000; Jarvis et al. 2001). Biomass and productivity of boreal forests have been examined mainly in the evergreen taiga established in the regions of nonpermafrost or discontinuous permafrost, e.g., interior Alaska (Van Cleve et al. 1983, 1986; Vogt et al. 1996), northern Canada (Gower et al. 2001; Bhatti et al. 2002; Bond-Lamberty et al. 2002), and northern Europe (Schulze 2000). In contrast, comparable studies are considerably limited in the boreal forests of Siberia, where three *Larix* species are growing separately in different locations and soils: each of two similar species, *Larix gmelinii* (Rupr.) Rupr. and *L. cajanderi* Mayr, dominates in the continuous permafrost regions in Central and Northeastern Siberia, respectively, while *Larix sibirica* L. grows mainly in the nonpermafrost regions of Western or Mountainous southern Siberia (Abaimov 1995; also see Chaps. 1, 3 and 4).

In Russia, total carbon pool of forest ecosystems has been assessed based on the data of National Forest Inventory, and was estimated to be in the order of 30–50 Pg C, excluding the amount in soil-C stock (Isaev et al. 1995; Alexeyev et al. 1995; Alexeyev and Birdsey 1998; Shvidenko and Nilsson 1999). These studies indicate that larch forests of Siberia occupy the largest proportion of Russian forests, about 42% in area and about a half of total C-pool. In the process of large-scale evaluation in carbon stock, however, the larch forests consisting of three species are often treated as one forest type. For example, a conversion factor from the unit of stem volume to that of dry mass, which is used for the calculation of C-pool from the Forest Inventory data, is assumed to be the same for these larch species. Also, a ratio of biomass allocation among components (stems, needles, root) is generally assumed to be constant (e.g., Isaev et al. 1995; Alexeyev et al. 1995). These assumptions seem to be due to lack of sufficient biomass data for these larch species that are measured in natural growth habitats. Particularly, knowledge about belowground carbon stocks and production for the two species (*L. gmelinii*, *L. cajanderi*) growing on continuous

A. Osawa et al. (eds.), *Permafrost Ecosystems: Siberian Larch Forests*,
Ecological Studies, Vol. 209, DOI 10.1007/978-1-4020-9693-8_6,

permafrost is still insufficient, since most of the previous studies have dealt with only the aboveground components (e.g., Pozdnyakov et al. 1969; Pozdnyakov 1975; Schulze et al. 1995).

We have recently studied structure, biomass, and net primary production of forests of these two larch species at locations in Central and Northeastern Siberia (Kajimoto et al. 1999, 2003, 2006; Osawa et al. 2003). Findings of these studies suggested that pathway to roots is important in biomass allocation, which differed substantially from that of the other boreal forests distributed in non or discontinuous-permafrost regions (Kajimoto et al. 2006). This implies that the processes of carbon accumulation and allocation in the *Larix* taiga are closely linked with the influence of specific soil environments in the region of permafrost. However, previous studies dealt mainly with old stands (> 100 years-old). Long-term processes of individual tree growth and stand-level carbon accumulation and allocation have not been well understood, including those at younger postfire growth stages.

In this chapter, the main objective is to characterize the processes of carbon accumulation and allocation, and that of net primary production of the *Larix* taiga on the Siberian permafrost. For this purpose, all data that are available to us at present are presented – previous data obtained mainly for old forests as mentioned above and new data for some young and old *L. gmelinii* stands. Based on these data, first, we discuss how the stand-level biomass accumulation, allocation, and productivity vary in relation to stand age and local site condition. As for changes in these variables along a stand age-sequence, we make comparisons between young (< 30 years-old) and old (> 100 years-old) growth stages. Second, we review available data of biomass for stands of *Larix gmelinii* and *L. cajanderi* (Usoltsev 2001), and overview their potential carbon stocks and allocation patterns. Finally, we discuss how the process of carbon accumulation in the permafrost *Larix* taiga is characterized, compared to those of evergreen taiga, which makes up the other boreal forest ecosystems in nonpermafrost regions.

6.2 Data Source and Analysis

6.2.1 Study Site

Field measurements and sampling were carried out in three different locations within the continuous permafrost region of Siberia: two sites of *L. cajanderi* forests in Northeastern Siberia, and one intensive study area of *L. gmelinii* forests in Central Siberia (Table 6.1).

Of the two study sites of *L. cajanderi* in Northeastern Siberia, one site was located on an almost flat area within the lower delta of Kolyma River near Chersky (69°N 160°E, ca. 100 m a.s.l.). Another site was on the midslope of a mountain on the upper reach of the Indigirka River near Oymyakon (63°N 145°E, 1,160 m a.s.l.). These two sites were near the northern and altitudinal treelines (i.e., forest-tundra vegetation), respectively. At each site, a typical old stand was selected for estimation

Table 6.1 Outline of the ten research sites of *Larix* forests, eight *L. gmelinii* stands at Tura in Central Siberia, and two *L. cajanderi* stands in Northeastern Siberia

	L. gmelinii forests at Tura								*L. cajanderi* forests	
	Young even-aged			Old even-aged			Old multiaged		Old multiaged	
Stand age (years-old)	10	14	26	105	105	105	174	>220	>155	>140
Stand name	CR1994	CR1990	CR1978	CF	W1	NF	CR1830	C1	Chersky	Oymyakon
Location	Site 2	Site 1	Site 3	Flux site	Site 1	Site 1	Site 2	Site 2		
Slope aspect	E	NW	E	N	W	NW	SE	E	N	E
Slope inclination (°)	<3	10–15	10–15	<3	<5	10–15	5–10	<5	<3	10
Plot size (m^2)	2	4	25	400	25	225	500	1,000	600	1,000
Number of plots	10	4	4	4	6	12	2	1	1	1
Tree density (ha^{-1})	395,500[a]	148,200[b]	13,700[b]	5,480[b]	5,670[b]	5,390[b]	1,620	1,910	1,930	850
	(97,050)	(15,550)	(2,560)	(560)	(840)	(320)				
Stem diameter *D* (cm)	–	–	2.73[a]	3.15[a]	2.24[a]	4.52[b]	9.46	6.83	5.93	6.57
			(0.30)	(0.09)	(0.18)	(0.23)				
Tree height *H* (m)	0.55[a]	1.47[a]	4.80[b]	3.41[c]	2.66[c]	5.54[b]	9.01	5.50	4.31	4.46
	(0.04)	(0.09)	(0.35)	(0.04)	(0.18)	(0.23)				
Crown area index CAI ($ha\ ha^{-1}$)	1.94[a]	3.18[b]	1.33[a]	0.18[c]	0.12[c]	0.28[c]	0.23	0.34	0.37	0.09
	(0.26)	(0.59)	(0.08)	(0.01)	(0.01)	(0.01)				

Ages (at 2004) of three old multiaged stands show the averaged ages of larch trees sampled in each stand; maximum age of sample tree is 281 years (C1), 178 years (Chersky), and 253 years (Oymyakon). Tree density, breast height stem diameter (*D*), and tree height (*H*) are the values for living individuals ($H > 1.3$ m); however, trees smaller than 1.3 m in height are also included for two younger stands (10 and 14 years-old). Crown area index (CAI) is defined as the sum of individual crown projection area expressed per unit land area. Except for the stands with one or two permanent plots, value of each parameter is mean of permanent plots (standard error (SE) is shown in parenthesis); values within one raw followed by same small letter are not significantly different between stands (at p=0.05, Tukey's HSD test). See Fig. 6.1 (also Fig. 1.2) for location of each stand at Tura. Data sources: CR1978 and CF (Kajimoto et al. 2007); W1, C1, Chersky and Oymyakon (Kajimoto et al. 2006); other sites (Kajimoto et al. unpublished data)

of above- and below-ground biomass, and for analysis of stem growth. These two stands were likely to have regenerated intensively after each stand-replacing fire, occurring about 155 years (Chersky) and 140 years (Oymyakon) ago, but a few older trees (> 200 years-old) were also present in these stands. Further information on these study sites such as ground vegetation, climate and soils are described elsewhere (Kajimoto et al. 2006; also see Chap. 8).

All study sites of *L. gmelinii* in Central Siberia were established around Tura, a village located at the junction of the Nizhnyaya Tunguska River and its branch, the Kochechum River (64°N 100°E, 160 m a.s.l.) (Fig. 6.1; also see Fig. 1.1). Biomass and net primary production were examined in eight stands of different age classes: three young (<30 years-old) and five old (> 100 years-old) stands (Table 6.1). All these young stands (called CR1994, CR1990, and CR1978; stand No. 1, 2, and 3, respectively, in Fig. 6.1) were even-aged (10, 14, 26 years-old in 2004) due to intensive stand-replacing fires at each site (see also Table 1.1, for summary of plot and site identification). As for definition of stand name used in this chapter, for example, 10 years-old stand where fire occurred in 1994 is referred to as CR1994. Among five old stands, three stands (called CF, W1, NF) were also even-aged and almost the same age (105 years-old in 2004) because they were likely to have been established as a result of large-scale fire disturbance (in late 1890s) in the region of

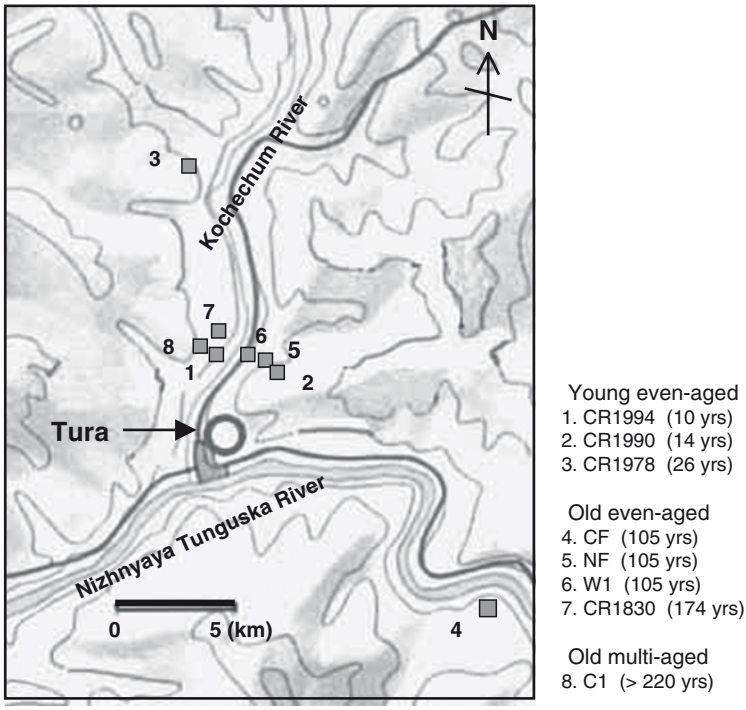

Fig. 6.1 Location map of the study stands of *Larix gmelinii* at Tura in Central Siberia. Outline of each site is described in Table 6.1 (also see Fig. 1.3)

the study (Abaimov, personal communication). Of these, one (CF; see stand No. 4 in Fig. 6.1) was located on nearly-flat area (< 3° in slope inclination) on Carbon Flux Site, while the other two stands (W1 and NF; stand No. 6 and 5) were located at the lower (< 5°) and middle (10–15°) parts of the same slope on Site 1, respectively (see also Fig. 1.3). For the other two old stands on Site 2, one (called CR1830; stand No. 7) was an even-aged stand (174 years-old), while the other (called C1; stand No. 8) was a multiaged stand (> ca. 220 years-old). This old multiaged stand was located near a recently burned, youngest stand (CR1994). Further information on these study sites around Tura is described elsewhere (see Chaps. 1, 2, 3 and 8).

6.2.2 Estimation of Above- and Below-Ground Biomass

Biomass of each stand was estimated with size-mass allometry of individual trees. The method was the same as that applied previously to the following four old stands: two *L. cajanderi* forests (Chersky, Oymyakon) in Northeastern Siberia, and two *L. gmelinii* stands at Tura (W1, C1) (Kajimoto et al.1999, 2006). Here, we briefly explain the method common to all stands, and additional site-specific procedures used for the three young (CR1994, CR1990, CR1978) and three old stands (CF, NF, CR1830) of *L. gmelinii*.

Number and size of permanent research plots established in these six *L. gmelinii* stands were as follows: $n=10$ (each plot 2 m^2) in CR1994; $n=4$ in CR1990 (4 m^2), CR1978 (25 m^2), and CF (400 m^2); $n=12$ in NF (225 m^2); and $n=2$ in CR1830 (500 m^2) (Table 6.1). Tree dimensions such as stem diameter at breast height (D) and tree height (H) were measured for living larch trees taller than 1.3 m; however, all trees were measured in two younger stands (CR1994, CR1990) regardless of stem size. Tree sampling was conducted for some selected larch trees that varied in size in each stand, except in 174 years-old stand (CR1830). In one young and two old stands, numbers of sampled trees were: $n=10$ (CR1978, CF) and $n=20$ (NF). Plot sizes and the numbers of sample trees in the other stands were described previously (Kajimoto et al. 1999, 2006; see Table 1).

For each sample tree, dry mass (oven-drying at 85°C) was determined separately for four components (stem, branch, needle, and coarse root). Coarse root was defined as roots larger than 5 mm in diameter. Dead parts of coarse roots, which were often observed for old sample trees (> 100 years), were excluded completely by visual inspection (see Chap. 16). In 10 years-old (CR1994) and 14 years-old (CR1990) stands, tree sampling was conducted twice (in 1994 and 2004) in order to estimate net primary production as the difference in biomass (details described below). Numbers of trees sampled were: $n=74$ in 1999, $n=31$ in 2004 (CR1994), $n=64$ in 1999, and $n=30$ in 2004 (CR1990). For these younger sample trees, dry mass was determined separately for three components (stem plus branch, needle and roots). Also, both coarse and fine root masses were measured together as roots, since roots of younger trees were mostly smaller than 5 mm in diameter.

Size-mass allometry ($y = A\,x^B$; x is size parameter, y is dry mass) were examined wR among the sample trees in each of five *L. gmelinii* stands, except for 174 years-old stand (CR1830). Figure 6.2 shows examples of the allometric relationships (i.e., dry mass of stem and/or roots) observed for the sample trees of these stands. Tree height (H) was used as an independent size parameter for two younger stands (CR1994 and CR1990) (Fig. 6.2a, b), while stem diameter (D) was used for the other stands, 26 years-old (CR1978) and two 105 years-old stands (CF, NF) (Fig. 6.2c–e). All these relationships were highly correlated ($r^2 > 0.95$; $p < 0.01$). It was also confirmed that site-specific allometry for dry mass of branch

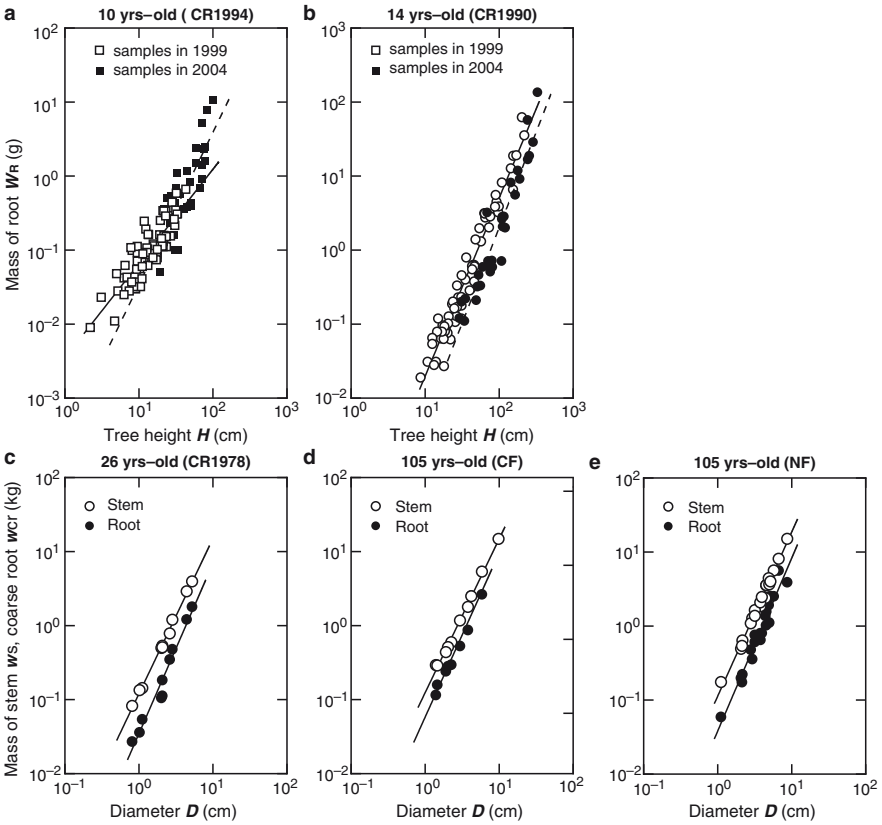

Fig. 6.2 Examples of allometric relationships between tree size parameters and dry mass of stem and/or root observed for sample trees of five *Larix gmelinii* stands at Tura. Relationship between tree height (H) – root mass (w_R; including both coarse and fine roots) is shown separately for individuals sampled at two different years in (**a**) 10-year-old stand (CR1994; $n = 74$ in 1999, $n = 30$ in 2004) and (**b**) 14-year-old stand (CR1990; $n = 64$ in 1999, $n = 31$ in 2004). Relationships between stem diameter (D), dry mass of stem (w_S), and coarse root (w_{CR}) are shown for sample trees in (**c**) 26-year-old (CR1978; $n = 10$), (**d**) 105-year-old (CF; $n = 10$), and (**e**) 105-year-old (NF; $n = 20$) stands. All regressions are significant ($r^2 > 0.95$; $p < 0.01$) (Kajimoto et al. unpublished data)

and needle was significant if these size parameters were used, and there were between-site differences in these regressions in some cases (Kajimoto et al. unpublished data). Thus, each component biomass of these five *L. gmelinii* stands was calculated by applying site-specific regressions to the tree census data. For only 174 years-old stand (CR1830), where tree sampling was not conducted, biomass was estimated by applying the site-common *D*-base allometric relationships that were previously derived by pooling the data of all sampled trees (total $n = 27$) in other four old larch stands (> 100 years-old; CK, OM, C1 and W1) (details see Kajimoto et al. 2006).

6.2.3 Estimation of Aboveground Net Primary Production

Aboveground net primary production (ANPP) is defined as the sum of annual biomass increment (Δy) and mortality (ΔL) of aboveground parts, if biomass loss due to grazing by herbivores is ignored. Among eight *L. gmelinii* stands in Tura, ANPP was previously assessed only for old multiaged stand (C1) (Kajimoto et al. 1999). In this previous study, ANPP was calculated as the sum of annual biomass increments of stem (Δy_S) and branch (Δy_B), and needle production; needle production was assumed to be equivalent to needle biomass (y_L), since litterfall (or mortality) was not measured in this stand. For other six *L. gmelinii* stands (i.e., except W1), litterfall rates of needles and branches were measured recently. Therefore, ANPP of these stands were estimated by the above definition ($\mathrm{ANPP} = \Delta y + \Delta L$). However, the following two components were excluded in the estimation of ANPP: biomass increment due to newly recruited individuals, and mortality due to death of individuals. Below, we describe the methods of litterfall measurement and estimation of biomass increments.

Litterfall was collected using the two types of litter traps during 1 year (2004–2005). A small square trap (0.04 m^2 in area) was set on the ground in two younger stands (CR1994, CR1990), while a triangular hanging-trap (1 m^2 in mouth area) was set at 70–80 cm above the ground in other four stands. Total number of traps differed according to size and number of permanent plots: $n = 6$ (CR1994), $n = 8$ (CR1990), $n = 8$ (CR1978), $n = 24$ (CF), $n = 36$ (NF), and $n = 8$ (CR1830). Collected litter was sorted into larch needles and branches, and other fractions (e.g., bark, leaves, and branches of broad-leaved species). Then their dry mass was determined after oven-drying at 85°C. Thus, mortality (ΔL) was calculated as the sum of annual litterfall rates of branch (ΔL_B) and needle (ΔL_L).

Aboveground biomass increments were estimated using slightly different methods between two younger stands and other four stands. For 10 years-old (CR1994) and 14 years-old (CR1990) stands, biomass of each component was estimated twice with a 5-year interval (in 1999 and 2004) as mentioned above (see Fig. 6.2a, b). Thus, annual biomass increments of stem (Δy_S), branch (Δy_B), and needle (Δy_L) were calculated directly as the difference of biomass estimates at these two sampling years. For other four stands (CR1978, CF, NF, CR1830), biomass increments

of stem (Δy_S) and branch (Δy_B) were estimated with a similar method applied previously to the old multiaged stand (C1) (Kajimoto et al. 1999). Here, an allometric relationship between stem dry mass (w_S) and annual stemwood volume increment (ΔV_S; averaged in recent 5 years) was derived using stem analysis data of five sampled trees. Then, coefficients of this regression were applied to estimation of both stem and branch biomass increment: mean bulk density of the larch stems (0.647 g cm^{-3}) was used in the conversion from stem volume to dry mass. In applying this method to four stands, we examined the w_S–ΔV_S allometry using the stem analysis data that were obtained for 10 young trees from 26 years-old stand (CR1978), and for 26 old trees (> 100 years-old) from two *L. gmelinii* (W1, C1) and two *L. cajanderi* (Chersky, Oymyakon) stands. It was recognized that the allometric relationships differed significantly between the young and old sample trees (Fig. 6.3) (Kajimoto et al. unpublished data). Thus, stem and branch biomass increments of 26 years-old stand were estimated with the coefficients of site-specific w_S–ΔV_S regression (dotted line in Fig. 6.3). On the other hand, biomass increments of stem and branches of four old stands were estimated with coefficients of site-common regression obtained from the data of old trees (solid line in Fig. 6.3), though stem analysis data of these stands were not available. For these four old stands, biomass increment of

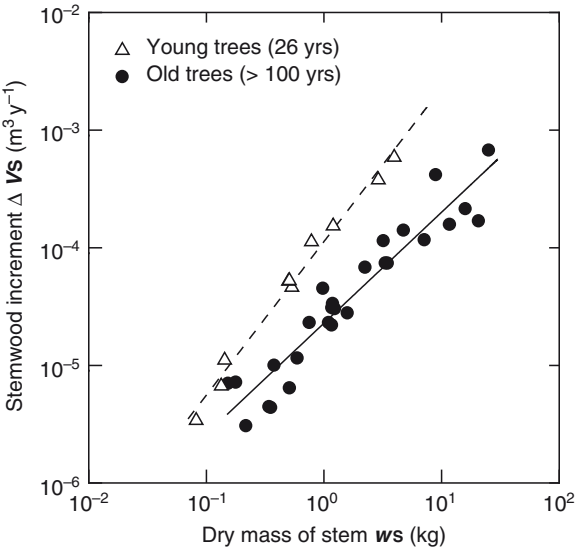

Fig. 6.3 Relationships between annual increment of stemwood volume (ΔV_S; mean of recent 5 years) and dry mass of stem (w_S) for sample trees of *Larix gmelinii*. *Open triangles* show data from 26-year-old stand (CR1978; $n = 10$), and *closed circles* show data from two old *L. gmelinii* (W1, C1) and two old *L. cajanderi* stands (Chersky, Oymyakon) (totally $n = 26$). Regression lines (*dotted*, *straight*) are approximated by a power-equation ($\Delta V_S = A\, w_S^{\,B}$) for data of young and old stands, respectively. Coefficients of two regressions (values A and B) are different significantly ($p < 0.01$; ANCOVA) (Kajimoto et al. unpublished data)

needles (Δy_L) was assumed to be zero, since needle biomass appeared to be stable as stand reaches a certain age (see Sect. 6.3).

6.3 Biomass

6.3.1 Aboveground Biomass

6.3.1.1 Local Scale Variation

Table 6.2 summarizes the estimates of component biomass for ten *Larix* stands in our study sites. Aboveground total biomass (y_{AT}) ranged from 3.1 to 27.7 Mg ha^{-1} for eight *L. gmelinii* forests in Tura. The y_{AT} values differed significantly among three young stands (< 30 years-old; CR1994, CR1990 and CR1978), indicating that aboveground biomass increases with stand age. In contrast, aboveground biomass differed largely among five old stands (> 100 years-old); the estimate of y_{AT} in three stands (NF, CR1830, C1) reached a similar level (23–27 Mg ha^{-1}), while the estimates of others (CF, W1) were as low as those of the younger stands. Aboveground biomass of two old *L. cajanderi* forests (Chersky, Oymyakon) fall within the range of the old *L. gmelinii* forests in Tura (Table 6.2).

Figure 6.4a compares the estimates of biomass in *L. gmelinii* forests with different ages; here, one 105 years-old stand (NF) is selected from three stands of the same age as the largest biomass was attained in this stand. This comparison simply indicates that aboveground carbon stock increases until a certain age (about 30 years), but it may become stable as the stand ages further.

The estimates of aboveground biomass vary greatly depending on sites, even among stands of similar age. As was seen in three 105 years-old stands, the value of y_{AT} differed about fourfold between two of them, 6.3 (W1) vs. 23.1 Mg ha^{-1} (NF) (Table 6.2). Tree density is almost the same (ca. 5,500 ha^{-1}) among three stands, but average tree size differs significantly (Table 6.1). For example, the average tree height of 2.7 m in W1, where total biomass is the smallest, is only a half of that of NF (5.5 m) where total biomass is the largest. Thus, between-stand variation of aboveground biomass may reflect differences in local site conditions, such as slope aspect and inclination. Biomass allocation also differed among five *L. gmelinii* stands, especially for three young forests (10, 14, and 26 years-old stands) (Fig. 6.4b). Change in carbon allocation with stand age will be discussed later (see Sect. 6.5).

Aboveground total biomass also differed greatly between two old *L. cajanderi* forests with similar ages (140- and 155-years-old stands): 16.3 Mg ha^{-1} (Chersky) vs. 7.6 Mg ha^{-1} (Oymyakon) (Table 6.2). However, the average tree size was nearly the same, though tree density differed by twofold: 1,930 ha^{-1} (Chersky) vs. 850 ha^{-1} (Oymyakon) (Table 6.1), suggesting that difference in tree density mainly affected the amount of aboveground carbon stock.

Table 6.2 Above- and below-ground biomass (Mg ha^{-1}) of the ten research stands of *Larix* in Central and Northeastern Siberia

		L. gmelinii forests a.t Tura								*L. cajanderi* forests	
		Young stands			Old even-aged				Old multiaged	Old multiaged	
Stand age (years-old)		10	14	26	105	105	105	174	>220	>155	>140
stand name		CR1994	CR1990	CR1978	CF	W1	NF	CR1830	C1	Chersky	Oymyakon
Stem	y_S	2.42	8.36	17.62	9.78	4.93	20.80	25.00	18.93	12.18	6.47
Branch	y_B	–	–	4.22	1.16	1.04	1.73	2.11	3.29	3.24	0.96
Needle	y_L	0.63	1.17	2.18	0.44	0.32	0.52	0.63	1.03	0.91	0.21
Above-total	y_{AT}	3.05[a]	9.53[b]	24.01[c]	11.38[b]	6.29[a, b]	23.06[c]	27.74	23.25	16.33	7.64
		(0.40)	(2.52)	(1.46)	(0.81)	(1.09)	(1.11)				
Coarse root	y_{CR}	–	–	6.21	5.14	2.98	8.32	9.84	11.72	10.92	2.89
Fine root	y_{FR}	–	–	–	–	4.10	–	–	5.90	–	–
Below-total	y_R	0.70[a]	1.68[a,b]	6.21[c]	5.14[c]	7.08	8.32[d]	9.84	17.62	10.92	2.89
		(0.09)	(0.44)	(0.23)	(0.41)	(0.52)	(0.57)				
Stand total	y	3.74	11.21	30.22	16.52	13.38	31.38	37.58	40.87	27.25	10.53
Top/root ratio	(y_{AT}/y_R)	4.4	5.8	3.9	2.2	2.1	2.8	2.8	2.0	1.5	2.6
Lear area index	LAI	0.78	1.46	2.70	0.55	0.37	0.65	0.78	1.28	1.13	0.26

For two younger *L. gmelinii* stands (10 and 14 years-old), each component biomass shows the estimate at sampling year of 2004. Stem biomass included branch biomass, and belowground biomass was not determined separately for coarse and fine roots. For the other stands, belowground biomass was estimated as only coarse roots; however, fine root biomass was estimated using core-sampling method for two *L. gmelinii* stands (W1, C1) (see Sect. 6.3.2). Each value is mean of permanent plots (n = 4–12), except for stands with only one or two plots. For the estimates of above- and below-ground total biomass (y_{AT}, y_R), SE is shown in parenthesis; values within one raw followed by same small letter are not significantly different between stands (at p=0.05, Tukey's HSD test). Leaf area index (LAI; m m^{-2}) was estimated by multiplying needle biomass by a mean specific leaf area (SLA = 124 cm^2 g (dry)$^{-1}$); this mean value was determined for needle samples taken at different crown positions of some *L. gmelinii* trees in old multiaged stand (C1) (Koike et al. unpublished data). Data sources: W1, C1, Chersky, and Oymyakon (Kajimoto et al. 2006); the other sites (Kajimoto et al. unpublished data)

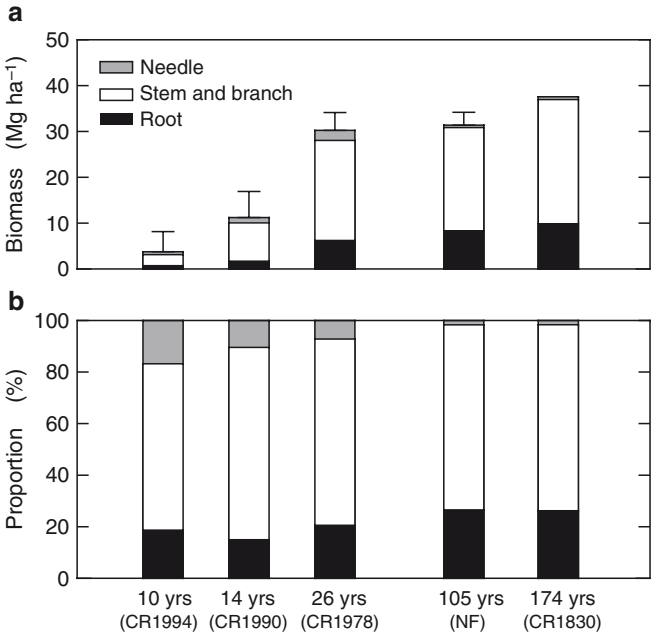

Fig. 6.4 Comparisons of (**a**) total biomass (*y*) and (**b**) its allocation among five *Larix gmelinii* stands at Tura. Here, data of one stand (NF) with the largest total biomass is selected as a representative from three 105-year-old stands (W1, CF, NF; see Table 6.2) (Kajimoto et al. unpublished data)

Figure 6.5 compares height growth curves of stems among the *Larix* stands, except for two youngest stands (10- and 14-years-old). The growth rate differed among the three 105 years-old stands in Tura (W1, CF, NF) (Fig. 6.5b–d): it was much smaller in W1 site where aboveground biomass was the smallest among the three. The evidence suggests that difference in aboveground total biomass among these old stands mainly reflects difference in individual growth rate in response to local site conditions.

Stem height growth pattern also differed among three 105 years-old stands. Trees of W1 (Fig. 6.5b) grew slowly throughout development, while those of CF (Fig. 6.5c) and NF (Fig. 6.5d) grew faster during the younger stage, and declined suddenly at mid age. When two stands (CF, NF) are compared, abrupt growth decline occurred slightly earlier in NF (i.e., ages 20–30 years) than in CF (25–50 years). Of these stands, NF is located at moderate slope (10–15° in inclination), while the others (W1, CF) are located at flat sites (<5°) (Table 6.1). Soil conditions are likely to differ among these stands due to difference in topographic location: soils are wetter (i.e., poorly drained) in the flat sites (W1, CF) than in the midslope (NF). Likewise, a similar relationship between stem growth pattern and topography was seen in two stands of *L. cajanderi* in Northeastern Siberia: trees on a flat site (Chersky) grew slowly from the beginning (Fig. 6.5e), while those at the midslope

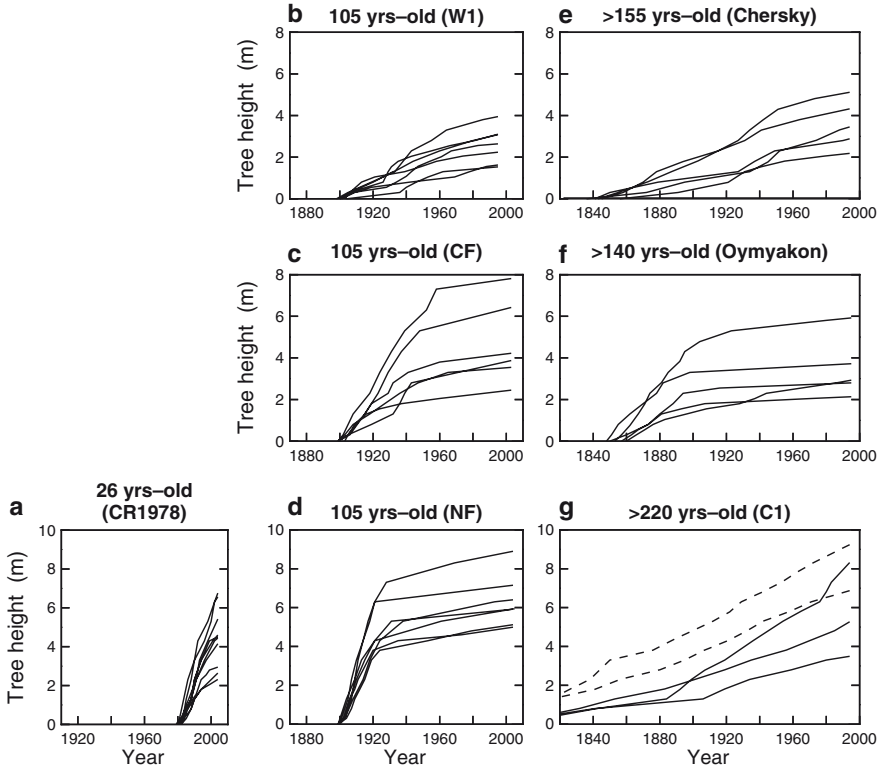

Fig. 6.5 Examples of stem height growth curves reconstructed for larch trees sampled in six study stands. (**a**) 26-year-old *Larix gmelinii* stand at Tura (CR1978; $n=10$). (**b**)–(**d**) Three 105-year-old *L. gmelinii* stands at Tura (W1, CF, and NF; $n=7$, 6, and 7, respectively). (**e**) >155-year-old *Larix cajanderi* stand (Chersky; $n=5$) and (**f**) >140-year-old *L. cajanderi* stand (Oymyakon; $n=5$) in Northeastern Siberia. (**g**) >220-year-old *L. gmelinii* stand at Tura (C1; $n=5$) (Kajimoto et al. unpublished data)

(Oymyakon) grew much faster until the stand age of 30–40 years (Fig. 6.5f). These comparisons suggest that local site conditions, such as soil water regime due to topography, may be a factor affecting individual growth and aboveground carbon stock.

6.3.1.2 Geographical Scale Variation

Figure 6.6 shows relationships between stand age and aboveground total and needle biomass for two larch species (*L. gmelinii*, *L. cajanderi*) in Central and Northeastern Siberia. Here, 93 stands with typical site indices in the region (IV or V; definition is shown in Sect. 7.2.2) are selected from data compiled by Usoltsev (2001). The data are plotted separately for the stands located in northern (64–72°N in latitude; closed circles) and southern regions (< 64°N; open circles). Aboveground total

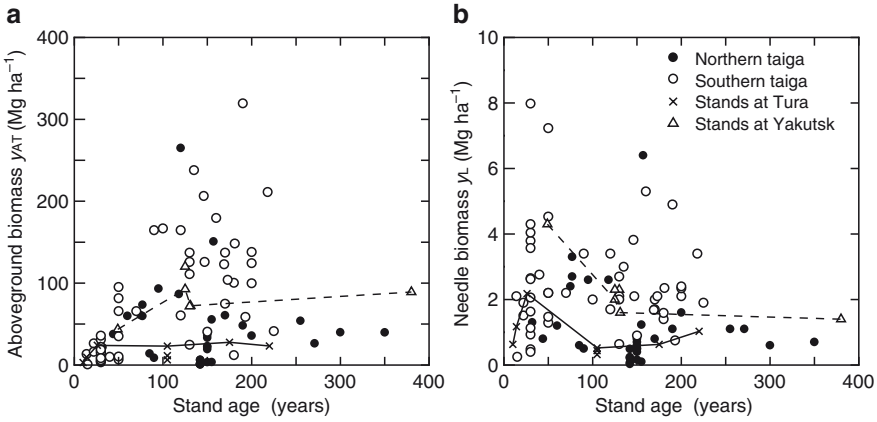

Fig. 6.6 Relationships between stand age and (**a**) aboveground biomass (y_{AT}) and (**b**) needle biomass (y_L) for stands of two larch species (*L. gmelinii*, *L. cajanderi*) in Siberia. Here, data of 93 stands with typical site index in the permafrost region (i.e., IV and V) are selected from the published dataset (Usoltsev 2001). *Filled* and *open circles* show stands located in northern (i.e., latitude > 64°; $n = 33$) and southern regions (< 64°; $n = 60$), respectively. *Open triangles* connected with *dotted line* show data of *L. gmelinii* stands near Yakutsk (Schulze et al. 1995). *Crosses* with *straight line* show data of *L. gmelinii* stands at Tura (present study; see Table 6.2)

biomass varied substantially even within the continuous permafrost region of Siberia, ranging from 1.0 to 180 Mg ha^{-1} (Fig. 6.6a). This variation, of course, may involve differences not only in stand age, but also other variables, such as tree density and local site condition (or individual growth potential) as was already discussed (also see Sect. 7.4).

At one location, for example, Schulze et al. (1995) indicated that aboveground biomass of larch forests near Yakutsk increased with stand age, but reached a stable level (ca. 90–100 Mg ha^{-1}) as the stand was older than 120–130 years (data are shown by triangles in Fig. 6.6a). Nevertheless, as far as old stands (> 100 years-old) are concerned, aboveground total biomass rarely exceed about 100 Mg ha^{-1} in the northern region, while they often reach 100–150 Mg ha^{-1} in the southern region (Fig. 6.6a). This implies that potential aboveground carbon stock varies along a latitudinal gradient within the *Larix* taiga: it tends to decrease gradually from the southern to northern regions (Usoltsev et al. 2002). The estimates of aboveground total biomass (< 30 Mg ha^{-1}) in some old *L. gmelinii* stands examined at Tura (64°N) are somewhat lower among the stands in northern taiga (data shown by crosses in Fig. 6.6a).

Such a geographical tendency is also observed for needle biomass (Fig. 6.6b). The estimates of needle biomass are smaller for stands in northern region than those in southern region, suggesting that forest productivity may become smaller toward the north (Usoltsev 2003). In both regions, however, needle biomass appears to be larger at younger stages, and declines sharply to a similar level (< 1–2 Mg ha^{-1}) as the stand ages > 100–150 years. For larch forests near Yakutsk, the needle biomass

peaked (ca. 4 Mg ha^{-1}) at 50 years-old stand, then decreased to about 2 Mg ha^{-1} in >120 years-old stands (data shown by triangles with dotted line in Fig. 6.6b; Schulze et al. 1995). In our *L. gmelinii* stands at Tura, needle biomass follows a similar trend along the stand age-sequence, though the peak of needle biomass appears to occur earlier (at 26 years-old stand; data shown by crosses with straight line in Fig. 6.6b).

6.3.2 Belowground Biomass

6.3.2.1 Coarse Root Biomass

Total root biomass (y_R) ranged from 0.7 to 17.6 Mg ha^{-1} for eight *L. gmelinii* stands at Tura (Table 6.2). The estimates of four stands (CR1978, CF, NF, CR1830) included only coarse root biomass (i.e., $y_R = y_{CR}$), while those of four other stands (CR1994, CR1990, W1, C1) included both coarse and fine root biomass (i.e., $y_R = y_{CR} + y_{FR}$). Thus, the estimates among these stands must be compared cautiously. Nevertheless, total root biomass in two younger stands, 0.7 and 1.7 Mg ha^{-1} in 10- and 14-years-old stands, is significantly smaller than the estimates of only coarse root biomass in 26 years-old stand, 6.2 Mg ha^{-1}, and in other old stands, >3.0 Mg ha^{-1} (Table 6.2). This indicates that belowground carbon stock as coarse roots increases sharply at earlier growth stage (< 30 years), showing a trend similar to aboveground carbon stock (Fig. 6.4a).

Coarse root biomass also varied largely among three 105 years-old *L. gmelinii* stands (W1, CF, NF). The estimate for NF stand at midslope (8.3 Mg ha^{-1}) was about twice as that of W1 stand located at flat terrain (3.0 Mg ha^{-1}) (Table 6.2). This difference might be primarily related to the differences in local site condition (e.g., soil water regime due to topography), as was already discussed for aboveground biomass (Sect. 6.3.1). However, the between-stand variation of coarse root biomass is relatively small compared to that of aboveground total biomass (about four times). Consequently, values of the aboveground total/root biomass ratio (i.e., top/root ratio, or y_{AT}/y_{CR}) of two 105 years-old stands on the flat terrain, 2.1 (W1) and 2.2 (CF), are somewhat smaller than those of the other 105 years-old stand on midslope, 2.8 (NF). For old *L. cajanderi* stands in Northeastern Siberia, top/root biomass ratio is also smaller in the stand on a flat terrain than that on midslope: 1.5 (Chersky) vs. 2.6 (Oymyakon) (Table 6.2). These comparisons suggest that local site conditions affect not only total carbon stock, but also pattern of carbon partitioning between aboveground parts and roots. Namely, belowground carbon allocation is likely to increase in poorly-drained flat sites where individual growth rate is relatively small (Fig. 6.5b, e). Such a pattern of biomass allocation in *Larix* trees seems different from, and opposite to, those reported for other coniferous trees. For example, biomass allocation into roots was larger (i.e., smaller top/root ratio) at well-drained sites than at poorly drained sites in subalpine species, such as *Abies amabilis* (e.g., Keyes and Grier 1981) and *Pinus contorta* (Comeau and Kimmins 1989).

6.3.2.2 Fine Root Biomass

Fine root biomass was previously estimated only in two stands of *L. gmelinii* at Tura, 105 years-old (W1) and >220 years-old (C1) stands, with the core sampling method (Kajimoto et al. 1999, 2003). Fine root biomass reached a relatively similar level, 4.1 Mg ha^{-1} (105 years-old) and 5.9 Mg ha^{-1} (>220 years-old), though coarse root biomass differed greatly between the two stands (Table 6.1). Proportion of fine roots in total root biomass (i.e., fine root ratio; y_{FR}/y_R) is somewhat larger in 105 years-old stand (0.58) than in >220 year-old stand (0.34) (Kajimoto et al. 2006). These values are as high as that reported for a 169 years-old *L. gmelinii* stand near Yakutsk (Kanazawa et al. 1994). Fine roots may make up about a half or more of belowground carbon stock in old stands of *L. gmelinii*, though there have been few studies that estimated biomass of coarse and fine roots separately in *Larix* taiga of Siberia (Usoltsev 2001).

Fine root biomass was estimated separately by root diameter classes in the >220 years-old *L. gmelinii* stand (C1) in Tura. Biomass of thick (3–5 mm in diameter) and thin roots (< 3 mm) was 2.2 and 3.6 Mg ha^{-1}, respectively (Kajimoto et al. 1999). The mean of thin roots biomass (< 3 mm) is smaller than that of fine roots (defined as roots < 2 mm) reported for some temperate coniferous (averaged 5.0 Mg ha^{-1}) or deciduous forests (4.4 Mg ha^{-1}), and similar to those for boreal forests (2.3 Mg ha^{-1}) (Jackson et al. 1997).

6.4 Net Primary Production

6.4.1 Aboveground Production

ANPP of six *L. gmelinii* stands in Tura are summarized in Table 6.3. ANPP increased rapidly with age in young stands, and peaked (3.63 Mg ha^{-1} year^{-1}) in 26 years-old stand (CR1978). The peak value is four to seven times of that (0.48–0.81 Mg ha^{-}1 year^{-1}) of two 105 years-old stands (CF, NF) or 174 years-old stand (CR1830). As shown in Fig. 6.7, aboveground net production tends to increase rapidly during the early growth stage (< 30 years), but declines substantially as stand ages (> 100 years).

Annual biomass increment (Δy) was mostly due to growth of stems (Δy_S), followed by branch (Δy_B); however, biomass increment of stem and branch was not determined separately in two younger stands (10- and 14-years-old) (Table 6.3). The proportion of biomass increment in ANPP (i.e., Δy/ANPP) exceeds 50% in young stands: 64% (10 years-old), 66% (14 years-old), and 56% (26 years-old; CR1978). In contrast, the proportion is slightly less than a half (46–47%) in 105 years-old (NF) and 174 years-old stands (CR1830). The difference suggests that allocation of annual carbon gain into growth of woody parts (especially stems) is larger in young stands than in old stands. Also, aboveground net assimilation rate, which was defined as net carbon gain per

Table 6.3 Aboveground net primary production (ANPP, Mg ha^{-1} year^{-1}) of six *L. gmelinii* stands at Tura in Central Siberia

		Young stands			Old stands		
Stand age (years-old)		10	14	26	105	105	174
Stand Name		CR1994	CR1990	CR1978	CF	NF	CR1830
Biomass increments							
Stem	Δy_S	0.461	0.789	1.776	0.152	0.311	0.345
Branch	Δy_B	–	–	0.272	0.020	0.030	0.034
Needle	Δy_L	0.106	−0.138	–	–	–	–
Total	Δy	0.567	0.651	2.048	0.172	0.341	0.379
Litterfall rate							
Branch	ΔL_B	0.048	0.022	0.060	0.043	0.053	0.087
Needle	ΔL_L	0.148	0.665	1.525	0.265	0.355	0.339
Total	ΔL	0.196	0.687	1.585	0.308	0.408	0.426
ANPP	$(\Delta y + \Delta L)$	0.763^{a,b}	1.338^{b}	3.633^{c}	0.480^{a}	0.749^{a,b}	0.805
		(0.080)	(0.504)	(0.070)	(0.020)	(0.028)	
ANAR		0.87	1.75	1.67	1.09	1.43	1.28

Value of ANPP is averaged for permanent plots of each stand (SE in parenthesis), except for 174 years-old stand (CR1830). Values with same small letter are not significantly different (p>0.05) between stands (Tukey's HSD test). For the two younger stands (10 and 14 years-old), stem biomass increment (Δy_S) included branch biomass increment (Δy_B). For the other stands, needle biomass increment (Δy_L) was assumed to be zero. Aboveground net assimilation rate (ANAR) is defined as net primary production per unit needle mass (i.e., ANPP/y_L) (Kajimoto et al. unpublished data)

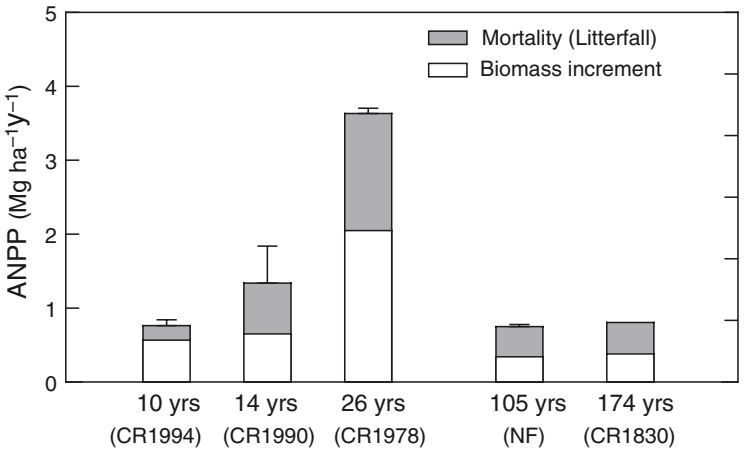

Fig. 6.7 Comparison of aboveground net primary production (ANPP) among five *Larix gmelinii* stands at Tura. Here, data of one stand (NF) with the largest ANPP is selected as a representative of three 105-year-old stands (W1, CF, NF; see Table 6.3) (Kajimoto et al. unpublished data)

unit needle mass (i.e., ANAR = ANPP/y_L), is higher (1.6–1.7 year^{-1}) in the two young stands (14- and 26-years-old) than in the old stands (1.1–1.4 year^{-1}) (Table 6.3). This suggests that as stand ages (> 100 years), annual carbon gain is allocated largely to needle production rather than to growth of woody parts. Similarly, stemwood volume increment per stem mass (relative growth rate of stem during recent 5 years, i.e., $\Delta V_s/w_S$; see Fig. 6.3) was much larger for the sample trees in the young stand (26 years-old, CR1978) than that in the old stands.

ANPP of *L. gmelinii* and *L. cajanderi* has been reported in literature, but it was mostly calculated simply by converting the biomass data with some assumptions or mathematical models (e.g., Shvidenko and Nilsson 1999; Usoltsev et al. 2002). Reliable data of ANPP obtained by the ecological summation method are still limited (methods see Sect. 6.2.3). The ANPP of the 220 years-old stand (1.3 Mg ha^{-1} year^{-1} of C1; Kajimoto et al. 1999) is larger than that (0.4–0.8 Mg ha^{-1} year^{-1}) of other old stands at Tura (>100 years-old; CF, NF, CR1830) (Table 6.3). The difference may be due to larger needle biomass (1.0 Mg ha^{-1}) in > 220 years-old stand compared to other old stands (Table 6.2). It may also be associated with higher individual growth rates in this old multiaged stand where ground-fire occurred several times in the past (i.e., until late 1900). Ground-fire disturbance might have enhanced growth of surviving trees through thinning and improved soil nutrient conditions (Chap. 4). Recent increase in stem height in the old stand (see Fig. 6.5g) may support this interpretation.

Another case study reported that aboveground net production was about 2.5 Mg ha^{-1} year^{-1} in a 169 years-old *L. gmelinii* stand near Yakutsk (Kanazawa et al. 1994). This estimate is much larger than that of old *L. gmelinii* stands at Tura (Table 6.3). However, site condition appeared better in the stand near Yakutsk than in the stands at Tura, since tree size and biomass were also much larger in Yakutsk: average tree height reached 16.9 m, and aboveground total (y_{AT}) and needle biomass (y_L) were 124 and 1.7 Mg ha^{-1}, respectively (Kanazawa et al. 1994).

A wealth of information on forest productivity is available for boreal forest ecosystems (e.g., Schulze et al 1999; Gower et al. 2001; Jarvis et al. 2001). Gower et al. (2001) compared the estimates of above- and below-ground net primary production among major types and regions of evergreen taiga. According to their data (see Tables 4 and 5 in Gower et al. 2001), ANPP ranges from 120 to 370 gC m^{-2} year^{-1} (or 2.4–7.4 Mg ha^{-1} year^{-1} on a dry mass basis) in mature stands (95–250 years-old) of evergreen taiga, such as black spruce (*Picea mariana*) and jack pine (*Pinus banksiana*) in Canada, white spruce (*Picea glauca*) in Alaska, and Norway spruce (*Picea abies*) and Scots pine (*Pinus sylvestris*) in northern Europe. These estimates include net production of understory and mosses. If the ANPP is expressed as the value only for tree components (i.e., woody biomass increments plus needle production or litterfall), the range becomes somewhat smaller (70–350 gC m^{-2} year^{-1}, or 1.4–7.0 Mg ha^{-1} year^{-1}). Some age-sequence studies in boreal forests also reported similar values of ANPP (only tree components), e.g., 100–150 gC m^{-2} year^{-1} in Scots pine forests (100–400 years-old) in Central Siberia (Wirth et al. 2002), and

63 and 110 gC m^{-2} $year^{-1}$ in black spruce forests (151 years-old) at two different soil conditions in interior Alaska (Bond-Lamberty et al. 2004). The range of ANPP in old *L. gmelinii* stands at Tura (0.4–0.8 Mg ha^{-1} $year^{-1}$, or ca. 20–40 gC m^{-2} $year^{-1}$) (Table 6.3) appears lower. Even for the peak value of the 26 years-old stand (about 180 gC m^{-2} $year^{-1}$), it corresponds to lower end of the ANPP range of the evergreen taiga. Potential productivity of permafrost *Larix* taiga in Central Siberia is likely to be the lowest among boreal forest ecosystems worldwide.

6.4.2 Belowground Production

As was mentioned earlier (Sect. 6.1), belowground net primary production (BNPP), or annual production of roots, has rarely been examined in the *Larix* taiga of Siberia by applying commonly used methods such as sequential core-sampling, in-growth core, and minirhizotron. Some fractions of BNPP were previously assessed only in a > 220 years-old *L. gmelinii* stand (C1) in Tura (Kajimoto et al. 1999). In the stand, the BNPP was estimated to be 0.48 Mg ha^{-1} $year^{-1}$, in which coarse and fine root production was 0.18 and 0.30 Mg ha^{-1} $year^{-1}$, respectively. The proportion of coarse root production is about a half of that of fine root production, though coarse root biomass is larger than fine root biomass (11.7 vs. 5.9 Mg ha^{-1}; Table 6.2). Coarse root production of this old stand (about 10 gC m^{-2} $year^{-1}$ in carbon base) is comparable to the range (10–30 gC m^{-2} $year^{-1}$) reported for some old stands of evergreen taiga in northern Canada and Europe (e.g., Gower et al. 2001). Furthermore, smaller proportion of coarse roots in BNPP (about 38%) in C1 agrees with the pattern suggested for the evergreen taiga: carbon allocation into fine root is much larger than that into coarse root (Gower et al. 2001).

It is noted, however, that the estimate of BNPP in the > 220 years-old *L. gmelinii* stand (C1) was calculated as the biomass increment of both coarse and fine roots (i.e., sum of secondary xylem thickening), and root mortality was ignored (Kajimoto et al. 1999). Production and mortality of very small roots occur simultaneously. Very small roots often turnover within 1 year also, as demonstrated in boreal evergreen conifer trees (e.g., black spruce) (Ruess et al. 1996, 2006; Steele et al. 1997). Therefore, true proportion of fine roots in total belowground production would be somewhat larger in the old larch stand (Kajimoto et al. 1999).

Recently, fine root production was assessed in two 105 years-old stands of *L. gmelinii* at Tura (CF, NF) by applying the in-growth coring method. Annual fine root production (i.e., mass of newly elongated roots into the in-growth core) reached about 1.5 (CF) and 0.8 (NF) Mg ha^{-1} $year^{-1}$ (Tokuchi et al. unpublished data). These estimates exceed the biomass increment of coarse and fine roots (0.18 and 0.30 Mg ha^{-1} $year^{-1}$) of the > 220-year-old stand (C1). If we roughly sum up these two values, BNPP in a typical old *L. gmelinii* forest in the study area would be in the order of 1–2 Mg ha^{-1} $year^{-1}$.

6.5 Carbon Allocation Pattern

For three young *L. gmelinii* stands in Tura (< 30 years-old; CR1994, CR1990, CR1978), relative proportion of needle biomass declined with increasing stand age (Fig. 6.4b), but top/root biomass ratio did not differ greatly (i.e., $y_{AT}/y_R = 3.9–5.8$) (Table 6.2). These patterns indicate that a trade-off of carbon allocation occurs mainly between the aboveground woody parts and needles during early growth stages. In other words, annual carbon investment priority might shift gradually from production of needle to those of stem and branch.

In contrast, old *Larix* stands (> 100 years-old) generally showed similar patterns of biomass allocation among the aboveground components (Table 6.2, Fig. 6.4b). Stems always make up the largest proportion (75–90% of aboveground total biomass), followed by branches (8–20%) and needles (2–5%). A small proportion of needle biomass was also reported for old *L. gmelinii* stands (> 120 years-old) located near Yakutsk in Northeastern Siberia: 1.6% (Kanazawa et al. 1994), 1.9–3.2% (Schulze et al. 1995), and 1.9–3.4% (Tsuno et al. 2001). However, small proportion of needle biomass does not mean that a priority of annual carbon allocation into needle production is reduced as stands age. For example, ANPP was much smaller in the old larch stands at Tura (CF, NF, CR1830) than in the young stands (Fig. 6.7), but its allocation into needle production (i.e., needle litterfall; 0.27–0.36 Mg ha^{-1} $year^{-1}$) was as high as that of aboveground woody parts (i.e., biomass increments of stem and branches; 0.17–0.38 Mg ha^{-1} $year^{-1}$) (Table 6.3). Consequently, top/root biomass ratio was much smaller in the old larch stands (2.1–2.8) than in young stands (3.9–5.8) (Table 6.2, Fig. 6.4b). Thus, priority of carbon allocation may shift from growth of stems and/or branches to that of roots as stand ages (> 30 years).

Top/root biomass ratio is known to vary by many factors even in a given forest. Factors that cause the variation include stand age (e.g., Smith and Resh 1999; Mund et al. 2002), soil water (e.g., Keyes and Grier 1981; Comeau and Kimmins 1989), and nutrient conditions (e.g., Grier et al. 1981; Gower et al. 1992; Haynes and Gower 1995). Nevertheless, top/root ratio generally ranges between 4 and 5 (or 20–25% in root proportion) for both conifers and broad-leaved species, and many forest types in different regions (tropical, temperate, boreal) (Karizumi 1974; Santantonio et al. 1977; Kurz et al. 1996; Cairns et al. 1997). This means that similar mass balance between aboveground parts and roots is achieved eventually in many forest ecosystems. However, such a standard rule may not apply in the *Larix* taiga in Siberia, because the top/root ratio of old larch stands in study sites at Tura are much smaller (mostly < 3.0) than this normal range.

Kajimoto et al. (2006) examined the relationship between aboveground total and coarse root biomass (y_{AT} vs. y_{CR}) in old stands of *L. gmelinii* and *L. cajanderi*, including four larch stands described in this chapter (W1, C1, CK and OM), then compared it to the relationship of Scots pine (*Pinus sylvestris*); those pine forests were established in discontinuous- or nonpermafrost regions in Siberia.

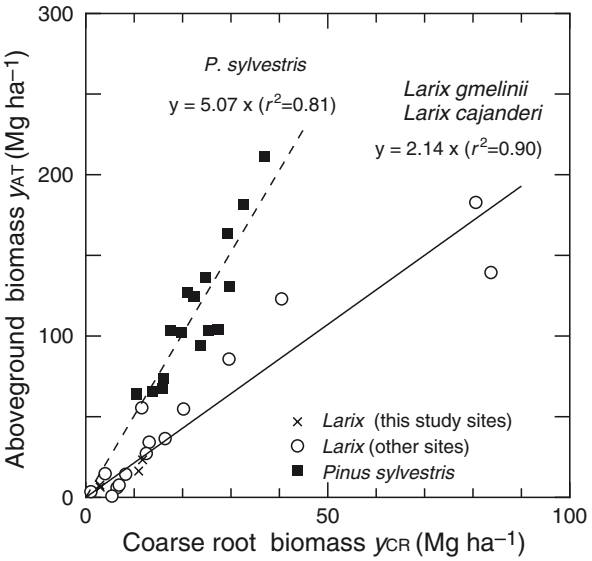

Fig. 6.8 Relationships between coarse root and aboveground total biomass for stands of two *Larix* species ($n=12$ for *L. gmelinii*, $n=7$ for *L. cajanderi*) and stands of Scots pine (*Pinus sylvestris*, $n=16$) in Siberia. Data of four old *Larix* stands in our study sites are shown by *crosses* (Chersky, Oymyakon, W1, and C1; see Table 6.2). *Solid* and *dotted lines* show the fitted linear regressions that are determined for *Larix* ($r^2=0.90$, $p<0.001$) and Scots pine ($r^2=0.81$, $p<0.001$), respectively. Slopes of these two regressions are different significantly ($p < 0.001$; ANCOVA) (redrawn from Kajimoto et al. 2006)

As shown in Fig. 6.8, the slope of this linear relationship for *Larix* (i.e., mean top/root ratio = 2.3) is significantly smaller than that for Scots pine (5.0). The difference suggests that, even in Siberia, very large carbon allocation into roots (or small top/root ratio) of old growth stands is achieved only in *Larix* taiga distributed in the continuous permafrost region. Rather root-oriented pattern of carbon allocation may be primarily explained as a positive growth response of larch trees against a constraint of available soil nutrients in the permafrost region (Kajimoto et al. 1999; see also Chaps. 8 and 12).

Larix sibirica, another species in boreal forest in Siberia, grows in the non-permafrost region of Siberia. Pozdynakov (1975) reported that top/root biomass ratio ranged 3.8–4.5 for the tree *L. sibirica* stands (> 80 years-old) (also see Usoltsev 2001). A similar value of top/root ratio (ca. 5.0) was also reported for young *L. sibirica* stands (32 years-old) that were planted in Iceland (Snorrason et al. 2002). Although available data of belowground biomass obtained under natural growth habitats of this larch species are restricted, its above-/belowground carbon allocation appears similar to that of other nonpermafrost boreal tree species (e.g., Scots pine), rather than the permafrost larch species (*L. gmelinii*, *L. cajanderi*).

6.6 Conclusions

Processes of carbon accumulation and allocation were examined in stands of two larch species (mainly *L. gmelinii*) growing in the Siberian permafrost region. Belowground processes of the *Larix* taiga still remain unclear – fine root production in particular. However, the following characteristic features are recognized:

- Potential carbon stock and ANPP of the permafrost larch forests at the old stage (>100 years old) are smaller than those of other boreal forests (i.e., evergreen taiga) distributed in the non or discontinuous permafrost regions.
- ANPP increases sharply and peaks at stand ages of about 30 years, but declines substantially as the stand ages further.
- Carbon allocation pattern differs between young (< 30 years old) and old growth stages, and root-oriented carbon allocation is achieved as the stand ages.

Among these features, low productivity might be primarily a result of environmental constraints that appear common to other high-latitude regions, such as low temperature and short growing season. In the *Larix* forests of Central Siberia, however, needle biomass is generally small (< 1.0 Mg ha^{-1}). The period of active carbon uptake by larch needles is restricted to less than 2 months, from mid-June to mid-August (Nakai et al. 2008; see also Chap. 10). The beginning of needle flush or stem diameter growth largely depends on the timing of soil-thawing in spring, and does not start simply in response to increasing air temperature (Kujansuu et al. 2007; see Chap. 17). Attributes conferred to deciduous species, coupled with the presence of permafrost, might have contributed to the lower potential of productivity.

The age-related change in ANPP agrees with the pattern found in many monospecific, even-aged forests (e.g. Smith and Resh 1999; Mund et al. 2002). Underlying mechanism of such age-related growth decline can be explained by several combined factors: reduction in photosynthetic capacity, nutrient limitation, and changes in top/root carbon allocation (Ryan et al. 1997). Available soil nutrients, especially nitrogen, are essentially limited in the permafrost *Larix* taiga of Siberia (Tokuchi et al. 2003; Kondo et al. 2004; also see Chaps. 8 and 12). As Schulze et al. (1995) demonstrated in the age-sequence study of *L. gmelinii* forests near Yakutsk, available soil-N may be reduced following stand development, and hence, limit biomass accumulation. Thus, the nutrient limitation hypothesis may primarily explain the age-related decline in biomass accumulation and/or ANPP in the *Larix* taiga. The inferred shift of carbon allocation pattern with stand age (i.e., from above- to root-oriented pattern) suggests that nutrient limitation is also linked to the hypothesis of allocation change: larch trees invest carbon to root system development for exploiting limited soil nutrients rather than to crown enlargement (Kajimoto et al. 2007; also see Chap. 16).

The root-oriented pattern of carbon allocation at the old growth stage implies that roots (i.e., coarse roots) function as important carbon sink in the permafrost *Larix* taiga (Kajimoto et al. 1999). Thus, even for the purpose of large-scale evaluation of forest carbon stock, especially for belowground C-pool, the permafrost

Larix ecosystem should be treated separately from other nonpermafrost forest types in Siberia (e.g., Scots pine and *Larix sibirica*).

Present data are still insufficient to discuss exactly how and when biomass and productivity change along a stand age-sequence in permafrost larch forests, since data from stands of intermediate age classes (i.e., 30–100 years-old) have not been available. Local-scale variations of biomass and productivity should also be examined further. It was observed that abrupt tree growth decline occurred at different timings among three 105 years-old stands (Sect. 6.3.1). This finding suggests that, even if age-related growth decline is likely to be caused by limitation in soil nutrients, start of such decline varies depending on local site conditions. Soil temperature and active layer thickness might be particularly important, since both factors vary together over stand development in the permafrost region (see Chaps. 7, 16, and 24). Further studies focusing on multiple linkages among soil environments, nutrients, tree growth, and temporal trends of these linkages are needed for further understanding of processes in carbon accumulation and allocation in the permafrost forest ecosystem.

References

Abaimov AP (1995) The larches of Siberian permafrost zone and their species peculiarities in progressive successions. In: Martinsson O (ed) Larch genetics and breeding: research findings and ecological-silvicultural demands. Swedish University of Agricultural Sciences, Umeå, pp 11–15

Alexeyev VA, Birdsey RA (1998) Carbon storage in forests and peatlands of Russia. USDA Forest Service, Northeastern Forest Experiment Station, GTR NE-244, 137pp

Alexeyev VA, Birdsey RA, Stakanov VD, Korotkov IA (1995) Carbon in vegetation of Russian forests: methods to estimate storage and geographical distribution. Water Air Soil Poll 82:271–282

Bhatti JS, Apps MJ, Jiang H (2002) Influence of nutrients, disturbance and site conditions on carbon stocks along a boreal forest transect in central Canada. Plant Soil 242:1–14

Bond-Lamberty B, Wang C, Gower ST (2002) Aboveground and belowground biomass and sapwood area allometric equations for six boreal tree species of northern Manitoba. Can J For Res 32:1441–1450

Bond-Lamberty B, Wang C, Gower ST (2004) Net primary production and net ecosystem production of a boreal black spruce wildfire chronosequence. Global Change Biol 10:473–483

Cairns MA, Brown S, Helmer EH, Baumgardner GA (1997) Root biomass allocation in the world's upland forests. Oecologia 111:1–11

Chapin FS III, Mcguire AD, Randerson J, Pielke SRR, Baldocchi D, Hobbie SE, Roulet N, Eugster W, Kasischke E, Rastetter EB, Zimov SA, Running SW (2000) Arctic and boreal ecosystems of western North America as components of the climate system. Global Change Biol 6:211–223

Comeau PG, Kimmins JP (1989) Above- and below-ground biomass and production lodgepole pine on sites with differing soil moisture regimes. Can J For Res 19:447–454

Goulden ML, Wofsy SC, Harden JW, Trumbore SE, Rill PM, Gower ST, Fries T, Daube BC, Fan S-M, Sutton DJ, Bazzaz A, Munger JW (1998) Sensitivity of boreal forest carbon balance to soil thaw. Science 279:214–217

Gower ST, Vogt KA, Grier CC (1992) Carbon dynamics of Rocky Mountain Douglas-fir: influence of water and nutrient availability. Ecol Monogr 62:43–65

Gower ST, Krankina O, Olson RJ, Apps M, Linder S, Wang C (2001) Net primary production and carbon allocation patterns of boreal forest ecosystems. Ecol Appl 11:1395–1411

Grier CC, Vogt KA, Keyes MR, Edmonds RL (1981) Biomass distribution and above- and below-ground production in young and mature *Abies amabilis* zone ecosystems of the Washington cascades. Can J For Res 11:155–167

Haynes BE, Gower ST (1995) Belowground carbon allocation in unfertilized and fertilized red pine plantations in northern Wisconsin. Tree Physiol 15:317–325

Isaev A, Korovin G, Zamolodchikov D, Utkin A, Pryaznikov A (1995) Carbon stock and deposition in phytomass of the Russian forests. Water Air Soil Poll 82:271–282

Jackson RB, Mooney HA, Schulze E-D (1997) A global budget for fine root biomass, surface area, and nutrient contents. Proc Natl Acad Sci USA 94:7362–7366

Jarvis PG, Saugier B, Schulze E-D (2001) Productivity of boreal forests. In: Roy J, Saugier B, Mooney HA (eds) Terrestrial global productivity. Academic Press, San Diego, pp 211–244

Kajimoto T, Matsuura Y, Sofronov MA, Volokitina AV, Mori S, Osawa A, Abaimov AP (1999) Above- and belowground biomass and net primary productivity of a *Larix gmelinii* stand near Tura, central Siberia. Tree Physiol 19:815–822

Kajimoto T, Matsuura Y, Osawa A, Prokushkin AS, Sofronov MA, Abaimov AP (2003) Root system development of *Larix gmelinii* trees affected by micro-scale conditions of permafrost soils in central Siberia. Plant Soil 255:281–292

Kajimoto T, Matsuura Y, Osawa A, Abaimov AP, Zyryanova OA, Isaev AP, Yefremov DP, Mori S, Koike T (2006) Size-mass allometry and biomass allocation of two larch species growing on the continuous permafrost region in Siberia. For Ecol Manage 222:314–325

Kajimoto T, Osawa A, Matsuura Y, Abaimov AP, Zyryanova OA, Kondo K, Tokuchi N, Hirobe M (2007) Individual-based measurement and analysis of root system development: case studies for *Larix gmelinii* trees growing on the permafrost region in Siberia. J Forest Res 12:103–112

Kanazawa Y, Osawa A, Ivanov BI, Maximov TC (1994) Biomass of a Larix gmelinii (Rupr.) Litv. stand in Spaskayapad, Yakutsk. In: Inoue G (ed) Proceedings of the second symposium on the joint Siberian permafrost studies between Japan and Russia in 1993. National Institute for Environmental Studies, Tsukuba, pp 153–158

Karizumi N (1974) The mechanism and function of tree root in the process of forest production. 1. Method of investigation and estimation of the root biomass. Bull Gov For Exp Sta 259:1–99

Keyes MR, Grier CC (1981) Above- and below-ground net production in 40-years-old Douglas-fir stands on low and high productivity sites. Can J For Res 11:599–605

Kondo K, Tokuchi N, Hirobe M, Kajimoto T, Matsuura Y, Osawa A, Abaimov AP (2004) Does nitrogen limiting factor of for plant growth in Larch forest in Tura, central Siberia? In: Tanaka H (ed) Proceeding of the fifth international workshop on global change: connection to the Arctic 2004 (GCCA5). Tsukuba University, Tsukuba, pp 195–198

Kujansuu J, Yasue K, Koike T, Abaimov AP, Kajimoto T, Takeda T, Tokumoto M, Matsuura Y (2007) Responses of ring widths and maximum densities of *Larix gmelinii* to climate on contrasting north- and south-facing slopes in central Siberia. Ecol Res 22:582–592

Kurz WA, Beukema SJ, Apps MJ (1996) Estimation of root biomass and dynamics for the carbon budget model of the Canadian forest sector. Can J For Res 26:1973–1979

Mund M, Kummetz E, Hein M, Bauer GA, Schulze E-D (2002) Growth and carbon stocks of a spruce forest chronosequence in central Europe. For Ecol Manage 171:275–296

Nakai Y, Matsuura Y, Kajimoto T, Abaimov AP, Yamamoto S, Zyryanova OA (2008) Eddy covariance CO2 flux above a Gmelin larch forest on continuous permafrost of Central Siberia during a growing season. Theor Appl Climatol 93:133–147

Osawa A, Abaimov AP, Matsuura Y, Kajimoto T, Zyryanova OA (2003) Anomalous patterns of stand development in larch forests of Siberia. Tohoku Geophys J 36:471–474

Pozdnyakov LK (1975) Larix dahurica. Nauka, Moscow, 310pp (in Russian)

Pozdnyakov LK, Protopopov VV, Gorbatenko VM (1969) Biological productivity of central Siberia and Yakutiya forests. Institute of Forest and Wood, Siberian Branch of the USSR Academy of Sciences, Krasnoyarsk, 156pp (in Russian)

Ruess RW, Van Cleve K, Yarie J, Viereck LA (1996) Contributions of fine root production and turnover to the carbon and nitrogen cycling in taiga forests of the Alaskan interior. Can J For Res 26:1326–1336

Ruess RW, Hendrick RL, Vogel JG, Sverinbjornsson B (2006) The role of fine roots in the functioning of Alaskan boreal forests. In: Chapin FS III, Oswood MW, Van Cleve K, Viereck LA, Verbyla DL (eds) Alaska's changing boreal forest. Oxford University Press, New York, pp 189–210

Ryan MG, Binkley D, Fownes JH (1997) Age-related decline in forest productivity: pattern and process. Adv Ecol Res 27:213–262

Santantonio D, Hermann RK, Overton WS (1977) Root biomass studies in forest ecosystems. Pedobiologia 17:1–31

Schulze E-D (ed) (2000) Carbon and nitrogen cycling in European forest ecosystems. Ecological studies, vol 142. Springer, Berlin, 500pp

Schulze E-D, Schulze W, Kelliher FM, Vygodskaya NN, Ziegler W, Kobak KI, Koch H, Arneth A, Kusnetsova WA, Sogatchev A, Issajev A, Bauer G, Hollinger DY (1995) Aboveground biomass and nitrogen nutrition in a chronosequence of pristine Dahurian *Larix* stands in eastern Siberia. Can J For Res 25:943–960

Schulze E-D, Lloyd J, Kelliher FM, Wirth C, Rebmann C, Luhker B, Mund M, Knohl A, Milyukova IM, Schulze W, Ziegler W, Varlagin AB, Cogachev AF, Valentini R, Dore S, Grigoriev S, Kolle O, Panfyorov MI, Tchebakova N, Vygodskaya NN (1999) Productivity of forests in Eurosiberian boreal region and their potential to act as a carbon sink – a synthesis. Global Change Biol 5:703–722

Shvidenko A, Nilsson S (1999) Phytomass, increment, mortality and carbon budget of Russian Forests. Interim Report IR-98-105/December, IIASA, Laxenburg, 25pp

Smith FW, Resh SC (1999) Age-related changes in production and below-ground carbon allocation in *Pinus contorta* forests. For Sci 45:333–341

Snorrason A, Sigurdsson BD, Gudbergsson G, Svavarsdottir K, Jonsson PH (2002) Carbon sequestration in forest plantations in Iceland. Icel Agr Sci 15:81–93

Steele SJ, Gower ST, Vogel JG, Norman JM (1997) Root mass, net primary production and turnover in aspen, jack pine and black spruce forests in Saskatchewan and Manitoba, Canada. Tree Physiol 17:577–587

Tokuchi N, Hirobe M, Kondo K, Prokushkin AS, Matsuura Y, Kajimoto T (2003) N cycling at a *Larix* stand in Tura, central Siberia – preliminary work. In: Matsumi Y (ed) Proceedings of the fourth international workshop on global change: connection to the Arctic 2003 (GCCA4). Nagoya University, Toyokawa, pp 139–143

Tsuno Y, Shibuya M, Saito H, Takahashi K, Sawamoto T, Hatano R, Isaev AP, Maximov TC (2001) Aboveground biomass, nitrogen and carbon contents in Larix stands in eastern Siberia. In: Fukuda M, Kobayashi Y (eds) Proceedings of the ninth symposium on the joint Siberian permafrost studies between Japan and Russia in 2000. Hokkaido University, Sapporo, pp 68–74

Usoltsev VA (2001) Forest biomass of northern Eurasia: data base and geography. Russian Academy of Sciences, Ural Branch, Botanical Garden, Yekaterinburg, 706pp (in Russian with English summary)

Usoltsev VA (2003) Forest biomass of northern Eurasia: the limits of productivity and their geography. Russian Academy of Sciences, Ural Branch, Botanical Garden, Yekaterinburg, 406pp (in Russian with English summary)

Usoltsev VA, Koltunova AI, Kajimoto T, Osawa A, Koike T (2002) Geographical gradients of annual biomass production from larch forests in northern Eurasia. Eurasian J For Res 5:55–62

Van Cleve K, Oliver L, Schlentner R, Viereck LA, Dyrness CT (1983) Productivity and nutrient cycling in taiga forest ecosystems. Can J For Res 13:747–766

Van Cleve K, Chapin FS III, Flanagan PW, Viereck LA, Dyrness CT (1986) Forest Ecosystems in the Alaskan Taiga. Ecological studies, vol 57. Springer, Berlin, 230pp

Vogt KA, Vogt DJ, Palmiotto PA, Boon P, O'Hara J, Asbjornsen H (1996) Review of root dynamics in forest ecosystems grouped by climate, climatic forest type and species. Plant Soil 187:159–219

Wirth C, Schulze E-D, Kusznetova V, Milyukova I, Hardes G, Siry M, Schulze B, Vygodskaya NN (2002) Comparing the influence of site quality, stand age, fire and climate on aboveground tree production in Siberian Scots pine forests. Tree Physiol 22:537–552

Chapter 7
Development of Stand Structure in Larch Forests

A. Osawa and T. Kajimoto

7.1 Introduction

Boreal forests of northern hemisphere are considered to be the major carbon sink in the world, and are potentially affecting carbon balance at large geographical scales (Kasischke and Stocks 2000; Schimel et al. 2001). This biome may be affected by warming air temperature, as the northern latitudes are where the effect of global warming is likely to be felt most strongly in the next several decades (Solomon et al. 2007). Therefore, better understanding of the patterns of forest development is relevant today, with respect to carbon sequestration of the ecosystems (Wirth et al. 2002).

One of the most influential characteristics of the environment of boreal forest biome is the permafrost – the perennially frozen soils at various thickness and spatial extent. As was detailed in Chap. 1, most of *Larix gmelinii* forests exist on the permafrost that is spread continuously. State of the permafrost could also change over time, and is not constant. Temporal change in the depth of soil active layer after forest fires shows a peculiar characteristic in boreal forests. Forest fires often remove most of the living biomass aboveground. Then, the soil becomes warmer by increased albedo and amount of direct solar radiation. This is followed by the deepening of the soil active layer(Abaimov et al. 1998). By stand age of 30–40 years, a layer of mosses develops gradually on the forest floor acting as effective insulation. The permafrost then rises toward the soil surface, recovering the predisturbance level (Kajimoto et al. 2007; see also Chaps. 4 and 16).

Tree morphology and stand structure may be affected by the changes in the soil active layer over time. For example, root development of trees must accommodate changes of the soil environment. Lateral roots develop at deeper parts of the soil (>30 cm) at the initial stage of stand growth. However, the deeper roots are gradually sealed into the frozen soil, and die (Kajimoto et al. 2003; see also Chap. 16). Then, new lateral roots develop adventitiously at shallower soil horizons as the trees grow. Therefore, development patterns of larch forests on Siberian permafrost may appear different from those of the even-aged forests of other biomes in the world. Patterns of stand development on continuous permafrost have rarely been studied outside of Siberia, since such ecosystems are rare (Zoltai 1975; Dyrness

A. Osawa et al. (eds.), *Permafrost Ecosystems: Siberian Larch Forests*,
Ecological studies, Vol. 209, DOI 10.1007/978-1-4020-9693-8_7,

et al. 1986). However, the potential to sequestrate a large amount of carbon in the vast areas of boreal forests, particularly in Siberia, justifies detailed examination of their stand development (Apps et al. 1993; Kasischke and Stocks 2000). The purpose of the present chapter is to summarize published data on the structure of *L. gmelinii* forests, combine them with additional observation, and suggest possible patterns of stand development of this species that grow on permafrost.

7.2 Approaches to Describe Stand Development in Larch Forests

Four separate sources of information will be used to characterize the stand development in *L. gmelinii*. First is published data of yield-density relationship that describe the patterns between stand density and aboveground biomass. Second is yield table data used in Russia that summarize possible effect of site condition on the relationship between stand yield and density. Third is our new observation on the changes in aboveground biomass and stand density inferred from a series of chronosequence stands. Measurement was also taken from additional stands to characterize tree size-stand density relationship of the species. Fourth is our published data on the estimated patterns of stand development over time that were drawn from various methods of quantitative stand reconstruction.

7.2.1 Study Site

An intensive study of larch forest structure and development was conducted for *L. gmelinii* at Tura (64°N, 100°E; ca.160 m a.s.l.) located in Evenkia Region of Central Siberia (Fig. 1.1). Data came from three sites (Sites 1, 2, and 3; see Fig. 1.3 and Table 1.1). Permafrost is distributed continuously with varying depth of soil active layer (see Chap. 1). Its depth increases dramatically after fire (up to 140 cm) in the upland sites of the present study area. Then, several decades later, recovery of the permafrost makes the depth of active layer reach a prefire level (30–70 cm) (Abaimov et al. 1998; Osawa et al. 2003)

7.2.2 Measurement of Chronosequence Plots

Even-aged stands with no signs of intermittent ground fires were selected for the study in Sites 1, 2, and 3 (Fig. 1.3). Rectangular plots of *L. gmelinii* forests of various sizes were established in six stands representing six forest ages of 10, 14, 26, 105, 174, and 266 years as of the year 2004. They developed after stand-replacing fires

of 1994, 1990, 1978, 1899, 1830, and 1740, and are referred to as plots CR1994, CR1990, CR1978, CR1899, CR1830, and C1, respectively (details see Table 1.1 and Fig. 6.1). All plots are on gentle slopes (ca. 5–15°) of NW to E aspects where the forest floor and shrub layer are characterized by relative abundance of *Pleurozium schreberi*, *Cladina stellaris*, *Vaccinium vitis-idaea*, *V. uliginosum*, *Duschekia fruticosa,* and *Ledum palustre* (Zyryanova and Abaimov, personal communication; see also Chaps. 2 and 5).

Site quality of *L. gmelinii* stands is quite variable, as being indicated by site index (Fig. 7.1). The stands that we analyzed as chronosequence and with the stand reconstruction technique were growing on one of the poorest site categories of site index Vb, an index representing a condition slightly worse than index Va shown in Fig. 7.1 (Abaimov et al. 1998; Usoltsev 2001). The site index is estimated in Russian forestry as mean tree height that is reached at a given time after stand establishment (Usoltsev 2002). The Vb site and a slightly better Va site are associated with continuous permafrost soils. Site index V represents even better growing condition (Fig. 7.1), and is also associated with permafrost. In contrast, the site index I through IV in Fig. 7.1 corresponds to relatively good sites, where the trees grow without the permafrost mostly in southern Siberia (Abaimov et al. 1998). A total of 33 chronosequence plots were established in stands of site index Vb. The plot C1 is an old multiaged stand that had experienced multiple surface fires in the past (Kajimoto et al. 1999; see also Table 1.1 and Chap. 6). It is not strictly considered a chronosequence with other Vb plots, but is included in this category for comparison.

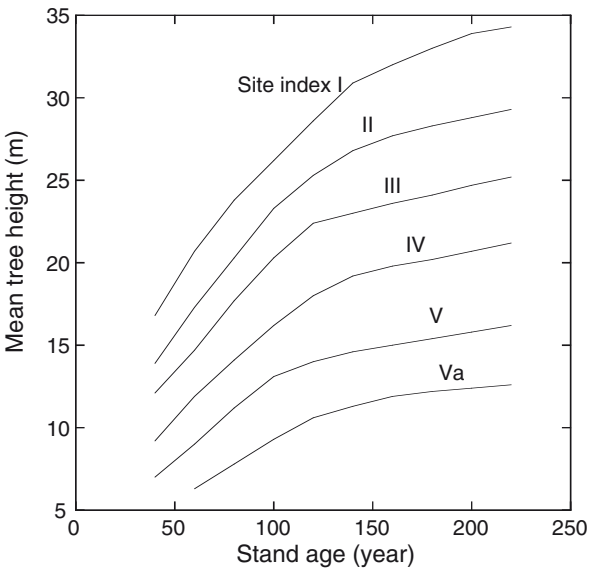

Fig. 7.1 Growth patterns of mean tree height in *Larix gmelinii*, defining site index of individual stands (data from Usoltsev 2002)

Aboveground dry biomass and stand density of *L. gmelinii* forests were estimated as follows. Stem diameter at breast height (dbh in cm), stem diameter at 0.3 m aboveground ($d_{0.3}$ in cm), tree height (h in cm), and height of crown base (h_B in cm) of all or selected individuals of various proportions were measured with rectangular plots of various sizes, so that more than 100 living trees were included in each plot. Aboveground biomass of individual trees was calculated with site-independent regression equations developed for the present study area (Osawa et al. unpublished data). Then, total aboveground biomass of a plot was computed. Stand density was estimated by counting the number of live trees in a plot.

Among the chronosequence plots on site index Vb, two in 105-year-old stand (CR1899) and two in 174-year-old stand (CR1830; see Table 1.1) were measured by the plot-less wandering quarter method (WQM; Catana 1963). Aboveground biomass of individual trees was estimated with the same method applied to the rectangular plots. Mean tree height, aboveground biomass, and stand density of these plots were then calculated.

7.2.3 Measurement of Additional Stands

Sixty stands of additional *L. gmelinii* forests were measured in Sites 1, 2, and 3, so that data from stands of various age and density are included. All stands were considered even-aged, and varied in canopy height, age, and/or stand density. Stand density, mean tree height, and mean dbh were estimated in each stand with the WQM (55 stands) or by the plot measurement (five stands). Then, aboveground biomass was calculated. Data from these stands were used for the analysis of yield-stand density relationship with the published data available (see Sect. 7.2.5). Maximum tree height was also estimated in fifteen stands, among the 60 that were investigated, by measuring the tallest tree that was selected by eye in the stand, when it was examined with the WQM. The maximum tree height data were used for the reconstruction of stand density (see Sect. 7.6.3).

7.2.4 Yield-Density and Yield Table Data

Published data were used for the analysis of yield-density relationship of *L. gmelinii*. Plot of such data commonly reveals the upper-boundary condition of the aboveground biomass (yield) vs. stand density relationship, suggesting the possible course of structural development when the stand tends to be crowded. We used data of 40 stands by Bondarev (1997) and 89 stands by Usoltsev (2001) measured or compiled for the species growing mostly in Central Siberia. All stands and 43 stands reported in Bondarev (1997) and Usoltsev (2001), respectively, were distributed in the region of continuous permafrost in northern part of Siberia. On the other hand, 46 stands in Usoltsev (2001) grew in southern Siberia where the effect of the

permafrost was negligible, and had better site index of I through IV. Yield table data given in Usoltsev (2002) were used to infer possible development patterns of *L. gmelinii* stands that grow on different sites. Trees generally attain greater height and biomass in a given number of years when they are present on sites of better quality. Possible effect of site condition on stand development will be examined with this data set.

7.2.5 Reconstructing Past Stand Structure

Patterns of structural development were studied for plot L14 located in Site 1 (see Table 1.1), a stand that we consider a typical forest in the region, which was regenerated naturally after a stand-replacing fire of some 100 years ago. A few methods of stand reconstruction techniques were employed for the examination. First is the stem analysis, an analysis of growth rings in individual trees. Second is the analysis of dead trees by harvesting and counting the number of rings at the ground level. This presents information on the pattern of tree mortality. Third is the quantitative reconstruction of stem size distribution, stand density, total stem volume, and stem volume growth of the whole stand; this quantitative method was proposed recently by Osawa et al. (2000a), and was first applied to the current study area.

A rectangular plot of 12 m × 18 m (plot L14) was established in an area of relatively dense *L. gmelinii* stand. Dead stems are abundant in the stand, indicating that the forest has been undergoing active self-thinning. All living trees were numbered, and their dbhs were measured. Small trees that did not reach the breast height were not measured, but their number was negligibly small. Fifteen largest trees (in dbh) and three smaller ones in the plot were cut at the ground level. Stem disks were collected at the following distances from the stem base: 0, 0.3, 1.3, 2.3 m, and upwards at 1-m intervals. Among these 18 harvested trees, stem analysis was conducted for five individuals of various sizes. Then, ring widths were measured along four radii of the breast height disks of the 15 largest trees that were harvested. There were 98 trees in the plot, or 4,120 trees ha^{-1}. Maximum tree height was 11.2 m. Maximum and mean dbh were 10.7 and 5.43 cm, respectively. Ages of the trees were between 95 and 97 years at the ground level, regardless of stem size. Charcoal was found in the forest floor. It suggests that the stand regenerated nearly simultaneously after a major forest fire that destroyed the previous stand.

All dead trees in plot L14 were marked and cut at the ground level. A stem disk was sawed out from each tree at the ground level. These stem disks were brought to the laboratory, sanded, and the number of growth rings was counted to estimate the time of tree death. A difference between 97 and the number of rings was assumed to be the year before present when the tree died, since the stand is considered even-aged, and became established 97 years ago. Decomposition rate of the dead stems appeared very slow, which allowed examination of nearly all stems that were collected. There were several stems in plot L14 that did not permit

detailed examination due to decay. However, the error associated with the lack of samples appears small. Consult Osawa et al. (2000a, 2005) for details of the quantitative method of reconstructing stand structure in the past that was applied in the present study

7.3 Yield-Density Relationship

There is a well-known rule in plant ecology that stand density (N) of dense populations of trees and yield (Y), as measured by either aboveground biomass, stem biomass, or stem volume for the whole stand, are related with a mathematical relationship,

$$Y = K \cdot N^{\gamma}, \tag{7.1}$$

where K is a real constant and γ is approximately $-1/2$. This relationship was first introduced to international literature by Yoda et al. (1963), and is called the $-3/2$ power law of self-thinning, the self-thinning rule, or similar terms (White and Harper 1970; Harper 1977; Westoby 1984; Weller 1987; Norberg 1988; Begon et al. 1996). It suggests that there should be a boundary condition for the possible combination of the values of stand density and yield. Plant populations can be at a state of any density vs. yield combinations, but they can never attain the yield above this boundary line for a given stand density (see Roscher et al. 2007 for more recent views). The relationship is expressed as a straight line with a slope of about $-1/2$, when Y and N are plotted on abscissa and ordinate, respectively, on double logarithmic coordinates. Many examples of plant populations have been presented that appear to obey the self-thinning rule (see reviews; Harper 1977; White 1980; Westoby 1984). The relationship has also been considered a general law in plant ecology (Hutchings 1983).

There has been debate on the generality of the self-thinning rule (Weller 1987; Osawa and Sugita 1989; Lonsdale 1990; Osawa and Allen 1993; Enquist et al. 1998), but it is nearly exclusively on the existence of a constant exponent γ. It has rarely been questioned as to the presence of the relationship of (7.1), particularly in natural plant populations. However, development of larch stands in Central Siberia may present a picture different from what has been conceived by studies of plant populations elsewhere.

Figure 7.2 shows plot of the aboveground biomass vs. stand density relationship for 144 stands of *L. gmelinii* that was compiled by Bondarev (1997) and Usoltsev (2001), along with 60 stands measured in the present study; a more complete analysis is presented by Osawa et al. (in preparation) with more than 300 stand data. The points are widely scattered in Fig. 7.2. A straight-line relationship of a possible boundary condition with a slope of approximately $-1/2$ is beginning to become apparent if we consider plots from all site categories (site index values of I through Vb). Our experience of examining self-thinning relationships for other tree species suggests that collection of data from 20 to 30 stands of natural forests of various

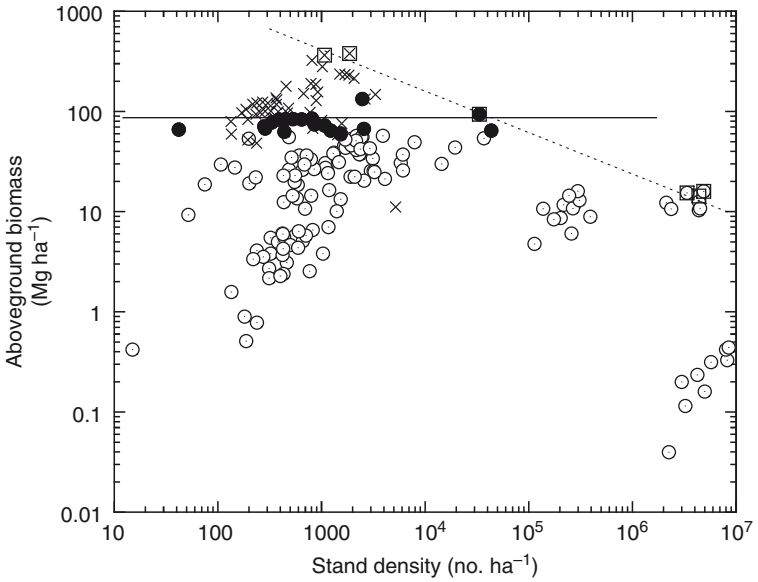

Fig. 7.2 Relationship of aboveground biomass and stand density for *Larix gmelinii*. The self-thinning boundary (*broken line*) was fitted through five stands by considering all stand data. The line of attainable maximum aboveground biomass (*solid line*) applies to the stands of site index V, Va, Vb, or worse (19 stands). Symbols represent the following: *open circle*, site index V, Va, Vb, or worse; cross, site index I, II, III, or IV; *open square*, stands used to fit the self-thinning boundary; *filled circle*, stands near the attainable maximum biomass in poor site condition

mean stem sizes that could be considered relatively dense in a study area is generally sufficient to define a self-thinning relationship. A similar collection of 100 stands should be considered more than adequate. See examples of the self-thinning relationships defined by such methods in Osawa and Allen (1993), Osawa (1995), Begin et al. (2001), and Osawa and Kurachi (2004). The fitted boundary line has a slope −0.39 with 95% Confidence Interval (−0.45, −0.34). The predicted slope was somewhat shallower than the theoretical value of −1/2.

The pattern of aboveground biomass-stand density relationship seems different for relatively sparse stands, when we limit the analysis for stands growing on the region of continuous permafrost (only stands with site index V, Va, Vb, and worse). It appears that the maximum yield that is attainable is nearly constant below the stand density of approximately 50,000 stems ha^{-2}. The second boundary line in Fig. 7.2 has a slope 0.01 with the ordinary least squares regression. The t value for testing the null hypothesis of slope = 0 is 0.718 with 17 degrees of freedom. Therefore, the null hypothesis cannot be rejected at the 5% level. We may call this constant level of biomass the attainable maximum aboveground biomass or asymptotic aboveground biomass. Presence of the attainable maximum aboveground biomass will be common because site index of nearly all stands in the region of continuous permafrost is restricted to V, Va, Vb, or worse.

If the above interpretation is true, this may indicate that the self-thinning relationship shows anomaly in stands growing over the permafrost. Schulze et al. (1995) suspected previously that the self-thinning slope may be unusually shallow in *L. gmelinii* stands that developed over the permafrost. Divergence of the self-thinning relationship may be observed under four situations. First, the attainable yield becomes constant (as in the case of present study) when the light level is reduced by shading. Cases were reported for two herb species that were grown experimentally: *Helianthus annuus* (White and Harper 1970) and *Lorium perenne* (Kays and Harper 1974). Second, the yield is greatly reduced, and the slope of the thinning relationship (7.1) becomes shallower when *Ocimum basilicum* is grown in sand under a nutrient poor condition (Morris and Myerscough 1991). Low levels of soil fertility were clearly shown to reduce both thinning intercept and gradient of the thinning slope in another experiment with *Ocimum basilicum* (Morris 1996). Such a diversion was not observed in growth experiments under various soil fertility levels in *Erigeron canadensis* (Yoda et al. 1963) and in *Brassica napus* and *Raphanus sativus* (White and Harper 1970). These older experiments have led to an interpretation that soil fertility levels do not affect the specific self-thinning relationship (Harper 1977). However, the experiments of Yoda et al. (1963) and White and Harper (1970) did not contain soils of very low fertility. Therefore, it is likely that sufficiently low supply of resources (be it light or nutrient) would not allow the plant populations to adhere to the classic self-thinning relationship (7.1). Rather, the yield becomes constant, or the thinning slope becomes shallower, for a wide range of stand density even without obvious effects of natural disturbances such as fire (Wirth et al. 2002).

Third, the yield appears constant for relatively low stand density in managed stands of beech and oak (White and Harper 1970). Harper (1977) interprets this as the result of selective cutting being conducted. The amount of new tree growth is compensated for by the wood volume removed by forestry operations, thereby maintaining more or less constant level of stand yield. Nakashizuka (1987) reported constant aboveground biomass in mature *Fagus crenata* forests in Japan at relatively low stand densities. The constant biomass may have been realized through limited resources (second situation). Management history and occurrence of natural disturbances are also possible reasons. Theoretical constructs of plant succession also advocate constant biomass in mature ecosystems (Odum 1969; Bormann and Likens 1979). This may be produced under the influence of limiting resources (Botkin et al. 1972) or of natural disturbances (Bormann and Likens 1979).

Fourth, the competition-density effect (Kira et al. 1953; Harper 1977) dictates that stands of the same age, but different densities at a time of observation, may show constant yield if mortality of individuals is not occurring.

For the present example of self-thinning in *L. gmelinii* populations, the light will not be a limiting resource, since leaf biomass of any *L. gmelinii* stand is relatively small (ca. 1–2 Mg ha^{-1} in dry mass; Kajimoto et al. 1999; see also Chap. 6). Light is usually abundant even near the forest floor and cannot be conceived as limiting growth and survival of the trees. The stands under consideration are also natural populations of trees with no forest management, and are undergoing active self-thinning.

The latter is evident from many dead standing stems in the stands. Therefore, the third and fourth explanations cannot be used as the reason for the constant yield in *L. gmelinii* populations, either. Majority of stands shown in Fig. 7.2 have never experienced forest fires when stand density is greater than 5,000 ha^{-1}. Tendency of biomass not exceeding a constant level is already evident in the density range of 5,000–50,000 stems ha^{-1}. Therefore, fire is not a likely cause of density reduction. Only one explanation is remaining, which is plausible. Soil fertility may be extremely low in Central Siberia where stands of *L. gmelinii* develop naturally. Evidence is abundant. First, soils of northern boreal forests and particularly those with permafrost are generally poor in nutrient condition (Van Cleve et al. 1983; Schulze et al. 1995). Soil analyses in the present study area indicate that it is indeed the case in Central Siberia (see also Chap. 8). Matsuura and Abaimov (2000) measured net nitrogen mineralization and net nitrification near plot L14 as the ranges between −0.38 and 0.43 gN $m^{-2}year^{-1}$ and between 0.10 and 0.35 gN $m^{-2}year^{-1}$, respectively. The values were extremely low; even lower than the values reported for other boreal forests and arctic tundra (Nadelhoffer et al. 1992; Van Cleve et al. 1993). That for net nitrogen mineralization even showed a negative figure. Matsuura and Abaimov (2000) suggested that the amount of mineral nitrogen that may become available for plant growth is very low, and much of the available nitrogen may have been absorbed by the soil microbes before it is taken up by the higher plants. See Chap. 12 for further discussion of nitrogen dynamics in the *L. gmelinii* ecosystems. Matsuura (personal communication) also indicated that nitrogen storage in living biomass and in soil active layer is correlated positively with depth of the active layer in midsummer. Therefore, available amount of nitrogen for plant growth is likely to become less as the stands develop and the level of permafrost starts to rise toward the ground surface.

In summary, development of stand yield is likely to have a peculiar pattern in natural stands of *L. gmelinii* in Central Siberia. They may follow the well-known self-thinning rule only during a short period after fire, when the small trees are growing in extremely dense condition. Stand development during much of the life of the trees at later stage of stand development may not follow the self-thinning rule. This must be born in mind when stand development is analyzed for species in Siberia.

7.4 Yield Table Data

Yield table data also suggest presence of the asymptotic aboveground biomass (Usoltsev 2002). The relationships between aboveground biomass and stand density of various site index classes throughout the range of the species are shown in Fig. 7.3. The biomass tends to reach the upper asymptote as stand density becomes smaller. Level of the maximum biomass appears higher for better sites.

The attainable maximum biomass is likely to be observed for an extended period only in stands of poor site conditions. Figure 7.2 shows stands for the site index V and worse conditions, since these sites (V, Va, Vb, and worse) commonly exist over

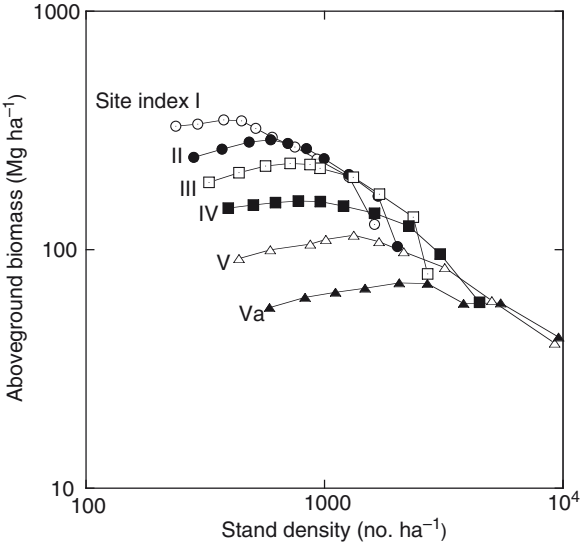

Fig. 7.3 Relationships of aboveground biomass and stand density for *Larix gmelinii* at various site index values (corresponding to various symbols). Better site qualities show increasingly larger values of maximum aboveground biomass at maturity

the permafrost. They correspond to some of the poorest site conditions among those possible for *L. gmelinii* (Usoltsev 2001, 2002). Therefore, appearance of the attainable maximum biomass may be a feature characteristic to the permafrost ecosystems. Leveling-off of aboveground biomass at lower stand density is also observed for better sites (site index I–IV in Fig. 7.3). However, generality of the pattern may be in question. Low density stands of high biomass nearly always represent old stands. The number of old stands sampled for study is usually small. Old stands are also likely to have been affected by various disturbances. Therefore, leveling-off of aboveground biomass in old stands could be a sampling artifact unless large number of stands are examined carefully in relation to disturbance history and management practices.

7.5 Chronosequence Data

Number of plots measured and plot area of each age category for the site index Vb are given in Table 7.1. Changes in mean tree height, aboveground biomass, and stand density observed in the present chronosequence are shown in Fig. 7.4. Mean tree height is approximately 8 m at stand age of 150 years in the Vb chronosequence site (Fig. 7.4a). Aboveground biomass of the Vb site increases rapidly after stand establishment. It reaches 39.4 Mg ha^{-1} at 26 years, then becomes more or less stable for over a century, ranging in the values between 42 and 48 Mg ha^{-1} (Fig. 7.4b).

Table 7.1 Stand characteristics of the chronosequence plots of *Larix gmelinii* used for the present study in Tura

Stand category[a]	Stand age[b] (years)	Number of plots	Plot area (m^2)
CR1994	10	15	1 or 2[c]
CR1990	14	4	4
CR1978	26	4	25
CR1899	105	5	400
CR1830	174	4	500
C1	266[d]	1	1,008

[a]Numerals after the letters CR represent the year of the forest fire when the previous stand was destroyed and the present stand became established. The plot C1 is an old uneven-aged forest that experienced multiple surface fires, but has survived (Kajimoto et al. 1999, 2007)
[b]Stand age is of year 2004
[c]Area of five plots was two square meters, whereas that of the rest was one square meter
[d]Maximum age of stand C1 follows estimation by Kajimoto et al. (1999)

The height and aboveground biomass were smaller in multiaged old stand (plot C1; shown by filled circle), probably due to additional tree mortality by ground fires and establishment of trees in younger age classes during stand development. Stand density declines rapidly over time in the Vb site class. The mean density was 440,000 ha^{-1} at stand age of 10 years. It declined to 28,700 ha^{-1} at age 26, then to 4,260 ha^{-1} at age 105 (Fig. 7.4c).

7.6 Reconstructed Stand Structure in the Past

Methods of stand reconstruction (Oliver and Stephens 1977; Osawa et al. 2000a) were applied for examining patterns of stand development in *L. gmelinii* forests. Reconstruction techniques were employed for obvious reasons. Although scientists in Russia (and former Soviet Union) have worked diligently examining ecology of boreal forests during the past several decades, the number of scientists has simply been too few to cover the whole territory of Siberia. There have been long-term studies of forest dynamics, including classic studies of larch and pine forests by Pozdynakov et al. (1969) and Pozdnyakov (1983, 1986). Fair number of permanent plots of forest stands has been employed for such studies. However, the number is simply not enough to describe variations in stand development. Long-term changes in forest structure, therefore, must be assessed by other means as well. The technique of stand reconstruction is well suited for research for boreal forest, because even-aged monospecific stands are predominant (e.g., Yarranton and Yarranton 1975; Carleton and Wannamaker 1987; Lussier et al. 2002). It is due to low diversity of tree species in the region, and the effect of frequent natural forest fires that reset plant succession. Even-agedness and the presence of annual growth rings, particularly, make the examination amenable.

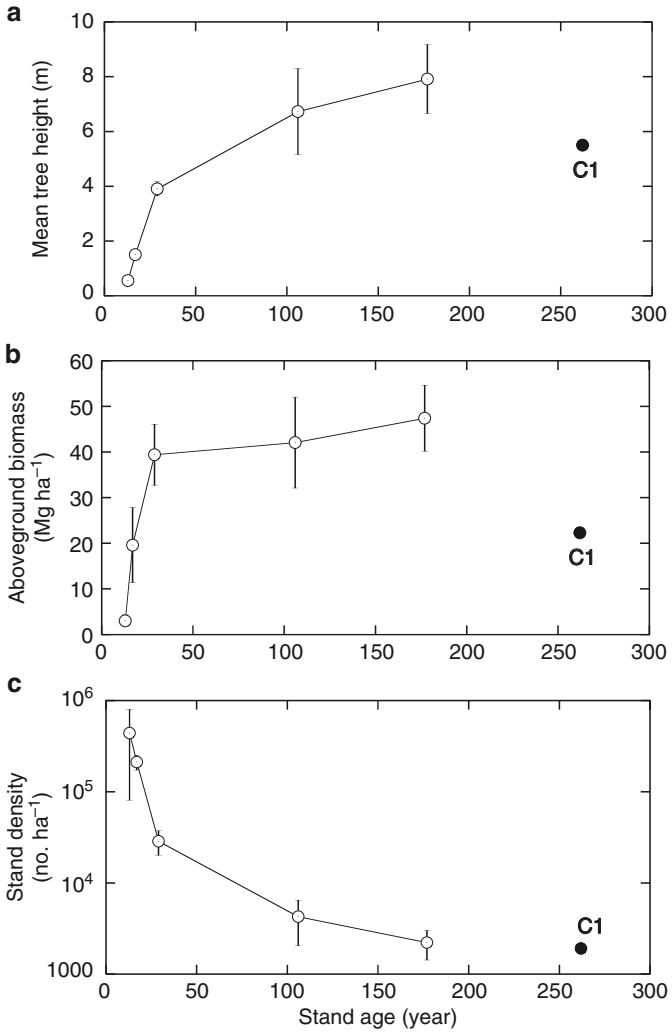

Fig. 7.4 Development patterns of (**a**) mean tree height, (**b**) aboveground biomass, and (**c**) stand density over time indicated for the chronosequence plots (*open circle*) at site index Vb. A *filled circle* indicates the uneven-aged stand (plot C1)

7.6.1 Height Growth

Figure 7.5 shows the reconstructed values of the mean height of canopy trees in relation to stand age in plot L14. There is a clear point of reflection at about 40 years when the height growth slowed substantially. The mean height increased about 3 m in 20 years before age 40, but after that the growth rate was reduced to only about 0.5 m in 20 years. This is consistent with the estimated (mean) height

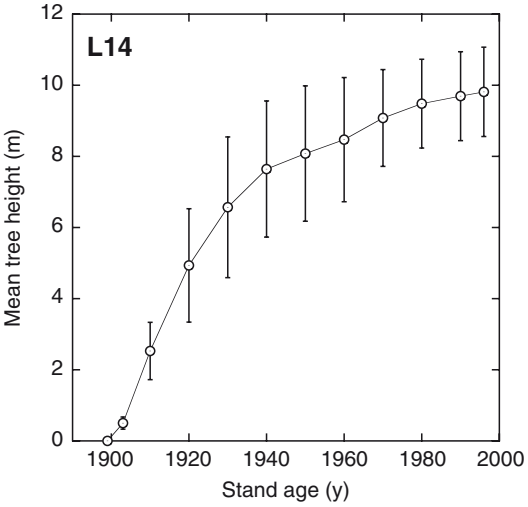

Fig. 7.5 Reconstructed development of maximum tree height in plot L14

growth from the chronosequence plots. It indicated reduction in the height growth rate at stand age of 30–40 years. Abrupt growth decline in stem height was also observed in a *L. gmelinii* stand (plot NF) near plot L14 at Site 1 (Fig. 1.3); growth decline in this stand occurred somewhat earlier (25–30 years; see Fig. 6.5d). As was interpreted previously (Kajimoto et al. 2007), the time of growth reduction is likely to coincide with the rise of permafrost in the soil.

7.6.2 Tree Mortality

Counting of growth rings in dead stems of plot L14 revealed that majority of the trees died between 1940 and 1965 when the trees were between 40 and 65 years old. The mortality jumped at age 40–45, and the highest values were at age 55–60 years (Fig. 7.6; see also Osawa et al. 1999). The dbh distributions of living trees and that of dead stems are shown in Fig. 7.7. It also shows the estimated tree mortality in relation to tree size (Fig. 7.7c). Largest proportion of trees died in the 3.5 cm dbh class (Fig. 7.7b). Tree mortality was relatively high in 5.5 and 6.5 cm classes also. In contrast, no trees died in the three largest classes (dbh > 8 cm). There was also no mortality in the smallest class; however, this may be due to decay of the smallest trees which had made examination of these individuals impossible (Osawa et al. 2000b).

The observed size dependency in tree mortality patterns suggests that a large number of relatively large individuals die in this ecosystem. Ford (1975) presented a pattern of size dependency in tree mortality of *Picea sitchensis* in monospecific plantations in UK. Only trees in the smallest size classes died in his study. Or the

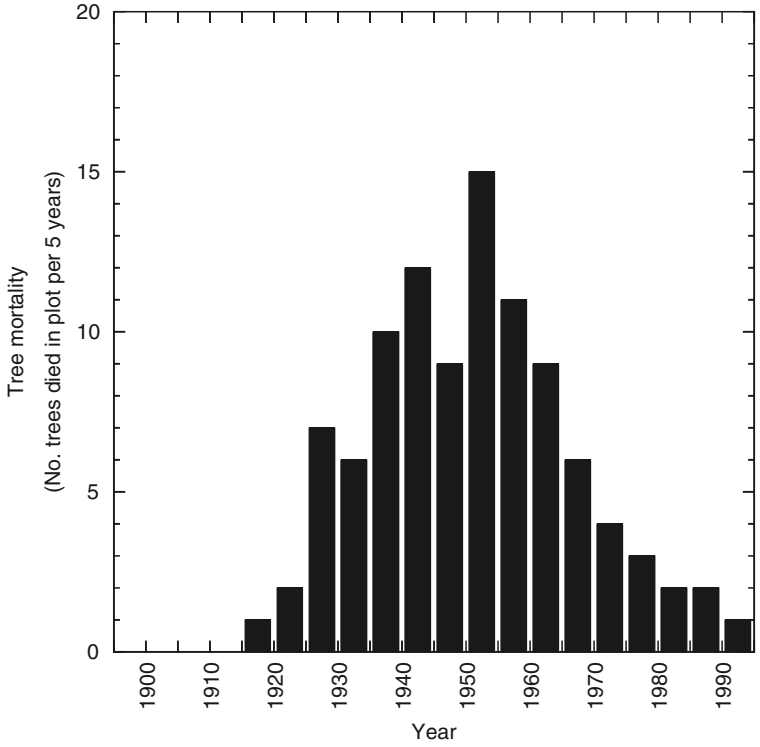

Fig. 7.6 Estimated tree mortality (number of trees died in the 0.0216 ha plot per 5 years) during development of a *Larix gmelinii* plot L14 (redrawn from Osawa et al. 1999)

death appeared in the smallest quarter of the size classes. Our observation of mortality in *L. gmelinii* in Siberia is different. Middle-size classes showed the greatest mortality. Only the largest few classes were free from tree death. Therefore, the mortality is widespread among trees of various sizes.

7.6.3 Reconstructed Stem Slenderness and Stand Density

Table 7.2 shows changes in the stem slenderness index, c (Osawa et al. 2000a), at various times during development of the plot L14. It has been shown (Osawa et al. 2000a) that stand density, N, is closely related to the slenderness index for a specific species and in a given region, and could be calculated for plot L14 as,

$$N = \frac{e^{1.72c}}{1.08H^2}, \tag{7.2}$$

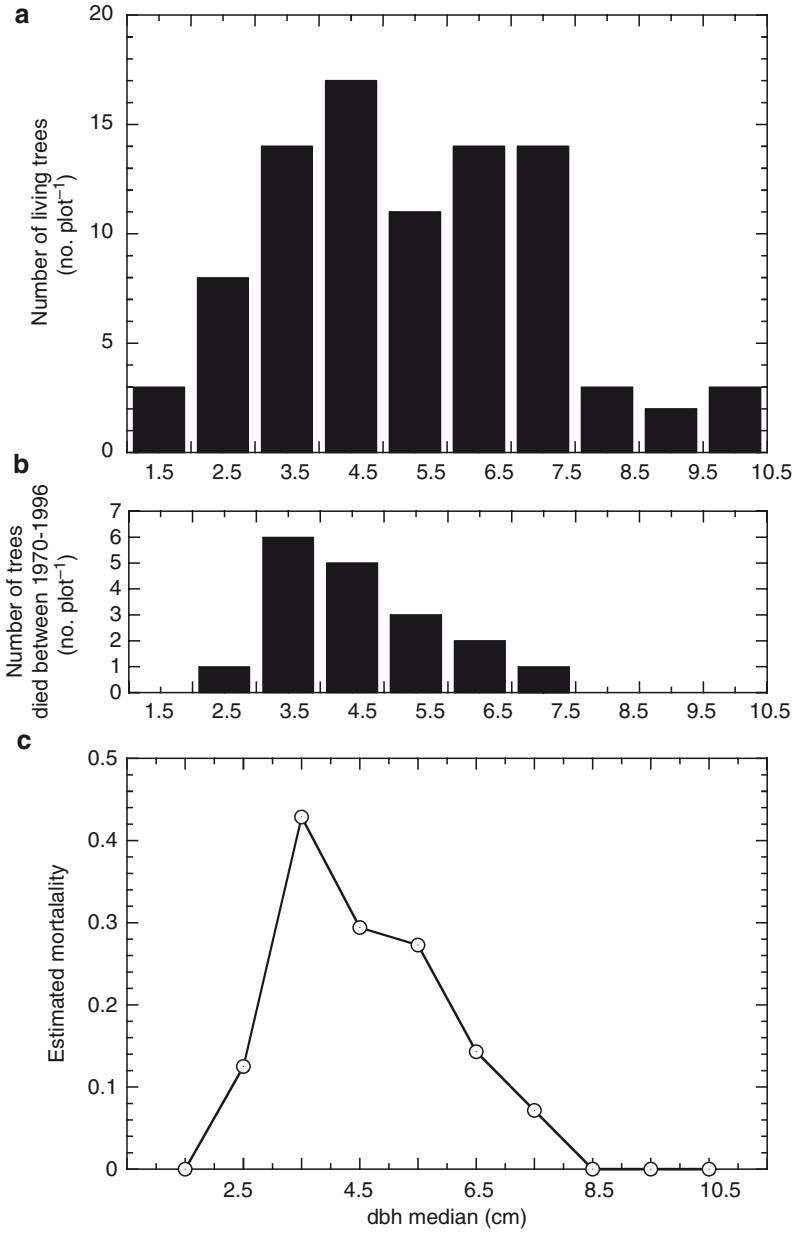

Fig. 7.7 Size (dbh) distribution patterns of trees in plot L14. (**a**) Number of living trees in 1996; (**b**) number of trees that died between 1970 and 1996; and (**c**) estimated tree mortality per dbh class as calculated by dividing the number in (**b**) by that in **(a)** of the same size class. It was assumed that stem growth between 1970 and 1996 was minimal (redrawn from Osawa et al. 2000b)

Table 7.2 Ranges of dbh and tree height (both at outside bark, and fresh condition) of five selected trees for stem analysis in plot L14, and the estimated values of the maximum tree height (H), stem slenderness index (c), and the R^2 of the regression relating tree height and dbh outside bark at fresh condition on double logarithmic coordinates with the fixed slope of 2/3 (from Osawa et al. 2000a)

Year	Range of dbh (cm)	Range of tree height (m)	H (m)	c (m cm$^{-2/3}$)	R^2
1920	5.93–2.61	6.75–3.46	6.75	1.91	0.92
1930	7.67–3.70	8.76–4.64	8.76	2.09	0.95
1940	8.79–4.12	9.89–5.35	9.89	2.17	0.95
1950	9.35–4.25	10.27–5.74	10.27	2.18	0.96
1960	9.61–4.43	10.49–5.98	10.49	2.20	0.96
1970	9.87–4.60	10.71–6.17	10.71	2.25	0.96
1980	10.07–4.67	10.92–6.27	10.92	2.27	0.92
1990	10.28–4.78	11.09–6.36	11.09	2.28	0.90
1996	10.40–5.01	11.18–6.40	11.18	2.28	0.88

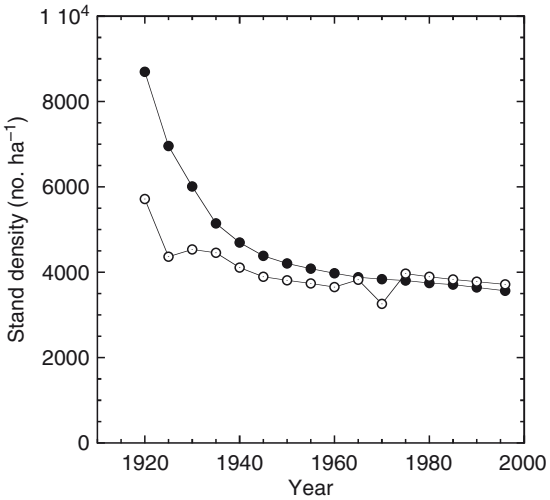

Fig. 7.8 Reconstructed changes in stand density of plot L14 between 1920 and 1996. *Open circles* and *filled circles* represent the estimates calculated with stem slenderness index in the past (current approach), and with the self-thinning assumption (details given in Osawa et al. 2000a), respectively (redrawn from Osawa et al. 2000a)

where H is the maximum tree height at the time for which the value of c was determined. The reconstructed changes of stand density over time for plot L14 are shown in Fig. 7.8. It was estimated that the stand had density of 5,716 trees ha^{-1} in 1920 when the trees were 19 years old. The stand density decreased relatively sharply to 4,110 trees ha^{-1} by 1940, but changed only slightly to 3,717 trees ha^{-1} by 1996. Stand density could not be estimated during the initial 19 years of stand development after stand initiation, mainly due to inability to estimate the stem

slenderness index when trees were small (< 130 cm tall). However, the estimated changes in stand density do suggest that the stem number decreased relatively rapidly for about 40 years in the initial part of stand development, but decreased only slightly between stand ages of 40 and 96 years. It may be interpreted that competition among individual trees was intense when trees were growing relatively rapidly under the condition of thick soil active layer, which may correspond to more abundant soil nutrient condition. In contrast, stem growth has been reduced greatly after the rise of the permafrost (considered to have happened around 1940), which has made inter-tree competition for light less intense, and thus, reduced tree mortality over a unit time period.

7.6.4 Reconstructed Stem Size Distribution

Figure 7.9 shows the $Y(w)$–$M(w)$ relationship, explained in Osawa et al. (2000), for plot L14. Data for six different times were indicated. It is clear that these two variables are related linearly for any given time in the past during stand development. Therefore, proposition of reconstructing stem size distribution as the –3/2 power distribution (Hozumi et al. 1968) appears warranted.

Table 7.3 presents estimates of various parameters describing structure of plot L14 at various times during stand development, including values of stand density, two parameters of the –3/2 power distribution, and maximum and minimum sizes of individuals in the stand. Finally, reconstructed stem size distribution for three occasions, 1940, 1970, and 1996, are shown in Fig. 7.10. Reconstructed stem volume data were converted to dbh information using appropriate time-dependent allometric relationships between these two variables. Patterns of all distributions are reverse-J shaped. This is because of our assumption of the size distribution function. General patterns and changes over time of the stem size distribution are depicted. There are limitations to the use of this distribution function. For example, a humped distribution pattern cannot be reproduced by the –3/2 power type. Other distribution functions must be employed in such a case. For discussions on applicability and limitation of the current approach for reconstruction of stem size distribution, see Osawa and Abaimov (2001) and Osawa et al. (2001).

7.6.5 Reconstructed Total Stem Volume and Stem Volume Growth

Figure 7.11a shows the time course of total stem volume for plot L14. The total stem volume of the stand has been increasing more or less steadily; however, the rate of growth decreased somewhat since 1970s. General decline of the growth is also seen in Fig. 7.11b, which describes the time course of stem volume growth for the same stand.

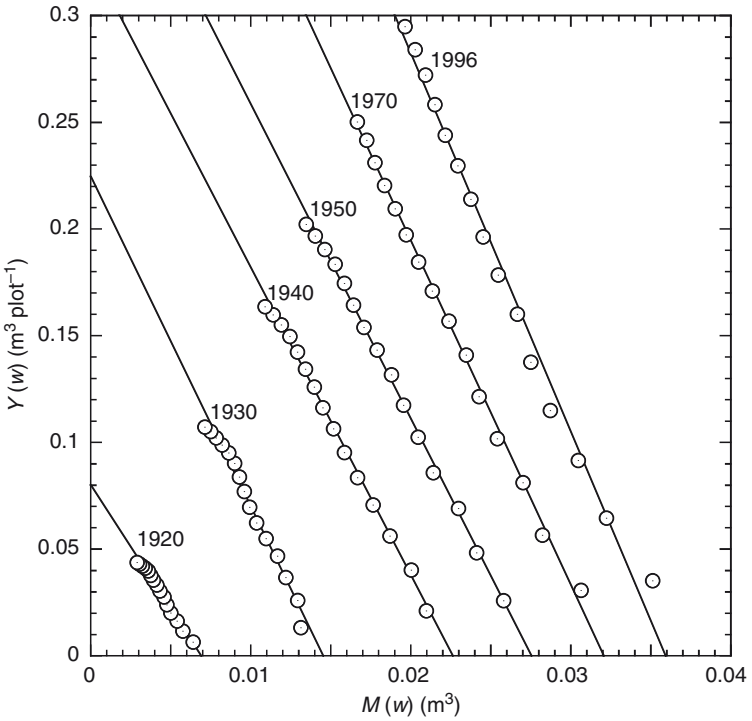

Fig. 7.9 The $Y(w)$ vs. $M(w)$ relationship for selected years during development of plot L14. The $Y(w)$ is expressed as the value for the plot area of 0.0216 ha (redrawn from Osawa et al. 2000a)

Figure 7.11b indicates that stem volume growth of the whole stand declined sharply around 1950 and around 1970. Also, it has continuously been at the low level since 1970, and particularly so during 1980s and 1990s. We can only speculate the causes. It is likely that the climate was not conductive to good growth during these periods of poor growth. E. Vaganov presented evidence that is supportive of this interpretation (personal communication). Analysis of tree-ring patterns for various sites in middle- and northern taiga of Evenkia region indicated growth patterns of the trees similar to the ones shown in Fig. 7.11b. The similarity should be interpreted by the fact that the growth patterns of trees are similar in the region regardless of sites and tree ages. A variable giving such a widespread pattern is likely to be the climate. Increased winter precipitation in recent years (Chap. 17) due to climate change may be a cause of delaying snow melt and shortening growth period for trees.

However, patterns of tree growth in plot L14 also indicated possible effect of stand development on the temporal changes in growth patterns. Examination of tree-height growth, stem volume growth, and total stem volume shows that the trees in this plot gained large amount of growth in tree height and stem volume until

Table 7.3 Parameters A and B of the $-3/2$ power distribution of stem volume and other variables that characterize the stand structure of plot L14 estimated for selected years between 1920 and 1996 (from Osawa et al. 2000a)

Year	A (plot m^{-3})	A (ha m^{-3})	B (m^{-3})	$\sqrt{B}(2A)^{-1}$ (m$^{3/2}$ha^{-1})	N (no. ha^{-1})	w_{max} (m^3, $\times 10^{-4}$)	w_{min} (m^3, $\times 10^{-4}$)	d_{max} (cm)	d_{min} (cm)
1920	12.51	0.2700	145.0	22.28	5,716	64	0.41	4.50	0.60
1930	4.45	0.0962	68.9	43.12	4,533	131	1.46	6.08	1.00
1940	3.06	0.0663	44.2	50.15	4,110	209	4.04	7.40	1.50
1950	2.46	0.0532	36.3	56.58	3,812	258	4.04	8.07	1.50
1960	2.17	0.0470	33.2	61.26	3,653	286	4.04	8.44	1.50
1970	1.93	0.0417	31.2	66.84	3,260	306	8.30	8.67	2.00
1980	1.77	0.0383	30.1	71.46	3,896	320	8.30	8.83	2.00
1990	1.64	0.0356	28.8	75.36	3,778	337	8.30	9.03	2.00
1996	1.57	0.0339	27.8	77.76	3,717	351	8.30	9.18	2.00

Note: The parameter A was first estimated for the plot area of 0.0216 ha (denoted as "plot" in the table), then converted to the value per hectare basis as shown in the table. N, stand density calculated with the stem slenderness index; w_{max} and w_{min}, stem volume for the largest and smallest living trees in the stand, respectively; d_{max} and d_{min}, maximum and minimum dbh of the trees in the stand, respectively. The w_{max} and d_{max} are the values obtained directly from stem analysis, whereas w_{min} and d_{min} were estimated as the smallest class boundaries with the present approach from the reconstructed tree size distribution and stand density. All stem volume and diameter data are for the air-dried condition

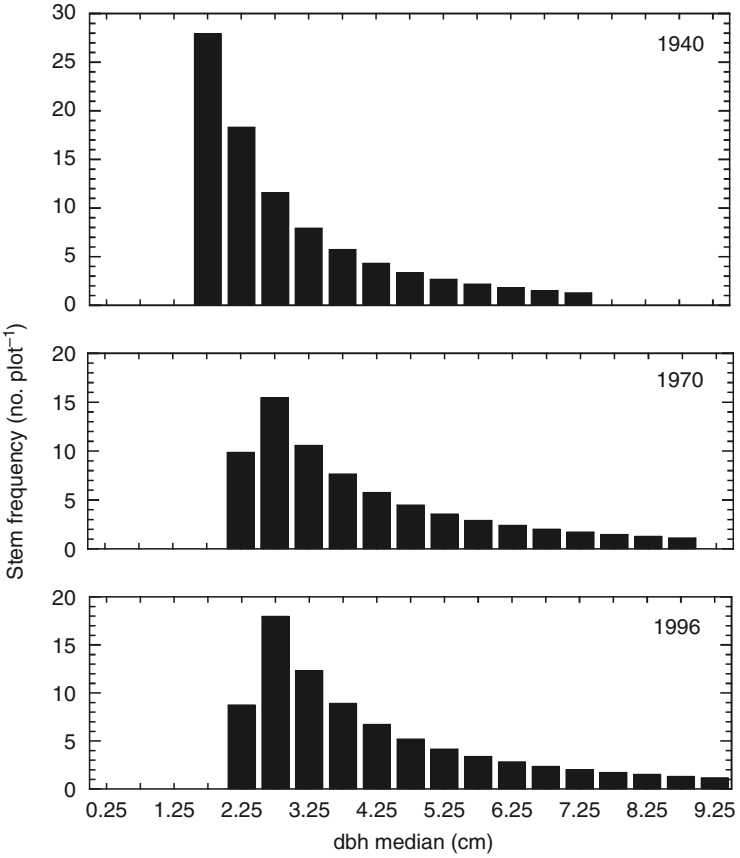

Fig. 7.10 Reconstructed patterns of stem dbh distribution in plot L14 at three selected years: 1940, 1970, and 1996 (redrawn from Osawa et al. 2000a)

around 1940, when the stem volume growth peaked and attained the highest value for the entire period of stand development. It was followed by abrupt reduction in height growth (Figs. 7.4a and 7.5) and stem volume growth (Fig. 7.11b). These growth patterns suggest that the level of permafrost was up to the prefire level by about 1940, reducing height as well as volume growth of the trees. Effects of both reduced nutrient availability and soil temperature may be related to the dwindling growth. Trees in this plot were about 40 years old in 1940. The *L. gmelinii* stands in the present study area also reach the maximum yield by stand age of about 30–40 years (Fig. 7.4b), and stop gaining further biomass in the aboveground portion of the ecosystem due partly to the raised level of tree mortality at that time (Fig. 7.6). This timing corroborates the time when the soil active layer becomes as shallow as the prefire thickness. Therefore, various patterns of stand development that were observed in the present analysis are in line with the notion that growth and structural changes of *L. gmelinii* forests are driven by the changes in soil active

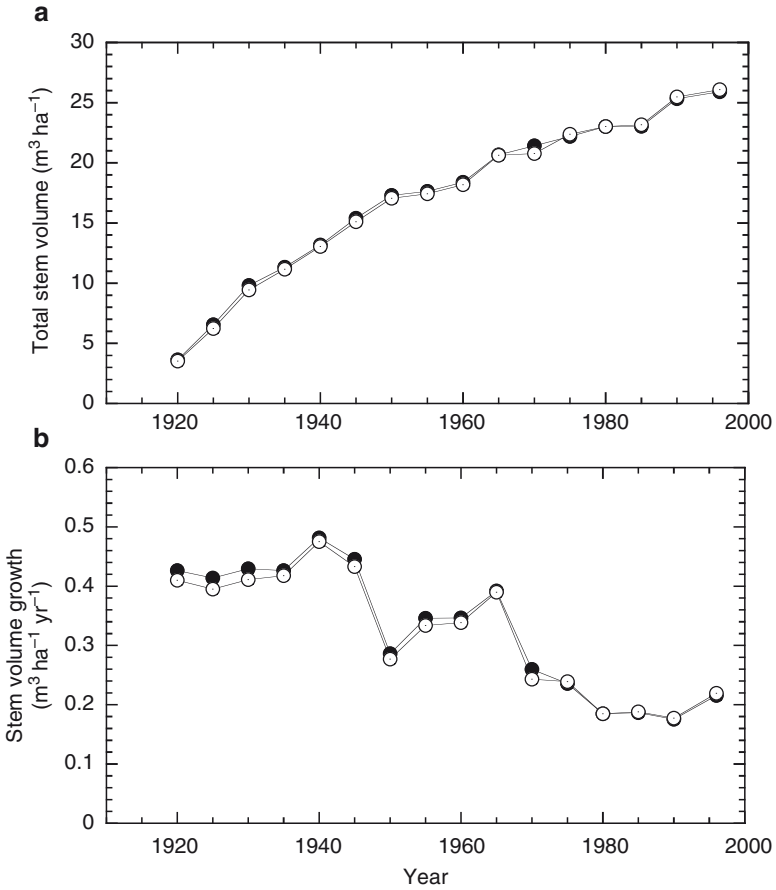

Fig. 7.11 Reconstructed changes over time of (**a**) total stem volume and (**b**) total stem volume growth of the trees in plot L14. Different symbols indicate the values estimated with two alternative methods (see also Fig. 7.8) (redrawn from Osawa et al. 2000a)

layer and the recovery of the permafrost after fire. Alternatively, apparent reduction in aboveground biomass growth after the rise of permafrost may be due to increased organic matter allocation to roots without substantial reduction in total net primary production (see Chap. 6). Root processes and patterns must be examined further to clarify this possibility.

7.6.6 Consideration on Accuracy of the Reconstruction Method

The above analysis of structural development in a *L. gmelinii* stand relies on the new method of stand reconstruction (Osawa et al. 2000a). There are three conditions that should be met if the reconstructed stand structure is to be accurate enough

for consideration. First, the method assumes a specific distribution function of stem sizes: the –3/2 power distribution. Therefore, tree sizes must conform to this particular function. If not, estimates may not be trusted. Second, fitting data to a distribution function introduces a statistical consideration. A distribution function is only an approximation when fitted to real data. We should expect that size data of all the trees in a stand and those of the largest ones, which we applied in the above analysis, may not always lead to the same size distributions. Then we may ask what proportion of the trees should be included in estimating the parameters of the stem size distribution successfully. Third, estimated values of total stem volume, stem volume growth, aboveground biomass, and other stand-level variables must also conform to those actually observed.

Osawa and Abaimov (2001) and Osawa et al. (2001) examined these three aspects of the method by utilizing data of stem sizes and aboveground biomass for 21 stands of *L. gmelinii* of Central Siberia and *Pinus banksiana* of northern Canada that considerably varied in stand density (range 1,290–3.32 million trees ha^{-1}) and canopy height (range 0.62–21.5 m). They calculated stem size distribution and various stand-level variables by using data of only a group of the largest trees in a stand and changing the proportion of the tree number to be included for the calculation from 50 to 10%, and then compared the obtained estimates to those observed in the actual stands. Thus, they tested accuracy of the method for the contemporary stands. Applicability of additional distribution function, beta-type distribution, was also examined in application to estimation of stem size distribution and stand variables.

Osawa and Abaimov (2001) showed that both −3/2 power and beta-type distributions of stem size distribution could be used for reconstruction from data of only the largest trees in a stand. This is the case, however, only when size distribution of all the individuals of the stand could be approximated by one of these distribution functions. Also, they indicated that information of the largest 20% of the trees in a stand is sufficient to estimate size patterns of all the trees, when the size distribution is approximated by the −3/2 power distribution. The necessary percentage increases to 30%, when beta-type function is utilized. In other words, when we used data of the largest X trees in a stand for reconstruction, estimates of size distribution may be accurate up to the time when stand density was $5X$, while assuming the −3/2 power function. When applying the beta-type distribution, the estimates may be accurate up to the stand condition of $3.3X$ trees per plot.

Accuracy of the method was also tested for estimation of total stem volume and aboveground biomass of the stand (Osawa et al. 2001). Ten percent of the largest trees in a stand should lead to acceptable estimates of total stem volume and aboveground biomass, when the −3/2 power distribution was assumed. Largest 30% of the trees were needed to calculate these variables successfully when the beta-type function was applied. It was also shown in a separate analysis (Osawa et al. 2000a) that error in estimating stand density is relatively insensitive to accuracy of the calculated total stem volume and stem volume growth of the stand. This is comforting, because appreciable error is expected in estimation of stand density of the past, but such error affects accuracy of the estimated total stem volume and stem volume

growth only a little. On the other hand, parameter *A* of the −3/2 power distribution (Table 7.3; see also Osawa et al. 2000a) is quite sensitive to the calculated values of stand variables. Thus, care should be exercised in fitting the distribution function to the stem size data.

The above analysis suggests that the present method of structural stand reconstruction can be applied with some confidence to even-aged monocultures of the boreal regions. However, there are other sources of error that have not been considered, but must be taken into account when the method is being applied. The method was tested so far with only the contemporary data, by comparing the calculated and observed values of stand structure at present. However, when we attempt to reconstruct the stand structure in the past, there are additional error associated with estimation of stem size, stem height, stand density, etc. of the past. These errors have not been addressed sufficiently. Comparisons of the reconstructed values of stand structure in the past and temporal data that were obtained in actual field measurements in the past are required as further tests on the accuracy of the present technique. A case of such comparison was presented for plantations of *Abies sachalininsis* growing in northern Japan (Osawa et al. 2005).

7.7 Conclusions

The above analyses of the published information, new data from stand measurement, and stand development by a structural reconstruction technique are all supporting the following interpretation on the patterns of stand development in *L. gmelinii* forests that grow on permafrost in Siberia. The patterns are unusual with respect to those we are familiar with in the ecosystems of lower latitudes in temperate regions or even in the southern boreal forests that lack the permafrost. The general characteristics of the stand development are summarized as the following four patterns:

- The stands follow the classic self-thinning relationship when they are young.
- The self-thinning phase lasts for a relatively short period, and is terminated by an abrupt reduction in stand growth at stand age of 30–40 years.
- Aboveground biomass of older stands approaches a constant value asymptotically, indicating the presence of the attainable maximum aboveground biomass.
- The attainable maximum aboveground biomass may vary depending on site condition.

The level of attainable maximum aboveground biomass increases as the site becomes better within the region of continuous permafrost. The causes that limit the amount of aboveground biomass in *L. gmelinii* forests on poor sites are important factors in understanding ecology of this species. As we have discussed, limitation in soil resources and cold soil temperature due to permafrost recovery are the possible mechanisms. However, they are still to be clarified in understanding details of the processes of stand development in *L. gmelinii*.

References

Abaimov AP, Lesinski JA, Martinsson O, Milyutin LI (1998) Variability and ecology of Siberian larch species. Swedish University of Agricultural Sciences, Department of Silviculture, Reports 43, Umeå, 118pp

Apps MJ, Kurz WA, Luxmoore RJ, Nilsson LO, Sedjo RA, Schmidt R, Simpson LG, Vinson TS (1993) Boreal forest and tundra. Water Air Soil Poll 70:39–53

Begin E, Begin J, Belanger L, Rivest LP, Tremblay S (2001) Balsam fir self-thinning relationship and its constancy among different ecological regions. Can J For Res 31:950–959

Begon M, Harper JL, Tawnsend CR (1996) Ecology, 3rd edn. Blackwell Science, Oxford

Bondarev A (1997) Age distribution patterns in open boreal Dahurian larch forests of Central Siberia. For Ecol Manage 93:205–214

Bormann FH, Likens GE (1979) Pattern and process in a forested ecosystem. Springer, Berlin

Botkin DB, Janak JF, Wallis JR (1972) Some ecological consequences of a computer model of forest growth. J Ecol 60:948–972

Carleton TJ, Wannamaker BA (1987) Mortality and self-thinning in postfire black spruce. Ann Bot 59:621–628

Catana HJ (1963) The wandering quarter method of estimating population density. Ecology 44:349–360

Dyrness CT, Viereck LA, Van Cleve K (1986) Fire in taiga communities of Interior Alaska. In: Van Cleve K, Chapin FS III, Flanagan PW, Viereck LA, Dyrness CT (eds) Forest ecosystems in the Alaskan taiga. Ecological Studies, vol 57, Springer, Berlin, pp 74–86

Enquist BJ, Brown JH, West GB (1998) Allometric scaling of plant energetics and population density. Nature 395:163–165

Ford ED (1975) Competition and stand structure in some even-aged plant monocultures. J Ecol 63:311–333

Harper JL (1977) Population biology of plants. Academic Press, London

Hozumi K, Shinozaki K, Tadaki Y (1968) Studies on the frequency distribution of the weight of individual trees in a forest stand I. A new approach toward the analysis of the distribution function and the −3/2th power distribution. Jpn J Ecol 18:10–20

Hutchings MJ (1983) Ecology's law in search of a theory. New Scient 98:765–767

Kajimoto T, Matsuura Y, Sofronov MA, Volokitina AV, Mori S, Osawa A, Abaimov AP (1999) Above- and belowground biomass and net primary productivity of a *Larix gmelinii* stand near Tura, central Siberia. Tree Physiol 19:815–822

Kajimoto T, Matsuura Y, Osawa A, Prokushkin AS, Sofronov MA, Abaimov AP (2003) Root system development of *Larix gmelinii* trees affected by micro-scale conditions of permafrost soils in central Siberia. Plant Soil 255:281–292

Kajimoto T, Osawa A, Matsuura Y, Abaimov AP, Zyryanova OA, Kondo K, Tokuchi N, Hirobe M (2007) Individual-based measurement and analysis of root system development: case studies for *Larix gmelinii* trees growing on the permafrost region in Siberia. J Forest Res 12:103–112

Kasischke ES, Stocks BJ (eds) (2000) Fire, climate change, and carbon cycling in the boreal forest. Ecological studies, vol 138. Springer, Berlin

Kays S, Harper JL (1974) The regulation of plant and tiller density in a grass sward. J Ecol 62:97–105

Kira T, Ogawa H, Sakazaki N (1953) Competition-yield-density interrelationship in regularly dispersed populations (intraspecific competition among higher plants I). J Inst Polytech, Osaka City University, Series D 4:1–16

Lonsdale WM (1990) The self-thinning rule: dead or alive? Ecology 71:1373–1388

Lussier J-M, Morin H, Gagnon R (2002) Mortality in black spruce stands of fire or clear-cut origin. Can J For Res 32:539–547

Matsuura Y, Abaimov AP (2000) Nitrogen mineralization in larch forest soils of continuous permafrost region, central Siberia – an implication for nitrogen economy of a larch forest stand.

In: Inoue G, Takenaka A (eds) Proceedings of the eighth symposium on the joint Siberian permafrost studies between Japan and Russia in 1999. National Institute for Environmental Studies, Tsukuba, pp 129–134
Morris EC (1996) Effect of localized placement of nutrients on root competition in self-thinning populations. Ann Bot 78:353–364
Morris EC, Myerscough PJ (1991) Self-thinning and competition intensity over a gradient of nutrient availability. J Ecol 79:903–923
Nadelhoffer KJ, Giblin AE, Shaver GR, Laundre JA (1992) Effects of temperature and substrate quality on element mineralization in six arctic soils. Ecology 72:242–253
Nakashizuka T (1987) Regeneration dynamics of beech forests in Japan. Vegetatio 69:169–175
Norberg RA (1988) Theory of growth geometry of plants and self-thinning of plant populations: geometric similarity, elastic similarity, and different growth modes of plant parts. Am Nat 131:202–256
Odum EP (1969) The strategy of ecosystem development. Science 164:262–270
Oliver CD, Stephens EP (1977) Reconstruction of a mixed species forest in central New England. Ecology 58:562–572
Osawa A (1995) Inverse relationship of crown fractal dimension to self-thinning exponent of tree populations: a hypothesis. Can J For Res 25:1608–1617
Osawa A, Abaimov AP (2001) Feasibility of estimating stem size distribution from measurement on the largest trees in even-aged pure stands. Can J For Res 31:910–918
Osawa A, Allen RB (1993) Allometric theory explains self-thinning relationships of mountain beech and red pine. Ecology 74:1020–1032
Osawa A, Kurachi N (2004) Spatial leaf distribution and self-thinning exponent of *Pinus banksiana* and *Populus tremuloides*. Trees 18:327–338
Osawa A, Sugita S (1989) The self-thinning rule: another interpretation of Weller's results. Ecology 70:279–283
Osawa A, Abaimov AP, Zyryanova OA (1999) Reconstructing past stand density in even-aged *Larix gmelinii* monocultures: comparison of three approaches. In: Shibuta M, Takahashi K, Inoue G (eds) Proceedings of the seventh symposium on the joint Siberian permafrost studies between Japan and Russia in 1998, Tsukuba, pp 21–24
Osawa A, Abaimov AP, Zyryanova OA (2000a) Reconstructing structural development of even-aged larch stands in Siberia. Can J For Res 30:580–588
Osawa A, Abaimov AP, Zyryanova OA (2000b) Tree size-density relationship and size-dependent mortality in Larix gmelinii stands. In: Inoue G, Takenaka A (eds) Proceedings of the eighth symposium on the joint Siberian permafrost studies between Japan and Russia in 1999. National Institute for Environmental Studies, Tsukuba, pp 36–41
Osawa A, Abaimov AP, Kajimoto T (2001) Feasibility of estimating total stem volume and above-ground biomass from measurement on the largest trees in even-aged pure stands. Can J For Res 31:2042–2048
Osawa A, Abaimov AP, Matsuura Y, Kajimoto T, Zyryanova OA (2003) Anomalous patterns of stand development in larch forests of Siberia. Tohoku Geophys J 36:471–474
Osawa A, Kurachi N, Matsuura Y, Jomura M, Kanazawa Y, Sanada M (2005) Testing a method for reconstructing structural development of even-aged *Abies sachalinensis* stand. Trees 19:680–694
Pozdnyakov LK (1983) Forests of the permafrost zone. Nauka, Novosibirsk (in Russian)
Pozdnyakov LK (1986) The permafrost forestry. Nauka, Novosibirsk (in Russian)
Pozdynakov LK, Protopopov VV, Gorbatenko VM (1969) Biological productivity of central Siberia and Yakutiya forests. Forest and Wood Institute, Siberian Branch of the USSR Academy of Sciences, Krasnoyarsk, 156pp (in Russian)
Roscher C, Schumacher J, Weisser WW, Schmid B, Schulze E-D (2007) Detecting the role of individual species for overyielding in experimental grassland communities composed of potentially dominant species. Oecologia 154:535–549
Schimel DS, House JI, Hibbard KA, Bousquet P, Ciais P, Peylin P, Braswell BH, Apps MJ, Baker D, Bondeau A, Canadell J, Churkina G, Cramer W, Denning AS, Field CB, Friedlingstein P,

Goodale C, Heimann M, Houghton RA, Melillo JM, Moore B III, Murdiyarso D, Noble I, Pacala SW, Prentice IC, Raupach MR, Rayner PJ, Scholes RJ, Steffen WL, Wirth C (2001) Recent patterns and mechanisms of carbon exchange by terrestrial ecosystems. Nature 414:169–172

Schulze E-D, Schulze W, Kelliher FM, Vygodskaya NN, Ziegler W, Kobak KI, Koch H, Arneth A, Kusnetsova WA, Sogatchev A, Issajev A, Bauer G, Hollinger DY (1995) Aboveground biomass and nitrogen nutrition in chronosequence of prestine Dahurian *Larix* stands in eastern Siberia. Can J For Res 25:943–960

Solomon S, Qin D, Manning M, Marquis M, Averyt K, Tignor MMB, Miller HL Jr, Chen Z (eds) (2007) Technical summary. In: Climate change 2007: the physical science basis. Contribution of Working Group 1 to the Fourth Assessment Report of the Intergovernmental Panel on Climate Change. Cambridge University Press, Cambridge, 142pp

Usoltsev VA (2001) Forest biomass of northern Eurasia: data base and geography. Russian Academy of Sciences, Ural Branch, Botanical Garden, Yekaterinburg, 706pp (in Russian with English summary)

Usoltsev VA (2002) Forest Biomass of Northern Eurasia: mensuration standards and geography. Russian Academy of Sciences, Ural Branch, Botanical Garden, Yekaterinburg (in Russian with English summary)

Van Cleve K, Dyrness CT, Viereck LA, Fox J, Chapin FS III, Oechel W (1983) Taiga ecosystems in interior Alaska. Bioscience 33:39–44

Van Cleve K, Yarie J, Erickson R (1993) Nitrogen mineralization and nitrification in successional ecosystems on the Tanana River floorplain, interior Alaska. Can J For Res 23:970–978

Weller DE (1987) A reevaluation of the −3/2 power rule of plant self-thinning. Ecol Monogr 57:23–43

Westoby M (1984) The self-thinning rule. Adv Ecol Res 14:167–225

White J (1980) Demographic factors in populations of plants. In: Solbrig OT (ed) Demography and evolution in plant populations. University of California Press, Berkeley

White J, Harper JL (1970) Correlated changes in plant size and number in plant populations. J Ecol 58:467–485

Wirth C, Schulze E-D, Luhker B, Grigoriev S, Siry M, Hardes G, Ziegler W, Backor M, Bauer G, Vygodskaya NN (2002) Fire and site type effects on the long-term carbon and nitrogen balance in prestine Siberian Scots pine forests. Plant Soil 242:41–63

Yarranton M, Yarranton GA (1975) Demography of jack pine stand. Can J Bot 53:310–314

Yoda K, Kira T, Ogawa H, Hozumi K (1963) Self-thinning in overcrowded pure stands under cultivated and natural conditions (Intraspecific competition among higher plants. XI. J Inst Polytech 14:107–129

Zoltai C (1975) Structure of subarctic forests on hummocky permafrost terrain in northwestern Canada. Can J For Res 5:1–9

Chapter 8
Soil Carbon and Nitrogen, and Characteristics of Soil Active Layer in Siberian Permafrost Region

Y. Matsuura and M. Hirobe

8.1 Introduction

Permafrost region of Siberia is mostly covered with larch forest or forest tundra. The permafrost-affected soils were generally classified as Cambisols (moderately developed soils) on plain topography and Leptosols (shallow and high gravel content soils) in mountainous topography (FAO 1993). The latest revision of soil classification systems of both USDA and FAO adopted permafrost as a diagnostic horizon, and created a new "soil order" (USDA) or a "main soil" (FAO) for permafrost-affected soils: Gelisols in the USDA classification system (Soil Survey Staff 1998), Cryosols in the FAO system (ISSS Working Group RB 1998), and Cryozems in the Russian system (V. V. Dokuchaev Soil Science Institute 2001; Naumov Ye 2004; Sokolov et al. 2004). There had been a few soil survey expeditions to the permafrost region of Siberia (e.g., Ivanova 1969), but most studies in the former Soviet Union focused on examination of podzolisation and humus chemistry. The results were published nearly exclusively in Russian language and were expressed in organic matter concentrations, not in carbon contents. No map coordinate data were generally available for the survey points in the literature. Though Alexeyev and Birdsey (1998) compiled soil carbon storage data for administrative unit of Russia, there were still uncertainties in soil bulk density, rock fragment ratio, fine earth content, etc. These are disadvantages of the available information if they are to be used in discussions of carbon or nutrient storage and dynamics.

Soils of larch forests commonly have thin A-horizon and dark-colored subsoil down to the permafrost table, with an acidic pH regime. Soils under severe continental climates with annual precipitation of only about 200–300 mm often show alkaline pH regimes and contain carbonate-C in the subsoil. For example, soils developed on thermokarst flat basin in central Yakutia (ca. 62°N, 130°E) have alkaline pH values into deeper subsoil horizons (Matsuura et al. 1994).

Soils of the permafrost region also tend to have low nutrient availability because of low soil temperature. Even if nutrient storage in the soil is abundant, nutrients in the soil active layer tend to be limited during a growing season, and much of the nutrients are bound in the frozen soil. For example, net nitrogen mineralization rate in Arctic tundra in North America was two to three orders of magnitude smaller

A. Osawa et al. (eds.), *Permafrost Ecosystems: Siberian Larch Forests*,
Ecological studies, Vol. 209, DOI 10.1007/978-1-4020-9693-8_8,

than that in tropical and temperate forests (Nadelhoffer et al. 1992). Low soil temperature apparently leads to low nutrient availability. In some cases, results of field incubation experiments for N mineralization indicated that immobilization process was dominant in the old larch (*Larix gmelinii*) forests on continuous permafrost regions in Central Siberia (Matsuura and Abaimov 2000; also see Chap. 12). Plants that grow in such severe nutrient conditions may have peculiar physiological traits, such as nutrient retranslocation (or resorption), to maintain nutritional requirements of individuals.

Previous studies have reported that these forests showed substantial variations in forest structure both spatially and chronologically (Schulze et al. 1995; Osawa et al. 2004). For such variations, availability of nutrients associated with permafrost dynamics over time is suggested to be a possible controlling factor through limitation of biomass increment (Van Cleve et al. 1983; Schulze et al. 1995). However, information is still limited for larch forest ecosystems of Siberia compared to boreal forests of other circumpolar regions.

In this chapter, first we describe soil carbon and nitrogen storage, and soil C/N ratio in larch forests of Central and Northeastern Siberia (see Chap. 1, for definition of the regions in Siberia), and discuss their regional-scale differences. These characteristics are still little known, and may be useful for understanding soil formation and carbon storage in the permafrost region. Second, variations of forest structure and soil properties were examined on a toposequence from hill-top (crest flat) to riverside. Topography is known as one of the most important factors for soil heterogeneity at a small spatial scale (Jenny 1980; Giblin et al. 1991). Therefore, it may contribute to spatial variations in the structure of larch forests. An objective is to clarify the extent of soil heterogeneity including nitrogen (N) availability along a toposequence, and to examine effects of soil heterogeneity on forest structure. Third, nutrient status (annual N cycling) in one old larch stand was inferred based on the data of needle N concentrations and its retranslocation rate before senescence.

8.2 Approaches to Describe Soil Properties

8.2.1 Soil Carbon and Nitrogen Storage, and Carbon Budget

Soil surveys were conducted in Central and Northeastern Siberia, where larch forest and forest tundra developed (see Fig. 1.2). The surveyed points were located at six different regions: Yakutian basin (62°N, 130°E), Lower Lena (72°N, 126°E), Kolyma lowland (69°N, 160°E), and upper Indigirka (63°N, 145°E) in Northeastern Siberia; and Putorana Mountains (67°N, 97°E); and around Tura (64°N, 100°E) in Central Siberia. At each site, field observation of soil profile was conducted by making representative profiles until permafrost table, along the topography or under typical vegetation. For example, Fig. 8.1 shows typical soil profiles in three locations, i.e., light-colored sandy texture soil in Yakutian basin (Fig. 8.1a),

Fig. 8.1 Typical soil profiles under larch forests; (**a**) in Yakutian basin, Northeastern Siberia (62° 09′N, 130° 38′E), (**b**) in Central Siberia (64° 19′N, 100° 14′E), and (**c**) earth hummock mound soil in forest tundra of Kolyma Lowland (68° 41′N, 160° 17′E). Profile (**a**) had light-colored sandy texture in the active layer. On the other hand, profile (**b**) had high rock fragment ratio in the active layer with loamy and/or clay loamy texture. In this profile (**b**), ice-filled cracks emerged at the bottom of the profile. The cross-section of earth hummock mound (**c**) showed thin A horizon (indicated by white small pins) and bowl-shaped subsoil with diffuse gley mottling (Photos: Y. Matsuura) *(see* Color Plates)

dark-colored with high rock fragment ratio and loamy soil in Tura, Central Siberia (Fig. 8.1b), and earth hummock soil in forest tundra of Kolyma Lowland (Fig. 8.1c).

Soils in active layers were sampled by using stainless steel cylindrical cores for estimation of bulk densities, fine earth ratios, and rock fragment ratios in each

horizon. Cubic block samples of permafrost were taken from the uppermost position of frozen table while avoiding surface contamination. Details of each site (location), sample procedures, and analysis are described elsewhere (Matsuura et al. 1994, 1997; Matsuura and Yefremov 1995, Matsuura and Abaimov 1999). Carbon and nitrogen contents of soil samples and of plant tissues of some major species from the ground vegetation were also determined using 2-mm sieved fine earth fraction and ground plant samples by dry combustion method (NC-800, Sumika Chemical Analysis Service, Osaka, Japan). Carbonate carbon in soil was determined by volumetric method (Allison and Moodie 1965), in case of soil effervescence reaction by diluted HCL drips. Soil organic carbon (SOC) and total nitrogen were estimated by multiplying the C, N contents, bulk density, fine earth ratio, rock fragment ratio, and thickness of horizon in each soil profile.

8.2.2 Soil Properties Along a Toposequence

Variations of soil properties along a toposequence were described in relation to soil active layer condition and other soil characteristics. The study site was at Site 1 near Tura (see Fig. 1.3) on a left bank of the Kochechum River, a branch of the Nizhnyaya Tunguska River. A total of 39 points was set at 30–50 m intervals along the slope from hill-top (crest flat) to riverside (Fig. 8.2).The first ten points

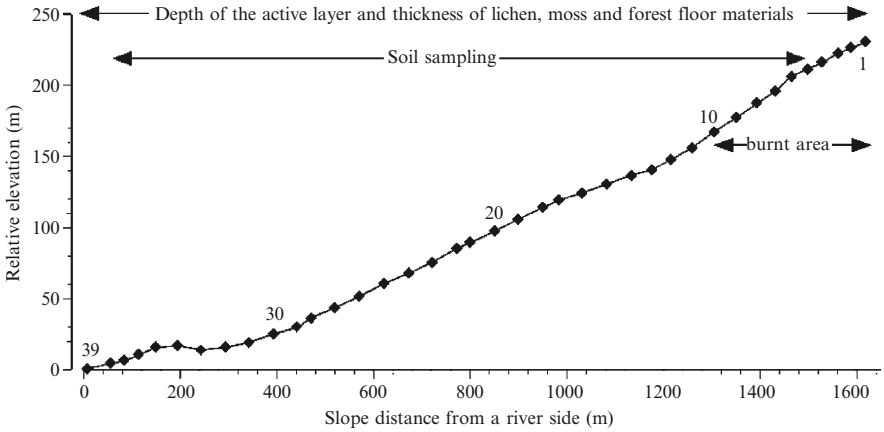

Fig. 8.2 Vertical cross-section of a riverside toposequence near Tura in Central Siberia (after Takenaka et al. 1999). Measurements of soil active layer depth and other variables were conducted at 39 points arranged from the top of the slope (no.1) to the riverside (no.39); soil sampling for chemical analysis was not conducted at the uppermost part of the slope (no.1–4). Most of the measurement points are located in even-aged *L. gmelinii* forest (ca. 105 years-old), except for the zone of recent burn (fire of 1990; no.1–10). Location and geomorphological map of the study slope (Site 1) are also shown in Figs. 1.3 and 2.3

from the hill-top were in an area burnt in 1990. The area including points 34 and 35 was bare ground where vegetation cover was removed by human activity. Other points were mostly located in *L. gmelinii* forests (about 105 years-old in 2004), except for the upper part of slope where young larch forest became reestablished after the intensive fire of 1990 (points 1–10; shown as burnt area in Fig. 8.2; see also Sect. 1.4).

Depth of soil active layer and thickness of lichen, moss, and forest floor materials were measured at all points along the toposequence (Fig. 8.2) in the summer of 1998, using a knocking cone penetrometer (Takenaka et al. 1999). As one of the indices related to forest structure, hemispherical photos were also taken at all points at the aboveground height of 1 m, and the percentage of canopy cover was analyzed by LIA32 (free software; Yamamoto 2003). The surface mineral soil (0–5 cm) was sampled at 34 points (between points 5 and 38) on the same toposequence in the late summer of 2003.

The concentrations of C and N in soil samples were analyzed by a NC analyzer (Sumika Chemical Analysis Service, NC900, Osaka, Japan). Soil pH was measured by a glass electrode in a 1:5 soil-water suspension. Available P was determined colorimetrically using a molybdate-ascorbic acid method (Olsen and Sommers 1982). The concentration of hot KCl-labile NH_4^+–N was calculated as the difference of NH_4^+–N concentrations between the initial and boiled extracts (Gianello and Bremner 1986). The concentration of NH_4^+–N in the extracts was determined colorimetrically by indophenol blue method (Keeny and Nelson 1982).

Principal component analysis was performed to compare the integrated index of soil chemical properties (SPSS 1999). In addition, to evaluate whether these new variables and the depth of soil active layer could explain the spatial variations of canopy cover percentage, multiple regression analysis was performed for the points except for the recently burnt area and the bare ground caused by human activity (SPSS 1999).

8.3 Soil Carbon and Nitrogen Storage

8.3.1 Carbon storage in Forest Ecosystems

Figure 8.3 compares carbon storage among three old larch stands located in three different regions of Siberia: Yakutsk, Tura (C1 in Site2), and near Chersky in Kolyma lowland (Matsuura et al. 2005). The *Larix cajanderi* stand (161 years-old) in Yakutsk had the largest forest biomass and the deepest active layer depth (1.15 m). The *L. cajanderi* stand (>155 years-old) in Kolyma lowland, which was located at forest-tundra transitional zone, had the smallest biomass and the shallowest active layer depth (0.38 m). Old multiaged *L. gmelinii* stand (>220 years-old) near Tura in Central Siberia showed intermediate level of biomass and active layer depth (0.77 m) among them.

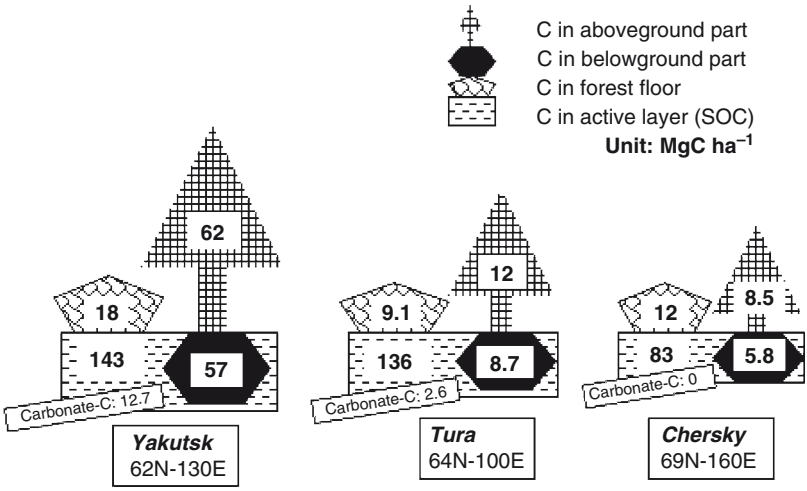

Fig. 8.3 Carbon storage diagram of three representative larch ecosystems in the continuous permafrost region of Siberia (modified from Matsuura et al. 2005). Carbonate-C is determined separately. The coordinates under the site names show approximate latitudes and longitudes. Original data source of plant biomass in each larch stand: Yakutsk (Kanazawa et al. 1994), Tura (Kajimoto et al. 1999), and Chersky (Kajimoto et al. 2006; see Table 6.2)

Both carbon storage in plant biomass and active layer depth in the stand seem unusually large at Yakutsk as compared to the ranges of these variables reported for the larch forests located at similar latitudes (see Sect. 6.3). On the other hand, northernmost larch stand in Chersky had the smallest carbon storage in plant biomass. As suggested by Kajimoto et al. (2006)(see also Chap. 6), carbon storage in belowground biomass was relatively high in all stands established in the permafrost region. Although total carbon storage of the ecosystem varied much among sites (from 110 to 280 Mg C ha^{-1}), the largest organic carbon reservoir was the soil compartment at all sites: 50 % (Yakutsk) to 80 % (Tura) of total carbon was stored in the soil active layer (Fig. 8.3).

8.3.2 SOC Storage and C/N Ratio in Central and Northeastern Siberia

Generally speaking, values of soil C/N ratio in boreal forests and tundra ecosystems are thought to be higher than those in other ecosystems of warmer climate regions (Post et al. 1982, 1985). Although soil C/N ratios in Northeastern Siberia varied much, the values were relatively low as compared to those in Central Siberia (Fig. 8.4). The mean C/N ratio of larch ecosystems in Northeastern Siberia and

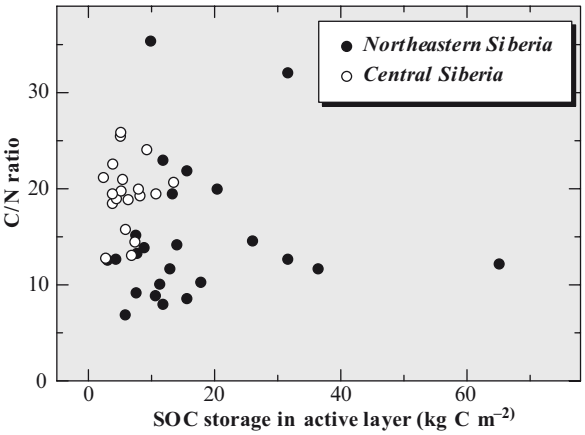

Fig. 8.4 Relationship between SOC storage and C/N ratio of soils in Northeastern (*filled circle*) and Central Siberia (*open circle*) (Matsuura et al., unpublished data)

Central Siberia was 14.8 ± 7.0 (mean±1 SD, $n = 24$) and 19.5 ± 3.6 (mean ±1 SD, $n = 19$), respectively. The mean soil C/N ratio of Northeastern Siberia was significantly lower than that of Central Siberia ($p = 0.0020$, Mann-Whitney's U-test).

The mean SOC storage of active layer in Central Siberia was 6.3 kg C m^{-2}, with a range from 2.5 to 13.6 kg C m^{-2}. Soil C storage often depends on the rock fragment content of the profile. Soils around Tura and forest tundra in Putorana Mountains had rather high rock fragment ratio in each horizon. Since soil parent material of larch ecosystems in Central Siberia was derived from old basalt lava flow (see Chap. 2), most of soil genesis had developed from *in situ* weathered rock fragment on the plateau with gently sloping topography (residual soils), not from particle-sorted thick deposits by river systems.

In contrast, the mean SOC storage in Northeastern Siberia was 16.8 kg C m^{-2}, which was significantly much larger than that (6.3 kg C m^{-2}) of Central Siberia ($p = 0.0001$, Mann-Whitney's U-test). The SOC storage regime in Northeastern Siberia also had wider range (from 3.12 to 65.2 kg C m^{-2}) than that in Central Siberia (<ca. 15 kg C m^{-2}; Fig. 8.4). Among the sites examined in Northeastern Siberia, soils which developed on thermokarst depression (i.e., alas) stored a large amount of SOC in the active layer (30–65 kg C m^{-2}), and the C/N ratio converged around 10–12 (see three data points that appear at far right in the middle portion of Fig. 8.4). Because multiterraced and plain topographies dominated in Yakutian Basin and Kolyma Lowland were created by large river systems, soils in Northeastern Siberia had extremely low rock fragment ratio in the soil matrix. Thus, high fine earth ratio and relatively large bulk density of soils may be responsible for the SOC to assume larger values.

Difference in soil characteristics, especially for SOC storage and C/N ratio, between soils derived from fluvial/lacustrine deposits and soils derived from *in situ*

weathered rock fragments seems to be critically important in the mechanism of nutrient cycling in larch ecosystems in the permafrost region. Soils of different C/N ratio may also respond differently to climate change through mineralization/immobilization processes in the future.

8.4 Soil Properties Along a Toposequence in a Larch Forest

8.4.1 Thickness of Soil Active Layer and Forest Floor, and Characteristics of Canopy Cover

On the riverside toposequence, the depth of soil active layer ranged from 22 to 148 cm, and the thickness of lichen, moss, and forest floor materials ranged from 2.5 to 22 cm (Fig. 8.5). The depth of soil active layer was deeper, and the thickness of lichen, moss, and forest floor materials was thinner in the recently burnt area than in the area that did not burn for about 100 years (Figs. 8.2 and 8.5a, b). Relationship between stand replacing fire and depth of soil active layer is also described elsewhere (e.g., Van Cleve et al. 1983). There was an inverse relationship between depth of soil active layer and thickness of lichen, moss, and forest floor materials (Fig. 8.5a, b; Takenaka et al. 1999). This inverse relationship might be primarily explained by the fact that thick moss layer insulates the soil due to its low bulk density and thermal conductivity (Van Cleve et al. 1983; see also Chap. 4). The percentage of canopy cover ranged from 33 to 66%, and showed a similar pattern to that of the thickness of lichen, moss, and forest floor materials along the toposequence (Fig. 8.5b, c). These results suggested that the depth of soil active layer in the larch forest ecosystem was affected greatly by burning of the organic soil and overstory trees, and was also closely related to chronological patterns of forest structure (i.e., extent of canopy development; see also Van Cleve et al. 1983).

8.4.2 Soil Chemical Properties

Soil chemical properties showed substantial variations on the riverside toposequence (Fig. 8.5, Table 8.1). However, soil chemical properties did not show clear difference between the area of recent burn and that of intact forest unburned during the past 100 years. Moreover, unlike other studies in both boreal and temperate regions (e.g., Hirobe et al. 1998; Giesler et al. 1998), soil chemical properties did not show any altitudinal trend along the toposequence. Giblin et al. (1991) also reported topographic variations in soil physico-chemical properties among six different ecosystem types occurring along a single toposequence in arctic Alaska. In our study site in Central Siberia, however, the overstory vegetation was composed of single species (*L. gmelinii*). Comparisons with these different ecosystems are

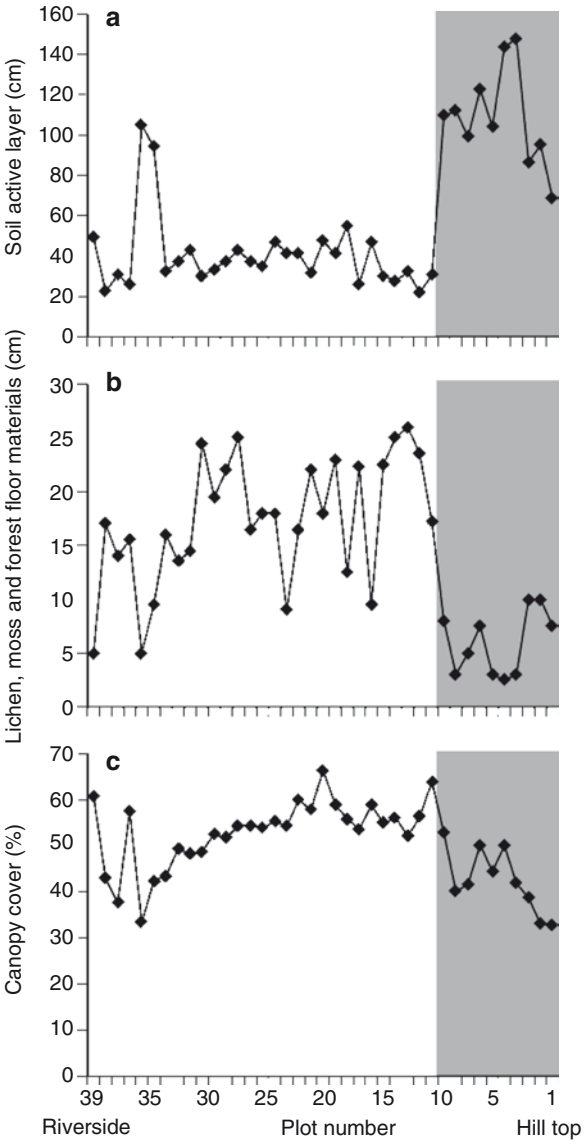

Fig. 8.5 Changes in (**a**) depth of soil active layer, (**b**) thickness of lichen, moss, and forest floor materials, and (**c**) percentage of canopy cover at the aboveground height of 1 m along a toposequence. Location of each observation point (no.1–39) is shown in Fig. 8.1, and the area burnt in 1990 at upper part of the slope (no. 1–10) was shown by shade (Takenaka et al. 1999; Hirobe et al., unpublished data)

difficult due to difference in species composition. Further field studies are required for discussing mechanisms so that no topographic variations in soil properties develop in the larch forest.

Table 8.1 Means and coefficient of variation [(SD/mean) × 100%] of soil chemical properties along a toposequence in Site 1 ($n = 34$) near Tura

	Mean (minimum–maximum)	CV
pH (H_2O)	5.81 (4.52–7.14)	11
Available P (mg-P/kg soil)	10.7 (4.23–37.3)	66
NH_4'–N pool (mg-N/kg soil)	47.8 (16.2–173.1)	66
Hot KCl labile NH_4'–N (mg-N/kg soil)	20.0 (0–64.7)	72
Total C (%)	7.80 (2.50–16.3)	72
Total N (%)	0.30 (0.12–0.66)	40
C/N ratio	26.3 (20.9–33.0)	13

8.4.3 Forest Structure and Soil Nutrient Properties

Principal component analysis of soil chemical properties along the toposequence (Fig. 8.2) showed that the first two principal components accounted for 74.1% of the total variance in the data (Table 8.2). The first principal component (PC1) accounted for 47.4% of the total variance and was highly correlated with available P concentration, NH_4^+–N pool, hot KCl labile NH_4^+–N concentration, and total C and N concentrations. The PC1 may show accumulation of organic matter and nutrient availability. The second principal component (PC2) accounted for 26.7% of the total variance and was highly correlated with pH and C/N ratio. The PC2 may show the quality of organic matter and physicochemical environment for soil microbes. For the points except recently burnt area and bare ground by human activity (see Fig. 8.2), the scores of the first two PCs and the depth of soil active layer were regressed against the percentage of canopy cover. The regression was not significant ($F = 2.12$, $p = 0.13$). The standard regression coefficients were −0.17 ($p = 0.40$), 0.34 ($p = 0.09$), and 0.33 ($p = 0.10$) for PC1, PC2, and the depth of soil active layer, respectively. Although the parameters could not significantly explain the variations of canopy cover percentage, the standard regression coefficients suggested that PC2 and the depth of soil active layer might be more important for controls of canopy cover percentage.

From these considerations, depth of soil active layer seems to be more important than local differences in soil chemical properties for the chronological differences in forest structure. For example, even in old forests of the same age (105 years-old) distributed along the toposequence (Fig. 8.2), larch trees on deeper soil active layer grew better, and formed closed canopy (i.e., larger canopy cover) at the stand level. In addition, the depth of soil active layer, which may cause local differences in soil organic matter quality and physicochemical environment for soil microbes, might also contribute to the spatial differences in forest structure.

Nutrient condition in permafrost larch ecosystems is related to low soil temperature regime during growing seasons, and to repeated freeze–thaw cycles in the soil active layer. Such soil temperature regime is likely to have affected forest structure and root system development of these ecosystems (see Chaps. 6, 7, and 16), and nutrient cycling through organic matter quality.

Table 8.2 The result of the principal component analysis of soil chemical properties along a toposequence in Site 1 near Tura. The first two principal components account for 74.1% of the variability in the entire data

	Loadings after varimax rotation[a]	
	PC1	PC2
pH (H_2O)	−0.09	−0.88
Available P	0.67	0.23
NH_4'–N pool	0.87	−0.15
Hot KCl labile NH_4'–N	0.65	−0.64
Total C	0.91	0.27
Total N	0.91	0.03
C/N ratio	0.15	0.73
Proportion (%)	47.4	26.7

[a]Loadings listed are simple correlations of the original variables with the new principal components, PC1 and PC2

Table 8.3 summarizes leaf (or needle) N status of various plants growing on the three permafrost larch ecosystems: Kolyma lowland and Yakutsk in Northeastern Siberia, and Tura in Central Siberia. Most of green leaf (or needle) N concentrations do not exceed 20 mg g^{-1}, including not only larches (*Larix gmelinii, L. cajanderi*), but also other evergreen trees (e.g., *Pinus pumila*) and woody shrubs (e.g., *Ledum palustre, Vaccinium uliginosum*). Nitrogen concentrations exceeding 20 mg g^{-1} were detected only for three species: two deciduous trees (*Betula exelis*; dwarf birch, and *Duschekia fruticosa*) and one herb (*Chamaenerion angustifolium*; fireweed).

For samples of *L. gmelinii* in Tura, the difference of N concentrations between green needle (15.8 mg g^{-1}) and litterfall needle (4.8 mg g^{-1}) reached 11 mg g^{-1} (Table 8.3). This indicates that about 70% of needle N was retranslocated to woody organs (branch or stem) before senescence in the concentration base. The high rate of N retranslocation was reported for Arctic tundra plants. According to the table summarized by Berendse and Jonasson (1992), N retranslocation before leaf shedding ranged from 39 to 74% in some shrub tree species (*Dryas octopetala*, *Ledum palustre*, *Betula nana*, and *Empetrum nigrum*).

Low quality of organic matter accumulating on the forest floor may be decomposed slowly and may also enhance a kind of conservative nutrient cycling pathway. Figure 8.6 shows rough estimate of the pattern of N cycling in a multiaged old *L. gmelinii* forest (Plot C1 in site 2); here, annual N cycling was calculated by combining the data of needle biomass and annual litterfall (see Tables 6.1 and 6.2), N mineralization rate estimated by *in situ* resin core incubation method (Matsuura and Abaimov 2000), and retranslocation rate of needle N (70%) as mentioned above. Total needle N during growing season was estimated for 15.8 kg N ha^{-1}, and N in litterfall was 4.8 kg N ha^{-1} $year^{-1}$. This N loss via litterfall must be replenished by available N uptake from the soil for the next spring growth. The diagram (Fig. 8.6) suggested that estimated supply of the maximum available N through mineralization processes in the soils (4.3 kg N ha^{-1} $year^{-1}$) was almost equivalent to, or slightly less than, the N loss via litterfall (4.8 kg N ha^{-1} $year^{-1}$)(Matsuura and

Table 8.3 Leaf carbon and nitrogen contents of plant species in Siberia (Matsuura et al., unpublished data)

species		location	carbon (mg g^{-1})	nitrogen (mg g^{-1})	C/N ratio
Larix gmelinii	Litterfall	Tura	503	4.83	104
	Green	*Tura	485 ± 9.6	15.8 ± 1.4	31
Larix cajanderi	Green	Yakutsk	491	17.3	28
Larix cajanderi	Green	**Kolyma	514 ± 13	19.0 ± 2.0	27
Ledum palustre	Current	Kolyma	571	11.8	48
	Current	Tura	557	13.2	42
Pinus pumila	(Current)	Kolyma	541	16.8	32
	(1-year)		510	11.3	45
	(2-year)		543	10.7	51
	(3-year)		543	10.0	54
Empetrum nigrum		Kolyma	551	7.09	78
Betula exilis		Kolyma	500	22.3	22
Vaccinium uliginosum		Tura	516	18.0	29
Duschekia fruticosa	Litterfall	Tura	503	13.4	38
	Green	Tura	514	31.8	16
Chamaedaphne calyculata		Tura	564	12.4	46
Chamaenerion angustifolium		Tura	460	21.5	21
Calamagrostis lapponica		Tura	394	13.3	30
Flavocetraria cucullata		Tura	456	3.5	130
Cladina rangiferina		Tura	450	1.9	237
Cladina stellaris		Tura	439	1.2	366

Sampling location: Kolyma (68°41′N, 160°16′E), Tura (64°19′N, 100°14′E)
Sample size: * $n = 12$; ** $n = 14$; no asterisks = 2

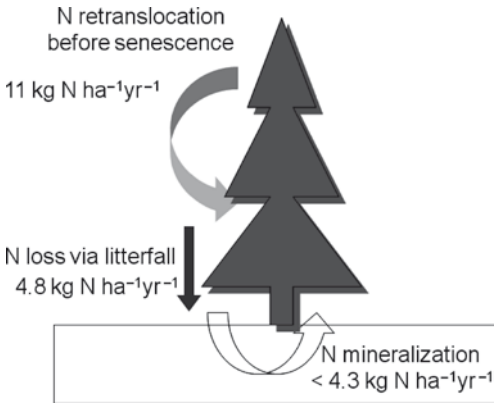

Fig. 8.6 Schematic diagram of nitrogen cycling estimated in a multiaged old *L. gmelinii* forest (>220 years old; plot C1) at Site 2 (Fig. 1.3) near Tura in Central Siberia (After Matsuura and Abaimov 2000; Matsuura et al., unpublished data)

Abaimov 2000). This means that N supply by mineralization in the soil may not meet the annual demand by trees: larches in the old forest might suffer from N deficit condition chronically. Therefore, their growth largely depends on the use of retranslocated N to meet annual demand of individual trees.

8.5 Conclusions

- Larch ecosystems on the continuous permafrost stored organic carbon mostly in the soil component (soil active layer). In the cases of three old larch forests, the proportion of SOC in the ecosystem total carbon stock was 50–80%, though the depth of soil active layer differed among the forests. High proportion of below-ground carbon storage, including plant biomass (roots), is a characteristic of the permafrost larch ecosystems.
- Storage patterns of soil C and N differed between Central and Northeastern Siberia, which were primarily associated with soils of different parent materials and different soil development processes between two regions. Residual soils developed in Central Siberian Plateau with high rock fragment content showed smaller SOC storage and high C/N ratio. In contrast, soils developed in Northeastern Siberia with fluvial/lacustrine deposit with low rock fragment showed larger SOC storage with lower C/N ratio.
- Fire disturbance enhances permafrost thawing and deepens soil active layer during a growing season. Variability in soil characteristics along a toposequence revealed that soil active layer depth and quality of soil organic matter might be important factors in the development of forest structure.
- Larch ecosystems on the continuous permafrost are likely to be nutrient-limited ecosystems at old stand age. Such a status of nutrient limitation was reflected in a tight nitrogen cycling: annual N supply by mineralization does not seem to meet the demand by the larch trees.

Acknowledgments We thank the late Dr. A. Abaimov of V.N. Sukachev Institute of Forest, whose leadership was instrumental in the successful research activities at Tura. We also thank O. Zyryanova, S. Prokushkin, A. Prokushkin, T. Bugaenko, O. Masyagina, and V. Zyryanov for cooperation. We are grateful to V. Borobikov for logistical support in field surveys, to A. Takenaka for the initiative to establish a long toposequence survey line at Site 1. N. Tokuchi, and K. Kondo for supporting our field survey and laboratory procedures in Japan. These activities were funded by Global Environmental Research Fund (S-1 and B-053), Ministry of the Environment, Japan, and by Ministry of Education, Culture, Sports and Technology Japan (No. 16405010 to M. Hirobe).

References

Alexeyev VA, Birdsey RA (1998) Carbon storage in forests and peatlands of Russia. USDA Forest Service, Northeastern Forest Experiment Station, GTR NE-244, 137pp

Allison LE, Moodie CD (1965) Carbonate. In: Black AC (ed) Methods of soil analysis. Part 2: chemical and microbiological properties. American Society of Agronomy, Madison, pp 1379–1396

Berendse F, Jonasson S (1992) Nutrient use and nutrient cycling in northern ecosystems. In: Chapin FS III, Jerreries RL, Reynolds JF, Shaver GR, Svoboda J (eds) Arctic ecosystems in a changing climate. Academic Press, San Diego, pp 337–356

FAO (1993) World soil resources. An explanatory note on the FAO World Soil Resources map. FAO, Rome, 64pp

Gianello C, Bremner JM (1986) A simple chemical method of assessing potentially available organic nitrogen in soil. Comm Soil Sci Plant Anal 17:195–214

Giblin AE, Nadelhoffer KJ, Shaver GR, Laundre JA, McKerrow AJ (1991) Biogeochemical diversity along a riverside toposequence in arctic Alaska. Ecol Monogr 61:415–435

Giesler R, Högberg M, Högberg P (1998) Soil chemistry and plants in Fennoscandian boreal forest as exemplified by a local gradient. Ecology 79:119–137

Hirobe M, Tokuchi N, Iwatsubo G (1998) Spatial variability of soil N transformations along a forest slope in a *Cryptomeria japonica* D. Don plantation. Eur J Soil Biol 34:123–131

ISSS Working Group RB (1998) World reference base for soil resources. In: Bridges EM, Batjes NH, Nachtergaele FO (eds) Atlas. ISRIC-FAO-ISSS-Acco Leuven, Belgium

Ivanova EN (ed) (1969) Soils of Eastern Siberia (translated by A Gourevitch). Israel Program for Scientific Translations Ltd, IPST Press, Jerusalem, 223pp

Jenny H (1980) State factor topography. In: Jenny H (ed) The soil resource, ecological studies 37. Springer, New York, pp 276–304

Kajimoto T, Matsuura Y, Sofronov MA, Volokitina AV, Mori S, Osawa A, Abaimov AP (1999) Above- and belowground biomass and net primary productivity of a Larix gmelinii stand near Tura, central Siberia. Tree Physiol 19:815–822

Kajimoto T, Matsuura Y, Osawa A, Abaimov AP, Zyryanova OA, Isaev AP, Yefremov DP, Mori S, Koike T (2006) Size-mass allometry and biomass allocation of two larch species growing on the continuous permafrost region in Siberia. For Ecol Manage 222:314–325

Kanazawa Y, Osawa A, Ivanov BI, Maximov TC (1994) Biomass of a Larix gmelinii (Rupr.) Litv. stand in Spaskayapad, Yakutsk. In: Inoue G (ed) Proceedings of the Second Symposium on the Joint Siberian Permafrost Studies between Japan and Russia in 1993. National Institute for Environmental Studies, Tsukuba, pp 153–158

Keeny DR, Nelson DW (1982) Nitrogen – inorganic forms. In: Page AL, Miller RH, Keeney DR (eds) Methods of soil analysis, part 2. ASA/SSSA, Madison, WI, pp 643–698

Matsuura Y, Abaimov AP (1999) Soil characteristics in Tura Experiment Forest, central Siberia. In: Shibuya M, Takahashi K, Inoue G (eds) Proceedings of the Seventh Symposium on the Joint Siberian Permafrost Studies between Japan and Russia in 1998. Tsukuba, Japan, pp 69–76

Matsuura Y, Abaimov AP (2000) Nitrogen mineralization in larch forest soils of continuous permafrost region, central Siberia – an implication for nitrogen economy of a larch stand. In: Inoue G, Takenaka A (eds) Proceedings of the Eighth Symposium Joint Siberian Permafrost Studies between Japan and Russia in 1999. Tsukuba, National Institute for Environmental Studies, pp 129–134

Matsuura Y, Yefremov DP (1995) Carbon and nitrogen storage of soils in a forest-tundra area of northern Sakha, Russia. In: Takahashi K, Osawa A, Kanazawa Y (eds) Proceedings of the Third Symposium on the Joint Siberian Permafrost Studies between Japan and Russia in 1994. Sapporo, Japan, pp 97–101

Matsuura Y, Sanada M, Ohta S, Desyatkin RV (1994) Carbon and nitrogen storage in soils developed on two different toposequence of the Lena River terrain. In: Inoue G (ed) Proceedings of the Second Symposium on the Joint Siberian Permafrost Studies between Japan and Russia in 1993. National Institute for Environmental Studies, Tsukuba, pp 177–182

Matsuura Y, Abaimov AP, Zyryanova OA, Isaev AP, Yefremov DP (1997) Carbon and nitrogen storage of mountain forest tundra soils in central and eastern Siberia. In: Inoue G, Takenaka A (eds) Proceedings of the Fifth Symposium on the Joint Siberian Permafrost Studies between Japan and Russia in 1996. National Institute for Environmental Studies, Tsukuba, pp 95–99

Matsuura Y, Kajimoto T, Osawa A, Abaimov AP (2005) Carbon storage in larch ecosystems in continuous permafrost region of Siberia. Phyton 45:51–54

Nadelhoffer KJ, Giblin AE, Shaver GR, Linkins AE (1992) Microbial processes and plant nutrient availability in arctic soils. In: Chapin FS III, Jerreries RL, Reynolds JF, Shaver GR, Svoboda J (eds) Arctic ecosystems in a changing climate. Academic, San Diego, pp 281–300

Naumov Ye M (2004) Soil and soil cover of northeastern Eurasia. In: Kimble JM (ed) Cryosols. Springer, Berlin, pp 161–183

Olsen SR, Sommers LE (1982) Phosphorus. In: Page AL, Miller RH, Keeney DR (eds) Methods of soil analysis, part 2. ASA/SSSA, Madison, pp 403–430

Osawa A, Abaimov AP, Kajimoto T, Matsuura Y, Zyryanova OA, Tokuchi N, Kondo K, Hirobe M (2004) Long-term development of larch forest ecosystems on continuous permafrost of Siberia: structural constraints and implications to carbon accumulation. In: Tanaka H (ed) Proceedings of the Fifth International Workshop on Global Change: Connection to the Arctic 2004 (GCCA5). Tsukuba University, Tsukuba, pp 53–55

Post WM, Emanuel WR, Zinke PJ, Stangenberger AG (1982) Soil carbon pools and world life zones. Nature 298:156–159

Post WM, Pastor J, Zinke PJ, Stangenberger AG (1985) Global patterns of soil nitrogen storage. Nature 317:613–616

Schulze E-D, Schulze W, Kelliher FM, Vygodskaya NN, Ziegler W, Kobak KI, Koch H, Arneth A, Kusnetsova WA, Sogatchev A, Issajev A, Bauer G, Hollinger DY (1995) Aboveground biomass and nitrogen nutrition in a chronosequence of pristine Dahurian *Larix* stands in eastern Siberia. Can J For Res 25:943–960

Soil Survey Staff (1998) Keys to soil taxonomy, 8th edn. USDA National Resources Conservation Service, Washington DC, 326pp

Sokolov IA, Ananko TV, Konyushkov DY (2004) The soil cover of Central Siberia. In: Kimble JM (ed) Cryosols. Springer, Berlin, pp 302–338

SPSS (1999) SPSS 10.0 for Windows. SPSS Inc, Chicago

Takenaka A, Matsuura Y, Abaimov AP (1999) The depth of active layer along a slope as affected by the fire history of ground vegetation. In: Shibuya M, Takahashi K, Inoue G (eds) Proceedings of the Seventh Symposium on the Joint Siberian Permafrost Studies between Japan and Russia in 1998. Tsukuba, Japan, pp 33–39

Van Cleve K, Dyrness CT, Viereck LA, Fox J, Chapin FS III, Oechel W (1983) Taiga ecosystems in interior Alaska. Bioscience 33:39–44

VV Dokuchaev Soil Science Institute (2001) Russian soil classification system (translated by Gerasimova M; Arnold RW (ed)), Moscow, 221 pp

Yamamoto K (2003) LIA for Win32 (LIA32). http://www.agr.nagoya-u.ac.jp/~shinkan/LIA32/index.html

Chapter 9
Soil Respiration in Larch Forests

T. Morishita, O.V. Masyagina, T. Koike, and Y. Matsuura

9.1 Introduction

Soil respiration is an important component process of the carbon cycle (Schlesinger and Andrews 2000). It is derived from both soil microbial respiration and plant root respiration (Luo and Zhou 2006). In boreal forests, substrate supply, soil temperature, and soil moisture control the soil respiration (Luo and Zhou 2006). The litterfall on the soil surface was found to have a liner relationship with an increase in soil respiration (Bowden et al. 1993; Boone et al. 1998; Maier and Kress 2000; Sulzman et al. 2005). Soil respiration responds to aboveground herbivory (Ruess et al. 1998), carbon supply from aboveground photosynthesis to roots (Högberg et al. 2001), fine root density (Shibistova et al. 2002), and availability of nutrients (Nadelhoffer 2000; Burton et al. 2000). Soil temperature strongly affects the soil respiration (Chen and Tian 2005). The soil respiration is also affected by soil moisture as very high soil moisture can block soil pores (Bouma and Bryla 2000), and very low soil moisture limits microbial and root respiration (Yuste et al. 2003). However, the soil respiration is not related to soil moisture in relatively mesic environments (e.g., Palmroth et al. 2005).

Most studies of soil respiration in boreal forests have been conducted in North America and Northern Europe, where the dominant conifer species are evergreen such as spruce, pine, and fir. These evergreen boreal forests are rarely distributed on continuous permafrost in Northern America (e.g., Alaska and Canada) (Weber and Van Cleve 2005). In Northern Europe, spruce and pine are the dominants on organic or podzolic soils with no permafrost (Hytteborn et al. 2005). In contrast, forests of the larch species (*Larix gmelinii* and *L. cajanderi*) are distributed mostly in continuous permafrost in Siberia (Abaimov et al. 1998, 2000). Kajimoto et al. (1999, 2006) reported that the biomass ratio of aboveground total to root in these *Larix* forests is much less than the ratio in other boreal species. The climate of Central and Northeastern Siberia is more severe than that of the other boreal forest regions because of lower temperature and lower precipitation (Abaimov and Sofronov 1996). They imply that soil respiration regime in permafrost *Larix* forests may be somewhat different from that in other evergreen boreal forests.

The magnitude of soil respiration was estimated based on about 100 sites by Kudeyarov and Kurganova (2005) in regions throughout Russia. They reported that

A. Osawa et al. (eds.), *Permafrost Ecosystems: Siberian Larch Forests*,
Ecological studies, Vol. 209, DOI 10.1007/978-1-4020-9693-8_1,

soil respiration rate during the growing season in different natural zones of Russia is similar (0.46–6.67 μmol $m^{-2} s^{-1}$). However, they did not cover fully the area of Russian forests, and suggested the necessity of conducting soil respiration measurements in Siberia, especially in permafrost regions, to improve the global estimate of soil respiration (Kudeyarov and Kurganova 2005; Davidson and Janssens 2006).

Therefore, objectives of this Chapter were to characterize soil respiration during a growing season in *Larix gmelinii* forest at Tura, Central Siberia. The rates of the soil respiration are compared with those of previous studies in other regions of the boreal forests. Also, studies on dynamics of other trace gases such as methane (CH_4) and nitrous oxide (N_2O) in Siberia are reviewed, and implications to evaluation of their global-scale emission rates are discussed.

9.2 Approaches to Study Soil Respiration

9.2.1 Study Site

The study site is located at Carbon Flux Site, 25 km upstream of the settlement of Tura along Nizhnyaya Tunguska River in Central Siberia (see Fig.1.3 and Table 1.1, this Vol.). Geographically, the site is located within and near the western edge of the continuous permafrost region (Abaimov et al. 1998). The climate is typically continental, characterized by large seasonal fluctuation of air temperature and small amount of annual precipitation (Lydolph 1977; Fig. 9.1, also see Chap. 1, this Vol.).

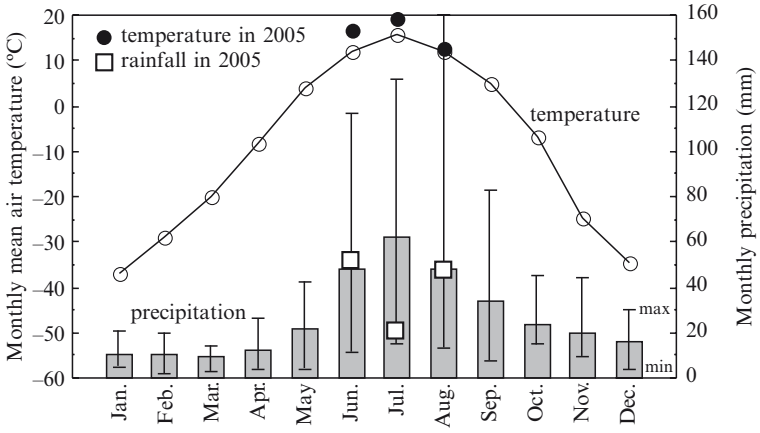

Fig. 9.1 Monthly mean air temperature (*open circle*) and precipitation (*bar*) according to the long-term record at Tura Meteorological Station (Lydolph 1977). Here, the data of mean air temperature (*black circle*) and precipitation (*open square*) for the summer of 2005 are also indicated (Morishita et al. 2006)

The soil type is classified as Gelisol in the World Reference base for soil resources (IUSS Working Group WRB 2006), with permafrost. The soil is completely frozen from mid-October to the beginning of May, and is thawed generally not more than 100 cm during the growing season. The study site mainly consists of a forest of *Larix gmelinii* trees of about 105 years old due to an extensive stand-replacing fire: tree density is 5,480 ha^{-1}, mean height is 3.41 m, and stand total biomass is 16.5 Mg ha^{-1} (Kajimoto et al. 2007; also see Tables 6.1, 6.2, this Vol.). The ground vegetation consists mainly of *Vaccinium vitis-idaea* (Lingonberry), *V. uliginosum* (Dwarf Blueberry), and *Ledum palustre* (Labrador tea). Patches of lichens and mosses cover the forest floor. They are 10–20 cm thick and composed mainly of *Cladina stellaris*, *Pleurozium schreberi*, and *Aulacomnium palustre*. The *Aulacomnium* patches are in relatively lower parts of the microtopography (5–10 cm) compared to those of other species. There is no clear difference in the thickness of the lichen and mosses among the species.

9.2.2 Measurement of Soil Respiration

Soil respiration was measured on June 2–3, July 18–19, and September 7–8, 2005. The soil respiration was measured by using the closed-chamber technique (Sawamoto et al. 2000; Morishita et al. 2003; Melling et al. 2005). Six stainless steel chambers, 25 cm in height and 20 cm in diameter, were set in a plot of ca. 20 m^2. Six patches were selected from the plot, two of which were patches of three major lichen and mosses: *Cladina stellaris*, *Pleurozium schreberi*, and *Aulacomnium palustre*. A chamber was installed at each patch. Before the measurement of the soil respiration, all green parts of the plants on the forest floor were carefully cut and removed in order to exclude live-plant respiration. The soil along the edge of each chamber was cut with a sharp knife. Then, the chamber was pushed into the soil to a depth of 3–5 cm to prevent leakage of gas from the bottom of the chamber. The chamber was left overnight to reduce the effect of disturbance. This duration was enough to establish an equilibrium state before the gas sampling (Melling et al. 2005).

Gas sampling commenced after the >24 h chamber equilibration. Initially, a 500-mL gas sample was collected with a syringe in a Tedlar® bag from the headspace of each chamber before sealed with an acrylic cover, and this sampling was regarded as being taken at the beginning of measurement (time 0 min). Another was collected 6 min after the chamber was sealed with the cover. The cover had two ports, one for gas sampling and the other for attaching a small bag to equilibrate the chamber pressure with the atmospheric pressure. The CO_2 concentration of each air sample was determined in the laboratory (described below).

Soil temperature and moisture were measured in each patch. Soil temperature was measured with a digital thermometer at a depth of 5 cm under the live lichens and moss layers. Frequently, soil temperature was measured not in the mineral soil, but in the humus layer. Soil moisture was measured as volumetric water content with a TDR (HydrosenseTM, Campbell Scientific Australia Pty. Ltd.) at depths of

0–12 cm near the chambers. All measurements were taken with three replications. However, we could not measure soil moisture in June because the probes could not be inserted into the soil due to soil freezing.

The daily change of the soil respiration was estimated by taking three measurements daily in the beginning of June, and nine measurements in the middle of July and beginning of September in 2005.

9.2.3 CO_2 Analysis and Calculation of Soil Respiration Rate

The CO_2 concentration in each bag was determined within a day of sampling using a portable infrared gas analyzer (LI–820, LI–COR). The gas analyzer was calibrated using a standard calibration gas mixture of 0 and 450 ppmv CO_2 in N_2. We used two-point regression of CO_2 concentrations in the headspace and air temperature in the chamber to estimate the soil respiration rate at each sampling point following the reports of Nakano et al. (2004) and Melling et al. (2005). The accuracy of this method was described by Melling et al. (2005). Before this study, we had confirmed that CO_2 concentration in the chamber increased linearly with increasing time in our study sites. The detectable limit of soil respiration rate in our study was 0.02 μmol $m^{-2} s^{-1}$.

9.2.4 Climate Condition of the Measurement Period

Monthly mean air temperature and precipitation with the long-term record at Tura Meteorological Station (Lydolph 1977) are shown in Fig. 9.1. The monthly mean temperatures in June (16.6°C) and July (19.0°C) in 2005 were higher ca. 4°C than those of the long-term record. The temperature in August 2005 (12.8°C) was similar to the record (12.0°C). The monthly mean precipitation in July (19.5 mm) was lower than that of the long-term record (62 mm), and the precipitations in June and August were similar to those recorded. Therefore, growing season in 2005 was hotter and drier compared with the norm.

Mean air temperatures during the measurement of soil respiration in June (16.9°C) and July (17.3°C) were similar to the respective monthly mean temperatures of 2005. The temperature during the measurement in September (10.3°C) was much higher than the monthly average (5.1°C), and was similar to that in August (12.8°C).

9.3 Soil Temperature, Moisture, and Respiration Rate

Daily changes of soil temperature, moisture, and soil respiration rate were shown in Fig. 9.2. The highest values of soil temperature were observed in the afternoon (Figs. 9.2a, b, and c). The lowest values of soil temperature were observed in the

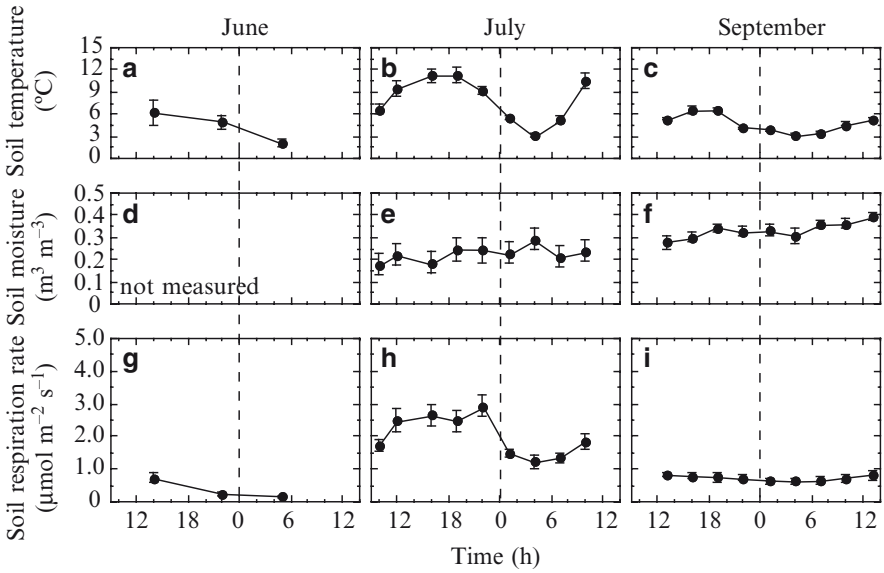

Fig. 9.2 Daily changes in soil respiration, soil temperature, and soil moisture in the *L. gmelinii* forest for the measurement period in June, July, and August 2005. Values are means (± 1 SE). (Morishita et al. 2006)

Table 9.1 Summary of soil temperature, soil moisture, and soil respiration in each measurement

	Soil temperature (°C)			Soil moisture ($m^3 m^{-3}$)			Soil respiration ($\mu mol\ m^{-2} s^{-1}$)		
	Mean	Min	Max	Mean	Min	Max	Mean	Min	Max
June	4.4	0.3	12.5	–	–	–	0.38	0.02	1.13
July	8.0	2.6	14.2	0.23	0.06	0.47	2.03	0.71	4.19
Sept	4.8	2.9	7.8	0.34	0.19	0.43	0.73	0.21	1.18

early morning around 4:00 (Figs. 9.2a, b, and c). The daily range of soil temperature (max. and min.) was larger in June (0.3 and 12.5°C) and July (2.6 and 14.2°C) than that in September (2.9 and 7.8°C) (Table 9.1). The highest soil temperature of all seasons was observed in July, but the lowest temperature in the early morning was not different among the months (Table 9.1). On the other hand, daily change in soil moisture was not clear (Fig. 9.2d, e and f). The daily averages of soil moisture were higher in September than in July (Table 9.1).

The daily changes in soil respiration were clear in July (Fig. 9.2h), but not in June (Fig. 9.2g) and September (Fig. 9.2i). The highest soil respiration was observed at different times. However, the lowest soil respiration was observed in early morning.

9.4 Relationship Between Soil Respiration and Soil Temperature and Moisture

Soil respiration was positively correlated with soil temperature ($R^2 = 0.46$, $p < 0.01$) (Fig. 9.3a) and negatively correlated with soil moisture ($R^2 = 0.43$, $p < 0.01$) (Fig. 9.3b), when all data were combined. Although soil temperature and soil moisture were correlated with each other ($R^2 = 0.27$, $p < 0.01$), the partial correlation coefficient was significant between soil respiration and soil temperature ($R^2 = 0.28$, $p < 0.01$) or soil moisture ($R^2 = 0.24$, $p < 0.01$).

The relationship between soil temperature and soil respiration was different among the months (Fig. 9.3c). For example, high soil temperature values in June (maximum 12.5°C) were similar to those (14.1°C) in July, but the soil respiration in June (1.13 μmol $m^{-2} s^{-1}$) was much less than that in July (more than ca.

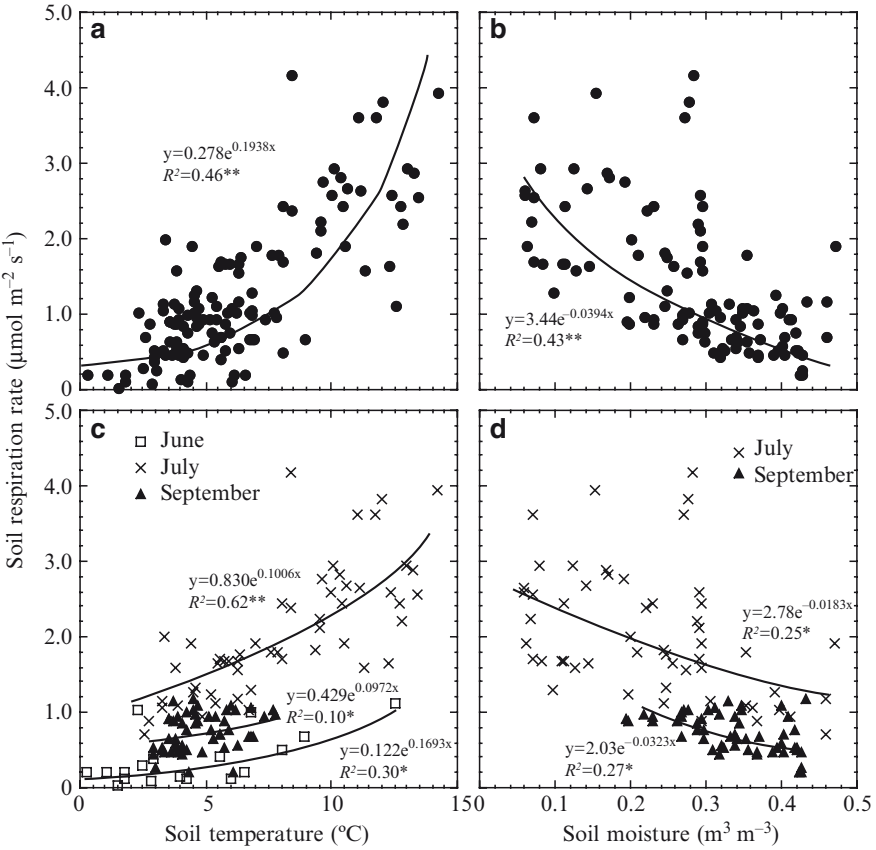

Fig. 9.3 Relationship between soil respiration and soil temperature in the *L. gmelinii* forest (Morishita et al. 2006)

1.5 μmol $m^{-2} s^{-1}$). On the other hand, when soil temperature was less than 5°C, soil respiration in July (0.7–2.0 μmol $m^{-2} s^{-1}$) was much higher than that in June (0.1–1.0 μmol m^{-2} s^{-1}) and September (0.2–1.2 μmol $m^{-2} s^{-1}$). For each month, the soil respiration was positively correlated with soil temperature ($p < 0.05$) as indicated by each regression curve (Fig. 9.3c). The relationship between soil moisture and soil respiration was also different among the months (Fig. 9.3d).

9.5 Seasonal Changes of Soil Respiration

According to the relationship between soil respiration and soil temperature, soil respiration rate under the same soil temperature tended to be different among seasons (Fig. 9.3c). It is considered that the frozen soil would affect soil respiration. In June, organic horizon had been thawed, but mineral horizon was still largely frozen. Sawamoto et al. (2000) reported that soil respiration rate per unit area was lower in the mineral horizon than that in the organic horizon in a *Larix gmelinii* forest near Yaktsuk in Northeastern Siberia. Furthermore, very low soil respiration was observed for the frozen soils in other boreal forests such as jack pine and black spruce forests near Thompson, Manitoba (Winston et al. 1997), a coniferous forest at high elevation between 3,400 and 3,700 m in Colorado Rockies (Brooks et al 2004), and a Scots pine forest in Finland (Ilvesniemi et al. 2005). These observations mean that frozen soils would emit small amounts of CO_2. Thus, the relatively low soil respiration at high soil temperature in June observed in the *L. gmelinii* forest of the present study, which was measured in the organic horizon, might have been caused by a relatively small contribution of soil respiration from the frozen mineral soil.

On the other hand, soil respiration rate in August and September was not as high as that in July under similar temperature conditions (Fig. 9.3c). Both microbial and root respiration were thought to be higher in July than those in other months by reflecting the amount of carbon supply and plant activity. In the stand of this study, litterfall of larch trees starts in late August or early September, and the soils start to freeze in the middle of September due to declining soil temperature near the ground surface (see Chap. 10, this Vol.). This means that much of the new litter would be decomposed in the next growing season. Maier and Kress (2000) manipulated the aboveground litterfall at the soil surface in a loblolly pine forest, and found a linear relationship between the increase in soil respiration and the amount of litter added to the soil surface. Similar relationships of litter input and soil respiration have been found in a mixed species forest in Massachusetts (Bowden et al. 1993; Boone et al. 1998; Sulzman et al. 2005). Therefore, when the soil is thawed and soil temperature increases in the warmer season, litter would decompose. Furthermore, peak fine-root elongation was observed in mid- to late- summer in Alaska (Tryon and Chapin 1983; Ruess et al. 1998) and in Siberia (Abaimov et al. 2000), when soil temperature was the highest. Root respiration increases exponentially with the increase in soil temperature (Burton et al. 1996). Soil respiration is also correlated positively

with fine root density (Shibistova et al. 2002). Högberg et al. (2001) reported that the amount of carbon allocation to roots controlled soil respiration in Scots pine forests. Thus, increase in fine root biomass, which enhances root respiration, and substrate supply (i.e., litterfall) might primarily explain the fact that soil respiration was higher in July than in the other months in the *L. gmelinii* stand.

9.6 Comparison of Soil Respiration in the Growing Season

The measured soil respiration in our *L. gmelinii* forest (0.38–2.03 μmol $m^{-2} s^{-1}$) was generally lower than those previously reported in the larch forests of Siberia. Yanagihara et al. (2000) reported that soil respiration ranged 0.6–12.6 μmol $m^{-2} s^{-1}$ on north- and south-facing slopes in >220 years-old *L. gmelinii* stands at Site 2 in Tura; these stands are located about 20 km northwest of the present study site (see Fig.1.3 and Table 1.1, this Vol.). They measured soil respiration in early August, and reported that soil respiration was higher on the south-facing slope (2.5–12 μmol $m^{-2} s^{-1}$) than on the north-facing slope (0.6–4.0 μmol $m^{-2} s^{-1}$) due to higher soil temperature and nitrogen content and lower moisture of the soil. The soil respiration rate in July of our study site was similar to their values on the north-facing slope, though our site was located on an almost flat area (<3° in slope inclination). Therefore, soil respiration rate differs by topography, and it may be higher in the south-facing slope due to higher soil temperature than in north-facing slope or in flat terrain in Central Siberia.

Nakai et al. (2008) reported that night-time net ecosystem exchange of CO_2 (NEE) in our *L. gmelinii* stand (plot CF) was mostly below 1 μmol $m^{-2} s^{-1}$ in early June, and within 2 μmol $m^{-2} s^{-1}$ between late June and early August in the growing season of 2004 (see also Chap. 10, this Vol.). The result indicates that ecosystem level respiration rates (i.e., -NEE in nighttime) are apparently about twice as large as our values of soil respiration, though the observation years are different. However, night-time ecosystem respiration should be higher than soil respiration in theory, since it includes not only soil respiration but also respiration of aboveground vegetation. Therefore, considering the fraction of vegetation respiration above the ground, the soil respiration rates measured by our closed-chamber method may not be in conflict with the estimate of ecosystem level respiration.

In a *L. gmelinii* forest on continuous permafrost in Yakutsk, Northeastern Siberia, Sawamoto et al. (2000) reported that soil respiration in severely burned forests (1.07–1.50 μmol $m^{-2} s^{-1}$ in July) was lower than that in intact forests (4.16–4.20 μmol $m^{-2} s^{-1}$) due to low rates of root and microbial respiration. Our results of soil respiration rate in the same season are comparable to their data, partly because our measurement followed the method identical to theirs: chamber size, forest floor preparation, collection of gas samples in chamber, and sampling time. The measured soil respiration in this study was similar to the values in severely burned forests, not in the intact forests, though our site consisted of old larch trees (about 100 years). Difference in biomass and soil environment might have caused the lower soil respiration in the present study. Aboveground biomass in larch forests of

Central Siberia (Kajimoto et al. 2006) is generally lower than that of other boreal forests (Cannell 1982). Matsuura (2006) reported that average C/N ratio in the soils of Northeastern Siberia can show anomalous values, compared to other boreal ecosystems when samples are taken in areas under the influence of large rivers (e.g., Lena River)(also see Chap. 8, this Vol.). The large soil respiration in the larch stand of Yakutsk may be influenced by these factors.

Soil respiration rate of the *L. gmelinii* forest in Central Siberia is lower than that of other, mostly nonpermafrost, boreal forests (Fig. 9.4). The total amount of soil respiration in all areas of Russia was estimated by Kudeyarov and Kurganova (2005) by referring to about 100 published reports. They suggested that the mean daily values of soil respiration during a growing season were not different between northern and southern taiga. However, the paper included only one datum from Yakutsk in Northeastern Siberia, which showed a higher soil respiration rate compared to that in this study.

Among three *Larix* species in Siberia, *Larix sibirica* is distributed mostly on discontinuous permafrost in Western Siberia, west of the Yenisei River, while *L. gmelinii* and *L. cajanderi* are distributed over the continuous permafrost region, east of the Yenisei River in Central and Northeastern Siberia (see Chaps. 1 and 3, this Vol.). Boreal forest is distributed over continuous permafrost only in Central and Northeastern Siberia. Thus, the deciduous habit of these two larch species and widespread distribution of the permafrost may affect soil respiration. The aboveground biomass in Central Siberia is generally lower than that in other boreal forests (Cannell 1982; also see Chap. 7, this Volume). On the other hand, root to aboveground biomass ratio was larger in Central Siberia than that in other boreal and

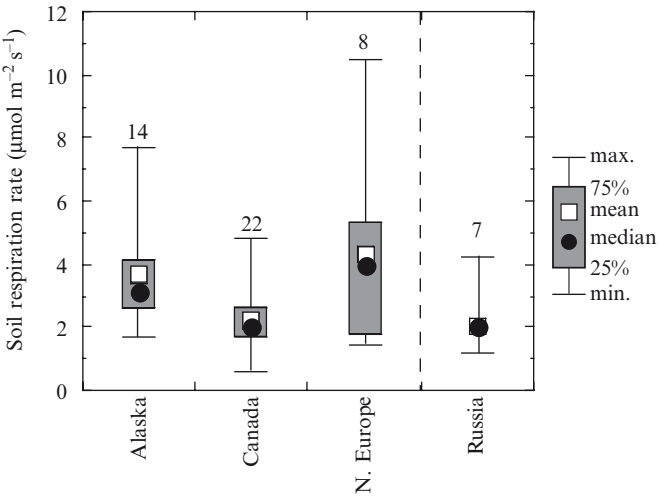

Fig. 9.4 Comparison of mean soil respiration rate (SR) during a growing season among boreal coniferous forests. Number of data is shown above each bar; individual values of SR are listed in Appendix A9.2

subalpine conifer forests. This pattern is considered to be due to low availability of soil-N (Kajimoto et al. 1999; also see Chap. 6, this Volume). According to our study, there were different relationships between soil respiration and soil temperature depending on the season. Presence of the permafrost and deciduous character of larch may be related to this pattern. Therefore, soil respiration of the boreal forest biome might have been overestimated due to omission of sites with low soil respiration values in the continuous permafrost zone. It is necessary to accumulate further data on soil respiration of the Siberian taiga that is likely to be affected by vegetation type, soil condition, and various other factors as indicated in recent reports (Kudeyarov and Kurganova 2005; Davidson and Janssens 2006).

9.7 Dynamics of Other Trace Gases in Larch Forests of Siberia

9.7.1 Methane (CH_4)

Methane (CH_4) is an important greenhouse gas with a contribution of about 18% in radiative forcing of global climate (IPCC 2007). Total CH_4 emission is estimated to be 582 Tg y^{-1} (IPCC 2007). Major sources of atmospheric CH_4 include the production and use of energy, biomass burning, rice fields, natural wetland systems, landfills, and enteric fermentation in animals and termites. The major sinks are considered to be the atmosphere and soils: 551 Tg y^{-1} is estimated to be consumed by the reaction of CH_4 with hydroxyl radicals in the atmosphere, while soils consume 30 Tg y^{-1} (IPCC 2007).

According to the latest estimation of CH_4 uptake by modeling (Curry 2007) and inventory data (Dutaur and Verchot 2007), CH_4 uptake in boreal forest soils accounts for 14 and 21% of the total CH_4 uptake by world's forest soils, referring to two methods. However, the CH_4 uptake by *Larix* taiga (*L. gmelinii*, *L. cajanderi*) over the continuous permafrost is not included in these estimates, though area of the larch forests is very large (see Sect. 9.1). At *L. gmelinii* forest in Yakutsk, Northeastern Siberia, Morishita et al. (2003) reported that CH_4 uptake in July ranged from −13 to −17 μg C m^{-2} h^{-1}. Such a CH_4 sink could appear as a large CH_4 source (0.6–7.0×10^3 μg C $m^{-2} h^{-1}$) after severe forest fires and thermokarst formation. The thermokarst increases CH_4 production and decreases CH_4 consumption by accumulation of salts and increase in soil moisture and soil organic carbon. At *L. gmelinii* stand of our study in Tura (CF), Central Siberia, Morishita et al. (2006) reported that CH_4 uptake in July ranged from −1.6 to −3.4 μg C $m^{-2} h^{-1}$. The value is much lower than that of the larch forest in Northeastern Siberia. Takakai et al. (2008) reported recently that annual CH_4 uptake ranged between −0.11 and −0.17 kg CH_4 $ha^{-1} y^{-1}$ in Northeastern Siberia. If the method of Dutaur and Verchot (2007) is applied, annual CH_4 uptake would reach the values between −0.07 and −0.16 kg CH_4 $ha^{-1} y^{-1}$ in our study stand of Central Siberia. These values of both *L. gmelinii* forests are one-tenth of those in the other boreal forests reported by Curry (2007) of −1.39 kg CH_4 $ha^{-1} y^{-1}$, and by Dutaur and Verchot (2007) of −1.66 kg CH_4 $ha^{-1} y^{-1}$.

9.7.2 Nitrous Oxide (N_2O)

Nitrous Oxide (N_2O) is an important greenhouse gas, contributing about 6% of radiative forcing in global climate (IPCC 2007). Total N_2O emission is estimated to be 17.7 Tg y^{-1} (IPCC 2007). Major sources of atmospheric N_2O include agriculture (2.8 Tg y^{-1}) and soils under natural vegetation (6.6 Tg y^{-1}) (IPCC 2007). However, uncertainty in estimation is still high due to large temporal and spatial variations.

Rate of N_2O emission in *Larix* taiga over continuous permafrost has rarely been examined. According to some recent reports, N_2O emission rate in *L. gmelinii* forest in Northeastern Siberia ranged from −2.1 to 1.0 μg N $m^{-2}h^{-1}$ in July in 2002 (Morishita et al. 2007) and −0.3–4.6 μg N $m^{-2}h^{-1}$ in growing season in 2004 and 2005 (Takakai et al. 2008). N_2O emission rate ranged from −0.4 to 1.0 μg N $m^{-2}h^{-1}$ in our old larch stand at Tura (plot CF) in Central Siberia (Morishita et al. 2006). These values are similar to those previously reported for other boreal forests: 0.22–1.3 μg N $m^{-2}h^{-1}$ (Klemedtsson et al. 1997; Corre et al. 1999).

N_2O uptake was observed in *L. gmelinii* forest in Northeastern and Central Siberia. Generally, N_2O consumption could occur under anaerobic condition due to a process of denitrification (Aulakh et al. 1992). However, the larch forest soils of Siberia are generally under aerobic condition as a result of low rainfall. Chapuis-Lardy et al. (2007) reviewed recently that N_2O consumption in soils is related to low inorganic N input into the soil and low availability of mineral N, but the exact relationships are still unclear. Nitrogen input and N mineralization are thought to be low in Central Siberia (see Chap. 12, this Vol.) probably due to low precipitation and low temperature, so that these may result in N_2O uptake into the soil.

9.8 Conclusions

Soil respiration was positively correlated with soil temperature and negatively correlated with soil moisture in a 105 years-old *L. gmelinii* forest in Central Siberia. Present estimates of the rate of soil respiration were smaller than those previously reported in other boreal forests. It was suggested that the differences in plant biomass and soil condition were important factors explaining the low values of the soil respiration in Central Siberia. The total value of soil respiration for the world's boreal forests may have been overestimated by ignoring the small values of soil respiration in the regions of continuous permafrost. In addition, there have been few studies of CH_4 and N_2O dynamics in the larch forests over continuous permafrost. Accumulating knowledge of the soil respiration, CH_4 uptake, and N_2O dynamics in boreal forests in the regions of continuous permafrost is deemed necessary for obtaining better estimates of their contribution at global scale.

Appendix A9.1 Soil respiration rates (SR; μmol $m^{-2} s^{-1}$) during a growing season measured in boreal forest ecosystems (>45°N)

Location			Vegetation	Age	Site condition	Measuring period	SR	Reference
Canada								
55° 53′N	98° 20′W	Manitoba	Black spruce	4	Dry0	May–Aug	1.30	Bond-Lamberty et al. 2004
55° 53′N	98° 20′W	Manitoba	Black spruce	7	Dry	May–Aug	0.60	Bond-Lamberty et al. 2004
55° 53′N	98° 20′W	Manitoba	Black spruce	13	Dry	May–Aug	1.98	Bond-Lamberty et al. 2004
55° 53′N	98° 20′W	Manitoba	Black spruce	21	Dry	May–Aug	2.75	Bond-Lamberty et al. 2004
55° 53′N	98° 20′W	Manitoba	Black spruce	38	Dry	May–Aug	2.20	Bond-Lamberty et al. 2004
55° 53′N	98° 20′W	Manitoba	Black spruce	72	Dry	May–Aug	2.27	Bond-Lamberty et al. 2004
55° 53′N	98° 20′W	Manitoba	Black spruce	152	Dry	May–Aug	1.85	Bond-Lamberty et al. 2004
55° 53′N	98° 20′W	Manitoba	Black spruce	4	Wet	May–Aug	0.66	Bond-Lamberty et al. 2004
55° 53′N	98° 20′W	Manitoba	Black spruce	7	Wet	May–Aug	2.36	Bond-Lamberty et al. 2004
55° 53′N	98° 20′W	Manitoba	Black spruce	13	Wet	May–Aug	1.65	Bond-Lamberty et al. 2004
55° 53′N	98° 20′W	Manitoba	Black spruce	21	Wet	May–Aug	3.20	Bond-Lamberty et al. 2004
55° 53′N	98° 20′W	Manitoba	Black spruce	38	Wet	May–Aug	2.08	Bond-Lamberty et al. 2004
55° 53′	98° 20′W	Manitoba	Black spruce	72	Wet	May–Aug	1.60	Bond-Lamberty et al. 2004
55° 53′	98° 20′W	Manitoba	Black spruce	152	Wet	May–Aug	1.67	Bond-Lamberty et al. 2004
54°–′N	105°–′W	Saskatchewan	Black spruce		Feather	May–Oct	2.81	O'Connell et al. 2003
54°–′N	105°–′W	Saskatchewan	Black spruce		Sphagnam	May–Oct	1.40	O'Connell et al. 2003
53° 92′N	104° 69′W		Jack pine			May–Sep	2.26	Striegl and Wickland 1998
47° 44′N	68° 09′W		Balsam fir	50	Mid	Apr–Dec	4.43	Lavigne et al. 2003
47° 19′N	71° 06′W		Balsam fir	60	Cool	Apr–Dec	3.12	Lavigne et al. 2003
46° 10′N	89° 40′W	Boulder	Red pine	31		Apr–Nov	1.92	Haynes and Gower 1995
46° 02′N	66° 23′W		Balsam fir	40	Warm	Apr–Dec	4.79	Lavigne et al. 2003
–			Black spruce			Aug–Sep	1.72	Rayment and Jarvis 1997
						Median	2.03	
						Mean	2.21	
Alaska								
64° 48′N	147° 52′W		Black spruce					Ruess et al. 2003

64° 48′N	147° 52′W		Black spruce					Ruess et al. 2003
64° 48′N	147° 52′W		Black spruce					Ruess et al. 2003
–			Black spruce					Bonan 1993
–			White spruce					Bonan 1993
63–65°N	142–148°W		Black spruce					Kane et al. 2006
63–65°N	142–148°W		Black spruce					Kane et al. 2006
63–65°N	142–148°W		Black spruce					Kane et al. 2006
63–65°N	142–148°W		Black spruce					Kane et al. 2006
63–65°N	142–148°W		Black spruce					Kane et al. 2006
63–65°N	142–148°W		Black spruce					Kane et al. 2006
63–65°N	142–148°W		Black spruce					Kane et al. 2006
63–65°N	142–148°W		Black spruce					Kane et al. 2006
63–65°N	142–148°W		Black spruce					Kane et al. 2006
Northern Europa								
64° 14′N	19° 46′E	Sweden	Scots pine	44–55		May–Nov.	1.69	Bhupinderpal-Singh et al. 2003
64° 14′N	19° 46′E	Aheden, Sweden	Scots pine	44–55		Jun.–Oct.	1.80	Hogberg et al. 2001
64° 07′N	19° 27′E	Flakaliden, Sweden	Norway spruce	40		May–Oct.	3.23	Eliasson et al. 2005
62° 47′N	30° 58′E	Finland	Spruce			May–Oct.	1.45	Niinisto et al. 2004
60° 05′N	17° 29′E	Uppsala, Sweden	Norway spruce/scots pine		CIP2	May–Oct.	10.51	Moren and Lindroth 2000
60° 05′N	17° 29′E	Uppsala, Sweden	Norway spruce/scots pine		C1	May–Oct.	5.08	Moren and Lindroth 2000
60° 05′N	17° 29′E	Uppsala, Sweden	Norway spruce/scots pine		C2	May–Oct.	4.73	Moren and Lindroth 2000
60° 05′N	17° 30′E	Uppsala, Sweden	Norway spruce			May–Oct.	6.04	Widen and Majdi 2001
						Median	3.98	
						2.49	4.32	
Russia								
62° 18′N	129° 06′N	Yakutsk	Larch		Loam	Jul.	4.20	Sawamoto et al. 2000

(continued)

Appendix A9.1 (continued)

Location			Vegetation	Age	Site condition	Measuring period	SR	Reference
62° 13′N	129° 10′E	Yakutsk	Larch		Sandy	Jul.	4.15	Sawamoto et al. 2000
60° 52′N	128° 16′E	Yakutsk				Jul.	2.40	Hollinger et al. 1998
61° N	89°E	Zotino			Sandy	Jul.	1.90	Kelliher et al. 1999
Northern Taiga				$n=8$			1.22	Kurganova and Kudeyarov 1998
Middle Taiga				$n=14$			1.55	Kurganova and Kudeyarov 1998
Sourthen Taiga				$n=81$			2.01	Kurganova and Kudeyarov 1998
						Median	2.01	
						Mean	2.49	

References

Abaimov AP, Sofronov MA (1996) The main trends of post-fire succession in near-tundra forests of central Siberia. In: Goldammer JG, Furyaev VV (eds) Fire in ecosystems of boreal Eurasia. Kluwer Academic Publishers, Dordrecht, pp 372–386

Abaimov AP, Lesinski JA, Martinsson O, Milyutin LI (1998) Variability and ecology of Siberian larch species. Swedish University of Agricultural Sciences, Department of Silviculture, Reports 43, Umeå, p 118

Abaimov AP, Zyryanova OA, Prokushkin SG, Koike T, Matsuura Y (2000) Forest ecosystems of the cryolithic zone of Siberia; regional features, mechanisms of stability and pyrogenic changes. Eurasian J Res 1:1–10

Aulakh MS, Doran JW, Mosier AR (1992) Soil denitrification: significance, measurement, and effects on management. In: Stewart BA (ed) Advances in soil science vol 18. Springer, Berlin Heidelberg New York, pp 1–58

Bhupinderpal-Singh NA, Lofvenius MO, Högberg MN, Mellander PE, Högberg P (2003) Tree root and soil heterotrophic respiration as revealed by girdling of boreal Scots pine forest: extending observations beyond the first year. Plant Cell Environ 26:1287–1296

Bonan GB (1993) Physiological controls of the carbon balance of boreal forest ecosystems. Can J For Res 23:1453–1471

Bond-Lamberty B, Wang CK, Gower ST (2004) Contribution of root respiration to soil surface CO_2 flux in a boreal black spruce chronosequence. Tree Physiol 24:1387–1395

Boone RD, Nadelhoffer KJ, Canary JD, Kaye JP (1998) Roots exert a strong influence on the temperature sensitivity of soil respiration. Nature 396:570–572

Bouma TJ, Bryla DR (2000) On the assessment of root and soil respiration for soils of different textures: interactions with soil moisture contents and soil CO_2 concentrations. Plant Soil 227:215–221

Bowden RD, Nadelhoffer KJ, Boone RD, Melillo JM, Garrison JB (1993) Contributions of above-ground litter, belowground litter, and root respiration to total soil respiration in a temperature mixed hardwood forest. Can J For Res 23:1402–1407

Brooks PD, McKnight D, Elder K (2004) Carbon limitation of soil respiration under winter snowpacks: potential feedbacks between growing season and winter carbon fluxes. Global Change Biol 11:231–238

Burton AJ, Pregitzer KS, Zogg GP, Zak DR (1996) Latitudinal variation in sugar maple fine root respiration. Can J For Res 26:1761–1768

Burton AJ, Pregitzer KS, Hendrick RL (2000) Relationships between fine root dynamics and nitrogen availability in Michigan northern hardwood forests. Oecologia 125:389–399

Cannell MGR (1982) World forest biomass and primary production data. Academic Press, New York

Chapuis-Lardy L, Wrage N, Metay A, Chotte JL, Bernoux M (2007) Soils, a sink for N_2O? a review. Global Change Biol 13:1–17

Chen H, Tian HQ (2005) Does a general temperature-dependent Q_{10} model of soil respiration exsist at biome and global scale? J Integr Plant Biol 47:1288–1302

Corre MD, Pennock DJ, Van Kessel C, Elliott DK (1999) Estimation of annual nitrous oxide emissions from a transitional grassland-forest region in Saskatchewan, Canada. Biogeochemistry 44:29–49

Curry C (2007) Modeling the soil consumption of atmospheric methane at the global scale. Global Biogeochem Cycles 21:GB4012

Davidson EA, Janssens IA (2006) Temperature sensitivity of soil carbon decomposition and feedbacks to climate change. Nature 440:165–173

Dutaur L, Verchot LV (2007) A global inventory of the soil CH4 sink. Global Biogeochem Cycles 21:GB4013

Eliasson PE, McMurtrie RE, Pepper DA, Stromgren M, Linder S, Agren GI (2005) The response of heterotrophic CO2 flux to soil warming. Global Change Biol 11:167–181

Haynes BE, Gower ST (1995) Belowground carbon allocation in unfertilized and fertilized red pine plantations in northern Wisconsin. Tree Physiol 15:317–325

Högberg P, Nordgren A, Buchmann N, Taylor AFS, Ekblad A, Högberg MN, Nyberg G, Ottosson-Lövenius M, Read DJ (2001) Large-scale forest girdling shows that current photosynthesis drives soil respiration. Nature 411:789–792

Hollinger DY, Kelliher FM, Schulze ED, Bauer G, Arneth A, Byers JN, Hunt JE, McSeveny TM, Kobak KI, Milukova I, Sogatchev A, Tatarinov F, Varlargin A, Ziegler W, Vygodskaya NN (1998) Forest-atmosphere carbon dioxide exchange in eastern Siberia. Agr Meteorol 90:291–306

Hytteborn H, Maslov AA, Nazimova DI, Rysin LP (2005) Boreal forests of Eurasia. In: Anderson F (ed) Ecosystems of the World 6 Coniferous forests. Elsevier, Amsterdam, pp 23–99

Ilvesniemi H, Kahkonen MA, Pumpanen J, Rannik U, Wittmann C, Peramaki M, Keronen P, Hari P, Vesala T, Salkinoja-Salonen M (2005) Wintertime CO_2 evolution from a boreal forest ecosystem. Boreal Environ Res 10:401–408

IPCC (2007) Climate change 2007: the scientific basis [http://www.ipcc.ch]

IUSS Working Group WRB (2006) World reference base for soil resources 2006. World Soil Resources. Reports No. 103, FAO, Rome

Kajimoto T, Matsuura Y, Sofronov MA, Volokitina AV, Mori S, Osawa A, Abaimov AP (1999) Above- and belowground biomass and net primary productivity of a *Larix gmelinii* stand near Tura, central Siberia. Tree Physiol 19:815–822

Kajimoto T, Matsuura Y, Osawa A, Abaimov AP, Zyryanova OA, Isaev AP, Yefremov DP, Mori S, Koike T (2006) Size-mass allometry and biomass allocation of two larch species growing on the continuous permafrost region in Siberia. For Ecol Manage 222:314–325

Kajimoto T, Osawa A, Matsuura Y, Abaimov AP, Zyryanova OA, Kondo K, Tokuchi N, Hirobe M (2007) Individual-based measurement and analysis of root system development: case studies for *Larix gmelinii* trees growing on the permafrost region in Siberia. J For Res 12:103–112

Kane ES, Valentine DW, Michaelson GJ, Fox JD, Ping CL (2006) Controls over pathways of carbon efflux from soils along climate and black spruce productivity gradients in interior Alaska. Soil Biol Biochem 38:1438–1450

Kelliher FM, Lloyd J, Arneth A, Luhker B, Byers JN, McSeveny TM, Milukova I, Grigoriev S, Panfyorov M, Sogatchev A, Varlargin A, Ziegler W, Bauer G, Wong SC, Schulze ED (1999) Carbon dioxide efflux density from the floor of a central Siberian pine forest. Agr Forest Meteorol 94:217–232

Klemedtsson L, Klemedtsson ÅK, Moldan F (1997) Nitrous oxide emission from Swedish forest soils in relation to liming and simulated increased N-deposition. Biol Fertil Soils 25:290–295

Kudeyarov VN, Kurganova IN (2005) Respiration of Russian soils: Database analysis, long-term monitoring, and general estimates. Eurasian Soil Sci 38:983–992

Kurganova IN, Kudeyarov VN (1998) Assessment of carbon dioxide effluxes from soils of the taiga zone of Russia. Eurasian Soil Sci 31:954–965

Lavigne MB, Boutin R, Foster RJ, Goodine G, Bernier PY, Robitaille G (2003) Soil respiration responses to temperature are controlled more by roots than by decomposition in balsam fir ecosystems. Can J For Res 33:1744–1753

Luo Y, Zhou X (2006) Substrate supply and ecosystem productivity. In: Luo Y, Zhou X (eds) Soil respiration and the environment. Academic Press, San Diego New York, pp 79–84

Lydolph PE (1977) Climates of the Soviet Union. World survey of climatology, vol 7. Elsevier, Amsterdam, p 417

Maier CA, Kress LW (2000) Soil CO_2 evolution and root respiration in 11 year-old loblolly pine (*Pinus taeda*) plantations as affected by moisture and nutrient availability. Can J For Res 30:347–359

Matsuura Y (2006) Comparative study on soil carbon storage of permafrost ecosystems in Northeastern Eurasia. In: Ryusuke H, Georg G (eds) Symptom of Environmental

Change in Siberian Permafrost Region. Hokkaido University Press, Sapporo, pp 103–107
Melling L, Hatano R, Goh KJ (2005) Soil CO_2 flux from three ecosystems in tropical peatland of Sarawak, Malaysia. Tellus B 57:1–11
Moren AS, Lindroth A (2000) CO_2 exchange at the floor of a boreal forest. Agr Forest Meteorol 101:1–14
Morishita T, Hatano R, Desyatkin RV (2003) CH_4 flux in an Alas ecosystem formed by forest disturbance near Yakustk, eastern Siberia, Russia. Soil Sci Plant Nutr 49:369–377
Morishita T, Matsuura Y, Zyryanova OA, Abaimov AP (2006) CO_2, CH_4, and N_2O fluxes from a larch forest soil in Central Siberia. In: Ryusuke H, Georg G (eds) Symptom of Environment Change in Siberian Permafrost Region. Hokkaido University Press, Sapporo, pp 1–9
Morishita T, Hatano R, Desyatkin RV (2007) N_2O flux in alas ecosystems formed by forest disturbance near Yakutsk, eastern Siberia, Russia. Eurasian J For Res 10:79–84
Nadelhoffer KJ (2000) The potential effects of nitrogen deposition on fine-root production in forest ecosystems. New Phytol 147:131–139
Nakai Y, Matsuura Y, Kajimoto T, Abaimov AP, Yamamoto S, Zyryanova OA (2008) Eddy covariance CO2 flux above a gmelin larch forest on continuous permafrost in central Siberia during a growing season. Theor Appl Climatol 93:133–147
Nakano T, Inoue G, Fukuda M (2004) Methane consumption and soil respiration by a birch forest soil in West Siberia. Tellus B 56:223–229
Niinisto SM, Silvola J, Kellomaki S (2004) Soil CO_2 efflux in a boreal pine forest under atmospheric CO_2 enrichment and air warming. Global Change Biol 10:1363–1376
O'Connell KEB, Gower ST, Norman JM (2003) Net ecosystem production of two contrasting boreal black spruce forest communities. Ecosystems 6:248–260
Palmroth S, Maier CA, McCarthy HR, Oishi AC, Kim HS, Johnsen KH, Katul GG, Oren R (2005) Contrasting responses to drought of forest floor CO_2 efflux in a Loblolly pine plantation and a nearby Oak-Hickory forest. Global Change Biol 11:421–434
Rayment MB, Jarvis PG (1997) An improved open chamber system for measuring soil CO_2 effluxes in the field. J Geophys Res 102(D24):28779–28784
Ruess RW, Hendrick RL, Bryant JP (1998) Regulation of fine root dynamics by mammalian browsers in early successional Alaskan taiga forests. Ecology 79:2706–2720
Ruess RW, Hendrick RL, Burton AJ, Pregitzer KS, Sveinbjornsson B, Allen ME, Maurer GE (2003) Coupling fine root dynamics with ecosystem carbon cycling in black spruce forests of interior Alaska. Ecol Monogr 73:643–662
Sawamoto T, Hatano R, Yajima T, Takahashi K, Isaev AP (2000) Soil respiration in Siberian taiga ecosystems with different histories of forest fire. Soil Sci Plant Nutr 46:31–42
Schlesinger WH, Andrews JA (2000) Soil respiration and the global carbon cycle. Biogeochemistry 48:7–20
Shibistova O, Lloyd J, Evgrafova S, Savushkina N, Zrazhevskaya G, Arneth A, Knohl A, Kolle O, Schulze ED (2002) Seasonal and spatial variability in soil CO_2 efflux rates for a central Siberian Pinus sylvestris forest. Tellus B 54:552–567
Striegl RG, Wickland KP (1998) Effects of a clear-cut harvest on soil respiration in a jack pine - lichen woodland. Can J For Res 28:534–539
Sulzman EW, Brant JB, Bowden RD, Lajtha K (2005) Contribution of aboveground litter, belowground litter, and rhizosphere respiration to total soil CO_2 efflux in an old growth coniferous forest. Biogeochemistry 73:231–256
Takakai F, Desyatkin AR, Lopez CML, Fedorov AN, Desyatkin RV, Hatano R (2008) CH_4 and N_2O emissions from a forest-alas ecosystem in the permafrost taiga forest region, eastern Siberia, Russia. J Geophys Res 113:G02002. doi:10.1029/2007JG000521
Tryon PR, Chapin FS (1983) Temperature control over root-growth and root biomass in taiga forest trees. Can J For Res 13:827–833
Weber MG, Van Cleve K (2005) The boreal forests of North America. In: Andersson F (ed) Ecosystems of the World 6 Coniferous Forests. Elsevier, Amsterdam, pp 101–130

Widen B, Majdi H (2001) Soil CO_2 efflux and root respiration at three sites in a mixed pine and spruce forest: seasonal and diurnal variation. Can J For Res 31:786–796

Winston GC, Sundquist ET, Stephens BB, Trumbore SE (1997) Winter CO_2 fluxes in a boreal forest. J Geophys Res 102(D24):28795–28804

Yanagihara Y, Koike T, Matsuura Y, Mori S, Shibata H, Satoh F, Masuyagina OV, Zyryanova OA, Prokushkin AS, Prokushkin SG, Abaimov AP (2000) Soil respiration rate on the constrasting north- and south-facing slopes of a larch forest in central Siberia. Eurasian J For Res 1:19–29

Yuste JC, Janssens IA, Carrara A, Meiresonne L, Ceulemans R (2003) Interactive effects of temperature and precipitation on soil respiration in a temperate maritime pine forest. Tree Physiol 23:1263–1270

Chapter 10
Net Ecosystem Exchange of CO_2 in Permafrost Larch Ecosystems

Y. Nakai

10.1 Introduction

Carbon dioxide exchange between the ecosystem and the atmosphere would be a major component for carbon budget at boreal forests. In this chapter, net ecosystem exchange (NEE) of CO_2 at a permafrost larch ecosystem will be discussed, based on a micrometeorological (tower flux) measurement. Movement of CO_2 from ecosystem to atmosphere is customarily labeled as positive. The micrometeorological measurement can obtain NEE with a half-hourly time-resolution at an ecosystem scale. These temporal and spatial scales are advantages in carbon, water, and energy budget studies over ecological measurements.

Most studies of recent micrometeorological NEE measurements in boreal forest regions have been conducted in evergreen coniferous ecosystems and in broad-leaved mixed forests of aspen, birch, and other species (Jarvis et al. 2001); see, for example, the Boreal ecosystem–atmosphere study (BOREAS) in Canada (Sellers et al. 1997), the northern hemisphere climate-processes land-surface experiment (NOPEX) in Scandinavia (Halldin et al. 1999), and the EuroSiberian Carbonflux (Schulze et al. 1999) and the TCOS-Siberia (e.g., Shibistova et al. 2002; Röser et al. 2002) projects in Siberia.

On the other hand, deciduous conifer, i.e., larch, has only a few series of continuous micrometeorological measurements of NEE taken in northern Eurasia such as Russia (Dolman et al. 2004; Machimura et al. 2005; Nakai et al. 2005), Mongolia (Li et al. 2005), China (Wang et al. 2005), and Japan (Hirano et al. 2003; Wang et al. 2004), in spite of its growing locations distributed over extended areas. In these studies, the measurements conducted over the continuous permafrost are very limited. One could easily imagine reasons why so few studies carry out continuous measurements in the permafrost larch ecosystems. They are in regions of extremely cold and continental climate, and at geographically remote locations. Consequently, micrometeorological NEE data from permafrost larch forests of Siberia are expected to be highly valuable to the studies of global carbon budget.

Some pioneering micrometeorological measurements at a few *Larix gmelinii* forests in Yakutia in Northeastern Siberia were reported in the literatures. The ecosystem exchange of water vapor (Kelliher et al. 1997) and carbon dioxide (Hollinger

A. Osawa et al. (eds.), *Permafrost Ecosystems: Siberian Larch Forests*,
Ecological studies, Vol. 209, DOI 10.1007/978-1-4020-9693-8_10,

et al. 1995, 1998) was assessed at a stand located at south of Yakutsk during midsummer. The GAME Siberia, CREST/WECNoF (Ohta 2005), and TCOS-Siberia projects had long-term measurements in a larch forest at Spasskaya Pad Experimental Site near Yakutsk in the continuous permafrost area. At this site, Ohta et al. (2001) reported year-round measurements of heat and water vapor fluxes. Also Ohta et al. (2008) measured the inter-annual variation of water balance (see also Chap. 13, this Vol.). Dolman et al. (2004) estimated seasonal variation in NEE. Machimura et al. (2005) estimated NEE of 80–130 gC m^{-2} for seasons from May to September by a micrometeorological measurement at Neleger near Yakutsk. However, the average tree size at these stands near Yakutsk was larger (e.g., heights >10 m) than the size typical of larch forests on Siberian permafrost. Generally, average tree heights in the canopy layer of old *L. gmelinii* stands do not exceed 10 m in the continuous permafrost regions of Central Siberia (Abaimov et al. 1998; Bondarev 1997; Kajimoto et al. 1999; see also Chap. 7, this Vol.).

As described above, recent information on NEE of larch forests in Siberia is still limited to stands with relatively large individuals near Yakutsk. To gain better understanding of NEE for typical permafrost larch ecosystems, there should be more sites for tower flux measurement in permafrost region of Siberian taiga. As one of such sites, a tower flux measurement was initiated in 2004 to observe energy, water, and CO_2 above a mature larch stand near Tura, Central Siberia (Nakai et al. 2004). This site may warrant a long-term study since it has stand structure typical of old *L. gmelinii* forests of the region and was established on a plateau. Recently, enough metainformation was also obtained by intensive and extensive ecological studies at sites near the flux tower (Zyryanova and Shitova 1999; Zyryanova et al. 2000; Kajimoto et al. 1999, 2003; Abaimov et al. 2000; Osawa et al. 2000, 2003, 2004; Matsuura and Abaimov 2000; Tokuchi et al. 2004; Matsuura et al. 2005; see also related chapters, this Vol.).

The objectives of this study were to estimate seasonal and annual carbon dioxide exchange and to evaluate whether the gmelin larch (*Larix gmelinii*) ecosystem functions as a carbon sink or source. For those purposes, measurement should be continued for many years. Measured data may be useful for understanding function of permafrost larch ecosystems. In this chapter, half-hourly, daily, and seasonal changes in NEE of a permafrost larch ecosystem are shown, based on the flux measurements at Tura in 2004 (Nakai et al. 2008).

10.2 Study Site for Micrometeorological Measurements

In 2002, a 105-year-old stand of larch (*Larix gmelinii*) forest (Carbon Flux Site in Fig. 1.3, this Vol.), east of the village of Tura, was selected for micrometeorological measurements. A 20-m high wooden tower was constructed in 2003 within the settlement of Tura, and this prefabricated structure was transported to the study site by a helicopter (Fig.10.1) in August 2003. The equipment was set up and flux measurements started in early June 2004 (Fig. 10.2).

Fig. 10.1 A helicopter transporting the wooden tower to the study site. The tower was landing on the ground (Photo: Y. Matsuura)

Fig. 10.2 The tower equipped with all devices (Photo: Y. Nakai) *(see* Color Plates)

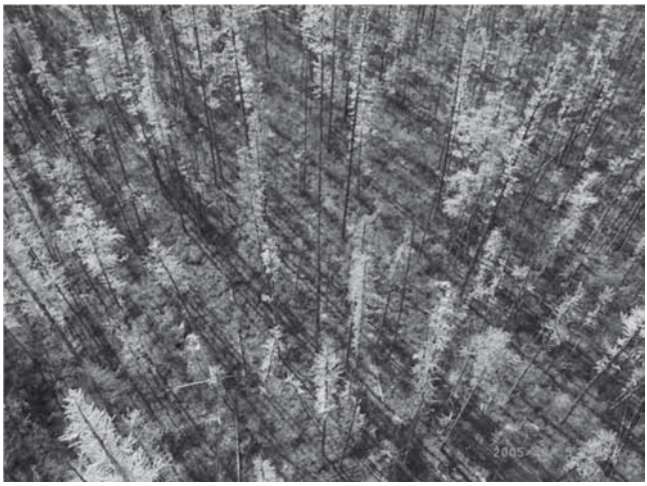

Fig. 10.3 Slender canopy of the larch trees in 105-year-old larch stand (Photo: Y. Nakai)

The site is on a slightly sloping terrace of the Nyzhnyaya Tunguska River with a northern aspect. It consists of a nearly even-aged stand of 105-year-old larch trees that originated from an intensive forest fire in late 1890s. The prevailing winds are westerly (Nakai et al. 2005). According to tree census data from four permanent plots near the flux tower (Kajimoto et al. 2004, 2007; see Table 6.1, this Vol.), stem density of living larch trees is about 5,480 trees ha^{-1}. Average diameter of the trees at breast height is 3.2 cm; mean tree height is 3.4 m. Individual tree crowns are slender and rarely overlap with one another (Fig. 10.3). Consequently, the stand has a very sparse canopy. Leaf biomass of the stand is 0.44 Mg ha^{-1}, and leaf area index (LAI; calculated as projected needle area) is ca. 0.6 ha ha^{-1} (details see Table 6.2, this Vol.). The leaves of the larch trees are nearly exclusively short shoot leaves and are often distributed throughout the length of the stem.

Soil type is cryosol with permafrost table existing within the upper one meter of the soil profile (Matsuura et al. 2005). The parent material is old fluvial deposit of the Nyzhnyaya Tungusuka River. Soil texture of the surface-active layer is clay rich. Ground surface is densely covered with lichen and moss as is seen commonly at high latitude boreal forests. This cover forms a thick porous layer of 10–30 cm in depth above the mineral soil, which functions as a heat insulator above the mineral soil. Climate data of Tura from a station with long-term observations (Lydolph 1977) are shown in Fig.10.4. According to the statistics of 1968–1995 observations at the station, annual mean air temperature is –9°C and annual total precipitation is 360 mm. About 45% of the annual precipitation falls between June and August. More detailed climatic information will be described in the next section.

Carbon dioxide, water vapor, heat, and momentum fluxes were measured at the top of the 20-m tall tower from June to early September, using the eddy covariance technique. Here, momentum flux can be calculated as covariance between horizontal

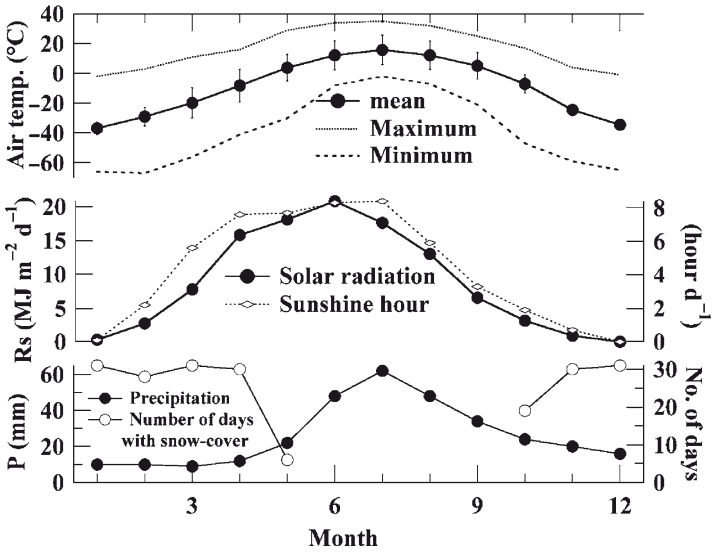

Fig. 10.4 Monthly climate variation of Tura. Error bar with monthly mean air temperature indicates mean daily difference. Data from Lydolph (1977)

wind and vertical wind. A three-dimensional sonic anemo-thermometer and a fast-response open-path infrared CO_2/H_2O gas analyzer (IRGA) were set at the top of the tower (see Table 10.1 for measurement sensors). Voltage signals from these eddy sensors were recorded at 10 Hz with a data logger (CR-5000, Campbell). The correction for angle of attack errors (Nakai et al. 2006) was applied to raw sonic wind data. Quality-control procedures designed by FFPRI FluxNet (Ohtani et al. 2005) were applied to the raw data as follows. First, graphs of the raw eddy time-series data plotted for an interval of every 30-min were visually checked. The noise-bearing data due to wetting on the sensor surfaces were excluded from further flux calculations. Second, within each half-hour observation, spikes and abnormal values out of plausible physical ranges, absolute variance, discontinuity, and stationarity were checked, using the procedures of Vickers and Mahrt (1997) and Foken and Wichura (1996). Coordinate axes for the wind field were rotated twice, so that the mean lateral and vertical velocities were zero (McMillen 1988). Humidity correction to sonic temperature and linear trends removal in scalar components (sonic temperature, water vapor, and CO_2 mixing ratio) were conducted. Water vapor and CO_2 fluxes were corrected for the air density effects using heat and water vapor fluctuation (WPL correction proposed by Webb et al. 1980). After the flux calculations, half-hourly fluxes with absolute angles of principal wind flow against a horizon >10°, measurable precipitation, or friction velocity <0.2 $m\,s^{-1}$ were excluded.

NEE between forest and the atmosphere can be computed as the sum of eddy covariance flux and storage change in CO_2 below the eddy flux measurement height (20 m in this case). The method by Hollinger et al. (1994) was employed for

Table 10.1 List of measurement items, heights, sensors for the micrometeorological observation

Measurement item	Height (m)	Sensor		
		Type	Model No.	Company
Fast response 3D-wind and sonic temperature	20 m = top of the tower	Sonic anemometer	R3	Gill
CO_2 and water vapor density		Open-path infrared gas analyzer	Li-7500	LiCor
Air temperature		Resistive platinum thermometer	HMP-45D	Vaisala
Relative humidity		Capacitive humidity sensor		
Wind speed and direction		Propeller anemometer	5103	R.M. Young
Rainfall		Tipping bucket rain gauge	T34	Ohta Keiki
Air pressure	18 m	Capacitive pressure sensor	PTB210	Vaisala
Shortwave – and Longwave radiation	20 m, down- & upward-	Radiation sensor	CNR1	Kip&Zonnen
Photosynthetic active radiation		Quantum sensor	Li-190SB	LiCor
Shortwave radiation at floor	1.1 m	Radiation sensor	CM03	Kip&Zonen
Photosynthetic active radiation at floor		Quantum sensor	Li-190SB	LiCor
Soil temperature	0.05, 0.1, 0.2, 0.4, 0.5 m	Resistive platinum thermometer	JIS-Pt100 4-wire	
Soil moisture		TDR sensor	CS616	Campbell
Soil heat flux	0.02, 0.05 m (depth)	Heat flux plate	HF-01	REBS

estimating the storage term since profile of CO_2 concentration was not measured at the site. However, the storage change in CO_2 should be verified by comparing it with profile measurements, because the estimates of storage changes here are uncertain, especially in half-hourly resolution.

Energy balance closure was examined to evaluate the surface flux measurements. The sum of turbulent energy fluxes is frequently less by 20% or more than the available radiative energy in many field measurements (e.g., Wilson et al. 2002). In this study, energy closure for quality-assured dataset was expressed by linear regressions as shown in Fig.10.5, where H is sensible heat flux, LE is latent heat flux, Rn is net radiation, and G is ground heat flux. *Left hand side* of Fig.10.5 (half-hourly time-resolution) revealed imbalance of total turbulent energy flux (H+LE) to some 40% of total radiative energy flux (Rn-G). On the other hand, right hand side of Fig.10.5 (daily time-resolution) shows much better agreement of total turbulent energy flux and total radiative energy flux. Such imbalance in half-hourly data might be due to the storage terms in sensible and latent heat fluxes, and to ignoring the latent heat of ice melting in the soil. Careful and detailed analysis of energy fluxes would still be needed for further discussion of energy balance closure.

Micrometeorological variables were also measured at the top of the tower: air temperature, relative humidity, wind speed and direction, precipitation, air pressure, shortwave, long-wave, and photosynthetic active radiation for both downward- and upward-direction. Soil temperature, moisture, and soil heat flux had been measured since late July 2004 (see Table 10.1 for measurement sensors with height or depth). For all micrometeorological variables, a half-hourly average was calculated and recorded with a data-logger (CR-10X, Campbell). Electricity for all devices was supplied with six solar panels (110 W maximum for each) through deep cycle batteries. A whole integrated measurement system (CFX-N1, Climatec, Inc.) had been operating steadily.

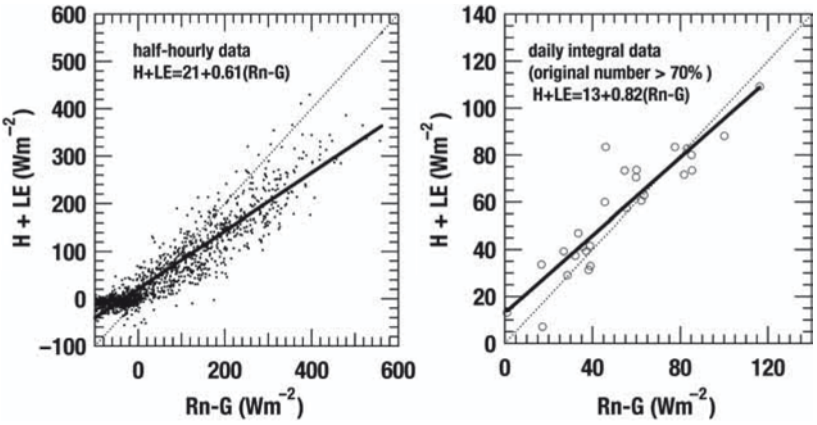

Fig. 10.5 Energy balance closure for observed energy fluxes. *H* sensible heat flux; *LE* latent heat flux; *Rn* net radiation; *G* ground heat flux; Total turbulent energy fluxes (H+LE) are plotted against total radiative energy fluxes (Rn-G)

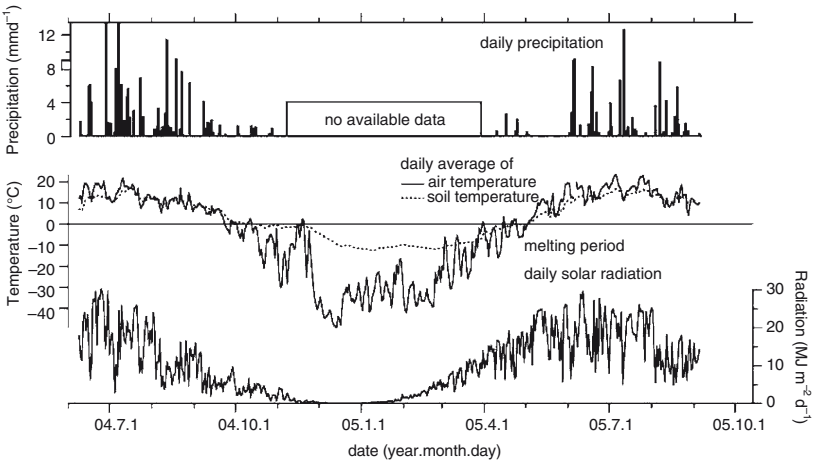

Fig. 10.6 Principal meteorological variations at Tura station of Russian Federal Service of Hydro-Meteorology from June 2004 to September 2005 (located in the residential area of Tura; see Fig. 1.3, this Vol.)

At Tura station of the Russian Federal Service of Hydro-Meteorology (located in a residential area of Tura; see Fig. 1.3, this Vol.), a year-round measurement was initiated for standard meteorological variables such as air temperature, humidity, solar radiation, wind speed, and precipitation. This provided additional meteorological data (Fig. 10.6) to those from the tower flux measurements. The year-round meteorological data help estimation of fluxes in early spring and late autumn when access to the tower site was difficult owing to instability of river ice, and provided basic data for annual NEE estimation (Nakai et al. 2007).

10.3 Meteorological Condition and Features of the Measurement Site

Monthly mean air temperature and total precipitation in the summer months (June, July, August) at the study site in 2004 are compared with the 30-year averages (1960–1989) recorded at the station of Russian Federal Service of Hydro-Meteorology in Tura (Table 10.2): monthly solar radiation in the summer 2004 is compared with climatic average values from Lydolph (1977). Mean monthly air temperature for 2004 was higher in June, but lower in July and August. Monthly precipitation was approximately half in June, but about the same in July and August. The temperature of the mineral soil surface under the lichen- or moss-litter layer, being affected by the permafrost, was nearly 0°C in June, and showed a maximum in July, decreasing in August, but was higher than that in June.

Daily climate variables are shown in Fig. 10.7. More than three quarters of the days in June were sunny (Fig. 10.7a). There were only several days of occasional showers.

Table 10.2 Meteorological characteristics of summer months at Tura, compared to long-term climatic mean values

	Year	June	July	August
Mean Air temperature (°C)	1960–89	12.4	16.9	13.1
	2004	16.0	14.5	10.8
Total Precipitation (mm)	1960–89	52	59	54
	2004	34	61	50
Total Solar radiation (MJ m^{-2})	[a]	624	546	390
	2004	624	524	326
Mean temperature at Mineral Soil surface (°C)	2004	1.5	4.8	3.1
Number of Day with precipitation >0 (mm d^{-1})	2004	9	18	16
Number of Days with maximum VPD[b] >1.5 kPa	2004	19	12	3

[a]Data from Lydolph (1977)
[b]Vapor pressure deficit

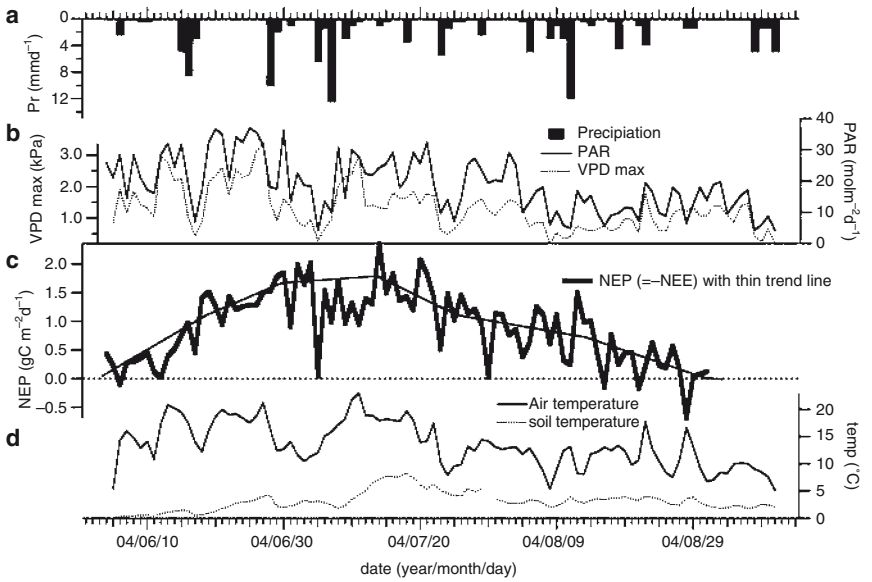

Fig. 10.7 Daily time-series of (**a**) precipitation (Pr), (**b**) daily maximum of vapor pressure deficit (VPDmax), photosynthetic active radiation (PAR), (**c**) net ecosystem production (NEP = −NEE), and (**d**) air temperature, and soil temperature (at 0.05 m depth of the mineral soil layer)

In both July and August, a majority of the days had rain, which was weaker and longer than in June. Total precipitation during the whole period was 125.5 mm (41 days with rainfall). In August, daily photosynthetic active radiation (PAR in Fig.10.7b) was considerably less than that in June and July, as the long-term average of monthly total

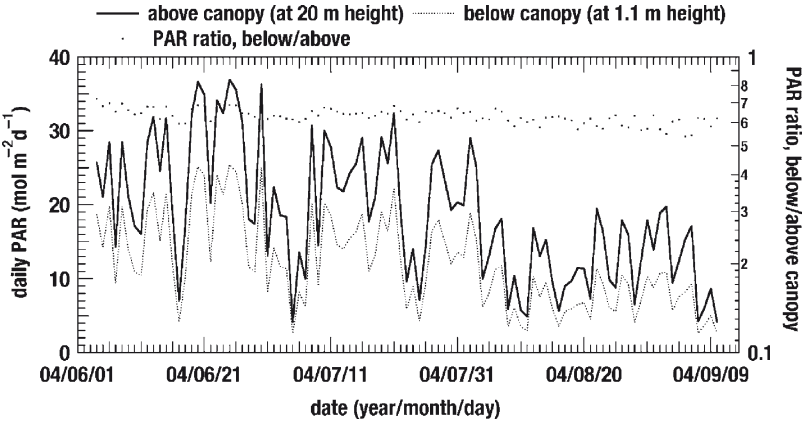

Fig. 10.8 Variation in daily photosynthetic active radiation (PAR) above (at 20 m height above ground) and below (at 1.1 m above the ground) the larch canopy

solar radiation reveals (Table 10.2). Average air temperature was 13.5°C throughout the measurement period (Fig. 10.7d). Daily maximum of vapor pressure deficit (VPDmax in Fig.10.7b) was generally higher in June and early July than in the later period.

Variations of the daily sums of photosynthetic active radiation (PAR) above the canopy (at 20 m height) and at the ground during the growing season are shown in Fig. 10.8. Day-to-day variations in PAR are large enough to obscure the seasonal change, though monthly PAR was the highest in June and lowest in August among the three months in summer. PAR at the ground was reduced to 55–70% of the global PAR above the canopy, as shown by PAR ratio (see dots in Fig. 10.8). This indicates that light interception by the larch canopy is not likely to limit the growth of ground vegetation. Dense ground vegetation under a sparse larch canopy in the permafrost forests might play a significant role in NEE, though seasonal variation in NEE during early growing season appears synchronized with larch needle development (for details see Sect. 10.4). Partitioning of CO_2 exchange into tree canopy and ground vegetation should be carried out to understand ecosystem function and its relationship to ecosystem structure.

10.4 Intensity and Seasonal Variations in Net Ecosystem Exchange and Larch Tree Phenology

Average diurnal cycles of NEE, PAR, and air temperature are indicated for each of 10-day periods in Fig. 10.9. Slightly negative NEE values of −1 μmol $m^{-2} s^{-1}$ at its minimum were observed during the daytime in early June. This indicates very weak net CO_2 uptake, though the open-path Infrared gas analyzer has a problem of

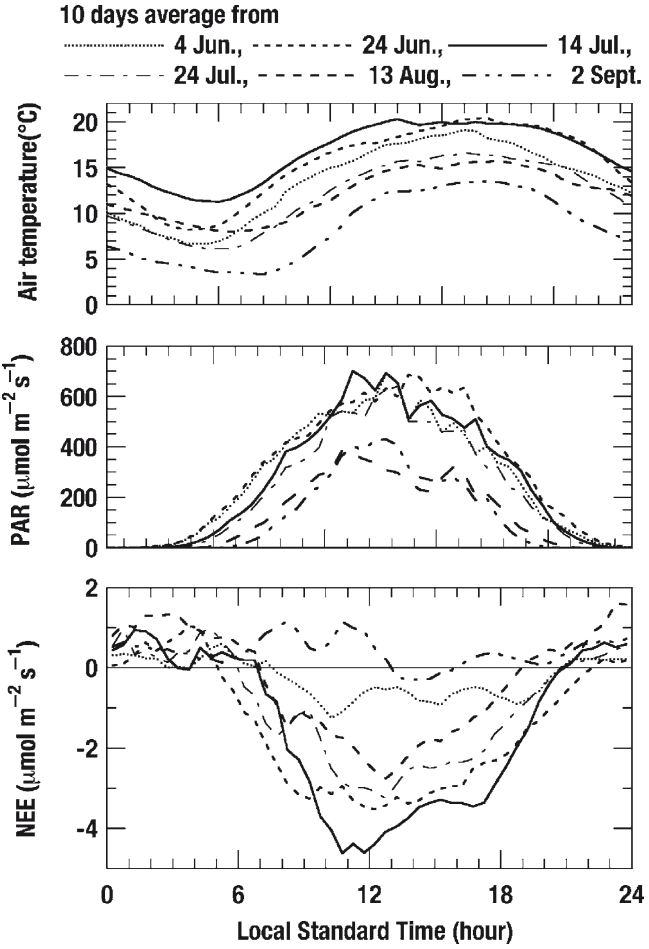

Fig. 10.9 Average diurnal cycles of NEE, PAR, and air temperature. Each line represents the average for 10-day periods: (a) 4–13 June; (b) 24 June–3 July; (c) 14–23 July; (d) 24 July–2 August; (e) 13–22 August; and (f) 2–11 September

underestimating NEE under a cold condition (e.g., Grelle and Burba 2007). In the beginning of June, soil surface started to melt and buds of larch trees had already broken. Larch needles did not flush for a few days after the bud break when air temperature was under 10°C, after which the needle flush began and was almost completed by the middle of June.

Daytime minimum of NEE reached −4 μmol $m^{-2} s^{-1}$ in late June (see lower graph in Fig.10.9). Furthermore, daytime minimum NEE of −5 μmol $m^{-2} s^{-1}$ was observed in mid July when NEE was at its lowest of the year and photosynthesis was likely to be most active. In late July, daytime minimum NEE became −3 μmol $m^{-2} s^{-1}$, which is equal to or larger than that in late June. In mid-August, NEE was little larger than

in late July, but still negative. The NEE was mostly in the positive range even during the daytime in early September when the leaves began to change color.

During four 10-day periods (10 days beginning on June 4, June 24, July14, and July 24), photosynthetic active radiation (PAR) showed similar values with each other (see middle graph in Fig. 10.9) – air temperature was probably high enough for photosynthesis (see upper graph in Fig. 10.9). However, NEE was clearly different with each other among these periods. Biological factors such as increased photosynthetic ability and CO_2 uptake of larch needles must promote Net Ecosystem Production (NEP = −NEE) from early June to early July, but the decrease in radiation and air temperature from mid-August to September should reduce the net uptake.

Later, based on daily integral of Net Ecosystem Production (NEP = −NEE), seasonal variation in NEE from the viewpoint of biological factors (such as photosynthetic ability) and environmental factors (such as air temperature and PAR) will be described again.

The relationship between NEE and absorbed PAR is approximated using a Michaelis-Menten type rectangular hyperbola (Ruimy et al. 1995):

$$\mathrm{NEE} = -P\max \cdot \frac{\mathrm{APAR}}{\mathrm{APAR} + \dfrac{P\max}{\alpha}} + Reco \tag{10.1}$$

where Pmax is maximum photosynthetic rate, α is initial light-use efficiency of the ecosystem, and Reco is ecosystem respiration. For light intensity of the ecosystem, absorbed photosynthetic active radiation (APAR) was used here, which was derived as incident PAR above the forest canopy minus reflective PAR. The relationship between daytime NEE and APAR was examined for every 10-day period, then it was approximated by applying Eq. (10.1). As shown in Fig.10.10, CO_2 uptake of the ecosystem was significantly lower in early June and early September than in other periods. Saturation of the CO_2 uptake against light intensity occurred approximately at APAR >500 μmol m^{-2} s^{-1} between mid-June and mid-August.

To estimate daily and seasonally integrated NEE, missing data of half-hourly NEE were filled with values (the so-called "gap-filling"). Here, gaps mean missing data due to device troubles or rejection by data quality control. The gaps that consisted of one or two points were filled with linear interpolation using data at both sides of each gap. For longer gaps during the daytime, regression models of Eq. (10.1) were used. Also, the longer gaps during nighttime were filled with a single exponential function, as follows:

$$\mathrm{NEE} = K_0 \,.\, exp\,(K_1 \,.\, Ta) \tag{10.2}$$

where k_0 and k_1 are coefficients, and Ta is air temperature. As a result of fitting Eq. (10.2) to whole available nighttime data, the most important index of temperature sensitivity of respiration $Q_{10} = \exp(k_1)$ was 2.1, and nighttime NEE at air temperature of 10°C was 1.1 μmol m^{-2} s^{-1}.

Time-series of the daily-integrated NEP (= −NEE), precipitation (Pr), global photosynthetic active radiation (PAR), daily maximum of vapor pressure deficit

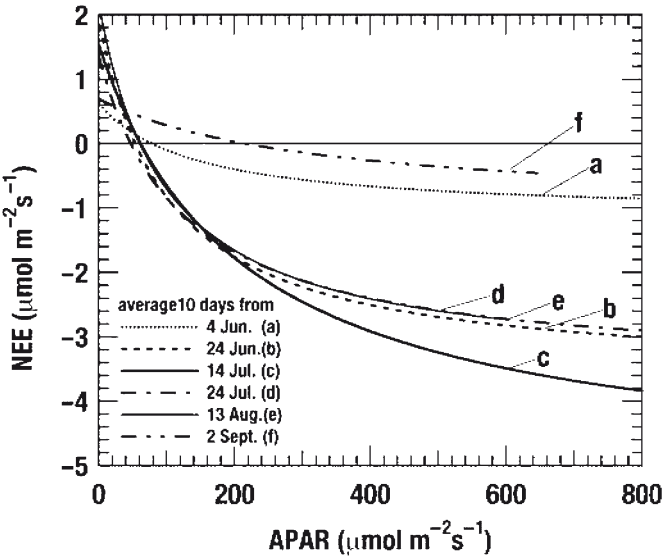

Fig. 10.10 Relationships between daytime net ecosystem exchange of CO_2 (NEE) and absorbed photosynthetic active radiation (APAR) for 10-day periods: (a) 4–13 June; (b) 24 June–3 July; (c) 14–23 July; (d) 24 July–2 August; (e) 13–22 August; and (f) 2–11 September. Each curve was fitted by Eq. (10.1)

(VPDmax), and daily average of air temperature and soil temperature are shown in Fig. 10.7. The cumulative NEP for the whole measurement period of 91 days was 76–78 gC m^{-2}. Daily NEP was near zero in early June, sharply increased by the end of June, and reached a seasonal maximum of 2.0 gC $m^{-2}d^{-1}$ between late June and mid-July. Thereafter, it decreased by late August, and became negative in early September. This seasonal variation indicates that net uptake by the ecosystem continued from early June to mid-August, reaching a maximum between late June and mid-July, and the ecosystem began to release CO_2 after late August.

Seasonal change in NEP during the early growing season could be primarily related to needle phenology of the larch trees. Namely, during a few-week-period of needle growth after bud-break in early and mid-June, daily net uptake sharply increased to the seasonal maximum (Fig. 10.7c), though no visible signs of seasonal growth were observed for the most species of ground vegetation (i.e., woody shrubs). This coincidence between the patterns of NEP and plant phenology suggests that net CO_2 uptake in the early growing season largely depends on photosynthetic activity of the larch trees. On the other hand, daily net CO_2 uptake decreased gradually from late July to the end of August. In this period, canopy photosynthetic activity may still have continued at least until late August, because senescence of larch needles occurred in early September or later. However, both air temperature and incident radiation have already begun to decline in late July (Fig. 10.7b, d), suggesting that NEE of the larch ecosystem might be mostly governed by seasonal changes in air temperature and incoming radiation rather than photosynthetic activities of larch needles during latter half of the growing season (late July to August).

The bud-break and flushing of *L. gmelinii* needles may be triggered by soil surface thawing in the spring (Kujansuu et al. 2007; also see Chap. 17, this Vol.). Air temperature and soil temperature data from 2004 to 2005 at Tura Hydro-meteorological Station (Fig. 10.6) show that thawing of the soil surface continued for several days (indicated as "melting period" in Fig. 10.6 when soil temperature remains near zero) and was completed in early May 2005, after which bud break occurred in mid-May near the station. Consequently, close relationships between the energy budgets over the soil surface and phenological characteristics could be a key issue in the CO_2 budget of larch ecosystems.

Daily maximum of half-hourly or hourly CO_2 uptake rates during midsummer reached 3–6 μmol $m^{-2} s^{-1}$. Table 10.3 lists the maximum values of half-hourly or hourly NEP (=−NEE) mainly for old larch forests and other boreal forests. The NEP value of *L. gmelinii* forest at Tura is considerably lower than that of other boreal forests. This may be primarily due to smaller leaf area index (LAI = ca. 0.6 ha ha^{-1}) of a typical old stand on permafrost compared to that of other forests (LAI = 1–4 ha ha^{-1}). Thus, cumulative NEP (70–80 gC m^{-2} for 91 days) during a growing season was also much lower than that (290 gC m^{-2} for 100 days) of the larch forest near Yakutsk with LAI of ca. 3.7 ha ha^{-1} (Dolman et al. 2004).

Lower cumulative value of CO_2 uptake could be associated not only with low LAI, but also with other environmental factors, such as short growing periods, typically beginning in late May or early June and ending in early September (i.e., only three months or less). Moreover, low soil temperature and shallow depth of soil active layer may make productivity of the larch forest lower. In fact, the maximum depth of soil active layer is shallower (ca. 0.7 m) in the present study site (Kajimoto et al. 2007) than in the larch forest near Yakutsk (1.2 m) (Dolman et al. 2004). In winter, NEE may be slightly positive due to gradual release of CO_2 from accumulated snow or frozen soils to the atmosphere as suggested in many forest ecosystems. Sum of such CO_2 release in winter is probably negligibly small in the stand of the present study (T. Morishita et al. personal communication). For further discussion of seasonal and annual NEE of typical old larch forests in the region, multi-year measurements are needed to ascertain how representative is the seasonal NEE during a single growing season. For evaluation of annual NEE, it is also necessary to estimate CO_2 exchange during winter by applying technically more difficult chamber measurements and continuous meteorological observations.

Additionally, water balance in the region of continuous permafrost is also globally an important theme (see Chap. 13, this Vol.). According to preliminary analysis, cumulative precipitation and evapotranspiration (probably without interception evaporation) were mostly comparable at the present study site during the measurement period. Daily evapotranspiration averaged 1.3 mm d^{-1} and reached the maximum of 2.4 mm d^{-1} (Y. Nakai, unpubl. data). Further analysis of water vapor fluxes, especially gap-filling, would still be needed for discussion of long-term evapotranspiration.

Table 10.3 Maximum NEP (half-hourly or hourly) at midday of midsummer, annual precipitation, and stand characteristics of boreal forests

Forest type	Location	Site ID (name)	Annual precipitation (mm)	Maximum NEP ($\mu mol\ m^{-2}\ s^{-1}$)	LAI	Stand height (m)	Mean DBH (cm)	Stand age (year)	Reference
Aspen	53.629°N, 106.200°W, 601 m a.s.l.	Boreal ecosystem–atmosphere study (BOREAS) SSA-OA	406	10–20	2.1	20	20.5	84	Black et al. (1996)
Black spruce	55.879°N, 98.484°W, 259 m a.s.l.	BOREAS NSA-OBS	517	4–10	2.3	9.1	8.5	155	Goulden et al. (1997)
Black spruce	53.987°N, 105.118°W, 629 m a.s.l.	BOREAS SSA-OBS	405	6–9	2.6	11	8	115	Jarvis et al. (1997)
Jack pine	53.916°N, 104.692°W, 579 m a.s.l.	BOREAS SSA-OJP,	405	8–12	1.4	13	17	65	Baldocchi et al. (1997)
Scot pine	61.850°N, 24.283°E, 181 m a.s.l.	Hyytiälä, Finland	709	10–16	4	14	–	40 plantation	Markkanen et al. (2001)
Scot pine	60.75°N, 89.23°E, 90 m a.s.l.	Zotino, Central Siberia	565	8–12	1.5	–	–	200	Lloyd et al. (2002)
birch	60.968°N, 89.717°E, 200 m a.s.l.	Zotino, Central Siberia	597	10–20	–	18	12	50	Meroni et al. (2002)
Mountain birch	69.467°N, 27.233°E, 280 m a.s.l.	Petsiko, northern Finland	–	4–7	2.5	3.5	–	–	Aurela et al. (2001)
Larch	48.4°N, 108.7°E, 1,630 m a.s.l.	Mongolia	282	7–10	2.2	20	15	>150	Li et al. (2005)

(continued)

Table 10.3 (continued)

Forest type	Location	Site ID (name)	Annual precipitation (mm)	Maximum NEP ($\mu mol\ m^{-2}\ s^{-1}$)	LAI	Stand height (m)	Mean DBH (cm)	Stand age (year)	Reference
Larch	42.7°N, 141.5°E, 125 m a.s.l.	Tomakomai, Hokkaido Japan	1,132	15–25	2.1	14	18	45	Wang et al. (2004)
Larch	45.3°N, 127.6°E, 340 m a.s.l.	Laoshan, China	724	20–35	2.5	18	–	–	Wang et al. (2005)
Larch (CP[a])	60.9°N, 128.3°E, 348 m a.s.l.	SW of Yakutsk	213	3–7	1.4	16	–	125	Hollinger et al. (1998)
Larch (CP[a])	62.3°N, 129.2°E, 220 m a.s.l.	Spasskaya Pad, Yakutsk	240	7–15	3.7	18	–	160	Dolman et al. (2004)
Larch (CP[a])	64.2°N, 100.5°E, 250 m a.s.l.	Tura, Central Siberia	360	3–5	0.6	3.5	3.1	105	Nakai et al. (2008)
High arctic fen, (CP[a])	74.5°N, 20.6°W, <200 m a.s.l.	Zackenberg, Greenland	214	2–4	1.1	0.13	–	–	Nordstroem et al. (2001)

[a]"CP" denotes continuous permafrost region

10.5 Conclusions

NEE of CO_2 in permafrost *Larix gmelinii* forests in Central Siberia can be summarized as follows.

- Information on carbon budget of larch forests is still limited compared to boreal forests in other regions. However, stable operation of tower flux measurements at remote sites is possible during growing seasons using the eddy covariance technique and solar power.
- Typical rates of CO_2 uptake and release by this 105-year-old are as follows: Maximum of half-hourly net CO_2 uptake rates during midsummer ranged from 3 to 5 μmol $m^{-2} s^{-1}$; Maximum of daily net uptake of CO_2 during the growing season was about 2 gC $m^{-2} d^{-1}$, occurring between late June and mid-July.
- In comparison to other boreal forests, magnitude of net CO_2 uptake and cumulative net CO_2 uptake were low. Lower net CO_2 uptake of this permafrost larch forest may be primarily associated with its small leaf area index, and is further influenced by the environmental factors characteristics to the permafrost region (e.g., low soil temperature, short growing season). Initiation and following increase in CO_2 uptake were closely related to phenological development of larch needles.

Directions that should be needed for further understanding of NEE of CO_2 in typical open-canopy old larch forests in the permafrost region of Siberia would be:

- To continue longer-term and multiyear measurements. This could clarify functions of permafrost larch forests.
- To partition entire ecosystem exchange into contributions of ground vegetation and of larch trees.
- To clarify and model phenology of larch trees in the permafrost Siberia.

Acknowledgments I appreciate the assistance of Y. Matsuura, T. Kajimoto, and A. Osawa for discussions and manuscript preparation. I am grateful to late A.P. Abaimov, O.A. Zyryanova, and colleagues of V.N. Sukachev Institute of Forest for their help in various aspects of the field work. Thanks are due to V.M. Borovikov and colleagues of Evenkia Department of Forestry in Tura for their support in logistics and instrumentation. I also thank T. Yorisaki, H. Tanaka, and staff of Climatec Inc. for system integration and instrumentation. I acknowledge Y. Ohtani, T. Watanabe, and Y. Yasuda for providing software resources. S. Yamamoto and N. Saigusa encouraged me greatly. This research was funded by the "Global environment research fund S-1," as "Integrated Study for Terrestrial Carbon Management of Asia in the twentyfirst Century based on Scientific Advancements (FY2002–2006)."

References

Abaimov AP, Lesinski JA, Martinsson O, Milyutin LI (1998) Variability and ecology of Siberian larch species. Swedish University of Agricultural Sciences, Department of Silviculture Reports 43, Umeå, p 118

Abaimov AP, Erkalov AV, Prokushkin SG, Matsuura Y, Osawa A, Kajimoto T, Takenaka A (2000) The conservation and quality of Gmelin larch seeds in cryolithic zone of Central Siberia. In: Inoue G, Takenaka A (eds) Proceedings of the Eighth Symposium on the Joint Siberian Permafrost Studies between Japan and Russia in 1999. National Institute for Environmental Studies, Tsukuba, pp 3–9

Aurela M, Tuovinen JP, Laurila T (2001) Net CO_2 exchange of a subarctic mountain birch ecosystem. Theor Appl Climatol 70:135–148

Baldocchi DD, Vogel CA, Hall B (1997) Seasonal variation of carbon dioxide exchange rates above and below a boreal jack pine forest. Agr For Meteorol 83:147–170

Black TA, den Hartog G, Neumann HH, Blanken PD, Yang PC, Russell C, Nesic Z, Lee X, Chen SG, Staebler R, Novak MD (1996) Annual cycles of water vapour and carbon dioxide fluxes in and above a boreal aspen forest. Global Change Biol 2:219–229

Bondarev A (1997) Age distribution patterns in open boreal Dahurican larch forests of Central Siberia. Forest Ecol Manage 93:205–214

Dolman AJ, Maximov TC, Moors EJ, Maximov AP, Elbers JA, Kononov AV, Waterloo MJ, van der Molen MK (2004) Net ecosystem exchange of carbon dioxide and water of far eastern Siberian Larch (*Larix cajanderii*) on permafrost. Biogeosciences 1:133–146

Foken Th, Wichura B (1996) Tools for quality asessment of surface-based flux measurements. Agr For Meteorol 78:83–105

Goulden ML, Daube BC, Fan S-M, Sutton DJ, Bazzaz A, Munger JW, Wofsy SC (1997) Physiological responses of a black spruce forest to weather. J Geophys Res 120:28987–28996

Grelle A, Burba G (2007) Fine-wire thermometer to correct CO_2 fluxes by open-path analyzers for artificial density fluctuations. Agric For Meteorol 147:48–57

Halldin S, Gryninig S-E, Gottschalk L, Jochum A, Lundin L-C, Van de Griend AA (1999) Energy, water and carbon exchange in a boreal forest landscape — NOPEX experiences. Agr Forest Meteorol 98–99:5–29

Hirano T, Hirata R, Fujinuma Y, Saigusa N, Yamamoto S, Harazono Y, Takada M, Inukai K, Inoue G (2003) CO_2 and water vapor exchange of a larch forest in northern Japan. Tellus 55B:244–257

Hollinger DY, Kelliher FM, Byers JN, Hunt JE, McSeveny TM, Weir PL (1994) Carbon dioxide exchange between an undisturbed old-growth temperate forest and the atmosphere. Ecology 75:134–150

Hollinger DY, Kelliher FM, Schulze E-D, Vygodskaya NN, Varlargin A, Milukova I, Byers JN, Sogatchev A, Hunt JE, McSeveny TM, Kobak KI, Bauer G, Arneth A (1995) Initial assessment of multi-scale measurements of CO_2 and H_2O flux in the Siberian taiga. J Biogeogr 22:425–431

Hollinger DY, Kelliher FM, Schulze ED, Bauer G, Arneth A, Byers JN, Hunt JE, McSeveny TM, Kobak KI, Milukova I, Sogatchev A, Tatarinov F, Varlargin A, Ziegler W, Vygodskaya NN (1998) Forest-atmosphere carbon dioxide exchange in eastern Siberia. Agr For Meteorol 90:291–306

Jarvis PG, Massheder JM, Hale SE, Moncrieff JB, Rayment M, Scott SL (1997) Seasonal variation of carbon dioxide, water vapor, and energy exchanges of a boreal black spruce forest. J Geophys Res 120:28953–28966

Jarvis PG, Saugier B, Schulze E-D (2001) Productivity of boreal forests. In: Roy J, Saugier B, Mooney HA (eds) Terrestrial global productivity. Academic Press, New York, pp 211–244

Kajimoto T, Matsuura Y, Sofronov MA, Volokitina AV, Mori S, Osawa A, Abaimov AP (1999) Above- and belowground biomass and net primary productivity of a *Larix gmelinii* stand near Tura, central Siberia. Tree Physiol 19:815–822

Kajimoto T, Matsuura Y, Osawa A, Prokushkin AS, Sofronov MA, Abaimov AP (2003) Root system development of *Larix gmelinii* trees affected by micro-scale conditions of permafrost soils in central Siberia. Plant Soil 255:281–292

Kajimoto T, Matsuura Y, Osawa A, Abaimov AP, Zyryanova OA, Ishii A, Kondo K, Tokuchi N (2004) Biomass and spatial patterns of individual root system in *Larix gmelinii* stands on

continuous permafrost region of central Siberia. In: Tanaka H (ed) Proceeding of the Fifth International Conference on Global Change: Connection to the Arctic (GCCA-5). Tsukuba University, Tsukuba, pp 187–190

Kajimoto T, Matsuura Y, Osawa A, Abaimov AP, Zyryanova OA, Isaev AP, Yefremov DP, Mori S, Koike T (2006) Size-mass allometry and biomass allocation of two larch species growing on the continuous permafrost region in Siberia. For Ecol Manage 222:314–325

Kajimoto T, Osawa A, Matsuura Y, Abaimov AP, Zyryanova OA, Kondo K, Tokuchi N, Hirobe M (2007) Individual-based measurement and analysis of root system development: case studies for *Larix gmelinii* trees growing on the permafrost region in Siberia. J For Res 12:103–112

Kelliher FM, Hollinger DY, Schulze E-D, Vygodskaya NN, Byers JN, Hunt JE, McSeveny TM, Milukova I, Sogatchev A, Varlargin A, Ziegler W, Arneth A, Bauer G (1997) Evaporation from an eastern Siberian larch forest. Agr For Meteorol 85:135–147

Kujansuu J, Yasue K, Koike T, Abaimov AP, Kajimoto T, Takeda T, Tokumoto M, Matsuura Y (2007) Responses of ring widths and maximum densities of *Larix gmelinii* to climate on contrasting north- and south-facing slopes in central Siberia. Ecol Res 22:582–592

Li S-G, Asanuma J, Kotani A, Eugster W, Davaa G, Oyunbaatar D, Sugita M (2005) Year-round measurements of net ecosystem CO_2 flux over a montane larch forest in Mongolia. J Geophys Res . doi:10.1029/2004JD005453

Lloyd J, Shibistova OB, Zolotoukhine D, Kolle O, Arneth A, Wirth C, Styles JM, Tchebakova NM, Schulze E-D (2002) Seasonal and annual variations in the photosynthetic productivity and carbon balance of a central Siberian pine forest. Tellus 54B:590–610

Lydolph PE (1977) Climates of the Soviet Union. World survey of climatology, vol 7. Elsevier, Amsterdam, p 417

Machimura T, Kobayashi Y, Iwahana G, Hirano T, Lopez L, Fukuda M (2005) Change of carbon dioxide budget during three years after deforestation in eastern Siberian larch forest. J Agric Meteorol 60:653–656

Markkanen T, Rannik Ü, Keronen P, Suni T, Vesala T (2001) Eddy covariance fluxes over a boreal Scots pine forest. Boreal Environ Res 6:65–78

Matsuura Y, Abaimov AP (2000) Nitrogen mineralization in larch forest soils of continuous permafrost region, Central Siberia: An implication for nitrogen economy of a larch forest stand. In: Inoue G, Takenaka A (eds) Proceedings of the Eighth Symposium on the Joint Siberian Permafrost Studies between Japan and Russia in 1999. National Institute for Environmental Studies, Tsukuba, pp 129–134

Matsuura Y, Kajimoto T, Osawa A, Abaimov AP (2005) Carbon storage in larch ecosystems in continuous permafrost region of Siberia. Phyton 45:51–54

McMillen RT (1988) An eddy correlation technique with extended applicability to non-simple terrain. Boundary-Layer Meteorol 43:231–245

Meroni M, Mollicone D, Belelli L, Manca G, Rosellini S, Stivanello S, Tirone G, Zompanti R, Tchebakova N, Schulze ED, Valentini R (2002) Carbon and water exchanges of regenerating forests in central Siberia. For Ecol Manage 169:115–122

Nakai Y, Matsuura Y, Kajimoto T, Abaimov AP, Yamamoto S (2004) CO_2 flux measurements above a larch forest in a continuous permafrost region of Central Siberia using eddy covariance techniques (preliminary results). In: Tanaka H (ed) Proceeding of the Fifth International Conference on Global Change Connection to the Arctic (GCCA5). Tsukuba University, Tsukuba, pp 160–163

Nakai Y, Matsuura Y, Kajimoto T, Abaimov AP, Yamamoto S (2005) Eddy covariance CO_2 flux above a Gmelin larch forest on continuous permafrost of Central Siberia during two Growing Seasons. In: Proceedings of the Sixth International Conference on Global Change Connection to the Arctic (GCCA6), Tokyo, pp 169–172

Nakai T, van der Molen MK, Gash JHC, Kodama Y (2006) Correction of sonic anemometer angle of attack errors. Agr For Meteorol 136:19–30

Nakai Y, Matsuura Y, Kajimoto T, Zyryanova OA, Yamamoto S (2007) Water and CO_2 exchange at a Gmelin larch forest on continuous permafrost of Central Siberia during growing Seasons.

Proceedings of the Seventh International Conference on Global Change Connection to the Arctic (GCCA7). International Arctic Research Center, University of Alaska, Fairbanks, pp 263–266

Nakai Y, Matsuura Y, Kajimoto T, Abaimov AP, Yamamoto S, Zyryanova OA (2008) Eddy covariance CO_2 flux above a Gmelin larch forest on continuous permafrost of Central Siberia during a growing season. Theor Appl Climatol 93:133–147

Nordstroem C, Soegaard H, Christensen TR, Friborg T, Hansen BU (2001) Seasonal carbon dioxide balance and respiration of a high-arctic fen ecosystem in NE-Greenland. Theor Appl Climatol 70:149–166

Ohta T (2005) Spatial variation of the parameters of canopy conductance model in temperate and boreal forests. Proceedings of the International Semi-Open Workshop on C/H_2O/Energy Balance and Climate over Boreal Regions with Special Emphasis on Eastern Eurasia. Yakutsk, Russia, pp 87–90

Ohta T, Hiyama T, Tanaka H, Kuwada T, Maximov TC, Ohata T, Fukushima Y (2001) Seasonal variation in the energy and water exchanges above and below a larch forest in eastern Siberia. Hydrol Proc 15:1459–1476

Ohta T, Maximov TC, Dolman AJ, Nakai T, van der Molen MK, Kononov AV, Maximov AP, Hiyama T, Iijima Y, Moors EJ, Tanaka H, Toba T, Yabuki H (2008) Interannual variation of water balance and summer evapotranspiration in an eastern Siberian larch forest over a 7-year period (1998–2006). Agr For Meteorol . doi:10.1016/j.agrformet.2008.04.012

Ohtani Y, Mizoguchi Y, Watanabe T, Yasuda Y (2005) Parameterization of NEP for gap filling in a cool-temperate coniferous forest in Fujiyoshida, Japan. J Agric Meteorol 60:769–772

Osawa A, Abaimov AP, Zyryanova OA (2000) Tree size-density relationship and size-dependent mortality in *Larix gmelinii stands*. In: Inoue G, Takenaka A (eds) Proceedings of the Eighth Symposium on the Joint Siberian Permafrost Studies between Japan and Russia in 1999, Tsukuba, pp 36–41, 2000

Osawa A, Abaimov AP, Matsuura Y, Kajimoto T, Zyryanova OA (2003) Anomalous patterns of stand development in larch forest of Siberia. Tohoku Geophysic J (Sci Rep Tohoku Univ Ser 5) 36:471–474

Osawa A, Abaimov AP, Kajimoto T, Matsuura Y, Zyryanova OA, Tokuchi N, Kondo K, Hirobe M (2004) Long-term development of larch forest ecosystems on continuous permafrost of Siberia: structural constraints and implications to carbon accumulation. In: Tanaka H (ed) Proceeding of the Fifth International Conference on Global Change: Connection to the Arctic (GCCA-5). Tsukuba University, Tsukuba, pp 53–56

Röser C, Montagnani L, Schulze E-D, Mollicone D, Kolle O, Meroni M, Papale D, Marchesini LB, Federici S, Valentini R (2002) Net CO_2 exchange rates in three different successional stages of the "Dark Taiga" of central Siberia. Tellus 54B:642–654

Ruimy A, Jarvis PG, Baldocchi DD, Saugier B (1995) CO_2 fluxes over plant canopies and solar radiation: a review. Adv Ecol Res 26:1–98

Schulze E-D, Lloyd J, Kelliher FM, Wirth C, Rebmann C, Luhker B, Mund M, Knohl A, Milyukova I, Schulze W, Ziegler W, Varlagin A, Sogachov A, Valentini R, Dore S, Grigoriev S, Kolle O, Tchebakova N, Vygodskaya NN (1999) Productivity of forests in the Eurosiberian boreal region and their potential to act as a carbon sink - a synthesis. Global Change Biol 5:703–722

Sellers PJ, Hall FG, Kelly RD, Black A, Baldocchi D, Berry J, Ryan M, Ranson KJ, Crill PM, Lettenmaier DP, Margolis H, Cihlar J, Newcomer J, Fitzjarrald D, Jarvis PG, Gower ST, Halliwell D, Williams D, Goodison B, Wickland DE, Guertin FE (1997) BOREAS in 1997: Experiment overview, scientific results, and future directions. J Geophys Res 120:28731–28769

Shibistova O, Lloyd J, Zrazhevskaya G, Arneth A, Kolle O, Knohl A, Astrakhantceva N, Shijneva I, Schmerler J (2002) Annual ecosystem respiration budget for a *Pinus sylvestris* stand in central Siberia. Tellus 54B:568–589

Tokuchi N, Kondo K, Hirobe M, Matsuura Y, Kajimoto T (2004) N cycling at Larix stand in Tura, Central Siberia –Spatial variability of soil N dynamics- In: Tanaka H (ed) Proceeding of the Fifth International Conference on Global Change: Connection to the Arctic (GCCA-5). Tsukuba University, Tsukuba, pp 207–209

Vickers D, Mahrt L (1997) Quality control and flux sampling problems for tower and aircraft data. J Atmos Ocean Tech 14:512–526

Wang H, Saigusa N, Yamamoto S, Kondo H, Hirano T, Toriyama A, Fujinuma Y (2004) Net ecosystem CO_2 exchange over a larch forest in Hokkaido, Japan. Atmos Environ 38:7021–7032

Wang H, Zu Y, Saigusa N, Yamamoto S, Kondo H, Yang F, Wang W (2005) CO2, water vapor and energy fluxes in a larch forest in northeast China. J Agric Meteorol 60:549–552

Webb EK, Pearman GI, Leuning R (1980) Correction of flux measurements for density effects due to heat and water vapor transfer. Q J Roy Meteorol Soc 106:85–100

Wilson K, Goldstein A, Falge E, Aubinet M, Baldocchi D, Berbigier P, Bernhofer C, Ceulemans R, Dolman H, Field C, Grelle A, Ibrom A, Law BE, Kowalski A, Meyers T, Moncrieff J, Monson R, Oechel W, Tenhunen J, Valentini R, Verma S (2002) Energy balance closure at FLUXNET sites. Agr For Meteorol 113:223–243

Zyryanova OA, Shitova SA (1999) Spatial distribution regularities of the central Evenkain larch forests: a cartographic model. In: Fukuda M (ed) Proceedings of the Fourth Symposium on the Joint Siberian Permafrost Studies between Japan and Russian in 1995. Hokkaido University, Sapporo, pp 65–69

Zyryanova OA, Abaimov AP, Bugaenko TN, Bugaenko NN (2000) Larch plant associations diversity of Central Siberian cryolithic zone and the development of the database. In: Inoue G, Takenaka A (eds) Proceedings of the eighth Symposium on the Joint Siberian Permafrost Studies between Japan and Russia in 1999. National Institute for Environmental Studies, Tsukuba, pp 83–89

Chapter 11
Behavior of Dissolved Organic Carbon in Larch Ecosystems

A.S. Prokushkin, S. Hobara, and S.G. Prokushkin

11.1 Introduction

Dissolved organic carbon (DOC) has a significant contribution to carbon cycling in terrestrial ecosystems and links terrestrial and aquatic environments (McDowell and Likens 1988; Neff and Asner 2001; Dittmar and Kattner 2003; Sondergaard et al. 2003). Permafrost-affected ecosystems, which hold 25–33% of the world's soil organic carbon (Hobbie et al. 2000), store significant part of this carbon temporarily in the surface layer of the ground as plant debris of different decomposition stages. This highly labile organic C may greatly exceed vegetation biomass (Prokushkin et al. 2006a, b; see also Chap. 8) and is most vulnerable to climate change (Schulze and Freibauer 2005). It is expected that along with climate-induced decomposition of this carbon pool, large amounts of dissolved organic matter will be released and transported to the oceans. Therefore, the transport of DOC from land to riverine systems and its chemical characteristics have received growing attention in the permafrost-dominated landscapes (Neff et al. 2006).

Production and release of DOC in non-permafrost forest ecosystems have been well documented (Kalbitz et al. 2000; McDowell 2003; Michalzik et al. 2003). In general, observed DOC concentrations and fluxes are the result from processes that release, such as leaching and desorption (Guggenberger et al. 1994; Michalzik and Matzner 1999; Michalzik et al. 2001; Guggenberger and Kaiser 2003), and remove DOC, such as adsorption and biodegradation (Kaiser and Guggenberger 2000; Kaiser et al. 2000). Local carbon stocks (Aitkenhead and McDowell 2000), properties of soils (Currie 1999; Cory et al. 2004), temperature, and moisture (Christ and David 1996) can modulate the DOC flux within a particular watershed. In permafrost-affected ecosystems, the sources and mechanisms of DOC export from watersheds are still under debate. Topography modulates heat flux to soils and strongly affects spatial variability in permafrost thawing rates and consequently decomposition rates of soil organic matter (SOM) (Prokushkin et al. 2005a, b, 2006a, b). Distinct terrigenic signatures (e.g., lignin, humic substances, and their isotopic composition) for different DOC sources in streams underline the importance of topography in driving spatial variability in the chemical structure of DOC that is reaching streams (White et al. 2002; Prokushkin et al. 2007).

A. Osawa et al. (eds.), *Permafrost Ecosystems: Siberian Larch Forests*,
Ecological studies, Vol. 209, DOI 10.1007/978-1-4020-9693-8_11,

Moreover, the seasonality of the export of DOC from forest ecosystems to surface waters is believed to depend on the active layer depth in permafrost soils (Woo and Winter 1993; MacLean et al. 1999; Prokushkin and Guggenberger 2007; Prokushkin et al. 2009) and microbial activity in these soils (Sorokin and Evgrafova 1999). However, so far few reports exist on the importance of these processes and mechanisms on DOC export from permafrost-affected ecosystems of Siberia.

The objective of the present study is to review and summarize major findings on DOC fluxes in larch ecosystems of Central Siberia, underlain by continuous permafrost.

11.2 Approaches to Study Dissolved Organic Carbon

11.2.1 Site Description

The present study was conducted at 5 km north of Tura settlement on the Kulingdakan watershed (64°17–19′N, 100°11–13′E) encompassed about 4,100 ha and a part of Site 1 (see Fig. 1.3). Watershed drains into a stream, which is a tributary of Kochechum River. Its basin consists of forested hills with table-like tops and boggy valley bottoms. The watershed geomorphology (elevation from 132 to 630 m, slope inclination of 12–15°) is typical for the Syverma plateau. The stream is approximately 8 km in length. The main channel near the junction with the Kochechum River is about 6 m wide and is characterized by step-pools with large pebbles and boulders. According to the long-term record at Tura (1928–2008), the average temperature for January (the coldest month) is −36.0°C, and that for July (the warmest month) is 16.6°C. Mean annual temperature is −9.0°C and mean annual precipitation is 369.6 mm (see also Chap. 1). About 40% of annual precipitation falls as snow. Intense snowmelt starts in mid-May and continues for about 2 weeks depending on the hydrologic and climatic conditions of the year. Various degrees of droughts characterize the summer climate. The entire watershed area is underlain by continuous permafrost and located at approximately 250 km distance from the edge of discontinuous permafrost distribution.

Vegetation of the watershed is typical for deciduous coniferous forests of Central Siberia (Abaimov 2005; see also Chap. 3). The overstory is formed by larch (*Larix gmelinii* (Rupr.) Rupr.) with occasional spruce (*Picea obovata* Ledeb.) and birch (*Betula pendula* L.) (see also Chaps. 2, 6, and 7). The ground vegetation is dominated by dwarf shrubs (*Ledum palustre* L., *Vaccinium vitis-idaea* L., and *Vaccinium uliginosum* L.), mosses (*Pleurozium schreberi* (Brid.) Mitt., *Hylocomium splendens* (Hedw.) B.S.G., and *Aulocomnium palustre* (Hedw.) Schwaegr.) and lichens (*Cladina* spp. and *Cetraria* spp.). Patches of *Sphagnum* spp. occur in waterlogged and shaded locations (see also Chap. 5). Approximately half of the watershed burned in 1990 by fire resulting in almost 100% mortality of larch trees.

Basalts and tuffs are the major soil forming parent materials conferring specific properties to soils of the region (Pokrovsky et al. 2005). Development of soils in the study area strongly depended on the permafrost regime inhibiting podzolization. All soils showed a mor-type organic layer (pH 3.8–5.0) of 4 cm (1–12 cm) thick on south-facing (SF) slopes and 7 cm (3–13 cm) thick on north-facing slopes. Inceptisols and Gelisols appeared on south- and north-facing slopes, respectively. Depth of the soil active layer, defined as a portion of the upper soil that thaws in summer, typically reaches maximum in September of up to about 0.5 m (0.2–0.7 m) on north facing slopes and about 1.0 m (0.6–1.4 m) on south facing slopes. In relief depressions active layer depth is restricted to the organic layer. Cryogenic microtopography (mounds and troughs) is the key cause of significant spatial variability of soil characteristics due to cryoturbation processes.

11.2.2 Soil and Water Sampling and Analyses

Examination of C stock and water-extractable organic carbon (OC) (henceforth referred to as water extractable organic carbon (WEOC); see Tokareva et al. 2006) content in organic and mineral layers of soils on the Kulingdakan watershed was conducted for stands of different classes (division distinguished by age and type of plant association) surveyed during 2003 and 2004 (Fig. 11.1). Within each class, three randomly located soil samples were taken from each of three topographic positions (ridge, slope, and riparian zone) (Tokareva et al. 2006).

Experimental plots (10 × 10 m each) for the analysis of ecosystem-scale DOC fluxes were selected at mid-elevation on north- and SF slopes of 12–13° inclination, referred to as NF and SF sites, respectively (Fig. 11.1); here, the NF plot differs from the plots labeled as NF1 through NF12 in Chaps. 1 and 6, but is located about 50 m down-slope (see Table 1.1 and Fig. 6.1). Sites were separated by a stream valley, which collected the DOC input from both slopes. Stand characteristics of the plots are presented in Table 11.1.

Organic layer and mineral soil up to permafrost were sampled randomly in triplicate at each position in the middle of the growing season. All samples were air-dried prior to analyses. Total carbon was measured by CuO-catalyzed dry combustion at 900°C (Elementar Vario Maxi CHNS analyzer, Elementar Analysensysteme GmbH, Hanau, Germany). All soil samples were free of carbonates, as shown by reaction with 10% H_3PO_4 and the CO_2 evolved was measured by IR absorption (C-mat 550 PC, Ströhlein GmbH, Kaarft, Germany). Content of water extractable organic carbon (WEOC) was measured in distilled water extracts of soil (1:10, soil:water) after 24 h of stirring.

Collection of soil solution samples for DOC analyses was conducted between 2001 and 2005 during a major part of frost-free period (25 May–25 September).

Organic layer seepage water: Solutes were collected beneath organic layer by zero-tension lysimeters ($n = 6$, area 80 cm^2) similar to those used by Hongve et al. (2000) and connected to 1 dm^3 PET bottle (flushed first with 0.1M HCl, then with

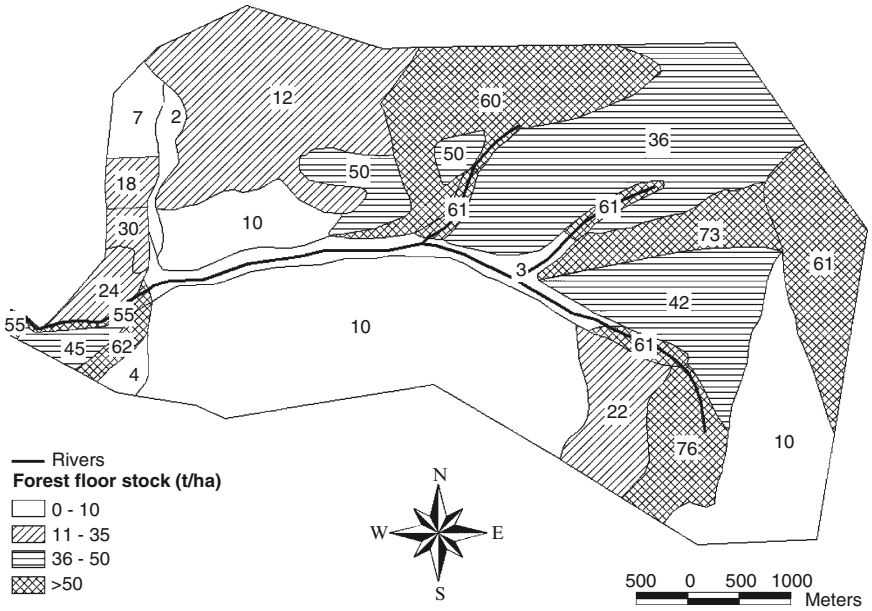

Fig. 11.1 Stocks of organic matter in the forest floor in forest categories in Kulingdakan watershed (Tokareva et al. 2006)

distilled water and finally with leachate). Sample collection was usually performed after rain events with some longer intervals (ca. 1 month).

Soil solution: Soil water was sampled by suction lysimeters (Eijkelkamp, the Netherlands) installed at the depths of 1, 5, and 20 cm at 4–7 day interval.

Stream and river water: Stream water sampling and discharge measurements were made daily using the methods that were previously described in Prokushkin et al. (2001). Kochechum river water was sampled at 5-day intervals during frost-free period (May–September) and monthly intervals during October–April. Discharges of the Nizhnyaya Tunguska and Tembenchi Rivers (1939–1989) were used to demonstrate annual hydrograph separation. The latter is a tributary of the Kochechum River.

DOC concentrations were determined by Shimadzu TOC-VCN (Shimadzu Corp., Kyoto, Japan).

Chemical composition of DOC was analyzed for lignin content (CuO oxidation) as described by Guggenberger et al. (1994) and by pyrolysis-GC-MS/IRMS (Kracht and Gleixner 2000; Prokushkin et al. 2007). Ultraviolet absorption of samples at 280 nm wavelength was measured by UV–Visible spectrophotometer (Cary 50 Scan Varian, Germany) and specific ultraviolet absorption (SUVA) was calculated as UV light absorption divided by DOC concentration in 1 m wide column ($l\ mgC^{-1}\ m^{-1}$).

Table 11.1 Stands characteristics of experimental plots on south- and north-facing slopes

Aspect	Elevation (m a.s.l.)	Slope angle (°)	Stand canopy				Forest floor				Active layer depth (cm)
			Age (years)	H (m)	DBH (cm)	Crown projection	Thickness (cm)	C (g m^{-2})	N (g m^{-2})	C/N	
South	215	12	83–100	10.0±2.5	8.2±3.0	0.53	4.2 ± 0.8	1,040 ± 44	34.3 ± 2.3	31	112 ± 7
							5.9 ± 1.1	1,256 ± 69	37.0 ± 2.0	34	86 ± 19
North	176	13	85–99	6.9±2.0	5.3±2.1	0.12	9.4 ± 2.2	1,325 ± 78	26.0 ± 1.5	51	64 ± 11
							10.8 ± 4.6	1,405 ± 90	23.7 ± 1.5	61	45 ± 22

Values are means ±SD. Values for the forest floor and active layer depth are given for mounds (numerator) and troughs (denominator). The canopy in both plots is larch (*L. gmelinii*). Active layer depth (depth of soil melting) is the value measured on September 14, 2002

11.3 DOC Content and Release in Soils

11.3.1 Soil Organic Matter Stocks and WEOC Content in Soils

Accumulation of organic C in organic layer of taiga soils appears to follow predictable patterns related to aspect and microtopography as a result of the interacting effects of temperature and moisture availability (Van Cleave and Yarie 1986; Hobbie 1996; Hobbie et al. 2000; Kawahigashi et al. 2004, Prokushkin et al. 2009). Our results (Fig. 11.1) show that the warmest, best-drained soils (SF slopes) in similar aged stands have usually thinner organic layers with lower stock of organic matter (18–70 Mg ha^{-1}) in the organic layer (Tokareva et al. 2006). The coldest, most poorly drained soils (e.g., stream valleys, north- and east-facing slopes) have the thickest organic layer and the highest organic matter accumulation (40–100 Mg ha^{-1}). These results are consistent with earlier results of Hobbie et al. (2000) and Kawahigashi et al. (2004), showing that increasing thickness of the O horizons reflects the difference in moisture conditions and thus probably microbial activity among the organic horizons. Because temperature and hydrologic conditions interact with both production and decomposition of organic matter, it is hard to determine which factor contributed the most in producing the spatial mosaic of C accumulation that we have documented. Soil drainage (i.e., dry conditions), for example, can both decrease moss productivity and accelerate organic matter decomposition, driving the site to lower accumulation of organic C (Hobbie 1996; Knorre et al. 2006). Conversely, an increase in organic layer thickness under cold conditions provides a potential positive feedback loop, as a thicker organic layer further insulates the soil from solar energy and makes the depth of the active layer decrease (Sofronov et al. 2000; also see Chap.4).

Carbon pool of the upper organic layer represents a major ecosystem source of DOC (Aitkenhead-Peterson et al. 2005). On the basis of single extraction procedure, water-soluble organic matter constitutes about 1% of total OC accumulated in organic soil layers (Fig. 11.2) and mosses. Interestingly, warmer aspects (i.e., SF slopes) revealed a larger content of WEOC in organic layers, which nevertheless was hidden by lower accumulation of total organic matter. Therefore, there was significant variability in WEOC stock in the watershed (Fig. 11.3) following aggregated accumulation of C within the organic layer. Total stock of WEOC in moss and organic layers within the watershed (including burnt and intact forest areas), representing the main ecosystem sources of mobile OC, was estimated as 0.24 MgC ha^{-1} (Tokareva et al. 2006).

These findings emphasize the significance of potentially mobile organic matter fraction in topsoils of permafrost terrains, which is also supposed to be replenished along with SOM decomposition and productivity of plants (Neff and Hooper 2002). Moreover, eight consequent extractions, when steady-state release was reached, led to doubling of this value (Tokareva et al. 2006).

In 1990, approximately 50% of watershed area was subjected to intense groundfire that resulted in combustion of 40–95% of organic matter accumulated in the

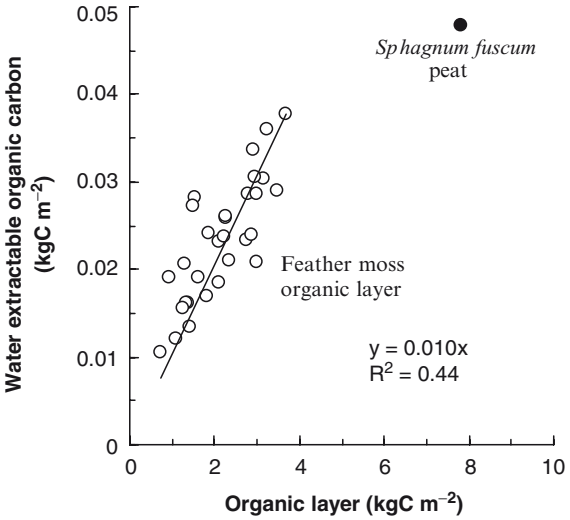

Fig. 11.2 Relationship between stock of water-extractable organic carbon (WEOC) and respective total organic carbon in the forest floor. *Black dot* represents the mean value for 50 cm deep peat of *Sphagnum fuscum*; regression line is derived excluding this datum (Prokushkin et al., unpubl. data)

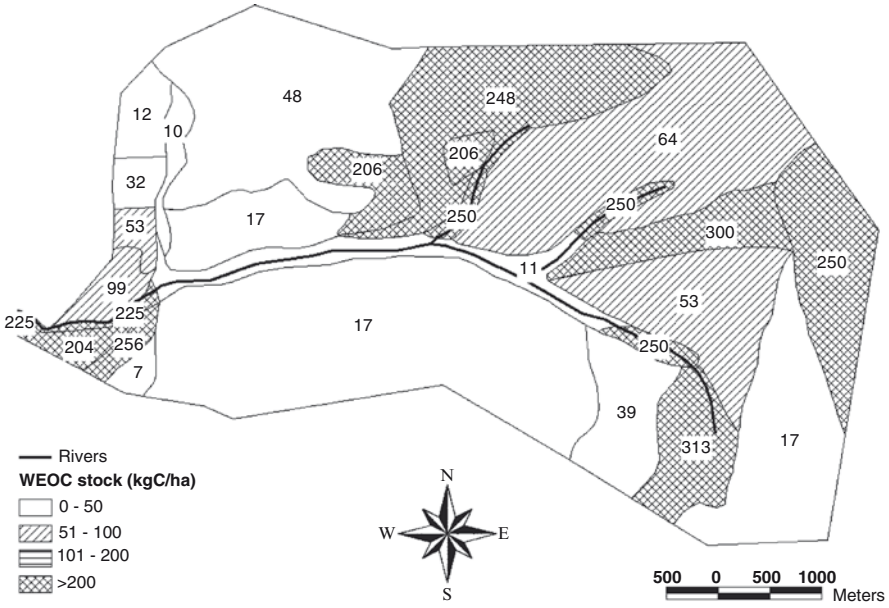

Fig. 11.3 Stocks of water-extractable organic carbon (WEOC) in the forest floor in various forest categories in Kulingdakan watershed (Tokareva et al. 2006)

ground vegetation and organic layer (Fig. 11.1). Including likely additional respiration losses during the first years after the fire, the loss totaled 1,800–2,400 gC m^{-2}. These estimates of fuel consumption are in the range of estimates for boreal North America (Randerson et al. 2006) and Siberia (Conard et al. 2002).

Combustion of organic layers greatly reduces the amount of mobile C fraction and export of DOC to the subsoil (Shibata et al. 2003). Within the Kulingdakan watershed, burned locations showed >90% decrease of WEOC stock in the organic layer (Fig. 11.3), whereas total OC loss was only 70% on average. These findings suggest that residual organic matter is likely to be composed of compounds that are less water soluble (e.g., black carbon, lignin etc.).

11.3.2 Soil DOC Concentrations and Fluxes

Concentrations of DOC in the organic layer seepage water from both SF and NF plots demonstrated inter-annual and more obvious inter-seasonal variation. Among individual collection dates, concentrations on the north-facing slope ranged from 16 to 71 mg Cl^{-1}. On the SF plot, DOC concentrations were significantly higher, ranging from 29 to 215 mg Cl^{-1}. In general, average DOC concentration for the whole measurement period was almost twofold higher in the seepage water on the SF than that on the NF plot (91 and 50 mg Cl^{-1}, correspondingly). Organic layer leachates of both slopes demonstrated seasonal changes of DOC concentrations with an increase from spring to autumn, which was more pronounced in the heat deficient north-facing slope (Fig.11.4).

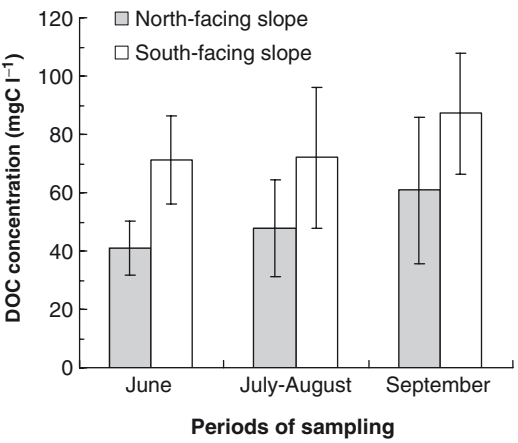

Fig. 11.4 Concentrations of DOC in leachates of forest floor during different periods of frost-free season on the north- and south-facing slopes. Data presented as a mean value with SD for six replicate lysimeters for every period during 2002–2005 field campaigns

Concentrations of DOC in solution percolating from the organic layer varied with both throughfall amounts and temperature on the NF plot, but were less related to either parameter on the SF plot. On both plots, DOC concentration tended to decline with increases in volume of leachate water, suggesting the presence of a dilution factor (Fig.11.5). Concentrations of DOC increased along with rising soil temperature on the north-facing slope (Fig.11.6a), but showed no or slightly negative response to temperature on the SF plot (Fig.11.6b), presumably because of

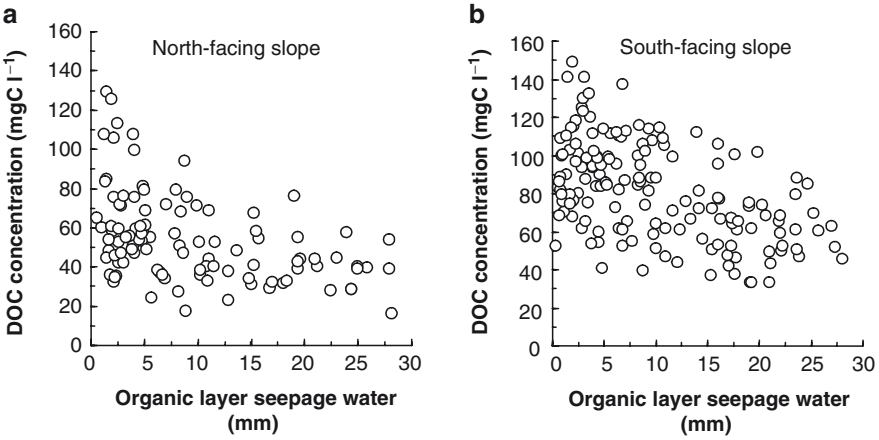

Fig. 11.5 Concentrations of DOC in leachates of forest floor of (**a**) north- and (**b**) south-facing slopes in relation to water volume percolated through forest floor (Prokushkin et al. 2008)

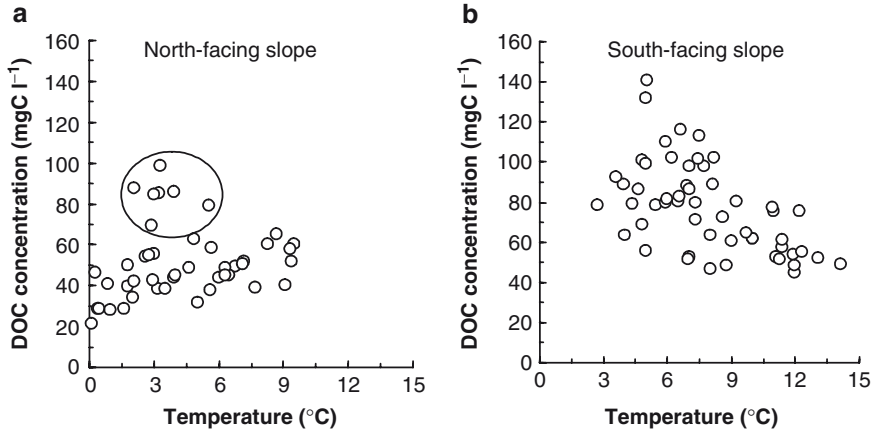

Fig. 11.6 Concentrations of DOC in leachates of forest floor of (**a**) north- and (**b**) south-facing slopes in relation to temperature at the interface between forest floor and mineral soil. Values in an oval represent those of the dry season of 2003 (Prokushkin et al. 2008)

decline in microbial activity with increasing drought stress. Therefore, yearly moisture regime is believed to control this trend, but has a site-specific effect. Under drought (i.e., July 2003), there was decrease in mobilized DOC in the SF plot. In contrast, higher DOC release was found in the NF plot. Autumnal increases in DOC values in organic layer seepage waters might be explained by a favorable combination of moisture and temperature driving the decomposition process.

DOC export from the organic horizon on the basis of individual percolation event ranged from 0.01 to about 3 gC m^{-2} on both SF and NF plots, and it was positively correlated with the volume of percolating soil solution (Fig. 11.7). In general, DOC flux from the organic horizon to the underlying mineral soil on the SF slope was approximately 1.5-fold higher than that on the north-facing slope (i.e., slope of linear regressions is 78 vs. 52 mgC mm^{-1}). Total DOC export during the frost-free season (2002–2005) ranged from 4.0 to 17.6 gC m^{-2} on the SF plot and from 2.2 to 8.9 gCm^{-2} on the NF plot. In 2006, the overall flux was the lowest because of a mid-summer drought (only 4 mm of leached water was measured from organic layer in July). Total DOC export from the organic horizon during the growing season in wetter years was about 1.5 higher than the total WEOC stock in moss and litter on the SF slope plot, but only 70% of that on the NF plot. DOC flux from the organic layer represented about 0.5% of total C stock on the NF plot, and respectively ca. 1.0% of C stock on the SF plot. These findings suggest higher mobility of C and elevated microbiological production of DOC within warmer environments.

Dissolved organic matter released from the organic layer is a very heterogeneous and complex mixture of organic molecules with different chemical characteristics (i.e., lignocellulose complex) (Schulten and Gleixner 1999; Gleixner et al. 2002). Recent application of pyrolysis-gas chromatography-mass spectrometry (Py-GC-MS) revealed distinct heterogeneity of organic matter translocating from

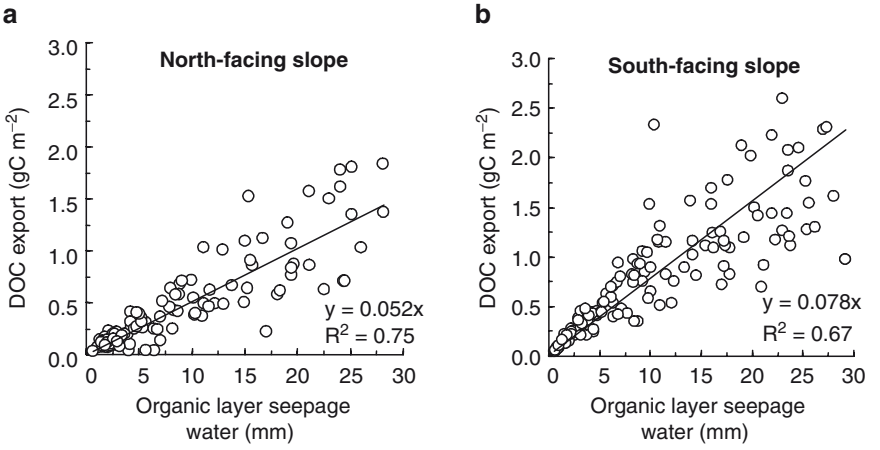

Fig. 11.7 DOC export from forest floor of (**a**) north- and (**b**) south-facing slopes in relation to water volume percolated through forest floor (Prokushkin et al. 2008)

organic layer to mineral soil as DOC in larch ecosystems. Even more detailed information has been obtained from examination of compound-specific isotope ratios acquired by isotope ratio mass spectrometry (IRMS) (Prokushkin et al. 2007).

DOC collected on north and SF slopes demonstrated significant Pearson correlation of both relative abundances and isotopic signatures of identified pyrolysis products, suggesting similar chemical characteristics of sources of DOC on these micro-climatically contrasting slopes. DOC from both locations demonstrated dominance of lignocellulose complex. Breakdown products of polysaccharides and phenols were the most abundant fraction comprising about 75% of all identified compounds (51 and 24%, respectively, Figs. 11.8a, c). At the same time, DOC from the SF plot contained higher amounts of "fresher" (2-furaldehyde, 5-methyl-2-furaldehyde, and 2-methoxyphenol) than that from the NF plot located on north-facing slope. Moreover, the average isotopic composition of pyrolysis products of DOC leached from the organic layer of the NF plot demonstrated overall enrichment (1.3‰) of DOC by ^{13}C relative to the SF plot. These findings suggest that DOC leached from the organic layer of colder north facing slopes is likely to have originated from more degraded material that escaped utilization by the microbial community (Kracht and Gleixner 2000) or stabilization. In contrast, presence of humified matter (e.g., methylmethoxyphenol and dimethylnaphthalin) identified in the S slope DOC indicates deeper transformation of organic matter at a warmer location (Prokushkin et al. 2007).

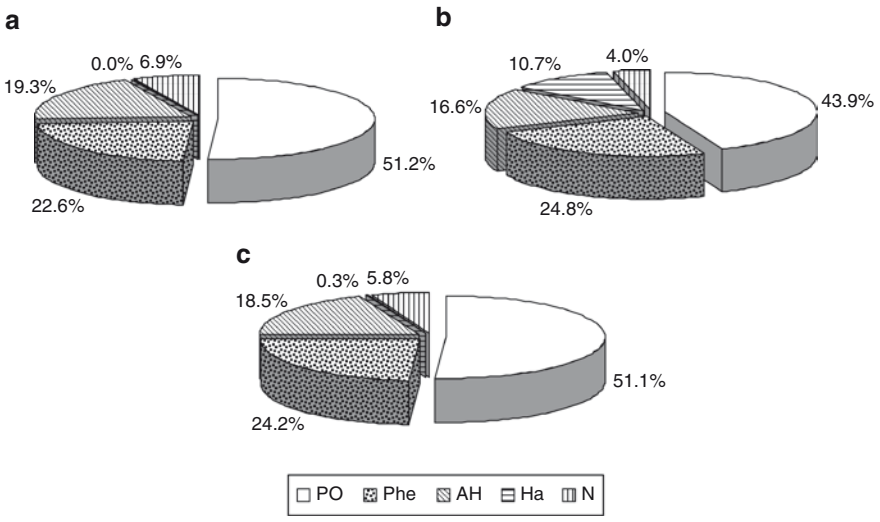

Fig. 11.8 Relative proportions of pyrolysis fractions of DOC (% of total relative abundances of identified compounds) in leachates of forest floor collected on (**a**) north- and (**c**) south-facing slopes, respectively, and (**b**) soil solution DOC collected on north-facing slope. Pyrolysis product fractions: polysaccharides (PO), phenolic compounds (Phe), aromatic hydrocarbons (AHC), humic substances (Ha), and nitrogen-containing compounds (N)

These results are consistent with previous studies, which showed that DOC production and CO_2 evolution increase with temperature (Christ and David 1996; Neff and Hooper 2002). Thus, it is likely that decomposition/oxidation of upper soil organic carbon, which leads to production of DOC in ecosystems limited by lower temperatures and excess soil moisture, would be enhanced under drier and warmer climate (Neff and Hooper 2002).

These increases may become substantial, as the projected rise in temperature is as much as 3–5°C in the next 50 years (Peterson et al. 2002). Depth of the active layer in Russian permafrost has already increased by 20 cm from 1956 to 1990 (Nikolaev and Fedorov 2004). The longer-term responses of organic soils and DOC flux in a warming climate are hard to predict, however. Changes in vegetation will undoubtedly be a result accompanied by changes in climate, and this will affect quality and quantity of organic matter entering the soil and thus production of DOC (Neff and Hooper 2002; Neff et al. 2006).

Models of vegetation response to warming in permafrost regions of Siberia suggest that initial stages of warming (1–2°C) may even accelerate moss production resulting in an increase in its thickness and insulating properties of the organic layer, cooling the soil by 0.5–1°C (Anisimov and Belolutskaya 2004). Continued warming that results in a shift toward more vascular vegetation in Central Siberia owing to higher summer air temperatures could lead to an increase of approximately 30% in the active layer depth.

Despite negative dependency between organic layer DOC concentration and the amount of percolated water, DOC concentration in mineral soil did not respond to precipitation events throughout the frost-free season (Prokushkin et al. 2008). However, there was a slight decrease in DOC concentration from June to September. In drier weather conditions (i.e., 2005 and 2006), there was no available water in all studied soil layers on the S-facing slope after mid-July (Fig. 11.9). In contrast, there was increase in DOC concentration in the soil solution during July at 5 and 20 cm depths in the wetter year of 2004. Therefore, moisture rather than temperature may drive production and mobilization of DOC in high latitude soils with low precipitation during a frost-free period (Prokushkin et al. 2005a).

In general, concentration of DOC is lower in soil solution than in seepage water from the organic layer. It suggests removal of DOC by microbial decomposition and/or adsorption (Kaiser and Guggenberger 2000; Guggenberger and Kaiser 2003; Kalbitz et al. 2005) on both slopes. However, the decrease in DOC concentration with soil depth was more apparent in the warmer SF slope.

Sorption of DOC on mineral phases is the key geochemical process for carbon preservation in soils (McDowell and Likens 1988). Across a broad range of ecosystems, most DOC leached from organic horizons is sorbed and retained in the subsoils (Kaiser and Guggenberger 2003; Kalbitz et al. 2000, 2005). The sorption depends much on contents of sesquioxides and amount of carbon previously accumulated in soils (Kaiser et al. 2000; Kawahigashi et al. 2006). In general, immobilization of DOC has been considered an important process in the formation of stabile OC due to its protection against microbial attack (Guggenberger and Kaiser 2003).

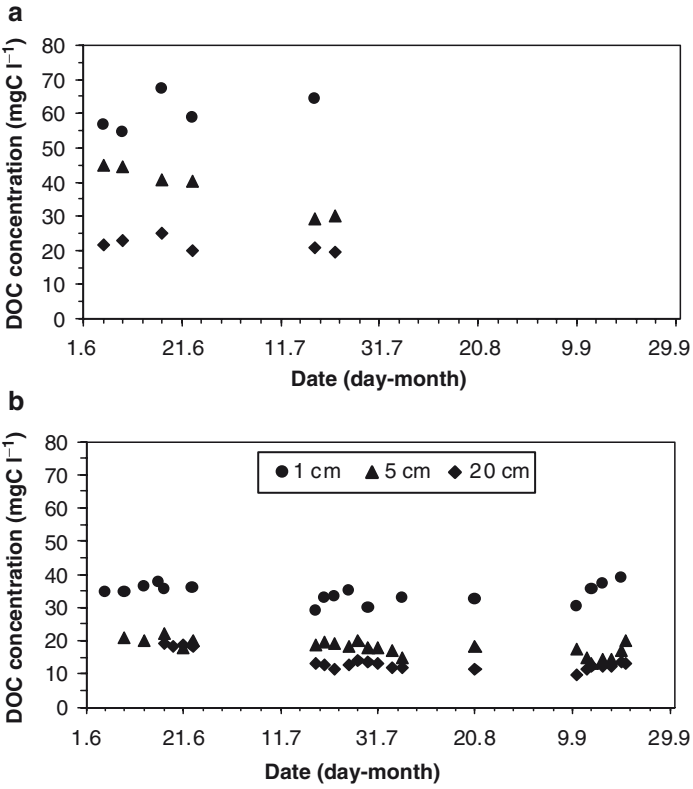

Fig. 11.9 Dynamics of DOC concentrations in mineral soil at three depths (1, 5, and 20 cm) on south- (*upper graph*) (**a**) and north-facing (*lower graph*) (**b**) slopes in 2005. There was no water suction from the soil of south-facing slope starting from mid-July

Sorption and mineralization of DOC in soil is not uniform because of heterogeneity and complex mixture of organic molecules with different chemical characteristics (Schulten and Gleixner 1999; Gleixner et al. 2002). Along with decrease in DOC concentrations along its passage through mineral soil (Fig. 11.9), there are major biochemical alterations of DOC composition (Fig. 11.8b). Hydrophobic compounds of high molecular weight and those rich in acidic functional groups and aromatic moieties are adsorbed most strongly (Kaiser et al. 2000; Kawahigashi et al. 2006). On the other hand, "new" substances were added to the soil solution in subsoil due to desorption of humified material and release of hydrophilic microbial products (Kawahigashi et al. 2004; Prokushkin et al. 2007).

Thus, warming in larch taiga of Central Siberia may lead to increased release of currently sequestered carbon through

1. Enhancement of temperature-controlled DOC production processes;
2. Raised precipitation, thereby increasing DOC mobilization from its large pool in the upper organic layer (Prokushkin et al. 2009).

However, fate of DOC in soils is largely determined by the hydraulic residence of DOC in soil and concurrent mineralization. As a result, although production and release of DOC from the organic layer is greater in warmer soils, the deeper active layer increases its contact with mineral soils and thus likelihood of DOC adsorption, leading to C stabilization in soil and/or microbial mineralization to CO_2.

11.4 Export of Terrestrial DOC to Riverine System

11.4.1 Seasonal Patterns of Riverine DOC Concentrations

There are several factors that distinguish runoff hydrology of the study area from more temperate regions: (1) snowmelt is the major hydrological event (Finlay et al. 2006), conveying about a half of the annual precipitation inputs to the catchment in a 2– 4-week period (Fig. 11.10); (2) deep drainage is restricted due to the presence of permafrost, thus enhancing near-surface water tables (Prokushkin et al. 2007; Prokushkin and Guggenberger 2007); (3) widespread occurrence of organic soils allows rapid translocation of water to the stream (Quinton et al. 2000; Carey and Woo 2001), and (4) matrix bypass mechanisms such as soil pipes (Gibson et al. 1993; Carey and Woo 2001) and inter-hummock flow (Quinton et al. 2000) may

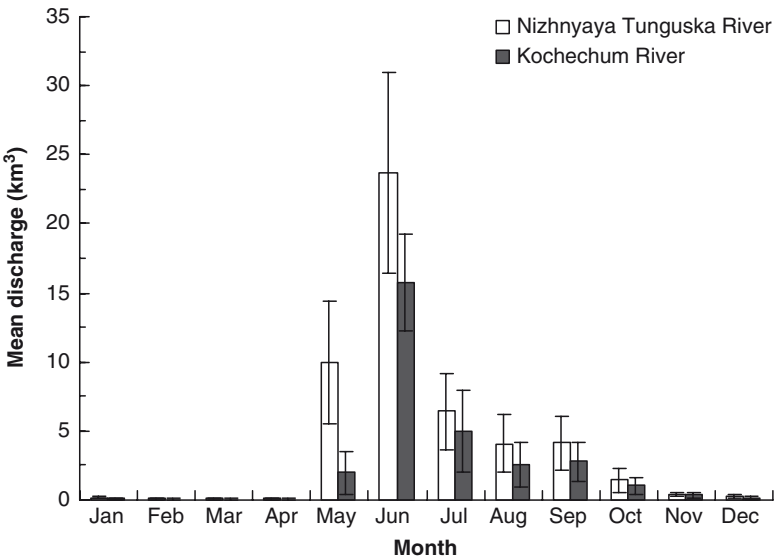

Fig. 11.10 Mean monthly discharge (1939–1995) of the Nizhnyaya Tunguska and Kochechum Rivers, representing the watersheds underlain by permafrost in Central Siberia (Data from http://www.r-arcticnet.sr.unh.edu)

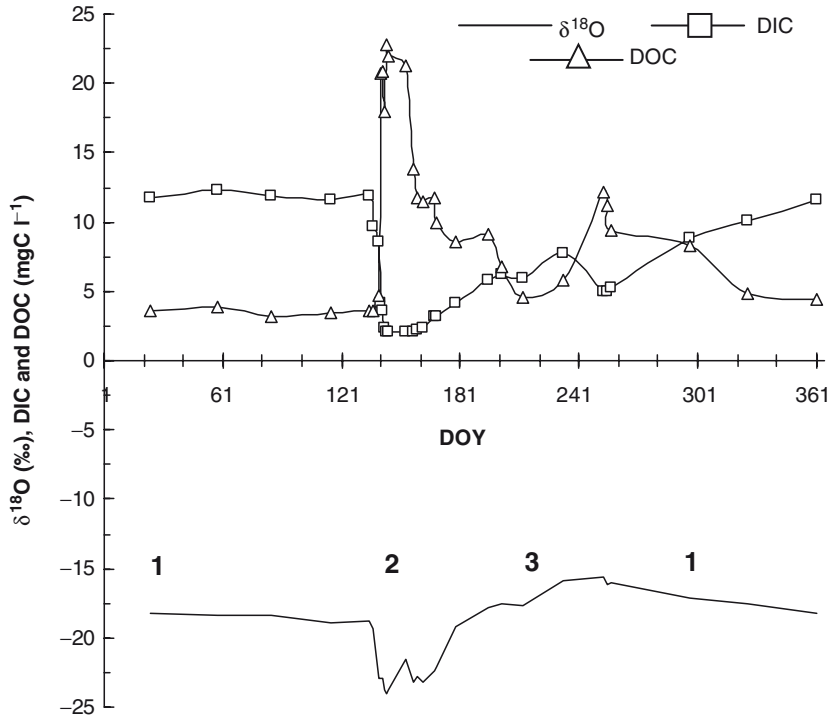

Fig. 11.11 Dynamics of $\delta^{18}O$ in water, concentrations of DIC and DOC in the Kochechum River (Central Siberia) in 2006: (1) winter; (2) spring flood; (3) summer and fall flow periods. DOY indicates Julian day

convey significant amounts of water during the melt period with wet antecedent conditions.

Based on seasonal patterns of discharge and chemical characteristics of DOC in subarctic streams and rivers, there is common division of annual hydrographs into spring flood, summer through autumn, and winter flow periods (Fig. 11.11). Though start and duration of these periods may vary greatly among basins and annually, such a separation is driven by distinct changes in sources and flowpaths of water and DOC in riverine systems (Finlay et al. 2006; Striegl et al. 2007).

During the entire observational period (May–September in 2001–2005), the DOC concentration in water of Kulingdakan stream varied from 8 to 32 mgC l^{-1} (Fig. 11.12). The maximum concentrations were obtained from snowmelt phase: May–early June (Table 11.2). Because of significant stream discharge, DOC export from the watershed in this period is above 140 mgC m^{-2} day^{-1} and is more than 40% of the total value for the entire frost-free period (Prokushkin and Guggenberger 2007).

Biochemical composition of stream DOC consisting of compounds of plant origin (polysaccharides are >40%, lignin and other polyphenolic compounds are about 26%), and products of microbiological synthesis (carbohydrates and uronic

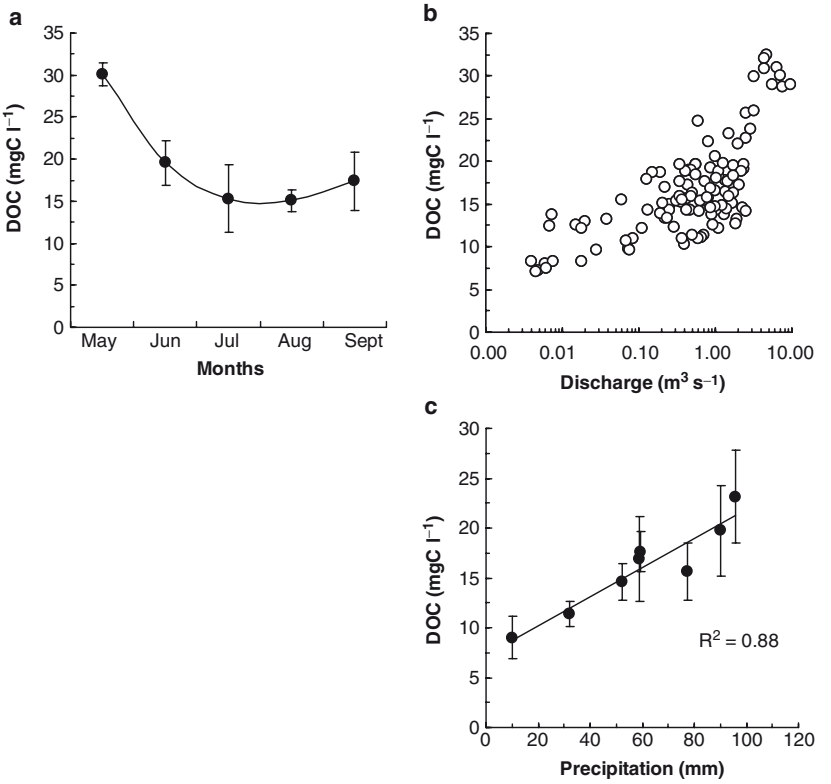

Fig. 11.12 Changes in (**a**) mean concentrations of DOC in the Kulingdakan stream from May to September in 2001–2005. Relationships between (**b**) stream DOC concentration and discharge, and (**c**) monthly mean DOC concentration and precipitation for July 1998–2005 (Prokushkin et al. 2009)

acids and humification) are <1 and 6%, respectively (Table 11.3). Above 20% is represented by aromatic hydrocarbons (AHC); about 5% belongs to nitrogen-bearing compounds (Prokushkin et al. 2007). Content of dissolved lignin (prevailing coniferous lignin) amounts to about 0.6 mg l^{-1} (Prokushkin and Guggenberger 2007). Therefore, DOC in the spring period is characterized by substantial aromatization (SUVA, Specific Ultraviolet Absorbance, 3.5 l mg C^{-1} m^{-1}), which indicates weak microbiological transformation of organic matter that enters the stream. Along with absolute domination of a hydrophobic fraction, it suggests sufficient DOC resistance to biodegradation in the aquatic environment.

In summer, monthly mean DOC concentration in the stream water decreased with increase in the thickness of active layer (Fig. 11.12a). However, precipitation still exerts significant control on DOC concentration in streams in this period. Low

Table 11.2 Averaged hydrological parameters, dissolved organic matter concentrations, and export in the Kulingdakan stream from May to September in 2001–2005 (Prokushkin and Guggenberger 2007)

Variables	May	June	July	August	September
Precipitation (mm)	28.4 ± 5.0	63.6 ± 24.2	60.0 ± 21.2	63.2 ± 31.5	38.6 ± 7.0
Stream flow (mm)	141.0 ± 37.4	28.3 ± 17.2	10.2 ± 8.5	26.5 ± 24.2	31.0 ± 7.6
DOC concentration (mg C l^{-1})	29.5 ± 2.4	19.6 ± 2.7	15.3 ± 4.0	15.7 ± 1.3	17.4 ± 3.5
DOC export (mg C m^{-2} day^{-1})	136.5 ± 24.7	58.6 ± 18.9	6.5 ± 4.1	17.0 ± 6.6	55.7 ± 26.2

Values are means ±SD

hydraulic conductivity of mineral soil horizons due to high content of clay fraction (>40%) and generally shallow active layer lead to dominance of surface runoff after strong rainstorms. Consequently, a positive relationship between stream discharge and DOC concentration in the stream has been observed (Fig. 11.12b). Our results also demonstrated that up to 70% of total DOC export from the watershed in summer occurs during the short-term stormflows. For example, release of the terrigenous DOC during a period of low flow is less than 0.1 mgC m^{-2} day^{-1}, whereas stormflows represent much larger flux – up to 100 mgC m^{-2} day^{-1}. The DOC export in July, averaged over 2001–2005, was only 0.20 (0.12 gC m^{-2} $month^{-1}$. In August, in spite of stream DOC concentrations close to those of July, increased stream discharges due to decreased evapotranspiration resulted in increased DOC export from the watershed of up to 0.5 gC m^{-2} $month^{-1}$ (0.15–0.88 gC m^{-2} $month^{-1}$).

Biochemical composition of DOC changes with the increase in stream discharge: increased aromatization (SUVA) from 2.0 to 2.5 lmg C^{-1} m^{-1}, and increased lignin and polysaccharide compounds concentrations (Table 11.3). The presence of specific chemical fingerprints of organic layer DOC in the stream, as well as isotopic (^{13}C) composition of those substances (e.g., 2-furaldehyde and 5-methyl-2-furaldehyde) clearly demonstrated importance of soil organic layers as a source of stream DOC at higher discharges (Prokushkin et al. 2007). Moreover, the analysis of pyrolysis breakdown products composition and their isotopic signatures suggests that SF slopes with deeper soil active layer do not have a significant hydrological connection to the stream during this time. Conversely, on the north-facing slope, the timing of lateral water flow and its DOC composition corresponds closely with the timing of streamflow freshet and stream DOC composition. Within the south aspects, upslope areas had increased infiltration capacities and deeper water tables as unsaturated seasonally frozen soils allow vertical infiltration. Conversely, within the northern aspects, the water table was within the organic layer perched above the mineral substrate at all sites. Thus, under the current conditions, composition and functional characteristics of stream DOC are mainly controlled by shallow soils developed at colder and wetter positions in the permafrost landscape. Deeper soils found in warmer and well-drained southern aspects effectively retain both water and DOC, resulting in lower export of both to rivers. Such findings suggest that warming and consequent deepening of the active layer will change not only the

chemical composition of DOC entering rivers, but also the summer export of water and dissolved organic matter (amount decreasing) from forested watersheds underlain by continuous permafrost in Siberia (Prokushkin et al. 2009).

Early autumn (September) is characterized by increased input of DOC to the stream (Table 11.2, Fig. 11.12), which is determined by the increased stream discharge due to excess soil moisture. The latter is considered to be a result of transition of plants to dormancy, low temperatures, and decreased evapotranspiration losses. Furthermore, still uncertain mechanisms may increase DOC concentrations in the organic layer in this period (Prokushkin et al. 2005a; Prokushkin et al. 2009). As a result, the total monthly (September) DOC export from the watershed basin increased to about 1.7 gC m^{-2}.

For the entire frost-free period, the average DOC removal from the watershed amounts to about 6 gC m^{-2}, varying from 3.0 gC m^{-2} in a dry year to 10.3 gC m^{-2} in a wet year (Prokushkin et al. 2008), or 80–420 MgC from the entire watershed. The latter values correspond to 12–40% of WEOC accumulated in moss and organic layers of the Kulingdakan watershed, and below 0.5% of total stock of OC of these layers. The major portion of annual DOC export from the catchment (up to 90%) occurs during flood events with little capacity of the soil to retain DOC (snowmelt, summer, and autumnal discharge peaks). In view of these findings, it is hypothesized that deepened active soil layer induced by warming will have a minor direct effect on annual export of DOC from the catchments. More profound effect of warming on DOC export from permafrost terrains at high latitudes is expected from the temperature-related changes in organic layer C stock or its combustion during wildfires.

Thus, there are two major controls on runoff and DOC export observed across the subarctic area: (1) permafrost distribution defines basin-contributing areas, as lateral flow is confined to permafrost-underlain terrains due to their ability to restrict deep percolation and (2) surface organic soils play a key role in rapidly conveying water to the stream. During the melt period, meltwater percolating from the snowpack in terrains with shallow permafrost soils infiltrates through the organic soil, since deeper infiltration is restricted by the impermeable permafrost table. In areas with a deeper active layer (e.g., SF slopes) or in the absence of frost (discontinuous or sporadic permafrost regions), percolation is uninhibited unless there are ice-rich layers at depth. The isotopic signature of river water at this time becomes strongly depleted with respect to $\delta^{18}O$ suggesting large snowmelt water input to streams (Fig. 11.11).

Chemically, DOC removed from the organic soils in the meltwater solution and flushed during this runoff pulse demonstrates enrichment in aromatic structures, originating from lignocellulose decomposition products (Prokushkin et al. 2007). This is attributed to relatively fresh organic matter entering the riverine systems. Such findings prove that organic solutes do not infiltrate to mineral soil and bypass the interaction with mineral soil that remains frozen till mid–June. As a result, more DOC reaches rivers; and therefore, subarctic river waters contain generally higher concentrations of DOC than rivers in permafrost-free areas. Furthermore, a peak in the DOC concentration is measured during spring breakup, when 40–80% of arctic

Table 11.3 Seasonal changes in the DOC composition in Kulingdakan stream based on the analysis of lignin (CuO oxidation) and pyrolysis-GC-MS (Prokushkin and Guggenberger 2007)

	Lignin			Groups of DOC pyrolysis products				
Season	Total (mg l^{-1})	*Vac/Val*	*V* (%)	PS	PhS	AHC	HS	NS
Snowmelt (May)	0.55	1.01	67.7	14.2/42.0	8.7/25.6	7.1/21.1	2.1/6.3	1.7/5.0
Early summer (June)	0.36	1.13	64.5	13.5/42.5	8.4/26.3	6.4/20.0	1.8/5.8	1.7/5.4
Summer low flow (July)	0.21	0.95	62.9	6.3/40.5	4.4/29.2	2.2/15.1	1.6/10.6	0.7/4.5
Summer storm flow (July)	0.46	1.46	49.0	13.7/45.7	7.8/26.2	5.7/18.9	1.5/5.0	1.3/4.2
Autumn flood (September)	0.33	0.93	61.1	–	–	–	–	–

Vac/Val is the acid/aldehyde ratio; *V* is sum of vanillyl derivatives of lignin (% of total lignin monomers); *PS* polysaccharides; *PhS* phenol substances; *AHC* aromatic hydrocarbons; *HS* humus substances; *NS* nitrogen-bearing substances; for these groups of DOC pyrolysis products are shown in numerator (mg l^{-1}) and in denominator (%)

river discharge occurs (Gordeev et al. 1996). Respectively, both streams and rivers of high latitudes release more than half of the annual DOC export during the 2–4 week long period of snow melt.

Reduced DOC export during summer through autumn in subarctic streams and rivers contradicts suggestions that rising temperature in northern latitudes will result in a significant increase in DOC flux to marine systems. Comparative analysis of watersheds with different extent of permafrost distribution in Alaska suggests reduction in DOC export under a warmer climate (MacLean et al. 1999). Recent data of Kawahigashi et al. (2004) provide further evidence of decreased riverine DOC export in Siberia due to significant drop in DOC concentrations in small streams along a gradient from continuous to discontinuous permafrost in the lower Yenisey River basin. Major alterations in biochemical composition (i.e., decrease in lignocellulose compounds, increase in hydrophilic fraction) that occur simultaneously confirm significant control of the thickness of the active layer and distribution of permafrost on flux, composition, and biodegradability of DOC in Siberian soils during the frost-free periods.

11.4.2 Implication for Global Change

There are two major scenarios of climate change at high latitudes (wet and dry), which have opposite effects on DOC export from terrestrial ecosystems.

First scenario is the consequence of a presumed increase in precipitation under "wet warming." It would significantly increase both generation of runoff and DOC export from permafrost terrains. Streams that are draining permafrost-dominated watersheds have "flashy" hydrology than those draining off permafrost-free watersheds (Woo and Winter 1993). Stormflows demonstrate an increase in DOC concentration (Fig. 11.12b) in high latitude streams, which indicates importance of near-surface pathways of runoff within catchments. Therefore, under a wetter climate, more of the runoff will be generated from soil organic layer resulting in higher concentrations of DOC within streams (Figs.11.12b, c) and increased overall export of DOC from watersheds.

Wildfires, assumed to be the main disturbance factor in the boreal biome, are tended to increase in frequency and severity under "dry warming" (Conard et al. 2002). In general, fires exert significant control on biogeochemical cycling within watersheds in permafrost terrains. Forested watersheds examined in Central Siberia demonstrated that presumably all basins of the region were affected by wildfires in the past. In terms of flux, DOC output from the recently burnt watershed in a dry year (2006) was only one-fifth of a watershed that burnt 100 years ago of which forest cover recovered since then. Decreased discharge and reduced DOC export have been suggested to result from larger water-holding capacity of the deepening active soil layer, which developed after the fire events, and combustion of the organic layer. Thus, under a drier climate, fires impose two limitations of DOC release from watersheds: (1) decreasing mobile C-source (combustion of organic layer), and (2)

decreased volume of draining water (increased water-holding capacity of soil). Comparable concentrations of DOC in streams draining from watersheds burnt 50 and 100 years ago corroborate earlier estimates of a recovery time of 50 years for ecosystem structures (species composition, soil temperature, etc.) (Abaimov 2005).

11.5 Conclusions

Forested basins of Central Siberia, underlain by continuous permafrost, export large amounts of terrigenous DOC. Clearly, the leaching of plant litter/upper soil organic layers and the leaching of deeper soil horizons produce different biogeochemical fingerprints, which can then be sought in the concentration and chemical composition of organic C species in streams.

Production and fate of DOC in larch ecosystems is largely influenced by the interaction between microbial activity, vegetation, and seasonal deepening of permafrost barrier to deep infiltration of solutes. Climate warming may cause increased DOC concentrations in streams supported by enhanced terrestrial primary production, increased production in organic topsoil, and release from thawing permafrost.

Although DOC fluxes are supposed to increase by temperature-related processes of DOC production, the increasing retention time of DOC in deepening mineral soil will most likely lead to the net decrease of DOC export to rivers due to its stabilization in the soil. Under this scenario, warming may result in the increased accumulation of C that is resistant to biodegradation in the deepened subsoil. Thus, adsorptive properties of the thawing soil distributed across Central Siberia will exert a major control on this process.

On the other hand, a major portion of DOC export (up to 90%) occurs during flood events with little soil potential to retain DOC (snowmelt, summer, and autumnal discharge peaks) suggesting little effect of warming on terrigenic DOC export values in the short term. More profound effect on DOC fluxes is believed to be caused by removal of the source matter of DOC – organic layer. In this context, another temperature-related factor influencing DOC export – wildfires (likely to increase in frequency with warming) will greatly decrease the DOC output from watersheds underlain by permafrost through reduction of the C pool in the upper organic layers.

Acknowledgments We thank all members of Tura experimental station, especially Viktor Borovikov and Sergey Tenishev, for fruitful discussions, useful hints during the designing phase of the field study, and crucial assistance during field campaigns. Anatoly Prokushkin highly appreciates valuable input of Georg Guggenberger and Gerd Gleixner in advancing biochemical analyses conducted under their supervision. Authors acknowledge Russian Fund of Basic Research for financial support provided for field studies in Central Evenkia during 2003–2007 (research grant nos. 03-04-48037, 05-05-64208, 07-04-00293, and expedition grant nos. 05-04-63097 and 07-04-10101). The possibility to conduct chemical characterization of DOC in Max-Planck Institute for Biogeochemistry (Jena, Germany) and Martin-Luther University (Halle, Germany) has been granted by DAAD and European Science

Foundation. We thank anonymous reviewers and Prof. E.-D. Schulze for their valuable comments in improving this chapter.

References

Abaimov AP (2005) Features and main trends of dynamics of forests and wood lands in permafrost zone of Siberia. Siberian Ecol J 4:663–675 (in Russian)

Aitkenhead JA, McDowell WH (2000) Soil C:N ratio as a predictor of annual riverine DOC flux at local and global scales. Global Biogeochem Cycles 14:127–138

Aitkenhead-Peterson JA, Alexander JE, Clair TA (2005) Dissolved organic carbon and dissolved organic nitrogen export from forested watersheds in Noca Scotia: identifying controlling factors. Global Biogeochem Cycles 19:GB4016

Anisimov OA, Belolutskaya MA (2004) Modeling of anthropogenic warming impact on permafrost: reflection of vegetation effect. Meteorologia i hydrologia 11:73–82 (in Russian)

Carey SK, Woo MK (2001) Slope runoff processes and flow generation in a subarctic, subalpine environment. J Hydrol 253:110–129

Christ MJ, David MB (1996) Temperature and moisture effects on the production of dissolved organic carbon in a Spodosol. Soil Biol Biochem 289:1191–1199

Conard SG, Sukhinin AI, Stocks BJ, Cahoon DR, Davidenko EP, Ivanova GA (2002) Determining effects of area burned and fire severity on carbon cycling and emissions in Siberia. Clim Change 55:197–211

Cory RM, Green SA, Pregitzer KS (2004) Dissolved organic matter concentration and composition in the forests and streams of Olympic National Park, WA. Biogeochemistry 67:269–288

Currie WS (1999) The responsive C and N biogeochemistry of the temperate forest floor. Trends Ecol Evol 14:316–320

Dittmar T, Kattner G (2003) The biogeochemistry of the river and shelf ecosystem of the Arctic Ocean: a review. Marine Chem 83:103–120

Finlay J, Neff J, Zimov S, Davydova A, Davydov S (2006) Snowmelt dominance of dissolved organic carbon in high-latitude watersheds: implications for characterization and flux of river DOC. Geophys Res Lett 33:L10401

Gibson JJ, Edwards TWD, Prowse TD (1993) Runoff generation in a high boreal wetland in Northern Canada. Nordic Hydrol 24:213–224

Gleixner G, Poirier N, Bol R, Balesdent J (2002) Molecular dynamics of organic matter in a cultivated soil. Org Geochem 33:357–366

Gordeev VV, Martin JM, Sidorov IS, Sidorova MV (1996) A reassessment of the Eurasian river input of water, sediment, major elements, and nutrients to the Arctic Ocean. Am J Sci 296:664–691

Guggenberger G, Kaiser K (2003) Dissolved organic matter in soil: challenging the paradigm of sorptive preservation. Geoderma 113:293–310

Guggenberger G, Zech W, Schulten HR (1994) Formation and mobilization pathways of dissolved organic-matter – Evidence from chemical structural studies of organic-matter fractions in acid forest floor solutions. Org Geochem 21:51–66

Hobbie SE (1996) Temperature and plant species control over litter decomposition in Alaskan tundra. Ecol Monogr 66:503–522

Hobbie SE, Trumbore SJP, SE RJR (2000) Controls over carbon storage and turnover in high-latitude soils. Global Change Biol 6:196–210

Hongve D, Van Hees PAW, Lunsdrom D (2000) Dissolved components in precipitation water percolated through forest litter. Europ J Soil Sci 51:667–677

Kaiser K, Guggenberger G (2000) The role of DOM sorption to mineral surfaces in the preservation of organic matter in soils. Organic Geochem 31:711–725

Kaiser K, Guggenberger G (2003) Mineral surfaces and soil organic matter. Eur J Soil Sci 54: 219–236

Kaiser K, Haumaier L, Zech W (2000) The sorption of organic matter in soils as affected by the nature of soil carbon. Soil Sci 165:305–313

Kalbitz K, Solinger S, Park JH, Michalzik B, Matzner E (2000) Controls on the dynamics of dissolved organic matter in soils: a review. Soil Sci 165:277–304

Kalbitz K, Schwesig D, Rethemeyer J, Matzner E (2005) Stabilization of dissolved organic matter by sorption to the mineral soiol. Soil Biol Biochem 37:1319–1331

Kawahigashi M, Kaiser K, Kalbitz K, Rodionov A, Guggenberger G (2004) Dissolved organic matter in small streams along a gradient from discontinuous to continuous permafrost. Global Change Biol 10:1576–1586

Kawahigashi M, Kaiser K, Rodionov A, Guggenberger G (2006) Sorption of dissolved organic matter by mineral soils of the Siberian forest tundra. Global Change Biol 12:1868–1877

Knorre AA, Kirdyanov AV, Vaganov EA (2006) Climatically induced interannual variability in aboveground production in forest-tundra and northern taiga of central Siberia. Oecologia 147:86–95

Kracht O, Gleixner G (2000) Isotope analysis of pyrolysis products from Sphagnum peat and dissolved organic matter from bog water. Org Geochem 31:645–654

MacLean R, Oswood MW, Irons JG III, McDowell WH (1999) The effect of permafrost on stream biogeochemistry: a case study of two streams in the Alaskan (U.S.A.) taiga. Biogeochemistry 47:239–267

McDowell WH (2003) Dissolved organic matter in soils - future directions and unanswered questions. Geoderma 113:179–186

McDowell WH, Likens GE (1988) Origin, composition, and flux of dissolved organic-carbon in the Hubbard Brook Valley. Ecol Monogr 58:177–195

Michalzik B, Matzner E (1999) Fluxes and dynamics of dissolved organic nitrogen and carbon in a spruce (*Picea abies* Karst.) forest ecosystem. Eur J Soil Sci 50:579–590

Michalzik B, Kalbitz K, Park JH, Solinger S, Matzner E (2001) Fluxes and concentrations of dissolved organic carbon and nitrogen – a synthesis for temperate forests. Biogeochemistry 52:173–205

Michalzik B, Tipping E, Mulder J, Lancho JFG, Matzner E, Bryant CL, Clarke N, Lofts S, Esteban MAV (2003) Modelling the production and transport of dissolved organic carbon in forest soils. Biogeochemistry 66:241–264

Neff JC, Asner GP (2001) Dissolved organic carbon in terrestrial ecosystems: synthesis and a model. Ecosystems 4:29–48

Neff JC, Hooper DU (2002) Vegetation and climate controls on potential CO_2, DOC and DON production in northern latitude soils. Global Change Biol 8:872–884

Neff JC, Finlay JC, Zimov SA, Davydov SP, Carrasco JJ, Schuur EAG, Davydova AI (2006) Seasonal changes in the age and structure of dissolved organic carbon in Siberian rivers and streams. Geophys Res Lett 33:L23401

Nikolaev AN, Fedorov PP (2004) The influence of climatic factors and thermal regime of permafrost-affected soils on radial increment of pine and larch trees in Central Yakutia. Lesovedenie 6:3–13 (in Russian)

Peterson BJ, Holmes RM, McClelland JW, Vorosmarty CJ, Lammers RB, Shiklomanov AI, Shiklomanov IA, Rahmstorf S (2002) Increasing river discharge to the Arctic Ocean. Science 298:2171–2173

Pokrovsky OS, Schott J, Kudryavtzev DI, Dupre B (2005) Basalt weathering in Central Siberia under permafrost conditions. Geochim Cosmochim Acta 69:5659–5680

Prokushkin AS, Guggenberger G (2007) Role of climate in removing dissolved organic matter from cryolithozone watersheds in central Siberia. Russian Meteorol Hydrol 32:404–412

Prokushkin AS, Shibata H, Prokushkin SG, Matsuura Y, Abaimov AP (2001) Dissolved organic carbon in coniferous forests of Central Siberia. Eurasian J For Res 2:45–58

Prokushkin AS, Kajimoto T, Prokushkin SG, McDowell WN, Abaimov AP, Matsuura Y (2005a) Climatic factors influencing fluxes of dissolved organic carbon from the forest floor in a continuous-permafrost Siberian watershed. Can J For Res 35:2129–2139

Prokushkin AS, Tokareva IV, Prokushkin SG, Abaimov AP (2005b) Input of dissolved organic carbon to soil of larch ecosystems in continuous permafrost region of Central Siberia. Lesovedenie 5:1–8 (in Russian)

Prokushkin AS, Gavrilenko IV, Abaimov AP, Prokushkin SG, Samusenko AV (2006a) Dissolved organic carbon in upland forested watersheds underlain by continuous permafrost in Central Siberia. Mitig Adapt Strateg Glob Change 11:223–240

Prokushkin AS, Gleixner G, McDowell WH, Ruehlow S, Schulze E-D (2007) Source- and substrate-specific export of dissolved organic matter from permafrost-dominated forested watershed in central Siberia. Global Biogeochem Cycles 21:GB4003

Prokushkin AS, Tokareva IV, Prokushkin SG, Abaimov AP, Guggenberger G (2008) Fluxes of dissolved organic matter in larch forests of permafrost zone of Siberia. Russian J Ecol 39:153–161

Prokushkin AS, Kawahigashi M, Tokareva IV (2009) Global warming and dissolved organic carbon release from permafrost soils. In: Margesin R (ed) Permafrost soils. Series soil biology, vol 16. Springer, Berlin, pp 237–250

Prokushkin SG, Abaimov AP, Prokushkin AS, Masyagina OV (2006b) Biomass of ground vegetation and litter in larch forests of cryolithozone of Central Siberia. Sibirskiy Ekologicheskiy Zhurnal 2:131–139 (in Russian)

Quinton WL, Gray DM, Marsh P (2000) Subsurface drainage from hummock-covered hillslopes in the arctic tundra. J Hydrol 237:113–125

Randerson JT, Liu H, Flaner MG, Chambers SD, Jin Y, Hess PG, Pfister G, Mack MC, Treseder KK, Welp LR, Chapin FS, Harden JW, Goulden ML, Lyons E, Neff JC, Schuur EAG, Zender CS (2006) The impact of boreal forest fire on climate warming. Science 314:1130–1132

Schulten HR, Gleixner G (1999) Analytical pyrolysis of humic substances and dissolved organic matter in aquatic systems: structure and origin. Water Res 3311:2489–2498

Schulze E-D, Freibauer A (2005) Environmental science – carbon unlocked from soils. Nature 437:205–206

Shibata H, Petrone KC, Hinzman LD, Boone RD (2003) Effect of fire on dissolved organic carbon and inorganic solutes in spruce forest in the permafrost region of interior Alaska. Soil Sci Plant Nutr 49:25–29

Sofronov MA, Volokitina AV, Kajimoto T, Matsuura Y, Uemura S (2000) Zonal peculiarities of forest vegetation controlled by fires in northern Siberia. Eurasian J For Res 1:51–57

Sondergaard M, Stedmon CA, Borch NH (2003) Fate of terrigenous dissolved organic matter (DOM) in estuaries: aggregation and bioavailability. Ophelia 57:161–176

Sorokin ND, Evgrafova SY (1999) Biological activity of forest cryogenic soils in Central Evenkia. Eurasian Soil Sci 32:578–582

Striegl RG, Dornblaser MM, Aiken GR, Wickland KP, Raymond PA (2007) Carbon export and cycling by the Yukon, Tanana, and Porcupine rivers, Alaska, 2001-2005. Water Resour Res 43(2):W02411

Tokareva IV, Prokushkin SG, Prokushkin AS (2006) Water soluble organic carbon on a forested watershed underlain by continuous permafrost and its export to stream. Forest Sci Tech 2:92–101

Van Cleave K, Yarie J (1986) Interaction of temperature, moisture and soil chemistry in controlling nutrient cycling and ecosystem development in the taiga of Alaska. In: Van Cleve K, Chapin FS III, Flanagan PW, Viereck LA, Dyrness CT (eds) Forest ecosystems in the Alaskan taiga. Springer, Berlin, pp 234–245

White D, Yoshikawa K, Garland DS (2002) Use of dissolved organic matter to support hydrologic investigations in a permafrost-dominated watershed. Cold Regions Sci Tech 35:27–33

Woo MK, Winter TC (1993) The role of permafrost and seasonal frost in the hydrology of northern wetland in North America. J Hydrol 141:5–31

Chapter 12
Soil Nitrogen Dynamics in Larch Ecosystem

N. Tokuchi, M. Hirobe, K. Kondo, H. Arai, S. Hobara, K. Fukushima, and Y. Matsuura

12.1 Introduction

About one-third of the stored soil carbon in the world is contained in large organic pools in northern taiga and tundra systems (Oechel and Billings 1992). In these ecosystems, at least 95% of the nutrients were incorporated in the soil (Marion et al. 1982). Therefore, plant growth or net primary production (NPP) is severely constrained by nutrient availability in high-latitude ecosystems, since the cold, wet conditions of arctic soils act to slow the release of nutrients (particularly inorganic N and P) from organic matter and the oxidation of organic C to CO_2 (Hobbie et al. 2002). These processes have led to the critical nutrient limitation on plant growth in these ecosystems (Shaver et al. 1992).

Most studies on productivity and nutrient cycling in arctic and subarctic regions were conducted in North America, especially in interior Alaska (e.g., Van Cleve et al 1983; Chapin et al. 2006). Those studies showed that nutrient pool in leaves and fine roots, which have rapid turnover rates, occupy less than 14% of the total nutrient pool (Jonasson and Michelsen 1996). Net mineralization measured with *in situ* buried bags often showed low or even negative values during the growing season (e.g., Giblin et al. 1991; Jonasson et al. 1999; Schmidt et al. 1999). Despite the large pools of N and P in the soil, net mineralization of N and P was generally low, and in most cases, lower than the plant uptake requirement (Schmidt et al. 2002). Recent estimates also suggested that the annual input of inorganic N (dry and wet deposition, N fixation and mineralization) could not account for the observed plant N uptake (Ruess et al. 1996).

Siberia is represented by a large area of arctic and subarctic ecosystems. The total area of Siberia is 13 million km^2 (Shvidenko and Nilsson 1994) which is about 30% greater than the entire area of Europe (10 million km^2 including European Russia; Stanner and Bourdeau 1995) and 12% greater than boreal North America (11.5 million km^2 of Canada and Alaska). Further, Siberia is much more extensively forested (6 million km^2) than Europe (3 million km^2) or boreal North America (5 million km^2). Therefore, Siberia is important in global C stock. In addition, forest ecosystems of Central Siberia are mostly on the continuous permafrost region, where the depth of soil active layer is generally shallow

A. Osawa et al. (eds.), *Permafrost Ecosystems: Siberian Larch Forests*,
Ecological studies, Vol. 209, DOI 10.1007/978-1-4020-9693-8_12,

(Chap. 1, this Vol.). This may lead to N and/or P limitation for plant growth in the region; however, there is not enough information on biogeochemistry in these forest ecosystems to confirm this.

Nonetheless, N deposition has gradually increased over the past few decades, and the change in N status will affect the rate of C sequestration in Siberian forests. The objective of this chapter is to describe results of a study, which was intended as a first step in the investigation of C sequestration in Siberian permafrost forest ecosystem, and was aimed to clarify the N status of the ecosystem. The amount of plant available N from soil was estimated by *in situ* measurements of N dynamics, and annual N requirements for vegetation growth were calculated through the ecological summation method used in estimation of forest productivity (see Chap. 6, this Vol.).

12.2 Approaches to Examination of Soil Nitrogen Dynamics and Status

Inorganic N dynamics in the soil is summarized in Fig.12.1. Soil inorganic N dynamics is characterized by the interactions among pool, production, and flux. The pool is defined by the amount of inorganic N at the initial time; the production is the amount of net mineralized N added to the pool since the initial time; and flux is the amount of N input and output from/to the soil compartment. Many studies expressed values of soil N pool and flux as per unit of soil weight or ion exchange resin (e.g., Nadelhoffer et al. 1991). With such units, it is often difficult to compare the values among studies. It is also difficult to understand the ecosystem N dynamics using these units. Therefore, measurements of all parameters are given in area-based units in this study.

12.2.1 Study Sites

The study was conducted at Carbon Flux Site (plot CF) – a 105-year-old stand of larch (*Larix gmelinii* (Rupr.) Rupr.) near Tura, Central Siberia (location of the site is described in Figs.1.1 and 1.3, and climate characteristics are described in Chaps. 1 and 10, this Vol.). Soil type is Gelisol with poor drainage. The soil is frozen from mid-October to the beginning of May. In this region, forests are generally dominated by ca. 100-year-old *L. gmelinii* larch with occasional tall shrub (*Duschekia fruticosa*). Ericaceous species and thick moss–lichen cover has developed on the forest floor. At this site, one of four permanent research plots (each 15×15 m^2) was selected for N flux measurements. The mean stem diameter at breast height of *L. gmelinii* was about 3.2 cm, and tree density was 5,480 trees ha^{-1} (for details see Table 6.1).

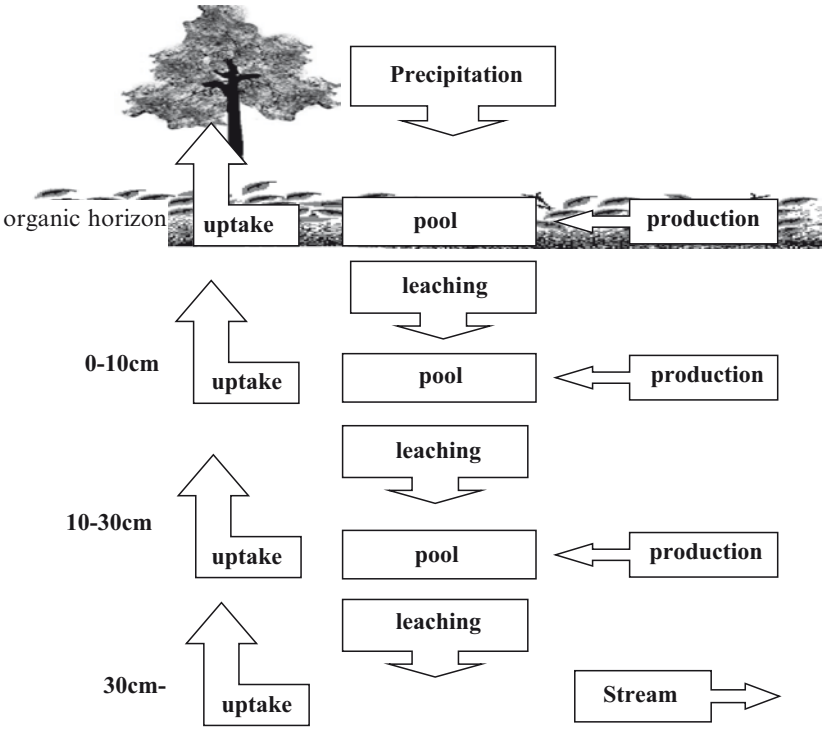

Fig. 12.1 Diagram of N dynamics in forest ecosystem

12.2.2 Soil N Mineralization, Leaching, and Status

Net mineralization rate, namely inorganic N production rate measured by *in situ* buried bag methods (Eno 1960), is one of the good predictors of productivity in temperate forest ecosystems (Nadelhoffer et al. 1984). Fresh samples collected from A_0, 0–10, and 10–30 cm soil horizons were put into polyethylene bags. The bags were buried in the same horizon where the soil was sampled. After one year, the soil samples in buried bags were collected and were extracted. The extracts were brought back to the laboratory, and NH_4^+ and NO_3^-–N concentrations were determined.

While *in situ* incubation rate is good predictor for productivity, there have been few data on *in situ* incubation rate compared to those on laboratory incubation rate. The laboratory incubation rate would be helpful. Unfortunately, there was no facility in Tura, and we measured the laboratory incubation rates in Japan. During the transportation from Tura to Japan, we could not control the sample temperature. Normally it took a week for transportation. Hence, we used the mineralization rate

by laboratory incubation as an index. In the laboratory, soil samples were kept at 25°C. The 4-week incubation period included transportation. After the incubation period, the samples were extracted and NH_4^+ and NO_3^--N concentrations were determined. Inorganic N leaching in soil was captured by the ion exchange resin for 2 years (Binkley and Matson 1983).

From the results of all measurements, we estimated available inorganic N for the vegetation using the following equation (Nadelhoffer et al. 1984; Tokuchi et al. 2007):

$$\text{Available N} = \text{Production N} + (\text{input N-output N})\text{-}\Delta\text{N pool} \quad (12.1)$$

where production N is in situ net mineralization, input N input is N leachate from upper horizon or precipitation N if the horizon is surface horizon, output N is N leachate from the soil surface, and ΔN pool is inorganic N pool at current sampling year minus inorganic N pool at previous sampling year. In this study,we examined the N acquisition of larch forest under a likely N limitation in this study site. Larch and *Duschekia* leaves and soil were sampled in the growing season of 2003. Samples of leaf and soil were grounded. The ground samples were analyzed for stable isotope ratios using an isotope ratio mass spectrometer (Kielland et al. 1998; Kielland 2001).

12.3 Soil Nitrogen Dynamics

12.3.1 Soil Inorganic N Pool

Soil inorganic N pools ranged from 1.0 to 8.1 kg N ha^{-1} in A_0 horizon, 5.9–22.6 kg N ha^{-1} in 0–10 cm horizon, and 11.4–34.0 kg N ha^{-1} in 10–30 cm horizon, respectively (Fig.12.2). NH_4^+ dominated inorganic N pool irrespective of horizons and years (data not presented). In interior Alaska, it has also been reported that extractable concentrations of NH_4^+ are typically one order of magnitude greater than that of NO_3^-.

The soil inorganic N pool sizes estimated for our old larch forest in Central Siberia (Fig. 12. 2) were in the range similar to those reported for boreal forests in northern Canada (Lamontagne 1998), but were larger than those of previous studies in tundra and/or in some boreal forests in Alaska (Table.12.1). Nitrogen pool in mineral soil was 6,580 kg N ha^{-1} in an old multi-aged (>220-year-old) *L. gmelinii* forest (plot C1) in Central Siberia (Matsuura et al., unpublished data), while it was 3,070 (ranged 1,920–4,060) kg N ha^{-1} in mineral soil of a black spruce forest in Alaska (Van Cleve et al. 1983). This suggests a large difference in N pool size between Siberia and Alaska. Also the N pool in aboveground biomass of the old multi-aged larch stand was 51 kg N ha^{-1} in Central Siberia (Matsuura et al., unpublished data), while it was 62.5 kg ha^{-1} in the black spruce forest in Alaska (Van Cleve et al. 1983). The proportion of the N pool in soil to above ground biomass in Siberian old larch forest was larger than that in Alaska, 129 vs. 49, respectively. This suggests that the quality of organic matter may be different

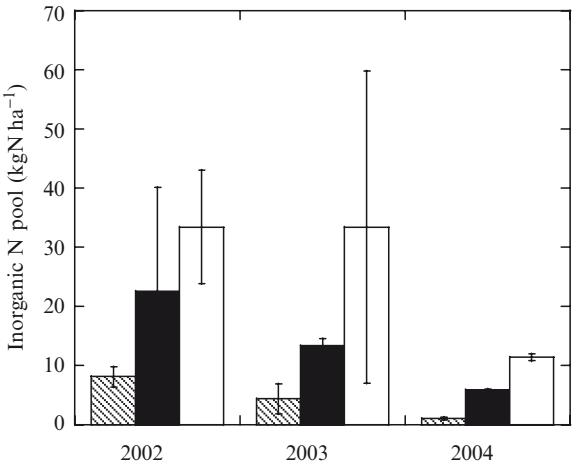

Fig. 12.2 Soil inorganic N pool from 2002 to 2004 in *L. gmelinii* forest in Central Siberia. *Gray bar* is for A_o horizon, *black bar* is for 0–10 cm horizon and *white bar* is for 10–30 cm horizon. Unit is kg N ha^{-1}. Data are mean ± SE ($n=4$)

between Central Siberia and Alaska. We need further research on the quality of organic matter in Siberia.

Although inorganic N pool was relatively large, it was not stable. Namely, there was high heterogeneity in soil inorganic N pool size among the plots in each observation year (Fig.12.2). Also, the total soil inorganic N pool size across the three horizons was significantly different among the observed years ($p < 0.05$).

Temperature is one of the essential environmental conditions influencing soil N dynamics. There was a significant correlation between summer air temperature (June–August) and inorganic N pool in each horizon, and inorganic N pool exponentially increased with summer air temperate in our old *L. gmelinii* forest (Fig. 12.3). In taiga soils, it was reported that N mineralization and nitrification do not respond significantly to temperature until it exceeds 15–20°C (Klingensmith and Van Cleve 1993). In our larch forest, the correlation coefficient was the highest between soil inorganic N pool and the highest mean monthly air temperature (July) ($r=0.862$ in A_0 horizon, $r=0.707$ in 0–10 cm soil depth and $r=0.548$ in 10–30 cm soil depth; Fig.12.3). Thus, one of the reasons of interannual variability of soil inorganic N pool is likely due to the fluctuation of air temperature in this larch forest.

In the relationship between soil inorganic N pool and summer soil temperature (data not presented), the correlation was stronger in the surface than in the deeper soil horizon, but the slope of the linear relationship was greater in the deeper horizon. This indicates that mineralization in the deeper soil responds more sharply to temperature than the surface soil: soil microbes in the deeper soil horizon may be more sensitive to temperature than that in the surface soil horizon.

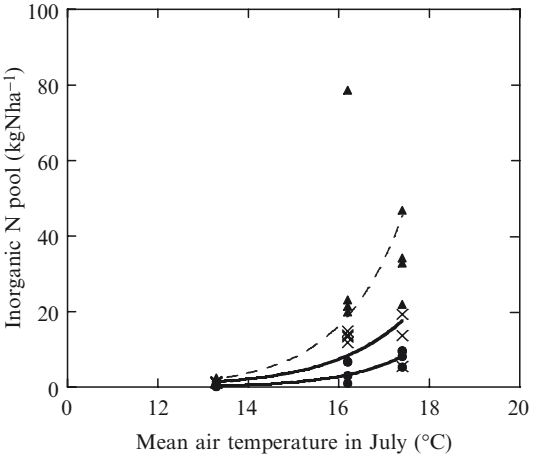

Fig. 12.3 Relationship between mean air temperature (June to August) and soil inorganic N pool in *L. gmelinii* forest. Regression curves are shown for each horizon among years (p <0.05). *Black circle* with *bold* line is for A_o horizon, cross with dashed line is for 0–10 cm horizon and *black triangle* with fine line is for 10–30 cm horizon

12.3.2 Soil N Mineralization

In the *in situ* buried bag method, net mineralization rate was variable among the soil horizons and years (Fig.12.4). Half of *in situ* net mineralization rates were negative. It means the immobilization of inorganic N was larger than the production of inorganic N. One of the reasons for strong immobilization seems due to the incubation period. The incubation period is longer than the previous studies. Thus, we checked the amount of one month *in situ* incubation in 2004. Even if incubation period was considered one month, the net in situ incubation rates also showed high variability and negative values; -0.22 ± 0.76 kg N ha^{-1} mo^{-1} in 0–10 cm soil. In the previous studies, the net mineralization measured with *in situ* buried bags often showed low or even negative values during the growing season in arctic and subarctic regions (Giblin et al. 1991; Jonasson et al. 1999; Schmidt et al. 1999). Thus, it is considered that the highly variable N mineralization rate and strong immobilization are the characteristics of soil N dynamics in cold regions including our study site in Central Siberia.

Net N mineralization rate by laboratory incubation varied among the years (Fig. 12.5). Net N mineralization by laboratory incubation was negative in 2002 in all soil horizons. It means that the immobilization of N exceeded the inorganic N production in 2002. On the other hand, N was mineralized in 2004 in all soil horizons. In 2003, N was immobilized in the surface and 10–30 cm depth, while N was mineralized in 0–10 cm depth. The periods of transport among years were similar. Based on both measurements of N mineralization rates, it could be summarized that N mineralization rate is variable among soil horizons and years, and immobilization process is dominant at this study site.

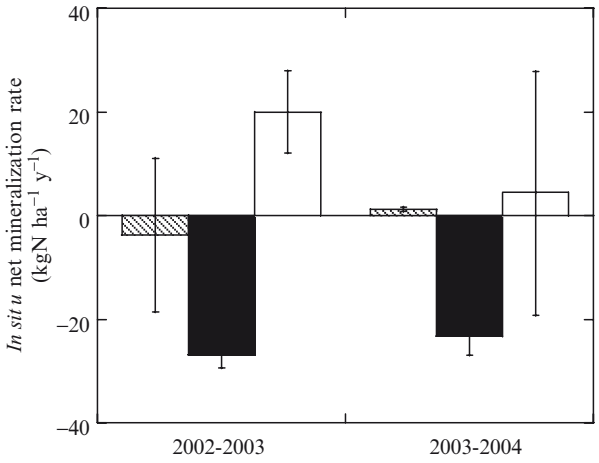

Fig. 12.4 *In situ* net N mineralization rate in larch forest ecosystem. *Gray bar* is for A_o horizon, *black bar* is for 0–10 cm horizon and *white bar* is for 10–30 cm horizon. Unit is kg N ha^{-1} y^{-1}. Data are mean ± SE ($n = 4$)

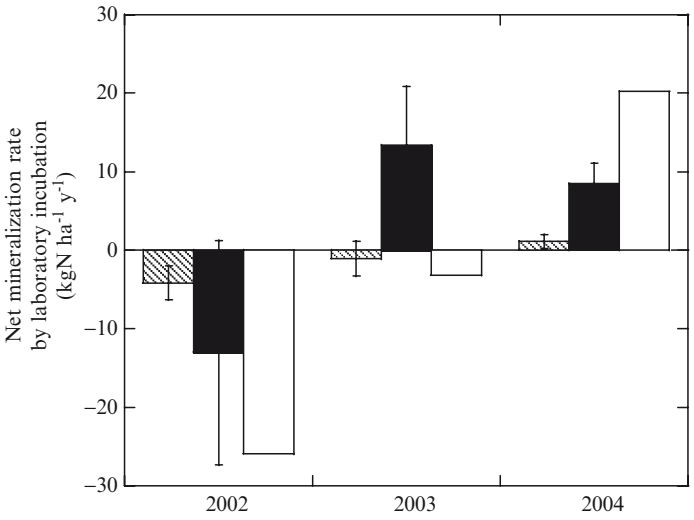

Fig. 12.5 Net N mineralization rate in laboratory incubation in *L. gmelinii* forest. *Gray bar* is for A_o horizon, *black bar* is for 0–10 cm horizon and white bar is for 10–30 cm horizon. Unit is kg N ha^{-1} y^{-1}. Data are mean ± SE ($n = 4$)

12.3.3 Controlling Factors on Soil N Dynamics

The trend of soil N mineralization tends to be different when estimated in the laboratory and through *in situ* incubation (Figs. 12.4 and 12.5). One of the possible reasons of the difference is the incubation period; 4 weeks for laboratory versus one

year for *in situ* incubation. It is considered that the incubation period influenced soil N transformation. We could discuss the short-term characteristics from the result of the laboratory incubation and the long-term characteristics from *in situ* incubation.

Based on the result of the laboratory incubation, N was immobilized in all soil horizons in 2002 (Fig. 12.5). In that year, soil inorganic N pool was the highest among all observation years (Fig. 12.2). In the short-term mineralization, the substrate for N mineralization tends to be exhausted. It is confirmed that in 2004 when soil inorganic N pool was the smallest, the N mineralization rate was the highest among the observation years.

As for the long-term mineralization characteristics, *in situ* soil N mineralization rate significantly correlated with soil inorganic pool size (p <0.05, Fig.12.6). Additionally, half of the *in situ* soil N mineralization rates were negative. This means that *in situ* soil N mineralization reflects the immobilization of the soil inorganic N pool. High immobilization of inorganic N suggests that a large proportion of the total C is available for microbes (Nadelhoffer et al. 1991). In terms of C availability, Schmidt et al. (2002) questioned the effectiveness of the buried bag method. The buried bag method prevents not only the uptake of nutrients by plant roots, but also the supply of labile carbon to soil microbes in the form of root exudates. However, they showed that the limitation of C was higher in bags than outside from a comparison of dissolved organic carbon (DOC) concentration between the inside and outside of the bags, and that C/N changed with microbial biomass change. They conclude that when N availability increases, the high immobilization of N in microbes would, probably, always take place regardless of the amount of available C (Schmidt et al. 2002). Therefore, it is hypothesized that there is a large available C pool for microbes in our *L. gmelinii* stand, and microbes would be the stronger competitor against plants for N uptake.

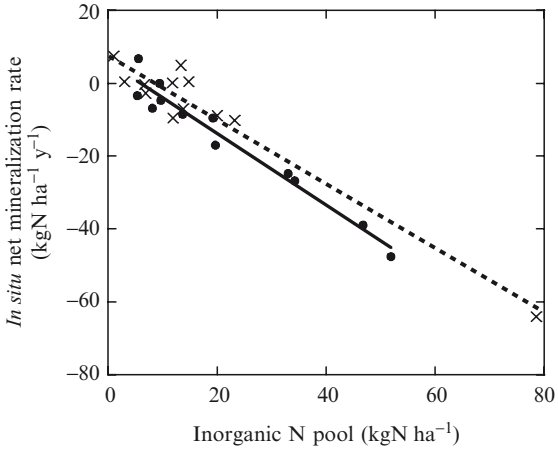

Fig. 12.6 Relationship between inorganic N pool and in situ net N mineralization. *Dashed line* is regression for the data of 2002–2003, and bold line is for 2003–2004 (p <0.001)

12.3.4 Inorganic N leaching in Soil

The values of annually captured inorganic N for 2 years were 1.90 and 1.97 kg N $ha^{-1}\,y^{-1}$ at the A_0 horizon, 1.70 and 1.95 kg N $ha^{-1}\,y^{-1}$ at the 10 cm soil depth, and 0.70 and 1.02 kg N $ha^{-1}\,y^{-1}$ at the 30 cm soil depth. The captured inorganic N amount decreased with soil depth, presumably because of the microbial and vegetative uptake. It resulted in low inorganic N concentration in the stream (lower than the detection limit, <1 μmol L^{-1}). Inorganic N loss from the soil was estimated as less than 0.1 kg N $ha^{-1}\,y^{-1}$. Few roots were present below 30 cm soil depth due to the permafrost in the old larch stand (see Chap. 16, this Vol.), indicating little uptake of N by vegetation at this horizon. One of the possible reasons of the discrepancy in inorganic N concentrations between 30 cm soil depth and the stream is denitrification occurring in the deeper soil horizons.

12.4 Soil Nitrogen Status in Larch Forest in Central Siberia

12.4.1 Available N

In 2002–2003, the estimated available N was −1.4, 14.6, −31.8, and 0.6 kg N $ha^{-1}\,y^{-1}$ at A_0 horizon, 0–10 cm horizon, 10–30 cm horizon, and under 30 cm horizon, respectively. Negative values were regarded as zero for available N. The total amount of available inorganic N was 15.2 kg N $ha^{-1}\,y^{-1}$ in 2002–2003. In 2003–2004, the estimated N was 15.3 kg N $ha^{-1}\,y^{-1}$.

In comparison, Ruess et al. (1996) estimated N uptake as the sum of net N mineralized plus input via precipitation and fixation. When we used the method of their calculation, available inorganic N was estimated as 7.3 kg N $ha^{-1}\,y^{-1}$ in 2002–2003 and 2.1 kg N $ha^{-1}\,y^{-1}$ in 2003–2004. These estimates of annual available N in this study (from 2.1 to 7.3 kg N $ha^{-1}\,y^{-1}$) is in a range similar to the annual N demand suggested for black spruce forest (9.2 kg N $ha^{-1}\,y^{-1}$) in upland sites in Alaska (Ruess et al. 1996).

12.4.2 The Possibility of N Limitation of Larch Forest in Central Siberia

In Central Siberia, Kajimoto et al. (1999) reported that NPP was 1.81 Mg $ha^{-1}\,y^{-1}$ in an old multi-aged *L. gmelinii* stand (> 220 years old; plot C1); NPP was estimated as the sum of annual woody biomass increment (stem, branch, and coarse root) and needle biomass (see also Chap. 6, this Vol.). N concentration in each component of the larch trees was 0.12% in stem, 0.35% in branch, 1.58% in green

needle, 0.24% in coarse root, and 0.76% in fine root (Matsuura et al., unpublished data), and N retranslocation ratio before needle senescence was about 70% (i.e., N concentration in needle litter fall was about 0.48%)(see Table 8.1, this Vol.). N retranslocation was subtracted from annual N increment to needles to obtain an estimate of N for foliage. Based on these values, the amount of N required for annual production of woody parts and needle (i.e., multiplying NPP by N concentration) would be about 8.1 kg N $ha^{-1} y^{-1}$ in this old multi-aged larch forest. However, the estimate of N demand seems underestimated, since it excludes the proportion for fine root production.

In the 105-year-old *L. gmelinii* stand of the present study (plot CF), N requirement (or annual plant uptake) can also be evaluated by applying the same values of N concentration in each component and N retranslocation rate. Aboveground net primarily production (ANPP) of this old stand is 0.48 Mg ha^{-1} (Table 6.3, this Vol.). Among belowground production, biomass increment of roots (both coarse and fine roots) due to secondary thickening was not estimated in the stand, and here it is assumed to be equivalent to that of >220-year-old stand (0.48 Mg ha^{-1}; Kajimoto et al. 1999). The amount of N that is required for annual production of aboveground components is 2.5 kg N $ha^{-1} y^{-1}$. Furthermore, fine root production was estimated at 0.76 Mg ha^{-1} by using in-growth core method in the stand (Tokuchi et al., unpublished data). When the fine root production is included, the N demand for the total belowground (both coarse and fine roots) reaches about 8.5 kg N $ha^{-1} y^{-1}$. Consequently, the estimated N requirement at the whole stand level is 11.0 kg N $ha^{-1} y^{-1}$. The value is slightly less than the annual N availability (averaged about 15.3 kg N $ha^{-1} y^{-1}$) estimated in this study. As compared to other ecosystems, however, the plant N uptake is in a order similar to those reported at high latitudes, such as tundra (Giblin et al. 1991; Jonasson et al. 1999), and larch (*L. gmelinii*) and Scots pine (*Pinus sylvestris*) mixed forests in Central Siberia (Shugalei and Vedrova 2004)(Table 12.1).

In this study, the N uptake of other plants on the forest floor was not estimated. However, aboveground biomass of forest floor was about 2.2 Mg ha^{-1} (Matsuura et al., unpublished data), which reached about 40% of aboveground biomass of larch trees (5.7 Mg ha^{-1}) in the old stand (see Table 6.2, this Vol.). This indicates that the annual N uptake by some woody shrubs, lichens, and mosses is not negligibly small. Therefore, it is possible that available inorganic N is likely a limiting factor for plant growth in the study area.

12.4.3 N Source of Larch Forest in Central Siberia Based on Isotopic signature

It is suggested that the isotopic change in plant organs is functionally caused by soil N turnover (Garten and Van Miegoet 1994). The isotopic signature of N in tissues of northern species provides evidence of niche differentiation regarding acquisition of different N forms (Schulze et al. 1994; Valentine et al. 2006).

Table 12.1 Comparison of N dynamics among arctic Tundra and boreal forest ecosystems

		Arctic tundra			Boreal forest		
		Alaska[a,b]	Scandinavia[e]	Alaska[f]	Canada[h]	Central Siberia[j]	Central Siberia[l]
				(Mixed forest)	(Pine, spruce)	(Larch, pine)	(Larch)
	[Soil horizon]						
N pool size	Organic horizon	0.8–2.6[c]	1.0	–	–	–	4.8–8.1
(kg N ha^{-1})	0–10 cm	–	–	–	–	21.1–39.8[k]	13.4–22.6
	10–30 cm	–	–	–	–	–	34.0–35.8
N production(kg N $ha^{-1} y^{-1}$)	Organic horizon	5.0[c]	0.5–1.1	4.0	3.9–6.3[i]	3.4–5.9	0.0
	0–10 cm	–	–	6.0[g]	–	–	0.0
	10–30 cm	–	–	–	–	–	0.0
Plant uptake N(kg N $ha^{-1} y^{-1}$)		1.0–23.0[d]	10.0	–	–	22.4–45.8[k]	11.1

[c]A_0 + mineral soil. [d]belowground + new uptake. [g]0–20 cm horizon. [i]include forest floor. [k]include mineral soil (averaged for 2 years). Data source: [a]Giblin et al. (1991), [b]Shaver and Chapin (1991); [e]Jonasson et al. (1999); [f]Van Cleve et al. (1993); [h]Lamontagne (1998); [j]Shugalei and Vedrova (2004); [l]Tokuchi et al. (2003)

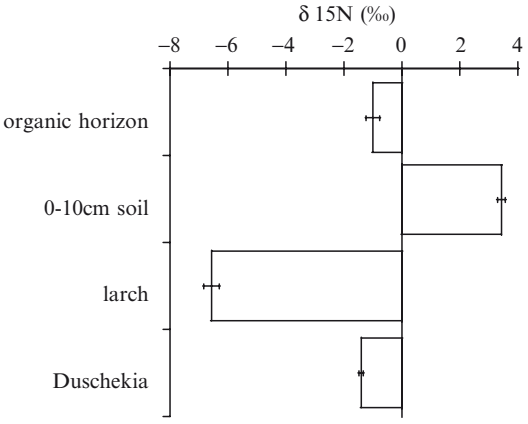

Fig. 12.7 Mean $\delta^{15}N$ values of soil (organic and 0–10 cm horizons) and leaves (*L. gmelinii* and *Duschekia fruticosa*) sampled in the larch forest ecosystem. Data are mean ± SE ($n = 8$) (Tokuchi et al., unpublished data)

In the larch forest of present study, $\delta^{15}N$ values were −1.01 ± 0.23‰ in the A_0 horizon, and 3.43 ± 0.38‰ in the 0–10 cm soil horizon (Fig.12.7). The leaf $\delta^{15}N$ values of larch and *Duschekia* were −6.56 ± 0.26 and −1.41 ± 0.04‰.

Even coexisting larch and *Duschekia* showed large difference in the leaf $\delta^{15}N$ values. *Duschekia* leaves showed $\delta^{15}N$ values close to that of atmospheric N_2 (=0‰), suggesting that *Duschekia* is likely to be fixing and using atmospheric N_2 (i.e., N_2 fixing species).

In Alaska, a large variation in foliar $\delta^{15}N$ values was observed among plant species (Nadelhoffer et al. 1996, Kielland et al. 1998; Kielland 2001). The most depleted $\delta^{15}N$ value was observed in *Picea mariana* (−9.7‰) and *Picea glauca* (−8.0 ‰) (Kielland et al. 1998; Kielland 2001), indicating that the *Picea* spp. were highly depleted in $\delta^{15}N$. The larch in Central Siberia showed a value of $\delta^{15}N$ similar to that of *Picea* in Alaska.

In both areas, there was a large discrepancy of $\delta^{15}N$ value between the leaf of *Picea* or larch and soil. It suggests that a long history of soil N processing should have enriched soils in ^{15}N via chronic losses of ^{14}N, while plant tissues are highly depleted in ^{15}N indicating a less direct pathway from soil into plant (Valentine et al. 2006).

12.5 Conclusions

Based on the present results it is possible that available inorganic N is likely to be a limiting factor for plant growth in this region. In Alaska, the annual net mineralization could account for half of the N taken up by plants (Schimel and Chapin 1996). Ruess et al. (1996) also indicated that inorganic N budget method was difficult to be applied in Alaska. A possible reason for the discrepancy between N

supply and demand is that boreal trees may absorb a part of their N demand as the organic form (Kielland 2001). In boreal surface soils, free amino acid concentrations are about 4–8 μg $N\,g^{-1}$ in dry weight (Kielland 2001; Jones and Kielland 2002), similar to the values in arctic tundra soils (Kielland 1994). Concentrations of dissolved organic N (DON) in mineral soil are typically two to three times greater than the concentration of NH_4^+ (Walker 1989; McFarland et al. 2002). Hobara and Hirobe (2007) also showed a significant amount of DON in Alaska. A probable gross rate must be DON ammonium > nitrate.

However, the available amount of organic N form for plants could not have been clarified until now. Also it is not clear whether the direct organic N uptake contributes to the large depletion of ^{15}N. If the organic N uptake is the major uptake process, there might be little discrepancy of the ^{15}N values between soil and vegetation. One possible explanation is the highly dynamic amino acid pool and plant uptake of the amino acids. For example, free amino acid turnover time in soils is about 1–12 h (Jones and Kielland 2002). However, there was not enough data on plant N use in Siberia. Therefore more research on organic N dynamics is needed using ^{15}N in this permafrost region.

Acknowledgments We are grateful for the help of O.A. Zyryanova, V.N. Sukachev Institute of Forest, Russian Academy of Sciences for collaboration. This study was partly supported by Integrated study for terrestrial carbon management of Asia in the twenty-first century based on scientific advancements (FY2002–2006), funded by the Ministry of Environment Japan.

References

Binkley D, Matson PA (1983) Ion exchange resin bag method for assessing forest soil N availability. Soil Sci Soc Am J 47:1050–1052

Chapin FS III, Oswood MW, Van Cleve K, Viereck LA, Verbyla DL (eds) (2006) Alaska's changing boreal forest. Oxford University Press, New York

Eno C (1960) Nitrate production in the field by incubating the soil in polyethylene bags. Soil Sci Soc Am Proc 24:277–279

Garten CT Jr, Van Miegoet H (1994) Relationships between soil nitrogen dynamics and natural ^{15}N abundance in plant foliage from Great Smoky Mountain National Park. Can J For Res 24:1636–1645

Giblin AE, Nadelhoffer KJ, Shaver GR, Laundre JA, McKerrow AJ (1991) Biogeochemical diversity along a riverside toposequence in arctic Alaska. Ecol Monogr 61:415–435

Hobara S, Hirobe M (2007) Fire effects on DOC and metal concentrations in an Alaskan boreal forest. In: Proceedings of the Seventh International Conference on Global Change: Connection to the Arctic (GCCA7). International Arctic Research Center, University of Alaska Fairbanks, pp 235–238

Hobbie SE, Nadelhoffer KJ, Högberg P (2002) A synthesis: The role of nutrients as constraints on carbon balances in boreal and arctic regions. Plant Soil 242:163–170

Jonasson S, Michelsen A (1996) Nutrient cycling in subarctic and arctic ecosystems, with special reference to the Abisko and TornetraÈsk region. Ecol Bull 45:45–52

Jonasson S, Michelsen A, Schmidt IK (1999) Coupling of nutrient cycling and carbon dynamics in the Arctic, integration of soil microbial and plant processes. Appl Soil Ecol 11:135–146

Jones DL, Kielland K (2002) Soil amino acid turnover dominates the nitrogen flux in permafrost-dominated taiga forest soils. Soil Biol Biochem 34:209–219

Kajimoto T, Matsuura Y, Sofronov MA, Volokitina AV, Mori S, Osawa A, Abaimov AP (1999) Above- and belowground biomass and net primary production of a *Larix gmelinii* stand near Tura, central Siberia. Tree Physiol 19:815–822

Kielland K (1994) Amino acid absorption by arctic plants: implications for plant nutrition and nitrogen cycling. Ecology 75:2373–2383

Kielland K (2001) Short-circuiting the nitrogen cycle; strategies of nitrogen uptake in plants from marginal ecosystems. In: Ae N, Arihara J, Okada K, Srinivasan A (eds) Plant nutrition acquisition: new perspectives. Springer, Berlin Heidelberg New York, pp 376–398

Kielland K, Barnett B, Schell D (1998) Intraseasonal variation in the delta N-15 signature of taiga trees and shrubs. Can J For Res 28:485–488

Klingensmith KM, Van Cleve K (1993) Patterns of nitrogen mineralization and nitrification in floodplain successional soils along the TananaRiver, interior Alaska. Can J For Res 23:964–969

Lamontagne S (1998) Nitrogen mineralization in upland Precambrian shield catchments: Contrasting the role of lichen-covered bedrock and forested areas. Biogeochemistry 41:53–69

Marion GM, Miller PC, Kummerow J, Oechel WC (1982) Competition for nitrogen in a tussock tundra ecosystem. Plant Soil 66:317–327

Matsuura Y, Kajimoto T, Osawa A, Abaimov AP (2005) Carbon storage in larch ecosystems in continuous permafrost region of Siberia. Phyton 45:51–54

McFarland JW, Ruess RW, Kielland K, Doyle AP (2002) Cycling dynamics of NH_4^+ and amino acid nitrogen in soils of a deciduous boreal forest ecosystem. Ecosystems 5:775–788

Nadelhoffer KJ, Aber JD, Mellilo JM (1984) Seasonal patterns of ammonium and nitrate uptake in nine temperate forest ecosystems. Plant Soil 80:321–335

Nadelhoffer KJ, Giblin AE, Shaver GR, Laundre JA (1991) Effects of temperate and substrate quality on element mineralization in six arctic soils. Ecology 72:242–253

Nadelhoffer K, Shaver GR, Fry B, Giblin AE, Johnson L, McKane R (1996) ^{15}N natural abundances and N use by tundra plants. Oecologia 107:386–394

Oechel WC, Billings WD (1992) Effects of global change on the carbon balance of arctic plants and ecosystems. In: Chapin FS III, Jefferies RL, Reynolds JF, Shaver GR, Svoboda J (eds) Arctic ecosystems in a changing climate. Academic Press, San Diego, pp 139–168

Ruess RW, Van Cleve K, Yarie J, Viereck LA (1996) Contributions of fine root production and turnover to the carbon and nitrogen cycling in taiga forests of the Alaskan interior. Can J For Res 26:1326–1336

Schimel JP, Chapin FS III (1996) Tundra plant uptake of amino acid and NH_4^+ nitrogen *in situ*: plants compete well for amino acid N. Ecology 77:2142–2147

Schmidt IK, Jonasson S, Michelsen A (1999) Mineralization and microbial immobilization of N and P in arctic soils in relation to season, temperature and nutrient amendment. Appl Soil Ecol 11:147–160

Schmidt IK, Jonasson S, Shaver GR, Michelsen A, Nordin A (2002) Mineralization and distribution of nutrients in plants and microbes in four arctic ecosystems: responses to warming. Plant Soil 242:93–106

Schulze E-D, Chapin FS III, Gebauer G (1994) Nitrogen nutrition and isotope differences among life forms at the northern treeline of Alaska. Oecologia 100:406–412

Shaver GR, Chapin FS III (1991) Production: biomass relationships and element cycling in contrasting arctic vegetation types. Ecol Monogr 61:1–31

Shaver GR, Bittlings WD, Chapin FS III, Giblin AE, Nadelhoffer KJ, Oechel WC, Rastetter EB (1992) Global change and the carbon balance of arctic ecosystems. Bioscience 42:433–441

Shugalei LS, Vedrova EF (2004) Nitrogen pool in northern-taiga larch forests of central Siberia. Biol Bull 31:247–256

Shvidenko A, Nilsson S (1994) What do we know about the Siberian forest ? Ambio 23:396–404

Stanner D, Bourdeau P (1995) Europe's Environment; the Dobris Assesment. European Environment Agency, Copenhagen

Tokuchi N, Hirobe M, Kondo K, Prokushkin AS, Matsuura Y, Kajimoto T (2003) N cycling at a *Larix* stand in Tura, central Siberia –preliminary work. In Proceedings of the Fourth International Conference on Global Change: Connection to the Arctic (GCCA4). Nagoya University, Toyokawa, pp 139–143 November 2003

Tokuchi N, Hirobe M, Nakanishi A, Wachirinrat C, Takeda H (2007) Comparison of soil N dynamics between dry dipterocarp forest and dry evergreen forest in Northeastern Thailand. Tropic 16:323–336

Valentine DW, Kielland K, Chapin FS III, McGuire AD, Van Cleve K (2006) Patterns of biogeochemistry in Alaskan boreal forests. In: Chapin FS III, Oswood MW, Van Cleve K, Viereck LA, Verbyla DL (eds) Alaska's changing boreal forest. Oxford University Press, New York

Van Cleve K, Oliver L, Schlentner RE, Viereck LA, Dyrness CT (1983) Productivity and nutrient cycling in taiga forest ecosystems. Can J For Res 13:747–766

Van Cleve K, Yarie J, Erickson R, Dyrness CT (1993) Nitrogen mineralization and nitrification in successional ecosystems on the Tanana River floodplain, interior Alaska. Can J For Res 23:970–978

Walker LR (1989) Soil nitrogen changes during primary succession on the Tanana River floodplain. Arct Alp Res 21:341–349

Chapter 13
Hydrological Aspects in a Siberian Larch Forest

T. Ohta

13.1 Introduction

Understanding the water cycle is crucial for ecological studies, because all life both depends on water and affects the water cycle. Energy exchanges between biomes and the atmosphere are also strongly tied to water cycles through evapotranspiration. Therefore, clarifying hydrological processes and features can greatly contribute to a deep understanding of ecological systems.

The high latitudes are characterized by low precipitation and short growing seasons due to the cold winter climate. Several studies have used general circulation models (GCMs) to examine the effects of high-latitude forests on water, energy, and carbon (WEC) cycles (e.g., Bonan et al. 1992, 1995) and have been followed by in situ observational studies. Some projects of WEC cycles have been carried out in high-latitude regions, including the northern hemisphere climate processes land surface experiment (NOPEX) on the Scandinavian Peninsula (Halldin et al. 1998) and the Boreal ecosystem-atmosphere study (BOREAS) in North America (Sellers et al. 1995). In Siberia, WEC cycles observations began in the late 1990s. The terrestrial carbon observation system-Siberia (TCOS-Siberia) study examined WEC exchanges in European Russia and Western Siberia (Schulze et al. 2002). Through intensive observations and analyses, the study revealed numerous characteristics not only of grasslands and bogs but also of forests, as well as distinctive characteristics of high-latitude WEC cycles. Examples of high-latitude WEC characteristics include relatively low evapotranspiration, the importance of tree phenology, and large contributions of understory vegetation.

Despite its having a more severe climate than the regions mentioned above, much of Northeastern Siberia is covered by taiga forests dominated by *Larix cajanderi* (Chap. 3, this Vol.). Yakutsk, located along the middle reaches of the Lena River, has an annual average temperature of only −10.2°C and annual precipitation of 235 mm. Moreover, extensive continuous permafrost exists in Northeastern Siberia, while relatively little permafrost exists in North America, Scandinavia, and Western Siberia (see Fig. 1.1. this Vol.). Therefore, the interactions between forests and permafrost in Northeastern Siberia likely result in unique hydrological features

A. Osawa et al. (eds.), *Permafrost Ecosystems: Siberian Larch Forests*,
Ecological studies, Vol. 209, DOI 10.1007/978-1-4020-9693-8_13,

in this region compared with other climate zones. As a first attempt to understand WEC cycles in Northeastern Siberia, Kelliher et al. (1997) conducted field studies for a short period during summer 1993 using an eddy correlation method. Long-term studies near Yakutsk have subsequently been carried out, including collaborative research between Russia and Japan as part of the global water and energy cycle experiment (GEWEX), Asian Monsoon Experiment-Siberia (GAME-Siberia; Lawford et al. 2004; Yasunari 2007), the Core Research for Evolutional Science and Technology (CREST)/Water and Energy Cycles in Northern Forests (WECNoF) project (http://www.agr.nagoya-u.ac.jp/~wecnof/), and the Russian–Dutch project PIN-Matra (Moors et al. 2006).

This chapter first discusses the hydrological characteristics of a Northeastern Siberian larch forest and then examines hydrological differences between permafrost and non-permafrost regions. Finally, the water cycle is estimated at a continental watershed scale using a land surface model (LSM) that incorporates in situ observations.

The water and energy balances are strongly related to the carbon dioxide exchange. Net ecosystem exchange of carbon dioxide in a permafrost larch stand is discussed by Y. Nakai (see Chap. 10, this Vol.).

13.2 Approaches to Study Stand-scale Hydrological Characteristics in a Larch Forest of Northeastern Siberia

13.2.1 Study Site for the Stand-scale Investigation

The observation site is located at the middle reaches of the Lena River, approximately 20 km north of Yakutsk city (62°N, 129°E, 220 m a.s.l.), and on the left bank of the river. This site, called Spasskaya Pad, is part of an experimental forest of the Institute of Biological Problems in the Cryolithozone, Russian Academy of Sciences. A 32-m-high meteorological tower was installed at the site in 1996, and full observations have been carried out since 1998. The topography is flat but inclining slightly northward.

The dominant overstory species is *Larix cajanderi*; the larch stand has a density of 840 trees ha^{-1}, a mean tree height of 18 m, and a leaf area index (LAI) of 1.56 $m^2 m^{-2}$. The forest floor is fully covered with *Vaccinium vitis-idaea*, with an LAI of approximately 2.0 $m^2 m^{-2}$. Roots are concentrated in a surface soil layer 0–20 cm deep; only 1.5% of the surface area of roots is distributed below 50 cm deep. *Larix cajanderi* is a deciduous species having clear phenological changes throughout a year. From 1998 to 2006, larch leaves started to flush from late April to late May (weeks of the year 16–21), and the canopy reached a mature condition during the following 2–4 weeks. The start of leaf fall varied yearly but generally occurred from late August to late September (weeks of the year 34–37), and almost all leaves had fallen by 10–20 days after the start of leaf fall.

Further details of the site have been provided by Ohta et al. (2001), Dolman et al. (2004), Hamada et al. (2004), and Ohta et al. (2008).

13.2.2 Measurement of Meteorological and Environmental Variables

Meteorological elements were measured at several heights on the 32-m-high tower, at six levels from 1998–2000 and at four levels since 2001. Downward and upward shortwave radiation (Sd, Su) and downward and upward longwave radiation (Ld, Lu) were observed at the top of the tower and above the forest floor. In addition, photosynthetically active radiation (PAR), both downward and upward (Pd, Pu), was measured at two levels. Wind direction was observed at the top of the tower only, while wind speed was observed at six or four levels using three-cup anemometers. Air temperature and relative humidity were measured at all levels, with ventilation.

Soil temperature (T_g) and soil water content (*SWC*) were also measured at several depths. Platinum resistance thermo-sensors were used to measure soil temperature, and time domain reflectometry (TDR) soil-moisture sensors were used to obtain *SWC*. Ohta et al. (2001) and Ohta et al. (2008) have reported details of these measurements.

13.2.3 Measurement of Water Vapor and Energy Fluxes

Water vapor and energy fluxes above the canopy were obtained by an eddy correlation method using a three-dimensional ultrasonic anemometer (3D-SAT) and an infrared gas analyzer (IRGA). Energy balance above a canopy was given as follows:

$$R_n - G = H + LE + J_a + J_s + J_w, \tag{13.1}$$

where *R*n is net all-wave radiation (W m^{-2}), *G* is ground heat flow (W m^{-2}), *H* is sensible heat flux (W m^{-2}), *LE* is latent heat flux (W m^{-2}), and J_a, J_s, J_w are heat storage in the air mass below the 3D-SAT and IRGA, in the soil layer between the soil surface and ground heat flow plate, and in the biomass. The J_a consists of sensible heat storage (J_h) and latent heat storage (J_l).

The relationship between available energy and the sum of turbulent fluxes and heat storage is given as

$$H + LE + J_a + J_s + J_w = \alpha(R_n - G) + \beta, \tag{13.2}$$

where α, β are coefficients. Energy balance is completely closed when α is 1.0 and β is 0.0. At the study site, α and β have values of 0.90 and −4.0, respectively. The value of α dropped to 0.75 when heat storages J_a, J_s, and J_w were ignored at the site (Ohta et al. 2001; Matsumoto et al. 2008a). The magnitudes of J_h and J_l were not small but led to small J_a, because these storages often had reverse directions and offset each other. This result implies that heat storage in the surface soil and biomass

is very important for energy balance in a Northeastern Siberian larch forest, because a sparse larch forest allows more radiation to penetrate under the canopy.

13.2.4 Evaluation of Hydrological Cycles in the Lena River Basin

Hydrological aspects at a continental watershed scale were investigated using an LSM and a distributed runoff model (DRM) coupled with the LSM. These models were applied over Central and Northeastern Siberia, including the Lena River and Kolyma River basins.

The LSM used was originally proposed by Yamazaki (2001) and developed to a watershed scale by Park et al. (2008). The model included three submodels for vegetation, snow, and soil processes. In the vegetation submodel, the canopy was divided into crown space and trunk space. The physiological responses to environmental variables were described by a Jarvis-type model. The parameters in the conductance responses are universal for all vegetation types in Far East Asia, from boreal to warm-temperate forests, based on the results obtained by Matsumoto et al. (2008b). Permafrost processes (i.e., melting and refreezing of the soil layer) were performed in the soil submodel. The watersheds analyzed were divided into $0.5 \times 0.5^{\circ}$ grids, and outputs from the LSM were obtained in each grid.

The DRM was originally described by Lu et al. (1989) and developed for Siberian rivers by Hatta et al. (2009). The runoff processes on slope and river channels were calculated in this model using a kinematic wave method. Hydraulic characteristics of channels were obtained from satellite data. Input for this DRM was outflow from a soil column simulated by the LSM described above. The DRM described not only the runoff processes but also breaking-up and freezing processes of river ice.

13.3 Seasonal and Interannual Variation of Energy Partitioning above the Siberian Larch Forest

Here, we discuss the partitioning characteristics of available radiation energy, $Rn - G$, into latent and sensible heat fluxes on seasonal and interannual temporal scales. Figure 13.1 shows the seasonal variation of net all-wave radiation; ground heat flow, including the energy for snowmelt; latent and sensible heat fluxes; and the Bowen ratio (the ratio of latent heat flux to sensible heat flux) above the canopy in 1998 based on daily values (Ohta et al. 2001). It shows only time series obtained over a dry canopy condition. The bar at the bottom of Fig. 13.1 shows the seasonal change of land surface conditions such as snow coverage and leaf phenology, which was determined by in situ observation.

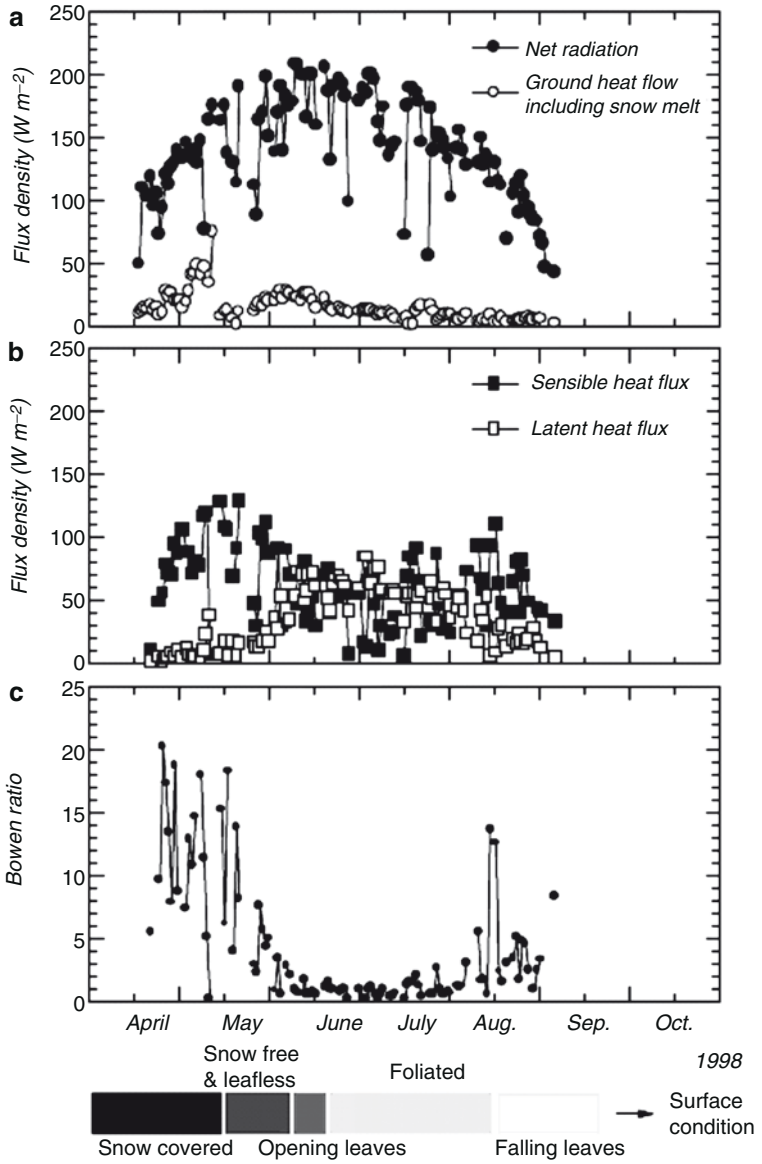

Fig. 13.1 Seasonal variation of energy budget components, Bowen ratios and land surface conditions obtained in the Siberian larch forest in 1998. (**a**) Net all-wave radiation (*filled circle*) and ground heat flow (*open circle*); (**b**) sensible heat flux (*filled square*) and latent heat flux (*open square*); and (**c**) Bowen ratios. (Ohta et al. 2001)

The latent heat flux remained low until the beginning of leaf emergence (i.e., bud break) at the end of May and then increased quickly toward the middle of June as the leaves opened and developed fully. The timing of leaf emergence of the larch trees almost agreed with the timing of permafrost thawing to depths of 10–20 cm. On the other hand, the sensible heat flux peaked in the middle of May and then dropped suddenly, even though net all-wave radiation was still increasing. Consequently, the time series of Bowen ratios (Fig. 13.1c) had a clear U-shape, with a minimum value of 1.0 during the growing season (June and July). This result indicates that the phenological effect on water and energy exchanges above the canopy is more significant than that of snow disappearance, although the soil surface condition became quite wet just after snow melt. Snow melt is a significant hydrological event from the viewpoint of runoff processes, but it does not have remarkable effects on the water and energy exchanges between forests and the atmosphere. Further, the minimum Bowen ratio (~1.0) was higher than that obtained at tropical and temperate forests, but typical for or somewhat lower than values at other boreal forests (e.g., Sellers et al. 1995; Kelliher et al. 1997, 1998; Tchebakova et al. 2002).

An evaporative fraction, presented by Barr et al. (2006), was used to examine the interannual energy balance features:

$$\Lambda = \frac{LE}{LE + H}, \tag{13.3}$$

where Λ is the evaporation fraction. Figure 13.2 shows the interannual time series of the latent and sensible heat fluxes above the canopy (upper panel) and the evaporative fraction (lower panel) (Ohta et al. 2008). Interannual fluctuation of latent heat flux was smaller than that of sensible heat flux. The evaporative fraction ranged from 0.379 to 0.678, with an average value of 0.477 and standard deviation (SD) of 0.182 during the growing season (June, July, and August). The corresponding Bowen ratios for these months were 1.10, 1.64, and 0.475, respectively.

As mentioned above, the average evaporative fraction was smaller in the Siberian larch forest than in temperate forests. Hamada et al. (2004) obtained similar Bowen ratios (1.0–2.0) in a Scots pine (*Pinus sylvestris*) forest located about 2 km south-east of the present study site of *L. cajanderi* forest during mid-summer of 2000. A small portion of available energy was partitioned to latent heat flux in the Siberian forest. However, the highest evaporative fraction was 0.678, which is equal to or somewhat larger than the values reported for several temperate forests (Kosugi et al. 2006, 2007). High evaporative fractions were found in wet years. These results imply that the low partitioning rate into latent heat flux is not an inherent characteristic of Siberian larch forest and that the portion of latent heat flux will increase under the more suitable growing conditions (e.g., higher soil water condition).

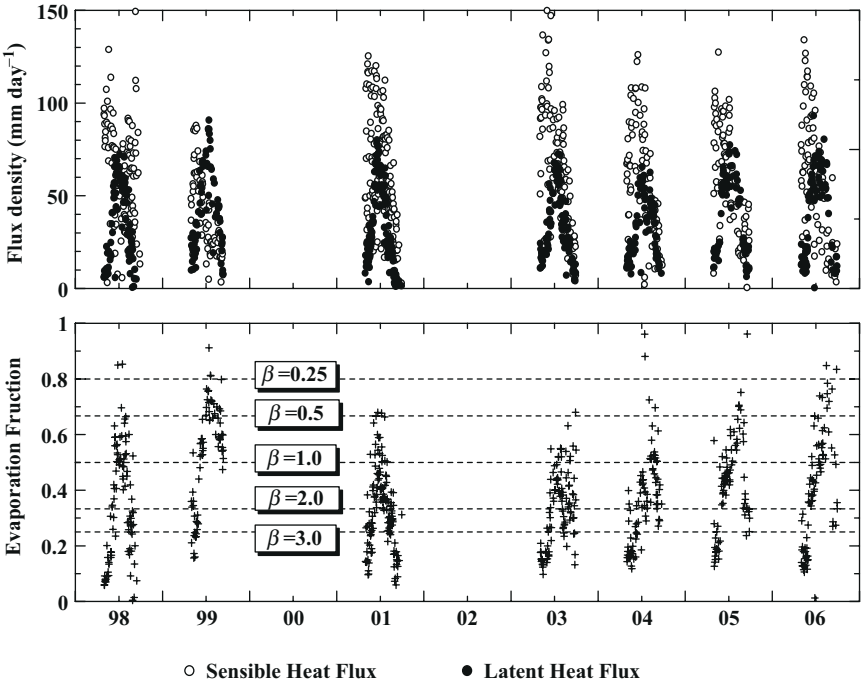

Fig. 13.2 Interannual variation of sensible heat flux (*open circle*) and latent heat flux (*filled circle*) (*upper panel*), and evaporative fraction (*lower panel*) over the Siberian larch forest during a period 1998–2006 (Ohta et al. 2008)

13.4 Water Balance of One-dimensional Scale in the Siberian Larch Forest

13.4.1 Interannual Variation

The water balance is described as follows:

$$P = E + \Delta S + R, \tag{13.4}$$

where P is the amount of precipitation (mm), E is the amount of evapotranspiration (mm), ΔS is the change in soil water storage between the first and the last day in a water budget period (mm), and R is the residual (mm). Positive R indicates runoff from a water balance system, while negative R indicates inflow into the system. In this section, because we focus on the temporal variation of the water balance in the Northeastern Siberian larch forest, the unit of each term in Eq.(13.4) is mm y^{-1}. Here, we define a water year as the 365 days from October 1 of the previous calendar

year to September 30 of the current year. That is, year "*N*" means the 365 days from October 1 of year "*N*-1" to September 30 of year "*N*."

Figure 13.3 shows the interannual variation of each water balance component presented in Eq.(13.4) (Ohta et al. 2008), and Table 13.1 presents the means and SDs of the components (Ohta et al. 2008). Evapotranspiration in the cold period from October to April is not included in the figure and the table because of the negative net all-wave radiation and very low temperatures. The annual precipitation amount ranged widely from 111 to 347 mm y^{-1} (SD = 82.3 mm). In comparison, the annual amount of evapotranspiration was relatively steady (SD = 19.7 mm), varying from 169 to 220 mm y^{-1}.

In non-permafrost regions with low annual precipitation (particularly areas with less than 500 mm y^{-1} of precipitation), the annual amount of evapotranspiration has been found to vary linearly with the annual precipitation amount, with a very slight deviation (Zhang et al. 2001). Figure 13.4 shows the empirical relationships between annual precipitation and annual evapotranspiration in watersheds covered

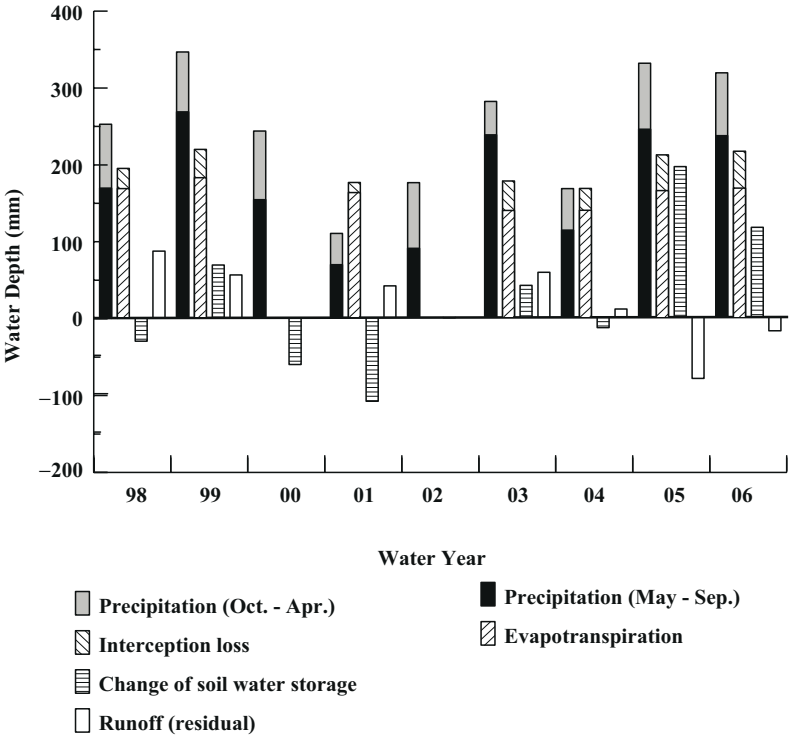

Fig. 13.3 Interannual variation of water balance components in the Siberian larch forest during a period 1998–2006. One water year is defined as 365 days from October 1 in the previous year to September 30 in the following year. (Ohta et al. 2008)

Table 13.1 Summary of the water balance in the Siberian larch forest during the period 1998–2006 (*left column*), 1998–2003 (*center column*), and 2004–2006 (*right column*) (Ohta et al. 2008)

	1998–2006		1998–2003		2004–2006	
	Mean	Standard deviation (SD)	Mean	SD	Mean	SD
Precipitation (mm)	259.2	82.3	248.4	86.3	273.6	78.4
October–April	69.0	18.3	63.7	19.3	76	14.2
May–September	190.3	70.1	184.7	76.8	197.6	59.9
Evapotranspiration (mm)	196.1	19.7	193.1	17.3	200.2	21.9
Change of soil water storage (mm)	39.6	94.1	−6.6	69.6	101.3	87.0
Residual (mm)	23.8	52.8	61.9	16.4	−27.0	38.4
Maximum thawing depth of permafrost (cm)	147.0	27.6	127.0	7.7	182.7	16.3
Date of maximum thawing depth	252.6	11.4	245.5	9.8	262.0	4.6

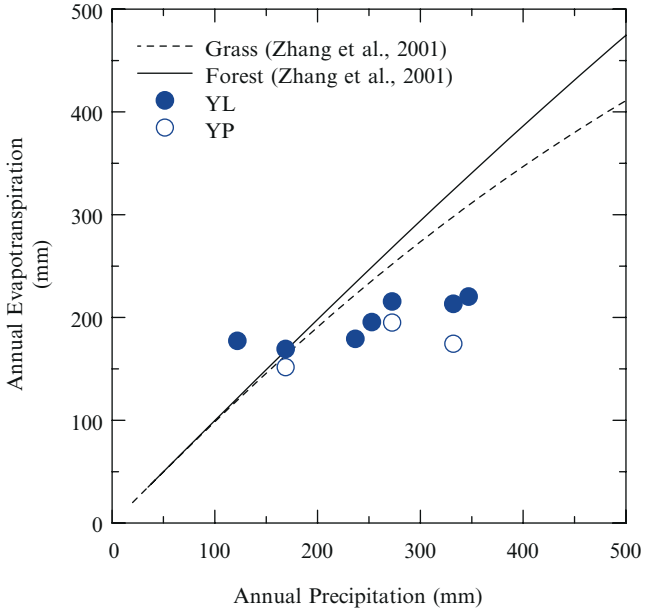

Fig. 13.4 Relationships between annual precipitation and evapotranspiration in the Siberian larch forest (*filled circle*) and pine forest (*open circle*). The solid and dashed lines indicate estimations by Zhang et al. (2001) for forested watersheds and grassland watersheds, respectively, located in a non-permafrost region. (Original data of larch and pine forests are from Ohta et al. 2008 and Hamada et al. 2004, respectively.).

with forests (solid line) and grass (dotted line) with an annual precipitation range of 0–500 mm y^{-1}, as obtained by Zhang et al. (2001). This figure also presents results for the larch forest (closed circles) and the nearby Scots pine forest (open circles) located approximately 2 km southeast of the larch forest (Hamada et al. 2004). Variation of evapotranspiration was much smaller in the Siberian forest ecosystem than in non-permafrost forests. This contrast is very important in understanding the effects of permafrost on hydrological aspects in this region.

Sugimoto et al. (2002) examined the water usage of larch stands near Yaktsuk using a stable isotope of oxygen, δO^{18}. They took water samples from precipitation, soil layers at several depths, and trees. The results showed that trees uptook precipitation water in wet years, but transpired permafrost meltwater in drought years. This result indicates that permafrost serves as a buffer for interannual fluctuation of precipitation.

As shown in Table 13.1, there was a significant difference in changes in soil water storageΔS and residual R and in the maximum thawing depth of permafrost between the periods 1998–2003 and 2004–2006. The change of SWC was very small, −6.6 mm, with a wide SD of 69.6 mm during 1998–2003. The residual indicated runoff of 61.9 mm during this period. By contrast, in 2004–2006 the changes of SWC significantly increased to 101.3 mm and the residual became a negative value of −27.0 mm. In addition, the thawing depth of permafrost was much deeper

in 2004–2006 than in 1998–2003. The negative residual indicates inflow into the water balance system and implies that the increase in SWC cannot be explained only by the approximately 25 mm increase in precipitation. Ohta et al. (2008) discussed several possible reasons for the negative residual, but the exact causes have not yet been determined. Regardless of the reasons, the soil water regime is a key factor in understanding hydrological features in the permafrost regions.

13.4.2 Annual Evapotranspiration and Environmental Variables

Here, we discuss environmental parameters affecting the interannual variation of evapotranspiration at the Siberian larch forest. Several previous reports have examined environmental variables affecting evapotranspiration on diurnal and seasonal scales in Siberian forests (Ohta et al. 2001; Hamada et al. 2004; Dolman et al. 2004). These studies have noted the importance of atmospheric water deficit in Northeastern Siberian larch and pine forests at these temporal scales. The variables affecting WEC cycles likely vary according to the spatiotemporal scale of focus (Baldocchi et al. 2001; Katul et al. 2001; Stoy et al. 2005). However, little is known about the environmental parameters affecting evapotranspiration at an interannual scale because of the lack of long-term data for permafrost regions.

Figure 13.5 shows the interannual variations of four environmental variables (short-wave radiation, air temperature, atmospheric water vapor deficit, and SWC) and evapotranspiration normalized by potential evaporation E/E_p, and their relationships. These values were averaged for the growing season (June, July, and August). No significant relationships were observed except for evapotranspiration and surface soil moisture content. It might seem surprising that we did not find a clear relationship between mean temperatures and E/E_p, because air temperature is considered to be one of the most important variables limiting evaporation in cold regions. Dolman et al. (2004) emphasized the importance of surface conductance for daily or seasonal variation of evapotranspiration; they reported that evapotranspiration was low when trees were exposed to very dry air, even if soil moisture did not limit stomata closure. However, we found no clear relationship between atmospheric water vapor pressure and E/E_p, as shown in Fig. 13.5c. These results basically agree with those obtained by Stoy et al. (2005), who found that the major environmental variables affecting WEC exchanges varied according to the temporal scale.

Figure 13.6 shows the time series of annual precipitation and SWC in the surface soil layer (0–50 cm) during June, July, and August. The interannual variation of SWC lagged that of annual precipitation by one year. Summer precipitation would be stored in the surface soil, which froze from late autumn to the following spring. Thus, the permafrost has a 1-year memory of precipitation and functions as a buffer for the interannual variation of precipitation. Because of this memory function, we could not find clear relationships between evapotranspiration and precipitation, and SWC was the most important factor for E/E_p. The interannual fluctuation of plant activity has also been examined by dendrochronology. Rigling et al. (2001) used tree-ring analyses to

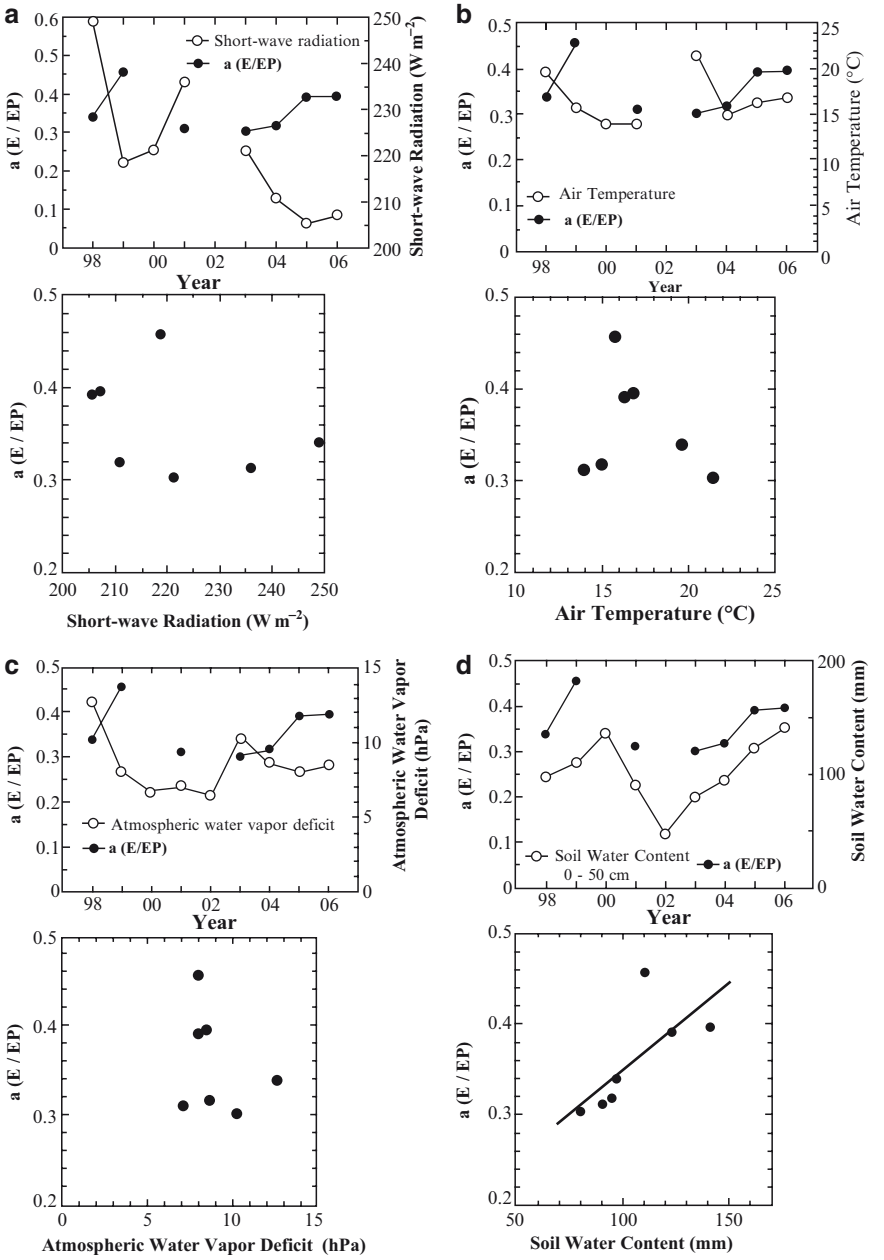

Fig. 13.5 Interannual time series and relationships of environmental variables and evapotranspiration normalized by potential evapotranspiration (E/Ep). (**a**) Shortwave radiation; (**b**) air temperature; (**c**) atmospheric water vapor deficit, and (**d**) soil water content (SWC). (Ohta et al. 2008)

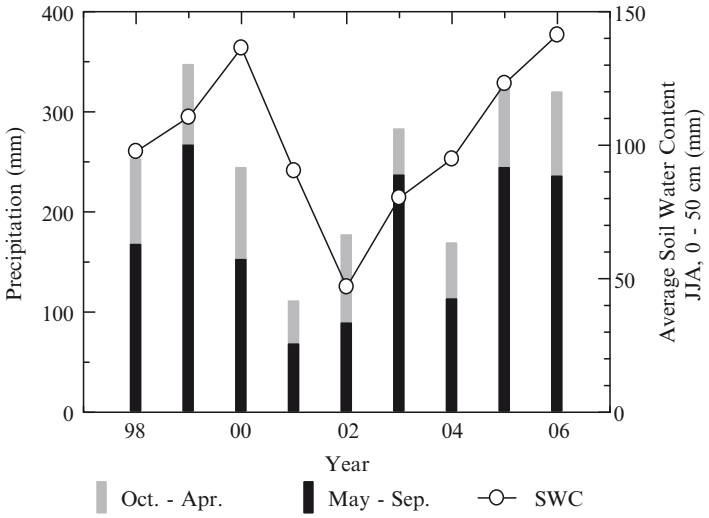

Fig. 13.6 Interannual variation of annual precipitation amount and SWC in the 0–50 cm depth layer. One water year is defined as 365 days from October 1 in the previous year to September 30 in the following year. (Ohta et al. 2008)

examine the relationships between climate and tree growth. They found that tree growth strongly corresponded to the amount of precipitation in the previous summer in Siberian forests. This result further demonstrates that frozen soil has a 1-year memory of precipitation. The 1-year time lag of SWC or plant activity is also found at the stand scale in the region of continuous permafrost in Central Siberia (see Chap. 17, this Vol.).

As mentioned previously, Siberian larch trees uptake permafrost melt water in drought years, and the permafrost reflects interannual variations of precipitation with a 1-year time lag. These two buffers result in the small interannual fluctuation of evapotranspiration, even in a region of relatively low precipitation, and in a significantly different relationship between annual precipitation and evapotranspiration compared with relationships obtained in non-permafrost regions (Zhang et al. 2001). A similar tendency might occur in photosynthetic activities in Siberian larch forests.

13.4.3 Water and Energy Exchange Differences between Non-permafrost and Permafrost Areas of Siberia

While Northeastern and Central Siberia are broadly covered with continuous permafrost, there is less permafrost in Western Siberia (Fig. 1.1, this Vol.). The distribution of the permafrost is also much more extensive in Northeastern Siberia than that in Central Siberia, where its distribution is either discontinuous or sporadic in the southern part of the region. However, few studies have investigated water and energy cycles in those regions. Tchebakova et al. (2002) investigated the water and energy exchanges

in a Scots pine (*Pinus sylvestris*) forest without permafrost at the Zotino site near the eastern boundary of Western Siberia. They examined seasonal variations of energy balance components. The seasonal time series of sensible heat roughly followed that of net all-wave radiation and did not show a clear peak just before the growing season, unlike in the larch forest in Northeastern Siberia. On the other hand, the course of latent heat flux was rather stable during the growing seasons. A similar time series was found at another Scots pine forest near Yakutsk in Northeastern Siberia with permafrost (Hamada et al. 2004). The differences in the seasonal variation of sensible and latent heat fluxes might have resulted from difference in the forest types, i.e., evergreen (pine) versus deciduous (larch), rather than the existence of permafrost.

The amount of evapotranspiration fluctuated from 147 to 196 mm during June, July, August, and September with annual precipitation of 188 to 209 mm in the same period (Tchebakova et al. 2002). The daily evapotranspiration rates were 0.6–2.0 mm d^{-1}. These rates were in the same range as that found in Northeastern Siberia, despite differences in forest types and permafrost existence, but lower than the range for Scandinavian boreal forests (Grelle et al. 1999). The range of fluctuation in evapotranspiration during the growing seasons was wider than that of the precipitation. This result shows clear difference in the interannual variation of evapotranspiration between permafrost (mentioned in Subsect. 13.4.1 and 13.4.2) and non-permafrost regions within the Siberian taiga.

Tchebakova et al. (2002) also concluded that low evapotranspiration of the Scots pine forest in Central Siberia was due to low LAI and low SWC. This conclusion qualitatively agrees with those obtained from the comparative analysis of boreal and temperate forests, as discussed in Subsect. 13.4.4. Surface conductance was controlled by atmospheric water vapor deficit rather than by SWC. This result also agrees with that found for a Northeastern Siberian pine forest (Hamada et al. 2004) where daily surface conductance was regulated by atmospheric water vapor deficit.

Several common features, including low evapotranspiration and low surface conductance, were found to be controlled by atmospheric water vapor deficit in larch forests of Northeastern Siberia and in pine forests of Central Siberia. On the other hand, there were different characteristics of the seasonal course of sensible and latent heat fluxes and the interannual variation of evapotranspiration. However, we cannot conclude which effect was more significant; forest types, existence of permafrost, or both.

13.4.4 Water and Energy Exchange in Different Environments and Climates

13.4.4.1 Seasonal Variations and Magnitudes among Climates

In recent decades, various single-site studies have examined canopy-atmosphere water and energy exchanges in different climates, e.g., tropical forest (Shuttleworth et al. 1984; Malhi et al. 2002; Kumagai et al. 2005), temperate forest (Verma et al. 1986; Kosugi et al. 2006), and boreal forest (Kelliher et al. 1997; Ohta et al. 2001).

These studies have suggested that the latent heat flux or evapotranspiration is generally smaller in boreal forests and that a larger part of available energy is consumed as sensible heat flux in high-latitude areas. However, the major factors characterizing hydrological aspects, especially evapotranspiration, have not yet been clarified.

Matsumoto et al. (2008a) examined differences in water and energy exchange characteristics at five forested sites, including Siberian larch and pine forests, in three climate zones: boreal, cool temperate, and warm temperate. Figure 13.7

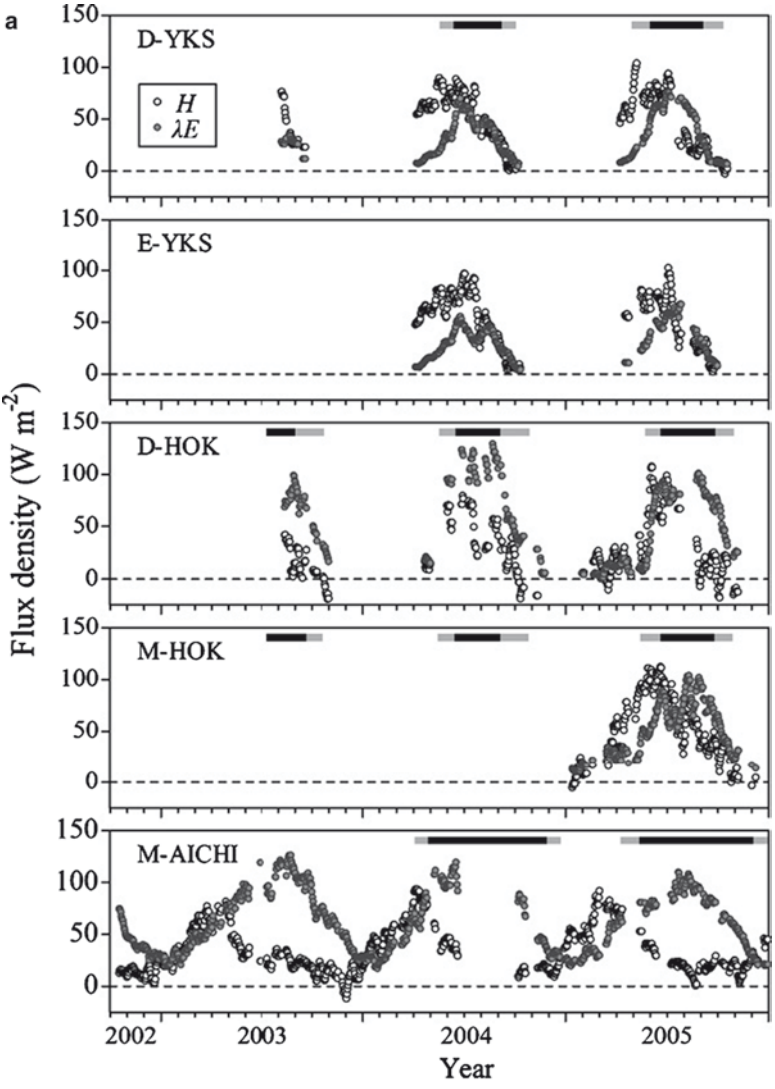

Fig. 13.7 Interannual variation of (**a**) sensible heat flux (*open circle*) and latent heat flux (*filled circle*) in the Siberian forests (*top two panels*), the cool-temperate forests (*middle two panels*), the warm-temperate forest (bottom panel); and (**b**) the evaporative fraction (Matsumoto et al. 2008a)

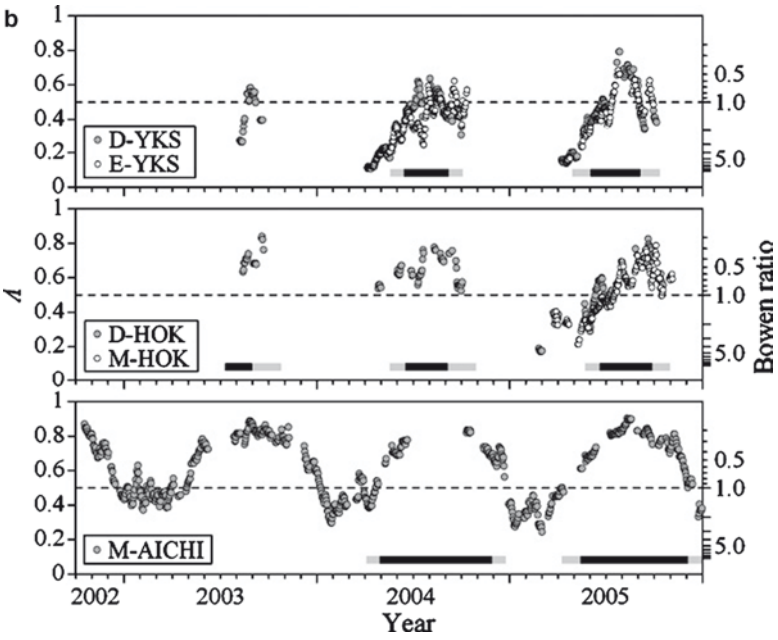

Fig. 13.7 (continued)

shows (**a**) time series of the latent and sensible heat fluxes and (**b**) the evaporative fraction Λ, defined by Eq. (13.3) and the Bowen ratio. They found no significant difference in the magnitude and seasonal variation between different forest types located in the same climate zone. However, there were remarkable differences in the exchanges of water and energy among the climate zones. Namely, the growing season, defined as the duration of $\Lambda \geq 0.5$ ($\beta < 1.0$), was longer at sites in the southern area. At northern sites, the magnitude of Λ was lower. The finding of smaller latent heat flux in the northern forests agrees with previous insights obtained from single-site studies. Maximum sensible heat flux occurred earlier than maximum latent heat flux, and time lag of the latent heat flux peak was shorter at northern sites. Regardless of the climate zone, the timing of maximum sensible heat flux coincided with that of leaf emergence of deciduous trees. In the warm-temperate forest, the sensible heat flux had a maximum value in April. Subsequently, the sensible heat flux decreased to only approximately 20–30 W m^{-2}, and the latent heat flux increased to more than 100 W m^{-2} in July and/or August. On the other hand, in the two boreal forests, maximum latent heat flux lagged the peak of sensible heat flux by only 2–4 weeks, and the sensible heat flux remained high (more than 50 W m^{-2}) and somewhat larger than the latent heat flux even during the mid-growing season in two boreal forests. The effect of atmospheric heating was more significant in the boreal forests than in the temperate forests.

13.4.4.2 Factors Controlling the Difference in Water and Energy Exchanges among Climate Zones

In this section, we discuss the major factors causing differences in water and energy exchanges among the climate zones mentioned above. Matsumoto et al. (2008a) compared the atmospheric and land-surface regulations of daily evapotranspiration (E_d; mm d^{-1}) based on potential evaporation (E_p) and an evapotranspiration coefficient (a). The relationship of the three variables is given as:

$$E_d = aE_p, \tag{13.5}$$

where E_p represents the atmospheric demand for evaporation under a given atmospheric condition and a indicates regulation of evapotranspiration by land surface processes.

Figure 13.8 shows the relationships between the evapotranspiration coefficient and daily evapotranspiration in July and August at each site. Solid lines indicate potential evaporation of 1–6 mm d^{-1}. The values of E_p ranged from 4–4.7 mm d^{-1} in the two Siberian forests and from 4–5.1 mm d^{-1} in the three temperate forests. The atmospheric demand for evaporation in the Siberian forests was quite similar to that in the temperate forests. This result indicates that there was no significant difference in the atmospheric demand for evaporation among the climates and that

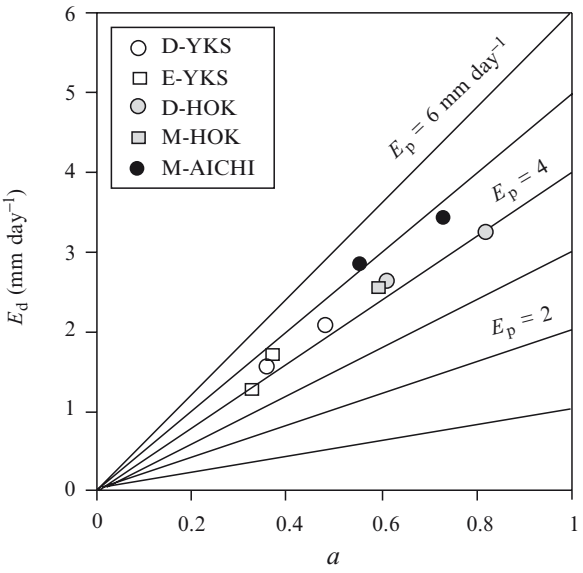

Fig. 13.8 Relationships between the evapotranspiration coefficient a and daily evapotranspiration rates at five forests in Siberia and temperate climate zones. *Solid lines* indicate potential evaporation for each value presented. (Matsumoto et al. 2008a)

the differences in water and energy exchange did not result from the atmospheric conditions. By contrast, the ranges of a values clearly differed between the boreal and temperate forests, with values of 0.3–0.5 in the Siberian forests and 0.6–0.8 in the temperate forests. These values indicate that evapotranspiration is strongly limited by land surface processes in the Siberian forests and that the evapotranspiration differences among the forests in three climates mainly resulted from the variation in land surface regulation.

Figure 13.9 shows the relationships between the parameter a and the atmospheric vapor pressure deficit (D), SWC (θ), or LAI, and a. Low atmospheric humidity and/or low SWC roughly induced the low evapotranspiration coefficient (Fig. 13.9a, b). However, a was lower in the Siberian forests than in the warm-temperate forest at the same ranges of θ and D. This difference can be explained by the difference in LAI (Fig. 13.9c): the forests with lower LAI had lower a, and there was no clear relationship between the other environmental factors and a.

The results reported by Matsumoto et al. (2008a) also suggested that low evapotranspiration in the Siberian forests might have resulted from land surface processes.

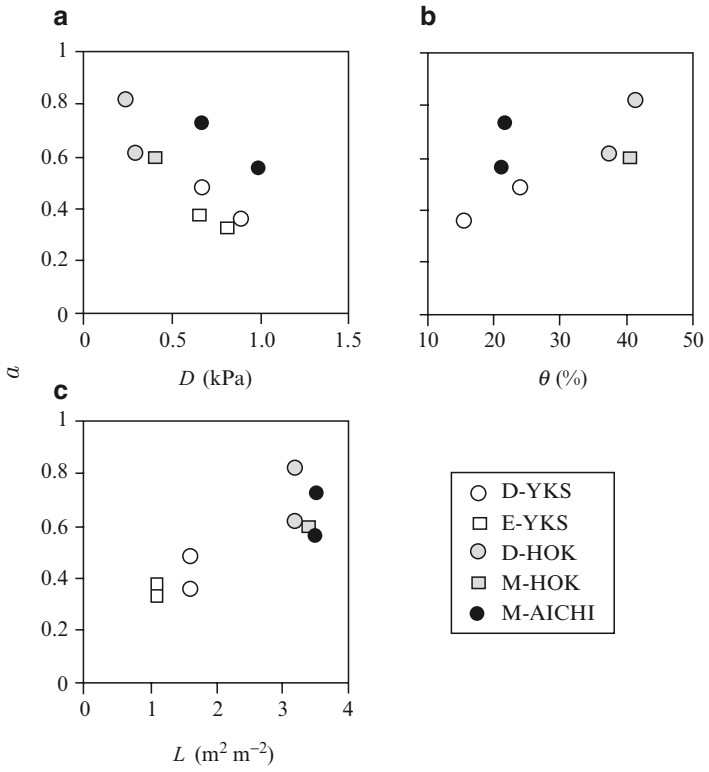

Fig. 13.9 Relationships between the evap\otranspiration coefficient a and (**a**) atmospheric water vapor deficit (D), (**b**) SWC (θ), and (**c**) leaf area index (LAI). Here, LAI is indicated as L according to the original figure (Matsumoto et al. 2008a)

In particular, atmospheric and soil moisture conditions and leaf mass (or LAI) appeared to strongly affect the differences in evapotranspiration among three climates considered. Lower leaf mass has a significant effect not only on evapotranspiration but also on net carbon exchange (see Chap. 10, this Vol.).

13.5 Evaluation of Hydrological Aspects in Northeastern Siberia

Previous sections have discussed hydrological aspects at the stand scale. However, regional characteristics cannot be understood only by stand-scale analyses. Here, we examine results obtained from the LSM and DRM analyses to understand regional-scale hydrological aspects over Central and Northeastern Siberia.

The results of the LSM (Park et al. 2008) and the DRM (Hatta et al. 2009) agreed well with the annual water balance and hydrographs at four major hydrological observation stations located along three tributaries and the mouth of the Lena River (results not shown). Table 13.2 shows the precipitation and evapotranspiration obtained by four studies. The evapotranspiration estimated by Park et al. (2008) agreed well with the results of previous studies, suggesting that Northeastern Siberia has unique surface conductance responses and supporting Matsumoto et al.'s (2008b) hypothesis that surface conductance responses against environmental variables are potentially similar throughout Siberia, despite wide variation in tree species and forest types. Figure 13.10 shows fields of mean net all-wave radiation, latent and sensible heat fluxes, and ground heat flow over Central and Northeastern Siberia during the period of 1986–2004 (Park et al. 2008). According to their results, energy consumption into the latent heat flux was twice as large (~25 $W\,m^{-2}$) in the boreal forests than in the tundra region. Tundra with low LAI might have low surface conductance due to rapid desiccation (Beringer et al. 2005). In addition, higher transpiration in the forested area would result from higher LAI compared with the tundra region. A dominant component of the energy balance in the boreal forest region was latent heat flux (~50 $W\,m^{-2}$), while a dominant component in the tundra region was sensible heat flux (~35 $W\,m^{-2}$). However, the magnitude of sensible heat flux was smaller in the tundra region than in the forest region

Table 13.2 Estimated annual precipitation and evapotranspiration in the Lena River basin

Precipitation (mm y^{-1})	Evapotranspiration (mm y^{-1})	Source
368.9	195.9	Park et al. (2008)
403.0	224.0[a]	Serreze et al. (2003)
	182.0[b]	Serreze et al. (2003)
350.0	160.0	Fukutomi et al. (2003)

The values of a and b were calculated by atmospheric water budget and water budget analyses using measured runoff datasets, respectively

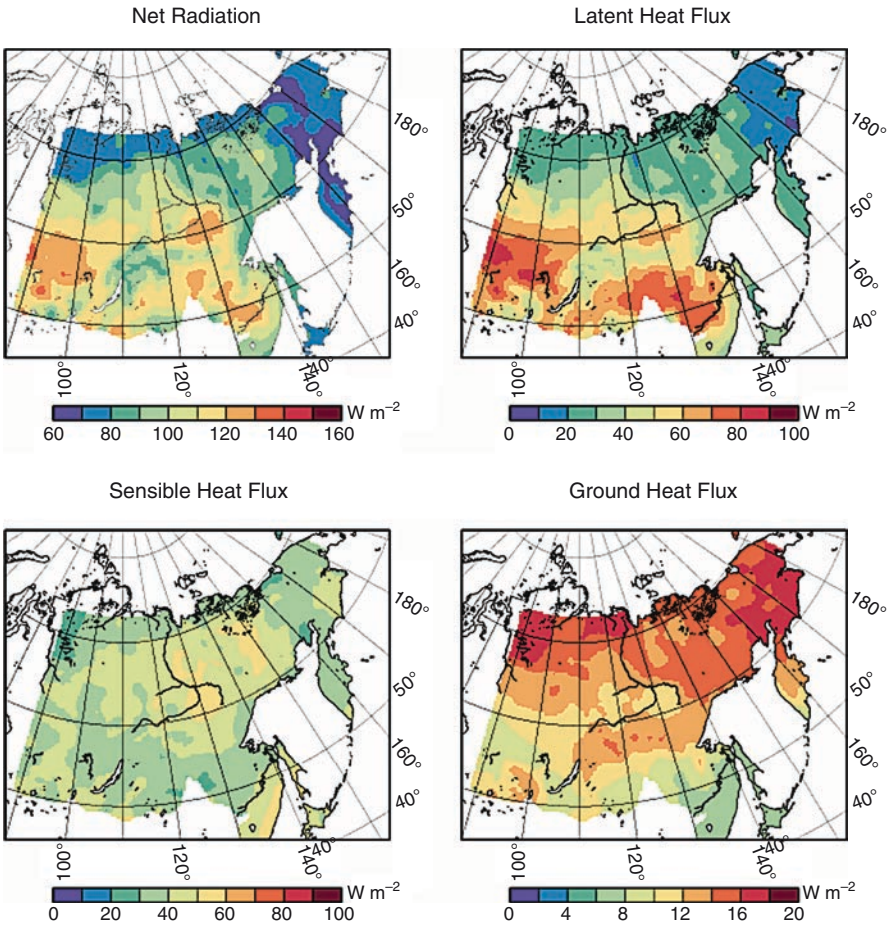

Fig. 13.10 Spatial mean distribution of net all-wave radiation, latent heat flux, sensible heat flux, and ground heat flow over Central and Northeastern Siberia during a period 1986–2004, estimated by a land surface model (Park et al. 2008) (*see* Color Plates)

(~45 W m^{-2}) because available energy, $Rn - G$, was much higher in the forest region (~110 W m^{-2}) than in the tundra region (~70 W m^{-2}) due to low albedo. The contrast in the energy balance between boreal forest and tundra occurred in the magnitude of net all-wave radiation due to albedo and in latent heat flux due to leaf mass.

Park et al. (2008) also examined the interannual variation of latent heat flux and its controlling factor over Northeastern Siberia. They found a significantly positive relationship between annual mean temperature during May–August and annual evapotranspiration over Northeastern Siberia. This implies that summer air temperature strongly controlled annual evapotranspiration, in agreement with results obtained by Suzuki et al. (2006) using the National Oceanic and Atmos pheric Administration (NOAA)/advanced very high resolution radiometer dataset.

These results contradict findings obtained at stand scales, mentioned in Subsect. 13.4.2 (Rigling et al. 2001; Ohta et al. 2008). Issues of spatial scaling may explain the difference. The model result has an advantage in that it spatially extends the representation, but at the cost of accuracy, for variables such as SWC. The opposite holds true for single-stand studies.

In addition, Park et al. (2008) showed a negative relationship between annual evapotranspiration and precipitation. Fukutomi et al. (2003) found an inverse relationship between these two variables in the Lena River basin, but they found no inverse relationship in the Ob and Yenisei watersheds. The Ob and Yenisei watersheds have much less permafrost coverage than the Lena watershed. This interesting contrast among the Siberian basins might result from permafrost conditions.

13.6 Conclusions

This section has focused on hydrological aspects of Northeastern Siberian forests, which strongly affect ecological characteristics. The seasonal and interannual variations of water and energy exchanges between forests and the atmosphere were discussed based on observations using an eddy covariance technique. The characteristics of Siberian forests were compared with those of forests located in other climate zones of East Asia. Finally, hydrological features over Central and Northeastern Siberia were examined based on results of the LSM analysis. Aspects of water and energy exchanges in Siberian forests are summarized as follows:

- The timing of latent heat flux increase and larch leaf emergence coincided. At the same time, sensible heat flux dropped, although net all-wave radiation continued to increase. However, the magnitude of latent heat flux was almost the same as that of sensible heat flux even in the mid-growing season. Snow melt did not significantly affect the water and energy exchanges between the forest and atmosphere, even in the mid-growing season, although snow melt was significant from a hydrological perspective.
- Annual evapotranspiration did not fluctuate widely, although annual precipitation showed a wide range. Annual evaporation rates were usually sensitive to changes in annual precipitation in non-permafrost regions, but the opposite was true in Northeastern Siberia. This difference in Northeastern Siberia was attributable to interactions between permafrost and vegetation. Interannual variation of surface soil water lagged that of annual precipitation by 1 year. In addition, trees can use permafrost melt water during drought years. Permafrost thus acts as a buffer against fluctuations in annual precipitation.
- The low evapotranspiration in the Siberian forests resulted from strong land surface regulation compared with that in temperate forests. Low SWC, high atmospheric water vapor deficit, and less leaf mass led to the low evapotranspiration rates in Northeastern Siberia.

- Annual evapotranspiration was strongly affected by soil moisture content. This characteristic resulted from the 1-year lag of soil moisture mentioned above. However, contradictions were found between the stand-scale analyses and watershed- or regional-scale investigations using an LSM or satellite data. Such discrepancies might have been due to issues with scaling.
- At a watershed scale, hydrometeorological aspects in the Siberian taiga region differed significantly from those in the tundra region. The magnitude of sensible heat flux in the tundra region was similar to that of latent heat flux in the Siberian taiga region, although the dominant turbulent flux component was sensible heat flux in the tundra region. However, the sensible heat flux was smaller in the tundra region than in the taiga region because of the high albedo of the former vegetation. In addition, a negative relationship between annual precipitation and evapotranspiration was only found in the Lena River basin. This interesting phenomenon might have resulted from the extensive permafrost in the Lena River basin.

As discussed above, hydrological aspects in Northeastern Siberia are strongly affected by interactions among the atmosphere, vegetation, and soil and are particularly affected by the existence of permafrost. Permafrost appears to function as a strong buffer for the wide fluctuations of annual precipitation in the region; by this permafrost buffer, the Siberian taiga forest can maintain stable evapotranspiration and probably photosynthesis. Several recent studies (e.g., Peterson et al. 2002; Yang et al. 2002; Serreze et al. 2003; McClelland et al. 2004) have reported increases in river runoff both in North America and Siberia. Runoff can be estimated as precipitation minus evapotranspiration; thus, understanding evapotranspiration processes will contribute to understanding of not only ecological features but also hydrological properties. Siberian forests also affect the spatial distribution of precipitation. Yoon and Cheng (2006) suggested that evapotranspiration from Siberian forests might maintain the rain belt along the high latitudes.

Woo et al. (2008) emphasized the importance of surface–subsurface processes in the hydrological processes of the permafrost region. Vegetation should also be considered in the examinations of the water cycles in this region. Understanding the interactions of hydrological and ecological factors will contribute to understandings of both of these scientific fields in the permafrost regions.

References

Baldocchi D, Falge E, Wilson K (2001) Asepctral analysis of biosphere-atmosphere trace gas flux densities and meteorological variables across hour to multi-year time scales. Agr For Meteorol 107:1–27

Barr AG, Morgenstern K, Black TA, McCaughey JH, Nesic Z (2006) Surface energy closure by the eddy-covariance method above three boreal stands and implication for the measurement of the CO2 flux. Agr For Meteorol 140:322–337

Beringer J, Chapin FS III, Thompson CC, McGuire AD (2005) Surface energy exchanges along a tundra-forest transition and feedbacks to climate. Agr For Meteorol 131:143–161

Bonan GB, Pollard D, Thompson SL (1992) Effects of boreal forest vegetation on global climate. Nature 359:716–718

Bonan GB, Chapin FS III, Thompson SL (1995) Boreal forest and tundra ecosystems as components of the climate system. Clim Change 29:145–167

Dolman AJ, Maximov TC, Moors EJ, Maximov AP, Elbers JA, Kononov AV, Waterloo MJ, van der Molen MK (2004) Net ecosystem exchange of carbon dioxide and water of far eastern Siberian Larch (*Larix cajanderii*) on permafrost. Biogeosciences 1:133–146

Fukutomi Y, Igarashi H, Masuda K, Yasunari T (2003) Interannual variability of summer water balance components in three major river basins of northern Eurasia. J Hydrometeorol 4:283–296

Grelle A, Lindroth A, Molder M (1999) Seasonal variation of boreal forest surface conductance and evaporation. Agr For Meteorol 98–99:563–578

Halldin S, Gottschalk L, Griend AA, Gryning S-E, Heikinheimo M, Hogstrom U, Jochum A, Lundin L-C (1998) NOPEX–a Northern hemisphere climate processes land surface. J Hydrol 212–213:172–187

Hamada S, Ohta T, Hiyam T, Kuwada T, Takahashi A, Maximov TC (2004) Hydrometeorological behaviour of pine and larch forests in eastern Siberia. Hydrol Proc 18:23–29

Hatta S, Hayakawa H, Park H, Yamazaki T, Yamamoto K, Ohta T (2009) Long term runoff analysis of the Lena river basin using a distributed hydrological model. J Jpn Soc Hydrol Water Resour 22:177–187 in Japanese with English abstract

Katul G, Lai C-T, Schafer K, Vidakovic B, Albertson J, Ellsworth D, Oren R (2001) Multiscale analysis of vegetation surface fluxes: from seconds to years. Adv Water Resour 24:1119–1132

Kelliher FM, Hollinger DY, Schulze E-D, Vygodskaya NN, Byers JN, Hunt JE, McSeveny TM, Milukova I, Sogatchev A, Varlargin A, Ziegler W, Arneth A, Bauer G (1997) Evaporation from an eastern Siberian larch forest. Agric For Meteorol 85:135–147

Kelliher FM, Lloyd J, Arneth A, Byers JN, McSeveny TM, Milukova I, Grigoriev S, Panfyorov M, Sogatchev A, Varlargin A, Ziegler W, Bauer G, Schulze E-D (1998) Evaporation from a central Siberian pine forest. J Hydrol 205:279–296

Kosugi Y, Takanashi S, Matsuo N, Tanaka K, Tanaka H (2006) Impact of leaf physiology on gas exchange in a Japanese evergreen broad-leaved forest. Agr For Meteorol 139:182–199

Kosugi Y, Takanashi S, Tanaka H, Ohkubo S, Tani M, Yano M, Katayama T (2007) Evapotranspiration over a Japanese cypress forest. I: Eddy covariance fluxes and surface conductance characteristics for 3 years. J Hydrol 337:269–283

Kumagai T, Saitoh TM, Sato Y, Takahashi H, Manfroi OJ, Morooka T, Kuraji K, Suzuki M, Yasunari T, Komatsu H (2005) Annual water balance and seasonality of evapotranspiration in a Bornean tropical rainforest. Agr For Meteorol 128:81–92

Lawford RG, Stewart R, Roads J, Isemer H-J, Manton M, Marengo J, Yasunari T, Benedict S, Koike T, Williams S (2004) Advancing global and continental-scale hydrometeorology. Bull Am Met Soc 85:1917–1930

Lu M, Koike T, Hayakawa N (1989) A rainfall-runoff model using distributed data of radar rain and altitude. Proceedings of Jpn Soc Civil Engin 411 II-12:135–142 (in Japanese with English abstract)

Malhi Y, Pegoraro E, Nobre AD, Pereira MGP, Grace J, Culf AD (2002) Energy and water dynamics of a central Amazonian rain forest. J Geophys Res 107(D20):LBA 45.1–LBA 45.17. doi:10.1029/2001JD000623

Matsumoto K, Ohta T, Nakai T, Kuwada T, Daikoku K, Iida S, Yabuki H, Kononov AV, van der Molen MK, Kodama Y, Maximov TC, Dolman AJ, Hattori S (2008a) Energy consumption and evapotranspiration at several boreal and temperate forests in the Far East. Agr For Meteorol . doi:10.1016/j.agrformet.2008.09.008

Matsumoto K, Ohta T, Nakai T, Kuwada T, Daikoku K, Iida S, Yabuki H, Kononov AV, van der Molen MK, Kodama Y, Maximov TC, Dolman AJ, Hattori S (2008b) Responses of surface conductance to forest environments in the Far East. Agr For Meteorol . doi:10.1016/j.agrformet.2008.09.009

McClelland JW, Holmes RM, Peterson BJ (2004) Increasing river discharge in the Eurasian Arctic: consideration of dams, permafrost thaw, and fires as potential agents of change. J Geophys Res 109:D18102. doi:10.1029/2004JD 004583

Moors EJ, Dolman H, Maximov TC, Jans W, Maximov A, Kononov A, Kruijt B, Nabuurs GJ (2006) Results of the PINMATRA project 2002-2004. In: Proceedings of Second International Workshop on C/H2O/Energy Balance and Climate over Boreal Regions with Special Emphasis on Eastern Siberia. pp 3–6 http://www.agr.nagoya-u.ac.jp/~wecnof/

Ohta T, Hiyama T, Tanaka H, Kuwada T, Maximov TC, Ohata T, Fukushima Y (2001) Seasonal variation in the energy and water exchanges above and below a larch forest in eastern Siberia. Hydrol Proc 15:1459–1476

Ohta T, Maximov TC, Dolman AJ, Nakai T, van der Molen MK, Kononov AV, Maximov AP, Hiyama T, Iijima Y, Moors EJ, Tanaka H, Toba T, Yabuki H (2008) Interannual variation of water balance and summer evapotranspiration in an eastern Siberian larch forest over a 7-year period (1998–2006). Agr For Meteorol . doi:10.1016/j.agrformet.2008.04.012

Park H, Yamazaki T, Yamamoto K, Ohta T (2008) Tempo-spatial characteristics of energy budget and evapotranspiration in the eastern Siberia. Agr For Meteorol . doi:10.1016/j.agrformet.2008.06.018

Peterson BJ, Holmes RM, McCelland JW, Vorosmarty CJ, Lammers RB, Shiklomanov AI, Shiklomanov IA, Rahmstorf S (2002) Increasing river discharge to the Arctic Ocean. Science 298:2171. doi:10.1126/science.1077445

Rigling A, Waldner PO, Forster T, Brake OU, Pouttu A (2001) Ecological interpretation of tree-ring width and intraanuual density fluctuations in *Pinus sylvestris* on dry sites in the central Apls and Siberia. Can J For Res 31:18–31

Schulze E-D, Vygodskaya NN, Tchebakova NM, Czimczik CI, Kozlov DN, Lloyd J, Mollicone D, Parfenova E, Sidorov KN, Varlagin AV, Wirth C (2002) The Eurosiberian transect: an introduction to the experimental region. Tellus 54B:421–428

Sellers P, Hall F, Margolis H, Kelly B, Baldocchi D, Hartog GD, Cihlar J, Ryan MG, Goodison B, Crill P, Ranson KJ, Lettenmaier D, Wickland DE (1995) The boreal ecosystem—atmosphere study (BOREAS): an overview and early results from the 1994 field year. Bull Am Meteorol Soc 76:1549–1577

Serreze MC, Bromwich DH, Clark MP, Etringer AJ, Zhang TZ, Lammers R (2003) Large-scale hydro-climatology of the terrestrial Arctic drainage system. J Geophys Res 108(D2):8160. doi:10.1029/2001JD000919

Shuttleworth WJ, Gash JHC, Lloyd CR, Moore CJ (1984) Eddy correlation measurements of energy partition for Amazonia. Q J Roy Meteorol Soc 110:1143–1162

Stoy PC, Katul GG, Siqueira MBS, Juang J-Y, Mccarthy HR, Kim H-S, Oishi AC, Oren R (2005) Variability in net ecosystem exchange from hourly to inter-annual time scales at adjacent pine and hardwood forests: a wavelet analysis. Tree Physiol 25:887–902

Sugimoto A, Yanagisawa N, Naito D, Fujita N, Maximov TC (2002) Importance of permafrost as a source of water for plants in east Siberian taiga. Ecol Res 17:493–503

Suzuki R, Xu J, Motoya K (2006) Global analyses of satellite derived vegetation index related to climatological wetness and warmth. Int J Climatol 26:425–438

Tchebakova NM, Kolle O, Zolotoukhine D, Arneth A, Styles JM, Vygodskaya NN, Schulze E-D, Shibistova O, Lloyd J (2002) Inter-annual and seasonal variations of energy and water vapour fluxes above *Pinus sylvestris* forest in the Siberian middle taiga. Tellus 54B:537–551

Verma SB, Baldocchi DD, Anderson DE, Matt DR, Clement RJ (1986) Eddy fluxes of CO2, water vapor, and sensible heat over a deciduous forest. Boundary-Layer Meteorol 36:71–91

Woo M-K, Kane DL, Carey SK, Yang D (2008) Progress in permafrost hydrology in the new millennium. Permafrost Periglac Proc 19:237–254

Yamazaki T (2001) A one-dimensional land surface model adaptable to intensely cold regions and is application in eastern Siberia. J Meteorol Soc Jpn 79:1107–1118

Yang D, Kane DL, Hinzman LD, Zhang X, Zhang T (2002) Siberian Lena river hydrologic regime and recent change. J Geophys Res 107(D23):4694. doi:10.1029/2002.JD002543

Yasunari T (2007) Role of land atmosphere interaction on Asian monsoon climate. J Meteorol Soc Jpn 85B:55–75

Yoon J-H, Cheng T-C (2006) Maintenance of the boreal forest rainbelts during northern summer. J Climate 19:1437–1449

Zhang L, Dawes WR, Walker GR (2001) Response of mean evapotranspiration to vegetation change at catchment scale. Water Resour Res 37:701–708

Part III
Tree Physiology and The Environment

Chapter 14
Photosynthetic Characteristics of Trees and Shrubs Growing on the North- and South-Facing Slopes in Central Siberia

T. Koike, S. Mori, O.A. Zyryanova, T. Kajimoto, Y. Matsuura, and A.P. Abaimov

14.1 Introduction

Larch species are distributed broadly in the permafrost region of eastern Eurasia. This area may be a key to regulating global CO_2 fixation and storage (Hollinger et al. 1998). Atmospheric CO_2 is still increasing yearly which may have caused the increase in ambient temperature since the early 1900s (Strain 1985; Mooney et al. 1991). In fact, the ambient temperature of higher latitudes between about 45 and 70°N increased 1.4–1.8°C during the last 30 years (Kasiscnke and Stocks 2000). This temperature increase may affect growth and development of woody plants native to Central and Northeastern Siberia also, where nitrogen is considered to be a major limiting factor for tree growth (Schulze et al. 1995; Matsuura and Abaimov 2000; also see Chap. 12). Therefore, existence and fate of the Siberian taiga may depend on the condition of the permafrost by way of water and nutrient supplies (Kojima 1994; Koike et al. 1998b).

Many experiments have demonstrated morphological and physiological acclimation of tree seedlings to environments that simulate the greenhouse effect (Oechel and Billings 1992; Ceulemans and Mousseau 1994; Saxe et al. 1998). However, these results of tree-level physiology cannot be readily scaled up to ecosystem processes, because the experiments included various artifacts, such as root restriction (e.g., Arp 1991) and position effects in a growth cabinet (Koike 1995). How can we predict future vegetation changes caused by the warming climate from experiments conducted under near natural conditions?

In an extremely harsh environment, such as timberline, micro-topography and other varying microenvironment (e.g., soil temperature) strongly influence plant growth and function (Häsler 1982; Hadley and Smith 1987; Koike et al. 1994; Körner 1999). According to the vegetation studies in northern Canada, permafrost typically exists on north-facing slopes with tundra vegetation, while south-facing slopes lack permafrost and support spruce forests with undergrowth of woody shrubs, mosses, and lichens. The latter can potentially develop on the north-facing slopes under the warmer climate (Smith 1985; Kojima 1994). Therefore, if the global temperature change continues, we may predict further warming conditions by examining contrasting responses of trees on north- and south-facing slopes, with an assumption that

A. Osawa et al. (eds.), *Permafrost Ecosystems: Siberian Larch Forests*,
Ecological studies, Vol. 209, DOI 10.1007/978-1-4020-9693-8_14,

patterns of precipitation do not change substantially. Soil temperature differs greatly between north- and south-facing slopes, which may simulate the present and future environments of the north-facing slope (Kojima 1994; Koike et al. 1994, 1998a, b).

We have studied species composition and physiological difference in larch (*Larix gmelinii*) and spruce (*Picea obovata*) trees growing on contrasting north- and south-facing slopes in Central Siberia (Koike et al. 1999). Soil respiration was also examined in those slopes (Yanagihara et al. 2000) as a model for predicting future changes in ecosystem physiology. Therefore, we may approximate present and future global-warming conditions by comparing contrasting responses of trees and shrubs on north- and south-facing slopes to light and soil temperature conditions. It is hypothesized that the net photosynthetic rate of trees on north-facing slopes may be lower because of low nutrient content in needles due to retardation of litter decomposition rate at low temperature. Consequently, this may be attributed to poor shoot (and root) development. Optimum temperature for net photosynthetic rate of trees that grew on the north-facing slopes may be lower than that of the south-facing slopes.

To assess these predictions, we measured ambient air and soil temperatures, and the temperature dependency of apparent (= net) photosynthetic rate in trees and shrubs growing on north- (about 20° inclination) and south-facing (about 25°) slopes at Tura Experiment Forest. Moreover, net photosynthetic rate and nutrient condition of larch and spruce trees on the two slopes and in the valley in between were analyzed in relation to light utilization capacity, nitrogen, and chlorophyll content in their foliage.

14.2 Study Site and Measurement of Foliar Ecophysiology

Our study site was located within and near the western edge of a continuous permafrost region at Tura in Central Siberia (ca. 64°N, 100°E; 160 m a.s.l.). There were contrasting north- and south-facing slopes across a small stream at Site 2 (Fig. 14.1; geographical location see Figs. 1.1 and 1.3). The average slope inclination ranged between 18° and 22°. Three belt-transects (about 10 m in width and 500–800 m in length) covering both slopes were made perpendicular to the general contour lines.

The dominant tree species was larch on both slopes. Old multiaged larch stand (>200 years-old) was distributed on the north-facing slope, while even-aged stand (ca. 180 years-old) covered the south-facing slope (Kujansuu et al. 2007; also see Chap. 17). Small-sized spruce (*Picea obovata*) was also present on the north-facing slope. Ground vegetation on the north-facing slope consisted of *Arctou erythrocarpus, Ledum palustre, Empetrum nigrum, Vaccinium vitis-idaea,* and *Carex* sp.; that on the south-facing slope was represented by *Vaccinium vitis-idaea, Vicia cracca, Calamagrotis lapponica,* and *Rosa acicularis.* Depth of active layer of the permafrost was measured by a steel pole (1 m in length and 1 cm in diameter). We measured the depth to be less than 80 cm, and generally in the range of 30–50 cm on the north-facing slope (see also Chaps. 1, 4, 5, and 9). As being reflected from conditions of shallower active layer of the north-facing slope, i.e., low temperature and

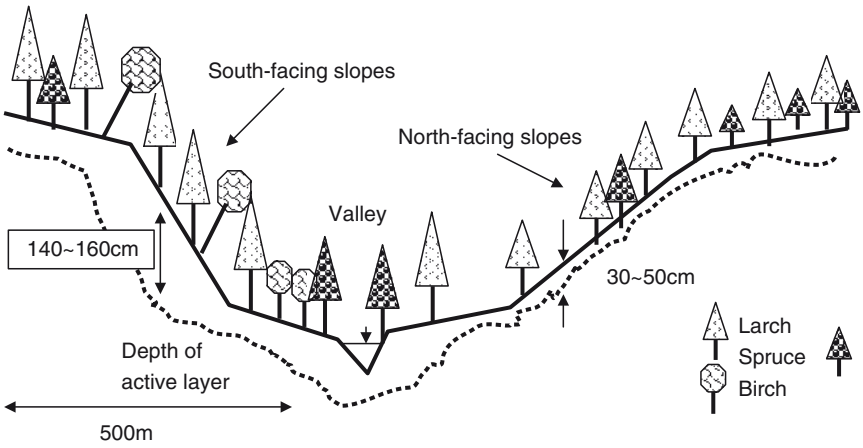

Fig. 14.1 Schematic representation of the study site at Tura Experimental Forest (Site 2), Central Siberia. Location of study site is shown in Fig. 1.3 (Chap. 1)

high soil moisture condition, forest floor was covered not only with woody plants but also with mosses and lichens. On the south-facing slopes, thickness of the active layer was estimated by soil excavation because the depth was beyond the length of the steel pole (Koike et al. 1998a, b).

Photosynthetic capacity and dark respiration of the plants were determined on both slopes. There was no electric power supply at the study sites. Therefore, we employed two simple chemicals for regulating temperature in the assimilation chamber, and for studying acclimation capacity in leaves to the contrasting microenvironments at north- and south-facing slopes. Measurement temperature in the chamber was regulated by a chemical coolant (NH_4NO_3) and pocket warmer (Fe-compound) from 7 to 38°C following the procedures of Terashima et al. (1993). Photosynthetic photon flux (PPF: wave length between 380 and 720 nm) was controlled by a shade cloth (Kurary, Osaka, Japan). Immediately after photosynthetic determination, dark respiration was measured by wrapping the chamber with aluminum foil.

Chlorophyll content of needles was extracted with 100% DMSO (dimethylsulfoxide)(Shinano et al. 1996). Needle nitrogen concentration was determined by a N/C analyzer (Sumica NT-800, Osaka, Japan). There were three replicates for each measurement. Net photosynthetic rate was determined with a potable porometer (LI-6200, Lincoln, NE, USA).

14.3 Environmental Conditions

Ambient temperature was monitored at 1.3 m above ground and soil temperature at 0–5 cm and at 10–15 cm beneath the surface of the moss and lichen layer with an auto-logging thermo-recorder. There was almost no difference in ambient temperature

between the north- and south-facing slopes. Temperature regime for soil respiration of the north-facing slope at both soil depths (0–5, 10–20 cm) was 2–5°C lower than that of the south-facing slope. Soil respiration is generally a function of soil temperature, which is strongly related not only to plant activities, but also to activities of microorganisms. Therefore, rate of soil respiration may be affected by the depth of the active layer. Soil condition of the two slopes was different, i.e., north-facing slope had a shallower active layer of less than 50 cm with lower nitrogen content (around 2.8 gN kg^{-1} within the active layer), while south-facing slopes had 100–160 cm of active layer with higher nitrogen content (about 4.5 gN kg^{-1})(Fig. 14.1) (Yanagihara et al. 2000).

Nutrients in soils may be the essential factor regulating the plant growth (Mooney et al. 1991). Therefore, characteristics of the two slopes may provide data for use in predicting the effect of the warming climate on vegetation in Central Siberia (see also Kojima 1994; Koike et al. 1998a, b). However, we could not assess the effect of pH levels on nutrient absorption by plants. Therefore, further study will be needed for the physiological responses of plants to high pH condition because of possible accumulation of nutrients on the soil surface that may proceed with the melting permafrost. Here, we show photosynthetic responses of trees and shrubs growing at the contrasting north- and south-facing slopes as they are likely to be affected by the different environmental conditions.

Light condition of the north-facing slopes may be dominant of diffuse light because about 30% of the canopy layer (in canopy projection area) in the larch (deciduous conifer) stand consisted of spruce (evergreen conifer) (data not presented). In general, these tendencies are usually dominant at north-facing slopes of mountains (e.g., Häsler 1982; Körner 1999). In contrast, incident sunlight often reaches to the forest floor in the south-facing slopes because of sparse canopy layer of overstory larch trees.

14.4 Photosynthetic Production and Shoot Morphology

Photosynthetic production can depend on temporal and spatial arrangement of the foliage, and duration of high photosynthetic activity before the beginning of leaf senescence. In this sense, we determined the shoot morphology and photosynthetic capacity of larch and spruce growing on the contrasting north- and south-facing slopes. Of course, photosynthetic rate is regulated by light condition and leaf longevity (Larcher 2003; Reich et al. 1995). According to a 3-year experiment, leaf age of *L. gmelinii* may be closely linked with the duration of P_{sat} (i.e., net photosynthetic rate at light saturation with ambient CO_2 concentration [CO_2] of around 375 ppm) as found in deciduous broad-leaved trees (Koike 1987, 1990). In general, leaf longevity is postponed in woody plants growing on more harsh condition. However, leaf longevity is sometimes diminished when plants grow under extremely poor nutrient conditions (Chapin 1980; Reich et al. 1995). Needle longevity of larch on the north-facing slope was about 10 days shorter than that on south-facing slope.

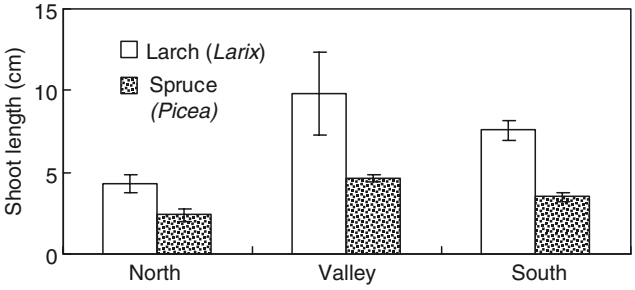

Fig. 14.2 Comparisons of annual shoot growth of larch (*Larix gmelinii*) and spruce (*Picea obovata*). North: north-facing slope; Valley: riverside; South: south-facing slope. Vertical bars in figure mean standard error. (after Koike et al. 1998b)

There were two types of shoots in larch, i.e., short-shoot and long-shoot. The former type is usually more abundant on north-facing slopes where tree growth rate is small, while the latter type is observed conspicuously in trees with large growth rate on south-facing slopes (Kujansuu et al. 2007).

Shoot internode length of larch and spruce on the south-facing slope was longer than that on the north-facing slope (Fig. 14.2). In larch, needle length for the south-facing slope was longer and the specific leaf area (SLA; $cm^2 g^{-1}$) was smaller. In contrast, spruce showed similar values in both needle length and SLA between the two slopes (not significant at $p = 0.05$). Needle color in larch and spruce on the north-facing slope was slightly darker than that on the south-facing slope, which may imply that needles of these conifers acclimate to catch the limited amount of light on the north-facing slope. Both needle length and shoot length were longer, especially larch, on the south-facing slope. These may directly reflect the difference in both physiology and nutrient status of the trees. It is considered that larch on the south-facing slope should have higher potential of biomass production under future greenhouse environment, especially under warm condition. However, potential response of the spruce may be smaller under the future condition of warmer environment.

14.5 Photosynthesis and Respiration of Trees and Shrubs

14.5.1 Dominant Tree Species

Larch and spruce are generally classified respectively as a light-demanding and a shade-tolerant conifer. However, characteristics of their photosynthetic function may be acclimated to specific microenvironments, such as shady north-facing slopes and sunny south-facing slopes. Photosynthetic rate of the trees planted on east- or south-facing slopes at timberline of Swiss Alps is usually higher than that

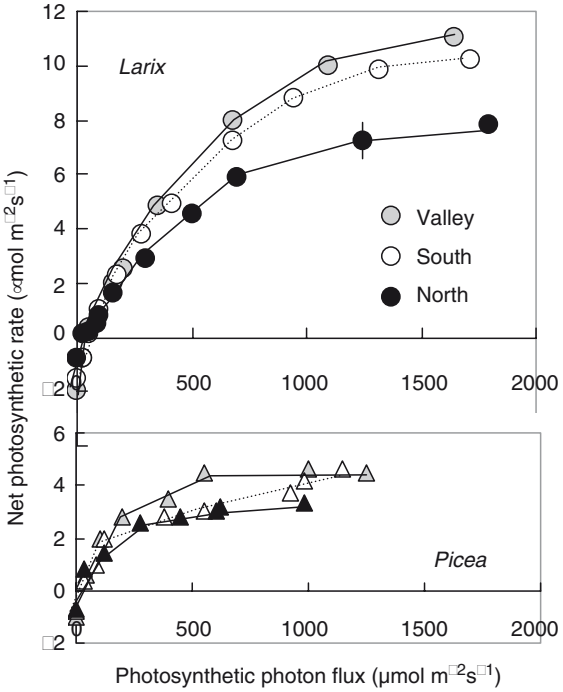

Fig. 14.3 Light-photosynthesis curves of larch (*Larix gmelinii*) and spruce (*Picea obovata*) on the north- and south-facing slopes. North: north-facing slope; Valley: riverside; South: south-facing slope (see Fig. 14.1). *Vertical bars* in figure mean standard error. (after Koike et al. 1998b)

on north-facing slopes (Koike et al. 1994). In Central Siberia, P_{sat} (net photosynthetic rate at the PPF saturation with ambient CO_2 concentration [CO_2]) of *L. gmelinii* and *P. obovata* that grew on the north-facing slope was significantly lower than that on the south-facing slope (Koike et al. 1999). Light saturation for net photosynthetic rate of the long-shoot needles of larch on both slopes occurred at around 1,300 μmole $m^{-2}s^{-1}$ (Fig. 14.3). In contrast, net photosynthetic rate of spruce was saturated at around 500 μmole $m^{-2}s^{-1}$. In larch, P_{sat} was larger for valley and south-facing slopes than north-facing slope (Fig. 14.3). There was no difference in the initial slope of light–photosynthetic curve of each species between the two slopes.

Optimum leaf temperature for photosynthesis was around 15–20°C for both species (Fig. 14.4). However, there was no temperature shift in the optimum temperature for photosynthesis of larch and spruce growing on the contrasting slopes. Reduction in net photosynthetic rate over the optimum temperature was the largest in larch on the south-facing slope. This may imply that stomatal regulation capacity of larch on the south-facing slope would be larger than the other. Photosynthetic adaptation (i.e., light and temperature responses) of trees on both slopes was relatively small, especially to temperature and light acclimation.

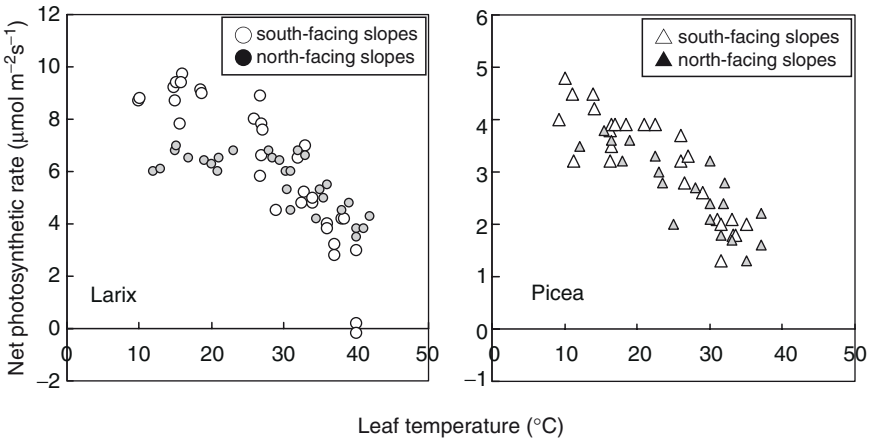

Fig. 14.4 Temperature dependency in the photosynthetic rate of larch (*Larix gmelinii*) and spruce (*Picea obovata*) growing on the north- and south-facing slopes

Respiration rate of larch needles was about 1.3 times higher than that of spruce needles developed on the north-facing slope. In larch, however, needle respiration on the north-facing slope was lower than that on the south-facing slope. Thermal coefficient (Q_{10}) of needle respiration rate was about 2 except for needles on the north-facing slope. There was a point of discontinuity around 15°C. Below the needle temperature of 15°C, Q_{10} of spruce needles was larger than 2. Respiration of spruce needles seems to have adaptation for energy production at a low temperature regime below 15°C. Evergreen needles of spruce may have greater adaptation capacity for temperature. The proportion of root respiration to total soil respiration is generally large (Boone et al. 1998).

Nutrient availability through nitrogen mineralization and other processes is an important factor for plant growth, especially on north-facing slopes (Näsholm et al. 1998). In fact, higher soil respiration was found on south-facing slopes of larch dominated stands at Tura Experimental Forest, Central Siberia (Yanagihara et al. 2000). In this sense, higher soil temperature on south-facing slopes may provide a favorable condition for establishment of relatively species-rich vegetation through decomposition of leaf litter. Trees on the south-facing slopes may produce nutrient-rich needles, then supply them as litter-fall to the ground. It is considered that foliage of trees and shrubs on south-facing slopes may have large amounts of nutrients available, if they have balanced nutrient conditions in needles (Oren and Schulze 1989). Under the nutrient rich condition of the south-facing slopes, physiological characteristics of photosynthesis and respiration lead to a prediction that larch may become more dominant in Central Siberia under a warm environment of the future induced by global climate change.

14.5.2 Nutrient Condition in Needles

As reflected in needle color, contents of nitrogen and chlorophyll in needles of larch and spruce growing on the south-facing slope were larger than those on the north-facing slope. Chlorophyll to nitrogen ratio (Chl/N) is one of the parameters, and represents nitrogen allocation to light harvesting protein (LHCP). The Chl/N ratio of larch and spruce needles on the north-facing slope was slightly larger than that on the south-facing slope during a latter part of the growing season in mid-August, but not earlier in the growing season. This means that light acclimation in the needles of larch and spruce occurred under a weak light accumulation during a lower position of incident sun light.

Nitrogen is the key element for photosynthetic activity; however, other nutrients also regulate physiological functions of plants. For example, light and CO_2 saturated photosynthetic rate of larch and spruce on north-facing slopes was lower, indicating that nutrient limitation might occur, especially ortho-phosphate deficiency in chloroplast (Sharkey 1985; Makino 1994; Koike et al. 1994; Tjoelker et al. 1998). Except for magnesium, elemental concentrations of potassium, phosphate, and calcium of larch needles on the south-facing slope and the valley were larger than those on the north-facing slope. Even though chlorophyll content in needles at the north-facing slope was larger (Koike et al. 1998b), there was no clear difference in magnesium concentration in the needles of both slopes. Magnesium is considered to be a key element for chlorophyll metabolism, so that both larch and spruce could keep enough amount of this element (data not presented).

14.5.3 Shrubs

Vegetation at high latitudes and on high mountains is usually affected by microenvironment through temperature and amount of solar radiation (e.g., Häsler 1982; Koike et al. 1994; Körner 1999). Microenvironment brings contrasting vegetation features, such as those on contrasting north- and south-facing slopes in Swiss Alps (Häsler 1982), Alaska, and northern Canada (Kojima 1994). In Siberia, many forest fires occur and the resulting ash contains many essential elements. Especially, process of vegetational recovery after forest fires is strongly dependent on microenvironment including nutrient condition through different degrees of resource requirements (Smith 1985). This environmental heterogeneity may provide several habitats for different types of plants.

In Central Siberia, vegetation is characterized by variation in shrubs and lichens in larch (*Larix gmelinii*) dominated forests, and spruce (*Picea obovata*) sometimes occurs on the north-facing slopes and/or wet sites especially along riversides and steams. Shrub and herb layers of a typical vegetation are composed of *Ledum palustre* and *Vaccinium vitis-idaea* on the north-facing slopes. It is composed of *Salix* sp.,

Betula nana, B. pendula, Deschekia fruticosa, V. vitis-idaea. Vacclaium uliginosum. Juniperus sp.*, and Lonicea* sp. on the south-facing slopes. After forest fires, the major species are seedlings of *L. gmelinii*, *Arctous elythrocarpa,* and *Epilobium* sp. on relatively moist sites (Yanagihara et al. 2000).

14.6 Light-Photosynthetic Curves

A set of light photosynthetic rates of some species of woody shrubs that grew on north- and south-facing slopes is shown in Figs. 14.5 and 14.6. Maximum net photosynthetic rate at light saturation (P_{sat}) of tree or these shrub species measured was in the order (from highest to lowest) of *Lonicea* sp., *Larix gmelinii, Betula nana, B. pendula, Duschekia fruticosa*, *Salix* sp., *Vaccinium uliginosum or V. vitis-idaea*, *Picea obovata,* and *Ledum palustre*. P_{sat} of *Juniperus sibirica* was the lowest among all species measured (Fig. 14.6). Among individuals of the same species, plants growing on the south-facing slopes had higher P_{sat} than those on the north-facing slopes. In general, maximum net photosynthetic rate (P_{sat}) is correlated positively with leaf mass per unit area (LMA; or reciprocal of SLA) (Reich et al. 1995). Accordingly, higher P_{sat} values on south-facing slope may be attributed to a larger value of LMA (or smaller SLA) (Koike et al. 1998b). However, there was little difference in P_{sat} of *L. gmelinii* found on both slopes in early part of a growing season (Koike et al. 1998b, 1999). In this sense, it may take some time for the larch needles to acclimate to diffuse low PPF condition of north-facing slopes.

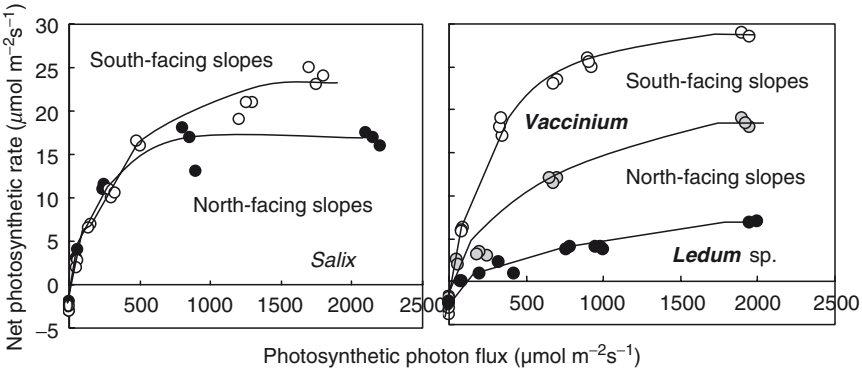

Fig. 14.5 Example of light-photosynthesis curves of some shrub species growing on the north- and south-facing slopes in the study site at Tura, Central Siberia. *Salix* sp.: same species in both slopes, but not identified exactly. *Vaccinium*: *Vaccinium vitis-idaea*. *Ledum* sp.: *Ledum pulstre* grows only on the south-facing slope. (Koike et al. 1998b, 1999, 2001; Koike et al., unpublished data)

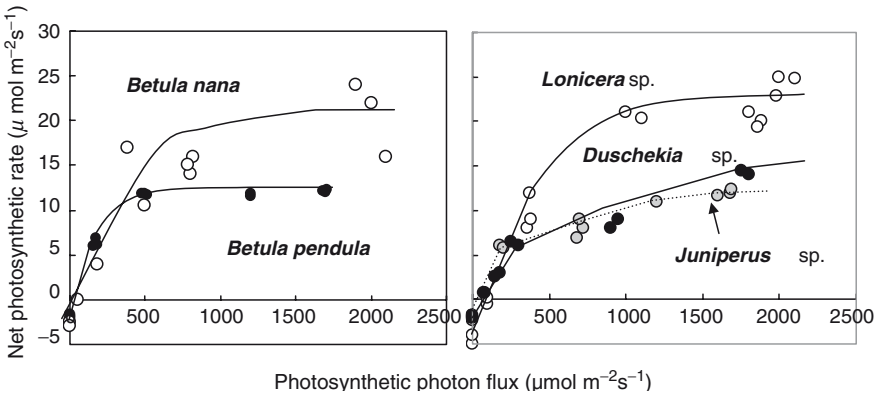

Fig. 14.6 Example of light-photosynthesis curves of some shrubs growing on the south-facing slope at the study site in Tura, Central Siberia. Among the examined species, *Juniperus* sp. (*Juniperus sibirica*) was found only on the south-facing slope (Koike et al. 1998b, 1999, 2001; Koike et al., unpublished data)

14.7 Chlorophyll Content

Chlorophyll content of leaves is one of the criteria of the light accumulating capacity of leaves (Larcher 2003). Leaf chlorophyll content of plants growing on contrasting slopes and in a community regenerating after a forest fire of 1994 (plot CR1994 on Site 2; see Fig. 1.3) was measured. On average, chlorophyll content of trees and shrubs on the south-facing slope was slightly larger than that on the north-facing slope (Koike et al. 1999). Chlorophyll content of *L. gmelinii* seedlings regenerated after a 1994 fire was the largest among the species tested (data not presented). Foliage nitrogen content was the highest in trees and shrubs at the 1994 burn site. Chlorophyll condition is also tightly connected to nitrogen status in the soil. In fact, mineralization of organic nitrogen may be accelerated there by higher soil temperature due to exposure to direct sunshine (Koike et al. 1998a, b; Matsuura and Abaimov 2000). After forest fires, regenerated seedlings and other plants had values of chlorophyll content similar to woody plants growing on the south-facing slope (Koike et al. 1999).

In general, chlorophyll b is tightly connected to light harvesting chlorophyll-protein complex (LHCP) (Larcher 2003). Therefore, chlorophyll a/b ratio is a good indicator of plants acclimating to shade environment (Kitaoka and Koike 2004). Amount of chlorophyll b in plants of north-facing slope was larger (thus chlorophyll a/b ratio smaller), which means that capacity of accumulating low PPF was larger in plants on the north-facing slope. Moreover, chlorophyll a/b ratio in plants of the south-facing slope was larger than that of the north-facing slope (Fig. 14.6). This may imply that light acclimation to low PPF occurred in plants on the north-facing slope where diffuse light is dominant. Tree canopies on different slopes may also alter light quality as well as light quantity differently (i.e., red/far-red ratio in light for understory plants) as found in a deciduous broadleaf forest (Lei et al. 1998).

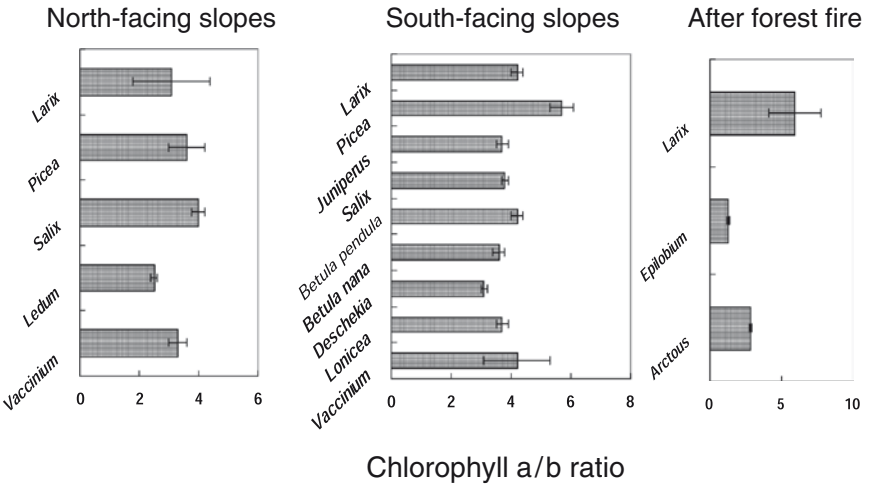

Fig. 14.7 Chlorophyll a/b ratio in trees and some shrubs growing on two contrasting slopes (*left*: north-facing, mid: south-facing) and nearby area that burned recently (*right*: young stand established after 1994 fire) (Koike et al. 1999)

The chlorophyll a/b ratio was the largest among all plants tested in seedlings of a young *L. gmelinii* stand regenerated after the 1994 fire (see right box in Fig. 14.7). This means that fire-regenerated larch seedlings have high acclimation to the open condition characterized by full sunlight and rich nutrient condition. Moreover, chlorophyll b is hardly degraded during leaf senescence (Koike 1990, 2004). In an open condition, chlorophyll b content of *L. gmelinii* was smaller. We expected a positive correlation between chlorophyll content and low PPF utilization capacity. Nevertheless, clear tendency was not found in the relationship between chlorophyll (a+b) or chlorophyll b and initial slope of the light curves. Of course, quantum yield in C_3 plants hardly changes with shade (Larcher 2003). Further study will be needed to elucidate the allocation pattern of nitrogen in the leaves in relation to light acclimation of shrubs native to Central Siberia.

14.8 Future Vegetation

Future vegetation is speculated in the area of Tura Experimental Forests in Central Siberia. After forest fires, depth of soil active layer becomes substantially deeper for some years with depth likely depending on fire intensity (Koike et al. 1998b; Makoto et al. 2007; Zyryanova et al. 2007; see also Chap. 4). According to a nutrient analysis of needles, young *L. gmelinii* seedlings regenerated after fire have higher nutrient content and larger shoot growth than seedlings of various species growing in a forest (Koike et al. 1998b). Based on the present analysis, nutrients in

soils and plants (Chapin et al. 1990) may be considered the determinant element pools for predicting future vegetation change. Furthermore, nutrient statuses of trees and tree growth are improved greatly with charcoal in the soil (Wardle et al. 1998; Makoto et al. 2009). In fact, larch seedlings regenerated after fire have higher nutrient concentration in the needles (Koike et al. 1998b). Further studies will be needed to analyze the ecological role of charcoal particles that are produced by forest fires (Wardle et al. 1998; Makoto et al. 2008; see also Chap. 21).

If greenhouse environment would progress further, depth of the soil active layer would become greater. This may lead to a large pool of available nutrients. Accordingly, larch as a light and nutrient demanding species might increase in plant size. We evaluated the temperature effects on the growth and gas exchange characteristics of tree species (e.g., larch, spruce) and shrub species, and on the contrasting north- and south-facing slopes at Tura Experiment Forest with an aim to estimate future vegetation changes and patterns of biomass production in Siberian "permafrost taiga." Soil temperature at 0–5 cm depth of the north-facing slope was 2–5°C lower than that of the south-facing slope. Needle lengths of larch and spruce on the north-facing slope were greater than those on the south-facing slope. Needle density was also different. Photosynthetic depression over the optimum temperature of larch growing on the south-facing slope was larger than that on the north-facing slope, which may imply that capacity of stomatal regulation was bigger in larch on the south-facing slope.

Light acclimation was found in the composition of chlorophyll a/b. Nitrogen concentration in needles of larch and spruce growing on the south-facing slope was higher than that on the north-facing slope. Shrubs showed high acclimation to shady condition at the north-facing slope with low chlorophyll a/b ratio. Based on the functional traits, it seems that larch may grow better in Central Siberia under the warm environment of the future that is likely to be induced by the global climate change. However, this change may also be regulated by the amounts and patterns of precipitation and the balance of evapotranspiration, which are out of the scope of the present chapter (see also Chaps. 13, 22, 23 and 24).

14.9 Conclusions

We compared photosynthetic light responses and leaf traits of larch, spruce, and representative shrub species growing on contrasting north- and south-facing slopes at Tura Experimental Forest in Central Siberia. We found clear difference in the depth of the "soil active layer" between two slopes, i.e., depth of active layer at the south-facing slope was around 150 cm, while that of the north-facing slope was around 30–40 cm. Based on this observation, possible changes in future vegetation were discussed with an assumption that future vegetation on the north-facing slope is what we see on the south-facing slope at present. Main findings are as follows:

- Length of internodes in trees (larch and spruce) on the north-facing slope was shorter than that on the south-facing slope.

- Light saturated photosynthetic rate of both species tested at the north-facing slope was lower than that at the south-facing slope.
- Chlorophyll content, Chl/Nitrogen ratio, and chlorophyll b content of leaves at north-facing slope were slightly larger than those at south-facing slope.

References

Arp WJ (1991) Effects of source-sink relations on photosynthetic acclimation to elevated CO_2. Plant Cell Environ 14:869–875

Boone RD, Nadelhoffer KJ, Canary JD, Kaye JP (1998) Roots exert a strong influence on the temperature sensitivity of soil respiration. Nature 396:570–572

Ceulemans R, Mousseau M (1994) Effects of elevated atmospheric CO_2 on woody plants. New Phytologist 127:425–446

Chapin FS III (1980) The mineral nutrition of wild plants. Ann Rev Ecol Syst 11:233–260

Chapin FS III, Schulze E-D, Mooney HA (1990) The ecology and economics of storage in plants. Ann Rev Ecol Syst 21:423–447

Hadley JL, Smith WK (1987) Influences Krummholz mat microclimate on needle physiolgy and survival. Oecologia 83:82–90

Häsler R (1982) Net photosynthesis and transpiration of *Pinus montana* at alpine timberline. Oecologia 54:14–22

Hollinger DY, Klliher FM, Schulze E-D, Bauer G, Arneth A, Byers JN, Hunt JE, McSeveny TM, Kobak KI, Milukova I, Sogatchev A, Tatarinov F, Varlargin A, Ziegler W, Vygodskaya VN (1998) Forest-atmosphere carbon dioxide exchange in eastern Siberia. Agr Forest Meteorol 90:291–306

Kasiscnke ES, Stocks BJ (2000) Fire, climate change, and carbon cycling in the boreal forest. Ecological studies, vol 138, Springer, Berlin, 461pp

Kitaoka S, Koike T (2004) Invasion of broadleaf tree species into a larch plantation: Seasonal light environment, photosynthesis, and nitrogen allocation. Physiologia Plantarum 121:604–611

Koike T (1987) Photosynthesis and expansion in leaves of the early, mid, and late successional tree species, birch, ash and maple. Photosynthetica 21:503–508

Koike T (1990) Autumn coloring, photosynthetic performance and leaf development of deciduous broad-leaved trees in relation to forest succession. Tree Physiol 7:21–32

Koike T (1995) Effects of CO_2 in interaction with temperature and soil fertility on the foliar phenology of alder, birch, and maple seedlings. Canadian Journal of Botany 73:149–157

Koike T (2004) Autumn coloration, carbon acquisition, and leaf senescence. In: Noodén LD (ed) Plant cell death processes. Elsevier, Amsterdam, pp 245–258

Koike T, Häsler R, Item H (1994) Leaf longevity and photosynthetic performance of Swiss stone pine and Norway spruce planted on the north- and east-facing slopes of the timberline of Stillberg/Switzerland. USDA INT-GTR 309, pp 78–80

Koike T, Mori S, Matsuura Y (1998a) An introduction to the study on effects of global warming in eastern Siberian taiga. Hoppo Ringyo (Northern Forestry) 50:241–244 (in Japanese)

Koike T, Mori S, Matsuura Y, Prokushkin SG, Zyranova OA, Kajimoto T, Abaimov AP (1998b) Photosynthesis and foliar nutrient dynamics in larch and spruce grown on contrasting north- and south-facing slopes in the Tura Experiment Forest in central Siberia. In: Mori S, Kanazawa Y, Matsuura Y, Inoue G (eds) Proceedings of the Sixth Symposium on the Joint Siberian Permafrost Studies between Japan and Russia in 1997. Tsukuba, pp 3–10

Koike T, Mori S, Matsuura Y, Prokushkin SG, Zyryanova OA, Kajimoto T, Sasa K, Abaimov AP (1999) Shoot growth and photosynthetic characteristics in larch and spruce affected by temperature of the contrasting north and south facing slopes in eastern Siberia. In: Shibuya M,

Takahashi K, Inoue G (eds) Proceedings of Seventh Symposium on the Joint Siberia Permafrost Studies between Japan and Russia in 1998. Tsukuba, pp 3–12

Koike T, Wang W, Kitaoka S, Mori S, Matsuura Y, Prokushkin AS, Zyryanova OA, Prokushkin SG, Abaimov AP (2001) Photosynthetic light curves of trees and shrubs grown under contrasting north-and south-facing slopes in central Siberia. In: Fukuda M, Kobayashi Y (eds) Proceedings of Ninth Symposium on the Joint Siberia Permafrost Studies between Japan and Russia in 2000. Hokkaido University, Sapporo, pp 35–41

Kojima S (1994) Boreal ecosystems and global climatic warming. Jpn J Ecol 44:105–113 (in Japanese)

Körner Ch (1999) Alpine plant life: functional plant ecology of high mountain ecosystems. Springer, Berlin

Kujansuu J, Yasue K, Koike T, Abaimov AP, Kajimoto T, Takeda T, Tokumoto M, Matsuura Y (2007) Responses of ring widths and maximum densities of *Larix gmelinii* to climate in contrasting north- and south-facing slopes in central Siberia. Ecological Research 22:582–592

Larcher W (2003) Physiological plant ecology, 4th edn. Springer, Berlin

Lei TT, Tabuchi R, Kitao M, Takahashi K, Koike T (1998) Effects of season, weather and vertical position on the light variation in quantity and quality in a Japanese deciduous broadleaf forest. J Sustainable For 6:35–55

Makino A (1994) Biochemistry of C_3-photosynthesis in High CO_2. J Plant Res 107:79–84

Makoto K, Nemilostiv YP, Zyryanova OA, Kajimoto T, Matsuura Y, Yoshida T, Satoh F, Sasa K, Koike T (2007) Regeneration after forest fires in mixed conifer broad-leaved forests of the Amur region of Far Eastern Russia: the relationship between species specific traits against fire and recent fire regimes. Eurasian J For Res 10:51–58

Makoto K, Kim YS, Nomura M, Shibata H, Satomura T, Kamiura T, Hojyo H, Takahashi H, Kotsuka C, Sakai R, Takagi K, Satoh F, Sasa K, Koike T (2008) Effects of prescribed burning on the available nitrogen and phosphorous in soil of a bamboo dominated forest in the Hokkaido. Trans Meet Jpn For Soc Hokkaido 56:29–32 (in Japanese)

Makoto K, Tamai Y, Kim YS, Koike T (2009) Buried charcoal layer and ectomycorrhizae cooperatively promote the growth of *Larix gmelinii* seedlings. Plant and Soil . doi:10.1007/s1114-009-0040-z

Matsuura Y, Abaimov AP (2000) Nitrogen mineralization in larch forest soils of continuous permafrost region, central Siberia -an implication for nitrogen economy of a larch forest stand. In: Inoue G, Takenaka A (eds) Proceedings of the Eighth Symposium on the Joint Siberia Permafrost Studies between Japan and Russia in 1999. National Institute for Environmental Studies, Tsukuba, pp 129–134

Mooney HA, Drake BG, Luxmoore RJ, Oechel WC, Pitelka LF (1991) Prediction of ecosystem responses to elevated CO_2 concentrations. BioScience 41:96–104

Näsholm T, Ekbald A, Nordln A, Glesler R, Högberg M, Högberg P (1998) Boreal forest plants take up organic nitrogen. Nature 392:914–916

Oechel WC, Billings WD (1992) Anticipated effects of global change on carbon balance of arctic plants and ecosystems. In: Chapin FS III, Jefferies R, Reynolds J, Shaver G, Svoboda J (eds) Arctic physiological processes in a changing climate. Academic, San Diego, pp 139–168

Oren R, Schulze E-D (1989) Nutritional disharmony and forest decline: a conceptual model. In: Schulze E-D, Lange OL, Oren R (eds) Air pollution and forest decline. Ecolgical Stuies, vol 77, Springer, Berlin, pp 425–443

Reich PB, Koike T, Gower ST, Schoettle AW (1995) Causes and consequences of variation in conifer leaf life-span. In: Smith WK, Hinckey TM (eds) Ecophysiology of coniferous forest. Academic, San Diego, pp 225–254

Saxe H, Ellsworth DS, Heath J (1998) Tree and forest functioning in an enriched CO_2 atmosphere. New Phytologist 139:395–436

Schulze E-D, Schulze W, Kelliher FM, Vygodskaya NN, Ziegler W, Kobak KI, Koch H, Ameth WA, Kusnetsova A, SoRatche A, Issajev A, Bauer G, Hollinger DY (1995) Aboveground

biomass and nitrogen nutrition in a chronosequence of pristine Dahurian *Larix* stands in eastern Siberia. Canadian Journal of Forest Research 25:943–960

Sharkey TD (1985) Photosynthesis in intact leaves of C_3 plants: physics, physiology and rate limitations. Botanical Review 51:53–105

Shinano T, Lei TT, Kawamukai T, Inoue MT, Koike T, Tadano T (1996) Dimethylsulfoxide method for the extraction of chlorophylls a and b from the leaves of wheat, field bean, dwarf bamboo, and oak. Photosynthetica 32:409–415

Smith WK (1985) Western montane forests. In: Chabot BF, Mooney HA (eds) Physiological ecology of North American plant communities. Chapman and Hall, New York, pp 95–126

Strain BR (1985) Direct effects of increasing CO_2 on plants and ecosystems. Trend Ecol Evol 2:18–21

Terashima I, Masuzawa T, Ohba H (1993) Photosynthetic characteristics of a giant alpine plant *Rheum nobile* Hook. et Thoms. and of some other alpine species measured at 4300m in the eastern Himalaya, Nepal. Oecologia 95:194–201

Tjoelker MG, Oleksyn J, Reich PB (1998) Seedlings of five boreal tree species differ in acclimation of net photosynthesis to elevated CO_2 and temperature. Tree Physiol 18:715–726

Wardle DA, Zackrisson O, Nilsson M-C (1998) The charcoal effect in boreal forests: mechanisms and ecological consequences. Oecologia 115:419–426

Yanagihara Y, Koike T, Matsuura Y, Mori S, Shibata H, Satoh F, Masyagina OV, Zyryanova OA, Prokushkin AS, Prokushkin SG, Abaimov AP (2000) Soil respiration rate on the contrasting north- and south-facing slopes of a larch forest in central Siberia. Eurasian J For Res 1:19–29

Zyryanova OA, Yabarov VT, Tchikhacheva TL, Koike T, Makoto K, Matsuura Y, Satoh F, Zyryanova VI (2007) The structure and biodiversity after fire disturbance in *Larix gmelinii* (Rupr.) Rupr. forests, northeastern Asia. Eurasian J For Res 10:19–29

Chapter 15
Respiration of Larch trees

S. Mori, S.G. Prokushkin, O.V. Masyagina, T. Ueda, A. Osawa, and T. Kajimoto

15.1 Introduction

Modeling of trees based on whole-plant physiology is a powerful tool to understand function and structure of forest ecosystems (Yoda et al. 1963; Hozumi and Shinozaki 1974; McCree 1983; Sievänen et al. 1988; Hagihara and Hozumi 1991; Mori and Hagihara 1991; Shugart et al. 1992; Watanabe et al. 2004). In particular, whole-plant carbon budget is a sensitive and biologically meaningful indicator to understand plant responses to environmental changes (McCree 1986, 1987; Adams et al. 1990; Gonzàlez-meler and Siedow 1999; Tjokelker et al., 1999). Single-leaf physiology does not predict plant growth and productivity, since individual leaves do not always reflect the physiological behavior of the whole-plant (Sims et al. 1994; Hikosaka et al. 1999). Nevertheless, whole-plant physiological characteristics have been measured only in crops, grasses, horticultural crops, and juvenile trees, whose body sizes are relatively small compared to mature forest trees (Geis 1971; Peters et al. 1974; Reicosky and Peters 1977; Garrity et al. 1984; Meyer et al. 1987; Dutton et al. 1988; Graham 1989; Berard and Thurtell 1990; Bower et al. 1998; Nogués et al., 2001). Because measurement of mature trees requires extensive set-up for controlling temperature and gas exchange, air conditioning units (Meyer et al. 1987) with supply of alternating current are commonly required. However, such a system is generally unavailable in the field in remote areas. In particular, boreal and tropical forests are usually located at remote sites, where elaborate measurement set-up cannot be operated. Therefore, a new system is necessary for measuring the whole-tree respiration with relatively simple equipment.

Respiratory consumption in forest ecosystems is thought to be the main parameter determining CO_2 budget (Valetini et al. 2000). Plant respiration is generally affected by a small number of environmental factors (mainly temperature) in contrast to photosynthesis (light, temperature, and other factors) (e.g., Sprugel et al. 1995). Therefore, plant respiration would be a good indicator to evaluate the carbon budget. Particularly, temperature dependency of whole-tree respiration will be an important information in predicting response of a given forest ecosystem to warming temperature. However, previous studies on whole-tree respiration have been generally

A. Osawa et al. (eds.), *Permafrost Ecosystems: Siberian Larch Forests*, Ecological studies, Vol. 209, DOI 10.1007/978-1-4020-9693-8_15,

restricted to night measurements without temperature controls (Ninomiya and Hozumi 1981, 1983a; Adu-bredu et al. 1996a, 1996b; Yokota and Hagihara 1996, 1998). Therefore, improvements are required of such methods in order to estimate both daytime and night respiration rates more accurately.

Such a system for whole-tree respiration measurement was developed for use in intact trees in the field, under regulated air-temperature. It uses a closed air-circulation system that does not require constant supply of alternating electric current. This method was then applied for trees in an old stand of *Larix gmelinii* (Rupr.) Rupr in Central Siberia. This species is distributed widely in the continuous permafrost region, often as monospecific stands (see Chap. 1), and seems to play a key role in terrestrial carbon cycling of boreal forests. Extent of annual carbon fixation and release by heterotrophic soil respiration in old larch forests in Siberia appears small (see Chaps. 6, 9, and 10), but the process of CO_2 consumption by autotrophic respiration still remains unclear.

In this chapter, we first introduce the new system for measuring whole-tree respiration, and discuss its methodological advantages and limitations. Second, we examine temperature dependency of *L. gmelinii* tree respiration and its variation in relation to individual size. Third, we estimate stand-level aboveground total respiration rate during a growing season, then discuss how the respiratory CO_2 release is associated with aboveground net primary production (ANPP) and net ecosystem production (NEP) in the permafrost larch forest.

15.2 Approaches and Measurement System

15.2.1 Study Site

Whole-tree aboveground respiration was measured in an old multiaged *L. gmelinii* stand (>220 years-old; plot C1) of Site 2 located near the settlement of Tura, Central Siberia (64°N, 100°E) (location see Fig. 1.3). Detailed characteristics of this stand are summarized in Fig. 6.1 and Table 6.1, and climate, and geological and floristic conditions of the study area are described elsewhere (Chaps. 1 and 2).

Measurement of whole-tree aboveground respiration was conducted during two summers (from July to August in 1997–1998). During the periods, thickness of soil active layer (i.e., depth from the ground surface to permafrost table) was about 30 cm.

15.2.2 Setting Whole-Plant Chamber

Sample trees (details see Sect. 15.2.6) were enclosed singly in a cylindrical whole-plant dark chamber. The chamber was fixed at 1.2 m in diameter, but its length was flexible from 4 to 9 m according to tree height. We framed the chamber using flexible

fiberglass rings (Fig. 15.1b), so that volume of the chamber is calculated easily. Around these sample trees, we constructed a wooden tower of about 10 m tall to hang the chamber (Figs. 15.1a and 15.2). The chamber was made of three kinds of films: 0.2 mm thick polyvinyl chloride transparent film at the very inside to keep CO_2 tightness, 0.03 mm thick polyvinyl chloride black film to achieve total darkness, and double layered 0.015 mm thick aluminum-coating films to reflect radiation.

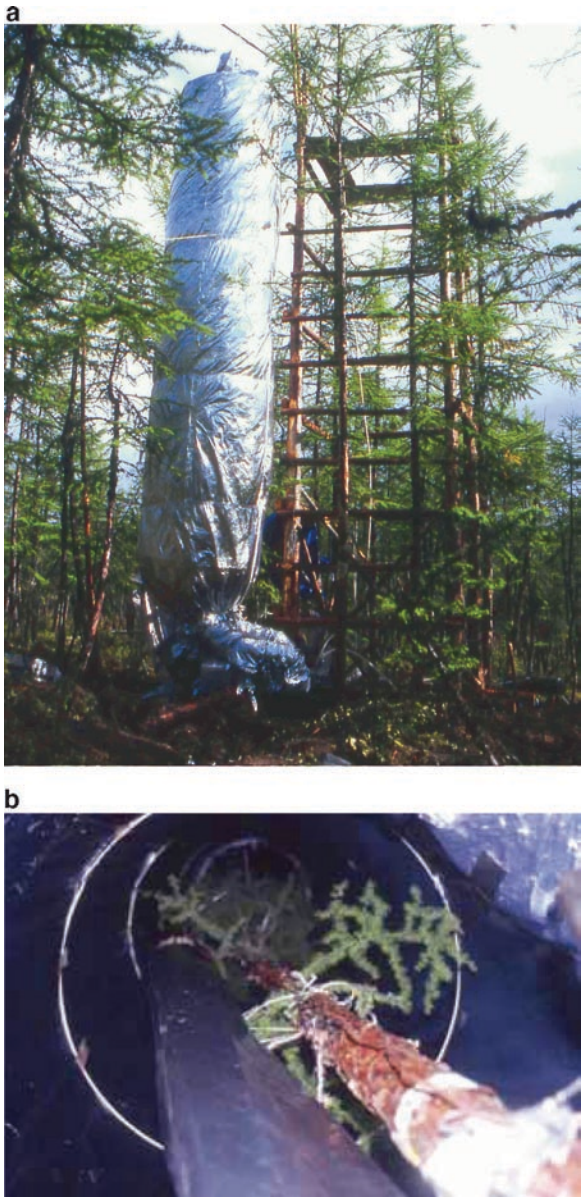

Fig. 15.1 A chamber enclosing a standing *L gmelinii* tree (No.2). (**a**) The chamber was hanged from a mast system set at the top of a wooden tower. (**b**) Inside view of a chamber. Volume, length, and diameter of the chamber were about 9 m^3, 8 m, and 1.2 m, respectively (photo: Mori)

After measuring larger trees, we cut and removed the bottom of the long chamber for enclosing smaller trees. The chamber volume ranged from 4.3 to 10 m^3.

15.2.3 Closed Air-Circulation System

A closed air-circulation was achieved by connecting the whole-plant chamber to a heat exchanger with air ducts of 20 cm in diameter (Fig. 15.2). After enclosing a sample tree, we circulated the enclosed air by an electric fan equipped at the upper part of the heat exchanger. As shown in Fig. 15.1b, launched air tracked up the air duct to the top of the chamber. The air duct bore small holes on the sidewall to avoid heterogeneous CO_2 concentration within the chamber. We set a bypass to the closed air-circulation system, which acted as a transient CO_2 scrubber. This was detached from the system by two air-shutters during measurement. We kept air-tightness at the connection of the stem and the chamber by clogging clay that does not absorb CO_2. A preliminarily test of air-leakage showed no decrease in CO_2 concentration at about 900 ppm for about 30 min.

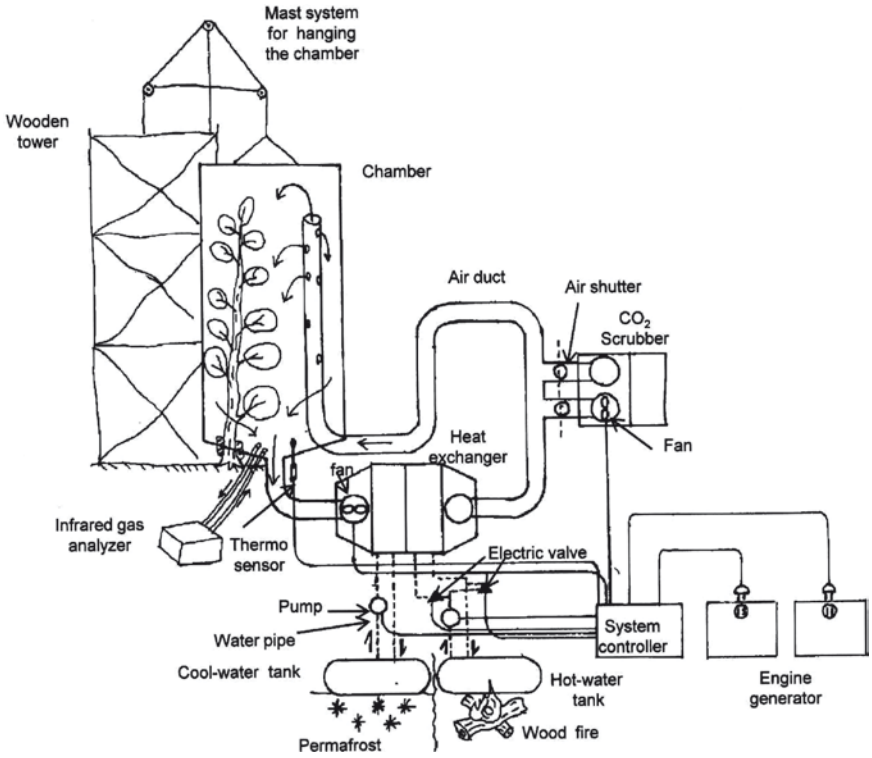

Fig. 15.2 Schematic representation of the system of whole-tree respiration measurement (modified from Mori et al. 1997)

15.2.4 CO_2 Scrubber

The scrubber consisted of an air filter filled with soda-lime granules to absorb CO_2 (Fig. 15.2). Before the measurement, we reduced CO_2 concentration within the system to the field level to avoid CO_2 leakage from the closed system. Bouma et al. (1997) reported that high CO_2 partial pressure did not disturb respiration. Therefore, we did not eliminate high CO_2 partial pressure in the closed system.

15.2.5 Temperature Control

To control air temperature within the chamber, we utilized natural heat energy generated from wood fire and permafrost (Fig. 15.2). Natural heat energy was captured by two steel water tanks of about 40 L each. The tank for cooling was buried under ground to have a direct contact with frozen soil (i.e., permafrost table was about 30 cm deep). The tank for hot water was heated by wood fire. We circulated the hot and cool water from the tanks to a heat exchanger through water pipes (Fig. 15.2). Hot water flow was continuously regulated by two electric water valves and the cool water flow by turning the water pump on and off through the PID controlled algorithm program on a personal computer. The air circulated about 50 times per hour in the largest-sized chamber; we confirmed that this rate was enough to maintain an even CO_2 environment within the chamber. Heating and cooling ability of the heat exchanger (Hokkaido DALTON Co., Sapporo, Japan) were 1 and 0.6 kW h^{-1}, respectively, when the air temperature and relative humidity within the chamber were 20°C and 60%, respectively. We operated the system using two handy engine generators of 5 kg and 352 VA power output (KH350HA, Kokusan Electric Co. Ltd., Shizuoka, Japan).

15.2.6 Measurement of Whole-Tree Respiration

Breast-height stem diameter (DBH) and tree height of six *L. gmelinii* trees examined were as follows: 9.6 cm and 8.8 m (No.1), 8.0 cm and 7.7 m (No.2), 7.6 cm and 6.9 m (No.3), 6.3 cm and 6.4 m (No.4), 3.4 cm and 4.2 m (No.5), and 3.0 cm and 4.1 m (No.6). Among them, two individuals (No.2, 4) were selected for assessing temperature dependency of respiration by changing air-temperature within the chamber at various levels (from ca.10 to 30°C). This measurement was conducted on the same day, and $n > 20$ datasets (respiration vs. temperature) were obtained for each tree. Respiration rates of the other four trees were measured at a given level of controlled-temperature (around 20°C).

For all trees, relatively short incubation period was applied, ranging from 20 to 60 s. CO_2 concentration within the chamber was measured every 2 s by the portable gas analyzer (LI-6200, LI-COR, Lincolon, USA). A whole-tree aboveground

respiration R (expressed by μmole mole^{-1} tree^{-1} s^{-1}) was calculated with the following equation:

$$R = V(273.2 / (273.2 + \theta))(10^3 / 22.4)\,\mathrm{d}C / \mathrm{d}t, \tag{15.1}$$

where V is chamber volume (m^3), θ is air-temperature inside chamber (°C), and dC is increment of CO_2 concentration during incubation time of dt. The term dC/dt indicates a mean increment rate of CO_2 concentration (μmole mole^{-1} tree^{-1} s^{-1}). The (15.1) assumes that respiration is measured under standard barometric pressure and the volume of enclosed tree was negligible compared to the chamber volume (Yokota et al. 1994).

15.3 System Response and Estimated Tree Respiration

15.3.1 Temperature Control of the System

For the sample trees No. 2 and No. 4, air temperature within the chamber was increased step by step according to the program. In the case of tree No.2 (Fig. 15.3), for example, we regulated air-temperature inside the chamber (shown by closed squares; chamber volume 8 m^3) to closely follow the programmed course of temperature (open squares) from 15 to 27°C. We also minimized overshooting of air temperature by the PID algorithm for realizing respiration measurement under stable air temperature. The temperature within this large chamber was efficiently controlled, even if the programmed temperature was about 10°C higher than the ambient air temperature (closed squares in Fig.15.3). Similar result was obtained for the other tree (No.4) (Mori et al., unpublished data). Thus, the temperature could be adjusted to a target value with good accuracy; however, temperature inside the chamber was affected slightly by the ambient temperature when the difference became greater than 10°C (see diversion of filled circles and open circles between 14:50 and 15:50 in Fig. 15.3).

15.3.2 Temperature Dependency of Whole-tree Respiration

Figure 15.4 shows an example of the relationship between incubation time and CO_2 concentration observed for a larger tree (No.2) under regulated temperature condition. The CO_2 concentration increased linearly with time, and its mean increment rate (dC/dt) was about 0.056 μmole mole^{-1} tree^{-1} s^{-1} as indicated by a linear regression (Fig. 15.4). Likewise, CO_2 emitted by respiration accumulated almost constantly within the chamber in all cases. Thus, we calculated mean CO_2 increment rate (dC/dt) at each controlled-temperature, then determined the whole-tree respiration rate (R) using the (15.1).

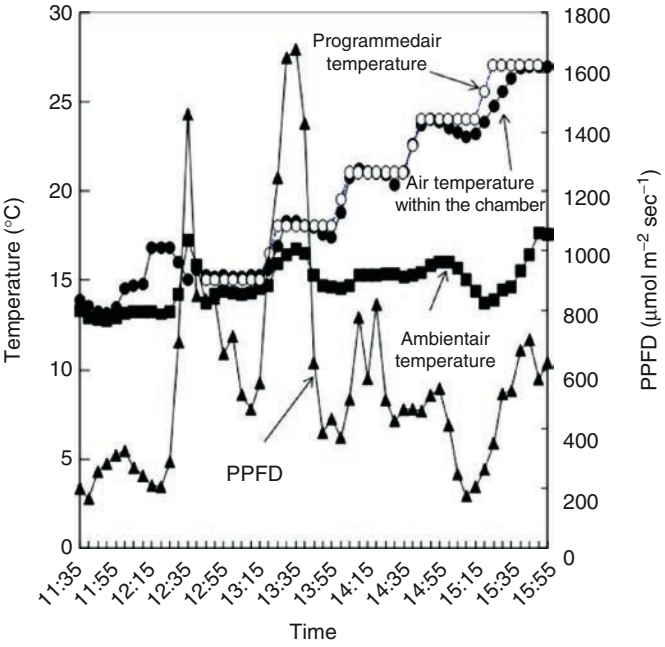

Fig. 15.3 Fluctuations in regulated air temperature within the chamber (*filled circle*), ambient air temperature (*filled square*), programmed air temperature (*open circle*), and photosynthetically active radiation (PPFD; *filled triangle*). Data were obtained from a large *L. gmelinii* tree (No.2) in mid-August (Mori et al., unpublished data)

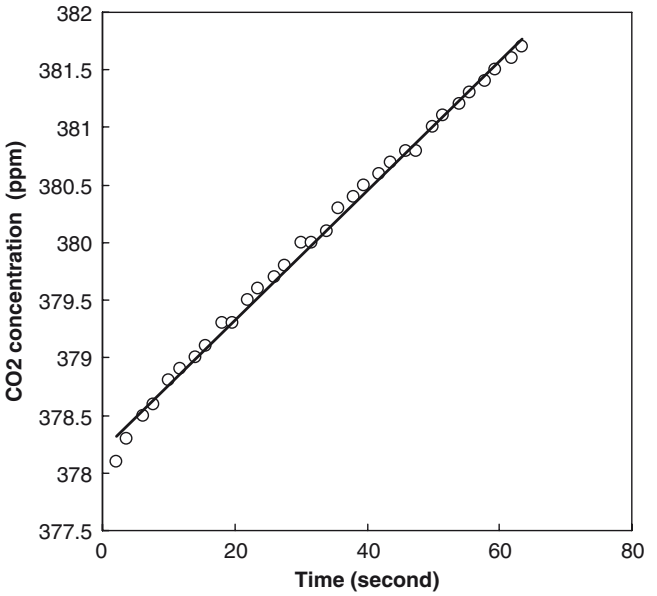

Fig. 15.4 An example of CO_2 increment (µmole mole^{-1} tree^{-1} s^{-1}) within the chamber. Data were obtained from a *L. gmelinii* tree No.4. Regression line was approximated by CO_2 [ppm] = $0.0562t + 378.2$ ($r^2 = 1.00$) (Mori et al. unpublished data)

Exponential relationships were found between whole-tree aboveground respiration (R) and air-temperature inside chamber for two sample trees (Fig. 15.5). The value of R for a given temperature was much higher in the larger individual (No.2; closed circles) than in the smaller one (No.4; open circles). However, temperature dependency of R did not differ significantly between these trees ($p > 0.05$), though the regression slope appeared somewhat larger in No.2 (0.074) than that in No.4 (0.054). According to each regression, the extent of respiration increase per temperature increase of 10°C (i.e., Q_{10} value) was calculated to be 2.1 (No.2) and 1.7 (No.4).

15.3.3 Size Dependency of Whole-tree Respiration

Whole-tree respiration rate at 20°C (R^*) was positively correlated with stem diameter (DBH) among the six trees examined. Here, R^* was the corrected respiration value by assuming $Q_{10} = 2$ in all examined trees; the assumption was based on the similarity of temperature dependency of whole-tree aboveground respiration in the two sample trees (Fig. 15.5). The difference of R^* reached nearly tenfold between the smallest (DBH = 3 cm) and the largest (10 cm) individuals.

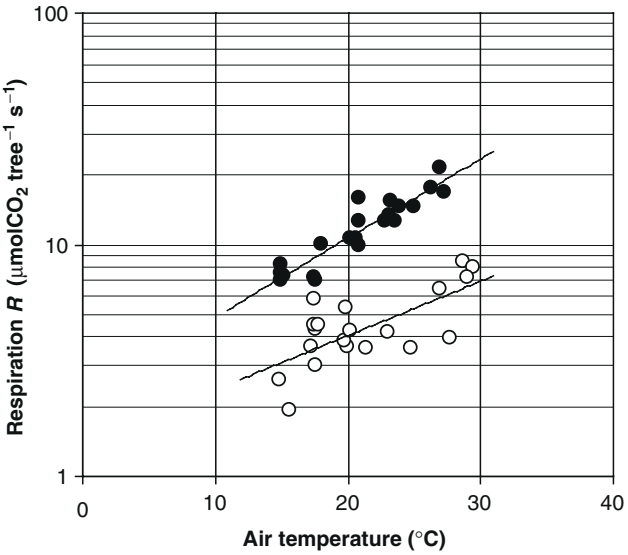

Fig. 15.5 Dependence of whole-plant respiration (R) on air-temperature (θ) for two *L. gmelinii* trees. Regression lines and symbols are as follows: $R = 2.22e^{0.074\theta}$ ($R^2 = 0.858$) for tree No.2 (*filled circle*), and $R = 1.38e^{0.054\theta}$ ($R^2 = 0.494$) for tree No.4 (*open circle*). Slopes of two regressions did not differ significantly ($F_{[1, 39]} = 2.54$, $p = 0.12$; ANCOVA) (Mori et al., unpublished data)

15.3.4 Estimation of Stand-Level Aboveground Respiration

We estimated stand-level respiration rate of the old multiaged *L. gmelinii* forest by applying the mean-sized method proposed by Ninomiya and Hozumi (1983b). Stand-level respiration is obtained by multiplying a respiration rate of the mean-sized tree by tree density of the forest. The estimate by this approach was reported to be similar to those estimated by two other methods (Ninomiya and Hozumi 1983b). Tree No.4 was selected as the mean tree, since its size was the closest to the mean DBH (6.3 vs. 6.8 cm) of the study stand.

Daily whole-tree aboveground respiration rate was calculated as the value at daily mean air-temperature by using the coefficients of regression between temperature and R for the sample tree (Fig. 15.5), and stand-level respiration was obtained by multiplying it by tree density (1,910 ha^{-1}). We assumed that respiration occurred potentially during four summer months (from early June to late September) when daily mean air-temperature generally exceeded 0°C. Then, annual stand-level aboveground respiration (R_{AT}) was estimated by summing up the daily respiration during this period. For evaluating the extent of year-to-year fluctuation of the estimates, we used air-temperature data that were recorded in the stand during four consecutive years (2001–2004) (see Fig. 16.7a, Chap. 16).

The estimate of stand-level aboveground respiration (R_{AT}) during these four seasons ranged from 2.23 to 2.81 $kgCO_2\ ha^{-1}\ year^{-1}$. On the basis of organic matter dry mass, the range corresponds to 1.37–1.73 Mg $ha^{-1}y^{-1}$, and is averaged 1.56 Mg $ha^{-1}y^{-1}$: a conversion factor = 0.614 was used (e.g., Yokota et al. 1994).

15.4 Evaluation of Measurement System

Present study applied a new closed air-circulation system to directly measure CO_2 release from aboveground parts of a whole tree. Our system has advantages compared to previous methods using a whole-tree enclosed chamber (e.g., Ninomiya and Hozumi 1981; Adu-bredu et al. 1996a; Yokota et al. 1994). First, the system enables us to determine the respiration rate at desirable and stable temperature levels in the field. Second, we do not need to consider dissolved CO_2 in water vapor which cannot be detected by infrared gas analyzer, since vapor from a plant body is considered negligible under the dark condition. Third, respiration rate is determined using one infrared gas analyzer. An open-system usually requires two analyzers to detect CO_2 concentration at both inlet and outlet of the system, and requires frequent calibration. Our closed system does not need to calibrate the CO_2 analyzer frequently. Lastly, the present system balances CO_2 concentration by attaching a CO_2 scrubber, by which leakage of CO_2 from the system can be ignored completely. Another improvement is the utilization of natural heat energy (i.e., permafrost and fire wood) for controlling air-temperature inside chamber. Although these energy sources may be applicable only in our study region, they enabled us to measure many sample trees in the field without an extensive unit of power-requiring air conditioning.

We used a dark chamber to solve problems specific to measurements of whole-plant respiration during a daytime. Because the up-streaming sap flow in the daytime cools down stem temperature near the ground, temperature of a whole plant body shows heterogeneity (Negisi 1974). Respiration rate of a lower part of the stem shows higher value than the other parts, which has a 44% share of the total stem respiration (Mori and Hagihara 1988, 1991). Sap-flow in the daytime probably interferes measurement of whole-plant respiration under a stable temperature. Hence, it was necessary to depress the sap flow of sample trees by a dark chamber. In the present system, temperature heterogeneity of the plant body was minimized. Therefore, the present set-up might serve as a better system to estimate respiratory potential of a whole-plant under a stable temperature.

However, limitations of the present system must also be considered. For example, an open system is suited to long-term monitoring of gas-exchange as demonstrated by Adu-bredu et al. (1997), while our closed system is not currently applicable to such continuous measurements. Therefore, modification of the present system to suit long-term monitoring of physiological dynamics should be considered a next challenge.

15.5 Aboveground Respiration and Production

The values of stand-level aboveground respiration (R_{AT} = 1.6 Mg ha^{-1}y^{-1}) estimated for the old *L. gmelinii* forest (plot C1) are somewhat larger than ANPP of the same stand (1.3 Mg ha^{-1} year^{-1})(Kajimoto et al. 1999), and those of other old stands (>100 years-old; 0.5–0.8 Mg ha^{-1} year^{-1})(see also Table 6.3). However, the estimate of stand-level aboveground respiration (R_{AT}) may be overestimated, because it includes respiration when *L. gmelinii* does not hold needles (i.e., early June and late September). In the study area, larch needles generally start to flush in late May or early June, but develop fully after mid-June (see Sect. 17.3). They begin to fall from early to mid-September. However, our estimate of stand-level aboveground respiration (R_{AT}) was based on the respiration rate at a whole-tree level (i.e., including needles). Individual respiration rate that was used for the present calculation of stand-level aboveground respiration (R_{AT}) was measured only for midsummer, when needles were fully developed and functioned actively. These considerations suggest that annual aboveground respiration rate of the stand and ANPP may be similar, or carbon loss due to aboveground respiratory consumption may be nearly balanced with annual net carbon gain (Fig. 15.6).

Present data are still limited in estimating stand-level aboveground larch respiration accurately due to both small sample size and short observation period. Nevertheless, the obtained stand-level aboveground respiration (R_{AT} = ca. 80 gC m^{-2} year^{-1} at carbon basis) falls in a value similar to net ecosystem production (NEP = 70–80 gC m^{-2} year^{-1}) estimated with the eddy covariance technique in another old stand (ca. 105 years-old) of *L. gmelinii* (plot CF in Carbon Flux Site) located in the same region (Nakai et al. 2008; details see Chap. 10).

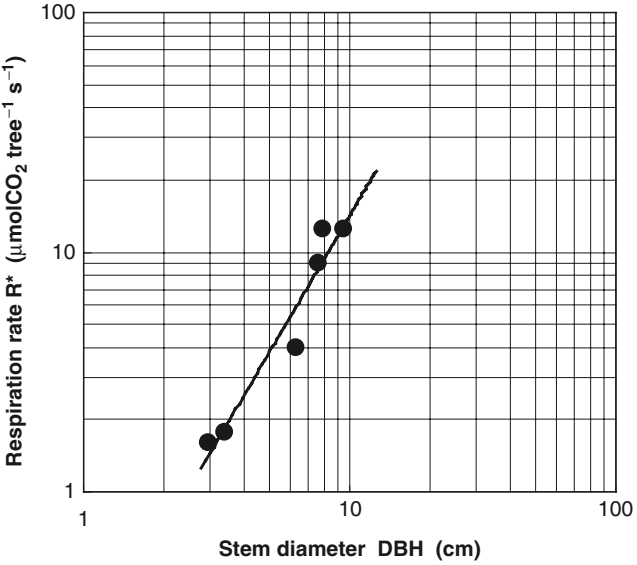

Fig. 15.6 Relationship between stem diameter at breast height (DBH) and aboveground respiration rate (R^*) for six *L. gmelinii* sample trees. The R^* values were corrected for temperature at 20°C; correction was made by assuming $Q_{10}=2$ (see Fig. 14.5). Regression line was significant ($r^2=0.94$, $p<0.01$) (Mori et al., unpublished data)

Similarity of these estimates suggests that aboveground respiratory CO_2 consumption of larch trees is a major component of ecosystem carbon flow.

However, NEP is a balance between carbon gain by plant photosynthesis and carbon release due not only to autotrophic respiration, but also to heterotrophic respiration. Without data of both elements, it is not possible to determine to what extent plant (larch) respiration contributes to total ecosystem carbon flux (see Chap. 24). Particularly, root respiration must be quantified, though its measurement under field conditions is generally difficult. According to our preliminarily trial of *in situ* measurement with a small chamber attached to intact roots, temperature dependency of root respiration maybe somewhat different from that of aboveground parts (Mori et al. 1997; Mori et al., unpublished data). Thus, further examination of both aboveground and root respiration is necessary to determine components of ecosystem respiration, and whether the permafrost larch forest is functioning as a carbon sink or source.

15.6 Conclusions

A new measurement system of whole-tree aboveground dark respiration was developed using a large cylindrical dark chamber, and was applied to an old *L. gmelinii* forest in Central Siberia. We used closed air-circulation system, and determined respiration

rate on the basis of CO_2 accumulation rate within the chamber system equipped with a CO_2 scrubber. To control air temperature within the chamber, we supplied hot and cool water by either heating or cooling the tanks with wood fire or permafrost. Although the present method has limitations, it also has methodological advantages: inside-chamber temperature was controlled easily at desirable levels, and relatively short time was required for measurement.

Whole-tree aboveground respiration rate increased with temperature, and its temperature dependency was similar between two individuals examined: Q_{10} value was nearly equal to 2. Based on the measurement of a mean-sized sample tree, stand-level aboveground respiration rate was estimated to be about 1.6 Mg $ha^{-1}y^{-1}$, by assuming that temperature dependency of respiration was constant and growing season was 4 months (from June to September). This estimate was evaluated in relation to the estimated ANPP in an old stand, suggesting that net carbon gain was nearly balanced with respiratory carbon release. It was also indicated that CO_2 release by aboveground larch respiration was a major component of total carbon flux in the permafrost larch forest ecosystem.

Acknowledgments. Authors thank their colleagues of V.N. Skachev Institute of Forest and Dr. Viktor M. Borovikov for their kind support during field measurement. This study was financially supported in part by Japan Environmental Agency.

References

Adams MB, Edward NT, Tayler GE Jr, Skkags BL (1990) Whole-plant ^{14}C-photosynthesis allocation in *Pinus taeda*: seasonal patterns at ambient and elevated ozone level. Can J For Res 20:152–158

Adu-bredu S, Yokota T, Hagihara A (1996a) Respiratory behaviour of young hinoki cypress (*Chamaecyparis obtuse*) trees under field condition. Ann Bot 77:623–628

Adu-bredu S, Yokota T, Hagihara A (1996b) Carbon balance of the areril parts of a young hinoki cypress (*Chamaecyparis obtuse*) stand. Tree Physiol 16:239–245

Adu-Bredu S, Yokota T, Hagihara A (1997) Long-term respiratory cost of maintenance and growth of field-grown young hinoki cypress (*Chamaecyparis obtusa*). Ann Bot 80:753–758

Berard RG, Thurtell GW (1990) Respiration measurements of maize plants using a whole-plant enclosure system. Agron J 82:641–643

Bouma TJ, Nielsen KL, Eissenstat DM, Lynch PL (1997) Soil CO_2 concentration does not affect growth or root respiration in bean or citrus. Plant Cell Environ 20:1495–1505

Bower JH, Jobling JJ, Patterson BD, Ryan DJ (1998) A method for measuring the respiration rate and respiratory quotient of detached plant tissue. Postharvest Biol Technol 13:263–270

Dutton RG, Jiao J, Tsujita MJ, Grodzinski B (1988) Whole plant CO_2 exchange measurements for nondestructive estimation of growth. Plant Physiol 86:355–358

Garrity DP, Sullivan CY, Watts DG (1984) Rapidly determining sorghum canopy photosynthetic rates with a mobile filed chamber. Agron J 76:163–165

Geis JW (1971) Carbon dioxide assimilation of hardwood seedlings in relation to community dynamics in central Illinois. 1 Filed measurements of photosynthesis and respiration. Oecologia 7:276–289

Gonzàlez-meler MA, Siedow JN (1999) Direct inhibition of mitochondrial respiratory enzymes by elevated CO_2: does it matter at the tissue or whole-plant level ? Tree Physiol 19:253–259

Graham MED (1989) The effect of increased transpiration on photosynthesis of corn. Part 1. A field portable single plant enclosure system. Agr Forest Meteorol 44:307–316
Hagihara A, Hozumi K (1991) Respiration. In: Ranghqavendra AS (ed) Physiology of trees. Wiley, New York, pp 87–110
Hikosaka K, Sudoh S, Hirose T (1999) Light acquisition and use by individuals competing in a dense stand of an annual herbs, *Xanthium canadense*. Oecologia 118:388–396
Hozumi K, Shinozaki K (1974) Studies on the frequency distribution of the weight of individual trees in a forest stand. 4. Estimation of the total function of a forest stand and a generalized mean plant weight. Jpn J Ecol 24:207–212
Kajimoto T, Matsuura Y, Sofronov MA, Volokitina AV, Mori S, Osawa A, Abaimov AP (1999) Above- and belowground biomass and net primary productivity of a *Larix gmelinii* stand near Tura, central Siberia. Tree Physiol 19:815–822
McCree KJ (1983) Carbon balance as a function of plant size in sorghum plants. Crop Sci 23:1173–1177
McCree KJ (1986) Measuring the whole-plant daily carbon balance. Photosynthetica 20:82–93
McCree KJ (1987) Whole plant carbon balance during osmotic adjustment to drought and salinity stress. Aust J Plant Physiol 13:33–43
Meyer WS, Reicosky DC, Barrs HD, Shell GSG (1987) A portable chamber for measuring canopy gas exchange of crops subject to different root conditions. Agron J 79:181–184
Mori S, Hagihara A (1988) Respiration in stems of hinoki (*Chamaecyparis obtusa*) trees. Jpn J Forest Soc 70:481–487
Mori S, Hagihara A (1991) Root respiration in a hinoki *(Chamaecyparis obtusa)* trees. Tree Physiol 8:217–225
Mori S, Prokushkin SG, Zyryanova OA, Abaimov AP, Kajimoto T, Ueda R (1997) Non-destructive measurement of whole plant respiration including underground parts in a Siberian larch forest. In: Inoue G, Takenaka A (eds) Proceedings of the Fifth Symposium on the Joint Siberian Permafrost Studies between Japan and Russia in 1996. National Institute for Environmental Studies, Tsukuba, pp 115–118
Nakai Y, Matsuura Y, Kajimoto T, Abaimov AP, Yamamoto S, Zyryanova OA (2008) Eddy covariance CO_2 flux above a Gmelin larch forest on continuous permafrost of Central Siberia during a growing season. Theor Appl Climatol 93:133–147
Negisi K (1974) Respiration rates in relation to diameter and age in stem or branch sections of young *Pinus densiflora* trees. Bull Tokyo Univ Forests 66:209–222
Ninomiya I, Hozumi K (1981) Respiration of forest trees. 1. Measurement of respiration of *Pins densi-thunbergii* Ueki by an enclosed standing tree method. Jpn J Forest Soc 63:8–18
Ninomiya I, Hozumi K (1983a) Respiration of forest trees. 2. Measurement of nighttime respiration in a *Chamaecyparis obtusa* plantation. Jpn J Forest Soc 65:193–200
Ninomiya I, Hozumi K (1983b) Respiration of forest trees. 3. Estimation of community respiration. J Jpn Forest Soc 65:275–281
Nogués S, Munné-bosch S, Casadesús J, López-carbonell M, Alegre L (2001) Daily time course of whole-shoot gas exchange rates in two drought-exposed Mediterranean shrubs. Tree Physiol 21:51–58
Peters DB, Clough BF, Graves RA, Stahl GR (1974) Measurement of dark respiration, evaporation, and photosynthesis in field plots. Agron J 66:460–462
Reicosky DC, Peters DB (1977) A portable chamber for rapid evapotranspiration measurements on field plots. Agron J 69:729–732
Shugart HH, Smith TM, Post WM (1992) The potential for application of individual-based physiology simulation models for assessing the effects of global change. Ann Rev Ecol Syst 23:15–38
Sievänen R, Bruk TE, Ek AR (1988) Construction of a stand growth model utilizing photosynthesis and respiration relationship in individual trees. Can J For Res 18:1027–1035
Sims DA, Gebauer RLE, Pearcy RW (1994) Scaling sun and shade photosynthetic acclimation of Alocasia macrorrhiza to whole-plant performance – 2. Simulation of carbon balance and growth at different photon flux densities. Plant Cell Environ 17:889–900

Sprugel DG, Ryan MG, Brooks JR, Vokt KA, Martin TN (1995) Respiration from the organ level to the stand. In: Smith WK, Hinkly TM (eds) Resource physiology of conifers. Academic, San Diego, pp 255–299

Tjokelker MG, Oleksyn J, Reich PB (1999) Acclimation of respiration to temperature and CO_2 in seedlings of boreal tree species in relation to plant size and relative growth rate. Global Change Biol 49:679–691

Valetini R, Matteucci G, Dolman AJ, Schulz E-D, Rebmann C, Moors EJ, Granier A, Gross P, Jensen NO, Pilegaard K, Lindroth A, Grelle A, Bernhofer C, Grünwald T, Aubinet M, Ceulemans R, Kowalski AS, Vesalsa T, Rannik Ü, Berbigier P, Loustau D, Guðmundsson J, Thorgeirsson H, Ibrom A, Morgenstern K, Clement R, Moncriff J, Montagnani L, Minerbi S, Jarvis PG (2000) Respiration as the main determinant of carbon balance in European forests. Nature 404:861–865

Watanabe T, Yokozawa M, Emori S, Takata K, Sumida A, Hara T (2004) Developing a multilayered integrated numerical model of surface physics – growing interaction (MINoSGI). Global Change Biol 10:963–982

Yoda K, Kira T, Ogawa H, Hozumi K (1963) Intraspecific competition among higher plants. 6. Self-thining in overcrowded pure stands under cultivated and natural conditions, Series D. J Inst Polytech Osaka City University 14:107–129

Yokota T, Hagihara A (1996) Dependence of the aboveground CO_2 exchange rate on tree size in field-grown hinoki cypress (*Chamecyparis obtusa*). J Plant Res 109:177–184

Yokota T, Hagihara A (1998) Changes in the relationship between tree size and aboveground respiration in field-grown hinoki cypress (*Chamecyparis obtusa*) trees over three years. Tree Physiol 18:37–43

Yokota T, Ogawa K, Hagihara A (1994) Dependence of the aboveground respiration of hinoki cypress (*Chamaecyparis obtuse*) on tree size. Tree Physiol 14:467–479

Chapter 16
Root System Development of Larch Trees Growing on Siberian Permafrost

T. Kajimoto

16.1 Introduction

Below-ground processes have been highlighted in the studies of carbon flux, nutrient cycling, and biodiversity in many terrestrial ecosystems under changing climates (e.g., Chapin and Ruess 2001; Schulze 2006). So far, as tree roots are concerned, much attention has recently been paid to the study of fine roots rather than coarse roots (Brunner and Godbold 2007), since fine roots are more important biologically, such as in resource uptake and mycorrhizal association (Vogt et al. 1996; Read and Perez-Moreno 2003). This trend is aided by improvements in observation techniques and/or devices (i.e., minirhizotron, digital image analyzer) that enable us to monitor fine root dynamics (e.g., Vogt and Persson 1991; Hendrick and Pregitzer 1996; Majdi 1996; Vogt et al. 1998; Johnson et al. 2001). In contrast, individual-based root observation (i.e., root system excavation), which requires laborious and time consuming work, seems outdated today, although many classical studies indicated advantages of this approach. For example, measurement of coarse root mass is essential in the estimation of stand-level below-ground biomass and production (e.g., Karizumi 1974; Santantonio et al. 1977; Deans 1981). Also, quantitative description of the spatial patterns of root systems (e.g., rooting map) tell us characteristics of species-specific strategies under local or microscale soil conditions in natural habitats (e.g., McMinn 1963; Eis 1974; Fayle 1975a, b; Karizumi 1979; Coutts 1983; Reynolds 1983; Kuiper and Coutts 1992; Drexhage and Gruber 1998).

Among these classical studies, some attempted to analyze root growth patterns using information of growth rings and discuss temporal patterns of root system development in monospecific conifer stands (Fayle 1975a, b; Coutts 1983; Kuiper and Coutts 1992). They also focused on the examination on below-ground space that was occupied by root systems (i.e., projection area, or width in horizontal spread), and its relationship to above-ground space that was occupied by tree crowns. These case studies demonstrated that analysis of temporal patterns in both root systems and crowns is a useful approach for understanding processes of above-/below-ground carbon partitioning. Furthermore, if corresponding stand-level indices of above- and below-ground space occupation are considered and

A. Osawa et al. (eds.), *Permafrost Ecosystems: Siberian Larch Forests*,
Ecological studies, Vol. 209, DOI 10.1007/978-1-4020-9693-8_16,

if age-related change in their relationship is examined, we may evaluate the mode of intertree competition against major target resources (i.e., light vs. soil nutrients) in a given forest ecosystem (Kajimoto et al. 2007).

From these viewpoints, field observations and analyses of individual root systems have been recently conducted for *Larix gmelinii* (Rupr.) Rupr. (Gmelin larch) trees growing on permafrost in Central Siberia (Kajimoto et al. 1999, 2003, 2006, 2007). Before these studies, it was known that larch trees often developed shallow root systems (e.g., see literature in Abaimov and Sofronov 1996). However, available information had been mostly qualitative, and processes of root system development had not been discussed in relation to soil environments. As was reported earlier (see Chaps. 6 and 7), tree growth, productivity, and development of *Larix* taiga are likely to be influenced largely by constraints of peculiar soil environments in the permafrost region (i.e., low soil temperature and nutrient limitation). Thus, in this chapter, a linkage between the development pattern of *L. gmelinii* root systems and permafrost soil environments in the region was discussed by synthesizing results of previous papers and other unpublished data. Topics focused for discussion are the following:

- How is spatial development of the root system affected by microscale conditions of soil temperature and water created by typical topography (i.e., hummock) in the study area?
- How is temporal development of the root system characterized?
- Is the extent of below-ground space occupation by root systems balanced or not with that of above-ground space occupation by crowns?
- How does the mode of intertree competition change following stand development?

16.2 Data Source

16.2.1 Study Site

Root systems of *L. gmelinii* were sampled in several stands located in Tura, Central Siberia (64°N 100°E; 160 m a.s.l.) (see Fig. 1.1). The root sampling was mainly aimed at estimating coarse root biomass (see Chap. 6), but the data were further employed for the analysis of individual root systems. In this chapter, the data on root systems obtained from the following four larch stands with different ages were used; one young stand (26-year old; abbreviated as CR1978), two old stands (ca. 105-year old; CF and W1), and one old multiaged stand (averaged ca. 220-year old; C1) (Fig. 1.2). Three stands (CR1978, CF, and W1) were almost even-aged due to rapid tree establishment after a stand-replacing fire at each site (details see Table 6.1). Common procedures used in root sampling and measurement, and definitions of some key parameters that were used for data analysis will be explained later in the text. Further details of the procedures were described elsewhere;

CR1978 and CF (Kajimoto et al. 2007), W1 (Kajimoto et al. 2003), and C1 (Kajimoto et al. 1999, 2003).

16.2.2 Methods of Root System Excavation and Measurements

Root sampling was conducted for selected trees with different sizes in each stand (n = 5–10 per stand) (Table 16.1; see examples in Fig. 16.1). Roots were excavated manually, including both coarse (≧ 5 mm in diameter) and fine roots (< 5 mm). Fine roots were traced carefully as far as practical, so that roots with diameters larger than 0.5–1 mm were mostly uncovered. For each root system, its horizontal projection was sketched as a map, and all living lateral roots (≧ 5 mm in basal diameter) occurring from the tap root (or lower part of the stem) were labeled (e.g., R1 and R2). Basal diameter and length of each lateral root were measured. Lateral root length was defined as the length from the basal portion to the boundary between coarse and fine roots (i.e., diameter = 5 mm) along the longest main axis. In this article, the term "lateral root" was used as a morphologically defined unit synonymous to a first-order root (e.g., Drexhage et al. 1999). Lateral root contains both parts of coarse and fine roots in terms of root diameter size (Kajimoto et al. 2007).

Table 16.1 Size dimensions of *L. gmelinii* root systems excavated in the four stands at Tura in Central Siberia. Stand age indicates the years (at 2004) that passed after each stand-replacing fire, except for old multiaged stand (C1), and tree age shows the range of trees sampled in each stand (details see Table 6.1)

	Young	Old		Old multiaged
	26-year old	105-year old	105year old	>220-year old
Stand age name	CR1978	W1	CF	C1
Number of sample trees	10	7	9	5
Tree age (year)	24–26	92–100	104–105	147–266
Tap root length (cm)	12.4 (8–19)	17.4 (13–22)	19.4 (13–29)	28.6 (19–40)
Number of lateral roots	9.3 (4–15)	8.6 (6–13)	9.0 (5–14)	7.0 (4–9)
Maximum root diameter (cm)	2.2 (0.8–5.9)	3.3 (1.8–5.6)	2.3 (1.0–4.4)	5.6 (3.0–8.1)
Maximum root length (cm)	128 (25–320)	170 (80–350)	206 (75–320)	218 (100–460)

Lateral root diameter is the value measured at basal portion for a longest lateral root. Lateral root length is the distance between basal and end portion of a part of coarse root (i.e., diameter > 5 mm, excluding fine roots). Value of each size parameter is mean of sample trees (range is shown in parenthesis). Data source: W1 and C1 (Kajimoto et al. 2003); CR1978 and CF (Kajimoto et al. unpublished data)

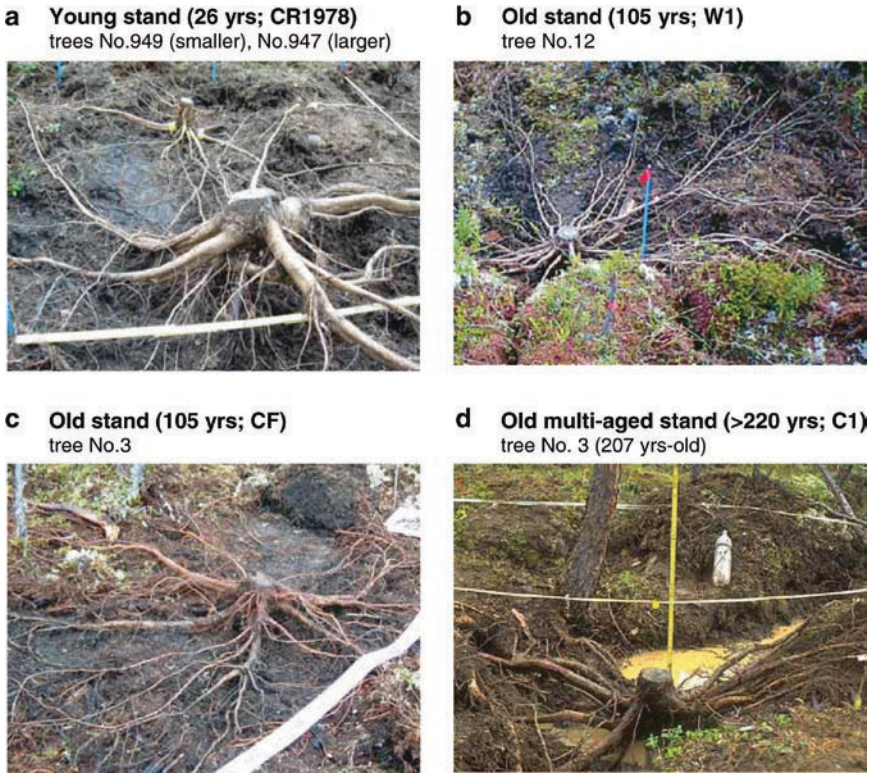

Fig. 16.1 Examples of *L. gmelinii* root systems excavated in four stands at Tura, Central Siberia. (**a**) Trees No. 947 (larger one; 25 years-old at sampling year, breast height diameter $D = 4.4$ cm) and No. 949 (smaller one; 24 years-old, $D = 2.1$ cm) in young stand (CR1978). (**b**) Tree No. 12 (99 years-old, $D = 3.2$ cm) of old stand (W1). (**c**) Tree No. 3 (105 years-old, $D = 5.9$ cm) of old stand (CF). (**d**) Tree No. 3 (207 years-old, $D = 7.7$ cm) of old multiaged stand (C1). Tap root length (i.e., depth of aborted tip portion) is 14 and 12 cm (No. 947 and No. 949 of CR1978, respectively), 19 cm (No. 12 of W1), 23 cm (No. 3 of CF), and 36 cm (No. 3 of C1) (photos: T. Kajimoto) (*see* Color Plates)

16.2.3 Parameters of Above- and Below-Ground Space Occupation

Horizontal rooting area (RA) was considered as the measure of below-ground space occupied by an individual root system. For each excavated tree, RA was defined as the area within approximately 30 cm along both sides of all lateral roots (i.e., parts of coarse root) and was calculated by imposing a square-combined closed polygon on each rooting map (minimum square $= 0.1 \times 0.1$ m^2) (see examples in Fig. 16.2). The definition was based on the observations that many fine roots occurred more or less continuously along the coarse lateral roots, and their lengths were mostly shorter than 30 cm for both young and mature trees (Kajimoto et al. 2003, 2007). Thus, RA covers the area where most of the active roots (i.e., living fine roots) are distributed; although, it ignores the space explored by a few extremely long fine roots (>30 cm).

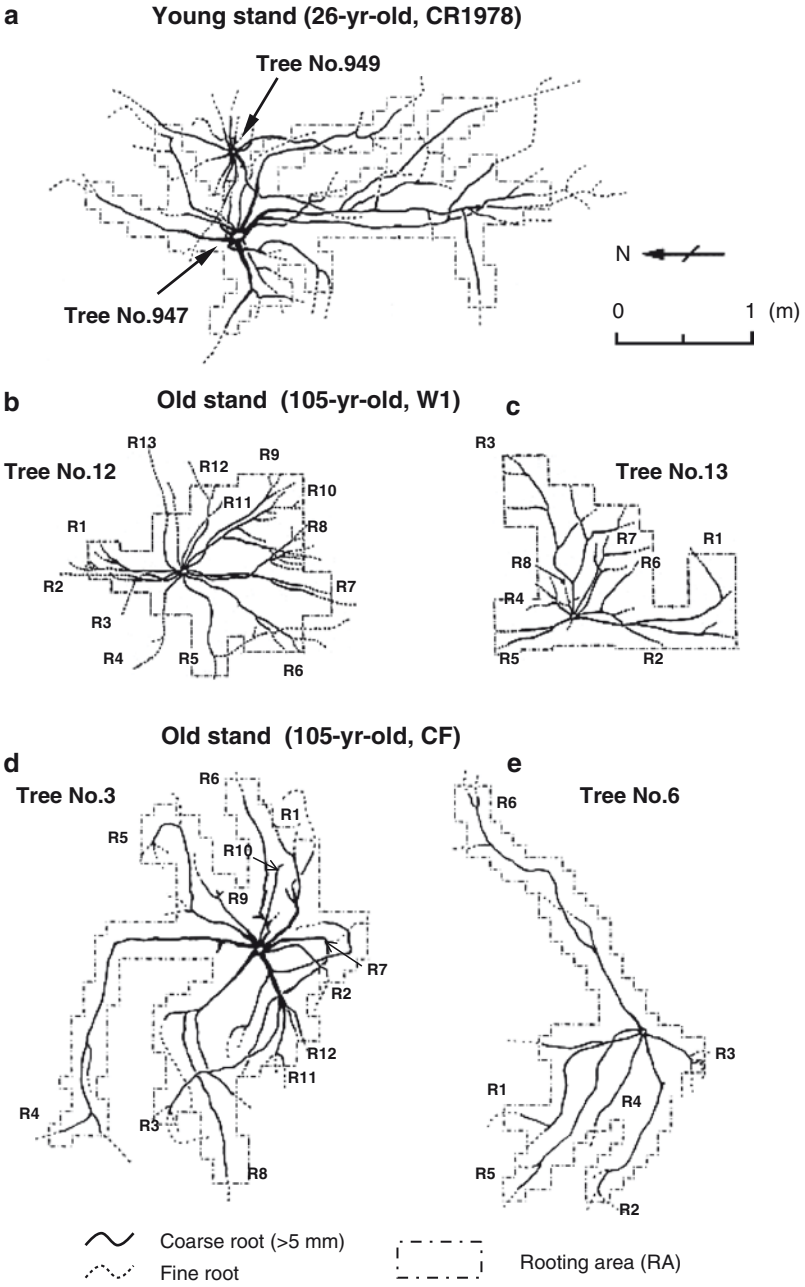

Fig. 16.2 Examples of horizontal projection maps of *L. gmelinii* root systems excavated in a young and two old stands. (**a**) Trees No. 947 and No. 949 of 26-year-old stand (CR1978). (**b**) Trees No. 12 and (**c**) No. 13 of 105-year-old stand (W1). (**d**) Trees No. 3 and (**e**) No. 6 of 105-year-old stand (CF). Ages and stem diameters of some trees are described in Fig. 16.1a–c. For some trees, labeled numbers (e.g., R1 and R2) of lateral roots within each root system are shown. Horizontal rooting area (RA) determined for each root system is shown by *dotted line* (from Kajimoto et al. 2003, 2007)

Rooting area index (RAI) was proposed as a stand-level measure of below-ground space occupied by root systems, and was expressed by the sum of RA per unit land area (i.e., $m^2 m^{-2}$). If RAI is equal to unity, the below-ground space is assumed to be occupied completely by the root systems, or root network is closed at the stand level. Note that RAI can exceed unity if there is substantial overlap of RA among adjacent trees. The RAI was estimated by applying the site-specific regression between stem diameter and RA that was derived from the data of excavated trees in each stand (see Sect. 16.6.2).

As for the corresponding parameters above ground, individual crown projection area (CA) and stand-level crown area index (CAI; $m^2 m^{-2}$) were determined. The CA was calculated as a circle using the average crown width along two radii. The CAI of each stand was estimated as the sum of CA values for all living trees in the permanent plots (the estimates of CAI are listed in Table 6.1).

16.2.4 Growth Pattern Analysis

Temporal development patterns of the root system were examined by applying growth ring analysis (i.e., in the same manner as for "stem growth analysis") to the lateral coarse roots. For each sample tree, root disks were taken from all lateral roots at their basal portions (i.e., just near tree stump). The numbers of annual rings were counted and then determined a period when each lateral root started to expand horizontally (i.e., root ages). Additionally, root disks were also sampled at further positions (20–30 cm intervals) along some lateral roots, and their elongation and diameter growth curves were reconstructed; this analysis was conducted only for a few selected trees in one 105-year-old stand (W1) and old multiaged stand (C1).

For each root disk sample, annual rings and their widths were measured along four radii using a dissecting microscope to 0.01 mm accuracy. However, reading annual rings of *L. gmelinii* roots was difficult in some cases. For example, very narrow rings were often found on smaller root disks (<ca. 1 cm in diameter). Missing rings also occurred especially for large roots (>ca. 3 cm diameter) that were taken near the basal portions; cross-sections were rather oval, and annual rings were compressed at right angle to ground surface. Similar features were examined for the roots of other conifer species (e.g., Fayle 1975b; Krause and Eckstein 1993; Richardson 2000). Thus, by applying cross-dating and other dendrochronogical techniques that were suggested in other reports, continuity of circumference on such root disk samples was carefully checked by referring to the ring count along the longest radius, and then, the number of rings was determined (Kajimoto et al. 1999).

16.3 Spatial Pattern of Individual Root System

All *L. gmelinii* trees excavated in both young and old stands developed superficial root systems (see examples in Fig. 16.1). Basically, the root system was composed of a short tap root and some horizontally spread lateral roots (average number is

7–9 per tree) (Table 16.1). Each tap root was already aborted at the tip portion (8–40 cm deep). Tap root length (average of sample trees) was longer in two 105-year-old stands (17 cm in W1, 19 cm in CF) or old multiaged stand (29 cm in C1) than that in the young stand (12 cm in CR1978).

For all root systems, lateral roots (both coarse and fines roots) were mostly distributed in upper soils (<10–15 cm deep) (also see Sect. 16.4.1). In two 105-year-old (W1, CF) and old multiaged stands (C1), lateral roots often grew in the litter layers or moss-lichen mats that covered the ground surface densely (e.g., Fig. 16.1b, c; see also Kajimoto et al. 1999, 2003). Vertically, root distribution of *L. gmelinii* was confined only in the upper parts of possible soil space that was expected from the soil depth of summer thawing (i.e., soil active layer) in each stand. For example, thickness of soil active layer was 53 cm (CR1978) and 64 cm (C1), and its range (measured at a number of points) was 20–50 cm (W1), and 30–80 cm (C1); although, these data were recorded in different seasons (from late July to late August) and/or years (Kajimoto et al. 2003, 2007; also see Chap. 8).

The sizes of lateral roots (e.g., diameter at basal portion, length) differed largely within each excavated root system, and their average values were also different among the sample trees in each stand (Table 16.1). In the case of 10 trees excavated in the 26-year-old stand (CR1978), the maximum root diameter and length (i.e., longest lateral root for each tree) ranged from 0.8 to 5.9 cm, and from 25 to 320 cm, respectively (Table 16.1). If the stand-average values were compared, the maximum root length was shorter in this young stand (128 cm) than in two 105-year-old stands (170 in W1, 206 cm in CF) or old multiaged stand (218 cm in C1).

Horizontally, lateral roots tended to expand into some specific directions for each examined tree. For example, two measured individuals of 26-year-old stand that were adjacent to each other expanded their lateral roots into either northern or southern directions (see tree No. 947 and 949 in Fig. 16.2a), suggesting that neighboring trees develop root systems that avoid one another in the dense young stand (i.e., tree density of plot CR1978 is 13,700 ha^{-1}; Table 6.1). However, such asymmetric pattern of lateral root expansion was also observed for some sample trees of two 105-year-old stands (Fig. 16.2b–e) or >220-year-old stand (Fig. 16.3; see Kajimoto et al. 1999) where trees grew much sparsely (density < ca. 5,000 ha^{-1}).

16.4 Effects of Microscale Soil Condition on Root Distribution

16.4.1 Topography and Soil Temperature

In arctic tundra, annual thaw–freeze cycle of soils (or cryoturbation) creates peculiar patterns on ground surface at variable scales, such as pingos, stony polygons, and soil hummocks (Williams and Smith 1989). Soil hummocks (also referred to as earth hummocks) often develop in the study sites at Tura in Central Siberia. Particularly, earth hummock was developed typically in old multiaged stand (C1):

mounds (each 1–2 m wide) were 50–70 cm higher than surrounding troughs. Spatial root distributions of the *L. gmelinii* trees sampled in the stand depended largely on such microtopography (Kajimoto et al. 1999, 2007).

For example, one medium-size tree (No. 3, 207-year old) expanded nine lateral roots (R1-R9) mostly into nearby elevated mounds other than troughs (Fig. 16.3). These lateral roots were distributed in the uppermost soils of the mounds (<10 cm in depth), except for places near the tree stump (<100 cm in distance) (Fig. 16.4). In the stand, microscale variation of soil temperature (at 10 cm depth) was examined along a line transect (5 m in length) across hummock topography (Fig. 16.5); the transect was located about 5 m apart from the place where root system of Tree No. 3 was excavated. The data indicate that monthly mean soil-temperatures were 7–8°C higher on the top of mounds (positions no. 8 or 9) than those at the bottom of trough (no. 6) during the summer 3 months (June–August) (Fig. 16.6a). Annual soil heat sum, which was defined as the sum of daily mean soil-temperature above 0°C (e.g., Van Cleve et al. 1981), also increased linearly with the relative height of observation positions: the values at the top of the mounds (1,000–1,200°C days) were about three or four times as those inside troughs (300–400°C days) (Fig. 16.6b). These observations suggest that larch trees expand lateral roots preferentially into warmer soils of mounds than into the colder troughs.

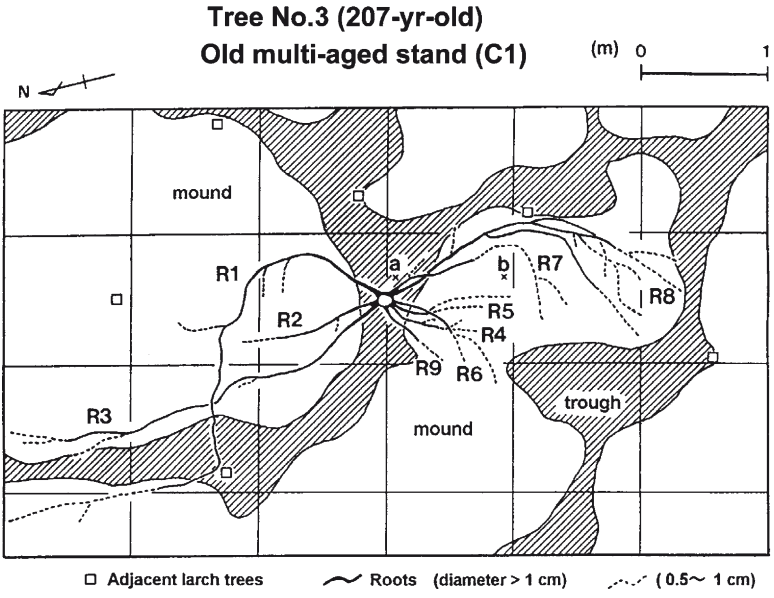

Fig. 16.3 Horizontal projection of root system of 207-year-old *L. gmelinii* tree excavated in the old multiaged stand (Tree No. 3, C1). Nine lateral roots are shown by the labeled numbers (R1–R9) (also see photo of the root system; Fig. 16.1d). *Shaded* and *white* areas show depressed troughs and elevated mounds; relative difference in elevation is about 60 cm between the bottom of trough ((**a**); just below tap root) and the top of nearby mound (**b**) (Kajimoto et al. 2007)

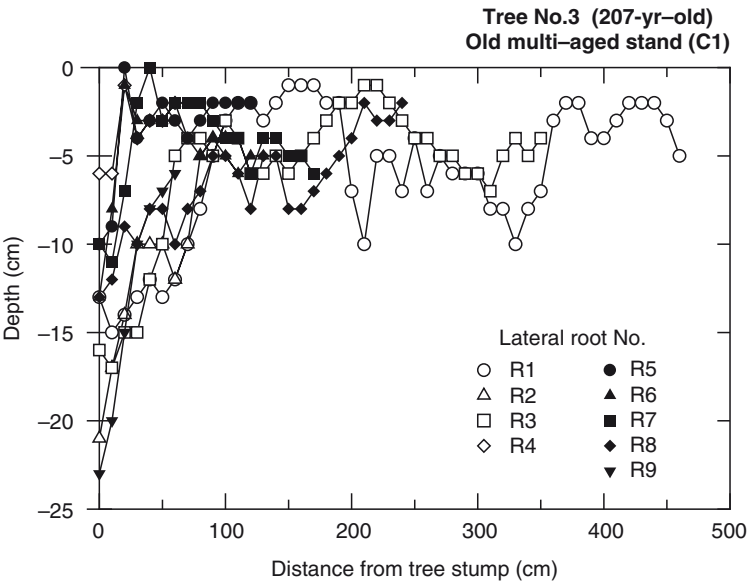

Fig. 16.4 Vertical distribution of nine lateral roots (R1–R9) of one *L. gmelinii* sample tree of the old multiaged stand (Tree No. 3, C1). Depth of each lateral root (vertical distance from ground surface) is plotted against horizontal distance at 10-cm intervals from the tree stump. Horizontal position of each lateral root is shown in Fig. 16.3 (Kajimoto et al. 2007)

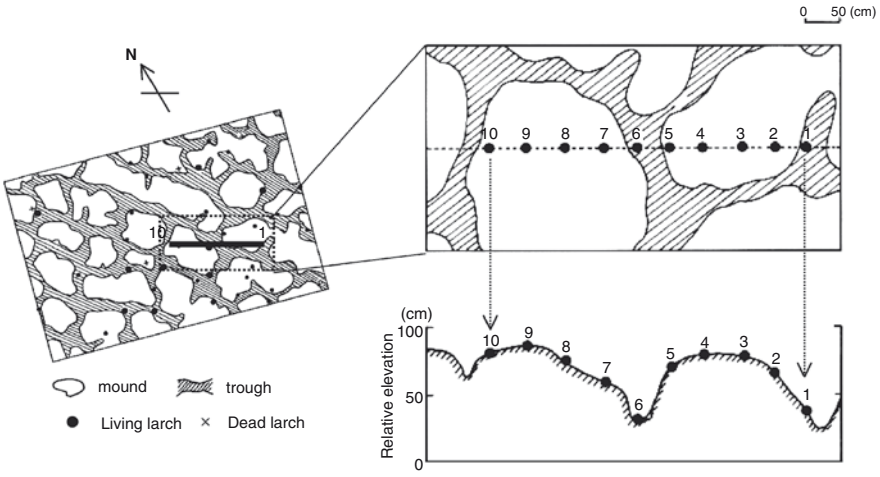

Fig. 16.5 Ground surface pattern and location of a line transect used for the measurement of soil-temperatures (10 cm deep) across hummocks in the old multiaged *L. gmelinii* stand (C1). Ten thermorecorders (Ondotori JR, T&D Ltd.) were installed at 50 cm intervals (positions no. 1–10) along the line (4.5 m in length), and soil-temperature was measured every hour from early September 1997 to late August 1998. The line was set about 5 m apart from the place where root system of tree No. 3 was excavated (the root system is shown in Figs. 16.1d and 16.3) (Kajimoto et al. unpublished data)

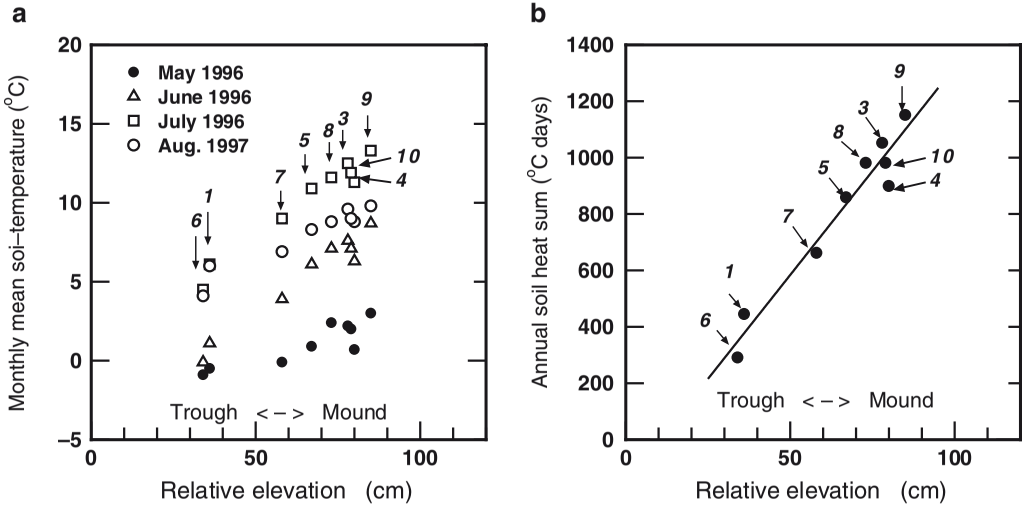

Fig. 16.6 Comparisons of (**a**) monthly mean soil-temperature and (**b**) annual soil heat sum among different positions across the hummock topography in the old multiaged *L. gmelinii* stand (C1). The data are plotted against relative elevations; small numbers indicate parts at the bottom of trough (e.g., position no. 1, 6), at the intermediate position between mound and trough (no. 5, 7), and on the tops of two mounds (no. 3, 8, 9) (see each position in Fig. 16.5). Annual soil heat sum (i.e., degree days) was defined as cumulative daily mean temperatures (above 0°C) during 1 year. Positive correlation was observed between relative elevation and soil heat sum ($n=9$, $r^2=0.95$, $p<0.01$); for calculation, position no. 2 was excluded due to lack of data in some periods. The regression slope was about 14.7°C days cm^{-1} (Kajimoto et al. unpublished data)

Unlike the old multiaged stand, hummocks are not developed conspicuously in the other old larch stands (W1, CF). However, similar microscale variations of soil temperature were observed. In the 105-year-old stand (W1), for example, daily mean soil-temperatures (at 10 cm depth) were 2–6°C higher on mounds than those inside troughs during the summer, where the mounds (only 10–30 cm higher than troughs) were covered with peat moss (*Sphagnum* sp.) or lichens (*Cladina* and *Cetraria* spp.), while the troughs were mainly covered with other moss (*Dicranum* spp.) (Kajimoto et al. 2003). Microscale variations of soil thermal regime were also reported for another 105-year-old stand (CF), which may be associated with the hummock topography and/or its corresponding specific moss/lichen types (see Chap. 9).

Soil-temperature condition might fluctuate interannually. However, the topography-related spatial variation of soil thermal regime is evident every year. In the old multiaged stand (C1), soil-temperature (at 10 cm depth) was also monitored at another hummock for 5 years (2001–2006). The data indicate that daily mean soil-temperature at top of the mounds increased sharply from mid- or late-May to early July, and peaked (>15°C) in mid-July every summer (Fig. 16.7b). The seasonal pattern closely followed that of the air-temperature (Fig. 16.7a). In contrast, soil-temperature inside a nearby trough started to increase much later (between mid- and late-June), and reached a seasonal peak (<10°C) in late July. The difference might be associated with the pattern that snow accumulates deeper in troughs than on mounds, and hence soil-thawing begins later and ends much later inside the troughs. As a result, thickness of soil active layer differs largely across hummock topography within this old stand: active layer is much shallower (<20 cm) inside depressed troughs than on elevated mounds (70–80 cm) (Sofronov et al. 2000; see Chap. 4).

Tryon and Chapin (1983) reported that black spruce (*Picea mariana* Mill. B.S.P.) and tamarack larch (*Larix laricina* (Du Roi) K. Koch) that grew in interior Alaska expanded roots mostly in upper soils, and elongation rates of their roots varied with the seasonal pattern of soil-temperature. Seasonal root growth of *L. gmelinii* might also be regulated largely by the soil thermal condition. Van Cleve et al. (1981, 1983a, b) reported that annual soil heat sum (above 0°C, at 10 cm deep) ranged from 480 to 1,300°C days for various boreal forests in interior Alaska. They also indicated that the value was relatively low (< ca. 700°C days) for black spruce stands that were established on lowlands with permafrost as compared with those of other forest types (>800°C days), such as white spruce (*Picea glauca* (Moench) Voss) and broadleaved deciduous species (e.g., *Populus tremuloides* Michx., *Betula papyrifera* Marsh.), which were mainly distributed on permafrost-free uplands. The range of soil heat sum (300–1,200°C days) that was recorded in the old multiaged *L. gmelinii* stand (C1) encompasses the whole range reported for the evergreen taiga. However, as was discussed earlier, rooting zone of *L. gmelinii* is restricted to the warmer, upper soils even on elevated mounds (>1,000°C days; Fig. 16.6b). This suggests that a threshold of soil heat sum that is sufficient for seasonal root growth of *L. gmelinii* might be as high as those of white spruce and broadleaved deciduous species in the Alaskan taiga.

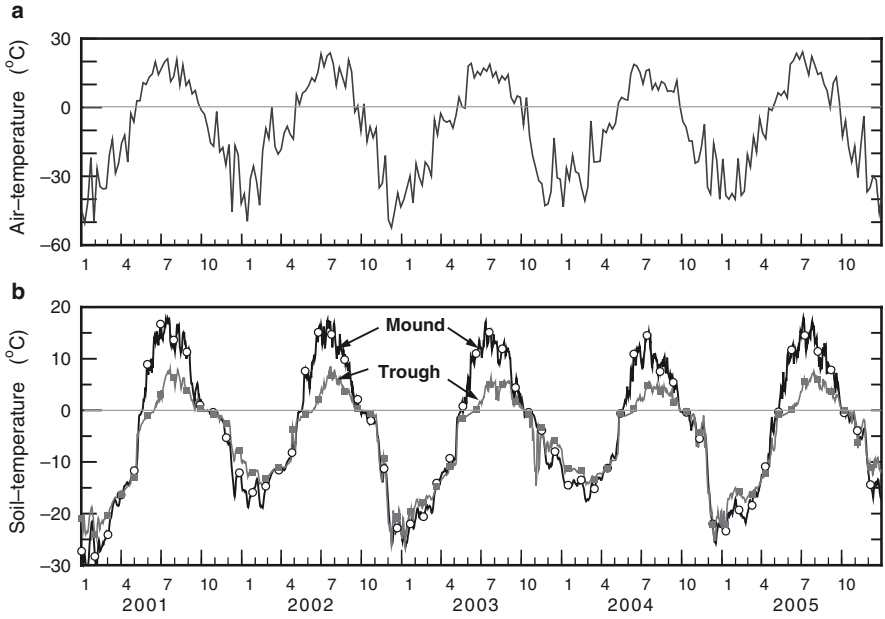

Fig. 16.7 Seasonal changes in (**a**) daily mean air-temperature and (**b**) soil-temperatures during recent 5 years (2001–2005) measured in the old multiaged *L. gmelinii* stand (C1). Soil temperatures (each 10 cm deep) were recorded using thermo-recorders (Ondotori JR, T&D Ltd.) at two positions across hummock topography; on the top of mound and inside nearby trough (relative elevation was about 50 cm). This measurement was conducted at about 15 m away from the line transect used for the measurement of soil-temperatures across hummock topography (see results in Figs. 16.5 and 16.6) (Kajimoto et al. unpublished data)

16.4.2 Topography and Soil Water

Soil water might be another external factor affecting spatial root development of *L. gmelinii*, since the hummocks create microscale variations of not only temperature but also water. Soils inside troughs are generally immersed with melting water from the thawing soils during summer: water begins to pool inside troughs even during root excavation (see Fig. 16.1d). In the old multiaged stand (C1), soil water suction (at 10 cm depth) was measured across a mound-trough topography using tensiometer with porous cups; the measurement was conducted in the same location where soil-temperature was monitored (Fig. 16.7b). According to the data on a mid-summer day (i.e., 5 days after last rainfall), soil water potential was almost stable inside trough, but it was reduced clearly at the top and/or middle parts of a nearby mound (Kajimoto et al. 2003). The difference indicates that soils inside troughs are immersed with water more than those on mounds. Thus, the fact that lateral roots of *L. gmelinii* rarely expanded into troughs (e.g., Fig. 16.3) might be associated with both conditions of low temperature and water logging (Kajimoto et al. 2007).

The superficial root systems of *L. gmelinii* are similar to those reported for two boreal conifer species, tamarack larch (*L. laricina*) and black spruce (*P. mariana*), which grow at poorly drained sites such as peatlands and lowlands in the evergreen taiga. In peatlands of Alberta in Canada, both species developed shallow root systems (< 30 cm deep), and their tap roots were aborted at the tip portions (Strong and La Roi 1983a, b; Lieffers and Rothwell 1987). These reports suggest that high water table mainly limits vertical root growth and may cause tap root abortion of these species. In Central Siberia, permafrost might play a role similar to water table as in sites of the evergreen taiga.

16.5 Temporal Pattern of Root System Development

16.5.1 Replacement of Root System

Formation of adventitious roots was reported for many *Larix* species (e.g., Cooper 1911; Islam and Macdonald 2004). In Central Siberia, *L. gmelinii* also produced roots adventitiously from tap root and/or lower part of stem, in both young and old stands (Figs. 16.8 and 16.9). Consequently, the root systems of all larch trees sampled in old stands (>100-year old) consisted of lateral roots of different ages (Kajimoto et al. 2003). As shown in Fig. 16.8, for example, the ages of five lateral roots (labeled No. R1–R5) of one 105-year-old tree (No. 1 of CF) ranged from 14 to 71 years; here, the root age means a time that passed after each lateral root started to expand. This example also indicates that the roots occurring at upper positions (No. R2 and R5) are relatively small and young (14 and 35 years) than those at lower positions (R1, R4, and R3; > 50 years), and that some dead roots remain near the bottom of the root system.

Similar relationship between lateral root age and its vertical position (i.e., depth in soil) was recognized for the other root-excavated larch trees (Fig. 16.10). For nine trees of two 105-year-old stands (W1, CF), the ages of lateral roots ranged between 10 and 80 years, and roots occurring at upper positions (>−5 cm in depth) were generally younger than those at lower positions (Fig. 16.10a, b). In the cases of two sample trees of old multiaged stand (No. 2, 3; C1), the ages of their lateral roots at lower positions were also older than those of the upper roots (Fig. 16.10c). These evidence indicate that *L. gmelinii* produces lateral roots successively from the lower to upper part of the tap root and/or stem.

The root age-depth diagram (Fig. 16.10) also shows that some older roots started to expand at similar periods within each root system. For example, at one 105-year-old stand (W1), four roots of tree No. 11 (shown by open circles) were initiated 64–65 years ago, and six roots of No. 13 (open triangles) and four roots of No. 14 (closed circles) did so 51–58 and 46–48 years ago, respectively (Fig. 16.10a). Likewise, such a tendency of simultaneous initiation of lateral roots can be observed for the sample trees of another 105-year-old stand (CF), e.g., for tree No. 1, the ages of five roots ranged 51–56 years among eleven lateral roots

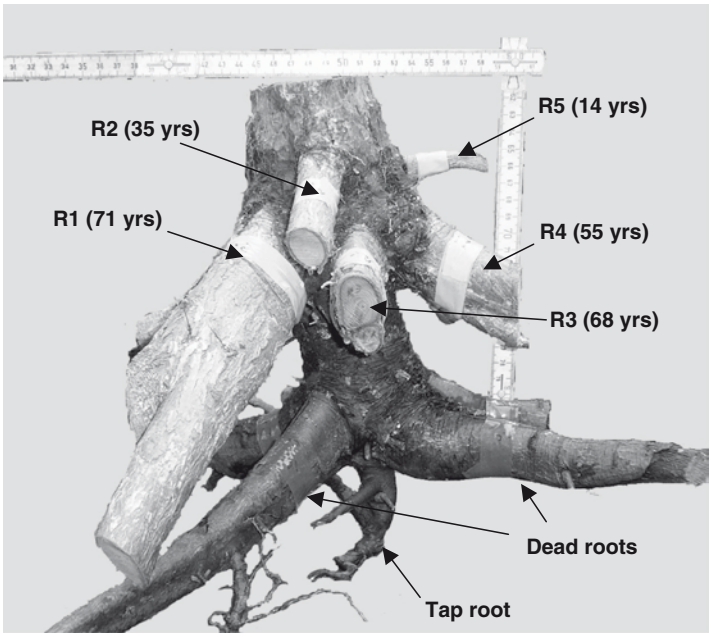

Fig. 16.8 Vertical profile of *L. gmelinii* root system excavated in the old stand (Tree No. 1, 105 years-old, CF). The root system consisted of 14 living lateral roots; here, ages of only five lateral roots (numbered R1–R5) are shown in parenthesis. Root age indicates the number of annual rings counted on the disk sample taken at basal portion (i.e., < 5 cm in distance from tree stump; see Sect. 16.2.2). Tap root was aborted at its tip (29 cm deep), and some dead lateral roots were observed at the bottom part of root system

that occurred at the depth of 10–15 cm (Fig. 16.10b). In the stand, ages of all lateral roots that occurred at such relatively deeper portion (below 15 cm in depth) fell in the range of 40–80 years, indicating that lateral root expansion started intensively after the stand age of 25 years. Mund et al. (2002) reported that sinker roots of old *Picea abies* trees (112-year old) started to grow vertically after the stand aged about 20 years.

As was seen in Fig. 16.8, some dead lateral roots were found in each excavated root system of the two 105-year-old stands (W1, CF). These dead roots were mostly located at the bottom of the root system, suggesting that they were among the roots developed initially just after tree establishment (i.e., about 100 years ago). Three individuals of old multiaged stand (tree No. 2, 3, 4; C1) have regenerated at least 200 years ago, but lacked living lateral roots that aged 160 years or more (Fig. 16.10c). However, some dead lateral roots also remained at the bottom of each root system, suggesting that initially occurring older roots might have already been dead, probably due to stresses under cold and wet soil conditions (see Sect. 16.4). In contrast, all the excavated root systems in 26-year-old stand (CR1978) were composed of only living and young (20–24 years) lateral roots (Kajimoto et al. unpublished data). In the young stand, successive replacement of root system from

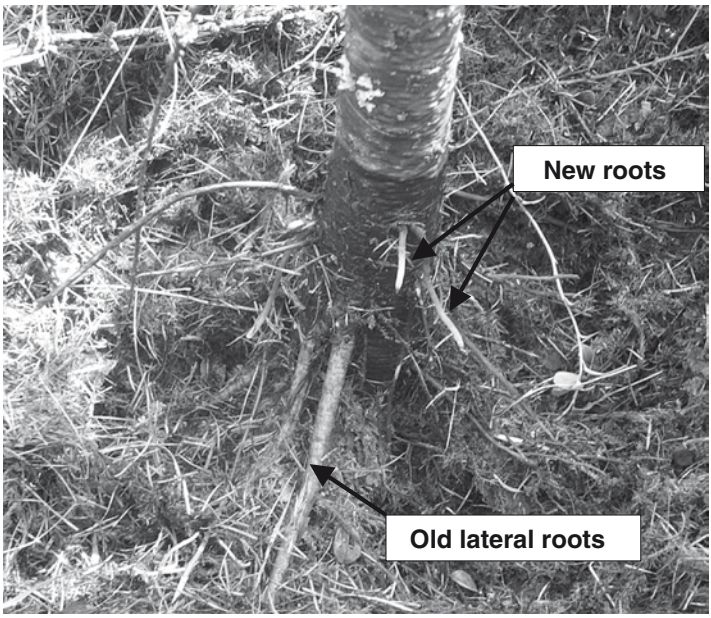

Fig. 16.9 Example of new lateral roots (i.e., adventitious roots) emerging from lower part of stem on young *L. gmelinii* tree (Tree No. 947, 25 years-old, CR1978). Root system of this young tree is shown in Fig. 16.1a (photo: mid-July in 2005, Kajimoto)

older roots to newly emerged roots, which were observed in the other old stands, may not have yet started.

16.5.2 Growth Rate and Pattern of Lateral Root

Elongation rates of lateral roots differed within a single root system of *L. gmelinii*. For example, mean annual rates of root elongation (i.e., root length/entire observation period) ranged from 1.0 to 11.4 cm year^{-1} (averaged 4.8 cm year^{-1}) for 13 lateral roots of 105-year-old tree (No. 12 of W1) (Fig. 16.11a). The elongation rates were smaller among roots of relatively older (>50 years) age-group (3–4 cm year^{-1}; R8, R9) than among younger (<50 years) roots (>7–8 cm year^{-1}; R5, R10). For one 207-year-old tree (No. 3, C1), the mean elongation rates were also relatively high in younger roots (10–23 cm year^{-1}; R4–R7) compared with those in older roots (2–8 cm year^{-1}; R1–R3, R8–R9) (Fig. 16.11b). Such smaller elongation rates were also observed in some older lateral roots (1–6 cm year^{-1}) of the other two old trees (No. 2, 6, C1) (Fig. 16.11c). The tendency suggests that elongation rates of lateral roots decline as they age.

The annual extension rates of *L. gmelinii* lateral roots were mostly less than 10 cm year^{-1}. The root extension rates are much lower than those (generally ranged

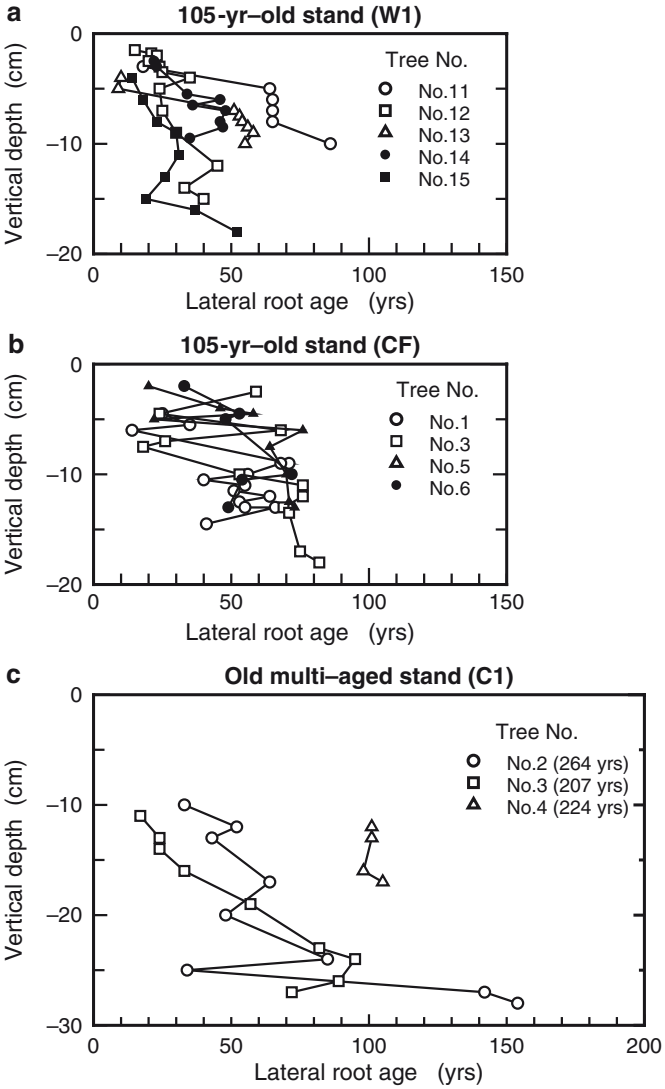

Fig. 16.10 Relationships between ages and vertical positions of lateral roots examined in some old *L. gmelinii* trees. (**a**) Five trees (No. 11–15) of old stand (105 years old, W1). (**b**) Four trees (No. 1, 3, 5, and 6) of old stand (105 years old, CF). (**c**) Three trees (No. 2, 3, and 4) of old multiaged stand (> 220 years old, C1). Vertical depth indicates the position where each lateral root occurs within each root system. The data are connected with line segments from the uppermost to the lowest root. Photos and/or rooting maps of these sample trees are shown elsewhere: Tree No. 12 of W1, No. 3 of CF, and No. 3 of C1 (see Fig. 16.1b–d), and No. 1 of CF (see Fig. 16.8) (original data of two stands, W1 and C1, are from Kajimoto et al. 2003; others are Kajimoto et al. unpublished data)

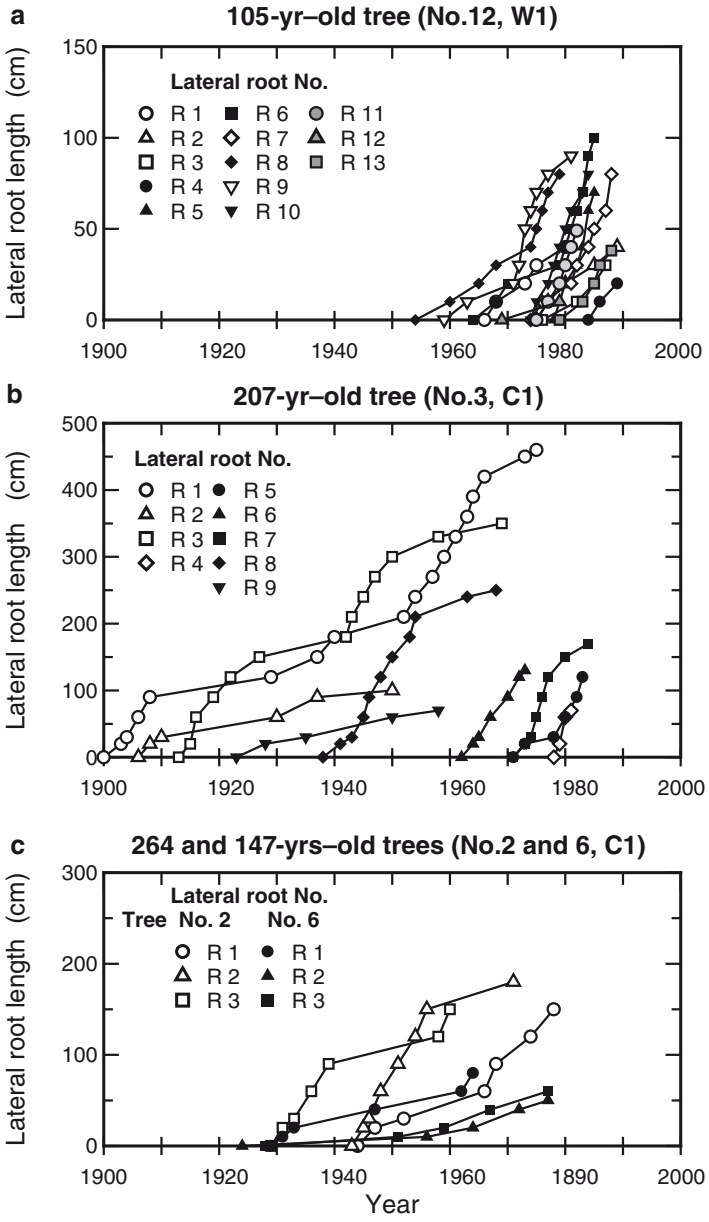

Fig. 16.11 Elongation growth curves of lateral roots reconstructed for some old *L. gmelinii* trees. (**a**) Thirteen lateral roots of Tree No. 12 (105 years old) of old stand (W1). (**b**) Nine lateral roots of Tree No. 3 (207 years old) of old multiaged stand (C1). (**c**) Three lateral roots of each of Tree No. 2 (264 years old) and No. 6 (147 years old) of old multiaged stand (C1) (original data of C1 from Kajimoto et al. 2007; others are Kajimoto et al. unpublished data)

10–80 cm year^{-1}) reported for other conifer species growing under climates milder than Siberia, such as *Pinus resinosa* Ait (Fayle 1975a), *Picea sitchensis* Bong. Carr. (Coutts 1983), and *Pseudotsuga menziesii* (Mirb.) Franco. (Kuiper and Coutts 1992) in North America, and *Picea abies* (Drexhage and Gruber 1998; Puhe 2003) in Eurasia.

Figure 16.12a shows diameter growth curves that were reconstructed for nine lateral roots (at basal portion) of one 207-year-old *L. gmelinii* tree (No. 3, C1). The pattern of root diameter growth varied largely within a root system, as was also seen

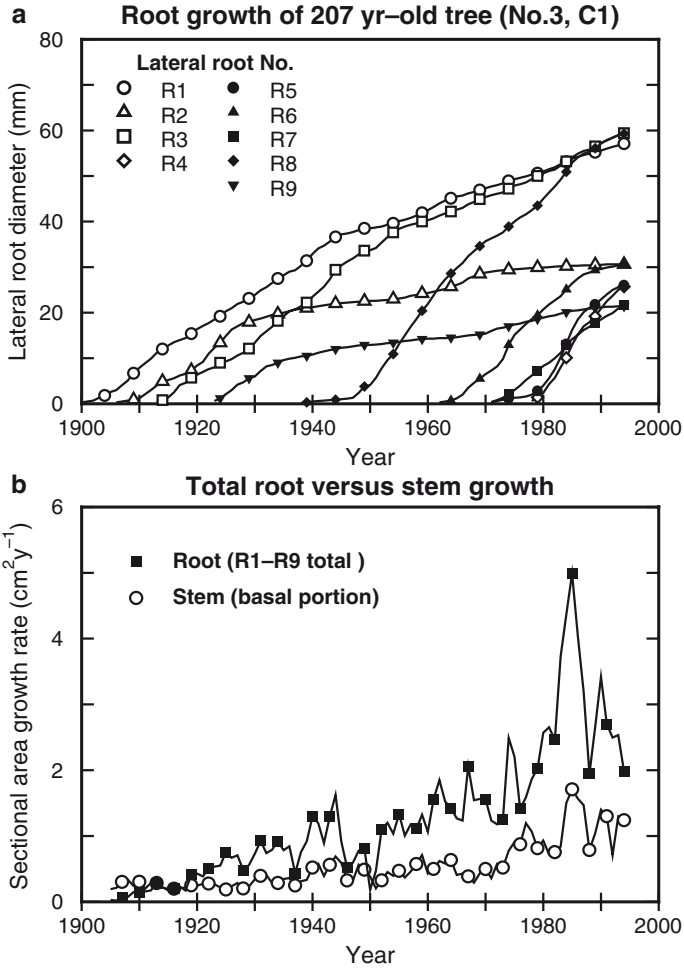

Fig. 16.12 (**a**) Diameter growth curves of nine lateral roots (R1–R9) at basal portions, and (**b**) changes in sectional area increments of total root (i.e., sum of these nine lateral roots) and stem (at basal portion) reconstructed for a 207-year-old *L. gmelinii* tree (No. 3) in the old multiaged stand (C1). Values of diameter and sectional area increments of both roots and stem were the averages; annual ring-widths were measured along four radii on each sample disk (Kajimoto unpublished data)

in their elongation growth patterns (Fig. 16.11b). Mean annual increments of root diameter, which was calculated by root diameter/entire observation period, ranged from 0.3 (R2) to 1.5 mm year^{-1} (R4). Four younger roots (No. R4–R7), which started to elongate after 1960, appears to keep higher diameter increments than the older roots (R1–R3, and R9) (Fig. 16.12a). However, these older lateral roots did not necessarily synchronize patterns in both elongation and diameter growth. Namely, two old roots, R1 (shown by open circle in Figs. 16.11b and 16.12a) and R3 (open square), grew much faster from early periods and maintained higher growth rates as compared to the other two roots, R2 (open triangle) and R9 (closed reverse triangle). A process of carbon allocation within the root system might cause such among-roots variation in growth rates or growth patterns (Kajimoto et al. 2007).

Carbon allocation process within root system still remains unclear, and should be further examined. As shown in Fig. 16.12b, a time trend of lateral root growth (i.e., sectional area increment at basal portion) examined for the 207-year-old tree (No. 3, C1) was fairly synchronized with that of stem if all lateral roots (R1–R9) were combined. This indicates that carbon allocation within the root system is primarily regulated at a whole-tree level, as was suggested for root systems of other conifer species (e.g., Fayle 1975b; Krause and Eckstein 1993; Drexhage et al. 1999). In other words, the amount of carbon allocation into a whole root system might be regulated or limited to attain a balance with allocation into above-ground parts (i.e., stem), although *L. gmelinii* tends to allocate annual photosynthetic production largely into roots as it grows (Kajimoto et al. 2006). Thus, the among-roots variation in growth rate and pattern (Fig. 16.11) suggests that the larch may allocate annual carbon gain into growth of one or two specific roots among similar-aged roots (e.g., R1 and R3 in Fig. 16.12a), and then expand newly emerged lateral roots at the expense of other growth-declined, older roots during development of the root system.

16.6 Below-ground Space Occupation by Root System

16.6.1 Relationship Between Root System and Crown

Old forests of *L. gmelinii* (>100-years old) in Central Siberia are generally sparse with open canopy. Individual crowns are thin and rarely overlap with their neighbors. This is reflected in the fact that extent of canopy closure, or crown projection area index (CAI) defined in this chapter, is generally lower than 0.4–0.5 $m^2 m^{-2}$ for old larch forests in the region (Abaimov and Sofronov 1996; Bondarev 1997). The values of CAI (0.1–0.3 $m^2 m^{-2}$) of three 105-year-old larch stands at Tura (W1, CF, C1) also fall in such range (see Table 6.1).

Figure 16.13 shows relationships between stem diameter at breast height (D) and crown projection area (CA) for sample trees of each of these study stands. The CA value for a given tree size is larger in 26-year-old stand (CR1978) than in two 105-year-old stands (W1 and CF), suggesting that *L. gmelinii* tends to hold a thin

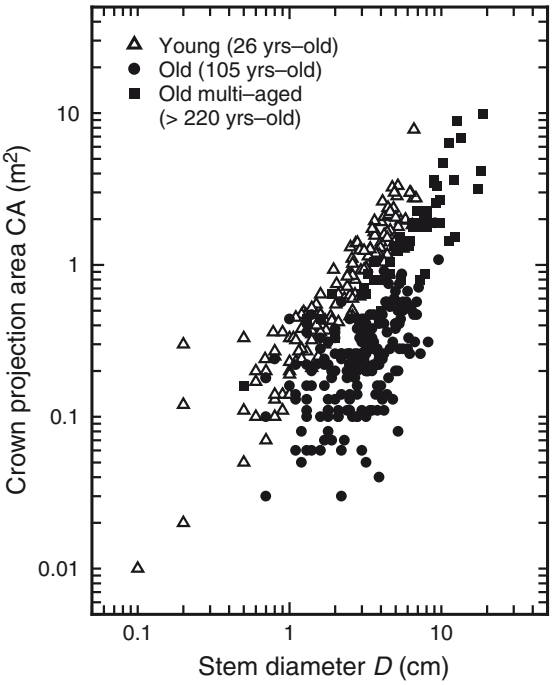

Fig. 16.13 Relationships between stem diameter at breast height (*D*) and crown projection area (CA) of living *L. gmelinii* trees in young (26 years-old, CR1978), old (105 years-old, CF) and old multiaged (>220 years-old, C1) stands. Here, tree census data for individuals taller than 1.3 m in permanent plots of each stand are used (Kajimoto et al. unpublished data)

crown even as it grows larger. In contrast, larch trees may continue to expand their root systems as they grow. Figure 16.14a shows that horizontal RA was about three or four times larger than the crown projection area (CA) for the sample trees of two old stands, while RA was nearly equivalent to CA (regression slope = 0.98) for those of young stand. A similar CA–RA relationship was also observed for the seven sample trees of another 105-year-old stand (W1) (Kajimoto et al. 2003). In addition, the size dependency of RA was similar between these two old stands (W1, CF), but was significantly different from that of young stand: RA of CR1978 was smaller than that of CF and C1 if similar-sized individuals ($D < 3$–4 cm) were compared (Fig. 16.14b). These discrepancies between young and old stands suggest that, after the stand age of about 30 years, the surviving trees mainly expand their root systems (Kajimoto et al. 2007). The CA–RA relationship that was found in the young *L. gmelinii* stand is similar to those reported for other monospecific conifer forests at relatively younger stages (10–60-year old), such as *Picea sitchensis* (Hinderson et al. 1983) and *Pseudotsuga menziesii* (McMinn 1963; Kuiper and Coutts 1992); in these conifer stands, individual RA (or width) rarely exceeded crown area.

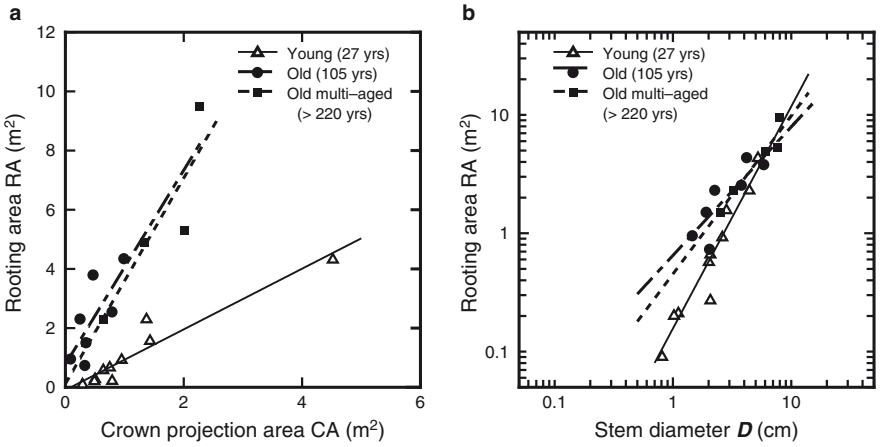

Fig. 16.14 Relationships between RA and (**a**) crown projection area (CA), and (**b**) breast height stem diameter (*D*), for *L. gmelinii* trees excavated in the young (26 years old, CR1978), old (105 years old, CF) and old multiaged (>220 years old, C1) stands. Regression lines are approximated by (**a**) linear and (**b**) log-log linear models, respectively. The coefficients of each regression are as follows: (**a**) RA = 1.02 CA − 0.10, $r^2 = 0.912$ (CR1978); RA = 3.30 CA + 0.77, $r^2 = 0.571$ (CF); RA = 3.48 CA + 0.12, $r^2 = 0.859$ (C1). (**b**) $RA = 0.16D^{1.93}$, $r^2 = 0.931$ (CR1978); $RA = 0.65D^{1.15}$, $r^2 = 0.730$ (CF); $RA = 0.45D^{1.35}$, $r^2 = 0.927$ (C1) (Kajimoto et al. 2007)

16.6.2 Stand-Level Root Network

RAI, which was estimated using site-specific *D*-RA regression (Fig. 16.14b), was the largest in the 26-year-old *L. gmelinii* stand (1.80 $m^2 m^{-2}$, CR1978), followed by 105-year-old stand (1.35 $m^2 m^{-2}$, CF) and >220-year-old stand (1.25 $m^2 m^{-2}$, C1) (Kajimoto et al. 2007). The RAI of another old stand (1.1 $m^2 m^{-2}$, W1; Kajimoto et al. 2003) was also as low as that of two old stands. All estimates of RAI exceed unity, indicating that stand-level root network is assumed to be closed in both young and old stands, although RAI of these old stands tends to be smaller than that of young stand. In contrast, the crown projection area index (CAI) exceeded unity only in the 26-year-old stand (1.33 $m^2 m^{-2}$), whereas those of the old stands were considerably less than unity (<0.3 $m^2 m^{-2}$) as was mentioned earlier (see Table 6.1). These comparisons suggest that canopy becomes open gradually due to tree mortality until the stand ages (>100-year old), but root network is kept fully closed. In other words, the stand at younger stage is over-crowded in both above- and below-ground spaces, but old stands are crowded only in below-ground space by surviving individuals.

16.7 Linkage with Postfire Permafrost Soil Environment

Patterns of postfire changes in soil physical properties such as soil temperature and thickness of soil active layer were well documented in evergreen taiga established on the permafrost in interior Alaska (e.g., Viereck 1982; Dyrness et al. 1986) and northern

Canada (e.g., Wein and Bliss 1973; Rouse 1976; Landhäusser and Wein 1993; Mackay 1995). According to these reports, soil temperature and active layer thickness increase sharply at once just after stand-replacing fires, since ground floor vegetation such as woody shrubs, mosses and lichens, and accumulated litter, that function as thermal insulator are eliminated (e.g., Viereck 1982; Oechel and Van Cleve 1986; see also Chap. 4). However, both temperature and active layer thickness subsequently decrease with recovery of floor vegetation as the stand ages, then return to prefire level. A return time of active layer thickness varies from about 10 years to several decades, depending on local conditions such as topography, fire intensity, and recovery rate of the floor vegetation. Likewise, these postfire changes in the soil environment also occur in the permafrost region in Central Siberia (Abaimov and Sofronov 1996; Gorbachev and Popova 1996; Sofronov et al. 2000). For example, Kharuk et al. (2005) examined various-aged stands of *L. gmelinii* (from a few years to >150-years old) in Central Siberia, and indicated that thickness of active soil layer decreased gradually (about 0.3 cm year^{-1}) with increase in stand age.

Figure 16.15 illustrates a concept that explains how temporal development of *L. gmelinii* root systems is linked to such postfire changes in permafrost soil environment (Kajimoto et al. 2003). There are distinct phases of root system development. First, when a dense seedling population becomes established after a stand-replacing fire, larch individuals grow roots vertically to some extent, and also start to expand lateral roots from the deeper part of the tap roots. This reflects the conditions of high soil temperature and deep active layer thickness. As the stand

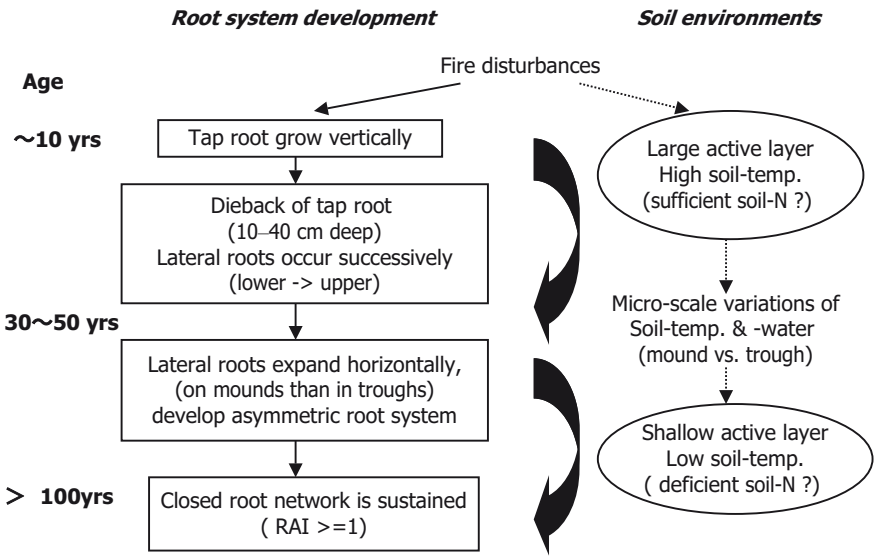

Fig. 16.15 Schematic diagram of a developmental process of individual root system of *L. gmelinii* in relation to postfire changes in soil environment in the permafrost larch taiga in Central Siberia (redrawn from Kajimoto et al. 2003)

develops, however, reduction in both temperature and active layer thickness limit vertical root growth, which results in death of the deeper portions of the tap root, or death of older and deeper lateral roots. Subsequently (after ca. 30 years), larch trees continue to expand lateral roots horizontally, especially into the warmer and drier soils on the elevated mounds. At this phase, they also replace lateral roots by growing new roots successively at upper positions of the tap root. Consequently, a fully closed root network would be maintained at the stand level due to horizontally spread individual root systems, at an old stand age (>100 years).

Associated with changes in these soil physical properties, nutrient conditions may also change with stand age. Generally, soil inorganic N-pool increases immediately after a stand-replacing fire (Grogan et al. 2000; Certini 2005), but declines to the prefire level within several years as a result of immobilization or uptake due to vegetation recovery (Wan et al. 2001; Smithwick et al. 2005). Soil nutrient, especially nitrogen, is essentially limited in the permafrost larch taiga in Siberia (e.g., Schulze et al. 1995; also see Chaps. 8 and 12). After the recovery of vegetation, constraint of available soil-N might become crucial and then limit individual growth. In the study site at Tura, height growth rates of *L. gmelinii* trees examined in two 105-year-old stands (W1 and CF) declined sharply at stand age of 30–50 years (see Figs. 6.5b, c and 7.5). The growth reduction occurred irrespective of difference in individual tree size, suggesting contributing effect of limitation in soil N. This period corresponds to the phase when larch trees start to replace the lateral roots successively (30–50 years; Fig. 16.15). The postfire change and limitation of available soil nutrients may trigger lateral root expansion, and hence affect temporal root system development of *L. gmelinii*.

16.8 Below-ground Competitive Interactions

As was mentioned earlier (Sect. 16.6.2), relationships between two indices of space occupation (CAI and RAI) change along stand age sequence, and old stands are suggested to be crowed only in the below-ground space. This implies shift in the mode of intertree competition following stand development in the permafrost *Larix* taiga. Namely, tree competition for available below-ground space or soil nutrients may become predominantly important more than above-ground competition for light after a stand age of about 30 years (Kajimoto et al. 2007). In other words, tree mortality may be caused not by shading among crowns but by competition among roots after this stand age.

Generally, root competition for soil resources (water, nutrients) is considered a size-symmetric (or two-sided) competition where two neighboring plants uptake resources evenly at the zone of influence (i.e., overlapped place of roots) even if they differ in size (e.g., Weiner 1990). There are still few evidence supporting this concept (Schwinning and Weiner 1998; Schenk 2006). However, the concept of size-symmetric competition means that larger individuals do not necessarily outcompete smaller ones when below-ground competition was dominant under

nutrient-poor condition. Such a mode of competition is likely to be occurring in monospecific, even-aged *L. gmelinii* forests in the permafrost taiga, since soil nutrients (e.g., nitrogen) are essentially limited (Schulze et al. 1995), and even smaller individuals can survive longer than larger ones during stand development (Osawa et al. 2003; also see Chap. 7). If so, it may be advantageous for larch trees to develop root systems that could explore limited soil resources by avoiding overlap with neighboring root systems, or by reducing root interference with neighbors. In other words, larger root system may not be necessarily advantageous for survivorship.

For further discussion of intertree competitive interference below the ground, more quantitative analyses are required regarding spatial arrangement of individual root systems. RAI of the present analysis indicates extent of closure in the root network at the stand level. However, it does not tell us how the root systems are interacting with one another, or to what extent the root systems are segregated or overlapped (Casper and Jackson 1997), and whether root competition actually occurs in response to depleted soil resources (Schenk et al. 1999; Casper et al. 2003). There are two possible approaches to address these questions. One approach is to examine spatial patterns of fine roots which uptake soil resources (e.g., Schmid and Kazda 2005). Another approach is to apply an intensive method of root excavation at whole-tree level, then visualize all root systems within a certain target area. Application of such intensive method has been few in forest ecosystems. However, this approach might be useful for quantitatively analyzing among-root interactions at the stand level, as was demonstrated in a monospecific shrub population of desert ecosystem (Brisson and Reynolds 1994).

16.9 Conclusions

Some characteristic features of *L. gmelinii* root system were suggested from the individual-based measurements and analysis.

- *L. gmelinii* trees generally develop superficial, horizontally spread root systems. The rooting depths in the study area in Central Siberia (<30–40 cm) are much shallower than those reported for other tree species in forest ecosystems worldwide (Stone and Kalisz 1991; Canadell et al. 1996; Schenk and Jackson 2002); exceptions are two boreal species (black spruce and tamarack larch) growing on specific conditions (see Sect. 16.4.2). The shallow root system of *L. gmelinii* is primarily a result of low soil temperature and potentially limited growing space (i.e., soil active layer) due to permafrost, and is further affected by microscale soil conditions of both temperature and water that are created by the peculiar topography (i.e., hummock) in the region of study.
- The temporal pattern of development in *L. gmelinii* root systems is closely linked to postfire changes of soil environment in the permafrost region. Larch trees gradually replace lateral roots with new roots (i.e., adventitious roots). This seems reflect constraints of soil physical properties (i.e., reductions in temperature

and active layer thickness) that might become crucial as the stand ages (to 30–50-year-old). Consequently, the larch continue to expand root systems horizontally (but not their crowns) so that the presumably limited soil nutrients are better exploited. Such a priority of root system development is supported by a process of carbon allocation at a whole-tree level (i.e., root-oriented carbon allocation).

- The analyses using two indices of space occupation of above (CAI) and below (RAI) the ground provide some insights into the mode of intertree competition that occurs in the permafrost larch taiga. The root systems of *L. gmelinii* are likely to be closed fully at the stand level ("closed root network") throughout stand development, suggesting predominance in below-ground intertree competition. The achievement of a closed root network seems to be primarily due to the effect of external factors (i.e., microscale soil conditions) on individual root system development (i.e., horizontally asymmetric distribution). This may also be affected by root competition among neighboring trees. However, the nature of below-ground intertree competition still remains unclear. To clarify these possible contributing processes, it is important to examine further the mechanisms related to patterns of tree mortality and stand development in the larch taiga on Siberian permafrost.

Acknowledgments I thank Y. Matsuura, A. Osawa, T. Miyaura, A.P. Abaimov, O.A. Zyryanova, A. S. Prokushkin, V.M. Borovikov, and other Japanese and Russian colleagues for their help during the field work. This study was partly supported by the fund of JSPS and RFBR under the Japan – "Russia Research Cooperative Program (FY2008–2009)."

References

Abaimov AP, Sofronov MA (1996) The main trends of post-fire succession in near-tundra forests of central Siberia. In: Goldammer JG, Furyaev VV (eds) Fire in ecosystems of boreal Eurasia. Kluwer Academic Publishers, Dordrecht, pp 372–386

Bondarev A (1997) Age distribution patterns in open boreal Dahurican larch forests of Central Siberia. For Ecol Manage 93:205–214

Brisson J, Reynolds JF (1994) The effect of neighbors on root distribution in a creosotebush (*Larrea Tridentata*) population. Ecology 75:1693–1702

Brunner I, Godbold DL (2007) Tree roots in a changing world. J Forest Res 12:78–82

Canadell J, Jackson RB, Ehleringer JR, Mooney HA, Sala OE, Schulze E-D (1996) Maximum rooting depth of vegetation types at the global scale. Oecologia 108:583–595

Casper BB, Jackson RB (1997) Plant competition underground. Annu Rev Ecol Syst 28:545–570

Casper BB, Schenk J, Jackson RB (2003) Defining a plant's belowground zone of influence. Ecology 84:2313–2321

Certini G (2005) Effects of fire on properties of forest soils: a review. Oecologia 143:1–10

Chapin FS III, Ruess RW (2001) The roots of the matter. Nature 411:749–752

Cooper WS (1911) Reproduction by layering among conifers. Bot Gaz 52:369–379

Coutts MP (1983) Development of the structural root system of Sitka spruce. Forestry 56:1–16

Deans JD (1981) Dynamics of coarse root production in a young plantation of *Picea sitchensis*. Forestry 54:139–155

Drexhage M, Gruber F (1998) Architecture of the skeletal root system of 40-year-old *Picea abies* on strongly acidified soils in the Harz Mountains (Germany). Can J For Res 28:13–22
Drexhage M, Huber F, Colin F (1999) Comparison of radial increment and volume growth in stems and roots of *Quercus petraea*. Plant Soil 217:101–110
Dyrness CT, Viereck LA, Van Cleve K (1986) Fire in taiga communities of Interior Alaska. In: Van Cleve K, Chapin FS III, Flanagan PW, Viereck LA, Dyrness CT (eds) Forest ecosystems in the Alaskan taiga. Ecological studies, vol 57. Springer, Berlin, pp 74–86
Eis S (1974) Root system morphology western hemlock, western red cedar, and Douglas-fir. Can J For Res 4:28–38
Fayle DCF (1975a) Extension and longitudinal growth during the development of red pine root systems. Can J For Res 5:109–121
Fayle DCF (1975b) Distribution of radial growth during the development of red pine root systems. Can J For Res 5:608–625
Gorbachev VN, Popova EP (1996) Fires and soil formation. In: Goldammer JG, Furyaev VV (eds) Fire in ecosystems of boreal Eurasia. Kluwer Academic Publishers, Dordrecht, pp 331–336
Grogan P, Bruns TD, Chapin FS III (2000) Fire effects on ecosystem nitrogen cycling in a Californian bishop pine forest. Oecologia 122:537–544
Hendrick RL, Pregitzer KS (1996) Application of minirhizotrons to understand root function in forests and other natural ecosystems. Plant Soil 185:293–304
Hinderson R, Ford ED, Renshaw E, Deans JD (1983) Morphology of the structural root system Sitka spruce 1. Analysis and quantitative description. Forestry 56:121–135
Islam MA, Macdonald SE (2004) Ecophysiological adaptation of black spruce (*Picea mariana*) and tamarack (*Larix laricina*) seedlings to flooding. Trees 18:35–42
Johnson MG, Tingey DT, Phillips DL, Storm MJ (2001) Advancing fine root research with minirhizotrons. Environ Exp Bot 45:263–289
Kajimoto T, Matsuura Y, Sofronov MA, Volokitina AV, Mori S, Osawa A, Abaimov AP (1999) Above- and belowground biomass and net primary productivity of a *Larix gmelinii* stand near Tura, central Siberia. Tree Physiol 19:815–822
Kajimoto T, Matsuura Y, Osawa A, Prokushkin AS, Sofronov MA, Abaimov AP (2003) Root system development of *Larix gmelinii* trees affected by micro-scale conditions of permafrost soils in central Siberia. Plant Soil 255:281–292
Kajimoto T, Matsuura Y, Osawa A, Abaimov AP, Zyryanova OA, Isaev AP, Yefremov DP, Mori S, Koike T (2006) Size-mass allometry and biomass allocation of two larch species growing on the continuous permafrost region in Siberia. For Ecol Manage 222:314–325
Kajimoto T, Osawa A, Matsuura Y, Abaimov AP, Zyryanova OA, Kondo K, Tokuchi N, Hirobe M (2007) Individual-based measurement and analysis of root system development: case studies for *Larix gmelinii* trees growing on the permafrost region in Siberia. J Forest Res 12: 103–112
Karizumi N (1974) The mechanism and function of tree root in the process of forest production. 1. Method of investigation and estimation of the root biomass. Bull Gov For Exp Sta 259:1–99
Karizumi N (1979) Illustrations of tree roots. Seibundo Shinkosha, Tokyo, pp 554–557 (in Japanese)
Kharuk VI, Dvinskaya ML, Ranson KJ (2005) The spatiotemporal pattern of firesin northern Taiga larch forests of Central Siberia. Russian J Ecol 36:302–311
Krause C, Eckstein D (1993) Dendrochronology of roots. Dendrochronologia 11:9–23
Kuiper LC, Coutts MP (1992) Spatial disposition and extension of the structural root system of Douglas-fir. For Ecol Manage 47:111–125
Landhäusser SM, Wein RW (1993) Postfire vegetation recovery and tree establishment at the arctic treeline: climate-change-vegetation-response hypotheses. J Ecol 81:665–672
Lieffers VJ, Rothwell RL (1987) Rooting of peatland black spruce and tamarack in relation to depth of water table. Can J Bot 65:817–821
Mackay JR (1995) Active layer changes (1968 to 1993) following the forest-tundra fire near Inuvik, N.W.T., Canada. Arct Alp Res 27:323–336

Majdi H (1996) Root sampling methods – applications and limitations of minirhizotron technique. Plant Soil 185:255–258
McMinn RG (1963) Characteristics of Douglas-fir root systems. Can J Bot 41:105–122
Mund M, Kummetz E, Hein M, Bauer GA, Schulze E-D (2002) Growth and carbon stocks of a spruce forest chronosequence in central Europe. For Ecol Manage 171:275–296
Oechel WC, Van Cleve K (1986) The role of bryophytes in nutrient cycling in the taiga. In: Van Cleve K, Chapin FS III, Flanagan PW, Viereck LA, Dyrness CT (eds) Forest ecosystems in the Alaskan taiga. Ecological studies, vol 57. Springer, Berlin, pp 121–137
Osawa A, Abaimov AP, Matsuura Y, Kajimoto T, Zyryanova OA (2003) Anomalous patterns of stand development in larch forests of Siberia. Tohoku Geophys J (Sci Rep Tohoku Univ Ser 5) 36:471–474
Puhe J (2003) Growth and development of the root system of Norway spruce (*Picea abies*) in forest stands – review. For Eco Manage 175:253–273
Read DJ, Perez-Moreno J (2003) Mycorrhizas and nutrient cycling in ecosystems – a journey towards relevance? New Phytol 157:475–492
Reynolds ERC (1983) The development of root systems analyzed by growth rings. Plant Soil 71:167–170
Richardson A (2000) Coarse root elongation rate estimates for interior Douglas-fir. Tree Physiol 20:825–829
Rouse WR (1976) Microclimatic changes accompanying burning in subarctic lichen woodland. Arct Alp Res 4:357–376
Santantonio D, Hermann RK, Overton WS (1977) Root biomass studies in forest ecosystems. Pedobiologia 17:1–31
Schenk HJ (2006) Root competition: beyond resource depletion. J Ecol 94:752–739
Schenk HJ, Jackson RB (2002) Rooting depths, lateral root spreads and below-ground/above-ground allometries of plants in water-limited ecosystems. J Ecol 90:480–494
Schenk HJ, Callaway RM, Mahall BE (1999) Spatial root segregation: are plants territorial? Adv Ecol Res 28:145–180
Schmid I, Kazda M (2005) Clustered root distribution in mature stands of *Fagus sylvatica* and *Picea abies*. Oecologia 144:25–31
Schulze E-D (2006) Biological control of the terrestrial carbon sink. Biogeosciences 3:147–166
Schulze E-D, Schulze W, Kelliher FM, Vygodskaya NN, Ziegler W, Kobak KI, Koch H, Arneth A, Kusnetsova WA, Sogatchev A, Issajev A, Bauer G, Hollinger DY (1995) Aboveground biomass and nitrogen nutrition in a chronosequence of pristine Dahurian *Larix* stands in eastern Siberia. Can J For Res 25:943–960
Schwinning S, Weiner J (1998) Mechanisms determining the degree of size asymmetry in competition among plants. Oecologia 113:447–455
Smithwick EAH, Turner MG, Mack MC, Chapin FS III (2005) Postfire soil N cycling in northern conifer forests affected by severe, stand-replacing wildfires. Ecosystems 8:163–181
Sofronov MA, Volokitina AV, Kajimoto T, Matsuura Y, Uemura S (2000) Zonal peculiarities of forest vegetation controlled by fires in northern Siberia. Eurasian J For Res 1:51–59
Stone EL, Kalisz PJ (1991) On the maximum extent of tree roots. For Ecol Manage 46:59–102
Strong WL, La Roi GH (1983a) Rooting depth and successional development of selected boreal forest communities. Can J For Res 13:577–588
Strong WL, La Roi GH (1983b) Root system morphology of common boreal forest trees in Alberta, Canada. Can J For Res 13:1164–1173
Tryon PR, Chapin FS III (1983) Temperature control over root growth and root biomass in taiga forest trees. Can J For Res 13:827–833
Van Cleve K, Barney R, Schlentner R (1981) Evidence of temperature control of production and nutrient cycling in two interior Alaska black spruce ecosystems. Can J For Res 11:258–273
Van Cleve K, Dyrness CT, Viereck LA, Fox J, Chapin FS III, Oechel W (1983a) Taiga ecosystems in Interior Alaska. Bioscience 33:39–44
Van Cleve K, Oliver L, Schlentner R, Viereck LA, Dyrness CT (1983b) Productivity and nutrient cycling in taiga forest ecosystems. Can J For Res 13:747–766

Viereck LA (1982) Effects of fire and firelines on active layer thickness and soil temperature in interior Alaska. In: Frech HM (ed) Proceedings of the fourth Canadian permafrost conference. National Research Council Canada, Ottawa, pp 123–135

Vogt KA, Persson H (1991) Measuring growth and development of roots. In: Lassoie JP, Hinckley TM (eds) Techniques and approaches forest tree ecophysiology. CRC Press, Boca Raton, pp 477–501

Vogt KA, Vogt DJ, Palmiotto PA, Boon P, O'Hara J, Asbjornsen H (1996) Review of root dynamics in forest ecosystems grouped by climate, climatic forest type and species. Plant Soil 187:159–219

Vogt KA, Vogt DJ, Bloomfield J (1998) Analysis of some direct and indirect methods for estimating root biomass and production of forests at an ecosystem level. Plant Soil 200:71–89

Wan S, Hui D, Luo Y (2001) Fire effects on nitrogen pools and dynamics in terrestrial ecosystems: a meta-analysis. Ecol Appl 11:1349–1365

Wein RW, Bliss LC (1973) Changes in arctic *Eriophorum* Tussock communities following fire. Ecology 54:845–852

Weiner J (1990) Asymmetric competition in plant populations. Trends Ecol Evol 5:360–364

Williams PJ, Smith MW (1989) The frozen earth. Fundamentals of geocryology. Cambridge University Press, Cambridge 306pp

Chapter 17
Seasonal Changes in Stem Radial Growth of *Larix gmelinii* in Central Siberia in Relation to its Climatic Responses

K. Yasue, J. Kujansuu, T. Kajimoto, Y. Nakai, T. Koike, A.P. Abaimov, and Y. Matsuura

17.1 Introduction

Tree stem is a major part of the carbon sink in forest ecosystems because of its large storage and long-term preservation. It may also have large potential as a factor in global carbon dynamics. Therefore, analysis of stem growth has drawn increasing attention, in which the study of radial growth responses in trees is an important subject to be understood in the effects of global warming on carbon storage in forests.

There have been several reports on climatic responses of larch radial growth in Siberia that were based on dendrochronological techniques. Significant correlations between spring temperatures and tree-ring widths for conifers (Vaganov et al. 1999), including major *Larix* species (*L. sibirica* Ledeb., *L. gmelinii* (Rupr.) Rupr. and *L. cajanderi* Mayr.) ,have been demonstrated at various locations in Siberian boreal forests (Kirdjanov and Zaharjevsky 1996; Naurzbaev and Vaganov 2000; Kirdyanov et al. 2003, 2007). Kirdyanov et al. (2003) showed that the estimated date of snowmelt was highly correlated with ring width, and postulated that the initiation of radial growth was initially controlled by snowmelt. Tree-ring density is also important as a tree-ring parameter in efforts to estimate the amount of carbon stored in tree trunks. Significant correlations between maximum density of tree rings and summer temperature have been described (Briffa et al. 1995; Kirdjanov and Zaharjevsky 1996; Kirdyanov et al. 2003, 2007). Because of their sensitivity to summer temperature, maximum densities were often used for past climate reconstructions (Briffa et al. 1995, 2001; Yasue et al. 2000).

In spite of reports on ring widths and maximum densities, the climatic effects on annual growth of xylem substance, representing the amount of fixed carbon, has not been described. In addition, there have been few reports on seasonality in radial growth in *L. gmelinii* trees growing on the permafrost. Observations on the seasonal radial growth of the species are limited in the nonpermafrost region, such as the vicinity of the city of Krasnojarsk in Central Siberia (Antonova and Stasova 1997). Observations in the regions of permafrost are necessary to understand mechanisms of how spring climate and snow conditions affect seasonal radial growth of *L. gmelinii*.

A. Osawa et al. (eds.), *Permafrost Ecosystems: Siberian Larch Forests*, Ecological studies, Vol. 209, DOI 10.1007/978-1-4020-9693-8_17,

Differences in topographical features, such as slope exposure, may also be the factor influencing tree-ring formation (Koike et al. 1998; Kirchhefer 2000). Koike et al. (1998) reported differences in shoot morphology, rates of photosynthesis, and nutrient conditions of *L. gmelinii* growing on soil active layers of different depths on contrasting north- and south-facing slopes in Central Siberia (see also Chap. 14). Because of changes in the depth of the active layer that might be expected to occur as a result of future climate change, it is important to identify responses of radial growth in larch trees to climate variables under different microsite conditions with varying depths of soil active layer.

In this chapter, we present results on (1) investigation on seasonal needle growth and stem radial growth over 2 years, and (2) dendroclimatic analyses on the responses of tree-ring parameters to climatic factors. In addition, limiting factors on radial growth in *L. gmelinii* that grow on the permafrost are discussed.

17.2 Approaches to Study Growth Phenology and Tree-Ring Responses to Climate

17.2.1 Study Sites

Two study sites were established in Tura Experiment Forest (64°19′N, 100°13′E; 200 m a.s.l.) of V.N. Sukachev Institute of Forest (Siberian Branch, Russian Academy of Science, Russia), on Central Siberian Plateau (see Fig. 1.1). The sites consisted of old *L. gmelinii* forests (over 100 years-old); one was located on north- to south-facing concave slopes across a small river in Site 2, and the other was located on gentle, north- to south-facing convex slopes on a small hill at southern end of Carbon Flux Site (Fig. 17.1; see also Fig. 1.3 and Table 1.1). The depth of

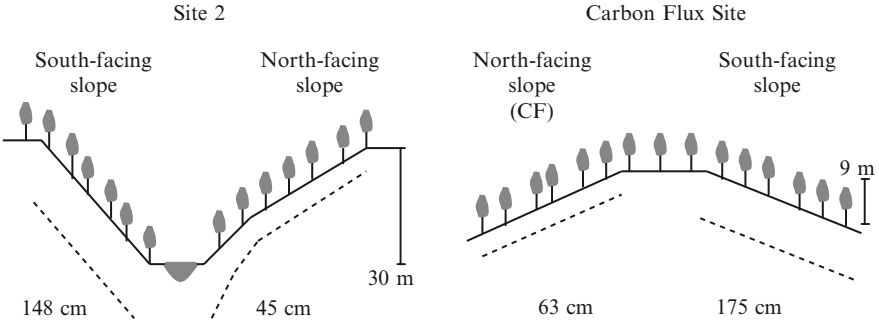

Fig. 17.1 Schematic representation of the study sites. Depths of soil active layers are indicated by *numerical values* and *dotted lines*, but are not shown to scale. The depths of the soil active layers at Site 2 were recorded in the summer of 1997 (Koike et al. 1998); those at Carbon flux site were recorded in the autumn of 2003 (modified from Kujansuu et al. (2007b))

soil active layer differed between the north- and south-facing slopes at both sites: deeper in south-facing slope than in north-facing slope (Koike et al. 1998; Kujansuu et al. 2007b).

17.2.2 Observations of Snow Melting, Needle Phenology, and Seasonal Radial Growth

Through the field observation from 2004 to 2005, we investigated (1) timing of snow disappearance at Site 2, (2) needle phenology of larch trees at Carbon flux site, and (3) seasonal changes in radial growth at Carbon flux site.

The timing of snow disappearance in both north- and south-facing slopes at Site 2 was observed during the spring season of 2004. An automatic camera (Kadec-Eye, Kona System, Sapporo, Japan) was fixed at about 5 m high on a tree standing at the north-facing slope. The camera angle was arranged so that both north- and south-facing slopes were included in the view (Fig. 17.2). Photos were taken daily at noon. Snow disappearance was defined as a condition where area of snow-cover becomes less than 10% for the observation area.

Needle phenology was observed at Carbon Flux Site during the growing seasons of 2004 and 2005. The photos were taken four times per day using another system of automatic camera (Climatec, Tokyo, Japan) (Fig. 17.3). The site for radial growth observation was also located near the area of needle phenology study.

Knife marking experiment was carried out to investigate seasonality of xylem formation in *L. gmelinii* at Tura. Two dominant trees (ca. 105 years-old in 2004) were chosen at Carbon flux site. The larch stand regenerated after a forest fire of late-1890s. The selected trees were relatively large (about 10 m in heights and 8 cm in DBH), and were expected to form wide-enough rings for measurement. A blade disposable cutter knife (Olfa, Japan) was inserted at a marking point and was removed immediately (Yoshimura et al. 1981; Kuroda and Kiyono 1997).

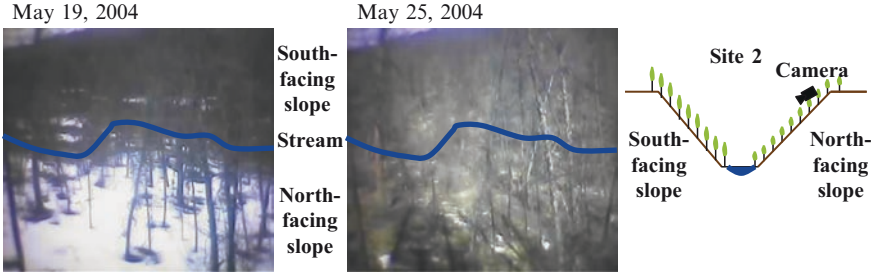

Fig. 17.2 Difference in snow disappearance date between north- and south-facing slopes at Site 2 in Tura, central Siberia. Daily photographs were taken by automatic camera during a spring season in 2004. Schematic representation of the camera setting is shown on the right-hand side (Yasue et al. unpublished data)

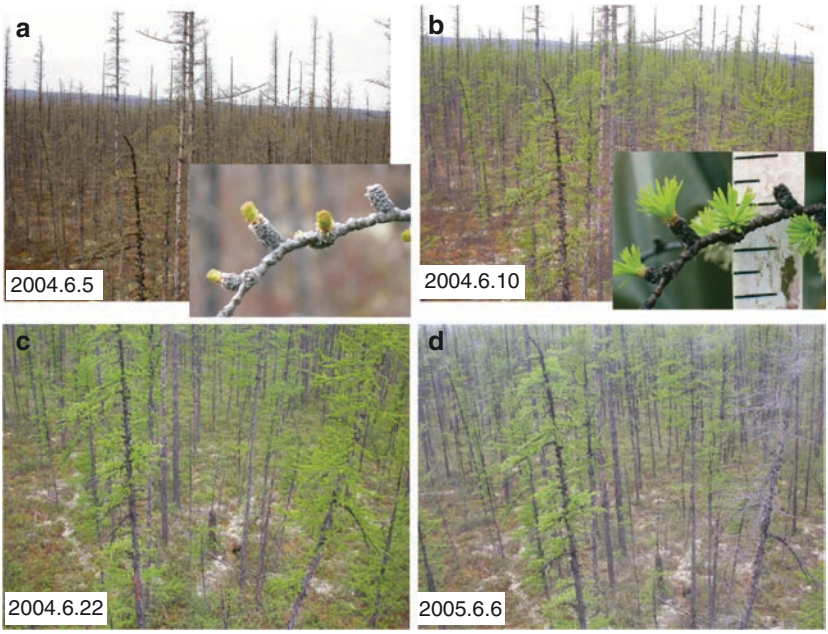

Fig. 17.3 Needle development of *Larix gmelinii* at Carbon flux site in Tura in 2004 (**a**–**c**) and 2005 (**d**) observed by automatic camera (Yasue et al. unpublished data) *See* Color Plate

The wounding operation was performed every ca. 10 days from end of May to end of September. The study was carried out over two seasons from 2004 to 2005. The trees were cut at stem base in September 2005. Wood blocks taken from the marking points were stored in 50% ethanol solution to extract resins that fills pores of tracheids. Transverse sections of 12 μm thickness were stained with 1% safranin solution and were mounted on glass. The sections were observed under light microscope and under polarized light microscope. The positions of cambial initials at the time of wounding were distinguished by immature tracheids at radial enlarging and secondary wall thickening (Fig. 17.4). Resin ducts (Yoshimura et al. 1981; Kuroda and Shimaji 1983) and flattened cells (Nobuchi et al. 1993) also helped to distinguish positions of cambial initials. Number of developed tracheids before wounding was counted for five radial files and averaged.

17.2.3 Analysis of Climatic Response of Radial Growth

To analyze climatic responses of radial growth statistically, tree-ring chronologies for two slopes (north- and south-facing) at each site were developed (Site 2 and Carbon Flux Site; see Fig. 17.1): four slopes were examined in total. Increment

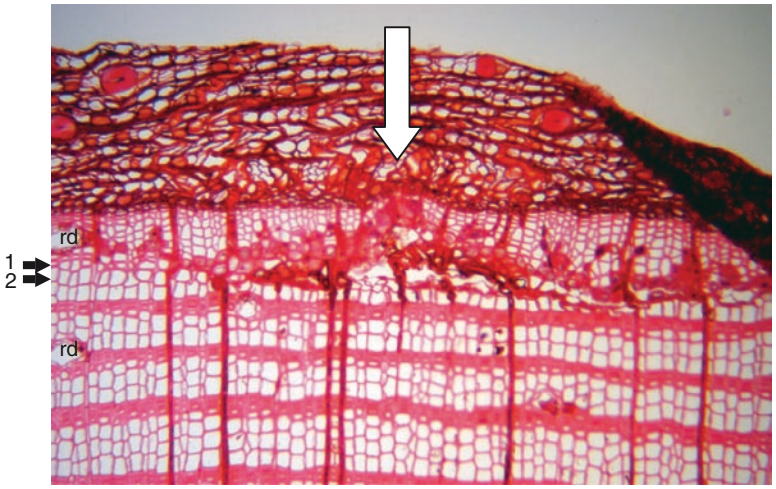

Fig. 17.4 Light micrograph of a transverse section of the area wounded on July 2, 2004. *Vertical thick arrow*, site of wounding; *Arrow 1*, position of cambial initials at the time of wounding; *Arrow 2*, position of initial of secondary layer deposition; rd, resin duct (Yasue et al. unpublished data)

cores or disks were extracted from 21 to 59 dominant trees per slope for examination (Kujansuu et al. 2007a, b; Table 17.1). Ring width, maximum density, and mean density were measured by standard X-ray technique for two directions for each tree. A series of tree-ring widths was cross-dated visually by using skeleton plot procedures and confirmed by a statistical method to ensure that correct dates have been assigned to the annual rings (Stokes and Smiley 1996). In addition, tree-ring mass was calculated by the product of ring width and ring mean density (Fig. 17.5). Then, ring width, maximum density, and tree-ring mass series were standardized by fitting smoothing splines (Cook and Peters 1981), with a 50% frequency-response cutoff of 80 years, for reduction of age-related trend and nonclimatic signals. The chronologies of ring width, maximum density, and tree-ring mass for each plot were developed by averaging the individual series by using a biweight robust mean.

Responses of tree-ring parameters to climatic variables were analyzed by calculating simple correlations. The climatic data used for the present calculations were obtained from Tura Meteorological Station (http://meteo.ru). Average daily mean temperatures for 10 consecutive days were used in the analysis, with a 2-day lag, starting from May 1 of the previous year. We chose to use the 10-days averaging because previous studies for *Larix* species (*L. sibirica*, *L. gmelinii*) in Siberia reported strong relationships between ring width and temperature in short time spans (Vaganov et al. 1999; Naurzbaev and Vaganov 2000; Kirdyanov et al. 2003; see also Chap. 18). Monthly precipitation data from May to September of the previous year and from May through August of the current year were also used. Winter precipitation was calculated as total precipitation from October of the previous year to April of the current year, because precipitation falls as snow. Analysis of tree-ring parameters

Table 17.1 Statistics of chronologies of *Larix gmelinii* at Site 2 and carbon flux site (modified from Kujansuu et al. 2007b)

	Ring width				Maximum ring density			
	Site 2		Carbon flux site		Site 2		Carbon flux site	
	North	South	North	South	North	South	North	South
Number of trees in chronology (radii)	58 (92)	59 (85)	21 (33)	26 (40)	19 (29)	27 (39)	21 (33)	26 (39)
Starting year of chronology	1621	1812	1920	1908	1811	1823	1920	1923
Standard chronology								
Mean sensitivity	0.22	0.24	0.23	0.17	0.06	0.05	0.05	0.04
Standard deviation	0.29	0.24	0.27	0.27	0.09	0.07	0.07	0.04
First-order autocorrelation	0.60	0.35	0.37	0.60	0.56	0.40	0.35	0.22
Correlation between trees[a]	0.34	0.48	0.45	0.42	0.32	0.38	0.34	0.30
Expressed population signal (EPS)	0.97	0.97	0.91	0.92	0.90	0.93	0.91	0.92
Minimum sample size for ESP 85%	12	12	12	13	13	12	12	13
Subsample signal strength > 0.85 (SSS)[b]	1800	1821	1921	1920	1895	1839	1923	1930
Residual chronology								
Mean sensitivity	0.25	0.26	0.26	0.22	0.07	0.06	0.05	0.04
Standard deviation	0.22	0.22	0.23	0.21	0.07	0.06	0.06	0.04
Correlation between trees[a]	0.37	0.52	0.44	0.41	0.36	0.39	0.33	0.33
Expressed population signal (EPS)	0.97	0.97	0.91	0.93	0.90	0.93	0.91	0.92
Minimum sample size for ESP 85%	12	12	12	12	13	12	12	12
Subsample signal strength > 0.85 (SSS)[b]	1800	1821	1921	1920	1895	1839	1923	1930

[a] Calculated for the common interval from 1930 to 2003

[b] Earliest year for which SSS of the chronology is greater than 85% of the original EPS

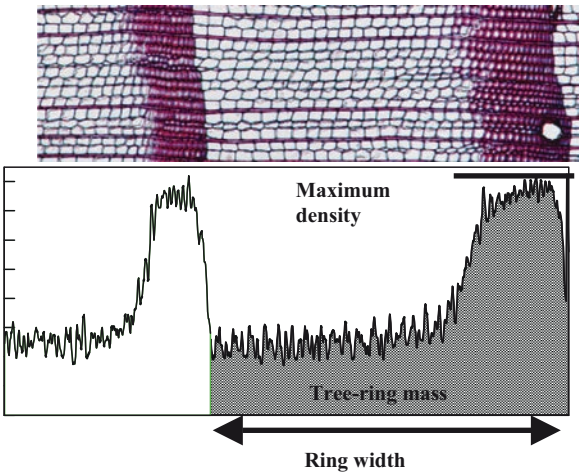

Fig. 17.5 Tree-ring parameters analyzed by X-ray densitometry. A density *curve* represents changes in diameter and cell wall thickness of tracheids in annual rings (Yasue et al. unpublished data)

and temperature covered a period from 1930 to 1995 (n = 65). That of tree-ring parameters and precipitation covered a period from 1939 to 1995 (n = 56).

17.3 Seasonal Changes in Snow Melting, Needle Phenology, and Radial Growth

In the spring of 2004, snow disappearance was observed on May 19 in the south-facing slope and on May 25 in the north-facing slope (Fig. 17.2). The results indicate about 1 week difference in the disappearance of snow cover between north- and south-facing slopes.

Needles flushed at the end of May and continued their development until mid June of 2004 (Fig. 17.3). On the other hand, in 2005, the needles had already been developed by the beginning of June when observation by an automatic camera was started. The difference can be attributed to difference in air temperature during an early season (from late May to mid June) between the two observation years: normal spring in 2004 and warm spring in 2005 (Fig. 17.6).

Knife marking experiment at Carbon Flux Site showed that cambial division started at the beginning of June in both years (Fig. 17.6). The cambial activity in 2004 ceased in mid July, whereas that in 2005 ceased in the beginning of August. There were few differences in the dates of reactivation in two sample trees in spite of about 2-week difference in needle development between the years. Results suggest that cambial initiation might not be sensitive to spring temperature. On the other hand, cell division ceased about 2 weeks earlier in normal spring of 2004 than in warm spring of 2005 (Fig. 17.6).

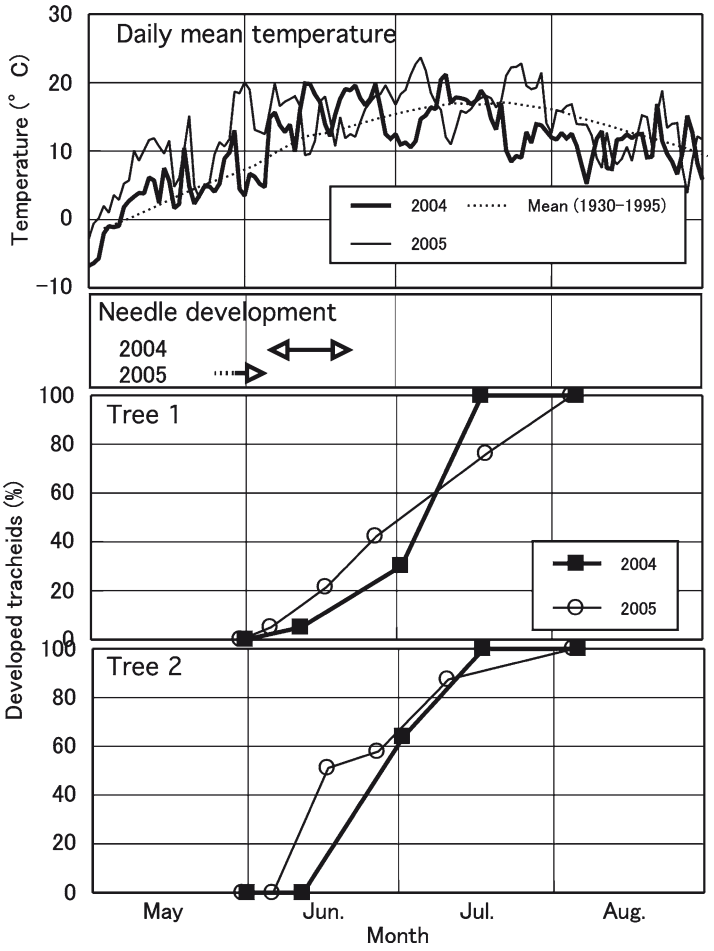

Fig.17.6 Tracheid development curves of two sample trees of *Larix gmelinii* at Carbon Flux Site in Tura, Central Siberia, and related daily mean temperature in 2004 and 2005. The period of needle development were shown in the middle (Yasue et al. unpublished data)

The longer duration of radial growth in 2005 may have been caused by ample supply of photosynthates that resulted from high spring temperature.

17.4 Climatic Responses of Radial Growth

Both residual and standard chronologies of ring widths were positively correlated with temperature from late May to mid June on all four slopes (Fig. 17.7). In contrast, standard chronologies of ring widths were negatively correlated with precipitation during the winter (from October to April) and in May on the north-facing

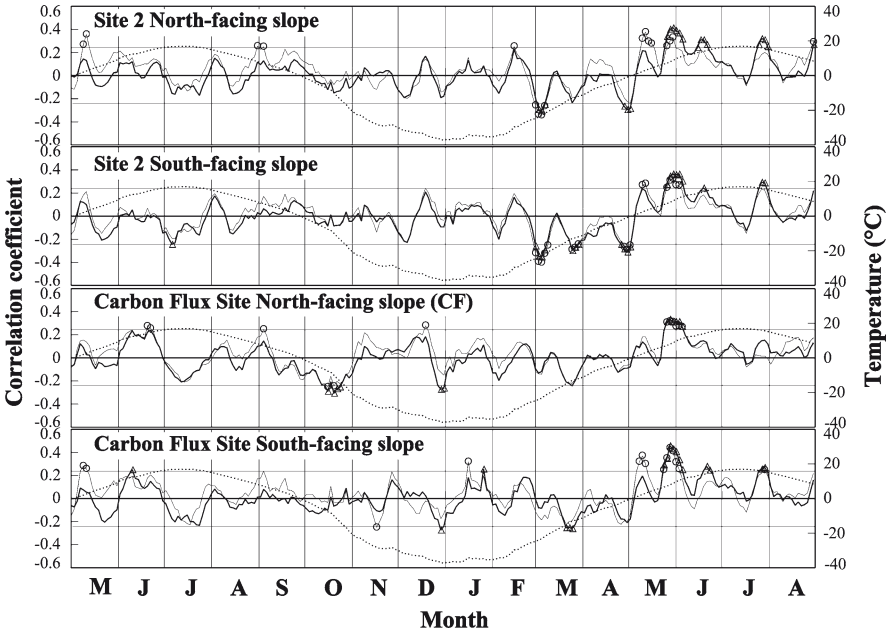

Fig. 17.7 Correlations between ring widths and 10-day average temperatures for *Larix gmelinii* on the north- and south-facing slopes at Site 2 and Carbon Flux Site in Tura, Central Siberia. The *thick* and *thin lines* indicate correlations of residual and standard chronologies, respectively. Each point represents the first day of a 10-day window with 2-day lag. *Horizontal lines* indicate bounds within which correlations are significant ($p = 0.05$). *Triangles* and *circles* indicate significant correlations ($p < 0.05$) of residual and standard chronologies, respectively. Sinusoidal curves show mean values of 10-day average temperatures, as calculated for the period from 1930 to 1995. *Letters* indicate months of the year (modified from Kujansuu et al. (2007b))

slope at Site 2 and on the south-facing slope at Carbon Flux Site, respectively (Fig. 17.8). The negative correlations with precipitation during winter and in May on some slopes suggested that delayed snowmelt in early spring may inhibit ring growth of *L. gmelinii*, and that effects of snow are likely to vary with topography. Difference in the responses to precipitation of winter and May existed between residual and standard chronologies (Kujansuu et al. 2007b). Weak correlations with residual chronologies indicate that precipitation of winter and May do not affect year-to-year (high-frequency) variations in ring widths. On the other hand, negative correlations between standard chronologies and precipitation of winter and May indicate possibility that low-frequency fluctuations in precipitation influence the radial growth (Kujansuu et al. 2007b).

Both residual and standard chronologies of maximum densities were positively correlated with temperature in early July on all four slopes (Fig. 17.9). Maximum densities were also positively correlated with precipitation during summer of the previous year on all slopes (Fig. 17.10). These suggest that no major differences

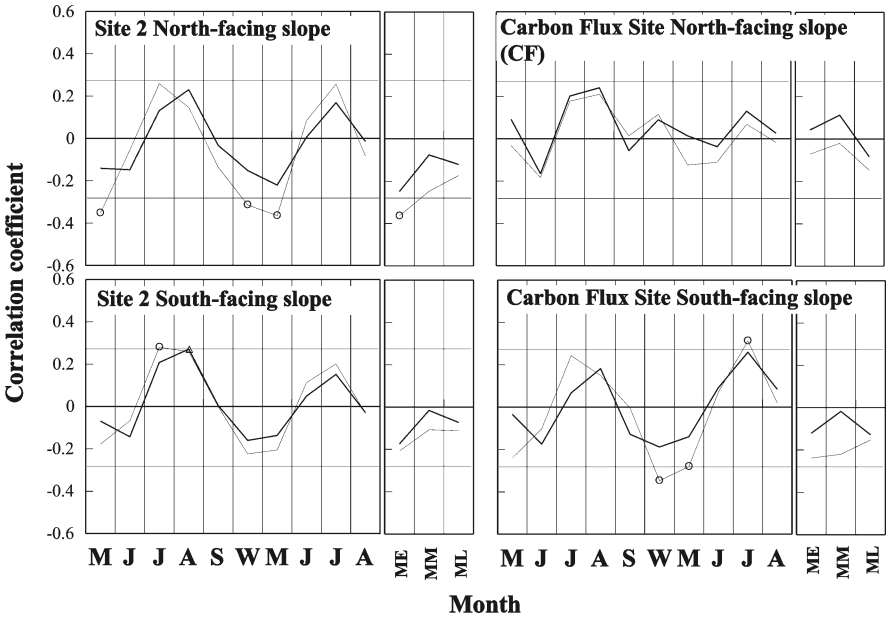

Fig. 17.8 Correlations between ring widths and precipitation for *Larix gmelinii* on the north- and south-facing slopes at Site 2 and Carbon Flux Site in Tura, Central Siberia. *Letters* indicate months of the year; W shows the sum of winter months (from October to April), and ME, MM, and ML indicate early May, mid May, and late May, respectively (modified from Kujansuu et al. (2007b))

exist in terms of responses of maximum density to climatic factors between the north- and south-facing slopes.

Standardized chronologies of tree-ring mass revealed positive correlations with temperature of mid May for both current and previous years, except for north-facing slope of Carbon Flux Site (Fig. 17.11). Tree-ring masses on both slopes at Site 2 were correlated with precipitation of previous May (Fig. 17.12). Tree-ring masses of north-facing slope of Site 2 and south-facing slope of Carbon Flux Site were correlated with winter (October–April) precipitation. Tree-ring masses of all sites except for south-facing slope of Site 2 were correlated with precipitation of current May. Tree-ring masses revealed positive correlations with summer temperature (June or July) of both previous and current growing seasons except for north-facing slope of Carbon Flux Site.

Tree-ring mass (Fig. 17.11) revealed similar responses to temperature of mid May that was also detected in the case of ring width (Kujansuu et al. 2007b). However, the period of significant correlation is quite short when compared with that for ring width. Weak correlation with summer temperature was observed. Responses to precipitation seem to be mixed for both ring width and maximum density, representing negative correlation with precipitation during winter and May and positive correlation with summer precipitation. The responses to precipitation also vary by sites.

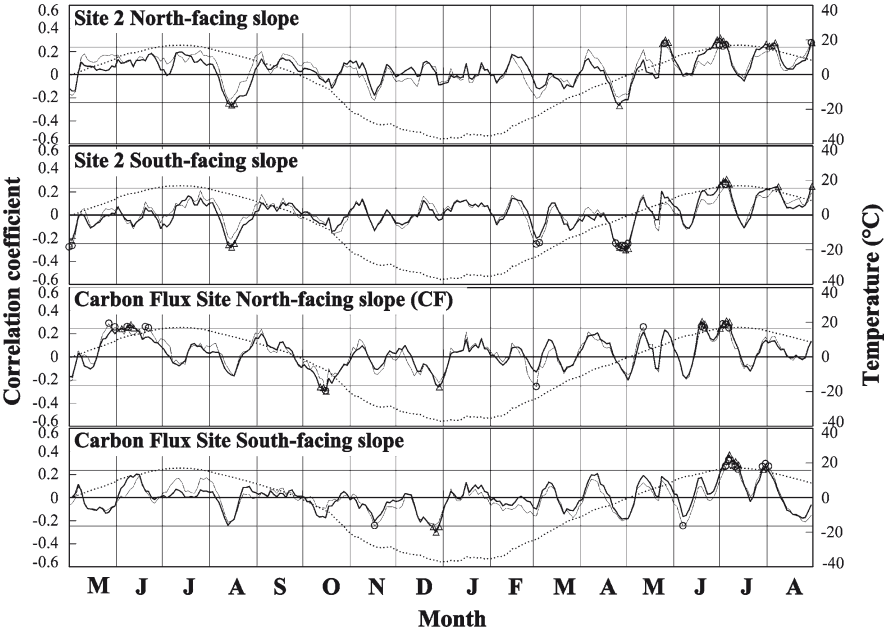

Fig. 17.9 Correlations between maximum densities and 10-day average temperatures for *Larix gmelinii* on the north- and south-facing slopes at Site 2 and Carbon Flux Site in Tura, central Siberia. *Letters* indicate months of the year (modified from Kujansuu et al. 2007b)

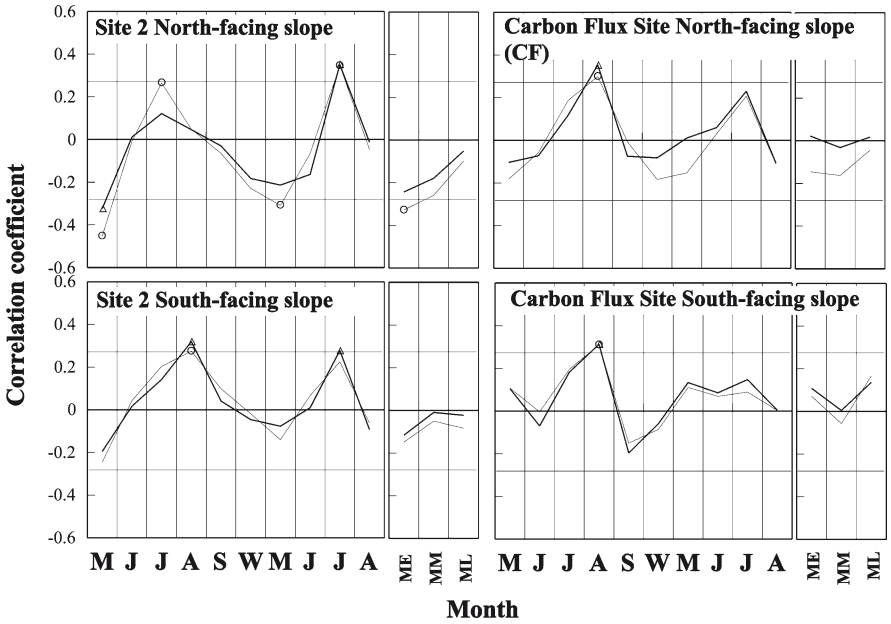

Fig. 17.10 Correlations between maximum densities and precipitation for *Larix gmelinii* on the north- and south-facing slopes at Site 2 and Carbon Flux Site in Tura, Central Siberia. *Letters* indicate months of the year; other letters (W, ME, MM, and ML) are the same in Fig. 17.8 (modified from Kujansuu et al. 2007b)

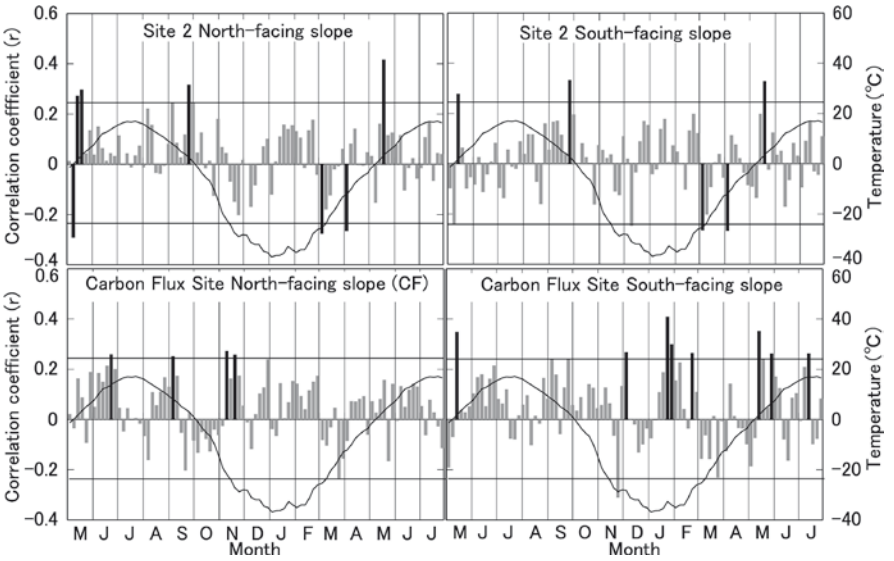

Fig. 17.11 Correlations between tree-ring mass and 10-day average temperatures for *Larix gmelinii* on the north- and south-facing slopes at Site 2 and Carbon Flux Site in Tura, central Siberia. Each *bar* represents the first day of a 10-day window with 2-day lag. *Horizontal lines* indicate bounds within which correlations are significant ($p = 0.05$). *Black bars* indicate significant correlations ($p < 0.05$). Sinusoidal curves show mean values of 10-day average temperatures, as calculated for the period from 1930 to 1995. *Letters* indicate months of the year (Yasue et al. unpublished data)

The patterns of climatic responses in tree-ring mass indicate that the most dominant limiting factor on carbon fixation is extent of snow accumulation in spring. Changes in precipitation of winter and early to mid May are likely to cause variation in snow accumulation in spring, because average temperature of early May remains below freezing. Delayed soil thawing caused by the accumulated snow in the spring might lead to decrease in the depth of soil active layer in the summer and to limit duration of root activity. Observations on the seasonal changes in radial growth indicated that warm spring did not lead to early initiation of cambial reactivation, but resulted in longer duration of cambial activity. These observations also support the above hypothesis on the effect of accumulated snow on stem growth. The roots of larch trees growing in nutrient-poor permafrost soils are thought to play an important role in their survival, as was indicated in large allocation of biomass to roots (Kajimoto et al. 1999; see also Chaps. 6 and 16). It may also be associated with slow rate of carbon turnover. Kagawa et al. (2006a, b) reported that assimilated carbon was carried-over and used to xylem development of the following years in a young *L. gmelinii* tree growing on permafrost in Northeastern Siberia, and the carbon turnover rate was slower than that of temperate trees. It can be hypothesized that delayed soil thawing inhibit (1) translocation of stored assimilates from roots to above ground parts, and (2) nutrient uptake by the roots.

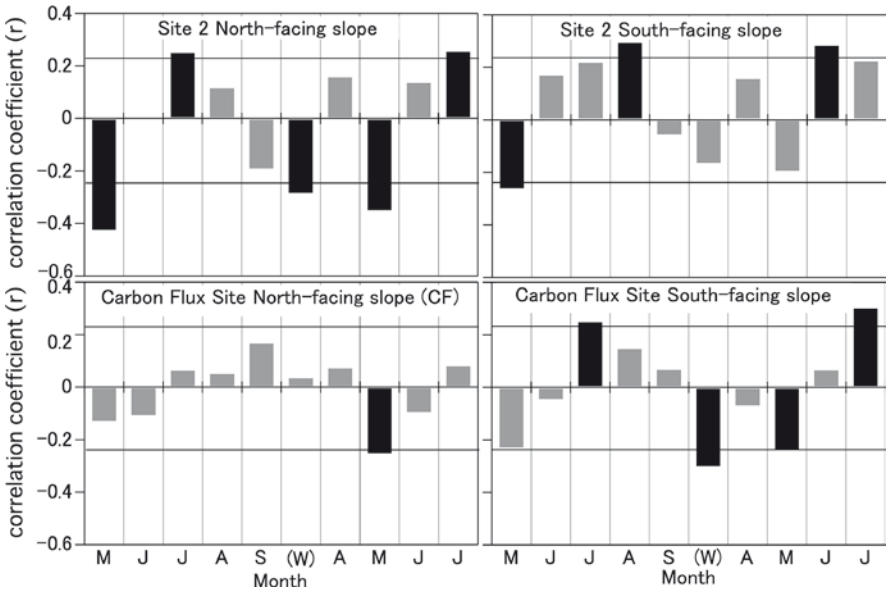

Fig. 17.12 Correlations between tree-ring mass and precipitation for *Larix gmelinii* on the north- and south-facing slopes at Site 2 and Carbon Flux Site in Tura, Central Siberia. W is Winter (October to April) accumulation. *Letters* indicate months of the year; other letters (W, ME, MM, and ML) are the same in Fig. 17.8 (Yasue et al. unpublished data)

Vaganov et al. (1999) and Kirdyanov et al. (2003) proposed that the date of snowmelt, being estimated from temperature and winter precipitation, had a significant effect on ring width (see also Chap. 18). They stated that recent trend of increasing precipitation in winter and delay in snowmelt could have a significant effect on radial growth of larch trees in Siberia. The present study revealed stronger effects of snow on tree-ring mass than those on ring width. This suggests that changes in spring temperatures and winter snow accumulation are important in assessing the effect of future changes in climate on carbon assimilation of *L. gmelinii* in Central Siberia. The study also confirmed the importance of microscale topography on growth of larch trees, which might also reflect local-scale difference in snow accumulation.

17.5 Conclusions

The effect of climatic factors on radial growth of *Larix gmelinii* in Tura in Central Siberia was analyzed with two approaches: (1) seasonal observation of needle development and radial growth and (2) dendrochronological analysis on climatic responses of tree-ring parameters. The needle development was about 2 weeks earlier in the warm spring of 2005 than in the normal spring of 2004. Cambial division

started in the beginning of June in both years. The cambial activity in 2004 ceased in the mid July, whereas that in 2005 ceased in the beginning of August. Therefore, cambial initiation might not be sensitive to spring temperature. On the other hand, longer duration of radial growth may be caused by sufficient supply of photosynthates. A dendroclimatological analysis of the climatic responses at two different sites revealed that precipitation of winter and May was the most dominant limiting factor on tree-ring mass, which represents total annual deposition of carbon on the tree stem. The delayed snowmelt in early spring might inhibit radial growth, and lead to decrease in carbon accumulation on stems of larch trees growing on the permafrost.

References

Antonova GF, Stasova VV (1997) Effects of environmental factors on wood formation in larch (*Larix sibirica* Ldb.) stems. Trees 11:462–468

Briffa KR, Jones PD, Schweingruber FH, Shiyatov SG, Cook ER (1995) Unusual twentieth-century summer warmth in a 1,000-year temperature record from Siberia. Nature 376:156–159

Briffa KR, Osborn TJ, Schweingruber FH, Harris IC, Jones PD, Shiyatov SG, Vaganov EA (2001) Low-frequency temperature variations from a northern tree ring density network. J Geophys Res 106 D: 2929–2941

Cook ER, Peters K (1981) The smoothing spline: a new approach to standardizing forest interior tree-ring width series for dendroclimatic studies. Tree-Ring Bull 41:45–53

Kagawa A, Sugimoto A, Maximov TC (2006a) Seasonal course of translocation, storage and remobilization of ^{13}C pulse-labeled photoassimilate in naturally growing *Larix gmelinii* saplings. New Phytol 171:793–804

Kagawa A, Sugimoto A, Maximov TC (2006b) $^{13}CO_2$ pulse-labelling of photoassimilates reveals carbon allocation within and between tree rings. Plant Cell Environ 29:1571–1584

Kajimoto T, Matsuura Y, Sofronov MA, Volokitina AV, Mori S, Osawa A, Abaimov AP (1999) Above- and belowground biomass and net primary productivity of a *Larix gmelinii* stand near Tura, central Siberia. Tree Physiol 19:815–822

Kirchhefer AJ (2000) The influence of slope aspect on tree-ring growth of *Pinus sylvestris* L. in northern Norway and its implications for climate reconstruction. Dendrochronologia 18:27–40

Kirdjanov AV, Zaharjevsky DV (1996) Dendroclimatological study on tree-ring width and maximum density chronologies from *Picea obovata* and *Larix sibirica* from the north of Krasnoyarsk region (Russia). Dendrochronologia 14:227–236

Kirdyanov AV, Hughes MK, Vaganov EA, Schweingruber FH, Silkin P (2003) The importance of early summer temperature and date of snowmelt for tree growth in the Siberian subarctic. Trees 17:61–69

Kirdyanov AV, Vaganov EA, Hughes MK (2007) Separating the climatic signal from tree-ring width and maximum latewood density records. Trees 21:37–44

Koike T, Mori S, Matsuura Y, Prokushkin SG, Zyranova OA, Kajimoto T, Abaimov AP (1998) Photosynthesis and foliar nutrient dynamics in larch and spruce grown on contrasting north- and south-facing slopes in the Tura Experiment Forest in Central Siberia. In: Mori S, Kanazawa Y, Matsuura Y, Inoue G (eds) Proceedings of the sixth symposium on the Joint Siberian Permafrost studies between Japan and Russia in 1997. Tsukuba, pp 3–10

Kujansuu J, Yasue K, Koike T, Abaimov AP, Kajimoto T, Takeda T, Tokumoto M, Matsuura Y (2007a) Climatic responses of tree-ring widths of *Larix gmelinii* on contrasting north- and south-facing slopes in central Siberia. J Wood Sci 53:87–93

Kujansuu J, Yasue K, Koike T, Abaimov AP, Kajimoto T, Takeda T, Tokumoto M, Matsuura Y (2007b) Responses of ring widths and maximum densities of *Larix gmelinii* to climate on contrasting north- and south-facing slopes in central Siberia. Eco Res 22:582–592

Kuroda K, Kiyono Y (1997) Seasonal rhythms of xylem growth measured by the wounding method and with a band-dendrometer: an instance of *Chamaecyparis obtsusa*. IAWA J 18:291–299

Kuroda K, Shimaji K (1983) Traumatic resin canal formation as a marker of xylem growth. For Sci 29:653–659

Naurzbaev MM, Vaganov EA (2000) Variation of early summer and annual temperature in east Taymir and Putoran (Siberia) over the last two millennia inferred from tree rings. J Geophys Res 105:7317–7326

Nobuchi T, Fujisawa T, Saiki H (1993) An application of the pinning method to the marking of the differentiating zone and to the estimation of the time course of annual ring formation in Sugi (*Cryptomeria japonica*). Mokuzai Gakkaishi 39:716–723

Stokes MA, Smiley TL (1996) An introduction to tree-ring dating. University of Chicago Press, Chicago

Vaganov EA, Hughes MK, Kirdyanov AV, Schweingruber FH, Silkin PP (1999) Influence of snowfall and melt timing on tree growth in subarctic Eurasia. Nature 400:149–151

Yasue K, Funada R, Kobayashi O, Ohtani J (2000) The effects of tracheid dimensions on variations in maximum density of *Picea glehnii* and relationships to climatic factors. Trees 14:223–229

Yoshimura K, Itoh T, Shimaji K (1981) Studies on the improvement of the pinning method for marking xylem growth (II). Pursuit of the time sequence of abnormal tissue formation in loblolly pine. Mokuzai Gakkaishi 27:755–760

Chapter 18
Dendrochronology of Larch Trees Growing on Siberian Permafrost

E.A. Vaganov and A.V. Kirdyanov

18.1 Introduction

Larch is the tree species most widely spread in the permafrost region of Siberia (Anonymous 1977; Dilis 1981; Koropachinskii 1983; Abaimov et al. 1997). Morphological and physiological features of the larch allowed it to adapt to severe conditions of climate, permafrost, and poor soils. The northern tree line of this species corresponds to the latitudinal timberline (Dilis 1981; Abaimov 1995). Tree-ring growth of larch at permafrost regions is characterized by features typical for the trees growing under strong influence of temperature (Vaganov et al. 1996). Dendrochronological method allows us to investigate various aspects of tree-ring formation at different locations under different conditions (Schweingruber 1996; see Chap. 17).

It was previously shown that forest-tundra (including northern open woodlands; definition see Fig. 1.2) and northern taiga ecosystems are very sensitive to global and regional environmental changes (Budiko and Izrael 1987; IPCC 2001). Use of dendrochronological techniques applied to the larch trees in the northern region gives a possibility to obtain retrospective patterns of climatic changes for vast territories (Schweingruber and Briffa 1996; Vaganov et al. 1996). As age of larch can be up to 600–700 years (Brown 1996; Vaganov et al. 1996) and some trees in the northern Siberia reach the age of more than 1,000 years (Vaganov et al. 1999b; Hughes et al. 2001), it is possible to investigate changes in some climatic parameters over hundreds and even thousands of years. Namely, a number of supra-long tree-ring chronologies were developed for the northern larch (Shiyatov 1993; Hantemirov 1999; Naurzbaev and Vaganov 2000). These chronologies are shown to be the most sensitive to summer temperature.

In the northern Siberian forest ecosystems, large portion of larch stand biomass is accumulated in above ground wood biomass (Bazilevich 1993). Therefore, changes in tree growth rate caused by environmental changes will be directly reflected in carbon storage of northern ecosystems (see Chaps. 6 and 24). Dendrochronological techniques give a possibility to follow year-to-year variability of stand dynamics, biomass accumulation in trees, and assess carbon capacity of

A. Osawa et al. (eds.), *Permafrost Ecosystems: Siberian Larch Forests*,
Ecological studies, Vol. 209, DOI 10.1007/978-1-4020-9693-8_18,

forest ecosystems (Graumlich et al. 1989; Vaganov and Hughes 2000; Knorre et al. 2006; see also Chap. 7).

Fire is another external factor, which is powerful enough to transform forest ecosystems (Furyaev et al. 2001; see also Chap. 4). Along with the climate, fires change ecological characteristics of the ecosystems, and their biogeochemical and hydrological cycles (Van Cleve and Viereck 1981; Crutzen and Goldammer 1993). Swetnam (1996), Arbatskaya (1998), Kharuk et al. (2007), and others showed that dendrochronological techniques are suitable for studying frequency of forest fires, their intensity, and occurrence. These investigations are extremely important for the northern latitudes because of great impact of fires not only on tree-ring growth but also in the context of stability and productivity of the permafrost ecosystems and their influence on global carbon balance.

The goal of this chapter is to analyze features of the variability in tree-ring structure of larch trees growing in the permafrost region of Siberia in relation to climate, and consider application of dendrochronological techniques to investigations of environmental changes.

18.2 Experimental Background

Tree-ring structure of larch (broadly speaking, *Larix sibirica* Ledeb in the west and *Larix gmelinii* (Rupr.) Rupr in the east of the Yenisei River; see also Chaps. 1 and 3) growing at 12 sites in permafrost zone in Siberia was studied (Fig. 18.1). The sites are located in the region bordered by 84°30′E in the west and 100°00′E in the east and between 63°40′N in the south and 71°20′N in the north. In the forest-tundra zone (see Fig. 1.2), wood samples (cores) were collected in 1991 in five lichen-moss-shrub larch and spruce-larch stands. In the northern taiga (Fig. 1.2), larch trees growing in seven moss and moss-shrub larch stands or stands with some admixture of Siberian pine (*Pinus sibirica* Du Tour) were sampled in 1993. Conditions at most sites were wet. Depth of soil active layer at the sites studied was up to 30–50 cm at the northern timberline and up to 60–90 cm at the sites on well-drained sandy soils in the northern taiga. Wood material from 10 to 20 trees per site was used in this study (Fig. 18.1).

For the collected wood samples, tree-ring width (TRW) was measured and processed according to the technique commonly practiced in dendrochronology (Cook and Kairiukstis 1990; Vaganov et al. 1996). For the material from five northern sites, tree-ring density was measured using the standard technique of soft X-ray densitometry (Schweingruber 1988). Cell size measurements for the last 100 years were carried out (Vaganov et al. 1996) at four sites. Both types of tree-ring structure data were obtained in three northern sites.

In Fig. 18.2a, a microphotograph of larch wood sample is presented. More than 90% of the larch wood consists of tracheids, organized in regular radial rows (Bannan 1955, 1957). Radial size of tracheids formed at the beginning of the growing season is greater (Fig. 18.2a, c). These earlywood cells are characterized by thin

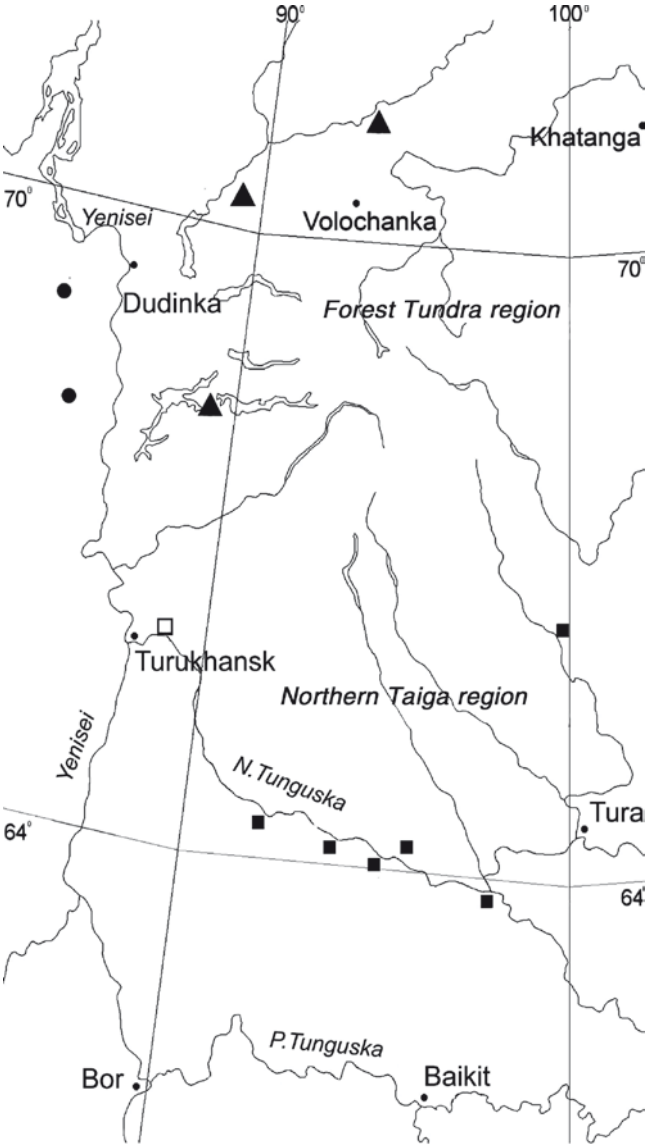

Fig. 18.1 Location of sites. The following tree-ring parameters were measured at a site: tree-ring width (TRW) (*filled square*), TRW and density (*filled circle*), TRW, density, and cell structure (*triangle*), TRW and cell structure (*open square*). Western sites are presented by Siberian larch and eastern sites by Gmelini larch

cell walls. Further to the border of the tree ring, tracheids of less radial size and greater cell wall thickness are formed. Latewood tracheids are characterized by smallest radial dimensions and thickest cell walls. Tracheid sizes and wall thickness

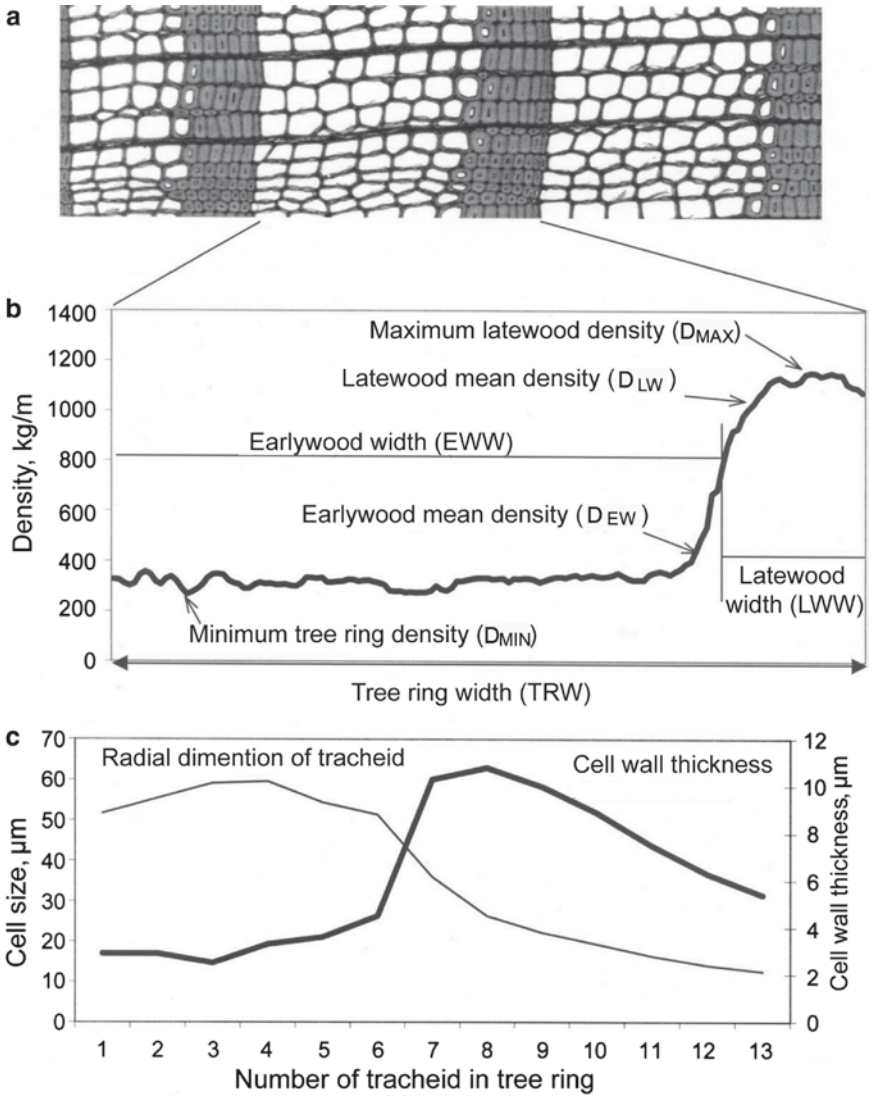

Fig. 18.2 (**a**) Microphotograph of wood sample with several tree rings, (**b**) density profile of one tree ring, and (**c**) intra-annual changes of radial cell size and cell wall thickness

define tree-ring density (Borovikov and Ugolev 1989; Yasue et al. 2000). Earlywood density is much less than latewood density (Fig. 18.2b).

The following parameters of density profile were used in this study to characterize density structure of each tree-ring (Schweingruber 1988): TRW, width of earlywood (EWW) and latewood (LWW), minimum (D_{MIN}) and maximum (D_{MAX}) tree-ring density and mean density of early- (D_{EW}) and latewood (D_{LW}). Cell structure

is described by radial size of tracheids typical for earlywood and latewood (Vaganov et al. 1996).

A series of year-to-year variations of each tree-ting parameter value (chronologies) was developed. Cross-dating of individual time series was visually performed to define the calendar year when each tree ring was formed. This procedure was carried out using TRW and maximum latewood density, as the most synchronous tree-ring parameters (Schweingruber 1988). Cross-dating was statistically verified with the program COFECHA (Cook and Peters 1981; Holmes 1994). Individual time series were processed to remove age-related trend and obtain site (master) and regional chronologies (Cook et al. 1990). In this study, tree-ring structure variability was compared at two dendroclimatic regions: the forest-tundra region (sites between the northern timberline and approximately 200 km to the south) and the northern taiga region (the middle flow of the Nizhnyaya Tunguska River). The regions were previously defined by Panyushkina et al. (1996) based on spatial–temporal variation analysis of tree-ring growth.

Standard dendrochronological statistics were calculated for the chronologies obtained to characterize strength of the environmental factors influencing and synchronizing tree-ring growth at the same site: correlation coefficient of individual chronologies with site time series, and coefficients of variation and sensitivity. The coefficient of sensitivity indicates year-to-year variability in tree-ring records and is calculated as the absolute difference between consecutive indices divided by their mean value (Fritts 1976). The higher these statistical parameters are, the greater the role of the environment in explaining tree-ring growth.

To investigate growth–climate relationship and to define those climatic factors that mainly influence tree-ring structure, correlation coefficients of tree-ring chronologies with monthly temperature and precipitation were calculated (Fritts 1976; Schweingruber 1996). Regional temperature for the forest-tundra region was derived as mean of monthly data from meteorological stations Dudinka (1906–1989) and Volochanka (1933–1989). Such averaging was possible due to high correlation between monthly temperature from different stations of the same region ($r = 0.87$–0.95 for the period from 1933 to 1990; $p < 0.001$). Similarity of monthly precipitation from different meteorological stations in the region is relatively low, but high enough (correlation is significant at $p < 0.01$) to obtain regional data. Tree-ring widths from the western part of northern taiga region were compared with data from Turukhansk (1877–1989) and regional TRW chronology obtained for the eastern part of northern taiga region with data from Tura (1929–1989). To investigate further the role of temperature in explaining tree-ring growth, tree-ring data from one northern site were compared with daily climatic data. Daily temperature from Khatanga (1933–1989) was used to obtain temperature of pentads (five consecutive days). These data were correlated with tree-ring parameter chronologies obtained for the nearest site at the northern timberline.

Multiple regression model based on different tree-ring parameter variability was established to reconstruct summer temperature changes in the forest-tundra region. Tree-ring parameters, contribution of which may explain changes in temperature, were included as independent variables in the model.

To analyze pre- and post-fire tree-ring growth dynamics and its important characteristics, additional wood material from trees having fire scars was collected in the northern taiga region. The "superimposed epochs" approach (Lough and Fritts 1987; Swetnam 1996) was used in this study.

18.3 Relationships of Tree-Ring Parameters Obtained for Larch Dendrochronological Network

Statistical parameters of tree-ring chronologies (Tables 18.1 and 18.2) indicate that in the north the correlation is high for the time series of TRW, EWW, LWW, D_{LW}, and D_{MAX} obtained for individual trees with the master chronologies. On the other hand, the correlation is quite low for D_{MIN}. Tree-ring density time series (D_{MAX}, D_{MIN}, D_{EW}, D_{LW}) are characterized by lower variability and sensitivity in comparison with width chronologies (TRW, EWW, LWW). The TRW data are less variable and sensitive in the northern taiga region than in the forest-tundra region. Cell size chronologies show variability comparable to that of density chronologies.

Data presented in Table 18.1 show that tree-ring density characteristics could be divided into three groups with similar values of statistical parameters: (1) TRW, EWW, LWW; (2) D_{MAX}, D_{LW}; and (3) D_{MIN}, D_{EW}. Comparative correlation analysis of chronologies obtained for the same tree-rings (Table 18.3) indicates that tree-ring parameters from exactly the same groups are correlated much better (in Table 18.3 correlation coefficients for one site are presented, but very similar results were obtained for all other sites with the tree-ring density data). Correlation between chronologies from two groups (D_{MIN}, D_{EW} and D_{MAX}, D_{LW}) is usually insignificant. Cell size chronologies show the highest positive relationship to TRW, EWW, and LWW (r up to 0.68; $p<0.01$). The D_{MIN} and D_{EW} are negatively correlated with parameters from the other groups.

Analysis of chronologies at the forest-tundra region indicates high similarity of tree-ring structure time-series obtained at different sites. Thus, correlation coefficients of TRW, D_{MAX}, and D_{MIN} larch chronologies from different sites for the common 1747–1989 period are 0.45–0.84, 0.64–0.90, and 0.30–0.52 ($p<0.001$), respectively. Similarity of TRW time series obtained for the eastern part of the northern taiga region is also high, $r=0.51$–0.80 ($p<0{,}001$). Cell size time series show high correlation (up to 0.68; $p<0.01$). In general, the greater the distance between sites, the lower the similarity between chronologies. The lowest values of the correlation in two regions were obtained for the most distant sites. However, highly significant ($p<0.001$) correlation coefficients between tree-ring parameter time-series from the different sites indicate presence of common environmental factors that influence and synchronize tree-ring growth and formation in the same region. To separate and strengthen the signal, master tree-ring chronologies were averaged in the regional time series.

Regional tree-ring chronologies for the forest-tundra region are presented in Fig. 18.3. Very narrow tree rings (1–3 tracheids per ring) are characterized by low

Table 18.1 Statistical characteristics of tree-ring width and density chronologies

Mean for individual chronologies				Master chronologies	
Tree-ring parameter	Correlation coefficient with master chronology	Coefficient of variation (%)	Coefficient of sensitivity	Coefficient of variation (%)	Coefficient of sensitivity
Forest-tundra region					
D_{EW}	0.486–0.549	8–14	0.065–0.111	4–8	0.040–0.076
D_{LW}	0.802–0.840	13–16	0.133–0.163	10–14	0.113–0.149
D_{MIN}	0.367–0.451	10–18	0.082–0.138	5–9	0.048–0.089
D_{MAX}	0.799–0.843	13–16	0.130–0.162	10–14	0.110–0.147
EWW	0.781–0.818	53–61	0.434–0.486	35–45	0.327–0.498
LWW	0.648–0.821	58–64	0.421–0.441	33–40	0.323–0.452
TRW	0.797–0.820	50–59	0.395–0.434	32–38	0.378–0.431
Northern taiga region					
TRW	0.605–0.709	60–69	0.260–0.401	23–29	0.271–0.318

Table 18.2 Statistical characteristics of cell size chronologies

Tree-ring parameter	Correlation coefficient with master chronology	Mean cell size (μm)	Standard deviation (μm)	Variation coefficient (%)	Coefficient of sensitivity
Forest-tundra region					
Earlywood cell size	0.67–0.77	40.5–50.9	4.31–5.83	10.1–11.4	0.090–0.130
Latewood cell size	0.64–0.81	17.7–19.2	2.70–3.10	15.1–16.2	0.135–0.176
Northern taiga region					
Earlywood cell size	0.68	47.6	5.80	12.2	0.134
Latewood cell size	0.76	15.0	2.56	17.0	0.157

D_{MAX}, TRW, and high D_{MIN} (for example, in 1644, 1742, 1807, 1819, 1837, 1889, 1907, 1974). Rings with low D_{MAX} and quite high TRW are so-called "light" rings (Schweingruber 1993). These generally wide tree rings with very narrow latewood (1–2 tracheids) and abnormally thin cell walls of latewood tracheids are formed during the years of unfavorable climate conditions such as early arrival of the autumn.

Table 18.3 Correlation of various tree-ring density structure chronologies from the same site during a period 1741–1990

	D_{EW}	D_{LW}	D_{MIN}	D_{MAX}	EWW	LWW
D_{LW}	0.161					
D_{MIN}	0.907[a]	−0.157				
D_{MAX}	0.122	0.992[a]	−0.199			
EWW	−0.565	0.441	−0.675[b]	0.482[b]		
LWW	−0.235	0.501	−0.404	0.520[b]	0.720[b]	
TRW	−0.501	0.483[b]	−0.635[b]	0520[b]	0.976[a]	0.846[a]

[a] Correlation coefficient is 0.800 or higher
[b] Correlation coefficient is not less than 0.450 at all sites studied

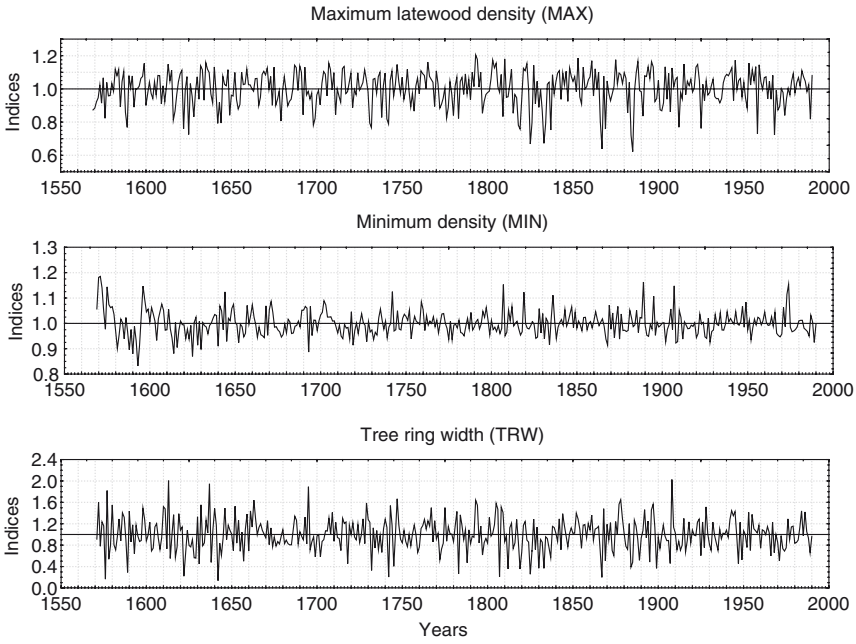

Fig. 18.3 Regional chronologies of tree-ring parameters obtained for the forest-tundra region

18.4 Effects of Climatic Factors on Radial Growth of Larch Trees

Results of dendroclimatic analysis of the tree-ring chronologies from the forest-tundra region (Fig. 18.4) show that summer temperature regime is the main climatic factor, which defines tree-ring growth in the north. Larch EWW, LWW, and TRW time-series correlate well with June and July temperature. The D_{MAX} and D_{LW} are significantly connected to temperature of the period from June to September. Larch D_{EW} time series shows significant correlation with August temperature, and D_{MIN} does

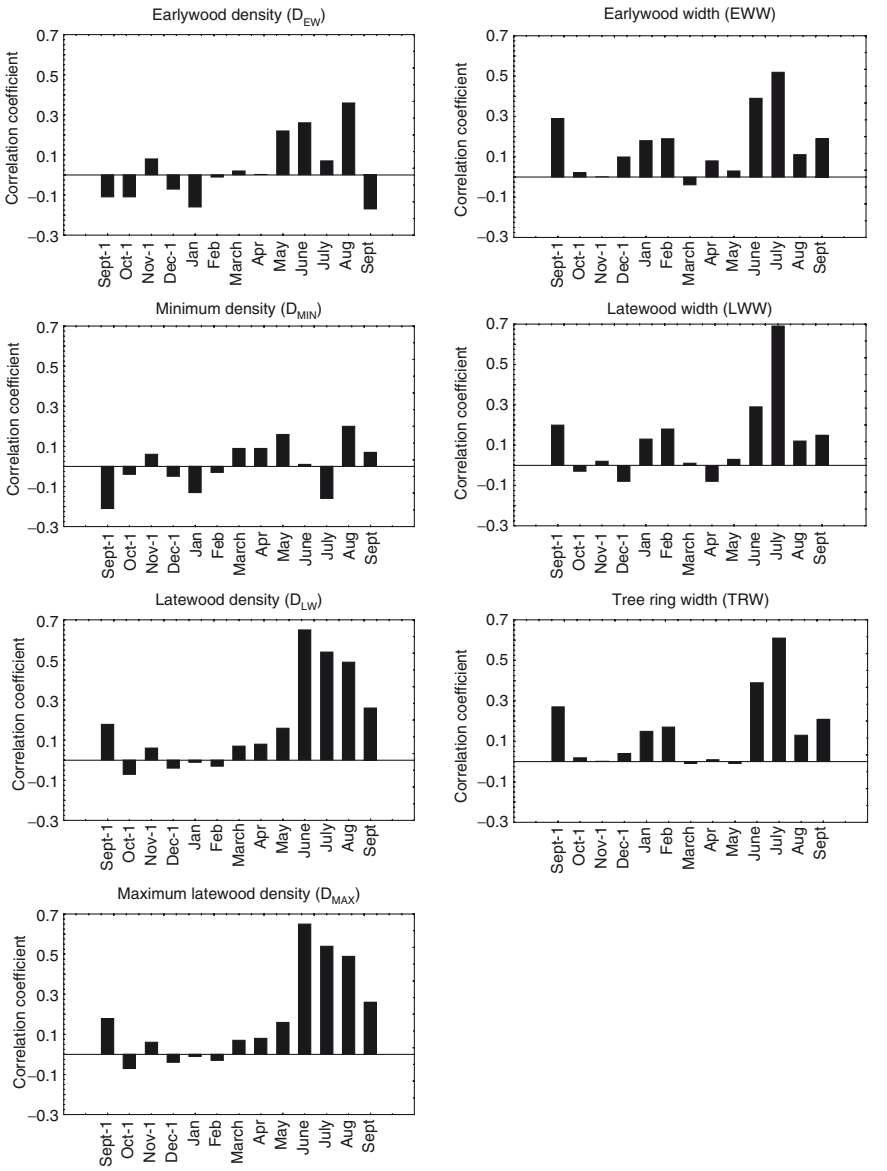

Fig. 18.4 Correlation of regional tree-ring chronologies obtained for the forest-tundra region with monthly temperature from September of previous year (Sept-1) until September of current year (Sept). Correlations with precipitation are insignificant and not shown

not correlate significantly with any climatic variables. There were no significant correlations found between the parameters of tree-ring structure and monthly precipitation.

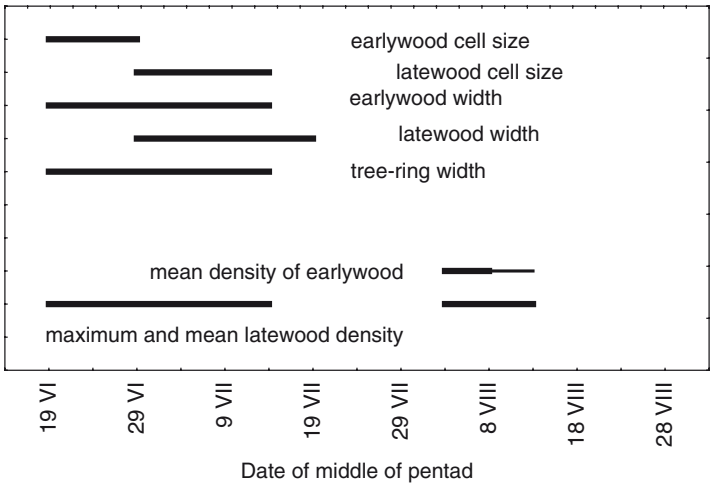

Fig. 18.5 Periods with significant correlation of tree-ring parameters with temperature of five consecutive days (pentads) in the forest-tundra region

Periods with significant correlation ($p < 0.05$) between tree-ring structure parameters of larch growing on the northern tree line and temperature of pentads during the growing season are presented in Fig. 18.5. Tracheid dimensions in different tree-ring zones are influenced by temperature of a short interval in the beginning of a growing season when those cells are being produced. Thus, the period when temperature influences latewood tracheid dimensions is shifted by 10 days in comparison to that for earlywood cell sizes (17 June–26 June for earlywood cell size and from 27 June till 11 July for latewood radial dimension). Similar shift of periods with important temperature is also obvious for EWW and LWW. The EWW is correlated with temperature from 17 June to 11 July, and LWW is influenced by temperature of a later period from 27 June to 16 July. The TRW is correlated significantly with temperature of the same period as EWW. Temperature of the period when cell walls are being formed influences mean earlywood density (1–10 August). Maximum and mean latewood densities record the temperature variations during the period of tracheid production and cell wall formation (17 June–11 July and 1–10 August).

Larch TRW chronologies obtained for the eastern and western parts of the region of the northern taiga respond to climate changes in different ways. Thus, regional chronology from the middle flow of the Nizhnyaya Tunguska River is significantly correlated with March–April temperature (negative correlation), June temperature (positive correlation), and May precipitation (negative influence) (Fig. 18.6a). Larch TRW chronology from the west of the region is correlated with June–July temperature. The connection to June temperature is stronger than that to July temperature (Fig. 18.6b).

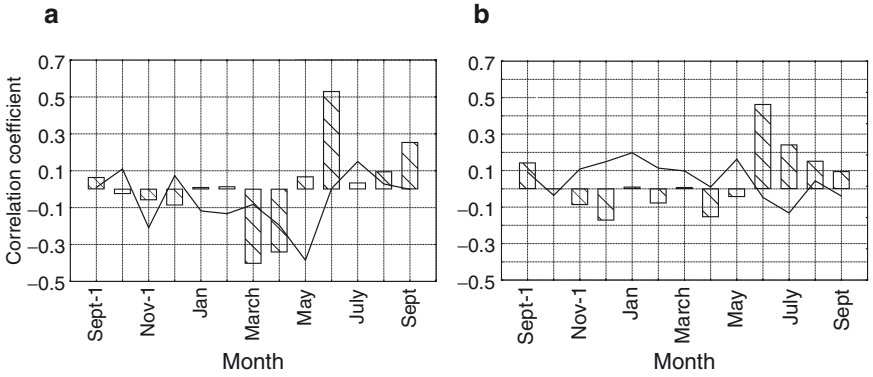

Fig. 18.6 Correlation coefficient of tree-ring width chronologies from (**a**) the east and (**b**) the west in the northern taiga region with monthly temperature (T – bars) and precipitation (P – line) of the nearest meteorological stations (**a**) Tura and (**b**) Turukhansk

18.5 Reconstruction of Summer Temperature Based on Regional Chronologies

Highly significant correlation obtained between tree-ring structure chronologies and various climatic parameters allows reconstruction of the climatic variables that are related to tree growth, primarily the summer temperature variation. As an example, reconstruction of June–August temperature in the forest-tundra region was obtained. The multiple regression was used with D_{MAX}, D_{MIN}, and TRW being the independent variables. The model was built for the period 1934–1989 (calibration period) and checked for 1906–1933 and 1906–1989 (verification periods). Statistical parameters of the model are the following: on the basis of tree-ring parameters, up to 75% of summer variation can be reconstructed ($F_{3,51}=49.7$, $p<0.000001$). Correlation of reconstructed and observed temperatures for the verification periods is not less than 0.84.

In Fig. 18.7, reconstructed June–August temperature is compared with instrumental data. The calculated mean temperature is 9.3°C; observed one is 9.5°C. Amplitude of instrumental data is 7.7°C (from 5.0 to 12.7°C). The calculated temperature is characterized by less variability of 5.6°C (from 5.8 to 11.4°C). It is about 73% of amplitude of the instrumental temperature. Coefficient of synchronization between observed and reconstructed temperature is 85%.

18.6 Effect of Ground Fires on Radial Tree Growth

An example of tree-ring width dynamics typically seen in larch ring growth in the northern taiga during pre- and post- forest fire periods is presented in Fig. 18.8. Results obtained for 15 trees and 10 fires are summarized. It is obvious that tree-ring

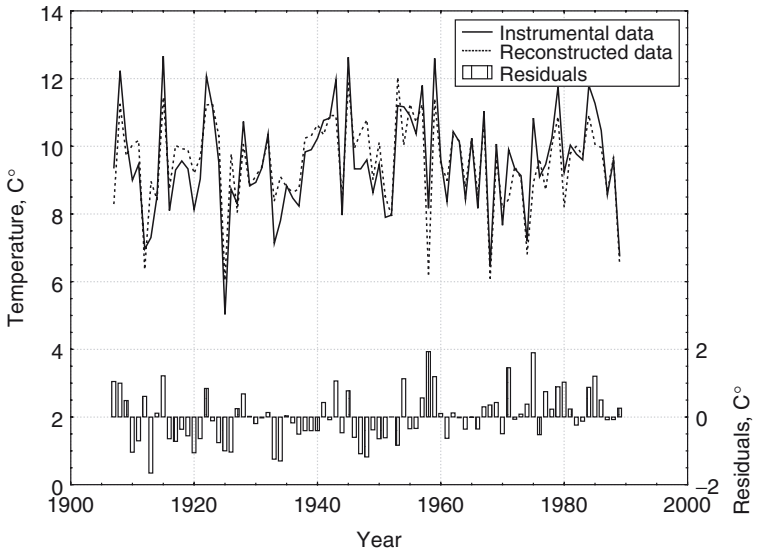

Fig. 18.7 Comparison of observed (*solid line*) and predicted (*dashed line*) summer (June–August) temperatures in the forest-tundra region of Central Siberia

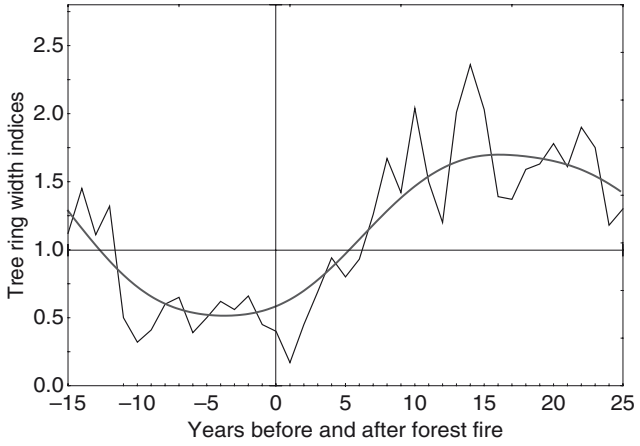

Fig. 18.8 Larch tree-ring growth before and after a forest fire in the northern taiga region

growth is depressed before fires due to increased thickness of the moss layer, which leads to a rise of the permafrost toward the soil surface (see also Chaps. 4, 8, and 24). Tree-ring width is minimal at the first year after fire. The depression can be up to 25–40% and is explained by damage of the tree and its root system. Then, tree-ring growth starts to increase. The rate of this increase and its duration usually depend on vegetation type of the stand and are associated with improvement of soil thermal

regime, regeneration of the root system, and restoration process of the forest floor destroyed by fire. In 15–25 years after fire, tree-ring growth starts to decrease again.

18.7 Features of Tree-Ring Growth on Siberian Permafrost

Climate is one of the main environmental factors that limits tree-ring growth over forest-tundra and northern taiga. Short vegetation period characterized by low temperature defines importance of summer temperature for tree-ring formation. Temperature regime is similar in vast territories, synchronizes tree-ring growth, and leads to high correlation of tree-ring chronologies established not only at the same site but also at sites up to 600 km apart (Vaganov et al. 1996). High sensitivity and variability of tree-ring chronologies obtained for these permafrost regions are also explained by strong climatic influence.

It is well known that tree-ring growth in the north shows a so-called "explosive" type when conditions of a very short period with constantly positive temperature in the beginning of the growing season defines structure of the tree ring formed during that year (Vaganov et al. 1999a; Kirdyanov et al. 2003; see also Chap. 17). Our data confirm that temperature at the beginning of a growth season is important for tracheid production (TRW). In other words, temperature defines cell production at the stage of cell division in the cambial zone. Radial cell sizes both in earlywood and latewood are also influenced by the early summer temperature. Temperature of a longer period affects density parameters. Significant correlation of latewood density with early summer temperature as well as temperature of some periods in August–September can be explained by the fact that enlargement and wall thickening stages of cell development require several weeks to complete the tracheid differentiation (1.5–2.5 months). Also, seasonal course of temperature is important for photosynthesis (quantity of substances assimilated during the summer) and consequently for development of cell wall thickness. So, for maximum latewood density, temperature of the period when photosynthesis and secondary wall thickening take place is also important. It is especially well seen, if the climatic signal in maximum latewood density is separated from that in tree-ring width (Kirdyanov et al. 2007). Earlywood density is influenced mainly by temperature during the cell wall formation period.

Vaganov et al. (1999a, b) and Kirdyanov et al. (2003) have shown that temperature variation is not the sole factor that defines tree growth at the northern timberline. The date of cambial initiation is another important climate-linked factor for tree-ring growth. This date is related to soil temperature, the date of snow melting, and consequently with winter precipitation. It was shown that both temperature and date of cambial initiation are important for tree-ring growth and cell production. In other words, even at regions with strong effect of summer temperature, tree growth response has a markedly "biological" character. So, in dendroclimatic studies, the actual date of cambial activation has to be taken into consideration to obtain results consistent with numerous findings on seasonal tree-ring formation (Lobjanidze 1961; Wilson and Howard 1968; Gregory 1971; Larson 1994; Vaganov et al. 2006; see also Chap. 17).

High sensitivity of tree growth in the north to temperature (Vaganov et al. 1996) provides a possibility to estimate natural climate changes during the preindustrial period and define the role of anthropogenic factor in the recent global temperature increase (Hughes 1995; Briffa et al. 2001). Many climate reconstructions on different spatial and temporal scales were recently published. Most of these reconstructions are based on either TRW only (e.g., Vaganov et al. 1996; Naurzbaev and Vaganov 2000; Esper et al. 2002) or combination of tree-ring width and other paleoclimate proxy data (e.g., Mann et al. 1998, 1999). Maximum tree-ring density is also widely used for temperature reconstructions (e.g., Schweingruber and Briffa 1996; Briffa et al. 1998a, b, 2001). However, our results show that information contained in tree-ring structure variation is more detailed and complete than that in tree-ring width and density variability (see also Kirdyanov et al. 2008). Different tree-ring parameters accumulate information on environmental changes that take place at different periods of a year. Statistics of climate factor reconstruction models show increase in reconstruction quality if several parameters of tree-ring structure are used. For example, the coefficient of determination (r^2) for the summer temperature reconstruction performed on the basis of TRW alone is not greater than 0.50 for the region studied. But in the case of multiple regression models, the explained variability (r^2) increases up to 0.75.

Forest fires influence northern ecosystem dynamics and tree-ring growth greatly. The fire-caused decrease in tree competition, destruction of ground layer, removal of organic matter (Abaimov et al. 2001), and also nutrient release from organic layers (Oechel and Van Cleve 1986) lead to considerable changes in tree-ring width (Fig. 18.8) and diameter growth curves (see Chap. 4). Such changes have to be taken into consideration in the dendroclimatic studies. Schweingruber (1996) attributed post-fire increase of tree-ring growth to decrease in tree competition. Our data indicate that post-fire tree growth dynamics is closely related to, and mainly associated with, recovery of the soil and regeneration of ground vegetation. It is confirmed by direct measurements that patterns of ground layer regeneration after fires at different intensities (Furyaev 1996; Prokushkin et al. 2006; see also Chap. 4) coincide with characteristic pattern of increase in post-fire tree-ring growth.

18.8 Conclusions

Analysis of tree-ring density and cell structure of larch trees growing in the permafrost region of Central Siberia shows that tree-ring growth in the forest-tundra and northern taiga is strongly influenced by climatic factors common to vast territories. Dendroclimatic analysis indicates summer temperature regime to be the main climatic factor that defines tree-ring growth in the region and up to 75% of summer (June–August) temperature variations can be reconstructed in the forest-tundra region from variability in tree-ring structure. Tree-ring width dynamics typical to annual growth of larch in northern taiga at pre- and post-forest fire periods is closely related to and mainly associated with after-fire permafrost dynamics and

recovery of ground vegetation. These and previously published data detect forest fire as another external factor greatly influencing tree-ring growth on permafrost.

Only the main aspects of dendrochronology of larch trees growing on Siberian permafrost were considered in this study. More studies are needed to estimate the influence of changing environment on larch tree-ring growth and wood production. It is becoming especially important because of increased anthropogenic impact on forest ecosystems in Eurasia, particularly in the remote regions of Siberia.

Acknowledgments: The authors thank P.P. Silkin for help in preparation of Fig. 18.2. The study was supported by RFBR (grant 07-04-00293), Swiss NSF (grants SCOPES IB74A0-110950 and IB73A0-111134), and ADPP 2.1.1/6131 (Scientific Potential of Russian High Education).

References

Abaimov AP (1995) The larches of Siberian permafrost zone and their species peculiarities in progressive successions. In: Martinsson O (ed) Larch genetics and breeding: research findings and ecological-silvicultural demands. Swedish University of Agricultural Sciences, Umeå, pp 11–15

Abaimov AP, Bondarev AI, Zyryanova OA, Shitova SA (1997) Polar forests of Krasnoyarsk region. Nauka, Novosibirsk (in Russian)

Abaimov AP, Prokushkin SG, Zyryanova OA, Kanazawa Y, Takakhashi K (2001) Ecological and forest-forming role of fires in the Siberian permafrost zone. Lesovedenie 5:50–59 (in Russian)

Anonymous (1977) Areals of trees and shrubs of USSR v. 1. Nauka, Leningrad (in Russian)

Arbatskaya MK (1998) Long-term changes in radial growth, climate and fire frequency in the central Siberian region. PhD thesis, Institute of Forest SB RAS, Krasnoyarsk (in Russian)

Bannan MW (1955) The vascular cambium and radial growth in *Thuja occidentalis* L. Can J Bot 33:113–138

Bannan MW (1957) The relative frequency of the different types of anticlinal divisions. Can J Bot 35:875–884

Bazilevich NI (1993) Biological productivity of Northern Eurasia ecosystems. Moscow, Nauka (in Russian)

Borovikov AM, Ugolev BN (1989) Hand-book on wood properties. Lesnaya promishlennost, Moscow (in Russian)

Briffa KR, Schweingruber FH, Jones PD, Osborn TJ, Harris IC, Shiyatov SG, Vaganov EA, Grudd H (1998a) Trees tell of past climates: but are they speaking less clearly today? Philos Trans R Soc London Ser B 353:65–73

Briffa KR, Schweingruber FH, Jones PD, Osborn TJ, Shiyatov SG, Vaganov EA (1998b) Reduced sensitivity of recent tree-growth to temperature at high northern latitudes. Nature 391:678–682

Briffa KR, Osborn TJ, Schweingruber FH, Harris IC, Jones PD, Shiyatov SG, Vaganov EA (2001) Low frequency temperature variations from a northern tree-ring density network. J Geophys Res 106:2929–2941

Brown PM (1996) OLDLIST: a database of maximum tree age. In: Dean JS, Meko DM, Swetnam TW (eds) Tree rings, environment and humanity. Radiocarbon (Special issue). The University of Arizona, Tucson, pp 727–731

Budiko MI, Izrael YuA (1987) Anthropogenic changes of climete. Gidrometeoizdet, Leningrad (in Russian)

Cook ER, Kairiukstis LA (eds) (1990) Methods of dendrochronology. Application in environmental sciences. Kluwer, Dordrecht

Cook ER, Peters K (1981) The smoothing spline: a new approach to standardizing forest interior tree-ring width series for dendroclimatic studies. Tree Ring Bull 41:45–53
Cook EH, Briffa KR, Shiyato SG, Mazepa VS (1990) Tree ring standardization and growth-trend estimation. In: Cook ER, Kairiuktis LA (eds) Methods of dendrochronology – application in environmental sciences. Kluwer, Dordrecht
Crutzen PJ, Goldammer JG (eds) (1993) Fire in the environment: the ecological, atmospheric and climatic importance of vegetation fires. Willey, New York
Dilis NV (1981) Larch/library: wood species. Lesnaya Promishlennost, Moscow (in Russian)
Esper J, Cook ER, Schweingruber FH (2002) Low-frequency signals in long tree-ring chronologies and the reconstruction of past temperature variability. Science 295:2250–2253
Fritts HC (1976) Tree-rings and climate. Academic, London
Furyaev VV (1996) Forest fire frequency and flammability of southern taiga in West and Central Siberia. Lesovedenie 6:44–53 (in Russian)
Furyaev VV, Vaganov EA, Tchebakova NM, Valendik EN (2001) Effects of fire and climate on succession and structural changes in the Siberian boreal Forest. Eurasian J For Res 2:1–15
Graumlich LJ, Brubaker LB, Grier CC (1989) Long-term trend in forest net productivity; Cascade Mountains, Washington. Ecology 70:405–410
Gregory RA (1971) Cambial activity in Alaskian white spruce. Am J Bot 58:160–171
Hantemirov RM (1999) Tree-ring reconstruction of summer temperatures on the north of Western Siberia over last 3248 years. Siberian Ecol J 2:185–191
Holmes RL (1994) Dendrochronology program library, version 1994. Laboratory of Tree-Ring Research, The University of Arizona, Tucson
Hughes MK (1995) Tree rings and the challenge of global change research. Tree rings from the past to the future. In: Ohta S, Fujii T, Okada N, Hughes MK, Eckstein D (eds) Proceedings of the International Workshop on Asian and Pacific Dendrochronology. Forestry and Forest Products Research Institute, Tsukuba
Hughes MK, Vaganov EA, Shiyatov SG, Touchman R, Naurzbaev MM, Funkouser G (2001) A 2500-year long temperature-sensetive tree-ring record in far north-eastern Eurasia. In: Dobbertin MK, Braeker OU (eds) Abstracts of International Conference on the Future of Dendrochronology. Swiss Federal Research Institute WSL, Davos
IPCC (2001) Contribution of Working Group I to the third assessment report of the Intergovernmental Panel on Climate Change. In: Houghton JT, Ding Y, Griggs DJ, Noguer M, van der Linden PJ, Dai X, Maskell K, Johnson CA (eds) Climate change 2001: the scientific basis. Cambrige University Press, Cambrige, New York
Kharuk VI, Ranson KJ, Dvinskaya ML (2007) Wildfires dynamic in the larch dominance zone. Geophys Res Lett 35:L01402. doi:10.1029/2007GL032291
Kirdyanov A, Hughes M, Vaganov E, Schweingruber F, Silkin P (2003) The importance of early summer temperature and date of snow melt for tree growth in Siberian Subarctic. Trees 17:61–69
Kirdyanov AV, Vaganov EA, Hughes MK (2007) Separating the climatic signal from tree-ring width and maximum latewood density records. Trees 21:37–44
Kirdyanov AV, Treydte KS, Nikolaev A, Helle G, Schleser GH (2008) Climate signals in tree-ring width, wood density and $\delta^{13}C$ from larches in Eastern Siberia (Russia). Chem Geol (including isotope geoscience). doi:10.1016/j.chemgeo.2008.01.023
Knorre AA, Kirdyanov AV, Vaganov EA (2006) Climatically-induced interannual variation in aboveground biomass productivity in the forest-tundra and northern taiga of central Siberia. Oecologia 147:86–95
Koropachinskii IYu (1983) Wood plants of Siberia. Nauka, Novosibirsk (in Russian)
Larson PR (1994) The vascular cambium. Development and structure. Springer, Berlin
Lobjanidze EO (1961) Cambium and tree ring formation. AS USSR, Tbilisi (in Russian)
Lough JM, Fritts HC (1987) An assessment of the possible effects of volcanic eruption on North America climate using tree-ring data, 1600 to 1900 AD. Clim Change 10:219–239
Mann ME, Bradley RS, Hughes MK (1998) Global scale temperature patterns and climate forcing over the past six centuries. Nature 392:779–787

Mann ME, Bradley RS, Hughes MK (1999) Northern Hemisphere temperatures during the past millenium: inferences, uncertainties and limitations. Geophys Res Lett 26:759–762

Naurzbaev MM, Vaganov EA (2000) Variation of summer and annual temperature in the East of Taymir and Putoran (Siberia) over the last two millennia inferred from tree-rings. J Geophys Res 105:7317–7327

Oechel WG, Van Cleve K (1986) The role of bryophytes in nutrient cycling in the Taiga. In: Van Cleve K, Chapin FS III, Flanagan PW, Viereck LA, Dyrness CT (eds) Forest ecosystems in the Alaskan Taiga. Springer, Berlin, pp 121–137

Panyushkina IP, Vaganov EA, Shishov VV (1996) Spatial-temporal variation of radial tree growth in the north of Middle Siberia in relation to climate. Dendrochronologia 14:115–126

Prokushkin AS, Knorre AA, Kirdyanov AV, Schulze E-D (2006) Productivity of mosses and organic matter accumulation in the litter of sphagnum larch forest in the permafrost zone. Russian J Ecol 37:225–232

Schweingruber FH (1988) Tree ring: basics and applications of dendrochronology. Reidel, Dordrecht

Schweingruber FH (1993) Trees and wood in dendrochronology. Springer, Berlin

Schweingruber FH (1996) Tree rings and environment: dendroecology. Haupt, Berne

Schweingruber FH, Briffa KR (1996) Tree-ring density networks for climate reconstruction. In: Jones PD, Bradley RS, Jouzel J (eds) Climatic variations and forcing mechanisms of the last 2000 years. NATO ASI Series 141. Springer, Berlin

Shiyatov SG (1993) The upper timberline dynamics during the last 1100 years in the polar Ural Mountains. In: Frenzel B (ed) Oscillations of the alpine and polar tree limits in the Holocene. Gustav Fischer, Stuttgart

Swetnam TW (1996) Fire and climate history in the Central Yenisei region, Siberia. In: Goldammer JG, Furyaev VV (eds) Fire in ecosystems of boreal Eurasia. Kluwer, Dordtrecht, pp 99–104

Vaganov EA, Hughes MK (2000) Tree rings and the global carbon cycle. In: Izrael YA, Semenov SM, Abakumov VA, Insarov GE (eds) Problems of ecological monitoring and ecosystem modeling, vol XVII. Gidrometeoizdat, St.Peterburg

Vaganov EA, Shiyatov SG, Mazepa VS (1996) Dendroclimatic investigation in Ural-Siberian Subarctic. Nauka, Novosibirsk (in Russian)

Vaganov EA, Hughes MK, Kirdyanov AV, Schweingruber FH, Silkin PP (1999a) Influence of snowfall and melt timing on tree growth in subarctic Eurasia. Nature 400:149–151

Vaganov EA, Naurzbaev MM, Eger IV (1999b) Age limit in larch trees in Siberia. Lesovedenie 6:66–70 (in Russian)

Vaganov EA, Hughes MK, Shashkin AV (eds) (2006) Growth dynamics of conifer tree-rings: images of past and future environments. Ecological studies, vol 183. Springer, Berlin

Van Cleve K, Viereck LA (1981) Forest succession in relation to nutrient cycling in the boreal forest of Alaska. In: West DC, Shugart HH, Botkin D (eds) Forest succession: concepts and application. Springer, Berlin

Wilson BF, Howard RA (1968) A computer model for cambial activity. For Sci 14:77–90

Yasue K, Funada R, Kobayashi O, Ohtani J (2000) The effect of tracheid dimentions on variations in maximum density of *Picea glehnii* and relationship to climatic factors. Trees 14:223–229

Part IV
Ecosystem Comparisons and Responses to Climate Change

Chapter 19
Characteristics of Larch Forests in Daxingan Mountains, Northeast China

F. Shi, K. Sasa, and T. Koike

19.1 Introduction

Daxingan Mountains are located in cold temperature region of northeast China, and are oriented from northeast to southwest direction. This area of China encompasses the southernmost distribution of continuous permafrost that extends from the Arctic region of Eurasia (see Fig. 1.1). The vegetation type is classified as deciduous conifer forest dominated by *Larix gmelinii* (Rupr.) Rupr. The major species accompanying *L. gmelinii* are *Betula platyphylla* Suk. and *Populus davidiana* Dode. These forests are extension of the larch forests of Central and Northeastern Siberia (Fukuda 1996; Kasischke and Stocks 2000). The climate in the region of Daxingan Mountains is more moderate than that of Northeastern Siberia. Therefore, the forest biomass and productivity are also higher than those of the Siberian counterpart. The climate differs among southern, middle, and northern regions within the Daxingan Mountains. It leads to regional-scale growth differences in the larch forests. For example, biomass and net primary productivity of *L. gmelinii* forests of ca. 30-year old in the southern region are 43.6 Mg ha^{-1} and 3.94 Mg ha^{-1} $year^{-1}$ higher than those in the northern region (Zhou 1991; Shi 1999). The biomass and net primary productivity of *L. gmelinii* forests of ca. 50-year old in the middle region are 6 Mg ha^{-1} and 1.24 Mg ha^{-1} $year^{-1}$ higher than those of the northern region.

An important factor affecting natural regeneration of *L. gmelinii* forests in Daxingan Mountains is forest fire. Natural regeneration is rare under the intact stand of mature *L. gmelinii*. But, once a forest fire occurs, natural regeneration begins quickly with seedlings of *L. gmelinii*, *B. platyphylla*, and *Populus davidiana*. Previous studies have shown that seedling density of these three species in an early stage of natural regeneration is strongly related to fire intensity in a *L. gmelinii* forest (Shi et al. 1996, 2000). Density of *L. gmelinii* seedlings would decrease with increasing fire intensity, while that of *B. platyphylla* will be larger with increasing fire intensity. If disturbance to the litter and soil on the ground surface is adequate, natural regeneration of *L. gmelinii* forests can be accelerated.

Light coniferous forest is usually used as a term for larch forests in order to distinguish it from evergreen forests composed of *Picea* and *Abies* species, where the

A. Osawa et al. (eds.), *Permafrost Ecosystems: Siberian Larch Forests*,
Ecological studies, Vol. 209, DOI 10.1007/978-1-4020-9693-8_19,

forest floor is rather dark (Shi 1999; Shi et al. 2000; see also Chap. 22). Large biomass and high primary productivity of the larch forests may be related to high adaptability of this species to low temperature as well as to efficient utilization of water from melting permafrost during hot and dry summer seasons (Zhou 1991; Xu 1998; Abaimov et al. 2000; Tchebakova et al. 2002). Mean net primary productivity in the regions of cold temperature is estimated to be about 8 Mg ha^{-1} $year^{-1}$ (Whittaker and Likens 1975). However, natural larch forests in the Daxingan Mountains show primary productivity higher than the larch stands of other regions (Kullervo 1990).

Studies of forest ecosystems have been focused on estimation of uptake, accumulation, and storage capacities of carbon (e.g., Roy et al. 2001; IPCC 2007). However, data from Far East Russia and China are still insufficient, considering a possibility that larch forest ecosystems of this region may be a large carbon sink, and may play an important role in moderating the increase in atmospheric CO_2 concentration. The sink capacity of young larch forests is usually greater than that of old forests (Shi and Matsuura 2001). Therefore, knowledge on productivity of young forests is of particular importance as well. Therefore, investigation of growth and stock of the larch species should be significant in estimating potential capacity of productivity and biomass in this region.

Several investigations have been carried out in Daxingan Mountains to assess biomass and primary productivity of larch forests (Han 1994; Hong et al. 1994; Liu et al. 1994; Wang and Feng 1994; Xu 1998; Zhao et al. 1996) and regeneration capacity after intensive forest fires (Uemura et al. 1990; Shi et al. 2000). Most of these studies were conducted in small areas, making it difficult for evaluation of total carbon budget of ecosystems under the effect of frequent forest fires.

In this chapter, data were presented on stand structure, biomass, and net primary production of *L. gmelinii* forests in the Daxingan Mountains, and variations of these parameters were discussed in relation to climatic zone, forest type, and age. Processes of postfire dynamics in larch forest ecosystems of this region were also discussed by focusing on growth response and regeneration trait of major component species.

19.2 Approaches to Study Biomass, Net Primary Production, and Regeneration

19.2.1 Study Sites

The Daxingan Mountains are located in the region of "extreme cold climate" in China, at latitudes between 46°26′ N and 53°34′ N, and longitudes between 119°30′ E and 127° E (Fig. 19.1). Monthly mean temperatures of less than 10°C last for about 9 months, while those over 10°C concentrate in a short period from May to August (ca. 70–100 days). Annual mean temperature varies from about −2 to −4°C. Maximum and minimum temperatures of the region are 39 and −52.3°C, respectively. Mean annual precipitation is in the range of 350–500 mm, most of which fall

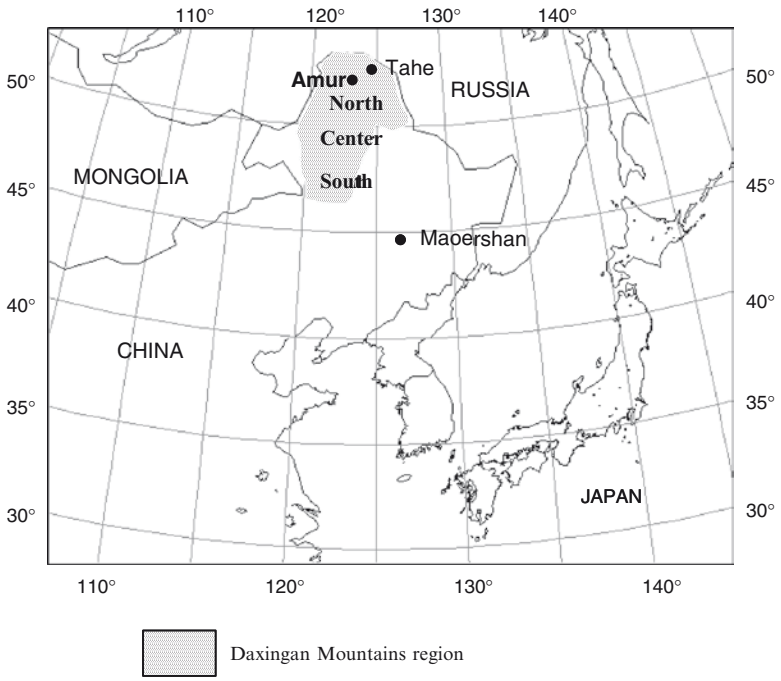

Fig. 19.1 Three climatic zones in the Daxingan Mountains in northeast China. The south climatic zone includes Aershan, Chuoer, Chuoyuan, Jiwen, and Alihe Forestry Bureaus; the central climatic zone includes Wuerqihan, Kuduer, Tulihe, Yitulihe, Keyihe, Genhe, and Ganhe Forestry Bureaus; the north climatic zone includes Tahe, Amur, Jinhe, Alongshan, Mangui Forestry Bureaus

in July and August. The climate is similar to that observed in Central Siberia (Abaimov et al. 2000; see also Sect. 1.2).

Temperature and precipitation regimes in the Daxingan Mountains vary considerably depending on the location, because southwest–northeast direction of the Mountains and prevailing direction of air mass movement from seaside as SE-monsoon to inner continental region. This contrasting climate condition can be summarized as follows: higher temperature and more precipitation associated with the southern region, and lower temperature and less precipitation found in the northern region. Mean annual temperature and precipitation are ca. −0.5°C, and 493 mm in the southern part; they are ca. −2.1°C and 231 mm in the northern part. Climate of the Daxingan Mountains was classified with thermal regimes (Guan 1988) as follows: south climatic zone, central climatic zone, and north climatic zone (Fig. 19.1). South climatic zone includes Aershan, Chuoer, Chuoyuan, Jiwen, and Alihe Forestry Bureaus within the Government Forest Management System of China. Central climatic zone includes Wuerqihan, Kuduer, Tulihe, Yitulihe, Keyihe, Genhe, and Ganhe Forestry Bureaus. North climatic zone includes Tahe, Amur, Jinhe, Alongshan, Mangui Forestry Bureaus.

Because of severe climate conditions of this region, forest ecosystems usually show simple stand structure and small species diversity. However, there are still differences between the southern and northern forests of the region, because of adaptation capacity of tree species to climate (Chabot and Mooney 1985). In the Daxingan Mountains, *L. gmelinii* (larch), *Pinus sylvestris* var. mongolica Litv. (pine), and *Betula platyphylla* (birch) can grow well; however, only *L. gmelinii* becomes the dominant species, and commonly form pure stands or mixed-species stands with *B. platyphylla*. This region can be considered the southern limit of the Siberian larch taiga (Shi et al. 2000).

The Daxingan Mountains are located at the southern limit of discontinuous permafrost zone (Xu 1998), where organic matter, such as litter-fall and coarse woody debris, decomposes slowly because of low temperature. As a result, large amount of litter is accumulated on the forest floor. Furthermore, thick peat layer is formed in some valleys and at high altitudes. Thickness of the peat reaches up to 2 m. Litter and peat might be the important components of carbon storage in this region. Therefore, the Daxingan Mountains is expected to be a large carbon reservoir, which may have significance in regulating carbon balance between the land and the atmosphere.

19.2.2 Estimation of Biomass and Net Primary Productivity

In this chapter, forests were classified into three age groups: young forest (<50 years) , middle age forest (50–100 years), and old forest (≥100 years). Biomass and primary productivity were measured in 355 standard plots (40×40 m) and from 1,051-sampled trees (Liu et al. 1994). Larch forests were divided into the following four types according to dominant species on the forest floor: *L. gmelinii*-herbage forests, *L. gmelinii-Rhododendron dauricum* L. forests, *L. gmelinii-Ledum palustre* Linn. Forests, and *L. gmelinii*-moss forests. In each forest type, aboveground biomass and primary productivity were estimated by the data of sample trees (e.g., tree size, component dry mass, and stem analysis) obtained from young, middle age, and old forests, respectively (details see Zhao et al. 1996). A similar study on estimation of forest biomass and net primary productivity in different forest types was carried out in Tahe Forestry Bureau (52°09′–53°23′ N, 123°20′–125°07′ E), located in the northeastern part of the Daxingan Mountains.

Biomass and primary productivity of *L. gmelinii* plantations were investigated in Maoershan Experimental Forest Station (45°21′–45°25′ N, 127°31′–127°34′ E) in the Zhangguangcai mountains, northeastern China (Ding et al. 1990). Biomass was estimated using an allometric relationship, i.e., $W = a\,(D^2H)^b$ (Shidei and Kira 1977; Han 1994), where W (kg), D (cm), and H (m) were dry mass of tree organ (stem, branch, or foliage), stem diameter at breast height, and tree height, respectively, and a and b were coefficients.

The study site was located in the Amur Forestry Bureau in the northern part of the Daxinganling Mountains (123°10′E, 52°45′N). Growing period of the trees is ca. 70–100 days from early June to end of August. Soil type is classified as the

brown conifer forest soil, and permafrost is distributed discontinuously (Hayashida 1989). The deepest soil active layer is approximately 2.5 m deep.

Dominant vegetation type in the Daxinganling Mountains is *Larix gmelinii* forest mixed with *Pinus sylvestris* var. mongolica, *Betula platyphylla*, and *Populus davidiana*. Shrub layer in the larch stands is generally dominated by *Ledum palustre* mixed with *Rhododendron dauricum*, *Rosa davurica*, and *Vaccinium vitis-idaea* (Chou and Liu 1995; Shi et al. 2000).

19.2.3 Examination of Postfire Forest Dynamics

A large-scale forest fire occurred in the Daxingan Mountains in May 1987. The burnt forest area was estimated as large as 1.34 million hectare (Shi et al. 1996). The volume of timber burnt was 0.38 billion m^3. The forest fire also caused about 14% decrease in forest coverage. At the same time, swampy sites appeared in many forested areas.

The Amur Forestry Bureau located in the central area of the Daxingan Mountains was affected by the forest fire of 1987. After the fire, site preparations were done in the spring of 1988 in order to observe regeneration processes of major component tree species after the disturbance. The burnt area was classified into three types according to fire intensity: light, intermediate, and heavy. The light fire means a ground surface fire, where trees were not burnt to the extent of causing mortality. Intermediate fire means the ground surface fire and partial crown fire, where some trees were killed. It also reduced growth of the dominant trees. Heavy fire means that trees were burnt to death nearly completely, where the burnt site changed into a denuded land.

In the site-prepared plots, disturbance furrows were made: each furrow is 40-cm-wide and 10-cm-deep, and distance between the furrows was 1 m. Further, natural regeneration plots without any site preparation were set up in three types of burnt areas.

Census of tree seedlings were conducted in these plots in June 1994 (the size of each plot was 20×20 m). Among these plots, four natural regeneration plots and four site-prepared plots were designated in the light fire area; five natural regeneration and five site-prepared ones in the intermediate fire area; and four natural regeneration and four site-prepared ones in the heavy fire area. Age of all seedlings was recorded in every plot.

19.3 Biomass, Productivity, and Stand Density

19.3.1 Biomass and Aboveground Net Primary Productivity in Different Climatic Zones

Aboveground biomass in the same age group of larch forests increased from north to south, and this tendency coincided with the change in climatic condition (Table 19.1). In the young forests, aboveground biomass was 85.4 Mg ha^{-1} in the southern climate zone, which was twice as large as that in the northern climate zone.

Table 19.1 Allocation of aboveground biomass in young and middle age forests at three different climatic zones of the Daxingan Mountains

			Biomass (Mg ha^{-1})				
Age group	Climate zone	Mean age	Bole wood	Bark	Branch	Leaf	Total aboveground
<50 year	North	34	29.1	5.9	4.4	2.6	41.8
	Central	29	39.8	7.9	6.4	2.6	56.7
	Southeast	29	63.6	9.0	9.0	3.8	85.4
	Mean		44.2	7.6	6.6	2.9	61.3
50–100 year	North	55	38.8	7.8	5.9	3.1	55.6
	Central	54	52.2	9.4	7.9	2.9	72.3
	Mean		45.5	8.6	6.9	3.0	64.0

Table 19.2 Aboveground productivity of young and middle age forests at three different climatic zones of the Daxingan Mountains

			Productivity (Mg ha^{-1} y^{-1})				
Age group	Climate zone	Mean age	Bole Wood	Bark	Branch	Leaf	Total aboveground
<50 year	North	34	2.3	0.4	0.3	2.6	5.3
	Central	29	3.6	0.6	0.5	2.6	7.3
	Southeast	29	4.9	0.6	0.6	3.8	9.9
	Mean		3.6	0.5	0.5	2.9	7.5
50–100 year	North	55	1.5	0.3	0.2	3.1	5.0
	Central	54	2.6	0.4	0.4	2.9	6.3
	Mean		2.0	0.3	0.3	3.0	5.7

Similar results were observed in the middle age forests: 72.3 Mg ha^{-1} in the central climatic zone, and was 16.7 Mg ha^{-1} higher than that in the northern climatic zone.

Aboveground net primary productivity (ANPP) increased along the climatic gradient from north to south (Table 19.2). The young forests showed the highest primary productivity (9.9 Mg ha^{-1} year^{-1}) in the southern climatic zone. As for the middle age forests, ANPP was 6.3 Mg ha^{-1} year^{-1} in the central climatic zone, which was 1.3 Mg ha^{-1} year^{-1} higher than that in the northern climatic zone.

19.3.2 Aboveground Biomass and Aboveground Net Primary Productivity in Different Forest Types

The forests of *L. gmelinii*-herbage type showed the largest values of both aboveground biomass and ANPP among the four vegetation types. The estimates of ANPP in *L. gmelinii-Rhododendron dauricum* forests were the second largest, followed by *L. gmelinii-Ledum palustre* and *L. gmelinii*-moss types. In each forest type, however, old forests usually had higher aboveground biomass and lower ANPP than young

or middle age forests. For example, biomass was 140.7 Mg ha^{-1} in *L. gmelinii-Ledum palustre* forest, but its ANPP was the lowest (3.5 Mg ha^{-1} year^{-1}) (Table 19.3).

19.3.3 Tree Density, Aboveground Biomass, and Aboveground Productivity in Relation to Forest Age

In young and middle age forests, tree density is commonly high with observed maximum of ca. 2,300 ha^{-1} (Fig. 19.2). However, the density decreases rapidly by forest age of 100 years, and was reduced to ca. 1,000 ha^{-1} in some cases. There is an increasing tendency in aboveground biomass from young to middle age forests (from 50 to 150 Mg ha^{-1} year^{-1}). In old forests, aboveground biomass reaches an asymptotic value of 100–130 Mg ha^{-1}.

ANPP increased only slightly in the early stage (i.e., between 20- and 40-year old; Fig. 19.2). The average ANPP over forests of all age-groups was about 5.0 Mg ha^{-1} year^{-1}. However, a slight decrease in aboveground productivity was observed in old stands (>100 years), with mean value of less than 4.0 Mg ha^{-1} year^{-1}.

19.3.4 Aboveground Biomass and Aboveground Net Primary Productivity of Larch Plantation

Larix gmelinii is a major species used for afforestation in northeastern China. Plantation of this species can occupy up to two-thirds of the total afforested area. Investigation carried out in Maoershan Experimental Forest Station, Zhanguangcai mountains (Ding et al. 1990), showed that the average aboveground biomass of young larch plantations (mean stand age 33 years) was 113.6 Mg ha^{-1}, and their mean ANPP was estimated to be 7.3 Mg ha^{-1}y^{-1} (Table 19.4). These values of biomass and ANPP were almost the same as those of natural larch forests in the central climatic zone, but were lower than those in the southern climatic zone (Tables 19.2 and 19.3)

There were significant relationships between D^2H and dry mass of each tree component (W), including root mass (Table 19.5). From these equations, the root biomass of the larch plantation could be calculated as 31.5 Mg ha^{-1}. It was about 28% of the aboveground biomass and 22% of the total biomass. Figure 19.3 shows the biomass ratios of tree organs measured in different areas.

Aboveground biomass of young and middle age forests in the Daxingan Mountains were 61.3 and 63.9 Mg ha^{-1}, respectively (Table 19.1). These values (average 62.6 Mg ha^{-1}) are slightly lower than the value averaged for boreal forests in the world (73 Mg ha^{-1}), but higher than that for Siberian boreal forests, including larch and Scot pine forests (56 Mg ha^{-1}; Jarvis et al. 2001). Comparisons of aboveground biomass and belowground biomass of other boreal forests are illustrated in Fig. 19.4.

Belowground biomass would account for a large percentage of total biomass. Kanazawa et al. (1994) reported that belowground biomass (109 Mg ha^{-1}; both

Table 19.3 Allocation of aboveground biomass and net primary productivity (NPP) among four different forest types at Tahe Forest Bureau of the Daxingan mountains

Forest type	Age[a] group	Mean Age (year)	Aboveground biomass (Mg ha^{-1})					
			Bole wood	Bark	Branch	Leaf	Total	NPP (Mg ha^{-1}y^{-1})
Larix gmelinii – herbage forests	Young	28	53.4	6.2	3.0	1.8	64.4	4.2
	Middle	58	117.7	14.2	11.5	3.8	147.1	6.4
	Mature	136	127.1	11.5	12.5	2.9	154.0	4.1
	Mean		99.4	10.6	9.0	2.8	121.8	4.9
Larix gmelinii – *Rhododendron dauricum* forests	Young	32	53.9	6.0	2.7	1.8	64.3	3.8
	Middle	63	102.3	12.5	8.9	3.4	127.0	5.5
	Mature	142	125.4	15.3	16.5	3.8	161.0	5.1
	Mean		93.9	11.2	9.3	3.0	117.5	4.8
Larix gmelinii – Ledum palustre forests	Young	34	62.7	7.3	3.3	2.2	75.4	4.4
	Middle	60	71.5	8.0	4.7	2.3	86.4	3.7
	Mature	152	119.4	9.8	9.0	2.5	140.7	3.5
	Mean		84.5	8.4	5.7	2.3	100.9	3.9
Larix gmelinii – moss forests	Young	34	45.1	3.9	2.6	1.1	52.7	2.7
	Middle	60	101.8	12.1	8.5	3.3	125.6	5.5
	Mature	171	92.4	10.9	9.3	2.9	115.4	3.6
	Mean		79.8	9.0	6.8	2.4	97.9	3.9

[a]Young: <50 year, Middle: 50–100 years, Mature: >100 years

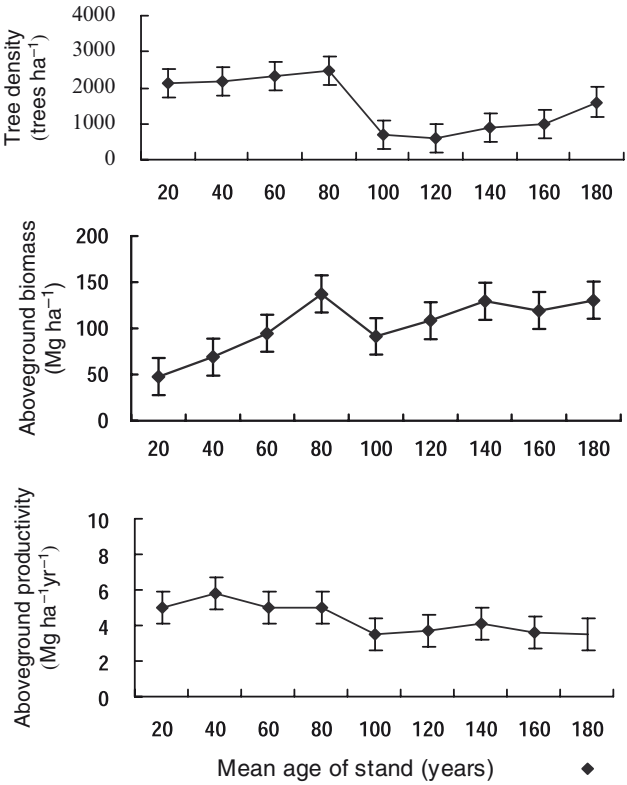

Fig. 19.2 Mean values of tree density, aboveground biomass, and productivity in relation to mean age of larch forests in the Daxingan Mountains

Table 19.4 Allocation of aboveground biomass and net primary productivity (NPP) of a young larch plantation stand at Maoershan of the Zhangguangcai Mountains

	Aboveground biomass (Mg ha^{-1})					
Mean age (year)	Bole wood	Bark	Branch	Leaf	Total	NPP (Mg ha^{-1} year^{-1})
33	93.8	8.4	8.7	2.8	113.6	7.3

Table 19.5 Estimated values of the variables in the regression analyses between the biomass of each organ of individual trees and D^2H Regression equation: $W = a\,(D^2H)^b$

Variable of regression analysis		Estimated value of regression variables				
		W_{wood}	W_{bark}	W_{branch}	W_{leaf}	W_{root}
Parameters	a	0.01258	0.02307	0.00136	0.01009	0.03615
	b	0.99331	0.70655	1.02797	0.64543	0.75995
Coefficient of determination	r^2	0.98	0.98	0.98	0.97	0.98

W is kg, D is cm, H is m

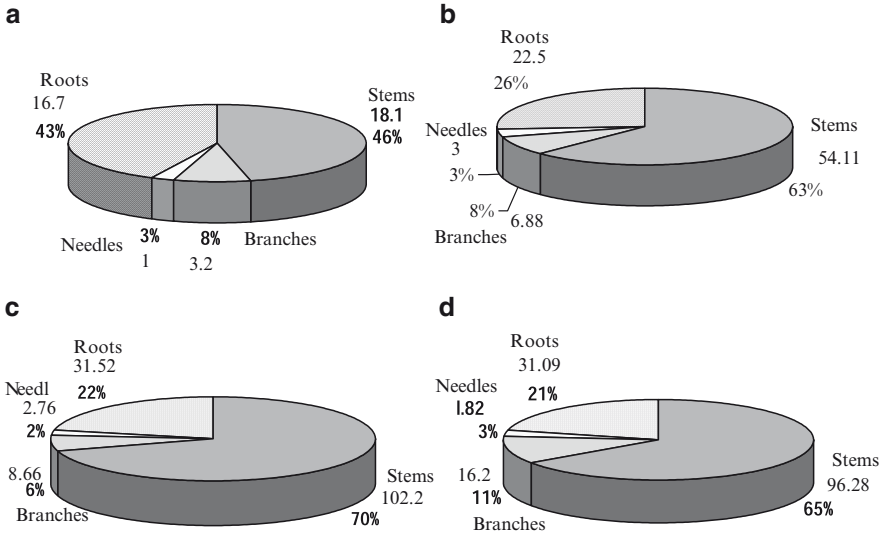

Fig. 19.3 Aboveground biomass and belowground biomass ratios in larch forests in different regions. Unit of biomass is Mg ha^{-1}. Data source: (**a**) Siberian old *Larix gmelinii* forest (Kajimoto et al. 1999); (**b**) middle age *Larix gmelinii* forests at Daxingan Mountains, northeast China and (**c**) young plantation of *Larix gmelinii* in Maoershan, northeast China (this study); (**d**) middle age *Larix leptolepis* (= *L. kaempferi*) forests in central Japan (Research Group on Forest Productivity of the Four Universities, 1964)

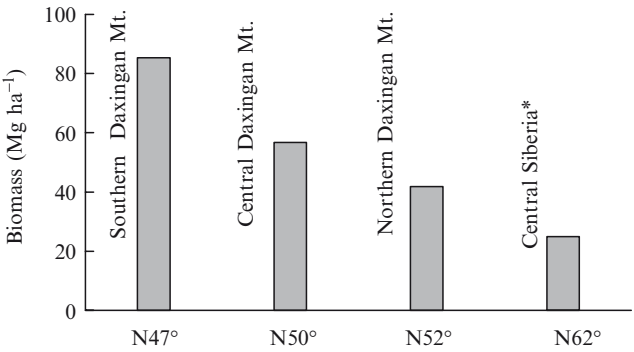

Fig. 19.4 Biomass of larch forests (30 year) at different latitudes. *Asterisk* – data from Shibuya et al. (2001a, b)

coarse and fine roots) of a 169-year-old mature *L. gmelinii* forest near Yaktsuk in Northeastern Siberia with deep soil active layer (>1 m) was 47% of the stand total biomass (232 Mg ha^{-1}). In larch stands of Siberia, tree density tended to be sparse and was affected by competition among roots because of infertile soil conditions and thin active layer of the soil over the permafrost.

Precise estimation for belowground biomass is more difficult than that of aboveground parts. Accordingly, previous studies on belowground biomass and primary productivity in the Daxingan Mountains are quite restricted. Han (1994) reported that belowground biomass and belowground net primary productivity of a larch-birch (*L. gmelinii- Betula phlatyphylla*) forest were about 5.74 Mg ha^{-1} (19.8% of total biomass) and 0.38 Mg ha^{-1} $year^{-1}$ (14.7% of total NPP). As listed in Table 19.6, the belowground biomass is quite variable among the boreal forest ecosystems. Jarvis et al. (2001) reported that the average root biomass was 36% (ranging 12–50%) of the aboveground biomass for some boreal forests in European Russia, Western Eutope, and North America. Ding et al. (1990) reported that belowground biomass and productivity of a *L. gmelinii* plantation in Maoershan Experimental Station were about 28.7 Mg ha^{-1} (21.4% of total biomass) and 1.20 Mg ha^{-1} $year^{-1}$ (14.6% of total NPP). In this study, the average belowground biomass of *L. gmelinii* was estimated to be about 22.5 Mg ha^{-1} throughout the Daxingan Mountains region (Table 19.6). The larch forest seems to develop well under cold climate conditions. The root biomass of larch forests in the Daxingan Mountains is slightly larger than that in Siberia and North America; but it is smaller than that in central Japan, European Russia, and western Europe. Biomass allocation of *L. gmelinii* and *L. kaempferi* to roots shows site- and species-specific patterns. Percentage of root biomass in *L. gmelinii* reaches 43–47% in Central and Northeastern Siberia (Kajimoto et al. 1999; Kanazawa et al. 1994; also see Chap. 6). Branches are quite similar among these different larch species. Biomass allocation to branches is ca. 5% smaller in *Larix gmelinii* than in *L. kaempferi* (Takahashi et al. 1968; Koike et al. 2001).

Large area of the Daxingan Mountains, with eight-degree range in latitude and two-degree range in longitude, includes various climatic and hydrological characteristics. In the southern climatic zone, ANPP of the young *L. gmelinii* forests was 9.9 Mg ha^{-1} $year^{-1}$ (Table 19.2), which coincides with near boreal conifer forests in northern Europe (9.0 Mg ha^{-1} $year^{-1}$); but it is less than boreal conifer forests in Japan (11.2 Mg ha^{-1} $year^{-1}$) (Shidei and Kira 1977). However, ANPP was only 2.7 Mg ha^{-1} $year^{-1}$ in the northern climatic zone. Kajimoto et al. (1999) reported that the ANPP of an old *L. gmelinii* forest established on permafrost in Central Siberia

Table 19.6 Average values of above- and belowground biomass of boreal forests

Areas	Aboveground biomass (Mg ha^{-1})	Belowground biomass (Mg ha^{-1})	Source
Daxingan Mountains	62.5	22.5	This study Research Group on Forest Productivity (1964)
Central Japan	116.3	31.09	
Siberia	56.0	20.2	Jarvis et al. (2001)
European Russia	91.0	32.8	Jarvis et al. (2001)
Western Europe	101.0	36.4	Jarvis et al. (2001)
North America	46.0	16.6	Jarvis et al. (2001)

belowground biomass is assumed to be 0.36 of aboveground biomass (Jarvis et al. 2001)

Table 19.7 Net primary production and its fractions estimated in some boreal forests

Parameters	Siberian boreal forests[a]	*Larix gmelinii* Forests in Central Siberia[b]	*Larix gmelinii* Forests in Daxingan mountains[c]
Wood net annual increment	0.81	0.32	2.66
Needles	0.88	1.01	3.00
Aboveground productivity	1.69	1.33	5.66
Coarse roots	0.32	0.18	–
Fine roots	1.13–2.44	0.30	–
Belowground Productivity	1.45–2.76	0.48	–
Total net productivity	3.14–4.45	1.81	–

Unit: Mg ha^{-1} $year^{-1}$
[a] From Jarvis et al. (2001)
[b] From Kajimoto et al. (1999)
[c] From the data of middle age forests (this study)

was 1.81 Mg ha^{-1} $year^{-1}$. Table 19.7 compares ANPP values of boreal forests between the Daxingan Mountains and Siberia. Among the larch forests of the same age (30 years), biomass increases clearly from Central Siberia to southern part of the Daxingan Mountains (Kajimoto et al. 1999; Shibuya et al. 2001a, b; Shi and Matsuura 2001). This implies that climatic factors, such as precipitation and temperature, would be the main limiting factors that cause the latitudinal gradient of productivity in larch forests within the Daxingan Mountains, because amount of precipitation and average temperature during a growing season increases from north to south at the similar longitude.

If ANPP of larch forests could be expressed as a combined function of precipitation and cumulative temperature, photosynthetic production would be estimated by these two climatic elements, when the amount of solar radiation stays constant. Therefore, the larch forests may have potential for increased productivity in the warming environment if water supply remains sufficient.

19.4 Regeneration of Larch-Dominant Forests after Forest Fires

Seedlings of four tree species regenerated naturally in burnt areas, previously of the larch forests. The species encountered are *Larix gmelinii*, *Pinus sylvestris* var. mongolica, *Betula platyphylla,* and *Populus davidiana*. Seedlings were very few during 3 years (1988–1990) immediately after the fire of 1987. No seedlings occurred in any of the natural regeneration plots in 1988; and less than 15 seedlings per hectare were recorded from 1989 to 1990. Number of *Larix gmelinii* seedlings had been increasing continuously from 1991 in most plots.

Number of seedlings after the light fire was more than those after the intermediate or heavy fires. Total number of seedlings was more than 1,750 per hectare in

Table 19.8 Total numbers of seedlings (per plot; 20×20 m) that occurred from 1988 to 1994 in the study sites of Daxingan Mountains. Figures in parenthesis show the number of seedlings per hectare

	Number of seedlings by fire severity class			
Species	Site preparation	Light	Intermediate	Heavy
Larix gmelinii	Nonprepared	122(3,050)	87(2,175)	71(1,775)
	Prepared	220(5,500)	128(3,200)	91(2,275)
Pinus sylvestris var. *mongolica*	Nonprepared	61(1,525)	58(1,450)	19(475)
	Prepared	36(900)	85(2,125)	23(575)
Betula platyphylla	Nonprepared	84(2,100)	123(3,075)	71(1,775)
	Prepared	95(2,375)	128(3,200)	139(3,475)
Populus davidiana	Nonprepared	7(175)	13(325)	24(600)
	Prepared	52(1,300)	42(1,050)	50(1,250)

all plots in 1993 and/or 1994 (Figs. 19.5–19.7). Regenerated seedlings of *Pinus sylvestris* var. *mongolica* were less than those of *Larix gmelinii* in all plots. Seedlings of *Betula platyphylla* were the most abundant on the prepared site after the heavy fire, which regenerated mainly from 1991 to 1993. Seedlings of *Populus davidiana* were relatively few; however, seedling establishment was successful in the heavily burnt area. The maximum number of seedlings of *Populus davidiana* was only 600 per hectare.

Figures 19.5–19.7 also indicate the effects of site preparation on regeneration of tree species. The site preparation markedly facilitated natural regeneration of the seedlings in *Larix gmelinii* in the prepared sites (see Sect. 19.2.3) and intermediate-fire sites. Regeneration started earlier in the site-prepared plots than those without site preparation. Moreover, numbers of regenerated seedlings in *Betula platyphylla* increased gradually in the prepared sites, and were more than those in sites without site preparation in 1994. However, numbers of seedlings in *Pinus sylvestris* var. mongolica, and *Populus davidiana* apparently did not increase on the prepared sites.

Total numbers of seedlings that occurred from 1988 to 1994 are shown in Table 19.8. Without site preparation, the number of seedlings in *Larix gmelinii* decreased with increasing fire intensity. However, the site preparation increased establishment of *Larix gmelinii* seedlings in all burnt areas. Regeneration characteristics of *Pinus sylvestris* var. mongolica were essentially the same as those of *Larix gmelinii*; but increase in seedling number was smaller. Seedling numbers in *Betula platyphylla* and *Populus davidiana* increased with site preparation.

19.5 Synthesis

There has been increase in air temperature of about 2°C in the last 30 years in the northern hemisphere. The increasing trend may continue in the future, especially in the regions of Siberia and Daxingan Mountains (Kasischke and Stocks, 2000).

Therefore, growth and dynamics of larch forests in this region should be monitored carefully. Future vegetation of the present larch-dominated forests may be something different, as model approaches suggest various patterns of future vegetation change in the region (see Chap. 22).

Tree density of old larch forests in the Daxingan Mountains declined sharply as the stand aged (>100 years) (Fig. 19.2a). This may be related to both natural self-thinning and frequently occurring forest fires (see also Chap. 7 for further interpretation). However, we could not reveal the reasons why tree density decreased sharply. Moreover, attention should be paid to fire history of the stands because soil fertility (i.e., nitrogen mineralization) may depend negatively on fire frequency (Matsuura and Abaimov 2000; Reich and Bolstad 2001). In the Daxingan Mountains, in fact, frequency and intensity of forest fires changed regeneration processes of larch forests greatly (Shi et al. 2000). For discussing reasons of the abrupt decline in tree density, it is necessary to understand interaction between fire frequency and speed of vegetation recovery.

Shrubs, such as *Ledum palustre*, form a thick vegetation cover and usually inhibit regeneration of natural *L. gmelinii* forests in the region of the present study. Forest fires eliminate such shrubs temporarily, enabling seedling recruitment, especially for light demanding species. In the areas of light and intermediate burn, the number of *L. gmelinii* seedlings was 5,500 and 3,200 ha^{-1}, respectively, with site preparation. These numbers may be sufficient for development of new larch stands without any further reforestation practices (Shi et al. 2000).

In the heavily burnt area, shrubs may not limit regeneration of tree species, since the original vegetation was lost completely. Therefore, the effect of site preparation on acceleration of natural regeneration was not clear in the heavy burns. Relative growth rate between 1988 and 1996 was greater at the heavily burnt area than the other areas. It may be because the number of seedlings was fewer there (Cao et al. 2000).

If fire is absent in the Daxinganling Mountains, spruce, not larch, would dominate because of its shade tolerance (Uemura et al. 1990). Berg and Chapin (1994) pointed out that deciduousness has an advantage in avoiding strong water deficit at needle flushing period in the permafrost region. As a tentative conclusion, dominance of *Larix* species in the Daxinganling Mountains at present may be determined by the physiological traits in water relations or shade tolerant capacities.

Of course, amount of seed supply from mother trees is another key factor that controls natural regeneration. The larch species generally have masting phenomena with approximately 3-year intervals in the present region of study. The masting of *L. gmelinii* was observed in 1993 around the study sites (Shi et al. 1996). Therefore, there was a regeneration peak in many plots in 1994. In the heavy-fire sites, the effect of site preparation (i.e., disturbance furrows) on regeneration of *Pinus sylvestris* var. mongolica and *Larix gmelinii* was not clear. This might have resulted partly from availability of few seeds. In contrast, regeneration of *Betula platyphylla* and *Populus davidiana* occurred well at the prepared sites, because they have high ability of sprouting and long-distance seed dispersal.

Vegetation recovery will occur by natural regeneration even at the heavily burned sites, if tree seeds are sufficiently dispersed. If seedling density is small,

reforestation practice becomes necessary. Also, typical light-demanding species, such as *Betula platyphylla* and *Populus davidiana*, will dominate many sites after heavy fires. It is necessary to continue the studies on quantitative aspects of forest dynamics and ecological characteristics of tree species for predicting vegetation changes of the study region under the effects of climatic change.

19.6 Conclusions

- Data on stand structure, biomass, and net primary production of *Larix gmelinii* forests at Daxingan Mountains, northeast China, were presented. Values of these parameters were compared among the climatic zone, forest type, and age. Then, processes of postfire forest dynamics of this region were discussed.
- Aboveground biomass for young *L. gmelinii* stands of the same age decreased from south to north: the value was 85.4 Mg ha^{-1} in the southern climatic zone, but it was about half the value in the northern climatic zone. For the middle age forests, aboveground biomass was 72.3 Mg ha^{-1} in the central climatic zone, which was 16.7 Mg ha^{-1} higher than that in the northern zone.
- ANPP was the highest in young stands in the southern climatic zone (9.9 Mg $ha^{-1}\,year^{-1}$). For the middle age forest, the value of 6.3 Mg $ha^{-1}\,year^{-1}$ in the central zone was 1.3 Mg $ha^{-1}\,year^{-1}$ higher than that in the northern zone.
- Old stands have higher aboveground biomass (100–130 Mg ha^{-1}), but low aboveground NPP (mean 4.0 Mg $ha^{-1}\,year^{-1}$).
- Aboveground biomass and aboveground NPP of young *L. gmelinii* plantations were 113.6 Mg ha^{-1} and 7.3 Mg $ha^{-1}\,year^{-1}$, respectively. These values were similar to those in natural stands of the central climatic zone.
- There is a clear latitudinal gradient of aboveground NPP from Central Siberia (1.81 Mg $ha^{-1}\,year^{-1}$) to southern climatic zone of Daxingan Mountains (9.9 Mg $ha^{-1}\,year^{-1}$).
- Number of regenerated *L. gmelinii* seedlings after light fire is generally sufficient (>1,750 ha^{-1}) in all plots regardless of site preparation. Also, site preparation increased establishment of *L. gmelinii* seedlings in all burnt areas.

References

Abaimov AP, Zyryanova OA, Prokushkin SG, Koike T, Matsuura Y (2000) Forest ecosystems of the cryolityhic Zone of Siberia; Regional Features, Mechanisms of Stability and Pyrogenic Changes. Eurasian J For Res 1:1–10

Berg EE, Chapin FS III (1994) Needle loss as a mechanism of winter drought avoidance in boreal conifers. Can J For Res 24:1144–1148

Cao C, Nakane K, Senoo T (2000) Diagnosis of vegetation recovery following major forest fire in Daxinganling, China, using NOAA/AVHRR data. Jpn J Ecol 50:1–12 (in Japanese with English summary)

Chabot BF, Mooney HA (1985) Physiological ecology of north American plant communities. Chapman and Hall, New York

Chou YL, Liu JW (1995) Deciduous and deciduous-evergreen forests in north eastern China. In: Box EO, Peet RK, Masuzawa T, Yamada I, Fujiwara K, Maycock PF (eds) Vegetation science in forestry. Handbook of vegetation science vol 12, Kluwer, Dordrecht, pp 307–315

Ding B, Liu S, Cai T (1990) Studies on biological productivity of artificial forests of Dahurian larch plantation. Acta Phytoecologica et Geobotanica Sinica 14(37):226–236 (in Chinese with English summary)

Fukuda M (1996) Far north Siberia. Iwanami-shoten, Tokyo (in Japanese)

Guan Y (1988) Zoning of original larch forest productivity of the Daxingan forestry administration bureau in Inner Mongolia autonomous region. Beijing Forestry University, Beijing (in Chinese)

Han M (1994) A study on biomass and net primary productivity in a Dahurian larch birch forest ecosystem. In: Zhou X (ed) Long-tem research on China's forest ecosystems. Northeast Forestry University Press, Harbin, pp 451–458 (in Chinese with English a summary)

Hayashida M (1989) Topography and soils in the Daxinganking Range. In: Tsuiii T (ed) Forest and fire in Daxinganling Range of China. Research Association for Natural Resources (RANR), Sapporo, pp 51–65 (in Japanese)

Hong Q, Chai Y, Wang Y, Zhao H, Hu C, Li F, Fan W (1994) Growth of natural larch forests in Tahe of Daxinan Mountains. J Northeast For Univ 20(2):92–97 (in Chinese with English a summary)

IPCC (2007) Assessing the physical science of climate change. (http://ipcc-wg1.ucar.edu/)

Jarvis PG, Saugier B, Schulze E-D (2001) Productivity of boreal forests. In: Roy J, Saugier B, Mooney HA (eds) Terrestrial global productivity. Academic, San Diego, pp 211–244

Kajimoto T, Matsuura Y, Sofronov MA, Volokitina AV, Mori S, Osawa A, Abaimov AP (1999) Above- and belowground biomass and net primary productivity of a *Larix gmelinii* stand near Tura, Central Siberia. Tree Physiol 19:815–822

Kanazawa Y, Osawa A, Ivanov BI, Maximov TC (1994) Biomass of a *Larix gmelinii* (Rupr.) Litv. stand in Spaskayapad, Yakutsk. In: Inoue G (ed) Proceedings of the Second Symposium on the Joint Siberian Permafrost Studies between Japan and Russia in 1993. National Institute for Environmental Studies, Tsukuba, pp 153–158

Kasischke ES, Stocks BJ (eds) (2000) Fire, climate change, and carbon cycling in the boreal forest. Ecological studies, vol 138. Springer, Berlin

Koike T, Hojyo H, Naniwa A, Ashiya D, Sugata S, Sugishita Y, Kobayashi M, Nomura M, Akibayashi Y, Nakajima J, Takagi K, Shibata H, Satoh F, Wang W, Takada M, Fujinuma Y, Shi F, Matsuura Y, Sasa K (2001) Basic data for CO_2 flux monitoring of a young larch plantation. Eurasian J For Res 2:65–79

Kullervo K (1990) The dynamics of boreal coniferous forests. Gummerus Kirja paino Oy Jyväskylä, Helsinki

Liu Z, Ma Q, Pan X (1994) A study on the biomass and productivity of the natural *Larix gmelinii* forests. Acta Phytoecol Sin 18(4):328–337 (in Chinese with English a summary)

Matsuura Y, Abaimov AP (2000) Nitrogen mineralization in larch forest soils of continuous permafrost region, central Siberia – An implication for nitrogen economy of a larch stand. In: Inoue G, Takenaka A (eds) Proceedings of the Eighth Symposium Joint Siberian Permafrost Studies between Japan and Russia in 1999. National Institute for Environmental Studies, Tsukuba, Japan, pp 129–134

Reich PB, Bolstad P (2001) Productivity of evergreen and deciduous temperate forests. In: Roy J, Saugier B, Mooney HA (eds) Terrestrial global productivity. Academic, San Diego, pp 245–283

Research Group on Forest Productivity of the Four Universities (1964) Studies on the productivity of forest. Part II Larch (*Larix leptplepis* Gord.) forests of Sinshu Distinct. Japan Forest Technology Association, Tokyo, 60pp

Roy J, Saugier B, Mooney HA (eds) (2001) Terrestrial global productivity. Academic, San Diego

Shi F (1999) Genetic ecology of *Larix* in northeast China. Northeast Forestry University Press, Harbin (in Japanese)

Shi F, Matsuura Y (2001) Biomass and productivity of *Larix gmelinii* forests Daxingan Mountains of China. Hoppo Ringyo (Northern Forestry) 53(5):4–6 (in Japanese)

Shi F, Kisanuki H, Suzuki K (1996) Initial regeneration stage of post-fire stand in Daxinganling Mountains of Northeast China. Proc Jpn For Soc 107:223–226 (in Japanese)

Shi F, Zu Y, Suzuki K, Yamamoto S, Nomura M, Sasa K (2000) Effects of site preparation on the regeneration of larch dominant forests after forest fire in the Daxinganling Mountain region, northeast China. Eurasian J For Res 1:11–17

Shibuya M, Sugiura T, Takahashi K, Sawamoto T, Hatano R, Cha J, Fukuyama K, Isaev AP, Maximov TC (2001a) Comparison of needle mass density in the tree crowns of *Larix gmelinii* and *Larix kaempferi* trees. Eurasian J For Res 2:39–44

Shibuya M, Tsuno Y, Saito H, Yajima T, Takahashi K, Sawamoto T, Hatano R, Cha J, Isaev AP, Moximov TC (2001b) Aboveground biomass and carbon sink in Eastern Siberia. Hoppo Ringyo (Northern Forestry) 53(9):1–4 (in Japanese)

Shidei T, Kira T (eds) (1977) Primary productivity of Japanese forests, JIBP vol 16. University of Tokyo Press, Tokyo

Takahashi N, Yanagisawa T, Kubota Y (1968) Production and utilization of hybrid larch, Series 8. Hokkaido Tree Breeding Association, Iwamizawa, 180pp (in Japanese)

Tchebakova NM, Kolle O, Zolotoukhine D, Arneth A, Styles JM, Vygogskaya NN, Schulze ED, Shibistova O, LLoyd J (2002) Inter-annual and seasonal variations of energy and water vapour fluxes above a *Pinus sylvestris* forest in the Siberian middle taiga. Tellus 54B:537–551

Uemura S, Tsuda S, Hasegawa S (1990) Effects of fire on the vegetation of Siberian taiga predominated by *Larix dahurica*. Can J For Res 20:547–553

Wang L, Feng L (1994) Biomass of herbage larch forest with variable density in Daxingan Mountain. In: Zhou X (ed) Long-tem research on Chinese forest ecosystems. NEFU Press, Harbin, pp 459–464 (in Chinese with English summary)

Whittaker RH, Likens GE (1975) Biosphere and man. In: Lieth H, Whittaker RH (eds) Primary productivity of the biosphere. Springer, Berlin, pp 305–328

Xu H (1998) Da Hinggan Ling mountains forests in China. Science, Beijing (in Chinese with English summary)

Zhao H, Wang Y, Chai Y, Hu C, Li F, Fan W (1996) On forest growth of northern slope of Daxinan Mountains. J Northeast For Univ 24(6):1–8 (in Chinese with English summary)

Zhou Y (1991) The vegetation of Daxingan Mountains in China. Science, Beijing (in Chinese)

Chapter 20
Carbon Dynamics of Larch Plantations in Northeastern China and Japan

M. Jomura, W.J. Wang, O.V. Masyagina, S. Homma, Y. Kanazawa, Y.G. Zu, and T. Koike

20.1 Introduction

Larix gmelinii (Rupr.) Rupr. is naturally distributed in central Siberia and have been artificially and experimentally planted for timber production in northern Asia. Its distribution ranges from permafrost to nonpermafrost areas (Abaimov et al. 1998; Kasischke and Stocks 2000). Recently, these forests have been studied widely from the viewpoint of CO_2 sequestration (Schulze et al. 1999). Several studies have treated carbon sequestration and accumulation capacity of the forest ecosystem to determine their sustainability as the carbon sink (e.g., Roy et al. 2001).

Carbon balance of a forest is the net result of CO_2 uptake by the process of photosynthesis and CO_2 emission through autotrophic and heterotrophic respiration. Photosynthates both from leaves and other chlorenchyma such as green cones are substrates for plant metabolism, and more than half of them are consumed by the autotrophic respiration by themselves and by other organs (Amthor and Baldocchi 2001). However, such data for larch trees are so limited, although the vast amount of forests in the northern biosphere might be a large carbon sink (Koike et al. 2000). The difference between photosynthesis and carbon lost by autotrophic respiration is net primary production (NPP), and the photosynthates are allocated to component parts of the plants. Carbon allocation determines growth pattern of trees, potential for future growth, and ability to tolerate environmental stresses. NPP in larch forest ecosystems in Russia (Kajimoto et al. 1999) and China (Shi et al. 2002; Zhou et al. 2002) have been reported, in which characteristics of carbon balance of the larch forests have been described (see also Chaps. 6 and 21, this Vol.).

Another important pathway of carbon is heterotrophic respiration estimated by soil respiration measurement. Soil respiration (CO_2 flux from soil surface) is the sum of respiration rates of soil microbes, roots, fauna, as well as inorganic chemical processes. To estimate whether ecosystems are operating as carbon sink or source, it is important to understand the balance of carbon sequestration and emission. Biometric-based net ecosystem production (NEP) is recently used to crosscheck micrometeorological-based net ecosystem exchange (NEE) between forest and the atmosphere because of many uncertainties in both measurements (e.g., Greco and Baldocchi 1996).

A. Osawa et al. (eds.), *Permafrost Ecosystems: Siberian Larch Forests*,
Ecological studies, Vol. 209, DOI 10.1007/978-1-4020-9693-8_20,

Three topics will be described in this chapter to understand the functional balance of carbon sequestration and emission in larch plantations of Eastern Asia: (1) biomass, NPP, and allocation pattern of carbohydrate, (2) photosynthesis and autotrophic respiration of main tree organs including green cones, and (3) soil respiration under CO_2 enhanced conditions and under thinning treatment.

20.2 Site Descriptions

Field measurements were carried out in four *Larix gmelinii* (Rupr.) Rupr. plantations at Hitsujigaoka, Sapporo, and Tomakomai in Hokkaido, northern Japan, and at Laoshan in northeastern China. Taxonomy of *Larix* species in Russian Far East and adjacent areas has not been settled. Therefore, conflicting views exist (Abaimov et al. 1998; see also Chap. 3, this Vol.). Hitujigaoka, Sapporo, and Tomakomai sites have a typical island climate with high precipitation and small variation in temperature. Immature volcanic ash and pumice comprise major part of the soils in all sites. General characteristics of the study sites are shown in Table 20.1.

Hitsujigaoka site is located in an experimental forest of Hokkaido Research Center, Forestry and Forest Products Research Institute (42°58′N, 141°23′E). The study area has gently sloped topography with black soil of volcanic ash origin. Larch trees were planted in 1972 (31-year old at the time of measurement) and stand density was high because of no thinning practiced since the planting. Biomass and NPP were estimated at the site.

Sapporo site is located in the Hokkaido University FACE (Free Air CO_2 Enrichment) experimental forest (43°06′N, 141°20′E). Having no walls, the FACE system allows plants to grow under realistic microclimate and CO_2 conditions expected to prevail in the near future (Masyagina et al. 2006b); general design of the FACE system was described in Hättenschwiler et al. (2002). All treatments of this experiment were studied with two soil types, each filling one-half of experimental or reference plot. One of the soil types was an infertile volcanic ash, and the other was a fertile brown forest soil. Both soil types are typical in Japan. Soil respiration measurement was carried out at the site.

Tomakomai site is located at Tomakomai Nathional Forest (42°44′N, 141°31′E). The site has a flat topography with gentle slopes. The soil is homogeneous, well-drained arenaceous soil derived from volcanic ash. Two plots were established at the site (Plots 1 and 2). Both stands were about 50 years old. Photosynthesis, autotrophic, and soil respiration measurements were carried out in the site.

Laoshan sites (45°20′N, 127°34′E) have a typical continental climate with low precipitation, large variation in temperature, and dark brown soil. They are in an experimental forest of Northeast Forestry University located in northeastern China. Biomass and NPP were estimated in two plots. Plot 1 is located on a slope facing southeast, where trees were planted in 1971 (35-year old). Broadleaved trees and understory vegetation are growing in the plot. Plot 2 lies in a flat area and trees were planted in 1985 (21-year old). Understory vegetation is present. Photosynthesis and

Table 20.1 Characteristics of four study sites of larch plantations

	Northern Japan				Northeastern China		
	Hitsujigaoka	Sapporo	Tomakomai		Laoshan		
			Plot 1	Plot 2	Plot 1	Plot 2	Plot 3
Site location	42°58′N, 141°23′E	43°06′N, 141°20′ E	42°44′N, 141°31′ E		45°20′N, 127°34′E		
Elevation (m)	150	17	115–140		340		
Vegetation type	*Larix gmelinii*	11 tree species including *Larix kaempheri*	*Larix kaempferi*	*Larix kaempferi* with *Picea jezoensis*	*Larix gmelinii* with broad-leaved trees	*Larix gmelinii*	*Larix gmelinii*
Slope inclination (°)	0	0	0	1–2	17	2	5
Temperature (C°)	7.2	9.4	7.3			2.8	
Precipitation (mm)	928	680	1,250			724	
Tree density (tree ha-1)	2,268	–	–	716[b]	1364	1,665	1,150
Age (years old)	31	4	49	50	35	21	35
Stem diameter at breast height(DBH) (cm) (min-max)	14.6 (9.1–20.1)	–	–	15.8	16.4 (8.1–29.3)	10.6 (4.4–21.0)	17.2 (SD:4.5)
Tree height H (m) (min-max)	14.0 (11.6–15.7)	0.95 (0.15–1.35)	18–20	18–20	17.0 (10.1–22.4)	11.3 (6.5–17.0)	15–18
Crown base height (m) (min-max)	9.9 (8.6–11.3)	–	–	8.9	10.2 (6.4–12.8)	5.8 (3.9–7.5)	–
Vegetation period	April to October					May to September	
Soil type	Black soil with volcanic ash	Infertile volcanic ash soil and brown	Immature volcanic ash soil			Dark brown soil	
Total organic C (kg m^{-3})	18.2[a]	–	2.62[a]	11.50	5.48[a]	7.33[a]	–
Total *N* (kg m^{-3})	1.36[a]	0.14–0.30[c]	0.19[a]	0.75	0.56[a]	0.74[a]	–
C/*N* ratio	13.4[a]	–	13.7[a]	15.3	9.78[a]	9.90[a]	–

(continued)

Table 20.1 (continued)

	Northern Japan				Northeastern China		
	Hitsujigaoka	Sapporo	Tomakomai		Laoshan		
			Plot 1	Plot 2	Plot 1	Plot 2	Plot 3
Biomass and net primary production (NPP)	X	–	–	–	X	X	–
Photosynthesis and autotrophic respiration	–	–	X	–	–	–	X
Soil respiration	–	X	–	X	–	–	X

Stem diameter, tree height, and crown base height are mean values. Temperature is annual mean value

[a] Y. Matsuura unpubl. data

[b] T. Hirano unpubl. data

[c] Eguchi et al. (2008)

[d] The "X" means that the variables were measured at the respective site

autotrophic respiration were also measured in another older larch stand (Plot 3; 35-year old) (Table 20.1).

20.3 Biomass and Net Primary Production

20.3.1 Estimation Procedures

Forest inventories were made at Hitsujigaoka and Laoshan sites, including measurements of diameter at breast height (DBH), tree height (*H*), and height of crown base of both larch and broadleaved trees. Five trees of various sizes were selected based on the DBH distribution. The selected trees were felled to estimate stand biomass and production. Each sample tree was separated into horizontal layers by cutting at 0.0, 0.3, and 1.3 m from its base. From 1.3 m above, the cutting interval was 1 m when live branches were attached to the stem, or 2 m when there were no branches. All branches were numbered, and their position attached to the stem was recorded after the cutting. Thereafter, the branches' diameter at the base, length, and length of the current shoot of each branch were measured. A stem fresh mass of each layer was measured by a spring balance. We obtained two sample disks from one end of each stem segment for estimating dry weight and tree ring analysis. Branch fresh mass was measured for each layer by a spring balance. Two branches from each layer were sampled for the dry mass estimation and branch ring analysis.

Leaves attached to branches of subsamples were separated from the branches after drying and weighed to calculate the ratio of leaf biomass to whole branch biomass. Leaf and branch biomass of each layer were estimated based on this ratio. To estimate biomass of the broadleaved trees, we cut three sample trees and treated them as in larch trees described earlier.

Whole root systems of three individuals were excavated; one sample tree was selected at both Hitsujigaoka and Laoshan sites. Parts of all roots were classified into either vertical or horizontal root according to an extending direction and were categorized into seven diameter (D) classes; $0 < D \leq 0.5$ cm, $0.5 < D \leq 1.0$ cm, $1.0 < D \leq 2.0$ cm, $2.0 < D \leq 3.0$ cm, $3.0 < D \leq 5.0$ cm, $5.0 < D < 7.0$ cm, $D > 7.0$ cm, and root stump. Fresh mass of composite of roots in each category was measured by a spring balance; then, subsamples were taken for estimating the dry mass. Other subsamples for root ring analysis were obtained. To estimate biomass of the remaining roots in the soil, 15 lateral roots were sampled (about 10–100 cm in length) for both vertical and horizontal parts. Then, a regression between root diameter at basal portion (i.e., just near the stump) and fresh mass of these roots was determined. Fresh mass of the remaining roots was estimated from this regression.

Fine root biomass was estimated at Laoshan site in September 2005 by the core sampling method with 5 cm core diameter to 10 cm soil depth of 0–5 cm and

5–10 cm. The cores were sampled at five points on the site. Fine roots were manually picked from the core sample, washed, and sorted into live and dead fragments by visual inspection. Subsamples taken from each organ were dried at 90°C to constant weight, and then the ratio of dry to fresh mass was determined.

To estimate biomass of the understory vegetation, five sample plots of 70 × 70 cm were established, and all above-ground parts were collected in the plots. The plants were separated into leaves and other organs, and fresh mass of each part was determined. The ratio of dry to fresh mass of each organ was obtained, and it was multiplied by the total fresh mass to estimate the total dry mass in each plot. Stand-level biomass and NPP were estimated using allometric relationships obtained for each organ at each site. The estimate of carbon-based biomass and NPP was calculated with an assumption that carbon content of each organ was 50% of dry mass.

Component of the NPP that is associated with stem increment was estimated with data from stem analysis. First, the current volume growth of the stem was calculated using the sampled stem disks; second, the ratio of disk volume to total volume without bark of the stem segment was calculated; and finally, the ratio was multiplied by mass of the stem disk to obtain an annual stem biomass production of that layer. Stem production of a tree was estimated by summing the stem biomass increment for each layer.

Annual branch production was also estimated using a branch ring analysis as a modified stem analysis. Since bud scales on branches are formed once a year, age of a branch segment can be distinguished easily by following the bud scale scars. Short shoots of a branch often accumulate the bud scale scars (Fig. 20.1) during their development. As the number of bud scale scar of a short shoot means the number of leaf flushings, age of a branch can also be distinguished easily by counting the number of piled up bud scale scars. The branches were classified into each age category according to the number of bud scale scars that had accumulated

Fig. 20.1 Bud scale scars of a short shoot on a larch (*L. gmelinii*) branch. (Photo: M. Jomura)

on the short shoot. Moreover, primary and secondary branches were also distinguished to take growth difference between them into account. About 10% of total number of branches was sampled among primary branches, and also among secondary branches. Annual rings of the branch samples were read using a digital camera (Fig. 20.2) and a digital scale software (Datapicker ver. 1.2) to obtain mean growth rate of their cross sectional area for each category. According to the examinations of sample tree (DBH: 17.28 cm, Height: 18.37 m) in Laoshan plot 1, growth rate of the main branch at different heights in the crown decreased with increasing age (Fig. 20.3) (Jomura et al., unpubl. data). The data also indicated

Fig. 20.2 Example of branch disk samples of larch (*L. gmelinii*) used for annual ring analysis (Photo: M. Jomura)

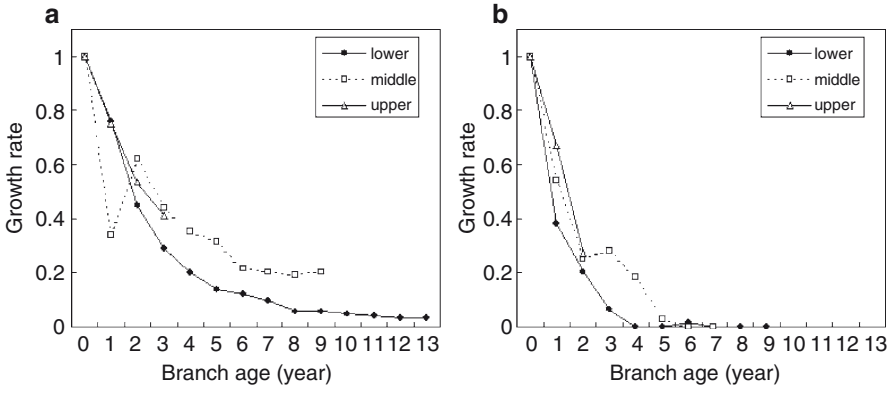

Fig. 20.3 Growth rate of primary (**a**) and secondary (**b**) branches (dry mass ratio of current-year branch to total branch) in relation to branch age at upper, middle and lower part of a crown of sample tree (diameter at breast height: 17.28 cm, Height: 18.37 m). (M. Jomura et al., unpubl. data)

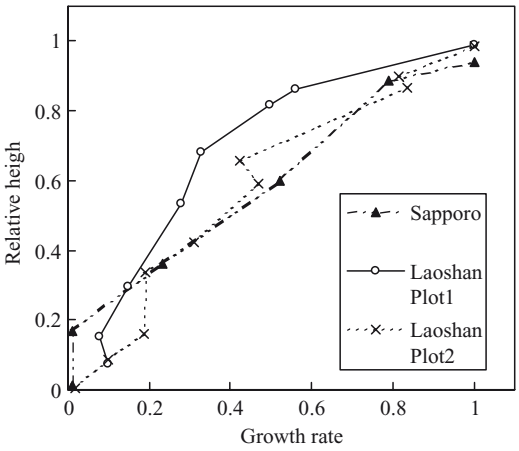

Fig. 20.4 Vertical distribution of growth rate of middle sized branches in three larch plantations, Sapporo (SP) and two plots of Laoshan (LS1–Plot 1, LS2–Plot 2) (M. Jomura et al., unpubl. data)

that growth rate of the main branch was higher than that of the other parts. Thus, annual branch production was estimated with these growth rates and biomass of each branch fraction. A vertical distribution of the ratios between the total branch production and branch biomass was shown in Fig. 20.4, indicating that a branch near the top of the crown had the highest ratio. The ratio decreased with lowering of the branch position in the crown.

Because larch is a deciduous tree, leaf biomass is assumed to be equal to annual leaf production. Root production was also estimated from root ring analysis using three whole root systems at Hitsujigaoka site (Plot 1) and two at Laoshan sites (Plots 1 and 2). Samples were divided into several diameter classes described above. Thereafter, subsamples were taken from each size class. It was assumed that the outermost ring was the current ring. Annual rings of subsamples were read and averaged to obtain current growth rate of cross sectional area in each size class. Root-mass increment was estimated by multiplying the averaged growth rate of subsamples by total dry mass of the roots in each class. Since most of broadleaved trees and understory vegetation in the study sites were deciduous species, their leaf biomass was also treated as their annual leaf production.

For the estimation of biomass, allometric relationships were examined between two size parameters (DBH and DBH^2H) and dry mass of stem, branch, leaf, and above-ground total. Similar approach was also applied to estimation of NPP. In both cases, a power function ($y = ax^b$ for each component mass or annual mass increment y with size parameter x) was used as an allometric equation. Coefficients a and b were obtained by the ordinary least squares method after logarithmic transformation of x and y. Fit of each regression was determined by coefficient of determination (r^2). In this study, individual tree biomass and mass increment of each organ were calculated with the developed allometric equations. Root biomass and its annual increment of nonharvested trees were estimated from the aboveground

Table 20.2 Coefficients of determination (r^2) in site-specific equations ($y = ax^b$) between two size parameters (DBH, DBH^2H) and dry mass of stem (W_s), leaf (W_l), branch (W_b), or aboveground total (W_{above}) for three larch plantations

x	y (Kg)	Hitsujigaoka	Laoshan Plot 1	Laoshan Plot 2
DBH	W_s	0.962[b]	0.989[c]	0.976[b]
(cm)	W_l	0.925[b]	0.862[a]	0.955[b]
	W_b	0.691[a]	0.970[b]	0.947[b]
	W_{above}	0.941[b]	0.993[c]	0.974[b]
DBH^2H	W_s	0.952[b]	0.996[c]	0.975[b]
(m^3)	W_l	0.906[a]	0.855[a]	0.959[b]
	W_b	0.647[a]	0.938[b]	0.943[b]
	W_{above}	0.921[b]	0.996[c]	0.972[b]

([a]$p < 0.1$, [b]$p < 0.05$, [c]$p < 0.01$) (M Jomura et al., unpubl. data)

total/root biomass ratio (i.e., top/root ratio). For top/root ratio of each site, the mean value of sample tree data ($n = 3$ in Hitsujigaoka site, $n = 4$ in Laoshan site) was used. Total stand biomass was estimated as the sum of stem, leaf, branch, and root biomass, and NPP was estimated as the sum of annual biomass increment of these components. Therefore, the derived value of NPP in the present study is composed of total increment of woody biomass and needle biomass, and it does not include a fraction due to tree mortality or grazing. The allometric relationship with DBH^2H as a size parameter was used for estimation of biomass and NPP of broadleaved trees. The top/root ratio of larch trees was adopted for estimating root biomass and NPP of broadleaved trees, because the proportion of broadleaved tree biomass to the total biomass was less than 2%.

All allometric equations and their statistics are summarized in Tables 20.2, 20.3, 20.4, and 20.5. Allometry of biomass of each organ for all site-specific relationships was statistically significant ($p < 0.05$, Table 20.2). Slopes of site-specific regressions using both DBH and DBH^2H did not differ among the three plots (Table 20.3). However, intercepts of all site-specific regressions using DBH differed significantly among the three plots. Site-common allometry using DBH^2H could be applicable for only above-ground biomass, although allocation patterns to stems, branches, and leaves were significantly different among the three sites. Allometry of biomass increment of each organ for all site-specific relationships was statistically significant except for the case of branch biomass at Hitsujigaoka site ($p < 0.05$; Table 20.4). No slopes of the allometry were significantly different. However, all intercepts of the allometry were different among the three sites (Table 20.5).

20.3.2 Biomass, Allocation, and Net primary production

Total biomass was estimated to be 77.3 ± 32.2 MgC ha^{-1} (Table 20.6). Stem biomass of larch trees occupied from 62 to 77% of total larch biomass in these three sites. Leaf and branch biomass of larch trees accounted for 2–4% and 8–18% of total larch biomass in these sites, respectively. Root biomass was 13–20% of total larch

Table 20.3 Coefficients of site-specific allometric equations ($y = a\ x^b$) between two size parameters (DBH and DBH^2H) and dry mass of stem (W_s), leaf (W_l), branch (W_b), or aboveground total (W_{above}) for three larch plantations

		Coefficients	Hitsujigaoka	Laoshan Plot 1	Laoshan Plot 2	*F* value	Site-common
DBH (cm)	W_s (kg)	a	4.121E−02	1.255E−01	1.759E−01	0.000[c]	6.877E−02
		b	2.675	2.393	2.116	0.267[ns]	2.535
		r^2	0.962	0.989	0.976		0.937
	W_l (kg)	a	1.251E−04	6.437E−04	5.498E−04	0.003[c]	2.476E−03
		b	3.610	2.870	3.229	0.741[ns]	2.497
		r^2	0.925	0.862	0.955		0.797
	W_b (kg)	a	1.350E−03	3.823E−03	1.677E−02	0.003[c]	5.356E−02
		b	3.236	2.799	2.554	0.774[ns]	1.930
		r^2	0.691	0.970	0.947		0.664
	W_{above} (kg)	a	3.623E−02	1.217E−01	1.725E−01	0.010[c]	1.032E−01
		b	2.788	2.443	2.242	0.400[ns]	2.453
		r^2	0.941	0.993	0.974		0.953
DBH^2H (m^3)	W_s (kg)	a	2.035E+02	2.175E+02	1.419E+02	0.070[a]	1.952E+02
		b	1.099	1.012	0.854	0.354[ns]	1.006
		r^2	0.952	0.996	0.975		0.969
	W_l (kg)	a	1.196E+01	4.897E+00	1.504E+01	0.001[c]	5.816E+00
		b	1.476	1.205	1.306	0.808[ns]	0.935
		r^2	0.906	0.855	0.959		0.734
	W_b (kg)	a	3.799E+01	2.302E+01	5.391E+01	0.005[c]	2.152E+01
		b	1.292	1.160	1.029	0.849[ns]	0.718
		r^2	0.647	0.938	0.943		0.604
	W_{above} (kg)	a	2.546E+02	2.464E+02	2.070E+02	0.428[ns]	2.248E+02
		b	1.140	1.031	0.904	0.532[ns]	0.966
		r^2	0.921	0.996	0.972		0.971

Comparisons of the coefficients among the stands were made by ANCOVA; significance level is shown in the column of *F* value ([a]p <0.1, [b]p <0.05, [c]p <0.01)
Site-common equation was derived by pooling all sample tree data (M Jomura et al., unpublished. data)

Table 20.4 Coefficients of determination (r^2) in site-specific allometric equations ($y = a\ x^b$) between two size parameters (DBH and DBH^2H) and annual production of each component (stem, leaf, branch, or aboveground total) for three larch plantations

x	y (Kg)	Hitsujigaoka	Laoshan Plot 1	Laoshan Plot 2
DBH (cm)	Stem	0.958[b]	0.889[a]	0.959[b]
	Leaf	0.925[b]	0.862[a]	0.955[b]
	Branch	0.652[ns]	0.956[b]	0.828[a]
	Above total	0.915[a]	0.978[b]	0.954[b]
DBH^2H (m^3)	Stem	0.944[b]	0.936[b]	0.956[b]
	Leaf	0.906[a]	0.855[a]	0.959[b]
	Branch	0.604[ns]	0.921[b]	0.821[a]
	Above total	0.891[a]	0.992[c]	0.952[b]

([a]p <0.1, [b]p <0.05, [c]p <0.01) (M Jomura et al., unpubl. data)

Table 20.5 Coefficients of site-specific allometric equations ($y = ax^b$) between two size parameters (DBH and DBH^2H) and annual production of each component (stem, leaf, branch, or aboveground total) for three larch plantations

x	y (Kg)	Coefficients	Hitsujigaoka	Laoshan Plot 1	Laoshan Plot2	*F* value	site-common
DBH	Stem	*a*	1.706E−04	3.362E−03	7.861E−03	0.000 [c]	3.294E−02
		b	3.571	2.618	2.599	0.383 [ns]	1.806
		r^2	0.958	0.889	0.959		0.522
	Leaf	*a*	1.251E−04	6.437E−04	5.498E−04	0.003 [c]	2.476E−03
		b	3.610	2.870	3.229	0.741 [ns]	2.497
		r^2	0.925	0.862	0.955		0.797
	Branch	*a*	1.632E−03	8.255E−04	9.987E−03	0.000 [c]	4.782E−02
		b	2.508	2.834	2.279	0.809 [ns]	1.418
		r^2	0.652	0.956	0.828		0.362
	Above total	*a*	6.866E−04	4.097E−03	1.506E−02	0.000 [c]	6.050E−02
		b	3.375	2.771	2.606	0.485 [ns]	1.848
		r^2	0.915	0.978	0.954		0.602
DBH^2H	Stem	*a*	1.448E+01	1.196E+01	2.909E+01	0.000 [c]	9.375E+00
		b	1.464	1.132	1.047	0.444 [ns]	0.705
		r^2	0.944	0.936	0.956		0.523
	Leaf	*a*	1.196E+01	4.897E+00	1.504E+01	0.001 [c]	5.816E+00
		b	1.476	1.205	1.306	0.808 [ns]	0.935
		r^2	0.906	0.855	0.959		0.734
	Branch	*a*	4.566E+00	5.536E+00	1.340E+01	0.001 [b]	3.940E+00
		b	0.998	1.172	0.916	0.806 [ns]	0.533
		r^2	0.604	0.921	0.821		0.336
	Above total	*a*	3.096E+01	2.314E+01	5.707E+01	0.000 [c]	1.924E+01
		b	1.375	1.176	1.050	0.583 [ns]	0.706
		r^2	0.891	0.992	0.952		0.577

Comparisons of the coefficients among the three stands were made by ANCOVA; significance level is shown in the column of *F* value ([a]p <0.1, [b]p <0.05, [c]p <0.01). (M Jomura et al., unpubl. data)

biomass, indicating top to root ratio of 4.0–6.6 in these sites. The allocation of total larch tree biomass to each organ is similar to those reported for middle-age (50 < age ≤ 100 years) forests of *Larix gmelinii* in Daxingan Mountains, a young plantation of *L. gmelinii* (≤50 years) in Maoershan, northeast China (Shi et al. 2002), and *Larix kaempferi* forests of central Japan (Research Group on Forest Productivity of the Four Universities 1964). However, the report in mature *L. gmelinii* (240 < age ≤ 280 years) forest in Central Siberia indicated that 46, 3, 8, and 43% of total biomass were allocated for stem, leaf, branch, and root, respectively (Kajimoto et al. 1999). Thus, proportions of stem and root in total biomass were considerably different between eastern Asia (northeast China and Japan) and Central Siberia, although the proportions of leaf and branch in total biomass were similar in these regions. These results suggest that stems of larch trees play the role of a large long-term carbon sink in northeast China and Japan.

Table 20.6 Biomass and net primary production (NPP) estimated in three larch plantations

		Hitsujigaoka		Laoshan Plot 1		Laoshan Plot 2	
		Site-specific	Site-common	Site-specific	Site-common	Site-specific	Site-common
Biomass	(MgC ha^{-1})						
Larch tree	Stem	63.8	67.8	73.9	66.6	24.6	27.1
	Leaf	2.5	2.2	1.5	2.1	1.4	0.9
	Branch	9.7	10.3	7.3	8.7	7.2	4.6
	Coarse root	19.1	15.3	12.5	14.7	6.4	6.2
	Fine root	–		0.7		–	
	Lrach total	95.1	95.6	95.9	92.0	39.6	38.8
Broad-leaved		–		0.4		–	
Understory vegetation		–		0.4		0.6	
Stand total		95.1		96.7		40.2	
Production (NPP)	(MgC ha^{-1} y^{-1})						
Larch tree	Stem	3.1	4.6	3.8	3.8	3.8	2.0
	Leaf	2.5	2.2	1.5	2.1	1.4	0.9
	Branch	1.6	2.3	1.5	1.7	2.1	1.0
	Root	2.1	1.7	2.2	1.4	0.8	0.7
	Lrach total	9.3	10.8	9.0	9.0	8.1	4.6
Broad-leaved		–		0.6		–	
Under layer		–		0.1		0.2	
Stand total		9.3		9.8		8.3	

Tow estimates using site-specific and site-common allometric equations are shown (see each equation in Tables 20.4, 20.5) (M Jomura et al., unpubl. data)

Top/root ratio in the three study sites was 5.2 ± 1.3. Mean value of the top to root ratio of temperate and boreal coniferous forests ($n = 260$) was 4.3 (Kurz et al. 1996). Thus, the top/root ratio in the three sites of the present study was a little larger than the reported value. The ratios for two *Larix kaempferi* plantations in Japan were reported to be 4.7 (Satoo 1970) and 3.7 (Kurachi et al. 1993). The reports of a natural forest of Daxingan Mountain and a plantation of Maoershan showed the ratio of 2.8 and 3.5, respectively (Shi et al. 2002; see also Chap. 19, this Vol.). In Siberian *L. gmelinii* forest, the ratio was reported to be 0.9 and 1.3 (Kajimoto et al. 1999, 2006) and 1.1 (Kanazawa et al. 1994), although much higher ratio was observed in young larch stand at Tura (see also Chap. 6, this Vol.). Thus, it is suggested that allocation into the root biomass increases latitudinally.

NPP of our study stands was estimated to be 9.1 ± 0.7 MgC ha^{-1} y^{-1} (Table 20.6). The NPP would be a little bit overestimated, because we assumed that amount of leaf biomass was equivalent to leaf mass in litter fall in these sites: reduction by translocation at leaf senescence was not included. Nutrient withdrawal at leaf senescence showed relatively large amounts (Carlyle 1986).

Proportions of the components of biomass increment included in total NPP (stem, leaf, branch, and root) were 41±7%, 20±6%, 20±5%, and 19±8% at three sites studied. These patterns suggest that stem growth was the main part of biomass increment. In Siberia, allocation to leaf and root was as large as 56 and 26% (Kajimoto et al. 1999). So, the allocation pattern of total NPP to each organ in our study sites differed considerably from that in Siberia. Biomass ratio of new stem to new leaf was 2.2±0.8 in this study. The mean value of this ratio for evergreen coniferous forest was 2.2 (n=29; White et al. 2000), which is similar to our values. Thus, carbon allocation pattern to stem and leaf production in northeastern China and northern Japan was almost equivalent to global mean of the evergreen coniferous forest.

Estimates of total larch tree biomass obtained by applying site-common allometric equation (Table 20.3) ranged from 38.8 to 95.6 MgC ha^{-1} (Table 20.6). When compared with estimates by the site-specific allometry, the difference between two estimates ranged from −0.6 to 3.4%. Production estimates by applying site-common allometry (Table 20.5) ranged from 4.6 to 10.8 MgC ha^{-1} y^{-1} (Table 20.6). The difference between the values by site-specific and site-common allometries ranged from −17 to 43%. Thus, biomass estimates could be obtained by applying both site-specific and site-common allometries for larch forest of China and Japan. However, production estimates could be better estimated with the site-specific allometry than the site-common equation.

20.4 Photosynthesis and Autotrophic Respiration

20.4.1 Data Source

Adult larch trees at two contrasting sites of Laoshan (Plot 3) in northeastern China and Tomakomai (Plot 1) in Northern Japan were chosen to study the long-term patterns of CO_2 exchange in heterophyllous leaves, cones, stems, and roots, because two sites are located at similar latitudes between 43 and 45° (Table 20.1), but under contrasting environments at relatively continental and maritime climates, respectively. In this section, similarities and differences in the characteristics of photosynthesis and autotrophic respiration, and their possible contribution to carbon budget are discussed when the trees are growing at such contrasting sites. All field data were measured by a Li-6400 system (LiCor Inc., NE, USA) during the vegetative period (Apr. or May to Sept. or Oct.) from 2000 to 2004. Details of the method for photosynthesis and respiration measurements could be found in Wang et al. (2001a, 2001b, 2003, 2006a, 2006b, 2006c) and Wang (2005)

20.4.2 Leaf Photosynthesis

The growing season at Tomakomai site is much longer than that at Laoshan site (Table 20.1). Light response curves of leaf photosynthesis showed such significant difference (Fig. 20.5), i.e., P_{sat} (net photosynthetic rate under saturated light) was

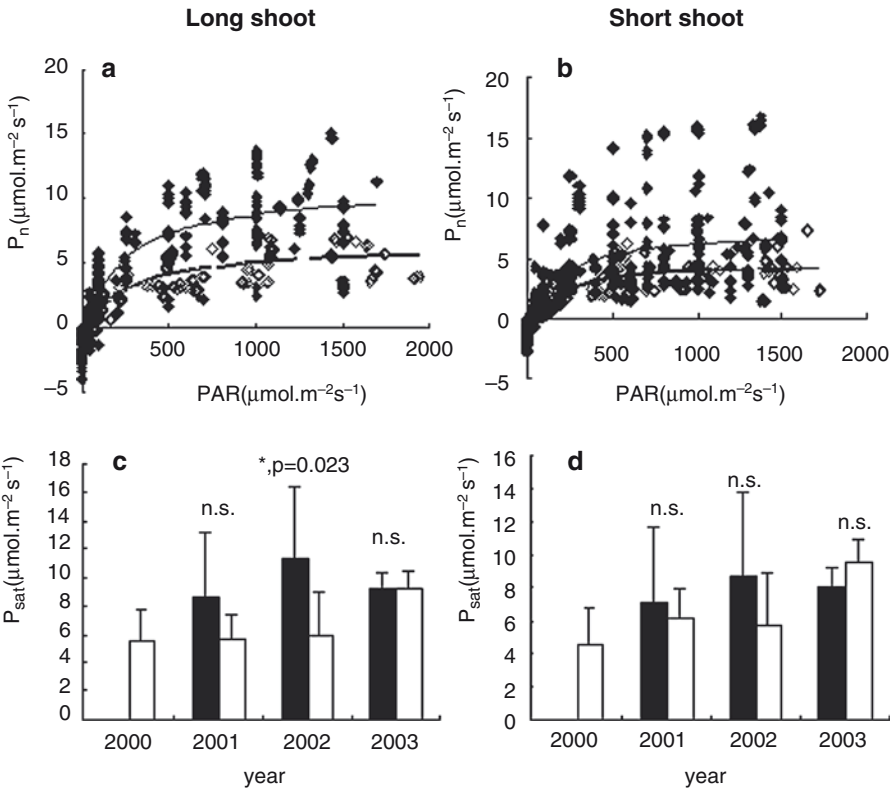

Fig. 20.5 Differences in light response curves of net photosynthetic rate P_n (**a, b**) and annual mean of net photosynthetic rate under saturated light, P_{sat} (**c, d**) for larch trees between two study sites, Laoshan in northeastern China (*L. gmelinii*) and Tomakomai in northern Japan (*L. kaempherii*). (**a**) and (**c**): data from long shoots. (**b**) and (**d**): data from short shoots. In (**a**) and (**b**), closed symbols represent the data of *L. gmelinii* at Laoshan, while open symbols represent the data of *L. kaempherii* at Tomakomai. The fitted curves are: (**a**) sunny long shoots at Laoshan (thin line), $y = 0.065\ x / (1 + 0.005\ x) - 1.77$ [$r^2 = 0.80$, $n = 521$]; sunny long shoots at Tomakomai (*bold line*), $y = 0.033\ x / (1 + 0.0056\ x) - 0.98$ [$r^2 = 0.84$, $n = 362$]. (**b**) sunny short shoots at Laoshan (*thin line*), $y = 0.052\ x / (1 + 0.006\ x) - 1.120$ [$r^2 = 0.53$, $n = 924$], sunny short shoots at Tomakomai, $y = 0.032\ x / (1 + 0.006\ x) - 0.657$ [$r^2 = 0.75$, $n = 322$]. All data were measured in the vegetative period from May to September. In (**a**) and (**b**), the data for Tomakomai were measured in 2000, those for Laoshan were measured in 2001 and 2002. In (**c**) and (**d**), black bars indicate annual mean P_{sat} at Laoshan, and white bars indicate annual mean P_{sat} at Tomakomai. Annual mean values in three years (2001–2003) at Tomakomai are calculated from monthly mean P_{sat} (May, June, August, and September) according to Kitaoka et al. (unpubl. data), and those in 2000 are based on W.J. Wang et al. (unpubl. data). All corresponding monthly data at Laoshan site are from W.J. Wang et al. (unpubl. data)

higher at Laoshan site than at Tomakomai site. This tendency was observed in both heterophyllous short shoots and long shoots (Fig 20.5). Moreover, much larger variation in P_{sat} at Laoshan site was observed. This may be related to the large climatic variation there, such as air temperature, humidity of air and soil, as well as total amount of precipitation.

Mean P_{sat} for short shoots and long shoots at Laoshan site ranged from 8 to 11 μmol $CO_2\,m^{-2}\,s^{-1}$, whereas those at Tomakomai site ranged from 4.5 to 9.5 μmol $CO_2\,m^{-2}\,s^{-1}$ (Fig 20.5). Exceptionally, higher P_{sat} was observed in 2003 at Tomakomai site; however, the reason could not be identified. The relatively high photosynthetic capacity as well as its large plasticity at Laoshan site may facilitate the larch shoots to maximize their carbon gain when the microenvironment is suitable for photosynthesis with the constraints of short vegetative period and harsh climatic condition. On the other hand, the longer vegetation period and relatively stable photosynthesis may strengthen the carbon gain of the larches at Tomakomai site (Table 20.7).

20.4.3 Cone Photosynthesis

The greenness of larch cones could allow photosynthesis in young cones in both sites. And, the substrate carbon was mainly from internal recycling of respiratory CO_2, which are different from that of leaf, the photosynthesized CO_2 are mainly from atmosphere CO_2 via stomata transportation (Wang et al. 2006a, 2006b). Stomata were observed on the scales of young larch cones; however, their regulatory function on photosynthesis was marginal compared to that of leaves, since it is unnecessary to control the entrances of CO_2 for photosynthesis (internal recycling). The internal recycling is manifested by the close correlation between intercellular CO_2 concentration (Ci) and photosynthesis in cones, but no such correlation was observed in leaves (Wang et al. 2006a, 2006b). Cone photosynthesis (P_{cone}: the differences between cone respiration; R_{cone}, in dark and in saturated light) was within similar magnitude at different sites, except for much higher rate observed in young cones at Laoshan site. The reason is that the cones were much younger at Laoshan than in Japan when the measurements were made (June at Tomakomai while May at Laoshan) (Table 20.7). The refixing ratio (P_{cone}/R_{cone}) of cone photosynthesis at Laoshan site ranged from near zero at the old stage to around 40% at the young stage, whereas it was as high as 71% at Tomakomai site. Although young cone has a much higher respiratory activity, their contribution to total forest carbon budget is negligible because of their low quantity compared with other organs in trees.

Through a rough upscaling, larch cones at Laoshan site could efflux 0.014 MgC $ha^{-1}\,y^{-1}$ at most (Wang 2005), which is much lower than that from roots and stems (Table 20.7). Calculation of total cone respiration and photosynthesis of the larch stand were carried out in 2004. By multiplying the cone projection area (0.8 cm^2 for young cone to 1.5 cm^2 for mature cone), cone density of a standard tree (200 $tree^{-1}$, a mean value of 18 trees), tree density of a forest (1150 ha^{-1}), day of a month, and mean cone respiration and photosynthesis, a rough estimate of total cone respiration was calculated to be 0.014 MgC $ha^{-1}\,y^{-1}$ (Wang 2005).

Table 20.7 Comparison of parameters associated with the rate of CO_2 exchange by cones, stems and roots in larch plantations at Laoshan in northeastern China and Tomakomai in northern Japan

Ogans	Parameters		Laoshan Plot 3	Tomakomai Plot1
Cones[a]	P_{cone}	Young	5.22 (1.8)	2.6 (0.7)
			(May – June, 2004)	(June, 2001 & 2004)
	(μmol CO_2 m^{-2} s^{-1})	Adult	1.4 (0.8)	0.8 (0.7)
			(July – Aug, 2004)	(July – Sept., 2001 & 2004)
		Old	0.1 (0.2)	0.04 (0.12)
			(late Aug., 2004)	(Oct. 2001)
	R_{cone}	Young	16.9 (3.69)	3.6 (0.8)
			(May – June, 2004)	(June, 2001 & 2004)
	(μmol CO_2 m^{-2} s^{-1})	Adult	4.8 (3.1)	2.6 (0.3)
			(July – Aug., 2004)	(July – Sept., 2001 & 2004)
		Old	0.1 (0.2)	2.0 (0.3)
			(late Aug., 2004)	(Oct., 2001)
	P_{cone}/R_{cone} (%)	Young	0.38	0.71 (0.04)
			(May – June, 2004)	(June, 2001 & 2004)
		Adult	0.29	0.28 (0.23)
			(July – Aug., 2004)	(July – Sept., 2001 & 2004)
		Old	0.01	0.02
			(late Aug., 2004)	(Oct., 2001)
Stems	R_{stem}[b](μmol CO_2 m^{-2} s^{-1})		2.8 (1.6)	2.0 (1.2)
			(May – Oct., 2001 & 2002)	(June – Oct., 2000)
	Q_{10}		2.2–3.5	2.6–3.8
			(May – Oct., 2001 & 2002)	(June – Oct., 2000)
	Annual sum of R_{stem}[c] (Mg C ha^{-1} yr^{-1})		3.31–3.60 (2001–2004)	[no data]
Roots	R_{soil} (μmol Co_2 m^{-2} s^{-1})		4.5 (2.7)	3.7 (1.6)
			(May – Oct., 2001 & 2002)	(June – Oct., 2000)
	R_{root}/R_{soil} (%)	Spring	14.2 (17.2)	31
			(April – May, 2001–2004)	(April – May, 2002 & 2003)
		Summer	38.2 (16.7)	40
			(June – Aug., 2001–2004)	(June – Aug., 2002 & 2003)
		Autumn	42.2 (14.8)	45
			(Sept. – Oct., 2001–2004)	(Sept. – Oct., 2002 & 2003)
		Microbes	1.89	[no data]
			(2001 – 2004)	
	Q_{10}	Microbes[b] roots(litters)	2.64 – 3.61 (2001 – 2004)	3.4 – 3.7

(continued)

Table 20.7 (continued)

Ogans	Parameters	Laoshan Plot 3	Tomakomai Plot1
	Annual sum of R_{soil} (Mg C $ha^{-1}\,y^{-1}$)	7.49 (0.70) [root = 2.26 (0.19)]	5.92 (5.5) [root; no data]

[a]Value based on the surface area of cones
[b]value based on stem surface area
[c]value based on ground area
Mean value with one standard deviation (in parentheses), or range is shown for each parameter (measurement period is shown below)
Data source: cones (Wang et al. 2006a), stems (Wang et al. 2003), and roots (Wang et al., unpubl. data) at Laoshan; cones (Wang et al. 2006b), stems and soil respiration (R_{soil})(Wang et al. 2001a, 2001b), R_{root}/R_{soil} ratio (Qu 2004), Q_{10} (Wang et al. 2001a, 2001b), and annual sum of R_{soil} (Shibata et al. 2005)

20.4.4 Stem Respiration

Stems show the largest biomass in the forest (see Sect. 20.3). Their autotrophic respiration at Laoshan site ($P_{stem} = 2.8\,\mu mol\ CO_2\,m^{-2}\,s^{-1}$) was higher than that at Tomakomai site ($2.0\,\mu mol\ CO_2\,m^{-2}\,s^{-1}$) (Table 20.7). However, their temperature sensitivity as manifested by the Q_{10} values was quite similar (2.3–3.5 vs. 2.6–3.8). By using stem temperature data recorded at a frequency of 2 times/hour, annual sum of CO_2 efflux from stems was calculated to be 3.31–3.60 MgC $ha^{-1}\,y^{-1}$ for larch trees at Laoshan site. This value is lower than that from soil system (i.e., annual sum of $R_{soil} = 7.49$ MgC $ha^{-1}\,y^{-1}$) but much higher than that from only roots (2.26 MgC $ha^{-1}\,y^{-1}$) in the same stand (Table 20.7).

20.4.5 Soil Respiration

Soil respiration at Laoshan site ($R_{soil} = 4.5\,\mu mol\ CO_2\,m^{-2}\,s^{-1}$) was more than 20% higher than that ($3.7\,\mu mol\ CO_2\,m^{-2}\,s^{-1}$) at Tomakomai site on average (Table 20.7). In both sites, proportion of root respiration to total soil respiration (R_{root}/R_{soil}) in spring was the lowest and increased with time in summer and autumn. No decreases were observed from summer to autumn (Table 20.7), which may be related to the time-lag effect of soil temperature in relation to air temperature.

The Q_{10} for respiration from soil microbes + roots (litters) was much higher than that from soil microbes alone (Table 20.7). Possibly, this finding indicates that roots may be more sensitive to temperature variation in local and global warming processes (Boone et al. 1998). However, the Q_{10} values of respiration from root or root + soil-microbes are even lower than those from soil-microbes alone by a review of 146 published Q_{10} values (Wang et al. 2006c). Thus, further investigation is necessary to obtain global estimates on temperature sensitivity of roots and soil microbes. In a review by Davidson and Janssens (2006), temperature sensitivity of soil respiration

is not related to temperature changes, but to differences in resource availability. Total CO_2 efflux from the soil system at Laoshan site (7.49 MgC $ha^{-1}\,y^{1}$) was one quarter higher than that (5.92 MgC $ha^{-1-}y^{1}$) at Tomakomai site. The efflux as the autotrophic respiration of roots at Laoshan site was 2.26 MgC $ha^{-1}\,y^{-1}$.

20.5 Soil Respiration and Environment

20.5.1 Enriched CO_2 experiment

In this section, results of experimental studies on soil respiration under enriched CO_2 concentration (FACE experiment) at Sapporo site are presented. Soil respiration was measured using a Li-6400 (LiCor Inc., NE, USA) connected to a soil respiration chamber (LI-6000-09, LiCor Inc., NE, USA). The six soil collars (10 cm in diameter and 6-cm length) were used as replicates in every treatment (totally 216 collars for the study). These collars were randomly placed, and inserted approximately 2.5 cm into the bare soil surface between plants. The treatments imposed were: (1) ambient CO_2 concentration (370 ppm) + volcanic soil; (2) elevated CO_2 concentration (550 ppm as a target CO_2 concentration at year 2040) + volcanic soil; (3) ambient CO_2 concentration + brown forest soil; (4) elevated CO_2 concentration + brown forest soil. Measurements were taken in July, August, and during a low activity season in October in 2005. Collar locations were rerandomized in the beginning of each measurement date. Soil temperature at 5-cm depth was recorded with thermocouple sensor attached to the respiration chamber at the time of measurement. After measuring respiration, soil was sampled from every collar for calculating mineral soil water content. We did not assess the effect of elevated CO_2 concentration on root biomass and root respiration rate. Root sampling was inadmissible, since the FACE experiment was considered to be a long-term program.

20.5.2 Effects of CO_2

Average respiration rate of volcanic soils exposed to elevated CO_2 concentration was about 7.3 μmol $CO_2\,m^{-2}\,s^{-1}$ at Sapporo site during a July–October period (Fig. 20.6b). This is significantly larger than the average value (about 4.4 μmol $CO_2\,m^{-2}\,s^{-1}$) for the volcanic soil under ambient CO_2 concentration (abbreviated as [CO_2] hereafter). Average respiration rate for the brown forest soils exposed to elevated [CO_2] was about 5.8 μmol $CO_2\,m^{-2}\,s^{-1}$, which was also higher than that exposed to ambient [CO_2], 4.4 μmol $CO_2\,m^{-2}\,s^{-1}$, although the difference was not significant in October (Fig. 20.6b) (Masyagina et al. 2006b). Variation of soil respiration was high (31–53%), and these observed rates of soil respiration are

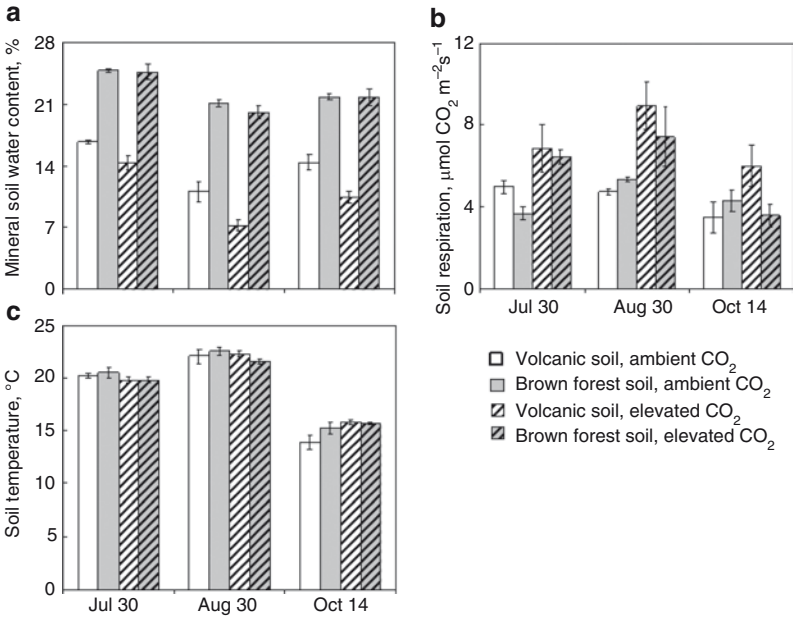

Fig. 20.6 Treatment effects on (**a**) soil respiration rate, (**b**) mineral soil water content, and (**c**) soil temperature of two soil types over three sampling dates during a growing season in larch plantation at Sapporo site. Data shown are treatment means ± SE. (Masyagina et al. 2006b)

close to the rates found by Butnor et al (2003) in loblolly pine stands (1–10.5 µmol $m^{-2} s^{-1}$ at ambient and elevated [CO_2]) and those by Lin et al. (1999) in Douglas-fir stands (2.5–4.5 µmol $CO_2 m^{-2} s^{-1}$ at ambient [CO_2] and 3.5–4.5 µmol $CO_2 m^{-2} s^{-1}$ at elevated [CO_2]).

Monthly averaged soil temperature ranged from 14 to 22°C during the growing season, and there were no statistically significant differences in soil temperature in relation to soil types and atmospheric [CO_2] conditions (Fig. 20.6c). Monthly averaged soil temperature increased 1.1 times from July to August and decreased 1.5 times from August to October ($p < 0.05$; Tukey HSD test). In spite of significant changes in soil temperature during vegetative period, we found only a significant negative correlation between the volcanic soil respiration and soil temperature (in July, $r = -0.67$, $p = 0.002$, $n = 18$; Table 20.8). Ball and Drake (1998) also detected no correlation between soil temperature and soil respiration.

Significant effect of [CO_2] on soil respiration rate has been found (Fig. 20.6b). Over the course of this research, monthly averaged soil respiration rates maintained at ambient [CO_2] were 1.4–1.9 times lower than that exposed to elevated [CO_2] conditions with exception in October, when no differences were observed in the soil respiration of brown forest soil due to [CO_2]. These results are in the middle of the range of stimulation (15–70%) of soil respiration reported for a variety of ecosystems exposed to elevated atmospheric CO_2 (Johnson et al. 1994; Vose et al. 1995;

Luo et al. 1996; Tjoelker et al. 1999; Pregitzer et al. 2000; Andrews and Schlesinger 2001; Butnor et al. 2003).

Because of inability to sample and analyze root biomass to assess the root respiration response to the elevated atmospheric [CO_2] in the present experiment, it was hard to suggest which of soil processes (root respiration, microbial respiration, decomposition, gas diffusion, etc.) are responsible for the increased soil respiration at the elevated [CO_2]. Though, it is known from literature that, in most cases, the elevated CO_2 treatment increased the contribution of root biomass (Johnson et al. 1994; Janssens et al. 1998; Ellsworth 1999; Tingey et al. 2000; Lukac et al. 2003). High-positive correlation between soil respiration and root biomass has been reported in a number of elevated-CO_2 studies (Johnson et al. 1994; Luo et al. 1996). In our study, model stands (larch with broad-leaved trees) are at a developing stage (4-year old)(Table 20.1). Therefore, significant increase of soil respiration found in our mixed stands under the elevated [CO_2] can be due to the increase in root biomass and proliferation of fine roots under the elevated CO_2 concentration. Another possibility suggested from stimulation of soil respiration in different biomes is increased rhizosphere microbial respiration and fine root turnover (Norby et al. 1992; Vose et al. 1995; Rouhier et al. 1996; Kubiske et al. 1998; Thomas et al. 1999).

There was no effect of soil type on soil respiration found during the growing season (i.e., depend on month and [CO_2], $p < 0.05$; Tukey HSD test). However, we also examined the effect of mineral soil water content (MSWC) on soil respiration in combination with change in [CO_2] conditions and soil type (Fig. 20.6a). Soil moisture is typically considered to be one of the key variables controlling soil respiration. Only a few negatively significant correlations between soil respiration and MSWC were found in our field experiment (Table 20.8): at elevated [CO_2] condition, brown soils with higher water content showed smaller respiration rates than volcanic soils with lower water content (see Fig. 20.6a, b). This is consistent with results from the tall grass prairie, where microbial activity (measured on disturbed samples) was correlated with soil moisture content (Williams et al. 2000).

20.5.3 Effects of Plantation Management

To examine the effects of thinning on soil respiration at Tomakomai site, we selected two plots in a mature plantation: a control and adjacent disturbed forest. The size of both control and disturbed sites was about 40 × 40 m. The thinning treatment (i.e., partial harvests) was made in January 2004, i.e., half a year before the respiration measurements. Thirty sample plots were established in the control site and 36 sample plots on the disturbed site. The size of sample plot was 1 × 1 m. Respiration measurements were combined with measurements of soil temperature, MSWC and other environmental variables. Soil respiration was measured at the end of July at all sites with a LI-6400 analyzer equipped with a soil respiration chamber (Li-Cor 6000-09). Measurements were made on fixed collars. Two soil cores of

Table 20.8 Results of correlation analysis of soil respiration at different level of atmospheric CO_2 concentration and hydrothermal parameters

	Soil respiration (μmol CO_2 m^{-2} s^{-1}) and mineral soil water content (%)			Soil respiration (μmol CO_2 m^{-2} s^{-1}) and soil temperature (°C)		
	r	*p*	*N*	*r*	*p*	*N*
A and V in July	0.31	0.209	18	0.15	0.153	18
A and BF in July	0.10	0.702	18	–0.08	0.757	18
E and V in July	–0.57*	0.015	18	–0.67*	0.002	18
E and BF in July	–0.27	0.272	18	–0.26	0.308	18
A and V in August	0.22	0.381	18	0.07	0.779	18
A and BF in August	0.14	0.583	18	–0.02	0.951	18
E and V in August	0.35	0.158	18	–0.15	0.546	18
E and BF in August	–0.53*	0.023	18	–0.07	0.782	18
A and V in October	0.44	0.066	18	0.44	0.069	18
A and BF in October	–0.59*	0.010	18	–0.24	0.338	18
E and V in October	–0.22	0.386	18	0.27	0.281	18
E and BF in October	–0.09	0.716	18	–0.34	0.163	18

A ambient [CO_2]; *E* elevated [CO_2]; *V* volcanic soil; *BF* brown forest soil
Values of *r* with asterisk are significant (*p <0.05)

small diameter (5 cm) were taken just after the respiration measurement from each collar (the same spot where respiration measurements were taken) to obtain estimates of soil texture, root density, mineral soil and litter water content and *C*/*N* value in the soil core.

Another factor affecting soil respiration is forest management (thinning and cutting) or strong wind disturbance. For example, harvesting or tree fall due to strong wind can lead to large heterogeneity of the ground surface that in turn causes spatial and temporal variability in soil respiration. To estimate the effects of thinning, soil respiration was studied in relation to soil temperature, mineral soil and litter water content, fine root density, litter density, and soil *C*/*N* after thinning (partial harvest) performed on a mature 50-year-old (as for 2003) larch plantation at Tomakomai National Forest, Hokkaido (Masyagina et al. 2006a).

The soil respiration rates observed in a larch plantation at control and thinned sites at Tomakomai display strong pattern of spatial variation (Figure 20.7) (Masyagina et al. 2006a). At the control site, variation of soil respiration (Cv = 19%, 5.6–12.1 μmol CO_2 m^{-2} s^{-1}) was less than that at the disturbed site (Cv = 33%, 4.5–19.8 μmol CO_2 m^{-2} s^{-1}). As mentioned, there are several possible causes of this large spatial heterogeneity: horizontal heterogeneity in the amount of roots, in litter thickness and in the *C*/*N* ratio, etc. The observed soil respiration rates are consistent with rates found in other ecosystems at similar temperatures (Klopatek 2002; Yim et al. 2003).

Forest management can influence the soil respiration rate in various ways: increasing, decreasing or not changing soil respiration. In this study, it was found that thinning management tends to increase soil respiration and leads to its large

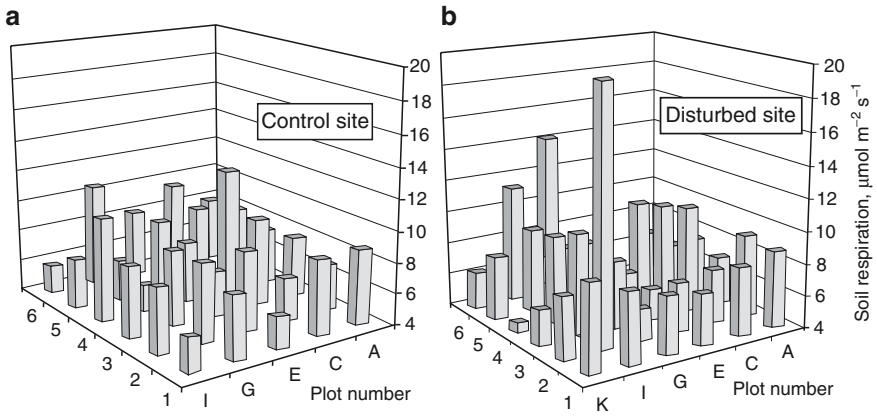

Fig. 20.7 Spatial variation of soil respiration (μmol $m^{-2} s^{-1}$) at (**a**) control and (**b**) disturbed sites in larch plantation at Sapporo site (Masyagina et al. 2006a)

variation after seven months of treatment. For example, after thinning, soil respiration rate was slightly but not significantly higher than that at control site, averaging about 8.3 μmol CO_2 $m^{-2} s^{-1}$ at disturbed site; this tendency is consistent with other studies reported for different coniferous ecosystems (Ohashi et al. 2000; Carter et al. 2002). The patterns of this increase can be attributed to stimulation of live roots and microflora activity, and increased decomposition associated with postharvesting, revegetation, and recolonization. In our study, the effect of thinning was not so large, because there was density reduction of only 33% of larch and 17% of broadleaved trees after the thinning operation. Therefore, the thinning was not so severe to cause crucial changes in soil respiration.

Dynamics of soil and litter are governed by complex interaction of factors that include soil respiration, litter input, climatic parameters, and soil *C* and *N* (Covington 1981). Concerning climatic factors, some authors propose that soil respiration depends mostly on soil temperature (Ohashi et al. 2000; Klopatek 2002; Gough and Seiler 2004); few studies assert that it depends strongly on soil moisture (Parker et al. 1983; Jiang et al. 2005). In our study, negative correlation between soil respiration and litter water content was observed at the disturbed site ($r = -0.41$, $p < 0.05$). These suggest high sensitivity of litter microbiota to moisture and its important role in decomposition processes in litter, especially after thinning. This is confirmed by the fact that most fine roots of larch trees are located in the litter layer; after thinning, they become damaged and start to decay. So, although soil respiration depends strongly on soil temperature and water content, these two factors do not contribute greatly to the spatial variability of soil respiration observed in this study. These relations suggest that the climatic factors influence temporal variability of soil respiration also, and even more strongly than the spatial variability.

Relationship between roots and soil respiration is obvious. In particular, respiration can be affected by variation in tree roots at different positions, and its relationships with soil temperature and moisture (Boone et al. 1998; Pangle and Seiler 2002).

Some studies nevertheless report no significant correlations between the roots and respiration (Gough and Seiler 2004). We also did not find any statistically close relationships between respiration and density of fine roots in either site. The mean value of fine root density at the control site was approximately 18% higher than at the disturbed site. It can be due to removal of larch biomass by 26% and biomass of broadleaved trees by 7% after the thinning operation in January 2004, but this difference was not statistically significant. The variation in root density was much greater at the disturbed site (Cv = 88%) than at the control site (Cv = 29%). According to Qu (2004), the proportion of root respiration in total soil respiration at a larch plantation ranged from 18 to 52%. Our study did not find any changes in the soil respiration rate after thinning. It is explained that by possible compensation of 18% reduction in fine root density following thinning by the increased microbial respiration as a result of decomposition of dead roots after felling. Toland and Zak (1994) similarly reported that acceleration of microbial respiration offsets a decline in root respiration in the first year of clear-cutting in northern hardwood forests. There have been similar findings in hardwood forest (Londo et al. 1999) and spruce-fir stands (Lytle and Cronan 1998). Clearly, the rapid decomposition of roots is able to compensate for the decrease in root respiration in the first year.

It has been found that litter density is significantly lower (by 15%, $t = 2.86$, $p = 0.006$) at the disturbed site (1150.5 g m^{-3}) than at the control site (1344.2 g m^{-3}). Thinning caused a large variation in litter density in the disturbed site (524.8–2057.5 g m^{-3}, Cv = 26%) with respect to control (965.0–1941.3 g m^{-3}, Cv = 18%). Qu (2004) states that the contribution of litter respiration to soil respiration varies from 8 to 32% at a larch plantation at Tomakomai National Forest. This indicates that litter decomposition is an important factor in the soil CO_2 flux. There was no significant correlation found between soil respiration and litter density at the control site, but there was positive correlation at the disturbed site ($r = 0.40$, $p < 0.05$).

According to a number of studies, the total *C* and *N* in the surface soil (0–10 cm) responded to harvesting. They declined during the first year after the harvest, and increased during the second year (Johnson 1992; Carter et al. 2002). Our findings agree with this conclusion, although major fluctuations may last for months or years before the soil *C* returns to preharvest levels. It has been found in the surface soil at seven months after thinning that, the *C* value was insignificantly higher (7%, *t*-test = −0.82, $p = 0.42$), and *N* was also significantly higher (18%, *t*-test = −3.29, $p = 0.002$) at the disturbed site ($C = 12.4\%$, $N = 0.91\%$) than at the control sites ($C = 11.5\%$, $N = 0.75\%$). Our results are consistent with the data reported by Qu (2004), in which the soil *C* in a larch plantation varied from 5 to 25%, and the soil *N* from 0.2 to 1.5%. The *C* and *N* content did not significantly influence the soil respiration rate at either site. In our study, the *C*/*N* ratio in the upper 10 cm of mineral soil remained fairly constant. The mean values of *C*/*N* were similar at the control and disturbed sites, taking values 15.3 and 13.5, respectively. The *C*/*N* ratio found in our study is lower than that observed by Carter et al. (2002) and Klopatek (2002). Similar to the report by Gough and Seiler (2004), we observed a significant positive correlation between soil respiration and soil *C*/*N* in the top 10 cm of mineral soil after thinning of larch plantation ($r = 0.39$, $p < 0.05$).

Thus, thinning treatment modified the physical and environmental conditions, along with changes in substrate availability, and probably caused the increase in soil microbial respiration, but also most likely a decline in root respiration following death of fine roots after the thinning. Some 18% loss in fine root density has been compensated for by the increased rates of heterotrophic respiration as a result of decomposition of dead roots after felling of the trees.

20.6 Conclusions

In this chapter, we described (1) biomass and allocation pattern of carbohydrate, (2) photosynthesis and autotrophic respiration of main tree organs, and (3) soil respiration under CO_2 enhanced conditions and under thinning treatment in four larch plantations (*L. gmelinii* or *L. kaempherii*) in Eastern Asia. Some characteristic features were suggested as follows:

- Total biomass of larch (*L. gmelinii*) plantation was not much different between northeastern China and northern Japan. Site common allometric relationship constructed for the sites in two countries showed good performance only in estimating total biomass. Allocation pattern of carbohydrate were affected by tree density and age of the stand rather than regional changes.
- From the view point of leaf photosynthesis and autotrophic respiration, the larch (*L. gmelinii*) trees at the continental site in northeastern China had higher photosynthesis and respiration of cones, stems and roots. Large variations were also observed, while the larch grown in northern Japan had contrastingly lower but relatively stable rates both in photosynthesis and respiration.
- Significant effects of CO_2 enrichment and thinning disturbance on soil respiration rate were found in young larch (*L. kaempherii*) plantation in northern Japan. Understanding influence of these disturbances on soil CO_2 exchange requires further knowledge on relative importance of various soil processes (such as root respiration, microbial reparation, and decomposition) on soil respiration.

References

Abaimov AP, Lesinski JA, Martinsson O, Milyutin LI (1998) Variability and ecology of Siberian larch species. Swedish University of Agricultural Sciences, Department of Silviculture, Reports 43, Umeå, p 118

Amthor JS, Baldocchi DD (2001) Terrestrial higher plant respiration and net primary production. In: Roy J, Saugier B, Mooney HA (eds) Terrestrial global productivity. Academic Press, San Diego, pp 33–59

Andrews JA, Schlesinger WH (2001) Soil CO_2 dynamics, acidification, and chemical weathering in a temperate forest with experimental CO_2 enrichment. Global Biogeochem Cycles 15:149–162

Ball AS, Drake BG (1998) Simulation of soil respiration by carbon dioxide enrichment of marsh vegetation. Soil Biol Biochem 30:1203–1205

Boone RD, Nadelhoffer KJ, Canary JD, Kaye JP (1998) Roots exert a strong influence on the temperature sensitivity of soil respiration. Nature 396:570–572

Butnor JR, Johnsen KH, Oren R, Katul GG (2003) Reduction of forest floor respiration by fertilization on both carbon dioxide-enriched and reference 17-year-old loblolly pine stands. Global Change Biol 9:849–861

Carlyle J (1986) Larch litter and nitrogen availability in mixed larch spruce stands. 1. nutrient withdrawal, redistribution, and leaching loss from larch foliage at senescence. Can J For Res 16:321–326

Carter MC, Dean TJ, Zhou M, Messina MG, Wang Z (2002) Short-term changes in soil C, N, and biota following harvesting and regeneration of loblolly pine (*Pinus taeda* L.). For Ecol Manage 164:67–88

Covington WW (1981) Changes in forest floor organic matter and nutrient content following clear cutting in northern hardwoods. Ecology 62:41–48

Davidson EA, Janssens IA (2006) Temperature sensitivity of soil carbon decomposition and feedbacks to climate change. Nature 440:165–173

Eguchi N, Morii N, Ueda T, Funada R, Takagi K, Hiura T, Sasa K, Koike T (2008) Changes in petiole hydraulic structure followed by the change in leaf water relations of birch and oak saplings exposed to free air CO_2 enrichment in northern Japan. Tree Physiol 28:287–295

Ellsworth DS (1999) CO_2 enrichment in a maturing pine forest: are CO_2 exchange and water status in the canopy affected. Plant Cell Environ 22:461–472

Gough CM, Seiler JR (2004) The influence of environmental, soil carbon, root, and stand characteristics on soil CO_2 efflux in loblolly pine (*Pinus taeda* L.) plantations located on the South Carolina Coastal Plain. For Ecol Manage 191:353–363

Greco S, Baldocchi DD (1996) Seasonal variations of CO_2 and water vapor exchange rates over a temperate deciduous forest. Global Change Biol 2:183–197

Hättenschwiler S, Handa T, Egli L, Asshoff R, Amman W, Körner C (2002) Atmospheric CO_2 enrichment of alpine treeline conifers. New Phytol 156:363–375

Janssens IA, Crookshanks M, Taylor G, Ceulemans R (1998) Elevated atmospheric CO_2 increases fine root production, respiration, rhizosphere respiration and soil CO_2 efflux in Scots pine seedlings. Global Change Biol 4:871–878

Jiang L, Shi F, Li B, Luo Y, Chen J, Chen J (2005) Separating rhizosphere respiration from total soil respiration in two larch plantations in northeastern China. Tree Physiol 25:1187–1195

Johnson DW (1992) Effects of forest management on soil carbon storage. Water Air Soil Pollut 64:83–120

Johnson DW, Geisinger DR, Walker RF, Newman J, Vose JM, Elliot K, Ball JT (1994) Soil pCO_2, soil respiration, and root activity in CO_2-fumigated and nitrogen-fertilized ponderosa pine. Plant Soil 165:129–138

Kajimoto T, Matsuura Y, Sofronov MA, Volokitina AV, Mori S, Osawa A, Abaimov AP (1999) Above- and belowground biomass and net primary productivity of a *Larix gmelinii* stand near Tura, central Siberia. Tree Physiol 19:815–822

Kajimoto T, Matsuura Y, Osawa A, Abaimov AP, Zyryanova OA, Isaev AP, Yefremov DP, Mori S, Kike T (2006) Size-mass allometry and biomass allocation of two larch species growing on the continuous permafrost region in Siberia. For Ecol Manage 222:314–325

Kanazawa Y, Osawa A, Ivanov BI, Maximov TC (1994) Biomass of a *Larix gmelinii* (Rupr.) Litv. Stand in Spaskayapad Yakutsk. In: Inoue G (ed) Proceedings of the Second Symposium on the Joint Siberian Permafrost Studies between Japan and Russia in 1993. National Institute for Environmental Studies, Tsukuba, pp 153–158

Kasischke ES, Stocks BJ (eds) (2000) Fire, climate change, and carbon cycling in the boreal forest. Ecological Studies, vol 138. Springer, Berlin Heidelberg New York

Klopatek JM (2002) Belowground carbon pools and processes in different age stands of Douglas fir. Tree Physiol 22:197–204

Koike T, Yazaki K, Funada R, Maruyama Y, Mori S, Sasa K (2000) Forest health and vitality in northern Japan: A history of larch plantation. Faculty Forestry, University of Joensuu, Research Notes 92, pp 49–60

Kubiske ME, Pregitzer KS, Zak DR, Mikan CJ (1998) Growth and C allocation of Populus tremuloides genotypes in response to atmospheric CO_2 and soil N availability. New Phytol 140:251–260

Kurachi N, Hagihara A, Hozumi K (1993) Canopy photosynthetic production in a Japanese larch forest 2. Estimation of the canopy photosynthetic production. Ecol Res 8:349–361

Kurz WA, Beukema SJ, Apps MJ (1996) Estimation of root biomass and dynamics for the Carbon Budget Model of the Canadian Forest Sector. Can J For Res 26:1973–1979

Lin G, Ehleringer JR, Rygiewicz PT, Johnson MG, Tingey DT (1999) Elevated CO_2 and temperature impacts on different components of soil CO_2 efflux in Douglas-fir terracosms. Global Change Biol 5:157–168

Londo AJ, Messina MG, Schoenholtz SH (1999) Harvesting effects on soil carbon content and efflux in an East Texas bottomland. Soil Sci Soc Am J 63:637–644

Lukac M, Calfapietra C, Godbold DL (2003) Production, turnover and mycorrhizal colonization of root systems of three Populus species grown under elevated CO_2 (POPFACE). Global Change Biol 9:838–848

Luo Y, Jackson RB, Field CB, Mooney HA (1996) Elevated CO_2 increases belowground respiration in California grasslands. Oecologia 108:130–137

Lytle DE, Cronan CS (1998) Comparative soil CO_2 evolution, litter decay, and root dynamics in clear-cut and uncut spruce-fir forest. For Ecol Manage 103:121–128

Masyagina OV, Hirano T, Ji DH, Choi DS, Qu L, Fujinuma Y, Sasa K, Matsuura Y, Prokushkin SG, Koike T (2006a) Effect of spatial variation of soil respiration rates following disturbance by timber harvesting in a larch plantation in northern Japan. For Sci Technology 2:80–91

Masyagina OV, Prokushkin SG, Qu L, Koike T (2006b) The response of the soil CO_2 emissions of a deciduous mixed stands in Hokkaido (Japan) to doubling of atmospheric carbon dioxide concentration. In: Proceedings of International Conference –Forest Ecosystems of Northeastern Asia and Their Dynamics, Vladivostok, pp 64–67, 2006

Norby RJ, Gunderson CA, Wullschleger SD, O'Neill EG, McCracken MK (1992) Productivity and compensatory responses of yellow-poplar trees in elevated CO_2. Nature 357:322–324

Ohashi M, Gyokusen K, Saito A (2000) Contribution of root respiration to total soil respiration in a Japanese cedar (*Cryptomeria japonica* D. Don) artificial forest. Ecol Res 15:323–333

Pangle RE, Seiler J (2002) Influence of seedling roots, environmental factors and soil characteristics on soil CO_2 efflux rates in a 2-year-old loblolly pine (*Pinus taeda* L.) plantation in the Virginia Piedmont. Environ Poll 116:85–96

Parker LW, Miller J, Steenberg Y, Whitford WG (1983) Soil respiration in a Chihuahuan Desert rangeland. Soil Biol Biochem 15:303–309

Pregitzer KS, Zak DR, Maziasz J, DeForest J, Curtis PS, Lussenhop J (2000) Fine root growth, mortality, and morphology in a factorial elevated atmospheric CO_2 x soil N availability experiment. Ecol Appl 10:18–33

Qu L (2004) Ecophysiological study on natural regeneration of the two larch species with special references to soil environment in larch forests. PhD thesis, Hokkaido University, Sapporo

Research Group on Forest Productivity of the Four Universities (1964) Studies on the productivity of forest. Part II Larch (*Larix leptplepis* Gord.) forests of Sinshu Distinct. Japan Forest Technology Association. Tokyo, p 60

Rouhier H, Billes G, Billes L, Bottner P (1996) Carbon fluxes in the rhizosphere of sweet chestnut seedlings (*Castanea sativa*) grown under two atmospheric CO_2 concentrations - C^{14} partitioning after pulse labelling. Plant Soil 180:101–111

Roy J, Saugier B, Mooney HA (eds) (2001) Terrestrial global productivity. Academic press, San Diego

Satoo T (1970) Primary production in a plantation of Japanese larch, Larix leptolepis: a summarized report of JPTF-66 KOIWAI. Jpn J For Soc 52:154–158

Schulze E-D, Loyd J, Kelliher FM, Wirth C, Rebmann C, Luhker B, Mund M, Knohl A, Milyukova IM, Schulze W, Ziegler W, Varlagin AB, Cogachev AF, Valentini R, Dore S, Grigoriev S, Kolle O, Panfyorov MI, Tchebakova N, Vygodskaya NN (1999) Productivity of forests in Eurosiberian boreal region and their potential to act as a carbon sink – a synthesis. Global Change Biol 5:703–722

Shi F, Qu L, Wang W, Matsuura Y, Koike T, Sasa K (2002) Aboveground biomass and productivity of *Larix gmelinii* forests in northeast China. Eurasian J For Res 5:23–32

Shibata H, Hiura T, Tanaka Y, Takagi K, Koike T (2005) Carbon cycling and budget in a forested basin of southwestern Hokkaido, northern Japan. Ecol Res 20:325–331

Thomas SM, Whitehead D, Reid JB, Cook FJ, Adams JA, Leckie AC (1999) Growth, loss and vertical distribution of *Pinus radiata* fine roots growing at ambient and elevated CO_2 concentration. Global Change Biol 5:107–121

Tingey DT, Phillips DL, Johnson MG (2000) Elevated CO_2 and conifer roots: effects on growth, life span and turnover. New Phytol 147:87–103

Tjoelker MG, Oleksyn J, Reich PB (1999) Acclimation of respiration to temperature and CO_2 in seedlings of boreal tree species in relation to plant size and relative growth rate. Global Change Biol 49:679–691

Toland DE, Zak DR (1994) Seasonal patterns of soil respiration in intact and clear-cut northern hardwood forests. Can J For Res 24:1711–1716

Vose JM, Elliott KJ, Johnson DW, Walker RF, Johnson MG, Tingey DT (1995) Effects of elevated CO_2 and N fertilization on soil respiration from ponderosa pine (*Pinus ponderosa*) in open-top chambers. Can J For Res 25:1243–1251

Wang WJ (2005) Physiological ecology of respiratory consumption of a larch (*Larix gmelinii*) forest in NE China. PhD thesis, Hokkaido University, Sapporo

Wang WJ, Kitaoka S, Shi FC, Matsuura Y, Sasa K, Koike T (2001a) Respiration of non-photosynthetic organs and forest soil in a Japanese larch plantation. Hokkaido Branch Trans Jpn For Soc 49:33–35 (in Japanese)

Wang WJ, Kitaoka S, Koike T, Quoreshi AM, Takagi K, Kayama M, Ishida N, Mamiya H, Shi F, Sasa K (2001b) Respiration of non-photosynthetic organs and forest soil of Japanese larch plantation and its contribution to CO_2 flux estimation. AsiaFlux Net 1:119–123

Wang WJ, Yang FJ, Zu YG, Wang HM, Takagi K, Sasa K, Koike T (2003) Stem respiration of a larch (*Larix gmelinii*) plantation in Northeast China. J Integrative Plant Biol 45:1387–1397

Wang WJ, Zu YG, Cui S, Hirano T, Watanabe Y, Koike T (2006a) Carbon dioxide exchange of larch (*Larix gmelinii*) cones during development. Tree Physiol 26:1363–1368

Wang WJ, Watanabe Y, Endo I, Kitaoka S, Koike T (2006b) Seasonal changes in the photosynthetic capacity of cones on a larch (*Larix kaempferi*) canopy. Photosynthetica 45:345–348

Wang WJ, Wang HM, Zu YG, Li XY, Koike T (2006c) Characteristics of the temperature coefficient, Q_{10}, for the respiration of non-photosynthetic organs and soils of forest ecosystems. Front For China 1:125–135

White MA, Thornton PE, Running SW, Nemani RR (2000) Parameterization and sensitivity analysis of the BIOME-BGC terrestrial ecosystem model: net primary production controls. Earth Interact 4:1–85

Williams M, Rice C, Owensby C (2000) Carbon dynamics and microbial activity in tallgrass prairie exposed to elevated CO_2 for 8 years. Plant Soil 227:127–137

Yim MH, Joo SJ, Shutou K, Nakane K (2003) Spatial variability of soil respiration in larch plantation: estimation of number of sampling points required. For Ecol Manage 175:585–588

Zhou G, Wnag Y, Jiang Y, Yang Z (2002) Estimating biomass and net primary production from forest inventory data: a case study of China's *Larix* forests. For Ecol Manage 169:149–157

Chapter 21
The Role of Ectomycorrhiza in Boreal Forest Ecosystem

L. Qu, K. Makoto, D.S. Choi, A.M. Quoreshi, and T. Koike

21.1 Introduction

The ectomycorrhizal fungi (ECM fungi) are both abundant and widespread in boreal forests. Host plant provides the assimilated carbon to the infecting ECM fungi. Many studies indicate that at most 10–30% of the assimilated carbon by the host plant photosynthesis may be used by the fungal partner for the production and sustenance of its external biomass (Smith and Read 1997). On the other hand, ECM fungi exude extracellular enzymes that are able to break down complex organic substances and consequently transmit the inorganic nutrients to their hosts. Such ECM activity results in greater plant growth under severe environmental conditions of the boreal forests (Read 1991; Chalot and Brun 1998). Tree seedlings infected with ECM can significantly improve their growth when compared with nonmycorrhizal seedlings.

Such symbiotic association between the host plant and ECM fungi is affected greatly by the environmental conditions in the forest ecosystem. In the Russian boreal forest, the permafrost soils and frequent forest fires are specific environmental factors (Chap. 1). Understanding ectomycorrhizal role in the ecosystem processes (i.e., carbon and nutrient cycling) in the Siberian forest requires knowledge on the ECM activities in the permafrost soils and in the postfire stands. Furthermore, it is also necessary to consider recent changes in the environmental conditions (e.g., rising atmospheric CO_2 concentration).

In this chapter, we first introduce physiology of the ECM plants associated with trade of nutrients and carbon – an overview of the ECM in boreal forests. Second, characteristics of ECM ecology in Siberian boreal forests, especially with respect to conditions of permafrost soil and forest fires, are examined, although previous knowledge appears to be limited. Finally, we show results of recent studies on the changes in symbiotic interactions between plants and ECM under the increased CO_2 concentration.

A. Osawa et al. (eds.), *Permafrost Ecosystems: Siberian Larch Forests*,
Ecological studies, Vol. 209, DOI 10.1007/978-1-4020-9693-8_21,

21.2 Physiology of Ectomycorrhizal Plants

There is a general agreement that ECM enhances the capacity of infected plants to absorb nutrients, and this can be especially important on infertile and adverse sites. The ECM root is characterized by the presence of three structural components, such as sheath or mantle, Hartig net, and hyphae (Smith and Read 1997). ECM increase uptake rates of nutrients by some mechanisms, including (1) increased physical access to soil with its thin mycelium, (2) changes in mycorrhizosphere or hyphosphere soil chemistry with the secretion of enzymes and organic acids (Van der Heijden and Sanders 2002), and (3) alteration of the bacterial community in the mycorrhizosphere (Rillig and Mummey 2006). Compared with nonmycorrhizal plants of the same species, ectomycorrhizal plants take up more organic N and P forms effectively, since ECM produces ecto-enzymes (Turnbull et al. 1996; Van der Heijden and Sanders 2002), and possibly through enhancing xylem loading to increase the amount of sulfate returned to roots for protein synthesis (Rennenberg 1999).

Khasa et al. (2001) reported increased seedling growth of larch, one of the dominant genera in Siberian forests, in both container-grown and bare-root nurseries as the levels of fertilizer increased. A similar phenomenon was found in hybrid Dahurian larch F1 (*Larix gmelinii* × *L. kaempferi*) (Qu et al. 2004; Choi et al. 2005; see also Chap. 3 for taxonomy of *Larix* in Siberia). Murata (1991) also reported that infection of *Suillus grebillei* and *Suillus laricinus* significantly enhanced the growth of *L. kaempferi* seedlings.

It was reported repeatedly that ECM mycelial systems enhance the nutrient uptake of N, P, K, Ca Zn, S, etc. (e.g., Frank 1894; Read 1983; Finlay 1993; Leake and Read 1997; Chalot and Brun 1998; Read and Perez-Moreno 2003; Lindahl et al. 2005). We summarize several ways of efficient nutrient uptake by ECM as follows:

First, the ECM mycelium is considered the physical extension of a root system. They significantly enhance the absorptive surface area and extract and transport nutrient from soil to plant. Van der Heijden and Sanders (2002) estimated that hyphae produced up to 60-fold increase in surface area of the root.

Second, secretion of enzymes that break down organic compounds is especially important in utilization of organic N and P (protein and amino acids) (Chalot and Brun 1998). Phosphate (P) is the major form of phosphorus available for uptake by plants. But it is relatively insoluble in mineral soil due to its biding to K, Ca, Mg, and Al, and therefore, is not readily transported by mass flow. ECM hyphae can explore the bulk soil and release the organic acids to decrease the rhizosphere pH. This decrease of soil pH by ECM results in increased mobilization of phosphate from K, Ca, and Mg in the rhizosphere (Lapeyrie et al. 1990, Watteau and Berthelin 1994, Olsson and Wallander 1998). Furthermore, the ECM mycelium system develops a large surface area and transports P to the host plant sufficiently (Allen 1991).

Third, ECM may act to increase N-fixation rates of N-fixing plants by alleviating other stresses imposed on those plants by selecting the bacterial population in the rhizosphere (Frey-Klett et al. 2007).

Fourth, ECM may also influence nutrient uptake indirectly through their effects on bacterial activity in the rhizosphere. Li et al. (1992) presented that N-fixing bacteria appear to be associated with specific types of ECM. In their papers,

nitrogenase activity of *Bacillus* sp (N-fixing bacteria) is enhanced with the addition of water extraction of ECM, and they suggest possibility of the importance of a nutritional relationship between this bacterium and ECM.

The ability of ECM mycelium to absorb water was also well documented (Duddridge et al. 1980; Read and Boyd 1986; Lamhamedi et al. 1992). Smith and Read (1997) have pointed out that nutrients become less and less available due to increasing tortuosity of the diffusion path associated with soil drying. Then, the hyphal contribution to nutrient and water uptake becomes increasingly important.

In addition, presence of the thick fungal mantle over the tissues of ectomycorrhizal root could be expected to provide a physical barrier to penetration by pathogens. Three-point-five percent of Russian larch seedlings that inoculated with ECM were damaged by Otiorhyneus larvae; however, 11.2% of noninoculated seedlings were damaged (Halldorsson et al. 2000).

21.3 Ectomycorrhizae in Boreal Forests

The boreal forest, or taiga, which cover about 9% ($13.7 \times 10^6 \text{km}^2$) of the land between 45 and 75° north (Czimczik et al. 2005), is the world's largest biome. It is characterized by cool climate and slow rate of decomposition. Thus, the organic residues of plants accumulate either as raw humus at the soil surface and within pores of shallow soils or as peat, sometimes to considerable depths (Read et al. 2004). The low mineralization rate by the microorganisms result in low availability of nutrient, especially nitrogen, in the boreal forest ecosystem (Näsholm et al. 1998). Thus, nitrogen (N) is the most important determinant of plant productivity in the boreal forest (Tamm 1991; Schulze et al. 1995). Therefore, the high capacity of ectomycorrhiza in utilizing organic substances reduces the chance of N limitation in plant productivity. As a result, low availability of N could be a characteristic feature of biomes dominated by the ECM plants (Smith and Read 1997). Read (1991) has hypothesized that the amount of soil organic matter present in an ecosystem may control the dominance of major mycorrhizal groups. He has suggested that ECM should be the most abundant in forests with a well-developed litter layer, since they produce enzymes that can mineralize organic materials such as proteins, cellulose, and phosphorus compounds (Abuzinadah and Read 1989; Read 1991).

Global importance of ECM requires no discussion. Pinaceae, Betulaceae, and Fagaceae predominantly form ECM roots, dominate in vast areas of boreal forests, and act as a huge carbon stock (Wielgolaski 2005; Thormann 2006).

21.4 Carbon Flux in Ectomycorrhizal Plants

It has generally been agreed that ECM plants can assimilate more carbon than non-ECM plants under the same growth condition. For example, Qu et al. (2004) reported that ECM larch seedlings that were inoculated with forest soil assimilated

6.5 and 18.0% more carbon to the stem in Japanese larch and in hybrid larch, respectively, than did the nonmycorrhizal seedlings. Of the total ^{14}C detected in needle, stem, and root fractions, ECM seedlings assimilated more carbon than the control seedlings. This may be due to the significantly higher photosynthetic rates of ECM seedlings of two larch species than the nonmycorrhizal seedlings. As a result, the dry mass of ECM seedlings was about 1.5 times larger than that of nonmycorrhizal seedlings. The C flux to ECM fungi from the host plants were estimated by various ways: comparing plants that are inoculated and noninoculated with fungi under the same plant growth rate; separating root systems into inoculated and noninoculated parts; measuring flow of ^{14}C-labeled assimilates into fungi. The dynamic carbon allocation could be studied by measuring ^{14}C-labeled assimilates in needle, stem, and root, respectively (Fig. 21.1). However, quantification of C flux into ECM plants has been quite variable due to wide variability of methodology, growing conditions, and species among studies. The first field estimate of the amount of carbon needed by fungal partner was presented by Harley (1971). He estimated that 10% of the wood production was used by the fungus. Fogel and Hunt (1983) estimated the fungal demand to be 24% of the annual throughput and Vogt et al. (1982) calculated that 15% of the primary production was used by the fungi. Finlay and Söderström (1989) accounted for turnover of ECM roots and the production of external mycelium, fungal mantle, and sporocarps, and calculated 15% of C flux into ECM tissues in a Swedish pine forest. The estimates of the C costs of mycorrhizal symbiosis vary between 4 and 20% of the carbon fixed in photosynthesis (Lambers et al. 1998). Field estimates of the C demand by ECM may be underestimated, because it is difficult to accurately measure the C demand of fruiting bodies and external hyphae supported by a tree or a community of trees

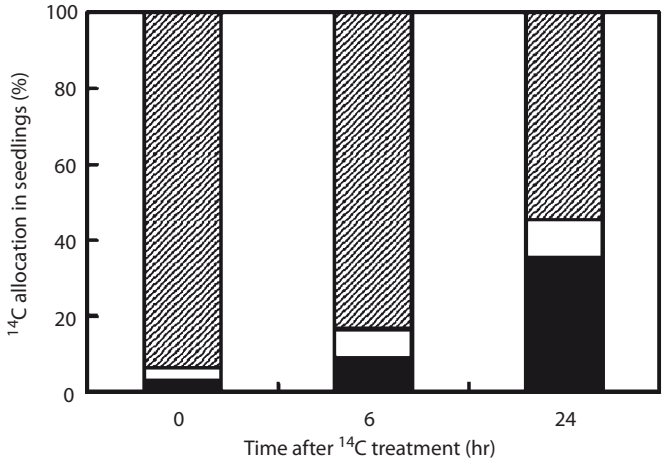

Fig. 21.1 Carbon allocation in hybrid larch (*Larix kaempferi* X *L. gmelinii*) infected with ectomycorrhiza (*Suillus grevillei*). The root means root plus ectomycorrhiza. (Modified from Qu et al. 2004)

(Rygiewicz and Andersen 1994; Tinker et al. 1994; Smith and Read 1997). Laboratory data with seedlings may overestimate C flux to ECM by not taking into account differences in root size or rates of root turnover between mycorrhizal and nonmycorrhizal plants (Durall et al. 1994; Tinker et al. 1994).

21.5 Ectomycorrhizae in Permafrost Soils, and after Forest Fires

Much of Siberian forests are on permafrost soils. Also, forest fire is strongly associated with tree regeneration as the main disturbance factor. How do these factors affect ECM? Although studies on ECM in Siberian forest ecosystems are limited, we summarize previous knowledge on the ecology of ECM in the permafrost soils and in postfire stands at different parts of Siberian boreal forests.

21.5.1 Ectomycorrhiza in Permafrost Soils

Upper layer of the permafrost soils, called "active layer," experiences annual freeze–thaw cycle (Chap. 4). Plants mainly develop their roots in this active layer and in the organic horizon in the Siberian permafrost soils (Kajimoto et al. 1999; see also Chap. 16). In addition to low temperature, ice segregation (or frost heave) in winter may act as a suppression factor (even as severe disturbance) for the ECM roots. However, the ECM appears to be abundant even under the extreme environment of the boreal forests in Siberia (Fig. 21.2). It is unclear how do the ECM roots survive and persist in such a severe condition.

Field studies on fine root dynamics typically find fresh ECM roots throughout winter in areas of regular soil freezing in *Abies amabilis* forest in the United States (Vogt et al. 1982) (average temperature in January is −3.2°). Also, Laiho and Mikola (1964) reported that many ECM species could survive the winter freeze in the nursery of central Finland (temperature in the end of October is −5°C). *Pisolithus tinctorius* mycelium was shown to survive subzero winter temperatures in the field at −7°C in the United States (Marx and Bryan 1975). It is observed that mycelium of *Thelephora terrestris* not only persist, but also continue to grow 0.7 mm day^{-1} in the roots of *Picea sitchensis* in a soil microcosm during winter in Scotland (when the soil temperature was −0.5°C) (Coutts and Nicoll 1990). On the other hand, *Laccaria proxima* is reported to disappear during autumn in a similar microcosm (Coutts and Nicoll 1990). Similarly, Tibbett et al. (2002) reported occurrence of some cold-intolerant ECM species (e.g., *Hebeloma* spp.).

From these results, it is suggested that there are freezing/cold-tolerant and intolerant ECM roots in the field. In Siberian forests, as the dominant larch is the ECM species, there should be cold/freeze-tolerant ECM communities. Under such conditions, ECM may develop a cold-tolerant metabolism. Such cold-tolerant ECM species

Fig. 21.2 The fruit bodies of ectomycorrhizal fungi in *Larix gmelinii* forest of the Tura Experimental Forest, Central Siberia (Photo: S. Mori)

may have enhanced the metabolism of the infected plants even in winter. For the function and persistence of ECM roots, some extracellular enzymes (phosphomonesterase) were reported to be released more by the ECM at low temperature of 2°C (Tibbet et al. 1998).

However, it is also observed that death of ECM roots is mainly due to soil movement with ground frost that broke the long roots (Laiho and Mikola 1964). This indicates that, in the active layer of the Siberian permafrost, frequent ice segregation and freeze–thaw cycle could damage the ECM root seriously. Furthermore, Iwahana et al. (2005) reported that, in the active layer of Northeastern Siberia, soil temperature reaches the minimum of −23°C, and continues to be at the sub-zero temperature for about seven months of the year. This temperature is much lower than that previously reported for the activity of ECM, and may severely influence it. Additional problem to apply results of the previous studies to Siberian situation is that most studies dealt with evergreen coniferous species. The main tree component

of Siberian forests is larch, a deciduous coniferous species. As these species cannot assimilate carbon in winter, seasonal patterns of carbon flux from the host to ECM would be different from those of evergreen conifers that grow in the milder climates. Such difference in host plant performance would affect metabolism of the ECM fungi in winter. Therefore, to understand ecology of ECM in Siberian forests, further studies are required focusing on the effects of (1) much lower soil temperature, (2) frequent freeze–thaw cycle, and (3) different seasonal C assimilation of host plant on ECM fungi.

21.5.2 Forest Fires and Ectomycorrhizae

As one of the main disturbance factors, forest fire plays an important role in establishment of boreal forests (e.g., Wardle et al. 1998; Kasischke and Stocks 2000). ECM is also reported to have an important role in seedling recruitment in burnt areas (e.g., Perry et al. 1989). Larch species mainly regenerate abundantly after forest fires in Siberia, and this species is known to develop symbiotic association with ECM. In Siberian forests, only few studies have examined ecology of ECM and its relationship to forest fire. At the same time, mushrooms are found abundantly in *Larix gmelinii* forests in Central Siberia. Even after intensive forest fires, rapid recovery of larch (*L. gmelinii*) populations is common (Zyryanova et al. 2001; Shi et al. 2002; see also Chaps. 5 and 19) with association of ECM (Mori and Quoreshi, unpubl. data). An example of ECM fungus (*Suillus grevillei*) in a postfire stand is shown in Fig. 21.2. Therefore, ECM communities may well be abundant in Siberian forests.

Generally, biomass and species richness of ECM fungi are reduced temporally by heat generated during burning (Tuininga and Dighton 2004; Martin-Pinto et al. 2006). However, they recover over time after fires (e.g., Palfner et al. 2005). During the recovery stage of ECM, there is succession within the fungal community. Dominance of specific ECM species is explained by tolerance to heat (Barr et al. 1999; Izzo et al. 2006) and characteristics of postfire soil conditions, e.g., high soil pH (Horikoshi 1986). Not only the soil pH, but also other soil properties (soil moisture, soil temperature, temporal nutrient supply as ash, and charcoal deposition) could be key factors for the dominance of specific ECM; however, relationships of these factors are still unclear (Makoto et al. in press).

Changes in fire regime are frequently reported in Russian forests in recent decades (e.g., Shvidenko and Nilsson 1996; Makoto et al. 2007). The changes include shifts in fire intensity and frequency that have been reported to result in altered effects on ECM biomass, host infection rate, and species richness (e.g., Cairney and Bastias 2007). Therefore, recent changes in fire behavior should result in changes of ECM communities in Russian boreal forests. The shift of fire intensity is also reported to affect physical and chemical properties of the soils. Prediction of the effects of fires on forest ecosystems require clarification of the relationships between various patterns of fire behavior and ECM performance.

21.6 Ectomycorrhizae and Elevated Atmosphere CO_2

Concentration of the atmospheric CO_2 has increased dramatically from 320 to 380 ppm during the last 50 years. The CO_2 concentration is increasing continually at 5% per year at present. Accordingly, many studies have been devoted to examination of the effects of elevated CO_2 concentration on plants. ECM depends on a host plant for its carbon acquisition. Therefore, any ambient CO_2 change affecting plants is likely to influence belowground processes, and increased carbon allocation to roots may affect ECM activity as well.

In return, ECM can influence carbon balance of the host plant via a number of processes, including net photosynthetic rate and mineral nutrition availability under the condition of elevated CO_2 concentration. These effects are due to improvements in nutrient relationship in plant body and sink activation, which could be the main factor in downregulation by the ECM under the elevated CO_2 environment. Choi et al. (2005) reported that ECM act to enhance net photosynthetic rate, water use efficiency, and P concentration of *Pinus densiflora*, *P. koraiensis,* and *L. kaempferi* seedlings at an elevated CO_2 condition. Particularly, the maximum photosynthetic rate and carboxylation efficiency of nonmycorrhizal seedlings grown at 72 Pa CO_2 (ca. 720 ppm) showed photosynthetic downregulation when compared with those grown at 36 Pa (ca. 360 ppm) CO_2. On the other hand, ECM seedlings showed no downregulation at the elevated CO_2 level.

The infection rate of ECM fungi on roots (percent root tips infected) has been pointed out to increase, no change, or decrease under high CO_2 concentrations (Diaz 1996; Hodge 1996; Staddon et al. 2002). Magnitude of responses due to ECM infection varies because of many factors including plant and fungal species composition. Lewis et al. (1994) presented that there were no significant effects of ECM infection on further ECM colonization, in spite of significant effects on root carbohydrate levels in *Pinus taeda* grown at elevated CO_2. However, hyphal length of ECM often increases under CO_2 enrichment, sometimes four- or fivefold from studies in greenhouse and in natural ecosystems (Treseder and Allen 2000). Kasai et al. (2000) suggest that EMF (ectomycorrhizal fungi) mass increased by CO_2 enrichment based on the ergosterol content analysis of fine roots. Increases in hyphal biomass and length under elevated CO_2 could imply greater nutrient uptake by plants, higher influx of C to ECM, alteration in C allocation among plant organs, and alteration of soil carbon storage due to decomposed C from ECM (Sanders et al. 1998; Rillig et al. 2002).

A question arises from these physiological considerations, if the boreal forest soil can store more carbon and so buffer the atmospheric CO_2 level in the world of increased CO_2 level. At present, there is growing interest in the effect of elevated CO_2 on ECM, which may be related to the "missing carbon sink" connected with the biotic belowground processes (Dyson 1992). Root mass consistently increased with elevated CO_2 condition (Bazzaz 1990). Larger mycorrhizal hyphae may act as extra sink of carbohydrate, and thus suppress or retard downregulation effects on photosynthesis (Lewis et al. 1994). It is predicted that total rhizodeposition of materials will increase.

Moreover, Gorissen (1996) showed that the roots cultivated at 700 ppm CO_2 were decomposed more slowly than those cultivated at 350 ppm CO_2. However, some studies found that differences in belowground C partitioning between mycorrhizal and nonmycorrhizal roots is greatly affected by fungal respiration (Rygiewicz and Andersen 1994; Colpaert et al. 1996; Ek 1997). Ek (1997) found that 43–64% of C allocated to mycelium was respired by external hyphae of ECM that is associated with birch. Rygiewicz and Andersen (1994) reported that total aboveground ^{14}C respiration by mycorrhizal seedlings was about 10% less than that by nonmycorrhizal seedlings, whereas belowground respiration of mycorrhizal seedlings was about 35% greater. The ectomycorrhiza reduced retention of C in the plant-fungus symbiosis by increasing C in roots and belowground respiration (Rygiewicz and Andersen 1994). In addition, greater total hyphal length in soil under the elevated CO_2 can influence a number of ecosystem characteristics, including physiochemical properties of the soil. In turn, these changes in soil quality can feed back to affect carbon flux, nutrient immobilization, and plant productivity (Rillig et al. 2002). It becomes urgent to investigate the effects of ectomycorrhiza on both sequestration and emission of carbon under the elevated atmospheric CO_2 condition in the future.

21.7 Conclusions

ECM is particularly important in the N-limiting biome of boreal forest ecosystems, since it could take up nutrients and water efficiently for its host plant. The important role of and further research on ECM necessary under changing environmental conditions are summarized as follows:

- Under the elevated CO_2 conditions, ECM would become a greater sink of photosynthates. Consequently, amount of carbon flow to soil might be increased. It is predicted that ECM might play an important role in carbon storage of boreal forests under the increased atmospheric CO_2 concentration.
- Along with increased atmospheric CO_2, the global warming is reported to influence forest fire regime, soil temperature, and melting of the permafrost soil. These multiple changes would intricately influence ECM activity in Siberian forests.
- More experiments and field studies on ECM ecology are urged to estimate the future role of ECM in Siberian forest ecosystems.

References

Abuzinadah RA, Read DJ (1989) The role of proteins in the nitrogen nutrition of ectomycorrhizal plants. IV. The utilization of peptides by birch (*Betula pendula* Roth.) infected with different mycorrhizal fungi. New Phytol 112:55–60

Allen MF (1991) The ecology of mycorrhiza. Cambridge University Press, Cambridge

Barr J, Horton TR, Kretzer AM, Bruns TD (1999) Mycorrhizal colonization of *Pinus muricata* from resistant propagules following a stand-replacing wildfire. New Phytol 143:409–418

Bazzaz FA (1990) The response of natural ecosystems to the rising global CO_2 levels. Ann Rev Ecol Syst 21:167–196

Cairney JWG, Bastias BA (2007) Influences of fire on forest soil fungal communities. Can J For Res 37:207–215

Chalot M, Brun A (1998) Physiology of organic nitrogen acquisition by ectomycorrhizal fungi and ectomycorrhizas. FEMS Microbial Rev 22:21–44

Choi DS, Kayama M, Chung DJ, Jin HO, Quoreshi AM, Maruyama Y, Koike T (2005) Mycorrhizal activities in *Pinus densiflora*, *P. koraiensis* and *Larix kaemferi* native to Korea raised under high CO_2 concentrations and water use efficiency. Phyton 45:139–144

Colpaert JV, Van Laere A, Van Assche JA (1996) Carbon and nitrogen allocation in ectomycorrhizal and non-mycorrhizal *Pinus sylvestris* L. seedlings. Tree Physiol 16:787–793

Coutts MP, Nicoll BC (1990) Growth and survival of shoots, roots and mycorrhizal mycelium in clonal Sitka spruce during the first growing season after planting. Can J For Res 20:861–868

Czimczik CI, Schmidt MWI, Schulze ED (2005) Effects of increasing fire frequency on black carbon and organic matter in podzols of Siberian Scots pine forests. Eur J Soi Sci 56:417–428

Diaz S (1996) Effects of elevated [CO_2] at the community-level mediated by root symbionts. Plant Soil 187:309–320

Duddridge JA, Malibari A, Read DJ (1980) Structure and function of mycorrhizal rhizomophs with special reference to their role in water transport. Nature 287:834–836

Durall DM, Jones MD, Tinker PB (1994) Allocation of C-14 carbon in ectomycorrhizal willow. New Phytol 128:109–114

Dyson F (1992) From Eros to Gaia. Pantheon Books, New York

Ek H (1997) The influence of nitrogen fertilization on the carbon economy of *Paxillus involutus* in ectomycorrhizal association with *Betula pendula*. New Phytol 135:133–142

Finlay RD (1993) Uptake and mycelial translocation of nutrients by ectomycorrhizal fungi. In: Read DJ, Lewis DH, Fitter AH, Alexander IJ (eds) Mycorrhiza in Ecosystems. Proceedings of the Third Eur Symp mycorrhizas. CAB International, Wallingford, pp 91–97

Finlay RD, Söderström B (1989) Mycorrhizal mycelia and their role in soil and plant communities. In: Clarholm M, Bergstrom L (eds) Ecology of arable land, perspectives and challenges, Development in plant and soil science, vol 39. Kluwer Academic Publishers, Dordrecht, pp 139–148

Fogel R, Hunt G (1983) Contribution of mycorrhiza and soil fungi to nutrient cycling in a Douglas-fir ecosystem. Can J For Res 13:219–232

Frank AB (1894) Die Bedeutung der Mycorrhizapilze für die gemeine Kiefer. Forstwissen Centralbl 16:1852–1890

Frey-Klett P, Garbaye J, Tarkka M (2007) The mycorrhiza helper bacteria revisited. New Phytol 176:22–36

Gorissen A (1996) Elevated CO_2 evokes quantitative and qualitative changes in carbon dynamics in a plant/soil system: mechanisms and implications. Plant Soil 187:289–298

Halldorsson G, Sverrisson H, Eyjolfsdottir GG, Oddsdottir ES (2000) Ectomycorrhizae reduce damage to Russian larch by Otiorhyncus larvae. Scand J For Res 15:354–358

Harley JL (1971) Fungi in ecosystems. J Appl Ecol 59:653–668

Hodge A (1996) Impacts of elevated CO_2 on mycorrhizal associations and implications for plant-growth. Biol Fertil Soils 23:388–398

Horikoshi T (1986) Mushroom in the burn out sites [YAKEATOKINOKO]. Hakkokogaku Kaishi 64: 225 (in Japanease)

Iwahana G, Machimura T, Kobayashi Y, Fedorov AN, Konstantinov PY, Fukuda M (2005) Influence of clear-cutting on thermal and hydrological regime in the active layer near Yakutsk, Eastern Siberia. J Geography Res 110:1–10

Izzo A, Canright M, Bruns TD (2006) The effects of heat treatments on ectomycorrrhizal resistant propagules and their ability to colonize bioassay seedlings. Mycol Res 110:196–202

Kajimoto T, Matsuura Y, Sofronov MA, Volokitina AV, Mori S, Osawa A, Abaimov AP (1999) Above- and belowground biomass and net primary productivity of a *Larix gmelinii* stand near Tura, central Siberia. Tree Physiol 19:815–822

Kasai K, Usami T, Lee J, Ishikawa S-H, Oikawa T (2000) Responses of ectomycorrhizal colonization and morphotype assemblage of *Quercus myrsinaefolia* seedlings to elevated air temperature and elevated atmospheric CO_2. Microbes Environ 15:197–207

Kasischke ES, Stocks BJ (eds) (2000) Fire, climate change, and carbon cycling in the boreal forest. Ecological Studies, vol 138. Springer, Berlin Heidelberg New York

Khasa PD, Sigler L, Chakravarty P, Dancik BP, Erickson L, Mc Curdy D (2001) Effects of fertilization on growth and ectomycorrhizal development of container-grown and bare-root nursery conifer seedlings. New For 22:179–197

Laiho O, Mikola P (1964) Studies on the effect of some eradicants on mycorrhizal development in forest nurseries. Acta For Fenn 77:1–34

Lambers H, Chapin FS III, Pons TL (1998) Plant physiological ecology. Springer, Berlin Heidelberg New York

Lamhamedi MS, Bernier PY, Fortin JA (1992) Hydraulic conductance and soil water potential at the soil root interface of *Pinus pinaster* seedlings inoculated with different dikaryons of *Pisolithus* sp. Tree Physiol 10:231–244

Lapeyrie F, Picatto C, Gerard J, Dexheimer J (1990) Tem study of intercellular and extracellular calcium-oxalate accumulation by ectomycorrhizal fungi in pure culture or in association with eucalyptus seedlings. Symbiosis 9:163–166

Leake JR, Read DJ (1997) Mycorrhizal fungi in terrestrial habitats. In: Wicklow DJ, Söderström B (eds) The Mycota IV. Environmental and microbial relationships. Springer, Berlin Heidelberg New York, pp 281–250

Lewis JD, Thomas RB, Strain BR (1994) Effects of elevated CO_2 on mycorrhizal colonization of loblolly pine (*Pinus taeda* L.) seedlings. Plant Soil 165:81–88

Lewis JD, Lucash M, Olszyk DM, Tingey DT (2004) Relationships between needle nitrogen concentration and photosynthetic responses of Dohglas-fir seedings to elevateal CO_2 and temperature. New Phytol 162:355–364

Li CY, Massicotte HB, Moore LVH (1992) Nitrogen-fixing *Bacillus* sp. associated with Douglas-fir tuberculate ectomycorrhizae. Plant Soil 140:35–40

Lindahl BD, Finlay RD, Cairney JWG (2005) Enzymatic activities of mycelia in mycorrhizal fungal communities. In: Dighton J, Oudemans P, White J (eds) The fungal community: its organization and role in the ecosystem. Marcel dekker, New York, pp 331–348

Makoto K, Nemilostiv YP, Zyryanova OA, Kajimoto T, Matsuura Y, Yoshida T, Satoh F, Sasa K, Koike T (2007) Regeneration after forest fires in mixed conifer broad-leaved forests of the Amur region of Far Eastern Russia: the relationship between species specific traits against fire and recent fire regimes. Eurasian J For Res 10:51–58

Makoto K, Kim YS, Tamai Y, Koike T (in press) Buried charcoal layer and ectomycorrhizae cooperatively promote the growth of Larix gmelinii seedlings. Plant and Soil DOI:10.1007/s11104-009-0040-z

Martin-Pinto P, Vaquerizo W, Penalver F, Olaizola J, Oria-de-Rueda JA (2006) Early effects of a wildfire on the diversity and production of fungal communities in Mediterranean vegetation types dominated by *Cistus ladanifer* and *Pinus pinaster* in Spain. For Ecol Manage 225:296–305

Marx DH, Bryan WC (1975) Growth and ectomycorrhizal development of loblolly pine seedlings in fumigated soil infested with fungal symbiont *Pisolithus tinctorius*. For Sci 21:245–254

Murata Y (1991) In vitro mycorrhizal synthesis on Japanese larch (*Larix leptolep sis* Gordon) seedlings and their growth. Bull Hokkaido Forest Res Inst 29:1–13

Näsholm T, Ekblad A, Nordin A, Giesler R, Högberg M, Högberg P (1998) Boreal forest plants take up organic nitrogen. Nature 392:914–916

Olsson PA, Wallander H (1998) Interactions between ectomycorrhizal fungi and the bacterial community in soils amended with various primary minerals. FEMS Microb Ecol 27:195–205

Palfner G, Casanova-Kathy MA, Read DJ (2005) The ectomycorrhizal community in a forest chronosequences of Sitka spruce [*Picea sitchensis* (Bong.) Carr.] in Northern England. Mycorrhiza 15:571–579

Perry DA, Margolis H, Choquette C, Molina R, Trappe JM (1989) Ectomycorrhizal mediation of competition between coniferous tree species. New Phytol 112:501–511

Qu LY, Shinano T, Quoreshi AM, Tamai Y, Osaki M, Koike T (2004) Allocation of ^{14}C-carbon in two species of larch seedlings infected with ectomycorrhizal fungi. Tree Physiol 24:1369–1376

Read DJ (1983) The biology of mycorrhiza in the Ericales. Can J Bot 61:985–1004

Read DJ (1991) Mycorrhizas in ecosystems. Experientia 47:376–391

Read DJ, Boyd R (1986) Water relations of mycorrhizal fungi and their host plants. In: Ayres P, Boddy L (eds) Water, fungi and plants. Cambridge University Press, Cambridge, pp 105–117

Read DJ, Perez-Moreno J (2003) Mycorrhizas and nutrient cycling in ecosystems – a journey towards relevance ? New Phytol 157:475–492

Read DJ, Leake JR, Perez-Moreno J (2004) Mycorrhizal fungi as drivers of ecosystem processes in heathland and boreal forest biomes. Can J Bot 82:1243–1263

Rennenberg H (1999) The significance of ectomycorrhizal fungi for sulfur nutriation of trees. Plant Soil 215:115–122

Rillig MC, Mummey DL (2006) Mycorrhizas and soil structure. New Phytol 171:41–53

Rillig MC, Treseder KK, Allen MF (2002) Global change and mycorrhizal fungi. In: Van der Heijden MGA, Sanders IR (eds) Mycorrhizal ecology. Springer, Berlin Heidelberg New York, pp 135–160

Rygiewicz PT, Andersen CP (1994) Mycorrhizae alter quality and quantity of carbon allocated below ground. Nature 369:58–60

Sanders IR, Steritwolf-Engel R, Van der Heijden MGA, Boller T, Wiemken A (1998) Increased allocation to external hyphae of arbuscular mycorrhizal fungi under CO_2 enrichment. Oecologia 117:496–503

Schulze E-D, Schulze W, Kelliher FM, Vygodskaya NN, Ziegler W, Kobak KI, Koch H, Arneth A, Kusnetsova WA, Sogatchev A, Issajev A, Bauer G, Hollinger DY (1995) Aboveground biomass and nitrogen nutrition in a chronosequence of pristine Dahurian *Larix* stands in eastern Siberia. Can J For Res 25:943–960

Shi F, Qu L, Wang W, Matsuura Y, Koike T, Sasa K (2002) Aboveground biomass and productivity of *Larix gmelinii* forests in northeast China. Eurasian J For Res 5:23–32

Shvidenko A, Nilsson S (1996) Expanding Forests but Declining Mature Coniferous Forests in Russia. IIASA Workingpaper WP 96-059

Smith SE, Read DJ (1997) Mycorrhizal Symbiosis, 2nd edn. Academic Press, London

Staddon PL, Heinemever A, Fitter AH (2002) Mycorrhizas and global environmental change: research at different scales. Plant Soil 244:256–261

Tamm TO (1991) Nitrogen in terrestrial systems. Springer, Berlin Heidelberg New York

Thormann MN (2006) The role of fungi in boreal peatlands. In: Wieder RK, Vitt DH (eds) Boreal peatland ecosystems. Ecological Studies, vol. 188, Springer, Berlin Heidelberg New York

Tibbet M, Sanders FE, Cainey JWG (1998) The effect of temperature and inorganic phosphorous supply on growth and acid phosphate production in arctic and temperate strains of ectomycorrhizal *Hebeloma* spp. in axenic culture. Mycol Res 102:129–135

Tibbett M, Sanders FE, Cairney JWG (2002) Low-temperature-induced changes in trehalose, mannitol and arabitol associated with enhanced tolerance to freezing in ectomycorrhizal basdiomycetes (*Hebeloma spp*.). Mycorrhiza 12:249–255

Tinker PB, Durall DM, Jones MD (1994) Carbon use efficiency in mycorrhizas: theory and sample calculations. New Phytol 128:115–122

Treseder KK, Allen MF (2000) Mycorrhizal fungi have a potential role in soil carbon storage under elevated CO_2 and nitrogen deposition. New Phytol 147:189–200

Tuininga AR, Dighton J (2004) Changes in ectomycorrhizal communities and nutrient availability following prescribed burns in two upland pine–oak forests in the New Jersey pine barrens. Can J For Res 34:1735–1765

Turnbull MH, Schmidt S, Erskine PD, Richards S, Stewart GB (1996) Root adaptation and nitrogen source acquisition in natural ecosystems. Tree Physiol 16:941–948

Van der Heijden MGA, Sanders IR (eds) (2002) Mycorrhizal Ecology. Springer, Berlin Heidelberg New York

Vogt KA, Grier CC, Meier CE, Edmonds RL (1982) Mycorrhiza role in net production and nutrient cycling in *Abies amabilis* ecosystems in western Washington. Ecology 63:370–380

Wardle DA, Zackrisson O, Nilson MC (1998) The charcoal effect in Boreal forests: mechanisms and ecological consequences. Oecologia 115:419–426

Watteau F, Berthelin J (1994) Microbial dissolution of iron and aluminum from soil minerals efficiency and specificity of hydroxamate siderophores compared to aliphatic acids. Eur J Soi Biol 30:1–9

Wielgolaski FE (2005) History and environment of the Nordic mountain birch. In: Wielgolaski FE (ed) Plant ecology, herbivory, and human impact in Nordic mountain birch forests. Ecological Studies, vol 180. Springer, Berlin Heidelberg New York

Zyryanova OA, Bugaenko TN, Buganenk NN, Koike T, Takenaka A (2001) Plant association diversity regeneration as related cryogenic microrelief and forest fires. In: Fukuda M, Kobayashi Y (eds) Proceedings of the Ninth Symposium on the Joint Siberian Permafrost Studies between Japan and Russia in 2000. Hokkaido University, Sapporo, pp 18–23

Chapter 22
From Vegetation Zones to Climatypes: Effects of Climate Warming on Siberian Ecosystems

N.M. Tchebakova, G.E. Rehfeldt, and E.I. Parfenova

22.1 Introduction

Evidence for global warming over the past 200 years is overwhelming, based on both direct weather observation and indirect physical and biological indicators such as retreating glaciers and snow/ice cover, increasing sea level, and longer growing seasons (IPCC 2001, 2007). On the background of global warming at a rate of 0.6°C during the twentieth century (IPCC 2001), the temperature increase in central Siberia is registered as large as 1–2°C on average for both in summer and winter in the high latitudes, and up to 2–5°C in winter alone in the south (Tchebakova and Parfenova 2006). Recent GCM projections of the Hadley Center (Gordon et al. 2000) for Central Siberia show an increase in temperature of 4–6°C in summer and 2–9°C in winter; an increase in precipitation is shown as much as 30% by 2090. In the south of Central Siberia, January temperature increases by 2000 have already exceeded those predicted by the Hadley Center scenario for 2090. July temperature increase rates for 2000 are of the same order of magnitude as predicted from scenarios 4–6°C for 100 years. Predicted change in rainfall is positive while registered change has been negative (Tchebakova et al. 2008). Predicted changes, moreover, could occur at a rate of 0.1–0.4°C per decade (Watson et al. 1996).

The rapid rate of change coupled with the large absolute amount of change is expected to have profound effects on plants of the boreal forests at all hierarchial levels: from forest zones (Tchebakova et al. 2003), to ecosystems (Guisan et al. 1995), to species (Iverson and Prasad 1998; Box et al. 1999), to populations within species (Rehfeldt et al. 1999b, 2002).

Our goals are to estimate effects of a warming climate on Siberian vegetation, at the highest level of organization, biomes, then at the intermediate level, species, and the lowest level, climatypes. The first considers the effects of global warming on zonal vegetation shifts, the second considers them on major Siberian tree species redistributions, and the third considers intraspecific effects across Siberia within both Siberian plains and the mountains in the south. We invoke Turesson's (1925) concept of climatypes, the climatic ecotypes that comprise species, and illustrate intraspecific effects for *Pinus sylvestris* and *Larix sibirica*.

A. Osawa et al. (eds.), *Permafrost Ecosystems: Siberian Larch Forests*,
Ecological studies, Vol. 209, DOI 10.1007/978-1-4020-9693-8_22,

22.2 Background

22.2.1 Study Area

Our studies deal with vegetation of Siberia and the forests in particular (within 60–140°E longitude and 50–75°N latitude), an area bounded by the Ural Mountains in the west, eastern Yakutia in the east, the Arctic ocean in the north, and the southern border of Russia in the south. The base map for this region was a 1 km (0.0083°) grid (GLOBE 1999).

22.2.2 Mapping Current and Future Climates

In this chapter, we use growing degree-days, above 5°C (GDD_5); negative degree-days, below 0°C (NDD_0); and an annual moisture index (AMI), the ratio of GDD_5 to mean annual precipitation. These three variables have proven to be instrumental for our previous analyses addressing plant responses to climate (Rehfeldt et al. 1999a, 2002; Tchebakova et al. 2003). From the physiologic viewpoint, GDD_5 represents temperature requirements for growth and development; NDD_0 defines cold tolerance, and AMI characterizes resistance to moisture stress. The present model does not take into account geographic variations of soils except for presence or absence of the continuous permafrost.

For mapping climates, we assembled temperature and precipitation records normalized for the period 1900–1964 from 1,063 weather stations with precipitation data and 812 weather stations with temperature data across Siberia (Reference books 1965–1970). Hutchinson's (2000) thin plate splines were used to produce climate surfaces of these variables on our base map at a resolution of 1 km. Climatic and topographic images were visualized using IDRISI32 (Eastman 2000). The AMI surface was calculated by dividing the GDD_5 image by the annual precipitation image.

For predictions of global warming, we used the greenhouse gas scenario (1% increase per year) from the Hadley Center, HadCM3GGa1 (Gordon et al. 2000), for the decade beginning in 2090. We chose this scenario as an extreme example of the vegetation changes that could take place in response to global warming: winter temperature increase of 3–9°C, summer temperature increase of 4–6°C, and annual precipitation changes between −4% and +25% over the study area. Future January and July temperatures and annual precipitation for each pixel were calculated by adding anomalies to the normalized monthly means (Reference books 1965–1970). Future values of climatic indices GDD_5 and NDD_0 were calculated using the following linear regressions calculated from contemporary data: GDD_5 was calculated from mean July temperature ($R^2 = 0.90$), and NDD_0 from January temperature ($R^2 = 0.96$). Future values of AMI were calculated directly by dividing the future GDD_5 image by the future annual precipitation image.

22.2.3 Permafrost

Permafrost covers 80% of Siberia and is the primary factor controlling the distribution of forests and their composition in Central Siberia and Yakutia (Pozdnyakov 1993). In the dry climate of Yakutia, forests are capable of developing in this region only because the melting of permafrost provides additional summer moisture to lands where otherwise the vegetation would be semidesert (Shumilova 1962). Permafrost also limits the northward and eastward spread of the dark-needled (*Picea obovata*, *Pinus sibirica*, *and Abies sibirica*) and also two light-needled (*L. sibirica* and *P. sylvestris)* species. Within the permafrost zone, spruce and pine can reach high latitudes on sandy soils along big river valleys and benches where permafrost may thaw deep enough (Shumilova 1962; Pozdnyakov 1993). Forests from both Siberian pine (*P. sibirica*) and fir (*A. sibirica*) are not found on continuous permafrost zone but found south of permafrost along discontinuous and island permafrost (Pozdnyakov 1993). Only *L. dahurica* (*L . gmelini* + *L. cajanderii*), by contrast, is capable of growing on shallow soils, which thaw as little as 10–30 cm during the growing season (Abaimov et al. 1999; see also Chap. 3).

Another factor limiting the tree species distribution in Siberia is forest fire. If even young dark-needled trees can emerge in some favorable habitats, frequent fire events in dry habitats fully eliminate their distribution (Polikarpov et al. 1998). Over the permafrost zone, only *L. dahurica* is adapted to fires, and successfully regenerates in burnt areas. Effects of forest fires on forest distribution were not modeled here.

In this study, we modeled permafrost influence on zones and tree species distribution. The current position of the active layer at the depth of 2 m across Siberia was predicted from the regression relating this layer from the map of Malevsky-Malevich et al. (2001) and our three climate variables ($R^2 = 0.70$). This regression is valid within the limits of contemporary climate. To map the permafrost border in the much warmer climate of 2090, we applied Stefan's theoretical formula (Dostavalov and Kudriavtsev 1967) predicting active layer changes from the ratio between GDD_5 in current and future climates.

22.2.4 Vegetation Zones

In our earlier study of global vegetation (Tchebakova et al. 1993), we applied the Budyko approach to predict the distribution of vegetation along two principal climatic variables, radiation balance and dryness index (a ratio of evapotranspiration to annual precipitation), which control vegetation zones (Budyko 1974). For the Siberian continental climate, low winter temperatures and permafrost are the crucial limiting factors controlling distribution of tree species distribution (Shumilova 1962). To account for these factors, the Siberian bioclimatic model of Tchebakova et al. (1994) was modified to predict vegetation zones (types) from the three bioclimatic parameters and permafrost (Tchebakova et al. 2003; Tchebakova and Parfenova 2006). Forest fire is not included in the model, because we consider only

climax vegetation depending on zonal climate. Fire controls forest successions within a climax vegetation type.

Major zonal (climax) vegetation types recognized by geobotanists on the plains of Central Siberia are as follows: (1) Tundra; (2) Forest-tundra; (3) Dark-needled (*Pinus sibirica, Picea obovata,* and *Abies sibirica*) taiga (subdivided into northern, middle, southern) on elevated tablelands; (4) Light-needled (*Larix sibirica* and *Larix gmelinii, Pinus sylvestris*) taiga (northern, middle, southern); (5) Birch (*Betula pendula* and *Betula pubescens*) and light-needled (*Larix sibirica* and *Pinus sylvestris*) subtaiga; (6) Birch (*Betula pendula* and *Betula pubescens*) and light-needled (*Larix sibirica* and *Pinus sylvestris*) forest-steppe; and (7) Steppe (Shumilova 1962; Nazimova 1995; see also Fig. 1.2 for a similar classification).

In our bioclimatic model (Table 22.1), the AMI separates vegetation into two large types, arboreal and nonarboreal (forests and steppes) and further subdivides the former type into dark-needled and light-needled forests by the AMI index. The cold parameter, NDD_0, equal to 3,500–4,000°C, also tends to separate dark-needled and light-needled tree species. And finally, the permafrost border limits dark-needled species from spreading eastward across Asia, although summers are sufficiently warm to allow survival as far east as Yakutia. The dark- and light-needled forest zones are further separated into latitudinal subzones (e.g. forest-tundra, northern, middle and southern taiga, forest-steppe) by GDD_5. Although temperate steppe, semidesert, broadleaf forest, and forest-steppe types are not found under current Siberian climate, these four classes are included in our model because of their potential importance under a warming climate. In total, therefore, our model considers 14 vegetation types, each of which can be defined climatically from the vegetation ordination in these three climatic variables (Table 22.1).

Table 22.1 Climatic limits for the modified Siberian vegetation model

	GDD_5		AMI		NDD_0	
Vegetation type	Lower limit	Upper limit	Lower limit	Upper limit	Lower limit	Upper limit
Tundra	None	<300	None	None	None	None
Forest-tundra and sparse taiga	300	500	None	None	None	None
Northern dark-needled taiga	500	800	None	<1.5	>−4,500	None
Northern dark-needled taiga	500	800	>1.5	None	None	<−4,500
Middle dark-needled taiga	800	1,050	None	<1.75	>−3,500	None
Middle light-needled taiga	800	1,050	>1.75	None	None	<−3,500
Southern dark-needled taiga and birch subtaiga	1,050	1,250	None	<2.25	None	None
Southern light-needled taiga and subtaiga	1,050	1,250	>2.25	None	None	None
Forest-steppe	1,250	1,650	None	<3.25	None	None
Steppe	1,250	1,650	>3.25	None	None	None
Semidesert/desert	>1,650	None	None	None	None	None
Broadleaf forest	1,250	1,650	None	<1.5	None	None
Temperate forest-steppe	>1,650	None	1.5	3.25	None	None

22.2.5 Major Forest-Forming Tree Species of Siberia

The forests across the vast territory of Siberia are composed largely of eight conifers (Pozdnyakov 1993): 49% *Larix spp.* of which 1% is *L. sukaczewi*, 13% is *L. sibirica*, and 83% is *L. gmelini* and *L. cajanderii*; and 3% of some far-eastern endemic larches; 13% *P. sylvestris*; 7% *Picea obovata*; 6% *Pinus sibirica*; 2% *Abies sibirica*; and 19% hardwoods and other species. The larches and the pine, therefore, are dominant tree species in the Siberian forests. These light-demanding species are commonly referenced in Russian literature as the light-needled conifers, which are opposed to the other three shade-tolerant conifers, spruce, cedar, and fir, which are referred to as the dark-needled species (Shumilova 1962). Siberian spruce dominates only in Western Siberia, both Siberian cedar and fir dominate on elevated tablelands (Yenisei Ridge) and in the southern mountains (the Altai-Sayan mountains). Only two tree species, *Larix gmelini* and *L. cajanderii*, dominate the forests in vast interior Siberia, the permafrost zone east of the Yenisei River. We consider results obtained from *L. gmelini* and *L. cajanderii* to be jointly applicable to their parental species, *L. daurica* (see Chap. 3).

22.2.6 Distributions of Pinus sylvestris and Larix Species

The contemporary potential and actual climate envelope of *P. sylvestris, L. sibirica, L. dahurica, and L. sukaczewii* and their climatypes was mapped using three variables: GDD_5, NDD_0, and AMI. Limits of distribution for these variables were approximated from the climatic extremes for provenances included in genecological studies established throughout the Soviet Union, limits of the breadth of transfer functions (see Rehfeldt et al. 2002), the relative climatic tolerances of species, and the climate estimated for extreme locations on range maps (Tchebakova et al. 2006).

Actual (realized) distributions are approximated by further reducing the climate envelopes according to the effects of habitat factors, permafrost, and interspecific competition among the species of *Larix*. The latter factors are recognized as the ecological factors most strongly influencing the distribution of the larches (Dylis 1981; Pozdnyakov 1993; Abaimov et al. 1998). Only *L. dahurica*, for instance, can survive on permafrost with depth of the soil active layer less than 1–2 m. As a result, *L. sibirica* and *L. dahurica* can dominate much of the Siberian forests, 50% of the forest areas in Central Siberia and 80% in Northeastern Siberia, respectively. In the warmer climates of Western Siberia, *L. sukaczewii* can be spread in the south and *L. sibirica* in the north with total 7% of the forest (Polikarpov et al. 1998).

Among larches, *L. sibirica* seems to be competitively superior to *L. daurica* (Polikarpov et al. 1986), outcompeting *L. daurica* on good sites. Yet, *L. sibirica* itself can be excluded from the warm and moist habitats in Trans-Urals by competition with *L. sukaczewii*, particularly on rich calcareous soils (Dylis 1981). And finally, both of these latter two larches displace *P. sylvestris* to poor sandy soils on

old alluvial terraces in Western Siberia or along the valleys of large Siberian rivers in the east (Pozdnyakov 1993).

To account for these ecological interactions, we reduced the size of the climatic envelope of the larches using geography of their distribution (Pozdnyakov 1993; Abaimov et al. 1998) according to the following algorithm: (1) the actual distribution of *L. dahurica* is limited by the climatic envelope on the cold fringe and by the permafrost border to the south and west; (2) the actual distribution of *L. sibirica* is determined by the permafrost border on the cold fringe and the climatic limits of *L. sukaczewii* on the warm fringe; (3) the actual distribution of *L. sukaczewii* is determined by its climatic envelope; and (4) the actual distribution of *Pinus sylvestris* is limited primarily by permafrost, although beyond the permafrost zone competition from *L. sibirica* and *L. sukaczewii* tends to relegate *P. sylvestris* only on sandy or boggy soils along wide river valleys.

22.2.7 Mapping Climatypes of Pinus sylvestris and Larix Species

Climatic envelopes were subdivided into climatypes by using the results of Rehfeldt et al. (2003). These results were based on common garden studies that had been established across the former Soviet Union. In such studies, seeds from numerous native populations are moved to and grown on an array of climatically disparate test sites. Because seeds are transferred along climatic gradients, such studies can also be viewed as climate-change experiments. Differential performance of populations then reflects adaptive differences that have accrued from natural selection in the climate of the provenance where the seeds originated. The results of such studies can be used to define a climatype as the climatic space occupied by a group of populations whose individuals are adapted to the same or similar climate.

The analyses of Rehfeldt et al. (2003) used published data across former Soviet Union within 46–86°N and 24–150°E on the height and survival of 313 populations of *P. sylvestris* that had been planted on 36 sites and of 130 populations of larch (63 of *L. sibirica,* 42 of *L. gmelinii*, and 25 of *L. sukaczewii*) planted on 8 sites. These data were used to develop transfer functions that predicted 12-year height from the difference in climate between the provenance of a population and the planting site. The functions were based on a Weibull model, which is Gaussian but can be asymmetric. For this study, three transfer functions driven by GDD_5, NDD_0, and AMI were developed. The transfer functions showed that height and survival decrease as the transferred distance either increased or decreased from an optimum value, which tended to be close to zero – the climate of the provenance. Confidence intervals about the vertex of the function were used to estimate the distance along climatic gradients that genotypes could be transferred without loss of growth potential or survival (Rehfeldt et al. 1999a). For *P. sylvestris,* these transfer distances were ±240 GDD_5, ±575 NDD_0, and ±0.6 units of AMI; for *L. sibirica* as ±325 GDD_5, ±1,150 NDD_0, and ±0.5 units of AMI; for *L. dahurica*, ±550 GDD_5, ±1,000 NDD_0, and ±1.2 units of AMI; and for *L. sukaczewii*, ±275 GDD_5, ±725 NDD_0, and ±1.0 units of AMI.

Table 22.2 Climatic limits, climatype breadth, and number of potential climatypes for the dominant conifers of Siberia for three climate indices (see Sect. 22.2.7)

Statistics		*Pinus sylvestris*	*Larix sibirica*	*Larix dahurica*	*Larix sukaczewii*
GDD_5 (°C)	Lower limit	600	650	400	800
	Upper limit	3,000	2,350	1,850	2,400
	Climatype breadth	480	650	1,100	550
	Number of classes	5	3	2	3
NDD_0 (°C)	Lower limit	−6,000	−4,500	−6,000	−2,200
	Upper limit	0	−1,200	−2,000	−300
	Climatype breadth	−1,150	−2,300	−2,000	−1,450
	Number of classes	6	2	2	2
AMI	Lower limit	0.6	0.8	0.9	1.0
	Upper limit	7.0	8.5	7.0	5.0
	Climatype breadth	1.2	1.0	2.4	2.0
	Number of classes	6	8	3	2
Total number of climatypes		180	48	12	12

It follows, therefore, that populations separated by the breadth of these transfer intervals tend to be genetically different for traits controlling growth and survival (Table 22.2). Climatypes are defined by subdividing the climatic envelope into classes bounded by these limits. For example, the 313 pine provenances used in these tests ranged from 626 to 2,916 GDD_5. Because the transfer functions suggested that the breadth of a climatype should be about 480 degree-days (240 × 2), 5 classes (2,290/480 = 4.77) are found. Six classes were needed for both NDD_0 and AMI. All possible combinations of these classes for three climatic indices produced an upper limit to the number of pine climatypes at 180. For the *L. sibirica*, there were 8 classes for the moisture index, 3 for GDD_5 and 2 for NDD_0, which produced a maximum of 48 climatypes; for *L. dahurica*, 3 for AMI, 2 for GDD_5, and 2 for NDD_0 for a total of 12; and for *L. sukaczewii*, 2 for AMI, 3 for GDD_5, and 2 for NDD_0 for a total of 12 (see Table 22.1). Tchebakova et al. (2003) summarized all possible climatypes for each species as combinations of growing degree-days above 5°C, negative degree-days below 0°C, and AMI.

Climatypes of the four species were mapped for all of Siberia using the climate maps of GDD_5, NDD_0, and AMI. Mapping was done for the contemporary climate and for the climate expected by the Hadley GCM for the decade beginning in 2090.

22.3 Effects of Global Warming on Vegetation Shifts

Changes in Siberian zonal vegetation were estimated by applying the Siberian vegetation model to the current climate and the climate change scenario for 2090, taking into consideration predicted changes in the distribution of permafrost (Table 22.3, Fig. 22.1).

In the contemporary climate of Siberia, taiga prevails on 65% of the area, 75% of which consists of light-needled taiga with *Larix sibirica* and *L. dahurica* being

Table 22.3 Vegetation change (%) in Siberia in a warmed climate

Vegetation zone[a]	Area (10^4 km^2) current	Proportion (%)	Area (10^4 km^2) 2090	Change (%)
Tundra	110.8	9.3	7.5	−93
Forest-tundra	91.3	7.7	12.2	−87
Northern dark taiga	1.9	0.2	10.9	+5-fold
Light northern taiga	191.1	16.1	48.6	−75
Dark middle taiga	52.7	4.4	10.2	−81
Light middle taiga	237.0	19.9	66.2	−72
Dark southern taiga	108.3	9.1	127.3	+18
Light southern taiga and subtaiga	98.6	8.3	87.0	−12
Forest-steppe	62.6	5.3	328.1	+5-fold
Steppe	139.2	11.7	176.5	+27
Drysteppe, semidesert	11.7	1.0	78.9	+7-fold
Temperate				
Broadleaved forest	0.03	0.0	2.4	–
Temperate forest-steppe	–	–	28.5	–
Temperate steppe	–	–	216.2	–

[a]No bare lands included

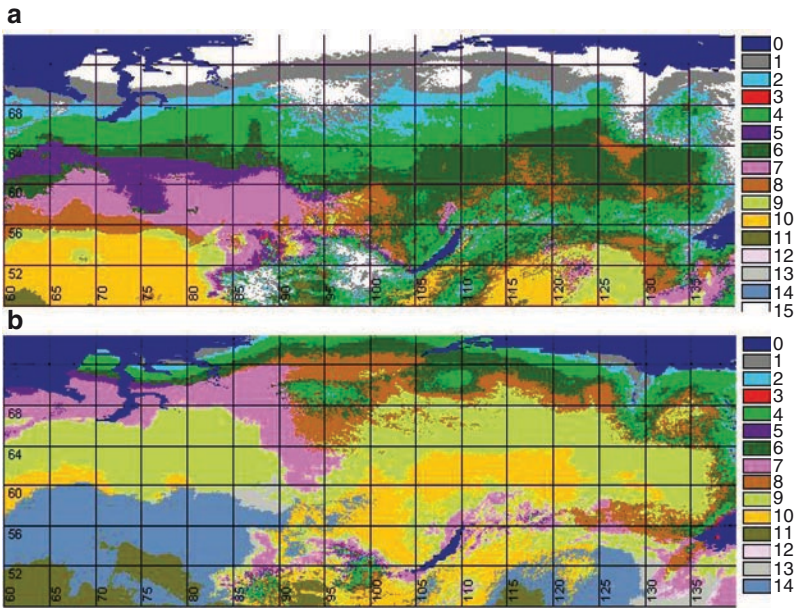

Fig. 22.1 Vegetation distribution in Siberia for the contemporary climate (**a**) and for the climate projected for the decade beginning in 2090 (**b**) (Soja et al. 2007). Numerals indicate the following: Water (0), tundra (1), forest-tundra (2), northern dark (3) and light (4) taiga, middle dark (5) and light (6) taiga, southern dark (7) and light (8) taiga, forest-steppe (9), steppe (10), dry steppe (11), broadleaved (12), temperate forest-steppe (13), and temperate steppe (14) *See* Color Plates

the domimant species. *Pinus sylvestris* can also dominate these forests in the warmer climates of the south or on sandy soils in middle and even northern taiga. Dark-needled taiga (25%) appears in moist and warm climates, such as in the West Siberian Plain, which is west of the Yenisei River, yet along the Yenisei Ridge at the mid-latitudes and in the Mountainous Southern Siberia. At the high latitudes of Putorana Mountains (north of the Artic Circle), only larch taiga can withstand the cold climate and permafrost. *Picea obovata* and *Pinus sibirica* may be mixed with *Larix* in the large river valleys, which tend to be warmer than the surrounding landscape. No grasslands occur north of 56°N (Fig. 22.1a). Nonarboreal types, tundra, and forest-tundra in the north and steppes and forest-steppes in the south, each cover about 17% of the area.

Fire and the melting of permafrost are considered to be the principal mechanisms that will shape new vegetation physiognomies (Polikarpov et al. 1998). In a warmed climate of 2090, taiga is predicted to shrink to half of the present area (Table 22.3, Fig. 22.1b). The southern treeline is being shaped by the forest fire, which rapidly promotes equilibrium between the vegetation and the climate. Tree decline in the southern taiga border in a dryer climate would facilitate the accumulation of woody debris. This accumulation, paired with increased weather suitable for fire, would result in a decreased fire return interval and an increased potential for severe and large fires. Predicted global warming will not be sufficient to melt permafrost deep enough to support dark-needled species in most of Siberia. Still, larch forests would dominate about 60% of Siberian taiga east of the Yenisei River, in Evenkia and in Yakutia. Forest-tundra and tundra should occupy only up to 1.5%. Although forest-steppe, steppe, and semidesert cover about 20% of the area in current climate of Siberia, these vegetation types would occupy more than 60% in the climate of 2090. In fact, large areas of steppe should cover the central Yakutian Plain and the Tungus Plateau, located more than 1,000 km north of the current steppe distribution.

Our Siberian vegetation model also shows that temperate vegetation types such as broadleaved forest, forest-steppe, and steppe climatic limits, which were derived from the global vegetation model (Tchebakova et al. 1993), currently do not exist in Siberia, although they should occur there in a warmed climate. The climate-change scenario we are using predicts the concomitant invasion of temperate broadleaved species such as linden into Western Siberia, which seems reasonable for a warmer climate. This is supported by Khotinsky (1977) who reconstructed mid-Holocene vegetation from pollen depositions and concluded that birch and other broad-leaved forests once were distributed east of the Ural Mountains as far as 70°E and 57°N into the West Siberian Plain.

22.4 Effects of Global Warming on Species Distributions

During the course of the century, the warming climate should become increasingly more suitable for *P. sylvestris*, *L. sibirica*, and *L. sukaczewii* but less favorable for *L. dahurica.* For the *Larix* genera as a whole, however, the climate of the future should

become only slightly more favorable than that of today. Figure 22.2 and Table 22.4 contain estimates of the climatic envelope and the actual distribution of these four conifers for contemporary climate and that expected for the decade beginning in 2090, according to the HadCM3GGa1 scenario of the Hadley Center.

The contemporary climatic envelope of *P. sylvestris* extends across approximately 68% of the area in Siberia, but a more realistic estimate of the actual distribution is only 38% (Table 22.4) because nearly half of the species distribution in Siberia includes sites within the permafrost zone where the species is rare (Fig. 22.2). By 2090, however, both the climatic envelope and the climate associated with the actual distribution should increase 1.5–2 times (Table 22.4), largely because of the melting of permafrost. An increase in area primarily would involve migration out of the valleys in Northeastern Siberia onto the plains and tablelands where it cannot exist today. Since these sites are included within the boundaries of the range map, the geographic extent of actual distribution we predict for the future is seen to be quite similar to the range map of today (Fig. 22.2). Because the future climate of this region is projected to be dry, competition with the dark-needled species should not be a factor because the dark-needled species do not occur under xeric conditions (Polikarpov et al. 1986). Yet, competition with *L. sibirica* should intensify, and this competition may limit the pine to the impoverished sandy soils. Our models also show that in the central part of Mountainous Southern Siberia, the climate suitable for *P. sylvestris* should move upwards in altitude by about 1,000 m by the last decade of the twenty-first century (Rehfeldt et al. 2004).

For *Larix*, all but the northernmost regions lie within the combined climatic envelopes of *L. sukaczwei*, *L. sibirica*, and *L. dahurica* in the contemporary climate (Table 22.4, Fig. 22.2). Estimates of the actual distributions suggest, in fact, that in total, 71% of Siberia is inhabitable by these species. As the climate warms, this estimate is expected to increase by only 4% by 2090. As was suggested in Fig. 22.2, the climate of the future in the southwest where *L. sukaczewii* now occurs should pass beyond the contemporary climatic envelope of all these species. This loss of habitat should be more than balanced by an increase in suitable lands to the north and northeast as the climate ameliorates. Nonetheless, the effects of global warming on the individual species of *Larix* are expected to differ greatly. Estimates of the

Table 22.4 Proportions of Siberia of conifer species (%, predicted actual distribution in parentheses) in the current climate and the climate projected by a GCM of the Hadley Center (HadCM3GGal) for the decade beginning in 2090 (Tchebakova et al. 2006)

	Area (% of total)	
Tree species	Contemporary climate	Future climate
Pinus sylvestris	68 (38)	87 (62)
Larix sibirica	58 (26)	71 (28)
Larix dahurica	60 (33)	38 (24)
Larix sukaczewii	12 (12)	26 (23)

Note that the first numerals in each cell include areas overlapping with distribution of other species, and do not add up to 100%

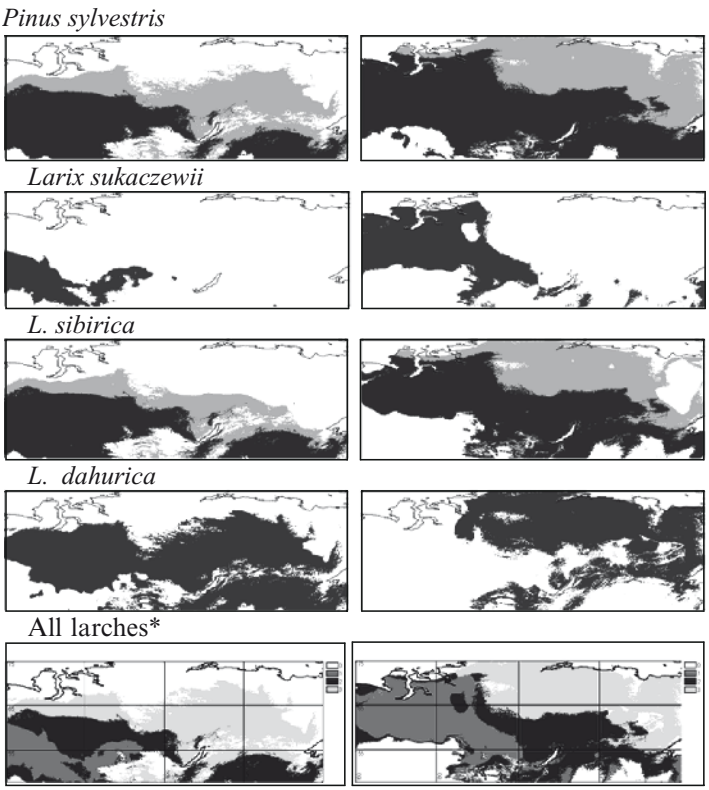

Fig. 22.2 Potential distributions of *P. sylvestris* and *Larix spp* modeled for the contemporary climate (*left*), and for the climate projected for the decade beginning in 2090 (*right*). *Gray* is part of the potential distribution of *L. sibirica* and *Pinus sylvestris* over the permafrost zone. *L. sukaczewii* occurs beyond the permafrost zone and *L. dahurica* occurs only on permafrost. (Asterisk) Actual distributions of *L. spp* depend on the effects of permafrost and interspecific competition among the larches (Tchebakova et al. 2006; shades of *gray*): *dark* – *L. sibirica*, *medium* – *L. sukaczewii*, *light* – *L. dahurica*

contemporary and future actual distributions suggest that lands climatically suitable for *L. sukaczewii* should increase by about 11%, those suited for *L. sibirica* should increase by a mere 2%, and those for which *L. dahurica* is suited should decrease by about 9% (Table 22.4, Fig. 22.2).

Unlike the projected future distribution of *P. sylvestris*, the future range limits of these three species of larch should be displaced considerable distances toward the east and northeast when future distributions approach an equilibrium with the novel climate (Fig. 22.2). Rough estimates from this figure suggest that the climate associated with the contemporary limits of distribution of *L. sukaczewii* and *L. sibirica* may be found as distant as 10° in latitude (about 700 km) toward the north by 2090. Estimates for *L. dahurica* are smaller because northward migration will halt at the Arctic Ocean.

22.5 Effects of Global Warming on Number, Size, and Distribution of Climatypes

Because climatypes are composed of genotypes physiologically attuned to climate, a change in climate will disrupt the relationship between the geographic distribution of plants and the distribution of their climatic optima. In assessing the effects of these changes, we assume that the vegetation of the future will move toward and eventually achieve the levels of adaptedness that typify the vegetation of today.

22.5.1 Pinus sylvestris

Of the 180 possible climatypes in the climatic envelope of *P. sylvestris,* most are small; only ten account for 55% of the species' climatic envelope and 63 comprise the species tri-variate envelope in Siberia (Table 22.5). As the climate of the future becomes more favorable to *P. sylvestris*, the number of climatypes suited to the future climate should increase to 101 by the end of the current century (Table 22.5). During this period, 15 of the contemporary climatypes should be lost, as the climate for which they are best suited dissipates. These 15, however, tend to be small, accounting for only 2% of the lands within the climatic envelope of today.

Meanwhile, 53 novel climatypes should appear in association with the appearance of climates currently not found in Siberia. While novel to Siberia, these climatypes undoubtedly exist today west of the Ural Mountains in Eastern Europe. These novel climatypes should make an important contribution to the future flora, accounting for approximately 36% of the species climatic envelope by the end of the century.

Of the 101 climatypes expected for the future, only one-half exist there today (Table 22.5). Nonetheless, like today's distribution of climatypes, those of the future should be dominated by a few large climatypes, the largest 10 of which should be suited to about 74% of the species climatic envelope.

Table 22.5 Effects of global warming on the number of climatypes in four Siberian species (Tchebakova et al. 2006)

Number of climatypes	*Pinus sylvestris*	*Larix sibirica*	*Larix dahurica*	*Larix sukaczewii*
Total possible	180	48	12	12
Contemporary climate	63	31	12	5
Future climate	101	42	12	10
Lost by 2090	15	3	0	0
Novel by 2090	53	14	0	5
Unchanged	48	28	12	5

While the number of climatypes suited to the future climate is increasing, the size and geographic position of the climatypes would also be changing. The five climatypes that currently dominate the pine forests of Siberia are expected to be reduced to approximately one-third of their contemporary distributions (Fig. 22.3). Of the five largest climatypes expected for the future, one is absent today and three are minor (<1%). Still, 48 climatypes that should exist in Siberia throughout the century should be suitable for about 63% of the future distribution. As shown in Fig. 22.3, however, the future location of climates inhabited by contemporary climatypes is expected to shift geographically. The shift, in fact, may amount to 500–1,000 km.

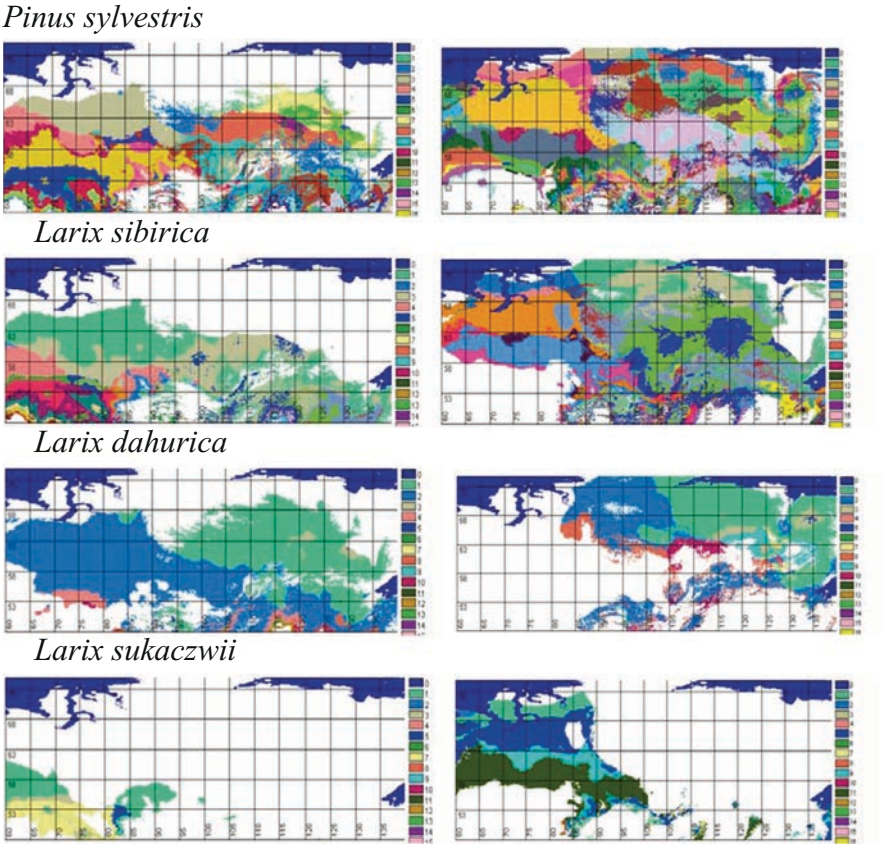

Fig. 22.3 Distributions of climatypes in Siberia for *Pinus sylvestris* and Siberian Larches (*Larix sibirica*, *L. dahurica,* and *L. sukaczewii*) in the contemporary climate (**a**) and in decade beginning in 2090 (**b**). For each species, one color corresponds to a single climatype of 180 possible climatypes for *Pinus sylvestris,* 48 for *Larix sibirica*, 12 for *L. dahurica*, and 12 for *L. sukaczewii* (see Table 22.5, Tchebakova et al. 2003) *See* Color Plates

22.5.2 *Larix sibirica*

Of the 48 possible climatypes, 31 comprise the species' contemporary climatic envelope in Siberia (Table 22.5). As with *P. sylvestris*, the contemporary envelope of *L. sibirica* is dominated by a small number of large climatypes. Five, in fact, account for 73% of the species' climatic distribution. Projected effects of global warming show that the proportion of Siberia climatically suitable for this species should increase slightly (Table 22.4) while their distribution should advance toward the east and north. As a result, the number of climatypes expected by the end of the century should increase from 31 to 42 (Table 22.5). Three minor climatypes (<0.5% of the area) are expected to disappear while 28 climatypes not presently in Siberia should appear. Twenty-eight climatypes should exist throughout the century, and these 28 should account for 73% of the future climatic envelope. However, the two huge climatypes of today should be reduced to one-fourth of their contemporary size, while the dominant climatype of the future currently comprises only 4% of the contemporary climatic envelope (Fig. 22.3).

22.5.3 *Larix dahurica*

Of the four species being considered, *L. dahurica* occurs in the coldest climates and is the only species endemic to permafrost; the cold fringe of its distribution thus borders the tundra. This means that the potential for migration to the northeast during global warming is limited ultimately by the presence of the Arctic Ocean. The most prominent effect of global warming, therefore, should be a reduction of the species climatic envelope to approximately 2/3 of its contemporary distribution by the end of the century (Table 22.4). As the envelope shrinks, however, the number of climatypes that comprise it should remain constant at 12, with neither new climatypes arising nor contemporary climatypes lost (Table 22.5). The two most important climatypes of today, which currently occupy 91% of the species climatic envelope, also are expected to be dominant at the end of the century but by then should occupy only 68%. As shown in Fig. 22.3 for one of the two, the future areal extent of these two climatypes should be reduced by about 50% while their geographic position shifts to the northeast.

22.5.4 *Larix sukaczewii*

Because projected effects of global warming on *L. sukaczewii* are similar to those on *L. sibirica*, anticipated effects on the number and distribution of climatypes are also similar. Because of an increase in the climatic envelope from 12% of Siberia to 26% (Table 22.4), the number of climatypes is expected to increase from 5 to 10

(Table 22.5). During the course of the century, the two climatypes that dominate the species envelope today (>89%) are expected to become insignificant by the end of the century (<13.5%). Meanwhile, the climate at the end of the century should become optimal for a single climatype, which is expected to account for 41% of the future climatic envelope. This climatype does not occur in Siberia today. Likewise, during the course of the century, four other novel climatypes should arise even though no contemporary climatypes are expected to be lost. The novel climatypes quite likely exist today west of the Ural Mountains.

22.6 Synthesis

It is well known that the distribution of forest trees is either directly or indirectly related to climate. It is also well known that genetic variability within species of forest trees is arranged along clines that parallel climatic gradients. It follows, therefore, that a change in climate will have prominent inter- and intra-specific effects across the landscape. In this paper, we estimate the future distribution of the climates in which the vegetation exists today. Potential biological impacts are qualified by use of the word "should."

Our analyses describe these effects for four of the dominant species of Siberia. The results show that if the vegetation of the future is to maintain the adaptedness characteristic of today's vegetation, species distributions will shift toward the north and east, regulated largely by the melting of permafrost. Maintaining adaptedness intraspecifically will require a concomitant redistribution of genetic variability across the landscape such that genotypes become realigned with their climatic optima.

Our analyses suggest that by the end of this century, the climate of Siberia should be more amenable for *P. sylvestris*, *L. sibirica,* and *L. sukaczewii* than it is today, but less suited for *L. dahurica*. As the melting of permafrost allows, *P. sylvestris* should migrate out of the broad valleys of northwest Siberia onto the plains and tablelands. The altitudinal displacement within the Mountainous Southern Siberia should approach 1,000 m. For *Larix*, the distribution of *L. dahurica* should shift toward the north and east, regulated by rates of permafrost thaw on the cold fringe and competitive exclusiveness of *L. sibirica* immigrants on the warm fringe. In the milder climates to the west, *L. sukaczewii* should advance into regions now occupied by *L. sibirica* but should be excluded from the advancing steppe on the southern front.

While the distributions of these species shift, the distribution of climatypes within species is expected to become reorganized so that optimal forest growth and productivity are to be maintained (Rehfeldt et al. 2001). The prominent climatypes of today should either be absent from or minor in the future forests. Likewise, the most prominent climatypes of the future seem to be either absent or minor in Siberia today. Even those climatypes that should remain on the landscape throughout the century are expected to change in position and importance. To be sure,

global warming as predicted by the Hadley GCM (HadCM3GGa1) should have widespread effects on the distribution of climatypes within these species.

Figure 22.3 illustrates the scope of the intraspecific effects expected from global warming. To be sure, the geographic position of the climates inhabited by contemporary climatypes may shift more than 1,000 km. As another indication of this scope, it is also instructive to assess the contemporary location of the climatypes expected to be of future importance in Siberia. Of the three *P. sylvestris* climatypes expected to dominate future forests, one, No. 40, is a minor component of the contemporary array. Nevertheless, this climatype is much more prevalent today toward the southwest in the foothills of the Altai Mountains, nearly 700 km away (Rehfeldt et al. 2004). Climatypes No. 82 and No. 88, which will be new to the Sayan Mountains, are currently present as isolated populations in Kazakhstan and Bashkiria, about 1,500 km and 20° of longitude to the west (Rehfeldt et al. 2004). And, for *L. sibirica,* climatype No. 20, which is to be of future importance, is present today in the Altai Republic. However, the climatic conditions with which this climatype is associated, can also be found west of the Ural Mountains in European Russia (Rehfeldt et al. 2004). Because the dominant larch west of the Ural Mountains is *L. sukaczewii,* it is possible that the future climates of Siberia may be suited to a mixture of larch species and their hybrids (see Abaimov et al. 1998; Chap. 3). Nevertheless, it is clear that the genotypes expected to be of importance to the future vegetation currently reside at long distances from their future habitat (Fig. 22.3). These distances further illustrate the magnitude and complexity of the intraspecific adjustments necessary for the forest vegetation of the future to become physiologically attuned to the novel climate.

These results are essentially the same as those obtained for *Pinus contorta* (Rehfeldt et al. 1999b) and *Picea engelmannii* (Rehfeldt et al. 2004) of western North America. The conclusion seems inescapable that global warming will initiate a redistribution of genetic variability within most species (Rehfeldt et al. 2004) such that in time genotypes also become redistributed. Response to climate-change, therefore, is much more than a shifting of species distributions (Davis and Shaw 2001; Davis et al. 2005). Indeed, effects of a changing climate reverberate throughout a species distribution as genetic variability becomes reshuffled across the landscape (Rehfeldt et al. 1999b, 2002).

The evolutionary processes by which these inter- and intraspecific changes will occur are well known (see Futyama 1979; Davis et al. 2005). While migration is the only feasible means by which immigration can take place, natural selection and gene flow are the processes most amenable to the restoration of population adaptedness (for discussion, see Rehfeldt et al. 1999b, 2001, 2003; Davis et al. 2005). One must be aware that genotypes physiologically attuned to a climatic regime are subject to selection and recombination during migration. Genotypes of sessile forest trees quite simply cannot track their climatic optima during times of change. There is no question, therefore, whether the vegetation is capable of adjusting to the predicted changes. However, evolutionary processes by which these adjustments will occur to accommodate the changes needed for Siberian forests require periods of time that far exceed the rates that the climate is expected to change.

At the interspecific level, migration of forest species in Siberia is largely dependent on rates of thawing of permafrost. These rates are much slower than the projected rates of climate change (Izrael et al. 2002), and as a result, a migration lag (Davis 1989) can be anticipated. One must also realize that migration through a closed forest canopy cannot commence until the physiological plasticity of the existing forest has been exhausted and the resulting forest demise creates the openings required for reproduction (Rehfeldt et al. 2001). Therefore, the fact that forest sites are currently occupied should exasperate the lag between the change in climate and the appropriate vegetation response. Thus, even the modern synthesis of plant migration, which proposes migration rates of as much as 1 km per year instead of a few meters per year (Clark et al. 1998; Higgins et al. 2003), is insufficient to account for the rates that must occur if the vegetation is to closely track the climate as it changes across Siberia.

At the intraspecific level, responses to selection can be rapid, but there are limits to the amount that genetic systems can change in a single generation of selection. Estimates for *P. contorta* (Rehfeldt et al. 2001) and *P. sylvestris* (Rehfeldt et al. 2002) suggest that 5–10 generations may be required for the evolutionary process to adjust to global warming. This process, therefore, may take several centuries even where species' distributions are not changing (see Rehfeldt et al. 2002).

These analyses on disparate species thus demonstrate the far-reaching effects of a changing climate on the ecological distribution and genetic composition of future forests. Forest zones and species boundaries are expected to change at the same time that genotypes within species will be redistributed. Because analogs to the future forests of Siberia exist contemporarily, one can confidently assume that the vegetation doubtlessly is capable of adjusting to the predicted changes. Current estimates, however, suggest that redistribution of forest zones, tree species, and their climatypes will require long periods to adjust to the amount of change being predicted. From the ecological perspective, therefore, it is the speed of warming rather than the absolute amount of warming that is most foreboding.

We believe that mitigating the effects of global warming will require a proactive stance by forest managers. Mankind must participate in the evolutionary processes to lessen the lag between the timing of the change and the appropriate response of the vegetation. Forest management as viewed by Noss (2001) during a changing climate will suffice only to the point where the amount of change exceeds plastic physiological systems to adjust. Because there is little doubt that the amount of change predicted for the world's temperate and boreal forests will exceed the plasticity of contemporary forests and cause widespread mortality in existing populations (see Rehfeldt et al. 1999b, 2002, 2003), managers will need to assist the natural processes to maintain the goods and services demanded of today's forests.

From the practical viewpoint, therefore, it seems obvious that maintaining optimal levels of productivity for Siberian forests will require the participation of mankind in the evolutionary processes to assist migration such that the appropriate species and their proper genotypes track their climatic optima in a timely manner. Assistance would take the form of massive planting programs to transfer seeds from their contemporary location to the future site of their climatic optima (see Rehfeldt

et al. 2004; St Clair and Howe 2007). Maps such as Fig. 22.3 can serve as blueprints for guiding the long-distant transport of seeds from their contemporary location to the novel location of their climatic optima for selected periods (e.g. 2020) during the coming decade.

22.7 Conclusions

Impacts of global warming on the Siberian vegetation will be pronounced if GCM scenarios are allowed to reach their 2090 projections. Effects should shift vegetation zones, alter species distributions, and produce populations within species that no longer are physiologically attuned to their environment.

Shifts in zonal vegetation could result in a taiga that is only one-half of the current area while steppe and semidesert vegetation should proliferate, increasing in area from about 20% of the total to 60%. The future climate may also be suited to temperate broadleaved species, which do not inhabit Siberia today. Fire and the melting of permafrost are viewed as the principal mechanisms promoting establishment of new vegetation and, therefore, the shifting vegetation zones.

The shifts in zonal vegetation will result from migration of species as they attempt to track their climatic optima. The 2090 climate of Siberia should be increasingly more suitable for *P. sylvestris*, *L. sibirica*, and *L. sukaczewii* but less favorable for *L. dahurica.* Suitability of the future habitat, however, will depend as much on permafrost melting, a process that lags behind the change in climate.

Genetic structure of species will be disrupted, as the changing climate becomes less and less suited to extant populations. The area suitable for the climatypes of today should undergo tremendous change as minor climatypes of today become important for the future. The future location of climates optimal for the climatypes of today is projected to recur at distances measured in hundreds of kilometers from their contemporary location.

Extent of the projected impacts is so profound that maintaining a semblance of equilibrium between plant distributions and climate will require humans to assist in plant migration.

Acknowledgment The study was partially supported by grant No. 06-05-65127 of the Russian Foundation for Basic Research.

References

Abaimov AP, Lesinski JA, Martinsson O, Milyutin LI (1998) Variability and ecology of Siberian larch species. Swedish University of Agricultural Sciences, Department of Silviculture, Reports 43, Umeå, 118pp

Abaimov AP, Prokushkin SG, Matsuura Y, Osawa A, Takenaka A, Kajimoto T (1999) Wildfire and cutting effect on larch ecosystem permafrost dynamics in central Siberia. In: Shibuya M,

Takahashi K, Inoue G (eds) Proceedings of the seventh symposium on the Joint Siberian Permafrost Studies between Japan and Russia in 1998. Tsukuba, Japan, pp 48–58
Box EO, Crumpacker DW, Hardin P (1999) Predicted effects of climatic change on distribution of ecologically important native tree and shrub species in Florida. Clim Change 41:213–248
Budyko MI (1974) Climate and life. Academic Press, New York 508pp
Clark JS, Fastie C, Hurtt G, Jackson ST, Johnson C, King GA, Lewis M, Lynch J, Pacala S, Prentice C, Schupp EW, Webb T, Wyckoff P (1998) Reid's paradox of rapid plant migration - dispersal theory and interpretation of paleoecological records. Bioscience 48:13–24
Davis MB (1989) Lags in vegetation response to greenhouse warming. Clim Change 15:75–82
Davis MB, Shaw RG (2001) Range shifts and adaptive responses to quaternary climate change. Science 292:673–679
Davis MB, Shaw RG, Etterson JR (2005) Evolutionary responses to changing climate. Ecology 86:1704–1714
Dostavalov BN, Kudriavtsev VA (1967) Basic permafrost science. Moscow University Press, Moscow, 404pp (in Russian)
Dylis NV (1981) Larch. Forestry Industry Press, Moscow, 97pp (in Russian)
Eastman JR (2000) IDRISI32 reference guide. Clark Labs, Worchester
Futyama DJ (1979) Evolutionary biology. Sinauer Associates, Sunderland
GLOBE Task Team: Hastings DA, Dunbar PK, Elphingstone GM, Bootz M, Murakami H, Maruyama H, Masaharu H, Holland P, Payne J, Bryant NA, Logan TL, Muller J-P, Schreier G, MacDonald JS (eds) (1999) The Global land one-kilometer base elevation (GLOBE) digital elevation model, Version 1.0. National Oceanic and Atmospheric Administration, National Geophysical Data Center, Boulder, Colorado. Digital data base on the World Wide Web (URL: http://www.ngdc.noaa.gov/seg/topo/globe.shtml)
Gordon C, Cooper C, Senior C (2000) The simulation of SST, sea-ice extents and ocean heat transport in a version of the Hadley Centre coupled model without flux adjustments. Clim Dyn 16:147–168
Guisan A, Holten JI, Spichiger R, Tessier L (eds) (1995) Potential ecological impacts of climate change in the Alps and Fennoscandian Mountains. Conservatoire et Jardin Botaniques de Geneve, Geneva, 195pp
Higgins SI, Clark JS, Nathan R, Hovestadt T, Schurr F, Fragoso JMV, Aguiar MR, Ribbens E, Lavorel S (2003) Forcasting plant migration rates: managing uncertainty for risk assessment. J Ecol 91:341–347
Hutchinson MF (2000) ANUSPLIN Version 4.1 User's Guide. Australian National University, Centre for Resource and Environmental Studies, Canberra
IPCC (2001) Climate change 2001: the scientific basis Working Group I contribution to the IPCC Third Assessment Report (URL: http://www.ipcc.ch/)
IPCC (2007) Climate change 2007: the Physical Science Basis. Working Group I contribution to the IPCC Forth Assessment Report (URL: http://www.ipcc.ch/)
Iverson LR, Prasad AM (1998) Predicting abundance of 80 tree species following climate change in the eastern United States. Ecol Monogr 68:465–485
Izrael YA, Pavlov AV, Anokhin YA (2002) Cryolithozone evolution under contemporary global climate change. Russian J Meteorol Hydrol 1:22–34
Khotinsky NA (1977) Holocene of Northern Eurasia. Nauka, Moscow, 200pp (in Russian)
Malevsky-Malevich SP, Molkentin EK, Nadyozhina ED, Sklyarevich OB (2001) Numerical simulation of permafrost parameters distribution. Cold Regions Sci Tech 32:1–11
Nazimova DI (1995) A climatic ordination of zonal classes of ecosystems as a basis for a generalized vegetation classification. Lesovedenie 4:63–73 (in Russian)
Noss RF (2001) Beyond Kyoto: forest management in a time of rapid climate change. Conserv Biol 15:578–590
Polikarpov NP, Andreeva NM, Nazimova DI, Sirotinina MA and Sofronov MA (1998) Formation composition of forest zones of Siberia as reflected through forest-forming tree species. Russian J For Sci 5: 3–11

Polikarpov NP, Tchebakova NM, Nazimova DI (1986) Climate and mountain forests of southern Siberia. Nauka, Novosibirsk, 225pp (in Russian)

Pozdnyakov LK (1993) Forestry on permafrost. Nauka, Novosibirsk, 192pp (in Russian)

Reference books on climate of the USSR (1965–1970) Gidrometeoizdat, Leningrad (in Russian)

Rehfeldt GE, Tchebakova NM, Barnhardt LK (1999a) Efficacy of climate transfer functions: introduction of Eurasian populations of *Larix* into Alberta. Can J For Res 29:1660–1668

Rehfeldt GE, Ying CC, Spittlehouse DL, Hamilton DL (1999b) Genetic responses to climate in *Pinus contorta*: niche breadth, climate change, and reforestation. Ecol Monogr 69:375–407

Rehfeldt GE, Ying CC, Wykoff WR (2001) Physiologic plasticity, evolution, and impacts of a changing climate on *Pinus contorta*. Clim Change 50:355–376

Rehfeldt GE, Tchebakova NM, Parfenova EI, Wykoff WR, Kouzmina NA, Milyutin LI (2002) Intraspecific responses to climate in *Pinus sylvestris*. Global Change Biol 8:1–18

Rehfeldt GE, Tchebakova NM, Milyutin LI, Parfenova EI, Wykoff WR, Kouzmina NA (2003) Assessing population responses to climate in *Pinus sylvestris* and *Larix* spp. of Eurasia with Climate-Transfer Models. Eurasian J For Res 6:83–98

Rehfeldt GE, Tchebakova NM, Parfenova EI (2004) Genetic responses to climate and climate change in conifers of the temperate and boreal forests. Recent Res Devel Gen Breeding 1:113–130

Shumilova LV (1962) Botanical geography of Siberia. Tomsk University Press, Tomsk, 440pp (in Russian)

Soja AJ, Tchebakova NM, French NHF, Flannigan MD, Shugart HH, Stocks BJ, Sukhinin AI, Parfenova EI, Chapin FS III, Stackhouse PW Jr (2007) Climate-induced boreal forest change: predictions versus current observations. Global Planet Change 56:274–296

St Clair B, Howe GT (2007) Genetic maladaptation of coastal Douglas-fir seedlings to future climates. Global Change Biol 13:1441–1454

Tchebakova MN, Parfenova EI (2006) Predicting forest shifting in a changed climate by the end of the 20th century. Comput Technol 7(3):77–86 (in Russian)

Tchebakova NM, Monserud R, Leemans R, Golovanov S (1993) A global vegetation model based on the climatological approach of Budyko. J Biogeogr 25:59–83

Tchebakova NM, Monserud R, Nazimova DI (1994) A Siberian vegetation model based on climatic parameters. Can J For Res 24:1597–1607

Tchebakova NM, Rehfeldt GE, Parfenova EI (2003) Redistribution of vegetation zones and populations of *Larix sibirica Ledeb*. and *Pinus sylvestris* L. in Central Siberia in a warming climate. Siberian Ecol J 10:677–686 (in Russian)

Tchebakova NM, Rehfeldt GE, Parfenova EI (2006) Impacts of climate change on the distribution of *Larix spp.* and *Pinus sylvestris* and their climatypes in Siberia. Mitigat Adapt Strat Glob Change 11(4):861–882

Tchebakova NM, Parfenova EI, Soja AJ (2008) Climate change and hot spots in forest shifts in central Siberia by the end the XXth century. Forest Snow Landscape Research (in press)

Turesson G (1925) The plant species in relation to habitat and climate. Hereditas 6:147–236

Watson R, Zinyowera M, Moss R, Dokken D (1996) Climate change 1995. Impacts, adaptations and mitigation of climate change: scientific-technical analyses. Cambridge University Press, Cambridge, 878pp

Chapter 23
Effects of Elevated CO_2 on Ecophysiological Responses of Larch Species Native to Northeast Eurasia

T. Koike, K. Yazaki, N. Eguchi, S. Kitaoka, and R. Funada

23.1 Introduction

Larch species are broadly distributed in the northern hemisphere, and dominate the landscape especially in the northeastern part of the Eurasian continent where permafrost is well developed (Abaimov et al. 1998, 2000; Kajimoto et al. 2003, 2006). Four species of larch, *Larix sibirica*, *L. gmelinii*, *L. cajanderi*, and *L. kaempferi*, predominate in the eastern Eurasia (Koike et al. 2000a; see Chap. 3). Taxonomy of *Larix* is still somewhat unsettled in the eastern half of Siberia, and particularly in the Far East of the Russian Federation. Although *Larix* in the latter region was not generally classified as *L. gmelinii* in Russia (Abaimov et al. 1998), the larches native to Sakhalin and Kuril Islands have customarily been referred to as *L. gmelinii* by some workers (Kurahashi 1988; Uemura et al. 1994; LePage and Basinger 1995; see also Chap. 3). Therefore, we describe the *Larix* species from Sakhalin and Kuril Islands, and that transplanted in Hokkaido, northern Japan, as *L. gmelinii* hereafter in this chapter.

With the increasing use of forests in this region, growth and regeneration patterns of larch seedlings may become strongly dependent on environmental changes. Moreover, atmospheric CO_2 concentration (hereafter abbreviated as [CO_2]) is increasing yearly due to the intensive use of tropical forests and of fossil fuel (IPCC 2007). After COP3 (Kyoto Protocol) (IGBP 1998), it is hoped that biomass productivity of larch forests and other forested ecosystems function as large carbon sink. In this sense, larch species are key plants for moderating [CO_2] based on their photosynthetic productivity.

For prediction of traits in future growth under the increasing [CO_2], it should be noted that values of light saturated photosynthetic rate under a given [CO_2] are similar in larch and birch; but not in Scots pine that photosynthesizes more or less independently of the treated [CO_2] (Koike et al. 2000b). The results show that there may be photosynthetic adjustment for high [CO_2] values in the deciduous trees, but not in the evergreen species. According to these studies, we should evaluate changes in future growth in larch, the dominant species, for predicting potential of atmospheric CO_2 fixation and its possible changes under the warmer climate and increasing [CO_2].

Stomatal conductance (gs) of plants decreases with increasing [CO_2]; however, responses of gs to drastic increase in the CO_2 level vary greatly among species

A. Osawa et al. (eds.), *Permafrost Ecosystems: Siberian Larch Forests*,
Ecological studies, Vol. 209, DOI 10.1007/978-1-4020-9693-8_23,

(Koike 1993; Yazaki et al. 2005). This may be induced by the decrease in the size of vessels or tracheids in xylem at high CO_2 concentration through decrease in water flow (Tyree and Zimmermann 2002; Koike 2003; Watanabe et al. 2008). Therefore, we expect changes in xylem structure in the larch species that grew under the elevated CO_2 level. If xylem structure should change with higher CO_2, a question arises if there is any change in specific gravity of xylem. To evaluate the effect of difference in WUE (water-use efficiency; see Larcher 2003), traits in nitrogen use, and xylem formation under the environment of elevated CO_2 concentration, seedlings of three larch species were raised under different CO_2 and nutrient levels. The species tested were two of the dominant species in Siberia (*Larix gmelinii* and *L. sibirica*) and a species in the maritime region of East Asia (*L. kaempferi*).

23.2 Growth Characteristics of Larch Species

Most larch species in Siberia or eastern Eurasia grow well on fertile soils (Schmidt 1992; Ota et al. 1993; Schulze et al. 1995; Koike and Tabuchi 1994; Abaimov et al. 2000; Koike et al. 2000a, 2000b; Shi et al. 2000). Larch is a typical light demanding conifer, and is characterized by high growth rates, especially in *L. kaempferi* (= *L. leptolepis*; Japanese larch), which originated in central Japan. The growth rate of *L. kaempferi* is the highest among the larch species in the world at midlatitude (Matyssek 1986). It is usually used as a breeding material for the development of high growth species (Matyssek and Schulze 1987, 1988). This species has been widely planted in Korea, northern Japan, and in Europe, and has been used as a breeding material (Koike et al. 2000a).

Larix gmelinii dominates in the forests of Central Siberia in mostly the region between the Yenisei and Lena Rivers (Korotkii et al. 2002). Its distribution also extends into northeastern China (Shi et al. 2000; see Chap. 19). These regions have cold and dry climates, and are characterized by the distribution of mostly continuous permafrost (Schmidt 1992; Abaimov et al. 1998, 2000; Koike et al. 2000b). This species also has been planted through northeastern parts of Eurasian continent, especially in northeast China. *Larix sibirica* is mainly found in areas west of the Yenisei River in Western Siberia, and in regions west of the Lake Baikal, where there is seasonal and discontinuous permafrost (details see Chaps. 1 and 3). In addition, the growth rate of *L. gmelinii* is slower than that of *L. sibirica* (Abaimov et al. 1998, 2000), though its early growth may show an opposite relationship (Martinsson, personal communication).

23.3 Photosynthetic Adjustment at Elevated [CO_2]

Evaluation of the traits in gas exchange was carried out as follows: 1- and 2-year-old seedlings of the three larch species were raised under the conditions of ambient [CO_2] (360 ppm) and elevated [CO_2] (720 ppm) with high (100 mg l^{-1} $week^{-1}$) and

low nutrient (100 mg l^{-1} mo^{-1}) levels (Koike et al. 2000b). Seeds of *L. gmelinii* and *L. sibirica* were collected from a botanical garden in the city of Yakutsk, Northeastern Siberia, and those of *L. kaempferi* were from Uryu Experimental Forest of Hokkaido University at Nayoro, Japan. All treatments were carried out in the phytotron at Forestry and Forest Products Research Institute of Japan. Photosynthesis and transpiration rates of six seedlings of each treatment were simultaneously determined to evaluate WUE with an A/Ci (assimilation rate and intercellular CO_2 concentration) relationship with a portable gas exchange system (LI-6400, NE, USA). Needle area (projected area) was measured with an image analyzer (EPSON, Tokyo, Japan). After the gas exchange measurement, nitrogen content of the needles was determined with a N/C analyzer (NC-900, Shimadzu, Kyoto, Japan) (Koike et al. 2000a).

The light saturated photosynthetic rate (Psat) of all seedlings at high [CO_2] was usually lower than that at ambient [CO_2]. Even though Psat at [CO_2] under which the seedlings had grown was higher at the elevated [CO_2] than that at the ambient [CO_2], the photosynthetic acclimation was found in the needles to the [CO_2] at which seedlings had been grown (Yazaki et al. 2001). A small increase in Psat of the whole crown at elevated [CO_2] was observed. It was considered due to the smaller specific needle area and structural and anatomical change of the needles (Eguchi et al. 2004).

High Psat was only observed at the beginning of [CO_2] treatment as was shown by Coleman et al. (1993) and Lei and Koike (2005). Moreover, Psat measured at the high level of [CO_2] under which the seedlings were grown was almost the same as the value of those grown under the ambient [CO_2] treatment (Fig. 23.1). This photosynthetic adjustment was first recognized for grass species in Alaskan tussock tundra by Tissue and Oechel (1987) and is widely found in several plant species when grown without any special nutrient treatment, i.e., photosynthetic "down regulation" (Koike 1993, 2006; Koike et al. 2000a, 2000b). Therefore, we cannot

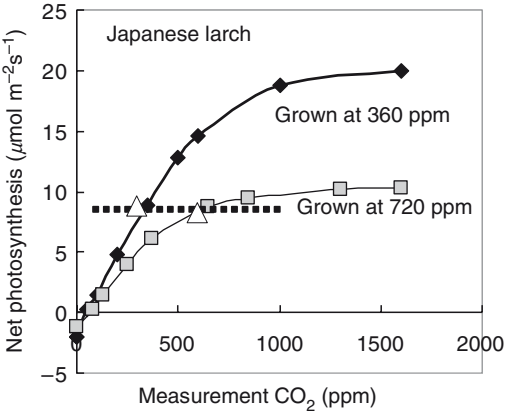

Fig. 23.1 Photosynthetic rate of Japanese larch (*Larix kaempferi*) grown at 360 or 720 ppm as a function of measured CO_2 concentration (Koike, unpublished data)

expect the high CO_2 fixation capacity of larch seedlings at moderate [CO_2] because there are several limitations of root expansion, enzyme level acclimation, extra-accumulation of photosynthates, etc. (Koike 1993; McConnaughay et al. 1993).

23.4 Nitrogen and Water Use Efficiency

At high [CO_2], three larch species (*Larix gmelinii, L. kaempferi, L. sibirica*) showed an increase in nitrogen use efficiency (NUE; net photosynthetic rate at light saturation per unit nitrogen, Larcher 2003). Because of high growth rate, nitrogen concentration of needles is diluted under the elevated [CO_2] (Coleman et al. 1993; Koike 1993). Among the three larch species, no difference in NUE was found (Fig. 23.2a). However, larch species native to Siberia had relatively high NUE. Therefore, photosynthetic rate of the larch in Central and Western Siberia may increase according to the increasing nitrogen deposition as noted by Valentini et al. (2000).

At present, there is low amount of precipitation (ca. 300–500 mm $year^{-1}$) in Central Siberia (Abaimov et al. 2000; see also Chaps. 1 and 10). With the changes in global climate, the patterns of precipitation are likely to change mainly at higher latitudes, and the direction of change is likely to be substantial reduction (see Chap. 22). How do the larch species respond to future environment of altered precipitation? Based on the analysis of A/Ci curve (Sharkey 1985; Koike et al. 1996), the stomatal limitation (Ls) of seedlings at 720 ppm was larger than that at 360 ppm. The highest Ls was found in *L. gmelinii* and the lowest was found in *L. kaempferi*. The Ls of *L. sibirica* was intermediate between them (Fig. 23.2b). This means that two larch species native to Siberia will be more resistant to desiccation in a future world of enriched [CO_2] through improved water use efficiency (WUE).

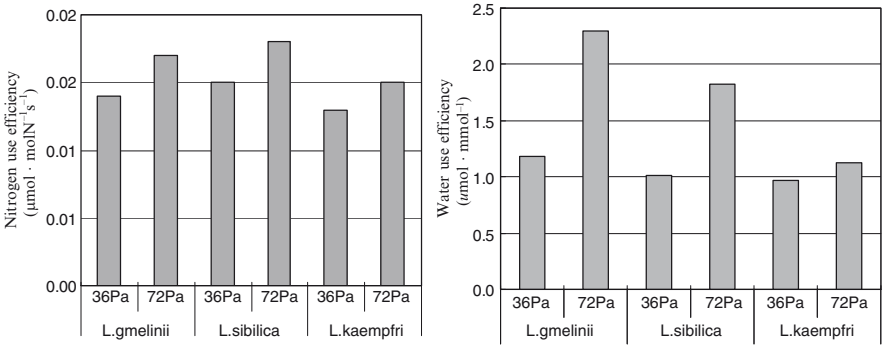

Fig. 23.2 Nitrogen (*left*; (**a**)) and water use efficiency (*right*; (**b**)) in three larch species raised at ambient and elevated CO_2 (after Koike et al. 2000a)

23.5 Xylem Formation

WUE of Siberian tree species increases under the environment of high [CO_2] (Koike et al. 1996). This means that water transport in xylem may decrease at high [CO_2], indicating possible decrease in vessel diameter (Koike 2006; Eguchi et al. 2008). In fact, tracheid size in conifer species decreased at high [CO_2] according to measurements in *L. kaempferi* and *L. sibirica* (Yazaki et al. 2001). Theoretical analysis in conifers also suggests occurrence of the same phenomenon (Roderick and Berry 2001).

Although enhanced [CO_2] may affect physiological and anatomical traits in *L. kaempferi*, tracheids and relative area of the cell-wall did not change in response to the elevated [CO_2] (Yazaki et al. 2004). Namely, there were no obvious differences in the thickness of the cell-wall or the relative area of the cell-wall between the seedlings grown at higher and ambient [CO_2]. Although the cell diameter after growth at the elevated [CO_2] was slightly larger than that after growth at ambient [CO_2], these increases had a minor effect on the relative area of the cell-wall. Therefore, the capacity for carbon fixation through cell-wall synthesis in tree stems may not be increased significantly in *L. kaempferi* that was exposed to elevated [CO_2]. In contrast, elevated [CO_2] affected stem shape by differentially altering shoot elongation and thickening. As the *L. kaempferi* seedlings acclimated to the [CO_2] under growth, increase in the amount of photosynthates gained was smaller than that in Psat in response to high [CO_2] of 720 ppm.

In *L. sibirica*, elevated [CO_2] enhanced stem diameter growth more than height growth, indicating that elevated [CO_2] affects the apical meristem and cambium differently or has different effects on cell division and cell expansion, or both. Changes in tracheid cell morphology in *L. sibirica* seemed to depend on changes in elongation rate of the shoots (Kinsman et al. (1996); Yazaki et al. 2001). Taylor et al. (1994) showed increase in the rate of leaf cell-expansion at elevated [CO_2] in a hybrid poplar. Thus, elevated [CO_2] may affect plant development not only by altering photosynthetic activity, but also by altering apical cell development.

Elevated [CO_2] had no significant effect on either stem height or diameter growth in *L. sibirica* seedlings (Yazaki et al. 2001). However, stem and diameter growth were enhanced by a high nutrient supply, which were also likely to be accelerated by high [CO_2] in the stands of *L. gmelinii* or *L. kaempferi*. (Yazaki et al. 2005). Enhanced [CO_2] increased width of the annual xylem ring and the number of cells in a radial file spanning the ring and tracheid lumen diameter, while it reduced cell-wall thickness (Fig. 23.3).

23.6 Rehabilitation with Larch Species

In the regions of Central and Northeastern Siberia, forest fires occur frequently during the growing season (Abaimov et al. 2000; see also Chap. 4). After a fire, natural regeneration is usually successful in most areas, but it depends on soil moisture

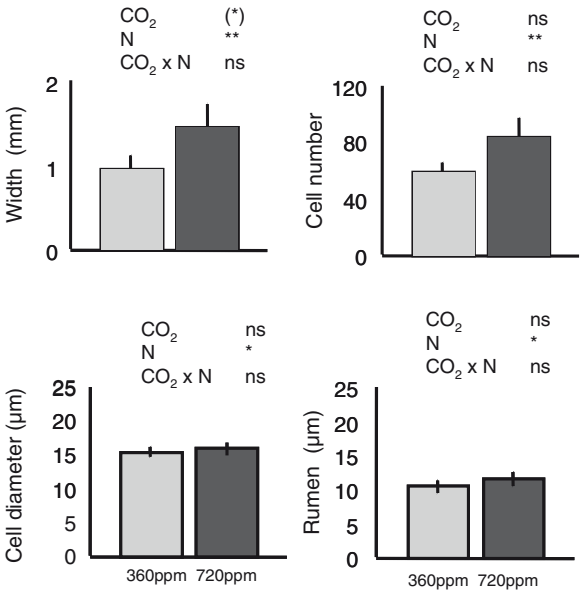

Fig. 23.3 Growth layer width, xylem cell number, cell diameter, and lumen diameter in *L. sibirica* grown at 360 or 720 ppm (after Yazaki et al. 2001)

condition and presence of abundant seed source (Shi et al. 2000; Yazaki et al. 2004) (Fig. 23.4). Based on phytotron studies (Koike et al. 2000b; Yazaki et al. 2005), capacity of CO_2 fixation in larch seedlings may be accelerated during the initial stage of natural regeneration when nutrient is still abundant (Abaimov et al. 2000; Korotkii et al. 2002; Qu et al. 2004).

As regeneration progresses, tree growth may decrease gradually due to competition among roots and shortage of nutrients, especially in the permafrost region (see Chap. 16). Photosynthetic capacity is also strongly regulated by nutrient conditions (Koike et al. 2000a, b; Yazaki et al. 2001). Therefore, the rate of CO_2 fixation in regenerated seedlings may decrease gradually even though [CO_2] may be increasing.

Larch seedlings need a relatively nutrient rich mesic habitat for their maximum growth, but they can survive on infertile volcanic ash soils, because of symbiosis with ectomycorrhiza. Under the enriched [CO_2], photosynthetic capacity of host plants (e.g., larch) may be enhanced when large amounts of photosynthates are translocated to symbiotic microorganisms such as ectomycorrhiza, which in turn supply nitrogen, phosphates, and water to the host plants (Quoreshi et al. 2003; Qu et al. 2004; Yazaki et al. 2004; see also Chap. 21). This symbiotic interaction may play an essential role in the success of forest rehabilitation in infertile soil conditions and is often a reason why larch species should be introduced as reforestation materials.

In northeast China and in Korean Peninsula, *L. kaempferi* has been planted for timber production. In Hokkaido, the northernmost major island of Japan, large

Fig. 23.4 Example of larch regeneration after forest fire in Central Siberia (photo: Koike)

areas of secondary forests of deciduous, broadleaved trees were cut and reforested with *L. kaempferi* during the past century. Recently, the role of the larch ecosystem has expanded from mere timber production to acting as the carbon sink because of its large distribution area in the northern hemisphere and high growth rate.

On the other hand, the *L. kaempferi* plantations in Hokkaido are examples of transplantation of an exotic species from central Japan to a new, local ecosystem. Indeed, *L. kaempferi* has a high susceptibility to shoot blight disease and grazing damage done by voles. Newly introduced species often suffer from several biological and physical problems. In 1954, a hybrid larch that was highly resistant to vole damage was discovered by chance at the Tokyo University Forest located in central Hokkaido.

Based on screening tests, it was found that Dahurian larch (*Larix gmelinii*) originated from the Kurile Islands had a higher resistance to both vole grazing and shoot blight disease, but those from Sakhalin Island did not (Kuromaru 2002; Ryu et al. 2009). In addition, *L. gmelinii* has greater resistance to frost than *L. kaempferi*. Such high tolerance of *L. gmelinii* to low temperature can be attributed to its phenological traits, namely early flush and early shedding of needles. The F_1 hybrid larch was produced by crossing *L. gmelinii* of the Kurile Islands (mother tree), with *L. kaempferi* (father tree). The chloroplast was inherited paternally from *L. kaempferi* (Shmidt et al. 1987) and the other growth characteristics, such as wood density and high resistance capacity, were inherited maternally from *L. gmelinii* (Hokkaido Regional Government 1987; Koike et al. (2000b)).

Recently, this F_1 hybrid larch was used as the planting stock throughout Hokkaido Island because of its high growth rate and high specific gravity of the stem. Most growth traits show intermediate characteristics between *L. gmelinii* and *L. gmelinii*. F_1 larch will be a promising species to fix atmospheric CO_2 more

quickly and to moderate global warming because of its high growth rate, high density, and resistance to several damages (Ryu et al. 2009).

23.7 Conclusions

Water use efficiency (WUE) and nitrogen use efficiency (NUE) of three larch species increased with enhanced [CO_2], but the increase in photosynthetic capacity was not long-lasting, which may be due to the effect of nutrient dilution in the plant body and nutrient limitation. The width of the annual ring and lumen size increased with high [CO_2], but no changes were found in the thickness of the cell-wall. Therefore, we cannot expect the naturally occurring larch species to play a role in fixing substantial amount of atmospheric CO_2 to moderate global warming, because they are likely to adapt to the new environment. On the other hand, F_1 (hybrid) larch may serve as a more effective fixer of atmospheric CO_2. Ectomycorrhiza should also be introduced and carefully used to accelerate the growth of larch seedlings, so that they can be effective in forest rehabilitation.

References

Abaimov AP, Lesinski JA, Martinsson O, Milyutin LI (1998) Variability and ecology of Siberian larch species. Swedish University of Agricultural Sciences Department of Silviculture Reports 43, Umeå, 123pp

Abaimov AP, Zyryanova OA, Prokushkin SG, Matsuura Y, Koike T (2000) Forest ecosystems of the cryolithic zone of Siberia; regional features, mechanisms of stability and pyrogenic changes. Eurasian J For Res 1:1–10

Coleman JS, McConnaughay KDM, Bazzaz FA (1993) Elevated CO_2 and plant nitrogen-use: Is reduced tissue nitrogen concentration size dependent ? Oecologia 93:195–200

Eguchi N, Fukatsu E, Funada R, Tobita H, Kitao M, Maruyama Y, Koike T (2004) Changes in morphology, anatomy and photosynthetic capacity of needles of Japanese larch (*Larix kaempferi*) seedlings grown in high CO_2 concentrations. Photosynthetica 42:173–178

Eguchi N, Morii N, Ueda T, Funada R, Takagi K, Hiura T, Sasa K, Koike T (2008) Changes in petiole hydraulic properties and leaf water flow in birch and oak saplings in a CO_2-enriched atmosphere. Tree Physiol 28:287–295

Hokkaido Regional Government (1987) Manual for plantation and tending in F1 larch plantation. Hokkaido Forestry Promotion Society, Sapporo, 165pp (in Japanese)

IGBP (1998) The terrestrial carbon cycle: implications for the Kyoto Protocol. Science 280:1393–1394

IPCC (2007) Assessing the physical science of climate change. (http://ipcc-wg1.ucar.edu/)

Kajimoto T, Matsuura Y, Osawa A, Prokushkin AS, Sofronov MA, Abaimov AP (2003) Root system development of *Larix gmelinii* trees affected by micro-scale conditions of permafrost soil in central Siberia. Plant Soil 255:281–292

Kajimoto T, Matsuura Y, Osawa A, Abaimov AP, Zyryanova OA, Mori S, Koike T (2006) Size-mass allometry and biomass allocation of two larch species growing on the continuous permafrost region in Siberia. For Ecol Manage 222:314–325

Kinsman EA, Lewis C, Davies MS, Young JE, Francis D, Thomas ID, Chorlton KH, Ougham HJ (1996) Effects of temperature and elevated CO_2 on cell division in shoot meristems: differential responses of two natural populations of *Dactylis glomerata* L. Plant Cell Environ 19:775–780

Koike T (1993) Ecophysiological responses of the northern tree species in Japan to elevated CO_2 concentrations and temperature. In: Oshima Y (ed) First IGBP Symposium. Japan Promotion of Sciences, Tokyo, pp 425–430

Koike T (2003) Responses of plants to environmental changes in earth. In: Muraoka H, Kachi N (eds) Light and water conditions affecting plant life – an introduction to plant physiological ecology. Bun'ichi Sogo, Tokyo, pp 119–138 (in Japanese)

Koike T (2006) Global warming and plant responses. In: Izuta T (ed) Plant under environmental stresses. Corona, Tokyo, pp 88–144 (in Japanese)

Koike T, Tabuchi R (1994) Ecophysiological studies of woody plants of Yakutia. In: Takahashi K (ed) Carbon storage and carbon dioxide budget in forest ecosystems. Interim Report of Joint Research Project between Japan and Russia. Forestry and Forest Products Research Institute, Sapporo, pp 59–71

Koike T, Lei TT, Maximov TC, Tabuchi R, Takahashi K, Ivanov BI (1996) Comparison of the photosynthetic capacity of Siberian and Japanese birch seedlings grown in elevated CO_2 and temperature. Tree Physiol 16:381–385

Koike T, Yazaki K, Funada R, Kitao M, Maruyama Y, Takahashi K, Maximov TC, Ivanov BI (2000a) Photosynthetic characteristics of Dahurian larch, Scotch pine and white birch seedlings native to eastern Siberia raised under elevated CO_2. Eurasian J For Res 1:31–37

Koike T, Yazaki K, Funada R, Maruyama Y, Mori S, Sasa K (2000b) Forest health and vitality in northern Japan – a case study on larch plantation. Faculty Forestry, University of Joensuu, Research Note 92, pp 49–60

Korotkii T, Prokushkin SG, Matsuura Y, Koike T (2002) Effects of soil temperature on the content of nitrogen compounds in seedlings of *Larix gmelinii* regenerated on permafrost in central Siberia. Eurasian J For Res 5:39–42

Kurahashi A (1988) Improvement of Larch by species hybridization. Bull Tokyo Univ For 79:1–94

Kuromaru M (2002) Interspecific hybridization of larch and its vegetative propagation in Japan. In: Rimbawanto A, Susanto M (eds) Proceedings: Advances in genetic improvement of tropical tree species. Japan International Cooperative Association, Tokyo, pp 131–135

Larcher W (2003) Physiological plant ecology, 4th edn. Springer, Berlin

Lei TT, Koike T (2005) Photosynthetic acclimation of birch, oak and maple seed lings to elevated CO_2 and the mediating effect of low growth irradiance. Phyton 45:145–152

LePage BA, Basinger JF (1995) The evolutionary history of the genus *Larix* (Pinaceae). In: Schmidt WC, McDonald KJ (eds) Ecology and management of *Larix* Forests: a look ahead. USDA Forest Service, Intermountain Research Station, GTR-INT-319, pp 19–29

Matyssek R (1986) Carbon, water and nitrogen relations in evergreen and deciduous conifers. Tree Physiol 2:177–187

Matyssek R, Schulze E-D (1987) Heterosis in hybrid larch (*Larix decidua* × *leptolepis*). II. Growth characteristics. Trees 1:225–231

Matyssek R, Schulze E-D (1988) Carbon uptake and respiration in above-ground parts of a *Larix decidua* x *leptolepis* tree. Trees 2:233–241

McConnaughay KDM, Bertson GM, Bazzaz FA (1993) Limitations to induced growth enrichment in pot studies. Oecologia 94:550–557

Ota S, Koike T, Osawa A, Sassa T, Takahashi K (1993) Forest environmental studies in Taiga developed on the permafrost region of Eastern Siberia. Shinrin Kagaku (Forest Science) 7:68–73 (in Japanese)

Qu LY, Kayama M, Kitaoka S, Akasaka M, Sasa K, Koike T (2004) Micro-environmental analysis of natural regeneration of larch in northern Japan. Eurasian J For Res 7:43–51

Quoreshi AM, Maruyama Y, Koike T (2003) The Role of mycorrhiza in forest ecosystems under CO_2-enriched atmosphere. Eurasian J For Res 6:171–176

Roderick ML, Berry SL (2001) Linking wood density with tree growth and environment: a theoretical analysis based on the motion of water. New Phytol 149:473–485

Ryu K, Watanabe M, Shibata H, Takagi K, Nomura M and Koike T (2009) Ecophysiological responses of the larch species in northern Japan to environmental changes as a base of afforestation. Landsc Ecol Eng 5:99–106

Schmidt WC (1992) Around the world with *Larix*: an introduction. In: Schmidt WC, McDonald KJ (eds) Ecology and management of *Larix* forests: a look ahead. USDA Forest Service, Intermountain Research Station, GRT-INT-319, pp 6–18

Schulze E-D, Schulze W, Kelliher FM, Vygodskaya NN, Ziegler W, Kobak KL, Koch H, Arneth A, Kusnetsova WA, Sogatchev A, Issajev A, Bauer G, Hollinger DY (1995) Aboveground biomass and nitrogen nutrition in a chronosequence of pristine Dahurian *Larix* stands in eastern Siberia. Can J For Res 25:943–960

Sharkey TD (1985) Photosynthesis in intact leaves of C3 plants: physics, physiology and rate limitations. Bot Rev 51:53–105

Shi FC, Zu YG, Suzuki K, Yamamoto S, Nomura M, Sasa K (2000) Effects of site preparation on the regeneration of larch dominant forests after a forest fire in the Daxinganling mountain region, northeast China. Eurasian J For Res 1:11–17

Shmidt A, Aleden T, Haellgren JE (1987) Paternal inheritance of chloroplast DNA in *Larix*. Plant Mol Biol 9:59–65

Taylor G, Ranasinghe S, Bosac C, Gardner SDL, Ferris R (1994) Elevated CO_2 and plant growth: cellular mechanisms and responses of whole plants. J Exp Bot 45:1761–1774

Tissue DL, Oechel WC (1987) Physiological response of *Eriophorum vaginatum* to field elevated CO_2 and temperature in the Alaskan tussock tundra. Ecology 68:401–410

Tyree MT, Zimmermann MH (2002) Xylem structure and the ascent of sap, 2nd edn. Springer, Berlin 283pp

Uemura S, Tsujii T, Ishizuka M, Volotovsky KA (1994) Timber limit vegetation of the Northernmost taiga in the Lena River basin, Eastern Siberia. In: Inoue G (ed) Proceedings of the Second Symposium on the Joint Siberian Permafrost studies between Japan and Russia. National Institute for Environmental Studies, Tsukuba, Japan, pp 116–121

Valentini R, Matteucci G, Dolman AJ, Schulze ED, Rebmann C, Moors EJ, Granier A, Gross P, Jensen NO, Pilegaard K, Lindroth A, Grelle A, Bernhofer C, Grünwald T, Aubinet M, Ceulemans R, Kowalski AS, Vesala T, Rannik U, Berbigier P, Loustau D, Gudmundsson J, Thorgeirsson H, Ibrom A, Morgenstern K, Clement R (2000) Respiration as the main determinant of carbon balance in European forests. Nature 404:861–865

Watanabe Y, Tobita H, Kitao M, Maruyama Y, Choi DS, Sasa K, Funada R, Koike T (2008) Effects of elevated CO_2 and nitrogen on wood structure related to water transport in seedlings of two deciduous broad-leaved tree species. Trees 22:403–411

Yazaki K, Funada R, Mori S, Maruyama Y, Abaimov AP, Kayama M, Koike T (2001) Growth and annual ring structure of *Larix sibirica* grown at different CO_2 concentration and nutrient supply. Tree Physiol 21:1223–1229

Yazaki K, Ishida S, Kawagishi T, Fukatsu E, Maruyama Y, Kitao M, Tobita H, Koike T, Funada R (2004) Effects of elevated CO_2 on growth, annual ring structure and photosynthesis in *Larix kaempferi* seedlings Tree Physiol 24:951–959

Yazaki K, Maruyama Y, Mori S, Koike T, Funada R (2005) Effects of elevated carbon dioxide concentration on wood structure and formation in trees. In: Omasa K, Nouchi I, De Kok LJ (eds) Plant responses to air pollution and global change. Springer, Tokyo, pp 89–97

Part V
Synthesis and Conclusion

Chapter 24
Characteristics of Permafrost Forests in Siberia and Potential Responses to Warming Climate

A. Osawa, Y. Matsuura, and T. Kajimoto

24.1 Introduction

The purpose of this chapter is to synthesize what have been reported in the preceding chapters, and to discuss (1) major characteristics in the structure, function, and development patterns of the larch forests that grow on permafrost, and (2) how their structure and function may change due to the warming climate.

Accumulated aboveground biomass of the permafrost larch forests is generally small. However, there are obvious patterns of variation depending on site conditions (Chap. 6). Development patterns of stand structure over time follows the well-known self-thinning rule in the permafrost forests; however, they also exhibit a phase of development that is unusual. Accordingly, we recognized that the larch ecosystems in the continuous permafrost region exhibit two growth phases that are distinctly different (Chap. 7). Morphology and growth patterns of root systems are also affected by the shift in the growth phase of the larch trees (Chap. 16). We show in the following sections that these changes in the patterns of stand development are closely tied to the changes in the condition of the permafrost that are occurring after a forest fire.

There is a great deal of uncertainty in the outcome of climate warming, which makes any prediction challenging in terms of both in time and space. For the sake of discussion, a 2 X CO_2 scenario that has often been used in GCM calculations is considered (Houghton et al. 1990; Gordon et al. 2000). More specifically, our warming earth is assumed to experience 1% increase per year of atmospheric CO_2 concentration for about 100 years, so that the CO_2 level would be a little bit more than doubled by the end of the twenty-first century (Gordon et al. 2000). According to the predictions by Tchebakova et al. (Chap. 22), the CO_2 enrichment of this magnitude is expected to make summer temperature of Central Siberia 4–6°C higher. The temperature increase can be even higher in winter: as much as 9°C. Precipitation is estimated to increase by about 30% in Central Siberia, although the prediction is less certain. The ecosystem changes that are dealt with here will be what we may see during the decade of 2090–2100. It is also noted that the predicted change of vegetation may be somewhat extreme (Chap. 22) corresponding to more dramatic climate change that we anticipate. Therefore, the expected vegetation change

A. Osawa et al. (eds.), *Permafrost Ecosystems: Siberian Larch Forests*,
Ecological studies, Vol. 209, DOI 10.1007/978-1-4020-9693-8_24,

could be more moderate in reality. This should be kept in mind when interpreting the predictions. We consider in this chapter only a biome currently dominated by *Larix gmelinii* or *L. cajanderi*, since this has been the focus of this book. Geographical extent of this biome at present nearly coincides with the area of continuous permafrost in Siberia (Fig. 1.1). Therefore, the fate of this biome is expected to depend on changes in both climate and future condition of the permafrost (Chap. 22). It is also necessary to take into account the hydrological characteristics of this region in relation to the presence of permafrost, and their relationship to function of the forest biome (Chap. 13).

24.2 Characteristics of Permafrost Forests in Siberia

24.2.1 Forest Fire and Dynamics of Ecosystem Development

Characteristics of forest stand development in the continuous permafrost zone of Siberia are constrained by forest fires and status of the frozen soils. Peculiar behavior of the permafrost shortly after the fire and its recovery over time are the key factors influencing forest development.

Tree species in the boreal forest are adapted to occurrence of forest fires (Wein and MacLean 1983; Van Cleve et al. 1986). Seeds of some species are very small with long silky hairs or wings (e.g. *Populus tremuloides*, *Betula pendula*), and can be dispersed long distance by wind. Seeds of other species have a fire-avoiding mechanism known as cone serotiny (Wein and MacLean 1983; Rudolph and Laidly 1990; see also Chap. 1). *Pinus banksiana* and *Picea mariana* of North America are good examples. As a result, dense even-aged communities of small number of tree species generally develop after fire. The new stands often consist of a single tree species (Osawa 1995). Therefore, postfire development of the forest follows the self-thinning rule (Osawa and Allen 1993; Osawa 1995) when the number of seedlings established after a fire is reasonably large (Chap. 7). *Larix gmelinii* growing near Tura, Central Siberia, is another good example exhibiting such a growth habit. Therefore, the larch stands often become established as dense seedling stands after fire, and increase in tree size and stand biomass while reducing stand density quickly through intraspecific competition (Fig. 24.1). Then, aboveground biomass reaches the maximum value by stand age of ca. 30 years, after which the biomass becomes more or less stable while stand density declines continuously (see Fig. 7.4b). The maximum value of aboveground biomass and the timing to reach the maximum biomass may vary somewhat depending on site conditions (Chaps. 6 and 7).

As illustrated in Fig. 24.1, these patterns of stand development are closely related to changes in the status of the permafrost. In the areas around Tura, depth of the soil active layer, the thawed part of the soil during a growing season, is in the range of 20–70 cm in the intact larch forests on the north-facing slope (see Chaps. 4, 6, 8, 11, and 16). However, forest fire changes the situation. The depth of the soil

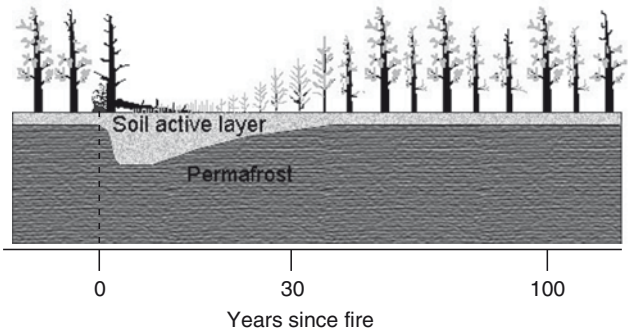

Fig. 24.1 Schematic representation of the pattern of larch forest development over time after a stand-replacing fire and changes in soil horizons that are underlain by continuous permafrost at Tura, Central Siberia. A fire is assumed to have occurred at year zero. Both horizontal and vertical axes are not to scale

active layer becomes 120–140 cm or more shortly after fire (see also Fig. 8.4a) due to decreased albedo and increased absorption of solar energy on the forest floor. The soil active layer stays deep for a few decades after that. It is during this period when rapid growth of seedlings and self-thinning by intraspecific competition occurs (Chap. 7). Presumably, soil is warmer and nutrient availability is greater at this stage (Chaps. 7 and 8). By ca. 30 years after fire, ground cover of mosses and other plants re-develops on the forest floor, acting as effective thermal insulator. It causes to cool the soil temperature, and allows the receded permafrost table to rise toward the ground surface (Fig. 24.1). Some 30 years is sufficient for the recovery of the previous permafrost table before the fire.

24.2.2 Ecosystem Carbon Budget

Patterns of carbon storage and flow in a 105-year-old *L. gmelinii* stand at Carbon Flux Site (plot CF; see Fig. 1.3) was evaluated by synthesizing data presented in the preceding chapters and other available data (Fig. 24.2). Most estimates are based on the measurements in the target stand, while others are inferred from data of separate old stands in the same region. There are still some uncertainties, such as root respiration (R_{bg}) and carbon efflux from soils due to litter decomposition by microbes (R_h; heterotrophic respiration). Net primary production (NPP) of the forest floor vegetation, such as shrubs, herbs, lichen, and mosses, was also not yet determined (shown by question marks in Fig. 24.2). Nevertheless, the diagram in Fig. 24.2 provides some characteristic features of the ecosystem carbon dynamics that could be achieved in a typical old larch forest (> ca. 100 years) in the region.

Ecosystem total carbon stock was about 92 MgC ha^{-1}, which was the sum of four components: soil organic carbon in the active layer (SOC; 70.9 MgC ha^{-1}), biomass of living plants as in larch trees (8.3 MgC ha^{-1}) and in vegetation at the forest floor

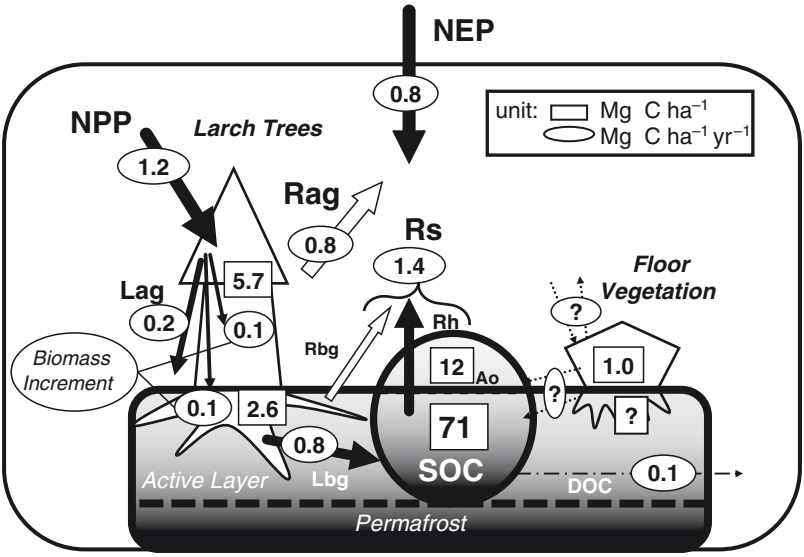

Fig. 24.2 Schematic diagram of ecosystem carbon budget in a 105-year-old *L. gmelinii* forest at Carbon Flux site in Tura, Central Siberia. Location and stand properties of the study forest (plot CF) is shown in Figs. 1.3 and 6.1, Table 6.1. Values in rectangular boxes indicate carbon stock (Mg C ha^{-1}), and values in ellipses attached to *arrows* indicate annual carbon flow (MgC ha^{-1} year^{-1}). The pathways as aboveground and belowground plant respiration were shown with open arrows, because they do not add up to calculation of net primary production (NPP), and are not used in estimation of net ecosystem production (NEP) if ecological summation method is used. The carbon stock and flow (e.g. plant biomass, NPP), which were originally estimated as dry matter, were converted to carbon-base values by multiplying by 0.5 (MgC ha^{-1}, MgC ha^{-1} year^{-1}). Data source and methods are as follows. Biomass and NPP was estimated for living larch trees; NPP was the sum of biomass increment and litterfall rate (L_{ab}) (see Tables 6.1 and 6.2). Biomass of floor vegetation (woody shrubs, herbs, mosses, and lichens) was estimated by harvest method (Matsuura and Kajimoto, unpublished data). Carbon in a compartment (Ao) was the sum of coarse woody debris (CWD; standing dead trees, and snags) and those in other dead materials (fine litter and raw humus); CWD was estimated in a subplot (16 × 16 m^2), and the other dead materials were determined at the same positions used for harvesting floor vegetation (Matsuura et al. 2004). Soil carbon storage (SOC) was the average value (n = 4); depth of active soil layer differed among the pits (mean 63 cm deep) (Matsuura, unpublished data; see Chap. 8). Aboveground respiration of larch trees was estimated based on the daily respiration rate determined for average size individual in the other old larch stand (plot C1); stand-level aboveground total respiration (R_{ab}) was the sum of daily respiration rates during a growing season (ca. 90 days) (see Chap. 14). Soil respiration rate was measured by closed chamber method, and total respiration rate during the growing season was calculated by applying the temperature–respiration relationship (Morishita et al. unpublished data; details of method see Chap. 9). Loss of dissolved organic carbon (DOC) from soil during soil-thawing period (i.e. nearly growing season) was evaluated in a watershed (Site 2) near Tura; the annually leached DOC was the average of several years (Prokushkin et al. 2005; see also Chap. 11). NEP was determined by eddy covariance technique during the growing season (Nakai et al. 2008; see also Chap. 10)

(1.0 MgC ha^{-1}), and organic carbon of dead materials (Ao; 11.7 MgC ha^{-1}) such as coarse woody debris (CWD), fine litter, and raw humus (Fig. 24.2). About 77% of ecosystem total carbon is stored in a thin layer of the thawed soil in summer (63 cm in depth).

If SOC is expressed as total organic carbon within the soil of 1 m depth (i.e. including the frozen soil at a deeper horizon), its relative proportion would be somewhat increased (82% of ecosystem total C) (Matsuura et al. unpublished data). The relative proportion of SOC is as high as the value for other boreal forests: soil C (down to 1 m depth) in ecosystem total C is 77% in Russia, 95% in Canada, and 84% in Alaska (Dixon et al. 1994). The comparison suggests that soil (active layer) is a major component of ecosystem C-pool even in the permafrost region. It is noted, however, that the absolute amount of organic carbon in both soil and vegetation in the old larch stand is much smaller than the value (281 and 83 MgC ha^{-1}) averaged for Russian boreal forests located mostly on nonpermafrost regions (Dixon et al. 1994).

As for the carbon flow, annually fixed carbon in larch trees was rather small (NPP; 1.2 MgC $ha^{-1}\,year^{-1}$), and was largely allocated into construction of two organs that are linked to resource uptake: needle and fine root (Fig. 24.2). Biomass increments of woody tissues are smaller (0.1 MgC $ha^{-1}\,year^{-1}$ for stem plus branch, and coarse root, respectively) than production of needles (L_{ag}; 0.2 MgC $ha^{-1}\,year^{-1}$) and fine roots (L_{bg}; 0.8 MgC $ha^{-1}\,year^{-1}$). Particularly, contribution of fine root production in NPP is large (ca. 60%). The pattern of high carbon allocation into fine roots agrees with those reported for boreal forests of other regions (see Sect. 6.4.2).

Net ecosystem exchange (NEE) of the old larch stand was estimated during a growing season (ca. 3 months) by eddy covariance technique (Nakai et al. 2008; see also Chap. 10), then net ecosystem production (NEP) was calculated as –NEE. The NEP estimate is slightly positive (0.8 MgC $ha^{-1}\,year^{-1}$) (Fig. 24.2). This indicates that the old larch forest may function as a net carbon sink. Valentini et al. (2000) reviewed data of NEE for various forest types in Europe (EUROFLUX network), and indicated that NEE tended to increase (or NEP decreased) with latitude. The NEE ranged between −2 and 2 MgC $ha^{-1}\,year^{-1}$ for the boreal forests located in the northernmost regions (60–65° in latitude). The NEP in the old *L. gmelinii* stand falls within this range. However, the absolute value of NEP in the larch forest is close to the detectable limit of accuracy when estimated from the CO_2 flux data (0.3 MgC $ha^{-1}\,year^{-1}$) (Valentini et al. 2000). Our estimate of the NEP does not include carbon efflux in winter, of which inclusion should further reduce the value somewhat. Also, the extent of inter-annual variation in NEP is unknown, which may be caused by the variations in climate variables such as temperature, precipitation, and duration of the growing season (e.g. Barr et al. 2002; Saigusa et al. 2008). Therefore, the old larch forest of the present investigation may be close to a steady state (NEP = 0) in terms of ecosystem carbon budget, rather than being a net carbon sink.

NEP is also defined as NPP minus heterotrophic respiration (R_h) and other pathways of carbon loss such as black carbon that has become inert and been segregated from the ecosystem carbon cycle, and dissolved organic carbon (DOC) seeped through the ecosystem (e.g. details see Schulze 2006; Chapin et al. 2006). We estimated NPP for larch trees (1.2 MgC $ha^{-1}\,year^{-1}$; see Chap. 6) and annual amount of DOC leaching from soil (0.1 MgC $ha^{-1}\,year^{-1}$; Prokushkin et al. 2005; also see

Chap. 11). Carbon efflux from soil as CO_2 was also measured using the closed chamber method (see Chap. 9), by which ecosystem-level soil respiration (R_s) during the growing season was estimated (1.4 MgC ha^{-1} year^{-1}) (Morishita et al. unpublished data) (Fig. 24.2). R_s is composed of respiration of plant roots (R_{bg}) and microbes (R_h). Thus, if the above-mentioned value of NEP is applied, heterotrophic respiration can be calculated as follows: R_h = NPP (1.2) −NEP (0.8) – leaching DOC (0.1) = 0.3 MgC ha^{-1} year^{-1}. Root respiration can also be given by the following equation: $R_{bg} = R_s$ (1.4) $- R_h$ (0.3) = 0.9 MgC ha^{-1} year^{-1}. The R_{bg} is nearly equivalent to the aboveground total respiration of larch trees (Rag; 0.8 MgC ha^{-1} year^{-1}; see Chap. 15).

According to the theoretical consideration, the proportion of heterotrophic respiration in total carbon efflux from soil (R_h/R_s ratio) would be about 0.2. The value suggests that contribution of root respiration is large in total amount of soil respiration. This may, in turn, imply that proportion of roots in total biomass is large (i.e. >30 %) in the old larch stand, compared with boreal forests of nonpermafrost regions (Kajimoto et al. 2006; see also Chap. 6). However, the inferred R_h/R_s (0.2) is apparently much smaller than the average ratio (0.65) suggested previously for boreal coniferous forests (Subke et al. 2006). Methodologically, separation of soil respiration (R_s) into these two components (R_{bg}, R_h) is difficult. Thus, general pattern of R_h/R_s ratio in major forest types is uncertain (e.g. Schulze 2006). Additional field studies and/or experiments (e.g. Högberg et al. 2001) are necessary for gaining further knowledge on partitioning soil respiration into that of roots and microbes.

It is necessary to be born in mind that parts of the ecosystem carbon dynamics (Fig. 24.2) still remains uncertain. Particularly, data on annual carbon flow through the forest floor vegetation (e.g. shrubs and mosses) are lacking. Such flows must be evaluated, since they may be significant in ecosystem NPP of boreal forests (O'Connell et al. 2003). A preliminary estimate of aboveground NPP by mosses, lichens, and shrubs at the forest floor suggested a value 0.2 MgC ha^{-1} year^{-1} (Fukuzaki 2008), approximately 17% of that of larch trees in the same ecosystem. Contribution by roots of the forest floor vegetation is still not included in this estimate. Therefore, further examination of the floor vegetation is likely to make the NPP value of the entire ecosystem even higher. It should also be noted that the absolute value of each component flow of carbon is mostly lower than 1.0 MgC ha^{-1} year^{-1}. This means that carbon moves slowly in the permafrost larch forest. Therefore, accuracy is important in evaluating the ecosystem C budget.

24.2.3 Comparison to Permafrost Forests of North America

The boreal forest biome does not generally occur over the continuous permafrost in North America as we described in Chap. 1 (see Fig. 1.1). Although species of *Picea* and/or *Larix* form the latitudinal tree line at the boundary of forest tundra and tundra biomes, this boundary roughly coincides with that of the continuous- and discontinuous-distribution zones of the permafrost (Brown et al. 1997). *Picea mariana* is

found at the tree line in Alaska (Van Cleve et al. 1986), Yukon Territory (Ritchie 1984; Kojima 1994), MacKenzie delta in Northwest Territories (Black and Bliss 1980; Ritchie 1984), and in northern Quebec (Payette and Gagnon 1979; Légère and Payette 1981; Penalba and Payette 1997). *Larix laricina* is also distributed widely in North America from the Atlantic coast to Alaska, and reaches the latitudinal timber line in Alaska, lower MacKenzie basin, northeastern Manitoba, southern shores of the Hudson's Bay, and in northern Quebec (Payette and Gagnon 1979; Légère and Payette 1981; Van Cleve et al. 1986; Johnston 1990; Penalba and Payette 1997).

An area that does not conform to this generalization is the lower MacKenzie River basin between ca. 65°N and 69°N, and between ca. 122°W and 135°W – the area bounded by Great Bear Lake and MacKenzie delta created by the MacKenzie and Peel Rivers (see Fig. 1.1; Burns and Honkala 1990). Here, *P. mariana* stands exhibit nearly closed-canopy or maximal biomass-stand density condition over the extended areas of continuous permafrost, but with narrow crowns and large size-variation in trees (Fig. 24.3).

Larix laricina is a member of the permafrost forest dominated by *P. mariana*. However, the *Larix* does not seem to form extended forest stands there. In this respect, distribution of *L. laricina* resembles that of *L. sibirica* in Western Siberia (Chap. 3) by being more abundant on permafrost-free soils. Therefore, a *Larix*

Fig. 24.3 *Picea mariana* forests over continuous permafrost in the lower MacKenzie River basin near 68°N, 134°W in Northwest Territories, Canada. (**a**) A stand of ca. 100 years old with maximal biomass-density condition judged by the self-thinning relationship; (**b**) a young, very dense stand with closed canopy condition; (**c**) an old, open-canopy stand at a relatively well-drained site with lichens (*Cladina* spp.) on the forest floor (photo: N. Kurachi)

species that occupies an ecological niche similar to that of *L. gmelinii* or *L cajanderi* appears missing from North America. On the other hand, no *Picea* species are known to grow extensively over the continuous permafrost in Siberia (Chap. 22). Therefore, the *Picea* species as hardy as *P. mariana* are missing from Siberia. How was this contrasting pattern developed? This is an interesting and unresolved question.

There have been studies suggesting why *P. mariana* can withstand severe environmental conditions more than *L. laricina*. The evergreen *Picea* produces greater amount of fine roots than the deciduous *Larix* (Gower et al. 2001), and may be better suited for nutrient uptake in the nutrient-limited environment. The value of foliar carbon isotope discrimination is less in *P. mariana* than in *Larix* species (Kloeppel et al. 1998), suggesting that *Picea* uses water more efficiently. These physiological characteristics may explain abundance of *P. mariana* on permafrost soils. On the other hand, *Larix* (including *L. laricina*) constructs a low-carbon-cost, well-illuminated, nitrogen-efficient canopy that can provide a carbon gain comparable with evergreen conifers (Tyrrell and Boerner 1987; Gower and Richards 1990; see also Chap. 8), allowing it to coexist with *Picea* species under severe environments. It has also been suggested that deciduousness of larch species serves as drought avoidance mechanism, and allow the larches to occupy permafrost soils (Berg and Chapin 1994). Then, why does *Larix laricina* not grow extensively to form more or less continuous canopies over the permafrost soils in North America? Ecological, pathological, or other mechanisms may be responsible for small abundance of *L. laricina* in the permafrost zone of North America. Comparative physiological and ecological studies of *Larix laricina*, *L. gmelinii*, *L. cajanderi*, *Picea mariana*, and *P. obovata* may be necessary to learn more of the reasons.

There has always been a contrast in major vegetation types during late Quaternary and in modern era between western and eastern parts of Beringia, the area between the Verkhoyansk Range in Northeastern Siberia and western Yukon Territory, Canada. Currently, forests are composed of the deciduous conifer, *Larix dahurica* (*L. cajanderi* in the nomenclature used in this book.; see Chaps. 1 and 3) in west Beringia, and mostly of *Picea mariana* and *P. glauca* in east Beringia (Anderson and Lozhkin 2001; Edwards et al. 2005). *Larix laricina* is the third conifer species present in east Beringia, but never forms a major component of the regional vegetation (Andreson and Lozhkin 2001). During Middle Wisconsian period (70–28 ka BP) in late Quaternary, *Larix* forests were widespread in west Beringia, but *Picea* was never abundant (Andreson and Lozhkin 2001; see their Table 2). On the other hand, the major vegetation was *Picea* forest in east Beringia during the same period. East Beringia was also covered with deciduous vegetation at times, but the main plants were shrubs of *Betula*, *Salix*, or *Alnus* (Andreson and Lozhkin 2001; their Table 3). Unlike west Beringia, *Larix* was never dominant (Ritchie 1977, 1982, 1985; Lacourse and Gajewski 2000). It is unclear why *Larix* species of west Beringia did not disperse to east Beringia through the Beringian land-bridge during this period. It is also unknown why the dominant *Picea* (particularly *P. mariana*) in east Beringia was unable to cross the land-bridge and spread toward west Beringia during late Quaternary.

24.3 Potential Responses to Warming Climate

24.3.1 Ecosystem Structure

First, the possible changes of the permafrost forests in terms of their physiognomy and distribution are discussed. Then, the changes at the finer scales will be described at the levels of hill slopes and individual stands.

24.3.1.1 Shift in Dominant Biome

Tchebakova et al. (Chap. 22) predicted that most of the permafrost forest biome will become forest-steppe or steppe biomes at the end of the twenty-first century. Super-dominance of *Larix gmelinii* and *L. cajanderi* is likely to give way to species of grasses. Tree density will become sparser as most communities are likely to become open forests, unless they turn into entirely treeless. The permafrost forest will expand its range northward toward the Arctic Ocean, but the area gained will be much less than that lost in the southern regions to steppe vegetation (Fig. 24.4). There may also be invasion of *Larix sibirica* into the southern region of contemporary permafrost forests (Fig. 22.2), up to the 60th parallel. Receding distribution of continuous permafrost is the major cause. However, *L. sibirica* will not form dense forests, because the main biome there will be a steppe.

Diversity of tree species will also become greater toward the southern and western borders of the presently permafrost forests. A pine species and some angiosperm trees have ability to expand into the regions where the permafrost becomes thin or discontinuous. *Pinus sibirica*, *Betula pendula*, and *B. pubescens* presently show some relative importance in the larch-dominated forests south of 63°N or west of 101°E. These species can become much more important, and may easily create mixed-species forests with the larches (Kharuk et al. 2007). On the other hand, *Pinus sylvestris* and dark-needle trees, such as *Picea obovata* and *Abies sibirica*, are not likely to invade the contemporary permafrost forest extensively, since the permafrost is expected to persist in much of the regions above the 60th parallel (Fig. 22.2). Increased frequency of forest fires in the warmer climate will also be detrimental to expansion of *Picea obovata* and *Abies sibirica* that are less adapted to fires for their thin bark and lack of fire-avoiding mechanism in mature seeds (e.g. cone serotiny of *Larix gmelinii*).

24.3.1.2 North- and South-Slope Ecosystems

The distribution of the tree species in space will not be uniform under the warmer climate, as it is also the case today. The landscape of Central and Northeastern Siberia is characterized by sloping plateaus and mountains (cf. Sect. 2.2). Relatively large areas of flat topography are rare, and are restricted to the zones along large rivers.

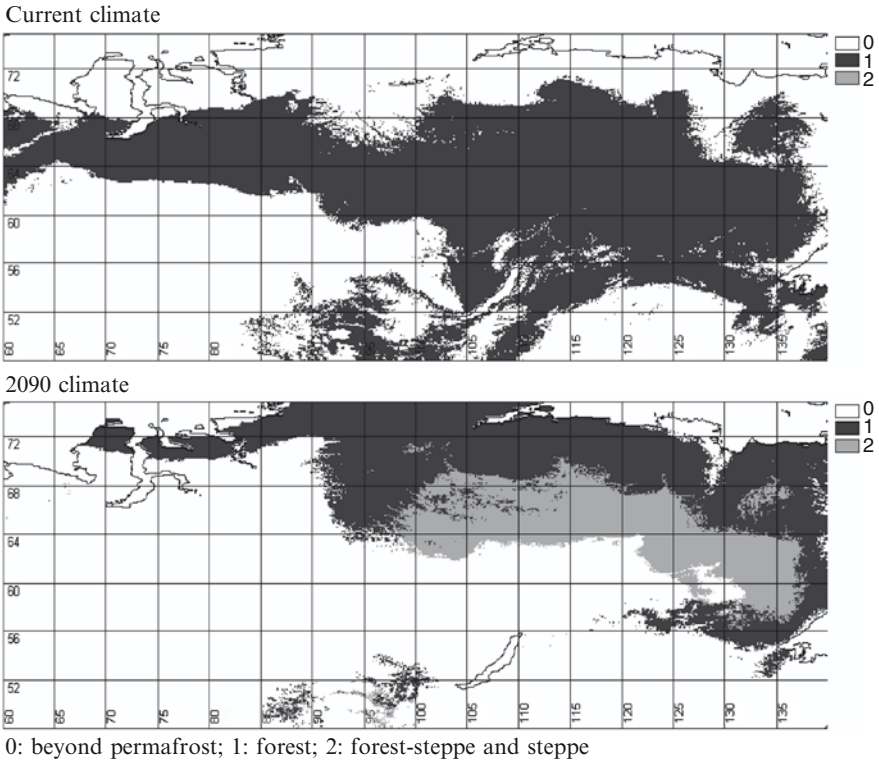

Fig. 24.4 Distribution of permafrost larch forests and forest-steppe or steppe vegetation in Siberia (**a**) under contemporary climate and (**b**) for the climate projected for the decade 2090–2100 by Tchebakova et al. (Chap. 22). Dark shade: permafrost larch forest including light taiga of *Larix gmelinii* and *L. cajanderi* at northern, middle, and southern Siberia, as well as forest-tundra of these larch species; Light shade: forest-steppe and steppe; No shade: biomes other than permafrost

Therefore, characteristics of the ecosystems vary depending on the aspect of these hill slopes. Distribution of different ecosystems on north- and south-facing slopes has been widely recognized in ecological literature (Barbour et al. 1980; Van Cleve et al. 1986; Kojima 1994). For example, colder north-slope with the underlain permafrost supports tundra vegetation, whereas warmer south-slope is dominated by forests of *Picea mariana* and *P. glauca* in the central part of Yukon Territory, Canada (Ritchie 1984; Kojima 1994).

Not only the amounts of solar radiation that slopes of different aspects receive, but also many other factors shall be involved in determining the distribution of plant communities. However, the vegetation on the south-slope at present may be considered a model representing what we may expect to see for the north-slope ecosystem under the warmer climate at the end of the twenty-first century. A simulation analysis of high latitude forests for Alaska, USA (Bonan et al. 1990) suggested that reduction of the permafrost by warmer climate will make the soil active

layer deep on the north-slope, leading to establishment of *Picea glauca* forests (Bonan et al. 1990). Following a similar argument, Kojima (1994) predicted for the north-slope of central Yukon Territory, Canada that *Picea mariana* forest or forest-tundra of this species may shift to respectable stands of *Picea glauca* and/or *P. mariana*. The north-slope is currently underlain by the permafrost; but the depth of soil active layer is likely to increase dramatically under the warmer climate. Increased depth of the active layer will still allow the soils to have sufficient moisture for good tree growth. Mesic soils also make the intensity of forest fires moderate, and much of the decomposing aboveground litter are kept from being consumed by fires. These conditions are amenable to development of coniferous forests of good stature. Therefore, one of the possible outcomes for the state of the north-slope vegetation in the warm world is something similar to those we presently see on the south-slope.

We observed around Tura in Central Siberia that forests are dominated nearly exclusively by *Larix gmelinii* regardless of slope aspect. However, we see short and thin trees on the north-facing slope, whereas south-facing slope commonly support stands of tall and thick trees, even for forests of a given stand age (Fig. 24.5a; see also Chaps. 14 and 17). The larch trees on the north-slope are growing on shallow soil active layer of only 30–50 cm deep (Fig. 24.5a) (Koike et al. 1998, 1999; see also Chaps. 4, 6, 7, 14 and 16). The soil on the north-slope is colder, and nutrient is less available than the south-slope (Chaps. 4, 6, 7, 11, 14, and 16). The canopy trees are often stunted, and show dieback (Chaps. 6, 7, and 16). On the other hand,

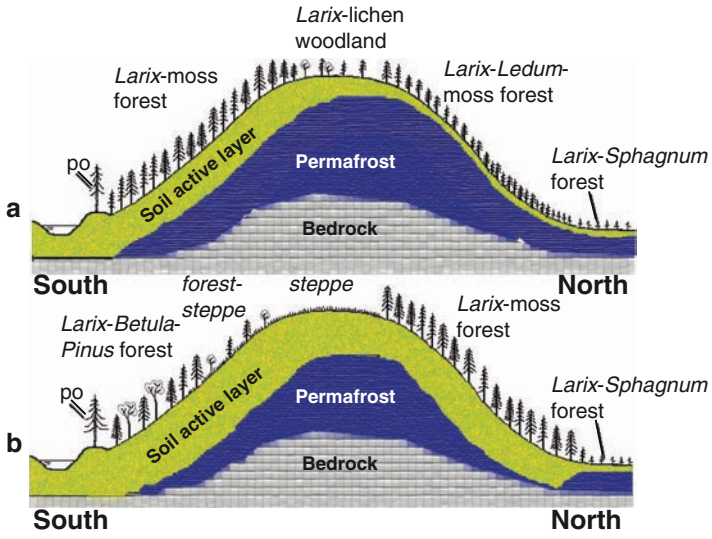

Fig. 24.5 Schematic representation of the distribution of vegetation on north- and south-facing slopes in northern taiga of Central Siberia: (**a**) present; (**b**) speculative prediction during the decade 2090–2100 under 2 X CO_2 scenario of atmospheric CO_2 concentration. The drawings are intended to show the vegetation around Tura at 64°N. Specific patterns of vegetation may vary depending on latitude and other factors

the larch trees on the south-slope are growing on warmer soils with soil active layer of 140 cm or deeper (Fig. 24.5a). Fallen leaves of *Duschekia fruticosa*, a shrub species, can also suppress development of the moss community by physically accumulating over it. These features of the forest floor generally indicate better nutrient condition of the south-slope.

Prediction of vegetation change on the south-slope appears more difficult. As was indicated by a simulation study for Alaska (Bonan et al. 1990), soils will become extremely dry on south-facing slopes. Then, the stands of *Picea glauca* on the south-slope will be replaced by those of *Populus* species or even by the steppe vegetation. Kojima (1994) suggested a possible outcome of the warmer climate under the 2 X CO_2 environment in central Yukon Territory. Increased exposure to fire will accelerate drying of the soils on the south-slope, and steppe may be the only vegetation that could be developed after frequent fires (Kojima 1994). However, *Populus tremuloides* and *Picea glauca* can also occupy lower part of the south-slope where the moisture condition is more moderate.

Analogy to the prediction in Yukon Territory suggests the following vegetation on the south-slope of Central Siberia at the end of the twenty-first century. Steppe will be the major type of vegetation as in the high latitude of North America. Tchebakova et al.'s prediction for Central Siberia indicates invasion by *Larix sibirica* at the latitudes lower than approximately 60°N (Chap. 22). It suggests that the permafrost is no longer present there continuously regardless of the slope aspect. On the other hand, areas north of the 60th parallel will still have the continuous permafrost, although *L. sibirica* is present at small abundance in the permafrost region of the Arctic in Western Siberia (see Fig. 22.2). Therefore, it is deduced that the south-slope has deep soil active layer, but the permafrost may be present underneath. A kind of vegetation possible under this condition is a mixed-species community of *Larix gmelinii*, *Betula pubescence*, *B. pendula*, and *Pinus sibirica* and/or *P. sylvestris*, with varying proportions of the species depending on situations (Fig. 24.5b). The trees will be shorter and sparser at upper slopes, approaching the steppe vegetation at the hill-top. Of course, there will be considerable variations depending on the latitude and local situations. The community of sparse *L. gmelinii* and *Sphagnum* mosses at a water-logged site may or may not be present on flat areas depending on changes in water regime of the site. The *Picea obovata* along the river banks will probably persist, since the local environmental condition is affected most strongly by the presence of rivers, and may not change drastically there (shown as Po in Fig. 24.5b). Accordingly, hydrological characteristics of the permafrost forest appear to have paramount importance. Potential effect of the warming climate on regional hydrology will be discussed later in this chapter (see Sect. 24.3.3.2).

24.3.1.3 Forest Dimension and Biomass

During the course of present investigation reported in the preceding chapters, we have observed that tree sizes differ dramatically in *Larix gmelinii* ecosystems in

Central Siberia depending on two factors. (1) The trees are generally bigger on south-slopes than on north-slopes, as was already described. (2) The trees tend to be significantly taller along rivers, streams, and lines of probable water movement. As a result, aerial view of the landscape in the northern taiga of Central Siberia show that areas of relatively short vegetation are commonly bounded by the lines of much taller trees along streams and water courses (Fig. 24.6). These two characteristics of tree sizes suggest possible changes in forest structure on the north-slope ecosystems under the warmer climate. Trees on the north-slope ecosystems are likely to become larger if structure of the north-slope communities approaches that of the south-slope in the future.

Appearance of larger trees along the streams and the lines of water movement is likely to suggest that those are the places of better nutrient availability. Chapin et al. (1988) reported a similar pattern in the Alaskan tussock tundra. Simultaneously, permafrost ecosystems are nutrient-limited in general (Chapin et al. 1988; Schulze et al. 1995). The predicted deepening of soil active layer on the north-slope is likely to ameliorate the generally nutrient poor condition of the permafrost ecosystems. What will happen seems predictable from the analogy to trees along the water-course. Trees are likely to become bigger due to the new condition of better nutrient availability.

Despite the discussions in the preceding part of this chapter, changes in tree size and stand biomass may be uncertain on the south-slope. Warmer environment should allow the trees to become larger if water is sufficient. However, trees could

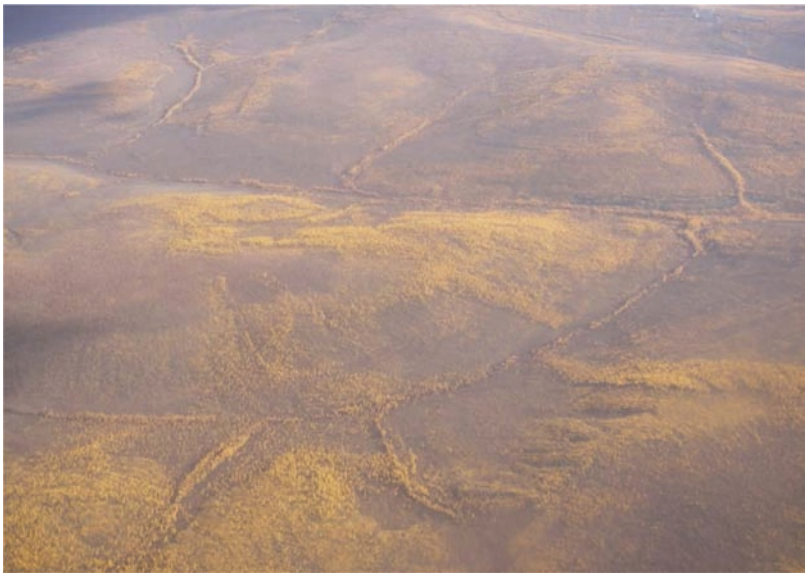

Fig. 24.6 Aerial view of the landscape near Tura in Central Siberia, where vegetation of relatively short trees are commonly bounded by the lines of much taller trees along streams and water courses (photo: Y. Matsuura)

become smaller and sparser if water becomes limited. The outcome at the end of the twenty-first century probably depends on latitude and local factors also.

24.3.2 Ecosystem Development

Following changes in the permafrost behavior and development patterns of stand structure may be predicted as the first qualitative approximation that may happen under the warmer climate. We limit the discussion to the permafrost larch forest on north-facing slopes, because most data in the previous chapters came from this site. The patterns of stand and permafrost development over time are depicted in Fig. 24.7a by reproducing the patterns already discussed (Fig. 24.1).

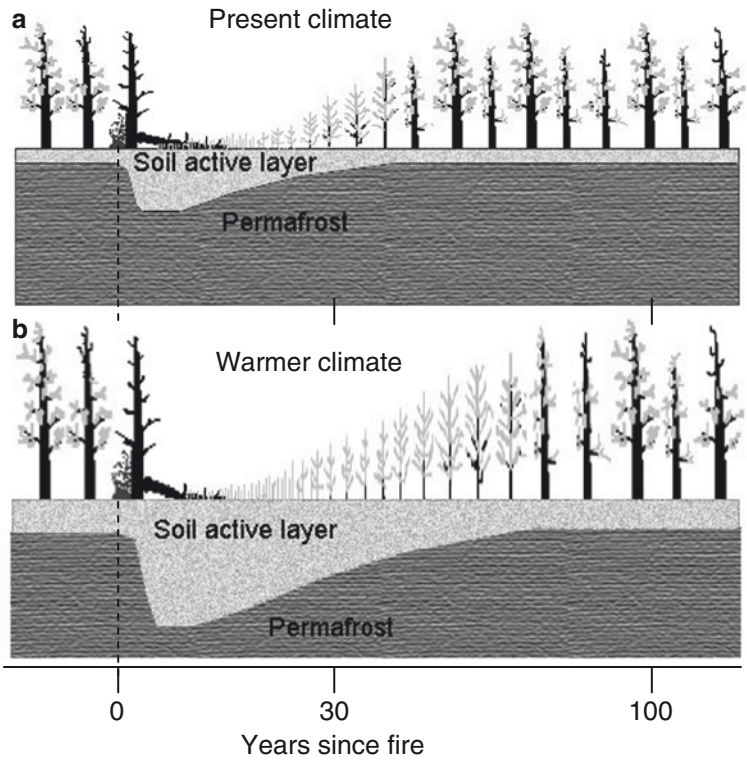

Fig. 24.7 Schematic representation of the patterns of larch forest development over time after a stand-replacing fire and changes in soil horizons that are underlain by continuous permafrost at Tura, Central Siberia. (**a**) Development pattern on a generally north-facing slope under the present climate; (**b**) development pattern also on north-facing slope under the warmer climate at the end of the twenty-first century with an assumption of increased tree growth. A fire is assumed to have occurred at year zero. Both horizontal and vertical axes are not to scale

Warmer climate would produce deeper soil active layer in the permafrost (Fig. 24.8). Analogy to present-day south-facing slope suggests that the active layer of an intact larch forest may become as deep as 120–140 cm or more on the north-slope (Fig. 24.7b). Note the deeper active layer just before the fire under the warmer climate (Fig. 24.7b), compared with the present climate (Fig. 24.7a). This would lead to two phenomena in the status of the permafrost over time. First, the depth of soil active layer becomes very deep after stand-replacing forest fires. The depth of more than 250 cm is probably not unrealistic under the warm climate (note the depth at ca. 10 years after fire; Fig. 24.7b). Second, deeper soil active layer just after the fire would create a longer period for recovery of the permafrost to the prefire depth and/or a longer period of higher surface soil temperature for less-restricted tree growth. Therefore, good tree growth with active self-thinning may continue much longer under the warmer climate. The result will be a larger average tree size and accumulation of greater aboveground biomass in the stand (Figs. 24.7b and 24.8). Better growth of the trees may be a result of improved soil nutrient availability in warmer surface soils (Fig. 24.8; see also Chaps. 9, 12, and 16).

However, these predictions may not be realized if other factors prevent the trees to grow better under the warmer climate. Shortened growing season due to heavier snow accumulation in winter (Chap. 17) and substantially reduced summer precipitation (Chaps. 13 and 22) are possibilities (Fig. 24.8). Obviously, further work is necessary to reach more definite conclusions.

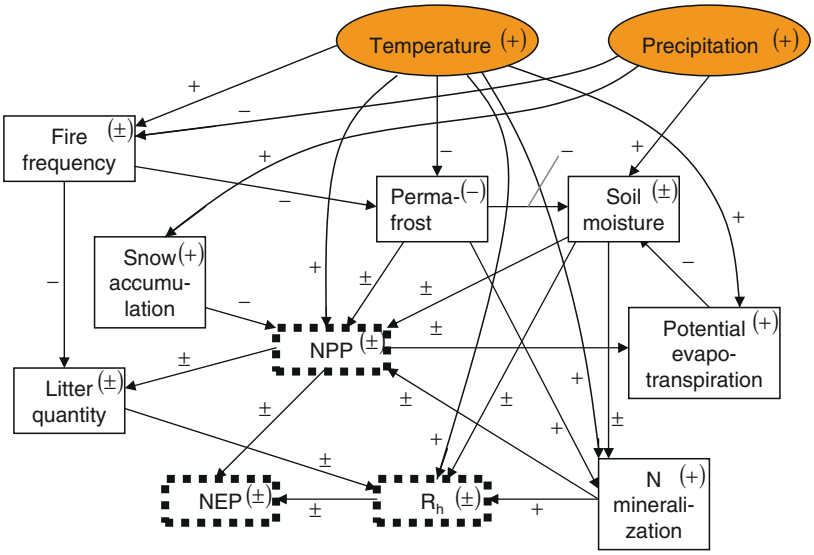

Fig. 24.8 Direct and indirect effects of temperature and precipitation (in oval symbols) on permafrost and vegetation, through changes in NPP, heterotrophic respiration (R_h), and net ecosystem production, and other components related to carbon exchange between permafrost forest ecosystem and the atmosphere. The plus (+), minus (−), and plus-minus (±) signs represent that the effect is to increase, decrease, or direction of change uncertain, respectively

24.3.3 Ecosystem Function

So far, we have discussed possible effects of climate warming on ecosystem structure between the levels of biomes and stands. The discussion was restricted to the world where the atmospheric CO_2 concentration is twice the present value. These changes will develop as a result of the accumulated effects on plant physiology, as well as on ecology of competing organisms. Therefore, potential effects of the warming on ecosystem function should also be considered to understand the changes in ecosystem structure that may develop over time. The preceding chapters of this volume have identified the following characteristics.

24.3.3.1 Biomass Allocation

Allocation of organic matter in trees is likely to be affected by the climate change. Stands, particularly on the north-slope, will allocate more biomass to aboveground organs under the warmer climate. Comparison of above- and belowground biomass allocation in various boreal forests suggests this possibility (Kajimoto et al. 1999, 2006; see also Chaps. 6 and 16). The ratio of aboveground biomass and root biomass (referred to as *T*/*R* ratio) is generally greater than 4 in *L. gmelinii* stands growing on relatively thick soil active layer (see Table 6.2). These stands are of young trees developing after the stand-replacing forest fires. However, stands of various tree species also show the *T/R* ratio of 4 or larger when growing without permafrost. This indicates that trees allocate more than 75% of organic matter to aboveground organs. Another example of *Pinus sylvestris* forest in the nonpermafrost region of southern Siberia showed the value 5, indicating aboveground mass allocation of 80%. In contrast, the *T/R* ratio of old *L. gmelinii* stands shows the values between 0.9 and 2.8. This means that the proportion of organic matter allocation to aboveground organs is between 47 and 73%. The tendency is clear. The trees allocate more organic matter to roots when growing over the permafrost soils with thin soil active layer. This is presumably to increase the absorbing surface of fine roots to capture more nutrients in the nutrient-poor environment of permafrost soils. Therefore, if the warming climate let the permafrost recede to deeper horizons, and makes the soil active layer thicker, it will be likely to cause increased biomass allocation to aboveground organs.

On the other hand, warmer soil temperature generally promotes increased fine root production (see Chaps. 9 and 20), suggesting allocation of more organic matter to belowground organs under the warmer climate. Clearly, this is a pattern opposite to that suggested in the previous paragraph. Increased fine root production may also mean more leaf biomass, which will lead to higher transpiration and lower soil moisture (Fig. 24.8). Therefore, the pattern of biomass allocation depends on hydrological characteristics of the site as well. Further work is necessary to clarify which patterns are more likely to occur under the warmer climate.

24.3.3.2 Hydrology

Regardless of a large fluctuation in annual precipitation, annual evapotranspiration was fairly stable in the continuous permafrost zone of Northeastern Siberia (Chap. 13). This is probably a result of the trees in larch forest to have an ability to use melt water from the permafrost during drought years (Chap. 13). Therefore, permafrost is acting as a buffer against fluctuations in annual precipitation. This characteristic in hydrology of the larch forests suggests that, even if the summer precipitation is reduced under the warmer climate, it is likely to have small effect on photosynthetic production of the larch trees for some time (perhaps decades). Only after substantial reduction of the permafrost, the effect of progressive drought will appear on tree growth (Fig. 24.8).

As was summarized by Ohta (Chap. 13), the low evapotranspiration in the Siberian forests resulted from its strong land surface regulation. In other words, low soil water content, high atmospheric water vapor deficit, and small leaf mass (and area) are inter-linked, and lead to low evapotranspiration rates in the permafrost forests of Siberia in drought years. These patterns suggest in return that potential increase in tree growth and tree size in warmer climate may lead to substantially increased evapotranspiration due to increased leaf biomass. This may then reduce the amount of available water for plants, and may feedback negatively to worsened tree growth (Fig. 24.8). In all, effect of the warming climate on hydrology of permafrost forests is still poorly understood. Reliable prediction rests on improved knowledge of the interaction among the atmosphere, vegetation, and permafrost soils.

24.3.3.3 Soil Respiration

The rate of soil respiration is known to increase with the increasing values of soil temperature (Chen and Tian 2005), aboveground litter fall (Bowden et al. 1993; Sulzman et al. 2005), and nutrient availability (Nadelhoffer 2000; Burton et al. 2000) (Fig. 24.8). However, very high or low soil moisture tend to inhibit soil respiration (Bouma and Bryla 2000; Yuste et al. 2003). All these parameters are likely to be affected by the warming climate. Therefore, amount of CO_2 efflux from the soil surface may change in the warmer world. A strong and nearly exponential relationship of soil respiration with temperature has been established by many studies, including a report by T. Morishita et al. (Chap. 9). Therefore, the warmer climate will generally be associated with higher rate of soil respiration (Fig. 24.8).

However, it is necessary to consider possible changes in the input of aboveground litter, belowground litter (fine root mortality), available nutrients in the soil, soil moisture, and other factors that may also affect soil respiration (Fig. 24.8; Davidson and Janssens 2006). Warmer soil temperature may facilitate mineralization of nitrogen and other soil nutrients. It may lead to increased production and turnover of fine roots. These characteristics are likely to facilitate increased microbial activity, thus increased soil respiration. However, these characteristics also

suggest increased plant-derived carbon inputs to soils, which may exceed increases in decomposition. Therefore, feedback to climate change may be either positive or negative (Fig. 24.8) (Davidson and Janssens 2006).

Possible deepening of the soil active layer on the north-facing slope that we discussed earlier in this chapter is likely to create warmer soils, increased nitrogen mineralization, and increased tree growth (Fig. 24.8). All these characteristics are likely to lead to increased production of leaves and other aboveground organs. Therefore, input of aboveground litter will increase. Then, the rate of soil respiration is likely to become greater.

On the other hand, excessive drying of the soils under the steppe or forest steppe vegetation on the south-facing slope and hill tops (Tchebakova et al.; Chap. 22) may create conditions dry enough to inhibit soil respiration.

Another scenario of decreased soil respiration comes from a possibility of tree growth reduction caused by increased winter precipitation under the warmer climate (Chap. 17). Reduced tree growth may lead to decrease in the amount of aboveground litter, then reduction in soil respiration. The increase in winter precipitation is likely to occur throughout the larch ecosystems of Siberia, affecting the landscape regardless of the slope aspect. Therefore, overall effect of climate warming on soil respiration is somewhat uncertain, particularly in cases of extreme increase in winter precipitation and/or development of excessive drought conditions.

24.3.3.4 DOC

Prokushkin et al. indicated (Chap. 11) that the warming climate is likely to increase the retention time of DOC in the deepened mineral soil due to subsidence of the permafrost to deeper horizons. Therefore, the warming may result in the increased accumulation of C in the subsoil. In addition, increased frequency of forest fires under the warmer climate will make the C pool smaller in upper organic horizons. Therefore, frequent fires will have an effect of reduced DOC output from the forested watersheds.

If the warming trend is associated with increased precipitation in the summer, however, the amount of DOC export from forests to streams will increase substantially (Chap. 11). This is due to the combined effect of increased runoff and associated higher concentration of DOC in the stream water. Therefore, the possible pattern of DOC export and retention will depend on the degree of increase in both air temperature and summer precipitation.

24.3.3.5 Delayed Snowmelt and Tree Growth

Yasue et al. showed (Chap. 17) that winter precipitation as snow has an effect of delaying the timing of snow melt and of shortening the period of growing season, which then cause reduction in tree-ring mass substantially (Fig. 24.8). A similar relationship was observed between the amount of winter precipitation and tree-ring

width in the same study area (Kujansuu et al. 2007a, b). This characteristic is something that has become apparent during the past several decades in high-latitude forests of the circum-polar region, but was absent previously (Vaganov et al. 1999; Kirdyanov et al. 2003). Therefore, changing climate of the region is the likely cause of increased snow fall and reduction in tree growth. A commonly observed correlation between tree-ring growth and summer air temperature has become weak also. We may argue that the increasing trend of winter precipitation eventually leads to reduced organic matter accumulation as forest biomass in the subarctic forests of Siberia.

24.3.3.6 Complex Interactions

As was summarized in Fig. 24.8, the effects of warming air temperature on various compartments of the permafrost forest ecosystem are complex. Direction of the effect is positive, negative, or uncertain, depending on the part of the ecosystem. The effect may also vary depending on the status of the permafrost: the warming climate may affect the forest production positively at the initial part of the climate change, but it may produce detrimental effects when the soil becomes too dry after receding of the permafrost in several decades or more. Our understanding is also poor at present regarding regional hydrology (Chaps. 13 and 17) and nitrogen nutrition in this ecosystem (Chap. 12). Further studies are necessary to narrow the uncertainties.

24.4 Conclusions

This study has identified the following characteristics of the permafrost larch forests of Central and Northeastern Siberia, and their potential responses to warming climate:

- Characteristics of forest stand development in the continuous permafrost zone of Siberia are constrained by forest fires and status of the frozen soils. Deepening of soil active layer shortly after fire and recovery of the permafrost table over time are the key factors influencing forest development.
- The old *Larix gmelinii* forest on the permafrost showed NEP value of 0.8 MgC ha^{-1} $year^{-1}$, with NPP and R_h of 1.2 and 0.3 MgC ha^{-1} $year^{-1}$, respectively, excluding carbon fixation by the forest floor plants. It is likely that this larch ecosystem is close to carbon neutral in which NEP is nearly zero.
- Tree species that occupy an ecological niche of *Larix gmelinii* or *L. cajanderi* in Siberia appear missing in North America. *Picea mariana* forms nearly closed-canopy or open-canopy stands over the permafrost, but appreciable region of its distribution over the continuous permafrost is restricted to a relatively small area of lower MacKenzie River basin in northwestern Canada.

- Region of the permafrost forests is likely to persist at latitudes above 60°N after a century of climate warming. Larch trees on northern slopes are likely to become larger in response to deepened soil active layer. Southern slopes are likely to become dry, so that larch communities may give way to mixed stands of smaller larch and *Betula* and *Pinus* species.
- Warming climate is likely to prolong the period of deep soil active layer after a forest fire, allowing the larches on more mesic north-slopes to become larger in size until recovery of the previous permafrost table.
- Allocation of large amount of assimilated organic matter into roots in permafrost forests may be altered by the warming climate. It is likely to be reduced; but opposite trend may also be possible. Direction of change in soil respiration, DOC export from the ecosystem, and tree growth by altered pattern of precipitation is also somewhat uncertain.
- Regardless of a large fluctuation in annual precipitation, annual evapotranspiration of permafrost forest was relatively stable in Siberia – probably a result of the larches to have an ability to use melt water from the permafrost during drought years.

Acknowledgments We thank Nadja Tchebakova for calculating distribution of future biomes in Siberia with her model, and producing Fig. 24.4.

References

Anderson PM, Lozhkin AV (2001) The stage 3 interstadial complex (Karginskii/middle Wisconsinan interval) of Beringia: variations in paleoenvironments and implications for paleoclimatic interpretations. Quaternary Science Reviews 20:93–125

Barbour MG, Burk JH, Pitts WD (1980) Terrestrial plant ecology. Benjamin/Cummings Publishing, Menlo Park

Barr AG, Griffis TJ, Black TA, Lee X, Staebler RM, Fuentes JD, Chen Z, Morgenstern K (2002) Comparing the carbon budgets of boreal and temperature deciduous forest stands. Can J For Res 32:813–822

Berg EE, Chapin FS III (1994) Needle loss as a mechanism of winter drought avoidance in boreal conifers. Can J For Res 24:1144–1148

Black RA, Bliss LC (1980) Reproductive ecology of *Picea mariana* (MILL.) BSP, at tree line near Inuvik, Northwest Territories, Canada. Ecol Monogr 50:331–354

Bonan GB, Shugart HH, Urban DL (1990) The sensitivity of some high-latitude boreal forests to climatic parameters. Clim Change 16:9–29

Bouma TJ, Bryla DR (2000) On the assessment of root and soil respiration for soils of different textures: interactions with soil moisture contents and soil CO2 concentrations. Plant Soil 227:215–221

Bowden RD, Nadelhoffer KJ, Boone RD, Melillo JM, Garrison JB (1993) Contributions of aboveground litter, belowground litter, and root respiration to total soil respiration in a temperate mixed hardwood forest. Can J For Res 23:1402–1407

Brown J, Ferrians OJ, Heginbottom JA, Melnikov ES (1997) Circum-arctic map of permafrost and ground-ice conditions. Circum-Pacific Map Series MAP CP-45, US Geological Survey

Burns RM, Honkala BH (eds) (1990) Silvics of North America. Agricultural Handbook 654. USDA, Forest Service, Washington, DC

Burton AJ, Pregitzer KS, Hendrick RL (2000) Relationships between fine root dynamics and nitrogen availability in Michigan northern hardwood forests. Oecologia 125:389–399

Chapin FS III, Fetcher N, Kielland K, Everett KR, Linkins AE (1988) Productivity and nutrient cycling of Alaskan tundra: enhancement by flowing soil water. Ecology 69:693–702

Chapin FS III, Woodwell GM, Randerson JT, Rastetter EB, Lovett GM, Baldocchi DD, Clark DA, Harmon ME, Schimel DS, Valentini R, Wirth C, Aber JD, Cole JJ, Goulden ML, Harden JW, Heimann M, Howarth RW, Matson PA, McGuire AD, Melillo JM, Mooney HA, Neff JC, Houghton RA, Pace ML, Ryan MG, Running SW, Sala OE, Schlesinger WH, Schulze E-D (2006) Reconciling carbon-cycle concepts, terminology, and methods. Ecosystems 9:1041–1050

Chen H, Tian HQ (2005) Does a general temperature-dependent Q_{10} model of soil respiration exist at biome and global scale? J Integr Plant Biol 47:1288–1302

Davidson EA, Janssens IA (2006) Temperature sensitivity of soil carbon decomposition and feedbacks to climate change. Nature 440:165–173

Dixon RK, Brown S, Houghton RA, Solomon AM, Trexler MC, Wisniewski J (1994) Carbon pools and flux of global forest ecosystems. Science 263:185–190

Edwards ME, Brubaker LB, Lozhkin AV, Anderson PM (2005) Structurally novel biomes: a response to past warming in Beringia. Ecology 86:1696–1703

Fukuzaki K (2008) Aboveground net primary production and biomass of forest floor vegetation (mosses, lichens, shrubs) in natural larch forest on Siberian permafrost. Thesis. Department of Forest Science, Faculty of Agriculture, Kyoto University, 20pp (in Japanese)

Gordon C, Cooper C, Senior C (2000) The simulation of SST, sea-ice extents and ocean heat transport in a version of the Hadley Centre coupled model without flux adjustments. Clim Dyn 16:147–168

Gower ST, Richards JH (1990) Larches: deciduous conifers in an evergreen world. Bioscience 40:818–826

Gower ST, Krankina O, Olson RJ, Apps M, Linder S, Wang C (2001) Net primary production and carbon allocation patterns of boreal forest ecosystems. Ecol Appl 11:1395–1411

Högberg P, Nordgren A, Buchmann N, Taylor AFS, Ekblad A, Högberg MN, Nyberg G, Ottosson-Lövenius M, Read DJ (2001) Large-scale forest girdling shows that current photosynthesis drives soil respiration. Nature 411:789–792

Houghton JT, Jenkins GJ, Ephraums JJ (1990) Climate change: the IPCC Scientific assessment. Cambridge University Press, Cambridge, MA

Johnston WF (1990) Larix laricina (Du Roi) K. Koch, Tamarack. In: Burns RM, Honkala BH (eds) Silvics of North America, Agricultural Handbook 654. USDA, Forest Service, Washington, DC

Kajimoto T, Matsuura Y, Sofronov MA, Volokitina AV, Mori S, Osawa A, Abaimov AP (1999) Above- and belowground biomass and net primary productivity of a *Larix gmelinii* stand near Tura, central Siberia. Tree Physiol 19:815–822

Kajimoto T, Matsuura Y, Osawa A, Abaimov AP, Zyryanova OA, Isaev AP, Yefremov DP, Mori S, Koike T (2006) Size-mass allometry and biomass allocation of two larch species growing on the continuous permafrost region in Siberia. For Ecol Manage 222:314–325

Kharuk VI, Ranson KJ, Dvinskaya M (2007) Evidence of evergreen conifer invasion into larch dominated forests during recent decades in Central Siberia. Eurasian J For Res 10:163–171

Kirdyanov AV, Hughes MK, Vaganov EA, Schweingruber FH, Silkin P (2003) The importance of early summer temperature and date of snowmelt for tree growth in the Siberian subarctic. Trees 17:61–69

Kloeppel BD, Gower ST, Treichel IW, Kharuk S (1998) Foliar carbon isotope discrimination in *Larix* species and sympatric evergreen conifers: a global comparison. Oecologia 114:153–159

Koike T, Mori S, Matsuura Y, Prokushkin SG, Zyranova OA, Kajimoto T, Abaimov AP (1998) Photosynthesis and foliar nutrient dynamics in larch and spruce grown on contrasting north- and south-facing slopes in the Tura Experiment Forest in central Siberia. In: Mori S, Kanazawa Y, Matsuura Y, Inoue G (eds) Proceedings of the sixth symposium on the Joint Siberian Permafrost studies between Japan and Russia in 1997. Tsukuba, pp 3–10

Koike T, Mori S, Matsuura Y, Prokushkin SG, Zyryanova OA, Kajimoto T, Sasa K, Abaimov AP (1999) Shoot growth and photosynthetic characteristics in larch and spruce affected by

temperature of the contrasting north and south facing slopes in eastern Siberia. In: Shibuya M, Takahashi K, Inoue G (eds) Proceedings of the seventh symposium on the Joint Siberia Permafrost studies between Japan and Russia in 1998, Tsukuba, pp 3–12

Kojima S (1994) Boreal ecosystems and global climate warming. Jpn J Ecol 44:105–113

Kujansuu J, Yasue K, Koike T, Abaimov AP, Kajimoto T, Takeda T, Tokumoto M, Matsuura Y (2007a) Responses of ring widths and maximum densities of *Larix gmelinii* to climate on contrasting north- and south-facing slopes in central Siberia. Ecol Res 22:582–592

Kujansuu J, Yasue K, Koike T, Abaimov AP, Kajimoto T, Takeda T, Tokumoto M, Matsuura Y (2007b) Climatic responses of tree-ring widths of *Larix gmelinii* on contrasting north-facing and south-facing slopes in central Siberia. J Wood Sci 53:87–93

Lacourse T, Gajewski K (2000) Late quaternary vegetation history of Sulphur Lake, southwest Yukon Territory, Canada. Arctic 53:27–35

Légère A, Payette S (1981) Ecology of a black spruce (*Picea mariana*) clonal population in the hemiarctic zone, northern Quebec: population dynamics and spatial development. Arct Alp Res 13:261–276

Matsuura Y, Kajimoto T, Osawa A, Abaimov AP, Zyryanova OA (2004) Coarse woody debris estimation in a *Larix gmelinii* stand in Tura, central Siberia. In: Proceedings of the seventh international conference on global change connection to the arctic (GCCA7). International Arctic Research Center, University of Alaska Fairbanks, pp 199–202

Nadelhoffer KJ (2000) The potential effects of nitrogen deposition on fine-root production in forest ecosystems. New Phytol 147:131–139

Nakai Y, Matsuura Y, Kajimoto T, Abaimov AP, Yamamoto S, Zyryanova OA (2008) Eddy covariance CO_2 flux above a Gmelin larch forest on continuous permafrost of Central Siberia during a growing season. Theor Appl Climatol 93:133–147

O'Connell KEB, Gower ST, Morman JM (2003) Comparison of net primary production and light-use dynamics of two boreal black spruce forest communities. Ecosystems 6:236–247

Osawa A (1995) Inverse relationship of crown fractal dimension to self-thinning exponent of tree populations: a hypothesis. Can J For Res 25:1608–1617

Osawa A, Allen RB (1993) Allometric theory explains self-thinning relationships of mountain beech and red pine. Ecology 74:1020–1032

Payette S, Gagnon R (1979) Tree-line dynamics in Ungava peninsula, northern Quebec. Holarct Ecol 2:239–248

Penalba MC, Payette S (1997) Late-Holocene expansion of eastern larch (*Larix laricina* [Du Roi] K. Koch) in northwestern Quebec. Quatern Res 48:114–121

Prokushkin AS, Kajimoto T, Prokushkin SG, McDowell WN, Abaimov AP, Matsuura Y (2005) Climatic factors influencing fluxes of dissolved organic carbon from the forest floor in a continuous-permafrost Siberian watershed. Can J For Res 35:2129–2139

Ritchie JC (1977) The modern and late Quaternary vegetation of the Campbell-dolomite uplands, near Inuvik, N.W.T. Canada. Ecol Monogr 47:401–423

Ritchie JC (1982) The modern and late-quaternary vegetation of the Doll area, north Yukon, Canada. New Phytol 90:563–603

Ritchie JC (1984) Past and present vegetation of the far northwest of Canada. University of Toronto Press, Toronto

Ritchie JC (1985) Late-Quaternary climatic and vegetational change in the lower MacKenzie basin, northwest Canada. Ecology 66:612–621

Rudolph TD, Laidly PR (1990) Pinus banksiana Lamb. Jack Pine. In: Burns RM, Honkala BH (eds) Silvics of North America, Agriculture Handbook 654. USDA Forest Service, Washington, DC

Saigusa N, Yamamoto S, Hirata R, Ohtani Y, Ide R, Asanuma J, Gamo M, Hirano T, Kondo H, Kosugi Y, Li S-G, Nakai Y, Takagi K, Tani M, Wang H (2008) Temporal and spatial variations in the seasonal patterns of CO_2 flux in boreal, temperate, and tropical forests in East Asia. Agr Forest Meteorol 148:700–713

Schulze E-D (2006) Biological control of the terrestrial carbon sink. Biogeoscience 3:147–166

Schulze E-D, Schulze W, Kelliher FM, Vygodskaya NN, Ziegler W, Kobak KI, Koch H, Arneth A, Kusnetsova WA, Sogatchev A, Issajev A, Bauer G, Hollinger DY (1995) Aboveground biomass

and nitrogen nutrition in a chronosequence of pristine Dahurian *Larix* stands in eastern Siberia. Can J For Res 25:943–960

Subke J-A, Inglima I, Cotrufo MF (2006) Trends and methodological impacts in soil CO_2 efflux partitioning: A metaanalytical review. Global Change Biol 12:9321–9943

Sulzman EW, Brant JB, Bowden RD, Lajtha K (2005) Contribution of aboveground litter, belowground litter, and rhizosphere respiration to total soil CO_2 efflux in an old growth coniferous forest. Biogeochemistry 73:231–256

Tyrrell LE, Boerner RE (1987) *Larix laricina* and *Picea mariana*: relationships among leaf lifespan, foliar nutrient patterns, nutrient conservation, and growth efficiency. Can J Bot 65:1570–1577

Vaganov EA, Hughes MK, Kirdyanov AV, Schweingruber FH, Silkin PP (1999) Influence of snowfall and melt timing on tree growth in subarctic Eurasia. Nature 400:149–151

Valentini R, Matteucci G, Dolman AJ, Schulze E-D, Rebmann C, Moors EJ, Granier A, Gross P, Jensen NO, Pilegaard K, Lindroth A, Grelle A, Bernhofer C, Grünwald T, Aubinet M, Ceulemans R, Kowalski AS, Vesala T, Rannik Ü, Berbigier P, Loustau D, Guðmundsson J, Thorgeirsson H, Ibrom A, Morgenstern K, Clement R, Moncrieff J, Montagnani L, Minerbi S, Jarvis PG (2000) Respiration as the main determinant of carbon balance in European forests. Nature 404:861–865

Van Cleve K, Chapin FS III, Flanagan PW, Viereck LA, Dyrness CT (eds) (1986) Forest ecosystems in the Alaskan taiga. Ecological Studies, vol 57. Springer, Berlin

Wein RW, MacLean D (1983) The role of fire in northern circumpolar ecosystems. Scope 18, Wiley, Toronto

Yuste JC, Janssens IA, Carrara A, Meiresonne L, Caulemans R (2003) Interactive effects of temperature and precipitation on soil respiration in a temperate maritime pine forest. Tree Physiol 23:1263–1270

Color Plates

Fig. 10.2 The tower equipped with all devices (Photo: Y. Nakai)

Fig. 2.4 Longitudinal rock fields on the west-side slope of the Kochechum River (photo: H. Daimaru)

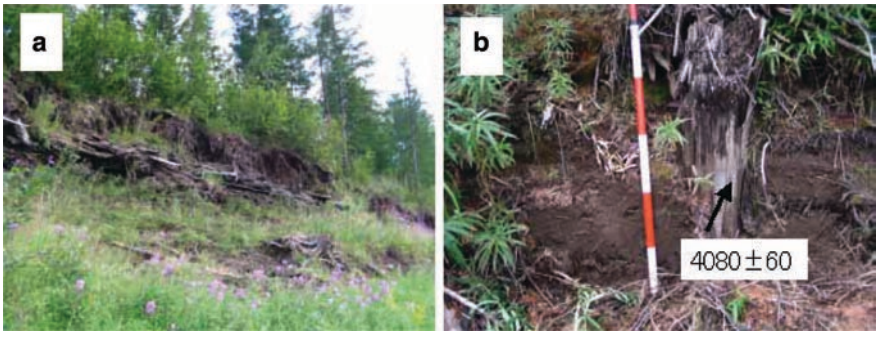

Fig. 2.8 (**a**) Ancient tree stumps and log jam buried by fluvial sand of the natural levee. (**b**) Most outside part of a buried wood stump was dated as 4,080 ± 60 yBP (Daimaru et al. unpublished data)

Fig. 8.1 Typical soil profiles under larch forests; (**a**) in Yakutian basin, Northeastern Siberia (62° 09′N, 130° 38′E), (**b**) in Central Siberia (64° 19′N, 100° 14′E), and (**c**) earth hummock mound soil in forest tundra of Kolyma Lowland (68° 41′N, 160° 17′E). Profile (**a**) had light-colored sandy texture in the active layer. On the other hand, profile (**b**) had high rock fragment ratio in the active layer with loamy and/or clay loamy texture. In this profile (**b**), ice-filled cracks emerged at the bottom of the profile. The cross-section of earth hummock mound (**c**) showed thin A horizon (indicated by white small pins) and bowl-shaped subsoil with diffuse gley mottling (Photos: Y. Matsuura)

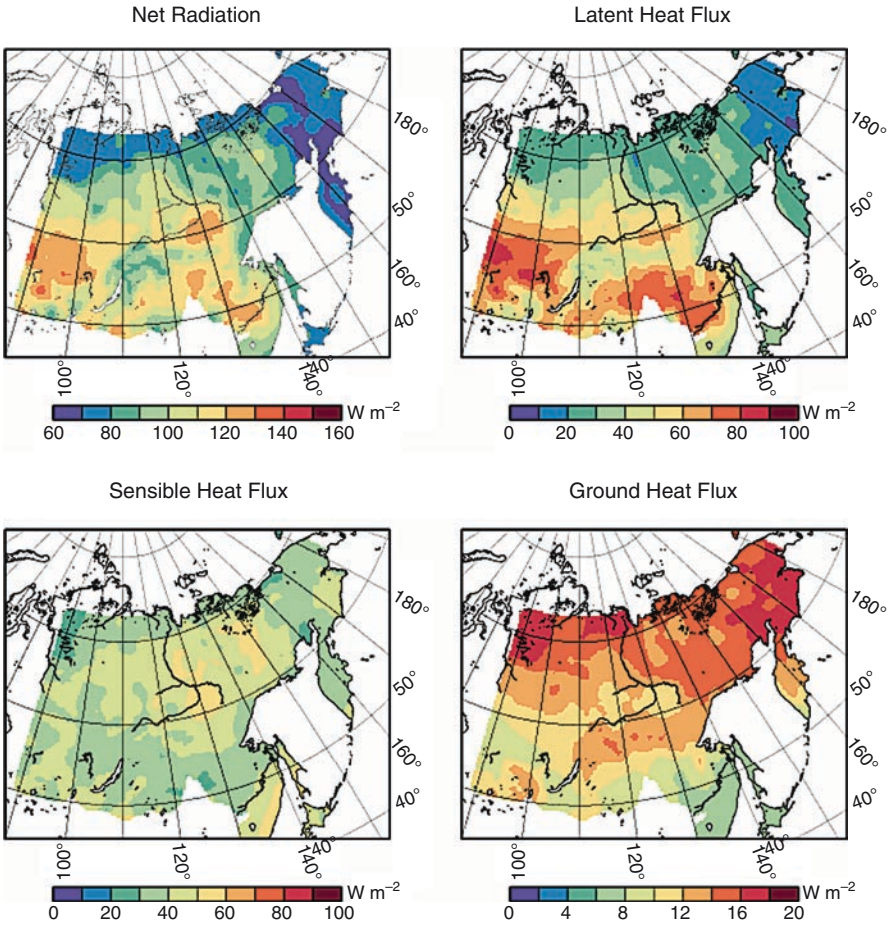

Fig. 13.10 Spatial mean distribution of net all-wave radiation, latent heat flux, sensible heat flux, and ground heat flow over Central and Northeastern Siberia during a period 1986–2004, estimated by a land surface model (Park et al. 2008)

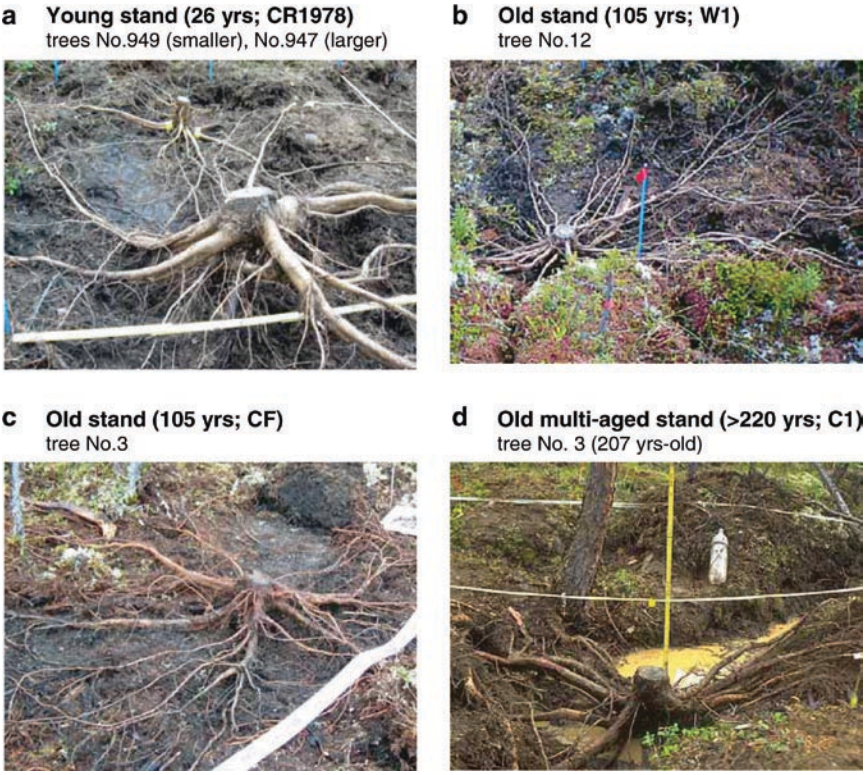

Fig. 16.1 Examples of *L. gmelinii* root systems excavated in four stands at Tura, Central Siberia. (**a**) Trees No. 947 (larger one; 25 years-old at sampling year, breast height diameter $D = 4.4$ cm) and No. 949 (smaller one; 24 years-old, $D = 2.1$ cm) in young stand (CR1978). (**b**) Tree No. 12 (99 years-old, $D = 3.2$ cm) of old stand (W1). (**c**) Tree No. 3 (105 years-old, $D = 5.9$ cm) of old stand (CF). (**d**) Tree No. 3 (207 years-old, $D = 7.7$ cm) of old multiaged stand (C1). Tap root length (i.e., depth of aborted tip portion) is 14 and 12 cm (No. 947 and No. 949 of CR1978, respectively), 19 cm (No. 12 of W1), 23 cm (No. 3 of CF), and 36 cm (No. 3 of C1) (photos: T. Kajimoto)

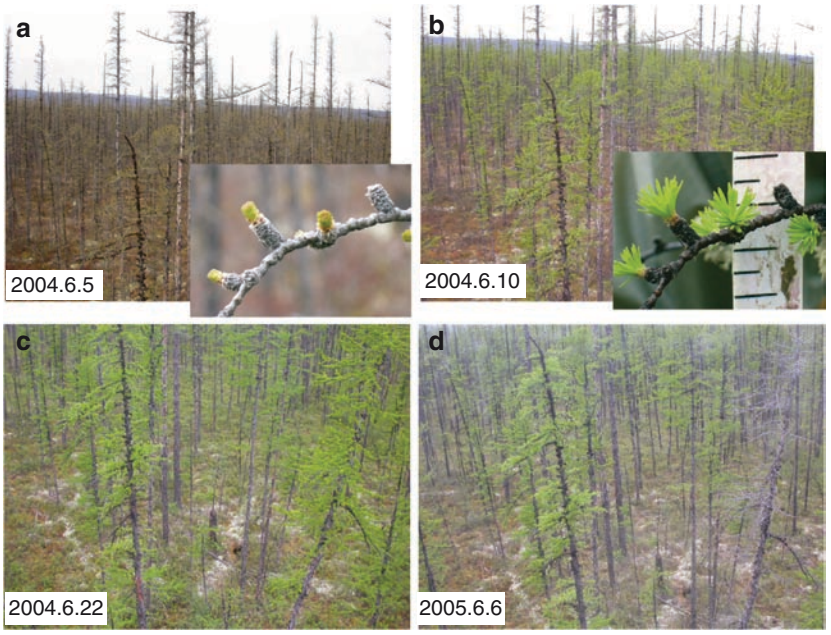

Fig. 17.3 Needle development of *Larix gmelinii* at Carbon flux site in Tura in 2004 (**a**–**c**) and 2005 (**d**) observed by automatic camera (Yasue et al. unpublished data)

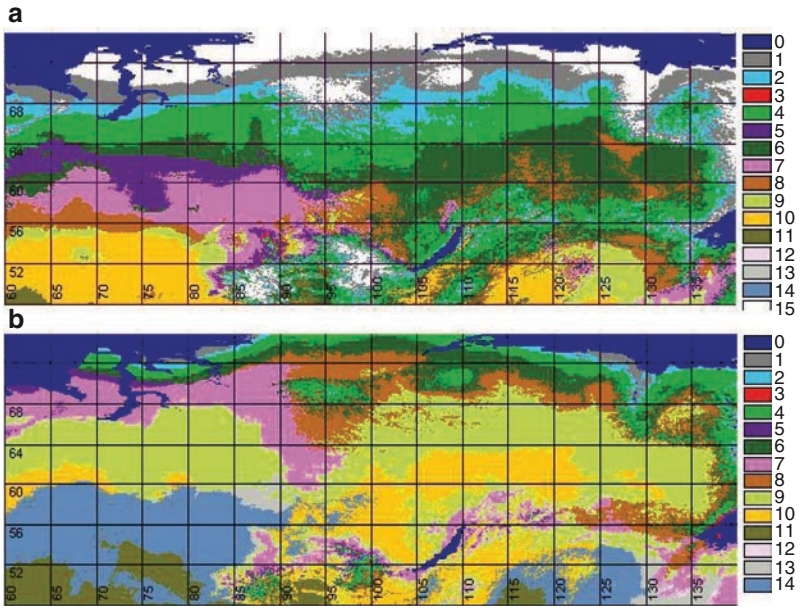

Fig. 22.1 Vegetation distribution in Siberia for the contemporary climate (**a**) and for the climate projected for the decade beginning in 2090 (**b**) (Soja et al. 2007). Numerals indicate the following: Water (0), tundra (1), forest-tundra (2), northern dark (3) and light (4) taiga, middle dark (5) and light (6) taiga, southern dark (7) and light (8) taiga, forest-steppe (9), steppe (10), dry steppe (11), broadleaved (12), temperate forest-steppe (13), and temperate steppe (14)

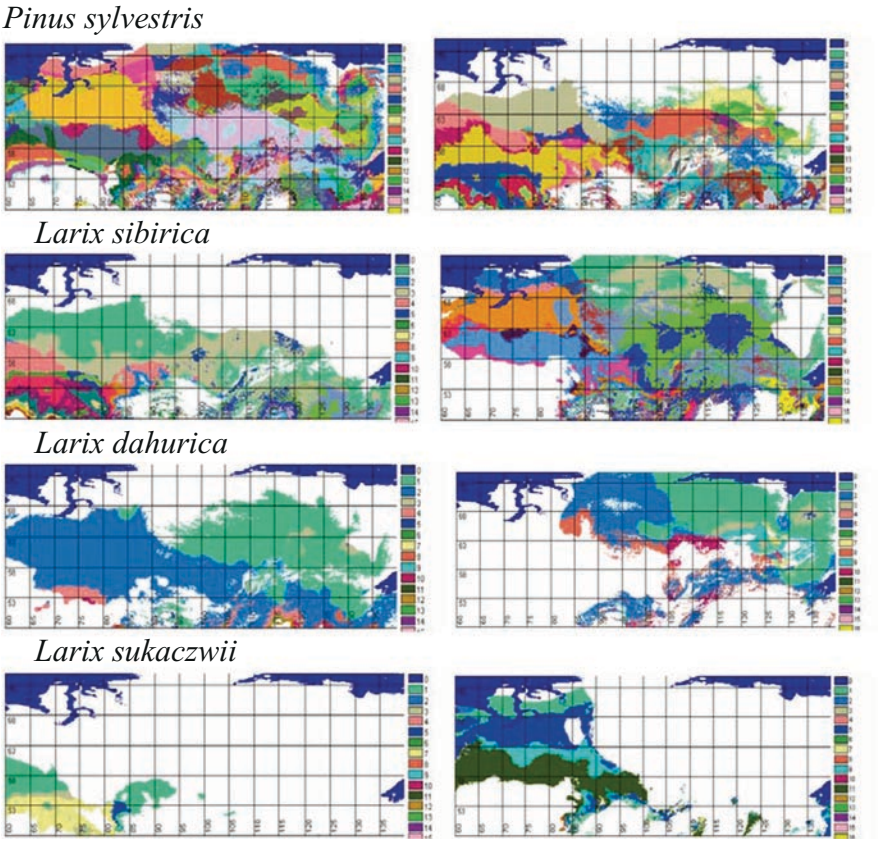

Fig. 22.3 Distributions of climatypes in Siberia for *Pinus sylvestris* and Siberian Larches (*Larix sibirica*, *L. dahurica,* and *L. sukaczewii*) in the contemporary climate (**a**) and in decade beginning in 2090 (**b**). For each species, one color corresponds to a single climatype of 180 possible climatypes for *Pinus sylvestris,* 48 for *Larix sibirica*, 12 for *L. dahurica*, and 12 for *L. sukaczewii* (see Table 22.5, Tchebakova et al. 2003)

Illustration and Table Credits

Fig. 1.2 After Fig. 2.8 in H. Hytteborn et al., Boreal forests of Eurasia, in F. Andersson (ed), Coniferous Forests, Ecosystems of the World 6, Page 42, Elsevier, Amsterdam (2005)

Fig. 2.1 After Fig. 1 in G. Czamanske et al., Demise of the Siberian plume: paleogeographic and paleotectonic reconstruction from the prevolcanic and volcanic record, northcentral Siberia. International Geology Review 40, Page 96, Taylor & Francis, Zug (1998)

Fig. 4.2 After Fig. 1 in M.A. Sofronov et al., Zonal peculiarities of forest vegeta-tion controlled by fires in Northern Siberia, in Eurasian Journal of Forest Research 1, Page 54, Hokkaido University, Sapporo (2000)

Fig. 4.3 After Fig. 1 in M.A. Sofronov et al., The ecological role of moss-lichen cover and thermal amelioration of larch forest ecosystems in the northern part of Siberia, in Eurasian Journal of Forest Research 7-1, Page 12, Hokkaido University, Sapporo (2004)

Fig. 4.4 After Fig. 2 in M.A. Sofronov et al., The ecological role of moss-lichen cover and thermal amelioration of larch forest ecosystems in the northern part of Siberia, in Eurasian Journal of Forest Research 7-1, Page 15, Hokkaido University, Sapporo (2004)

Fig. 4.5 After Fig. 3 in M.A. Sofronov et al., The ecological role of moss-lichen cover and thermal amelioration of larch forest ecosystems in the northern part of Siberia, in Eurasian Journal of Forest Research 7-1, Page 16, Hokkaido University, Sapporo (2004)

Fig. 4.7 After Fig. 4 in M.A. Sofronov et al., The ecological role of moss-lichen cover and thermal amelioration of larch forest ecosystems in the northern part of Siberia, in Eurasian Journal of Forest Research 7-1, Page 18, Hokkaido University, Sapporo (2004)

Fig. 6.8 After Fig. 3, in T. Kajimoto et al., Size-mass allometry and biomass al-location of two larch species growing on the continuous permafrost region in Siberia, in Forest Ecology and Management 222, Page 322, Elsevier, Oxford (2006)

Fig. 7.8 After Fig. 2 in A. Osawa et al., Reconstructing structural development of even-aged larch stands in Siberia, in Canadian Journal of Forest Research 30, Page 584, NRC Research Press, Ottawa (2000)

Fig. 7.9 After Fig. 3 in A. Osawa et al., Reconstructing structural development of even-aged larch stands in Siberia, in Canadian Journal of Forest Research 30, Page 585, NRC Research Press, Ottawa (2000)

Fig. 7.10 After Fig. 4 in A. Osawa et al., Reconstructing structural development of even-aged larch stands in Siberia, in Canadian Journal of Forest Research 30, Page 585, NRC Research Press, Ottawa (2000)

Fig. 7.11 After Fig. 5 in A. Osawa et al., Reconstructing structural development of even-aged larch stands in Siberia, in Canadian Journal of Forest Research 30, Page 586, NRC Research Press, Ottawa (2000)

Table 7.2 After Table 1 in A. Osawa et al., Reconstructing structural develop-ment of even-aged larch stands in Siberia, in Canadian Journal of Forest Research 30, Page 584, NRC Research Press, Ottawa (2000)

Table 7.3 After Table 2 in A. Osawa et al., Reconstructing structural develop-ment of even-aged larch stands in Siberia, in Canadian Journal of Forest Research 30, Page 585, NRC Research Press, Ottawa (2000)

Fig. 11.6 After Fig. 2 in A. Prokushkin et al., Fluxes of dissolved organic matter in larch forests in the cryolithozone of Central Siberia, in Russian Journal of Ecology 39, Page 153, Pleiades Publishing, Ltd., Moscow (2008)

Fig. 11.7 After Fig. 3 in A. Prokushkin et al., Fluxes of dissolved organic matter in larch forests in the cryolithozone of Central Siberia, in Russian Journal of Ecology 39, Page 154, Pleiades Publishing, Ltd., Moscow (2008)

Fig. 11.12 After Fig. 16.7 in A. Prokushkin et al., Global warming and dissolved organic carbon release from permafrost soils, in Margesin Rosa (ed), Permafrost Soils, Page 245, Springer, Dordrecht, (2009)

Fig. 13.1 After Fig. 5, in T. Ohta et al., Seasonal variation in the energy and wa-ter exchanges above and below a larch forest in eastern Siberia, in Hydrological Processes 15, Page 1467, Wiley-Blackwell, Oxford (2001)

Fig. 13.2 After Fig. 3, in T. Ohta et al., Interannual variation of water balance and summer evapotranspiration in an eastern Siberian larch forest over a 7-year period (1998-2006), in Agricultural and Forest Meteorology 148, Page 1946, Elsevier, Oxford (2008)

Fig. 13.3 After Fig. 4, in T. Ohta et al., Interannual variation of water balance and summer evapotranspiration in an eastern Siberian larch forest over a 7-year period (1998-2006), in Agricultural and Forest Meteorology 148, Page 1947, Elsevier, Oxford (2008)

Fig. 13.5 After Fig. 8, in T. Ohta et al., Interannual variation of water balance and summer evapotranspiration in an eastern Siberian larch forest over a 7-year period (1998-2006), in Agricultural and Forest Meteorology 148, Page 1949, Elsevier, Oxford (2008)

Fig. 13.6 After Fig. 9, in T. Ohta et al., Interannual variation of water balance and summer evapotranspiration in an eastern Siberian larch forest over a 7-year period (1998-2006), in Agricultural and Forest Meteorology 148, Page 1950, Elsevier, Oxford (2008)

Fig. 13.7 After Fig. 5, in K. Matsumoto et al., Energy consumption and evapotranspiration at several boreal and temperate forests in the Far East, in Agricultural and Forest Meteorology 148, Page 1985, Elsevier, Oxford (2008)

Fig. 13. 8 After Fig. 9, in K. Matsumoto et al., Energy consumption and evapotranspiration at several boreal and temperate forests in the Far East, in Agricultural and Forest Meteorology 148, Page 1987, Elsevier, Oxford (2008)

Fig. 13. 9 After Fig. 10, in K. Matsumoto et al., Energy consumption and evapotranspiration at several boreal and temperate forests in the Far East, in Agricultural and Forest Meteorology 148, Page 1987, Elsevier, Oxford (2008)

Fig. 13.10 After Fig. 3, in H. Park et al., Tempo-spatial characteristics of energy budget in the eastern Siberia, in Agricultural and Forest Meteorology 148, Page 1996, Elsevier, Oxford (2008)

Table 13.1 After Table 2, in T. Ohta et al., Interannual variation of water balance and summer evapotranspiration in an eastern Siberian larch forest over a 7-year period (1998-2006), in Agricultural and Forest Meteorology 148, Page 1947, Elsevier, Oxford (2008)

Table 13.2 After Table 3, in H. Park et al., Tempo-spatial characteristics of en-ergy budget in the eastern Siberia, in Agricultural and Forest Meteorology 148, Page 1998, Elsevier, Oxford (2008)

Fig. 16.1(d) After Fig. 1(B), in T. Kajimoto et al., Root system development of Larix gmelinii trees affected by micro-scale conditions of permafrost soils in central Siberia, in Plant and Soil 255, Page 284, Springer, Dordrecht (2003)

Fig. 16.2(b), (c) After Fig. 2b (No.12, No.13), in T. Kajimoto et al., Root system development of Larix gmelinii trees affected by micro-scale conditions of permafrost soils in central Siberia, in Plant and Soil 255, Page 287, Springer, Dordrecht (2003)

Fig. 16.2(a), (d), and (e) After Fig. 2A-D, in T. Kajimoto et al., Individual-based measurement and analysis of root system development: case studies for Larix gmelinii trees growing on the permafrost region in Siberia, in Journal of Forest Research 12, Page 106, Springer Japan, Tokyo (2007)

Fig. 16.3 After Fig. 1, in T. Kajimoto et al., Individual-based measurement and analysis of root system development: case studies for Larix gmelinii trees growing on the permafrost region in Siberia, in Journal of Forest Research 12, Page 106, Springer Japan, Tokyo (2007)

Fig. 16.4 After Fig. 3, in T. Kajimoto et al., Individual-based measurement and analysis of root system development: case studies for Larix gmelinii trees growing on the permafrost region in Siberia, in Journal of Forest Research 12, Page 107, Springer Japan, Tokyo (2007)

Fig. 16.10(a) and (c) After Fig. 4A-B, in T. Kajimoto et al., Root system development of Larix gmelinii trees affected by micro-scale conditions of permafrost soils in central Siberia, in Plant and Soil 255, Page 288, Springer, Dordrecht (2003)

Fig. 16.11(b) and (c) After Fig. 4A-B, in T. Kajimoto et al., Individual-based measurement and analysis of root system development: case studies for Larix gmelinii trees growing on the permafrost region in Siberia, in Journal of Forest Research 12, Pages 108, Springer Japan, Tokyo (2007)

Fig. 16.14 After Fig. 6A-B, in T. Kajimoto et al., Individual-based measurement and analysis of root system development: case studies for Larix gmelinii trees growing on the permafrost region in Siberia, in Journal of Forest Research 12, Page 109, Springer Japan, Tokyo (2007)

Fig. 16.15 After Fig. 7, in T. Kajimoto et al., Root system development of Larix gmelinii trees affected by micro-scale conditions of permafrost soils in central Siberia, in Plant and Soil 255, Page 290, Springer, Dordrecht (2003)

Fig. 17.1 After Fig. 2, in J. Kujansuu et al., Responses of ring widths and maximum densities of Larix gmelinii to climate on contrasting north- and south-facing slopes in central Siberia, in Ecological Research 22, Page 584, Springer Japan, Tokyo (2007)

Fig. 17.7 After Fig. 5, in J. Kujansuu et al., Responses of ring widths and maximum densities of Larix gmelinii to climate on contrasting north- and south-facing slopes in central Siberia, in Ecological Research 22, Page 587, Springer Japan, Tokyo (2007)

Fig. 17.8 After Fig. 6, in J. Kujansuu et al., Responses of ring widths and maximum densities of Larix gmelinii to climate on contrasting north- and south-facing slopes in central Siberia, in Ecological Research 22, Page 588, Springer Japan, Tokyo (2007)

Fig. 17.9 After Fig. 8, in J. Kujansuu et al., Responses of ring widths and maximum densities of Larix gmelinii to climate on contrasting north- and south-facing slopes in central Siberia, in Ecological Research 22, Page 590, Springer Japan, Tokyo (2007)

Fig. 17.10 After Fig. 9, in J. Kujansuu et al., Responses of ring widths and maximum densities of Larix gmelinii to climate on contrasting north- and south-facing slopes in central Siberia, in Ecological Research 22, Page 591, Springer Japan, Tokyo (2007)

Fig. 22.1 After Fig. 9, in Soja et al., Climate-induced boreal forest change: Predictions versus current observations, Global and Planetary Change 56, Page 284, Elsevier, Oxford (2007)

Fig. 22.2 After Figs. 1b, 1c, 2b, and 2c, in N. Tchebakova, Impacts of climate change on the distribution of Larix spp. and Pinus sylvestris and their climatypes in Siberia, in Mitigation and Adaptation Strategies for Global Change 11(4), Pages 866, 867, Springer, Dordrecht (2006)

Table 22.2 After Table I, in N. Tchebakova, Impacts of climate change on the dis-tribution of Larix spp. and Pinus sylvestris and their climatypes in Siberia, in Mitigation and Adaptation Strategies for Global Change 11(4), Page 865, Springer, Dordrecht (2006)

Table 22.4 After Table III, in N. Tchebakova, Impacts of climate change on the distribution of Larix spp. and Pinus sylvestris and their climatypes in Siberia, in Mitigation and Adaptation Strategies for Global Change 11(4), Pages 873, Springer, Dordrecht (2006)

Table 22.5 After Table IV, in N. Tchebakova, Impacts of climate change on the distribution of Larix spp. and Pinus sylvestris and their climatypes in Siberia, in Mitigation and Adaptation Strategies for Global Change 11(4), Pages 875, Springer, Dordrecht (2006)

Species Index

Subject Index